

DOCUMENT RESUME

ED 058 455

VT 014 596

TITLE Exploring in Aerospace Rocketry. An Introduction to the Fundamentals of Rocketry.

INSTITUTION National Aeronautics and Space Administration, Cleveland, Ohio. Lewis Research Center.

REPORT NO NASA-EP-88

PUB DATE 71

NOTE 366p.

AVAILABLE FROM Superintendent of Documents, U.S. Government Printing Office, Washington, D.C. 20402 (Stock No. 3300-0394; NAS1.19:88, \$3.25)

EDRS PRICE MF-\$0.65 HC-\$13.16

DESCRIPTORS Aerospace Industry; *Aerospace Technology; *Curriculum Guides; Illustrations; *Industrial Education; Instructional Materials; Occupational Guidance; *Resource Materials; *Textbooks

IDENTIFIERS *Rocketry

ABSTRACT

This curriculum guide is based on 2 years of lectures and projects of a contemporary, special-interest aerospace program for promising students, ages 15-19. The program uses technical lectures, project activities and field trips to introduce students to the real engineering world of pioneering aerospace achievement, and the variety of skills and careers it involves. This book can be used as a curriculum resource for high school and college teachers, and may be helpful to curriculum committees and textbook writers. Teachers in various disciplines can use selected chapters to enrich or supplement regular courses, including applied mathematics, physics, chemistry and biology. With modification, some of the material could be useful industrial arts and vocational education courses. The 22 chapters are supplemented with numerous illustrations, photographs, charts, and line drawings. A related document is available as VT 014 597. (CD)

ED 058455



SURPRI
DUPLIC.

SCOPE OF INTEREST NOTICE

The ERIC Facility has assigned this document for processing to:

In our judgement, this document is also of interest to the clearinghouses noted to the right. Indexing should reflect their special points of view.

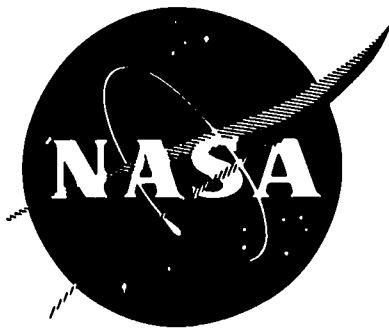
VT

CG

4 - OCT 27
Cop 07

EXPLORING IN AEROSPACE ROCKETRY

An Introduction to the Fundamentals of Rocketry



VT014596

NATIONAL AERONAUTICS AND SPACE ADMINISTRATION

ED 058455

U.S. DEPARTMENT OF HEALTH,
EDUCATION & WELFARE
OFFICE OF EDUCATION
THIS DOCUMENT HAS BEEN REPRO-
DUCED EXACTLY AS RECEIVED FROM
THE PERSON OR ORGANIZATION ORIG-
INATING IT. POINTS OF VIEW OR OPIN-
IONS STATED DO NOT NECESSARILY
REPRESENT OFFICIAL OFFICE OF EDU-
CATION POSITION OR POLICY.

EXPLORING IN AEROSPACE ROCKETRY

**an Introduction to the Fundamentals of Rocketry
developed at the NASA Lewis Research Center, Cleveland, Ohio**

**National Aeronautics and Space Administration, Washington, D.C. 20546
1971**

For sale by the Superintendent of Documents, U.S. Government Printing Office
Washington, D.C., 20402 - Price \$8.25
Stock Number 8800-0394

PREFACE

"Exploring in Aerospace Rocketry" is an educational publication based on the lectures and projects conducted during 2 years of the NASA-Lewis Aerospace Explorer program. (A similar publication, titled "Exploring in Aeronautics" (NASA EP-89), is based on the activities of 1 year during which the program focused on aeronautics.) This publication is intended not only to provide a basic explanation of some of the fundamentals of rocketry but also to stimulate other government agencies, educational institutions, private industry, and business to establish career-motivation programs within their own particular fields of activity.

The Lewis Aerospace Explorer program was started in December 1965 by the Director of the NASA-Lewis Research Center. The principal objective of this program is to provide promising students from local schools an opportunity for vocational guidance and motivation for a wide range of technical professions in the aerospace field. Each year, candidates (ages 15 to 19 years) for the program are selected by school officials on the basis of their demonstrated interest and proficiency in mathematics and science. NASA's intent is to take these young people outside the academic classroom and to expose them to the real engineering world of pioneering aerospace achievement. This transposition is made by introducing the youths to the kind of men, skills, thinking, planning, organization, and action necessary for successful mission accomplishment. Focus is on the interdisciplinary character of the aerospace teams. Specifically, NASA is attempting to expose the young people to the great variety of skills and careers that are integrated into and have impact on the general aerospace field.

The program format consists of technical lectures (illustrated with slides, motion pictures, demonstrations, etc.), project activities, and field trips. In the lectures, basic physical principles are explained, and unique analytical and experimental tools of the business are described. In the project activities, the youths learn by doing. Projects are assigned, planned, implemented, and analyzed, and the results are reported in considerable detail. In effect, the youths are exposed to a realistic "research-and-development" environment. The field trips help the participants to better understand various facets of science and technology.

Throughout the program, communication (both oral and written) is highly emphasized. The ability to communicate effectively is an important requirement for almost any career. For realistic exercises in communication, the young people in the program maintain pro-

ject notebooks, give oral progress reports, and conduct research-and-development conferences, or symposia.

The success of the program is reflected in the attendance, interest, active participation, and enthusiasm of the young people themselves. Most of those who complete the program continue on through college, pursuing careers of their choice. We at NASA hope, of course, that some of these young people will choose careers in aerospace engineering. However, the program is achieving its objective merely by arousing the interest of these young people and helping them in a realistic way to explore various career possibilities.

NASA-Lewis employee participation in the program is considerable. Many employees enthusiastically and sincerely work with the young people and help them in their scientific endeavors. Thus, the youths are exposed to a wide range of aerospace-oriented personnel - technicians, engineers, scientists, and administrators. The time and effort donated to the program by these NASA employees is their personal contribution to the future well-being and success of our youth and our nation.

Those employees who lectured to the Explorers are identified herein as the authors of the chapters. These lecturers also served as associate advisers on the various project activities. Other employees who donated their time and talent to the program included Dr. Abe Silverstein (Explorer Post sponsor); W. G. Mirshak, William J. Ratvasky, Larry E. Smith, John F. Staggs, and Richard S. Williams (all associate advisers on projects); Harold D. Wharton (institutional representative); John C. Evvard, Bruce R. Leonard, Roger W. Luidens, Roy A. Maurer, John L. Pollack, and Calvin W. Weiss (all members of Program-Project Committee); Joseph F. Hobzek, Jr., William A. Brahms, Donald A. Kelsey, Clair R. King, L. L. Manley, and Horace C. Moore, Jr., (all members of Explorer Post Committee); and Clifford W. Brooks (photographer for the program and associate adviser on projects).

James F. Connors
Director of Technical Services
(Adviser, Lewis Aerospace Explorer Post)

INTRODUCTION

Rockets have been used for centuries. By 1000 B.C., and perhaps as early as 3000 B.C., the Chinese had developed rockets for display and for use in warfare. As early as the 2nd century A.D., science fiction was written about imaginary rocket trips to the Moon. Early in the 20th century, Robert H. Goddard began a study of the use of rockets for reaching extreme altitudes, and his work laid the foundation for much of our present rocket technology. The development of rockets sophisticated enough to lift men to the Moon and return them to Earth has captured the attention of people everywhere. The study of the principles of rocketry is quite appropriate, therefore, for those who wish to understand the space age.

This book could be used as a curriculum resource for teachers in high schools and colleges. It might also be helpful to curriculum committees and textbook writers. It discusses many topics which teachers in various disciplines can use to enrich or supplement their regular courses. Many applications of the laws of physics are evident throughout the chapters. Examples of applied mathematics are abundant. Applications of chemistry will be found in the chapters on thermodynamics, materials, and propellants. Material related to biology will be found in the chapter on biomedical engineering. In general, these applications will be most meaningful with students of high ability.

The book could be used as the basis for an elective course in rocketry. Teachers who are interested in this possibility will want to do some reading in related literature in order to identify numerical problems which can be used to reinforce the concepts presented.

Some of the material, if presented at a lower level of sophistication, could be useful in industrial arts and vocational education courses. Students and adults who are hobbyists in model rocketry will find much of the book relevant to their interests.

It is hoped that one outcome of the use of this book, and of the companion volume, "Exploring in Aeronautics" (NASA EP-89), will be to stimulate the interest and imagination of capable students so that many of them will be interested in following developments in the rapidly changing aerospace field.

CONTENTS

| Chapter | | Page |
|---------|--|------|
| | PREFACE | iii |
| | INTRODUCTION | v |
| 1 | AEROSPACE ENVIRONMENT John C. Evvard Atmosphere. Space and planetary environments. Earth-Sun relations. Van Allen radiation belts. Solar winds. Thermal radiation. Meteoroid hazards. Solar flares. | 1 |
| 2 | PROPULSION FUNDAMENTALS James F. Connors Newton's Second Law of Motion (Force = Mass \times Acceleration). Newton's Third Law of Motion (Action = Reaction). Thrust. Momentum. Exhaust velocity. Specific impulse. Nozzle flow and thrust performance. | 29 |
| 3 | CALCULATION OF ROCKET VERTICAL-FLIGHT PERFORMANCE John C. Evvard Simplified calculation procedure for determining altitude for powered and coasting vertical flight for single and multistaged model rockets. | 45 |
| 4 | THERMODYNAMICS Marshall C. Burrows Propellant fundamentals. Injection. Mixing and vaporization. Ignition. Combustion. Heat transfer. Methods of cooling. Unstable processes. | 61 |
| 5 | MATERIALS William D. Klopp High-temperature throat inserts for rocket nozzles. Weld fractures in rocket casings. Lightweight, shatterproof fuel tanks. | 79 |

| Chapter | | Page |
|---------|--|------|
| 6 | SOLID-PROPELLANT ROCKET SYSTEMS Joseph F. McBride History. Propellant grain types and designs. Motor cases. Ignition devices. Nozzles. Steering control. | 95 |
| 7 | LIQUID-PROPELLANT ROCKET SYSTEMS E. William Conrad Propellants. Tankage. Pumps. Drives. Coolant systems. Injectors. Combustion chambers. Nozzles. Associated plumbing. | 111 |
| 8 | ZERO-GRAVITY EFFECTS William J. Masica Effects of gravity on fluid dynamical behavior in tanks of liquid rocket systems. Surface tension. Vapor-liquid interface. Heat transfer. Zero-gravity facilities. | 127 |
| 9 | ROCKET TRAJECTORIES, DRAG, AND STABILITY Roger W. Luidens Powered, coasting, and parachute trajectories. Drag. Static stability. Centers of pressure and gravity of model rockets. Orbital and escape velocities. | 143 |
| 10 | SPACE MISSIONS Richard J. Weber Requirements for manned and unmanned missions. Sounding rockets. Planetary flyby missions. Planetary landing modules. | 161 |
| 11 | LAUNCH VEHICLES Arthur V. Zimmerman Booster and upper stages. Systems. Launch sites. Vehicle performance. Staging requirements. NASA launch vehicles and their lifting capabilities. | 171 |



| Chapter | Page |
|---|------|
| <p>12 INERTIAL GUIDANCE SYSTEMS 187 Daniel J. Shramo</p> <p>Navigation. Inertial navigation system. Gyroscope. Gyroscopic drift. Accelerometers.</p> | |
| <p>13 TRACKING 209 John L. Pollack</p> <p>Observations and measurements from ground stations. Instruments. Tri- angulation. Altitude and range determinations. Range layout.</p> | |
| <p>14 ROCKET LAUNCH PHOTOGRAPHY 225 William A. Bowles</p> <p>The camera as a documentation and flight recording tool. Photographic techniques. Optical instrumentation.</p> | |
| <p>15 ROCKET MEASUREMENTS AND INSTRUMENTATION 237 Clarence C. Gettelman</p> <p>Rocket performance variables expressed in terms of measurable quantities. Measurement of force, pressure, temperature, and volume flow rate.</p> | |
| <p>16 ELEMENTS OF COMPUTERS 249 Robert L. Miller</p> <p>Principles of analog and digital computers. Applications. Machine lan- guage - logic. Storage and memory systems. Programming. Illustrations of representative facilities.</p> | |
| <p>17 ROCKET TESTING AND EVALUATION IN GROUND FACILITIES . . . 261 John H. Povolny</p> <p>Test facilities. Static firings. Thermal-vacuum testing of systems and components. Structural dynamics. Reliability and quality assurance.</p> | |

| Chapter | | Page |
|---------|---|------|
| 18 | LAUNCH OPERATIONS Maynard I. Weston Teamwork. Communications. Scheduling. Range safety requirements. Procedures. Operations. Global tracking networks. | 281 |
| 19 | NUCLEAR ROCKETS A. F. Lietzke Principles. Fission heating of hydrogen. Reactor concepts. Specific impulse potential. Comparisons with chemical rockets. | 301 |
| 20 | ELECTRIC PROPULSION Harold Kaufman Propulsion principles. Ionization methods. Electrostatic acceleration. Continuous-low-thrust missions. Comparison of high-specific-impulse electric engines with chemical and nuclear rocket systems. Power requirements. | 313 |
| 21 | BIOMEDICAL ENGINEERING Kirby W. Hiller Engineering principles and technology applied to the fields of biology and medicine in the areas of diagnostics, treatment, prosthetics, and biological research. Physiology of the human circulatory system. | 333 |
| 22 | PROJECTS IN ROCKETRY James F. Connors Projects in propulsion, electronics, model-rocket launch operations, aerodynamics, payloads and recovery, and tracking. | 355 |

1. AEROSPACE ENVIRONMENT

John C. Evvard*

In the broad sense, the word "space" is all-inclusive. It includes the Sun, the Earth, and the other planets of the solar system. It includes the one hundred billion stars or more in our own galaxy, which we label the "Milky Way." It includes all the other galaxies of the universe which we see as nebulae. The great nebula in Andromeda is shown in figure 1-1. Certainly there are billions of stars in this disk-shaped conglomeration, some of which may have planets and living, intelligent beings. If the environment near these billions of stars is right for living forms, then life might exist on some of them, but this is a challenge for the future. Our solar system probably is not unique even in our own galaxy, and we know that there are billions of galaxies in the universe.



CS-17763

Figure 1-1. - Great nebula in Andromeda.

*Associate Director for Research.

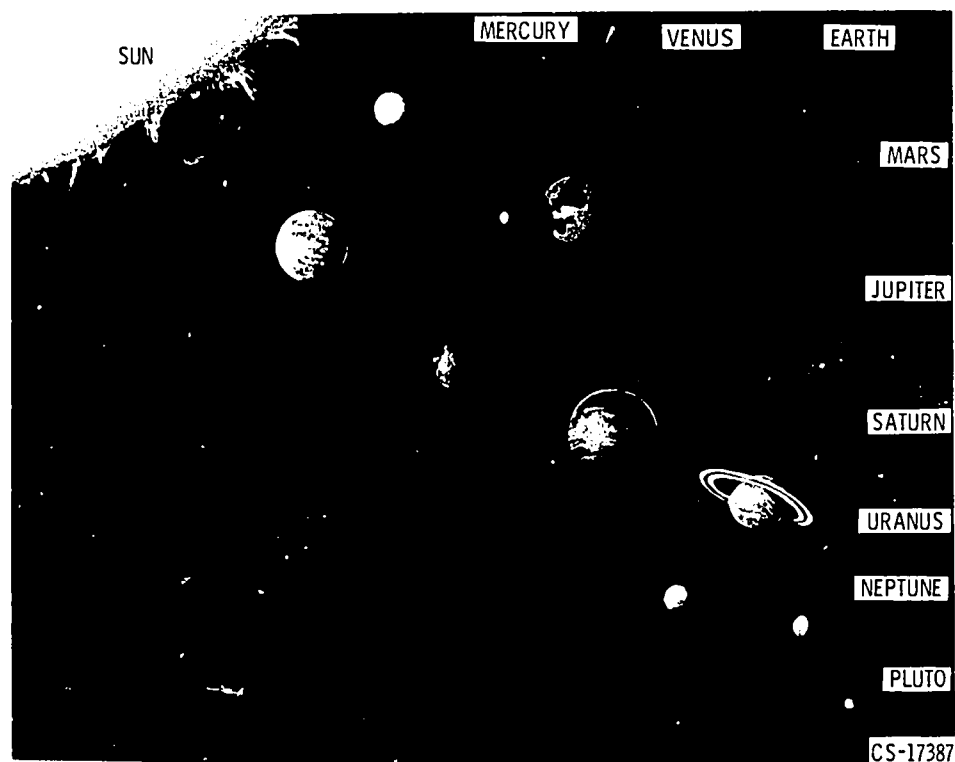


Figure 1-2. - Planets of the solar system.

The space environment includes all matter or the related lack of matter in the high-vacuum regions between the planetary and stellar mass concentrations. It likewise includes all excursions of matter through these regions and the influence that these meteoroidal excursions might have on a space ship contained therein. It includes all radiation, such as light, radiowaves, X-rays, and electromagnetic radiation. It includes all force fields, such as gravity, electrostatic attractions, and magnetic fields. Space environment must also include the probabilities of cosmic rays, solar winds, and lethal radiations associated with solar flares.

Solar space (fig. 1-2) is our primary concern. The Sun, which has a diameter of approximately 864 000 miles is the most important star to mankind. It is the principal source of energy in our solar system. While the internal temperature of this gigantic thermonuclear reactor is approximately 25 000 000^o F, the temperature of the photosphere (the luminous surface visible to the unaided eye) is only about 10 000^o F.

The Sun (fig. 1-3), however, is far from being a quiet, well-behaved source of heat and light. Intense storms project giant tongues of material into space (beyond the solar corona) at temperatures of millions of degrees. There are magnetic storms associated with sunspots that vary according to cycles of approximately 11 years. The Sun rotates on its axis and carries these sunspots across its surface in a 27-day period. Each of these periods influences the environment, weather, and atmospheres of the planets. In addition, the solar prominences project streams of charged particles and

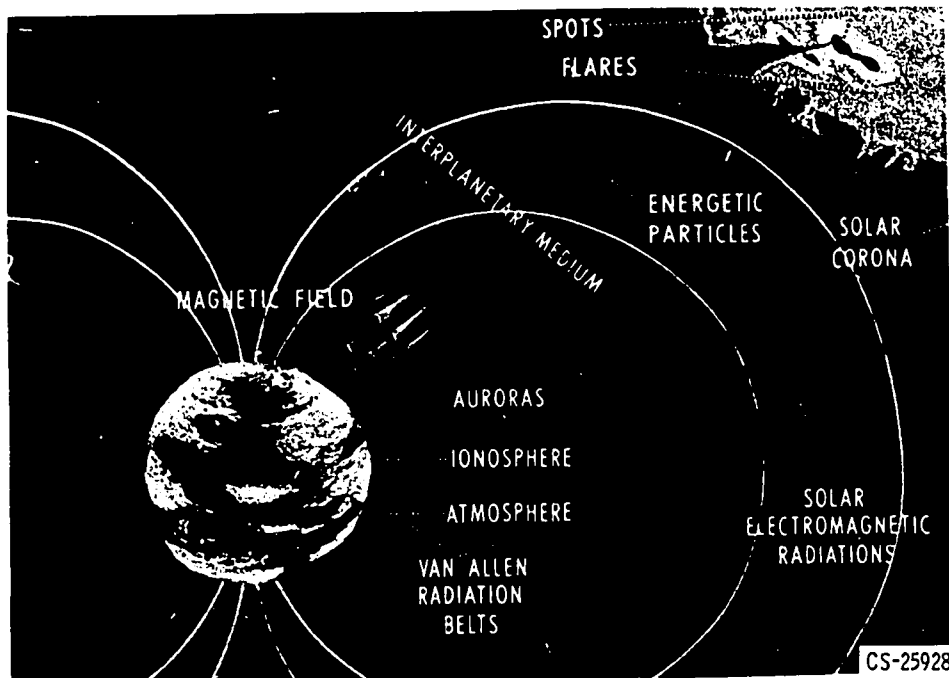


Figure 1-3. - Solar system environment.

magnetism outward to bathe the planets in a varying solar atmosphere. This solar atmosphere monotonically decreases in intensity as we proceed outward from the Sun's surface past the planets Mercury, Venus, Earth, Mars, Jupiter, Saturn, Uranus, Neptune, and Pluto. The Earth's magnetic field traps some of these charged particles to generate the Van Allen belts.

The intensity of radiation such as light and heat varies inversely as the square of the distance from the Sun. At the Earth's distance of 93 000 000 miles from the Sun (1 astronomical unit), the solar energy is 1.34 kilowatts per square meter. If this value were to increase by only 10 percent, the Earth's weather would be drastically altered, with the result that the polar ice caps would melt. A 5-percent decrease in the orbital diameter of the Earth would cause this effect. An increase in the Earth's orbital diameter would produce opposite and equally drastic results.

The known planets in the solar system have distances from the Sun ranging from 0.387 astronomical unit for the planet Mercury to 39.52 astronomical units for the planet Pluto. Therefore, the radiant energy intensity received by a spacecraft moving across the realms of solar space would vary by a factor of 10 000 in making a trip from Mercury to Pluto. The planet Pluto is so far removed even from Earth (more than 300 light-minutes) that the probability of manned flight beyond the solar system is questionable indeed. The nearest star is about 4.3 light-years away. (A light-year is the distance that light, with a velocity of approximately 186 000 miles per second, will travel in 1 year.)

It was mentioned previously that the space environment includes all of the force fields contained therein. One of these force fields, the gravitational attraction, holds very special significance. The force of gravity between two masses varies as the inverse square of the distance between them, and this relation is shown by the equation

$$f = G \frac{m_1 m_2}{r^2} \quad (1)$$

where f is the force of gravity, G is the gravitational constant, m_1 and m_2 are the two masses, and r is the distance between them. Because of this force, the planets are held in orbits around the Sun. For the general case, a planet will travel in an elliptical orbit around the Sun. The radius vector of a particular planet sweeps out equal areas in equal times. The square of the orbital period of a planet is proportional to the cube of the distance of that planet from the Sun. Crudely speaking, a planet remains in orbit because the centrifugal force associated with the speed of the planet and the curvature of the path just balances the gravitational attraction. If the planet were not moving, it would quickly fall into the parent body to become part of it.

The gravitational attraction of the Sun and planets also serves as a gigantic pump to remove most of the nonorbiting material from space; thus, it builds up life-sustaining atmospheres on the planets and leaves very high vacuum conditions in the regions between the planets. We must recognize, however, that this gravitational pump is not perfect, so that even the high vacuum regions may be regarded as the outer fringes of the solar and planetary atmospheres.

At the surface of the Earth, or sea level, our atmosphere exerts a pressure of 14.7 pounds per square inch (1 atmosphere); this pressure represents the weight of the atmosphere on each square inch of surface area. Atmospheric pressure decreases approximately by a factor of 2 for each 16 000-foot increase in altitude. This means that at each successive 16 000-foot step in altitude (starting from sea level) the pressure is one half the value of the preceding step, or level. Therefore, according to this general rule, the pressure is 1 atmosphere at sea level, 1/2 atmosphere at approximately 16 000 feet, 1/4 atmosphere at approximately 32 000 feet, etc. However, this rule provides only rough approximations of the actual values, shown in the following table:

| Pressure, atm | Altitude, ft |
|------------------|-----------------|
| 1/2 | 18 000 |
| 1/4 | 34 000 |
| 1/8 | 48 000 |
| 1/16 | 63 000 |

The pressure is roughly 0.01 atmosphere at 100 000 feet and it is 10^{-11} atmosphere at 300 miles. The rule lacks precision because of the temperature variations in the atmosphere. From 0 to 35 000 feet, the temperature of the atmosphere decreases approximately 3.5° F for each 1000 feet. From 35 000 to 100 000 feet, the temperature is nearly constant at -67° F.

The atmosphere is a mixture of oxygen, nitrogen, carbon dioxide, water vapor, etc. Each of these gases has a different weight, so one might expect the heavier gases to sink toward sea level and the lighter gases to float toward the heavens. Actually, the turbulence of the weather band around the Earth produces so much mixing that the atmospheric composition does not change much up to an altitude of about 100 miles. There is a distinct helium band (fig. 1-4) at 600 miles that blends into a hydrogen layer at higher altitudes. Atomic oxygen and ozone can be formed below 600 miles, and ionization is probable. The variation in atmospheric composition with altitude implies that the absorption of the radiated energy of the solar spectrum will also vary with altitude. Furthermore, when that energy is absorbed, chemical compounds are formed that intensify or modify the absorption characteristics of the atmosphere. The resulting composition, in combination with the Earth's magnetic field and the solar intensities, leads to our weather, to our radio transmission, and to other phenomena such as northern lights, magnetic storms, etc.

Visible radiation and radio waves penetrate the atmosphere to add heat to the Earth's surface. All other forms of radiation are generally absorbed before they reach the surface. The upper atmosphere can reach very high temperature levels, but, of course, the density is low.

Infrared radiation can be transmitted when the skies are clear, but it is absorbed by cloud cover. This is why on a clear night, even though the air temperature is above

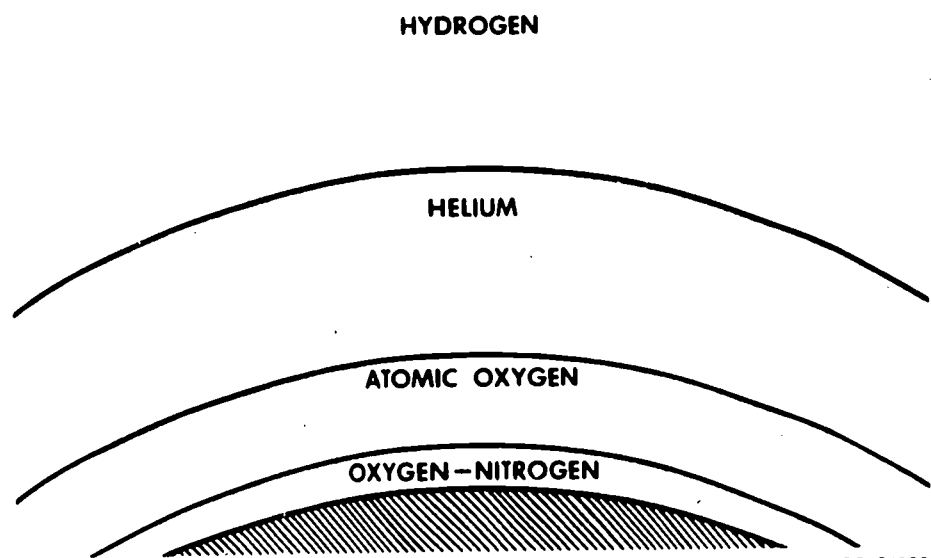


Figure 1-4. - Atmospheric composition.

CS-26322

freezing, frost can result if sufficient infrared heat of the Earth's vegetation is radiated into space to lower the planet surface temperature below the freezing point.

The atmosphere is opaque to ultraviolet rays with wavelengths below 2900 angstrom units. These rays cause the ionization in the ionosphere and generate the ozone layer at an altitude of about 15 miles, but they do not penetrate the ozone layer. The absorption of the ultraviolet rays explains the rise in temperature of the chemosphere, the air layer that overlaps and lies above the stratosphere. At higher altitudes, ionization, X-ray absorption, cosmic-ray absorption, and other complicated processes probably influence the heat and mass transfer and radio-wave reflection characteristics of our atmosphere.

Radio transmission depends on several different kinds of waves (fig. 1-5). The ground wave is that part of the total radiation that is directly affected by the presence of the Earth and its surface features. The two components of the ground wave are the Earth guided wave and the space wave. The tropospheric waves are those that are refracted and reflected by the troposphere. This refraction is due to changes in the index of refraction between the boundaries of air masses of differing temperature and moisture content. The ionospheric wave is that part of the total electromagnetic radiation that is directed through or reflected and refracted by the ionosphere. For nearby communication, the ground waves serve. For larger distances, refraction of the sky waves through the ionosphere is required. As shown in figure 1-5, a greater amount of bending is required to receive the signal at R_1 than at R_2 . A skip zone of no received signal occurs between the limit on the ground-wave propagation distance and the bending limit position of the sky-wave receiver.

The refractive index is close to 1 in the troposphere so that refraction is generally slight. With an increase of altitude, layers of ionization are formed by the action of

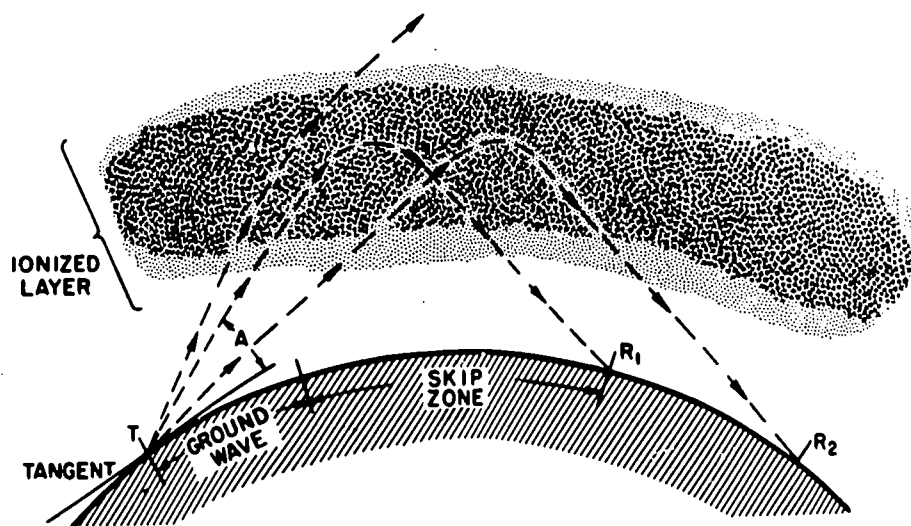


Figure 1-5. - Refraction of sky wave.

CS-16077

ultraviolet light on oxygen, nitrogen oxide, etc. Free electrons are therefore available to change the dielectric constant and the conductivity of the region for the relatively low frequencies of radio transmission. Much greater refraction of radio waves occurs in the ionosphere than in the troposphere.

Layers of ionization have been observed by reflection of radio waves, and they are designated as the D, E, F1, and F2 layers. The D ionization layer, at altitudes of 40 to 50 miles, only persists in the daytime, and the intensity of ionization is proportional to the height of the Sun. In this layer the density of ions and electrons is so high that recombination quickly occurs in the absence of the Sun's radiation. The E layer is largely due to ionized oxygen atoms at altitudes of 60 to 80 miles. The intensity of ionization is greatest at local noon and is almost zero at night. The F layers have their maximum ionization at an altitude of about 175 miles. Here the density of ions is so low that recombination with electrons takes place only slowly. The minimum ionization intensity occurs just before sunrise. In the daytime, there are two F layers.

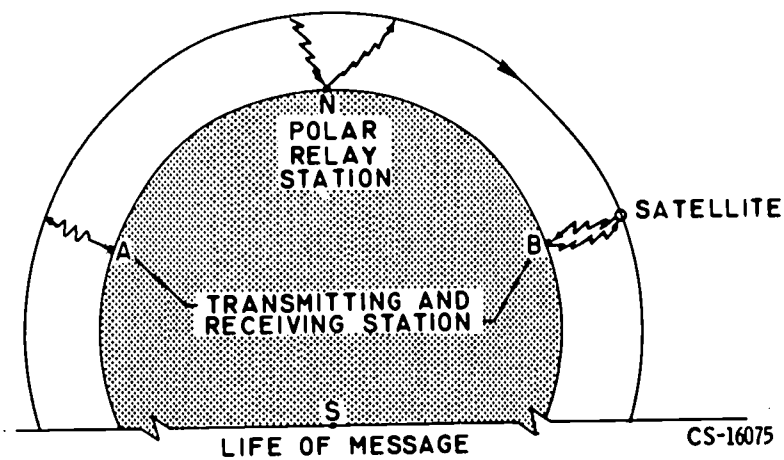
In the ionosphere, the degree of ionization depends on the intensity of the solar radiations. Therefore, ionization varies from nighttime to daytime, from summer to winter, with the 28-day period of the Sun's rotation, and with the 11-year sunspot cycle. Ionization is greatest during the period of maximum sunspot activity. The ionosphere is also strongly influenced by magnetic storms that may last several days. These so-called storms include unusual disturbances in the Earth's magnetic field along with accompanying disturbances in the ionosphere.

For a given ion density, the degree of refraction becomes less as the wavelength becomes shorter. Bending of the waves is less at high frequency than at low frequency because of the inertia of the ionization electrons. At the very high frequencies corresponding to TV channels, this bending is so slight that the wave does not return to Earth. This condition leads to the so-called "line of sight" limitation on radio waves.

It is evident that the conditions in the ionosphere are subject to the whims of the solar weather. By monitoring the conditions of the ionosphere with radio wave reflections, the long-distance communication networks can choose frequencies for best reception by use of extensive correlations. The Bureau of Standards also publishes prediction charts 3 months in advance on the usable frequencies above 3.5 megacycles for long-distance communications.

The use of satellites and high frequencies would allow long-distance radio-communication systems to be free from the vagaries of the Sun. Because the wave would be transmitted through the atmosphere, the system would be dependable irrespective of solar disturbances, seasons, time of year, sunspot cycles, etc. The Telstar, Relay, and Early Bird satellites are dramatic experiments demonstrating the feasibility of such communication systems.

Various types of satellites can be used as links in a communication system. One



1. TRANSMITTED AT A, RECORDED
2. RETRANSMITTED, RECEIVED AT B
3. RELAYED AT POLE TO OTHER SATELLITES

Figure 1-6. - Operation of message relay satellite.

type is the message relay satellite shown in figure 1-6. In this system the satellite contains a tape recorder, and messages transmitted from ground station A, when the satellite is over that point, are recorded and stored by the satellite. Later, when the satellite passes over ground station B to which the messages are addressed, that station triggers the relay with a command signal, and the satellite transmits the messages which it has stored. While ground station B is receiving messages from the satellite, the station may also be transmitting, on a different frequency, other messages to be carried by the satellite to other ground stations. Also, messages may be relayed from one satellite to another by means of a polar relay station.

The first example of a message relay satellite, and the world's first communications satellite, was Project Score, which was launched by the United States on December 18, 1958. This satellite was used to deliver President Eisenhower's Christmas message to the world on December 24, 1958. Message relay satellites might be used to relay military dispatches or as links in a rapid mail system.

Passive satellites can serve in a communication network if there are enough of them. In this system, the signal transmitted from a ground station to a satellite is reflected down to other ground stations. Satellites of this type include the Echo balloon configurations, the wire dipoles of Project Westford, and proposed balloons shaped to improve the signal reflection strength. Passive satellites generally must be at fairly low altitudes in order to give sufficient signal strength at the receiver. This problem arises because the strength of the signal transmitted to the satellite, even with a very good antenna, essentially diminishes as the inverse square of the distance, and the strength of the reflected signal returning to Earth diminishes at the same rate. Thus, the signal strength at the receiving station is proportional to the inverse fourth power

of the altitude. Hence, altitudes of several thousand miles are about the upper limit. Since individual satellites at these low altitudes do not remain in best signal-reflecting position for very long, many satellites would have to be employed to maintain continuous communication between any two stations.

Active satellites, such as Telstar and Relay, receive and amplify the signal before transmitting it back to a ground station. Therefore, these satellites can be used at much higher altitudes than the passive satellites. A satellite which is placed into an equatorial west-to-east orbit at an altitude of 22 300 miles is said to be in a stationary orbit; that is, its orbital period coincides with that of the Earth's rotation, and the satellite remains nearly stationary in the sky relative to the Earth. This type of satellite is known as a synchronous satellite. Syncom, shown in figure 1-7, is the first synchronous active repeater communications satellite. A single synchronous satellite can provide communication for nearly a hemisphere; three such satellites can cover the entire Earth, except for a small region around the poles. Syncom currently provides our most reliable system of communication with our forces in Viet Nam.

The faint, general illumination of the sky visible from the ground on a clear, moonless night is known as airglow. This light source originates at an altitude of approximately 90 to 100 kilometers and is caused initially by a triple collision of oxygen atoms. In the high vacuum of space, one of these oxygen atoms retains electrons in an elevated energy level; that is, the atom assumes a metastable state. Some time later, this forbidden neutral oxygen atom releases its energy at a wavelength of 5577 angstroms

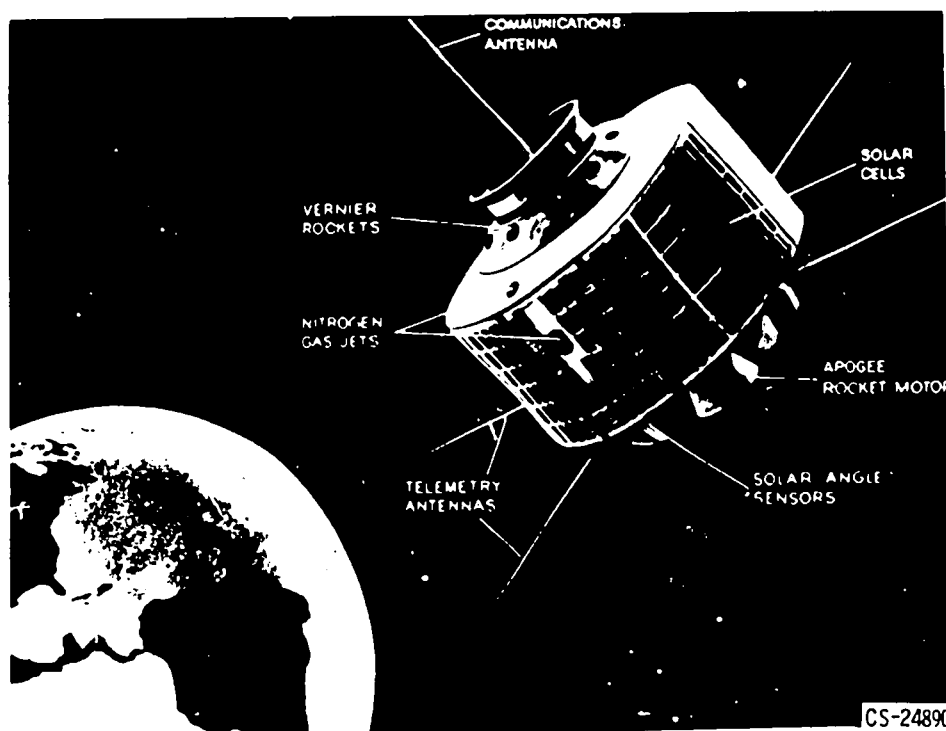


Figure 1-7. - Syncom satellite.

to produce the airglow. Conclusive proof of the cause of airglow was provided by astronaut M. Scott Carpenter, who, during his orbital flight on May 24, 1962, observed the airglow through a special filter which passed light only at a wavelength of 5577 ± 10 angstroms.

This airglow is by far the best horizon for the astronauts. Because stars can be seen between the airglow and the Earth, astronaut Carpenter was able to determine the altitude of this airglow horizon quite accurately by noting the exact time when individual known stars entered and left the airglow region. Since the altitude and position of the Mercury capsule were known, the rest of the computation followed in a straightforward manner.

What can the astronaut see from a satellite? He certainly can see the heavens unhampered by the turbulence of the atmosphere; stars, therefore, do not twinkle. He can get a marvelous view of the Earth's cloud cover and weather patterns; perhaps he can even detect hurricanes in their formation (fig. 1-8) before ground-based stations can do so. (Fig. 1-8 is not the best cloud-cover picture that has been obtained, but it is the first photograph of a hurricane in the making taken from a rocket.) The Tiros satellites, which have provided much better pictures than figure 8, have demonstrated their ability to aid in the observation and mapping of worldwide weather patterns. These satellites were used to locate accurately the center of a tropical storm after conventional tracking methods had provided a 500-kilometer error in its location. The break in an Australian heat wave was predicted accurately from data provided by Tiros II, and hurricane Esther was discovered by Tiros III. These contributions will be followed by others from more sophisticated satellites such as Nimbus and, still later, Aeros.

Gross weather patterns are definitely visible to an astronaut, but his ability to detect details and Earth surface characteristics has certain limitations. The quality of



Figure 1-8. - Rocket view from 100-mile altitude.

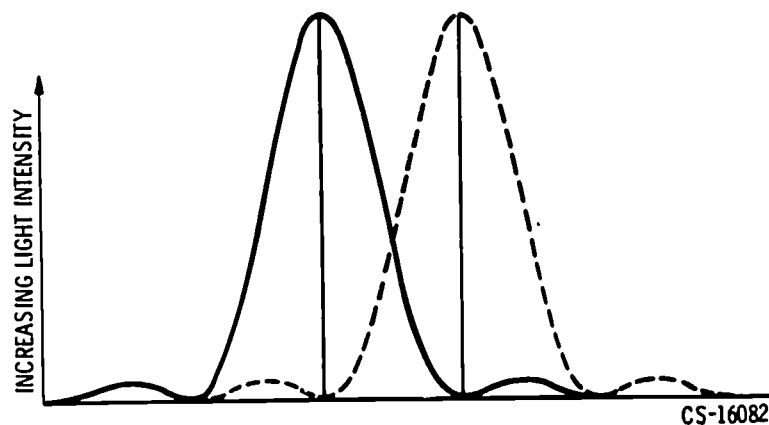


Figure 1-9. - Diffraction pattern of two point light sources (circular aperture).

the image from an optical or radar viewing system is limited by the fact that electromagnetic radiations have wavelike characteristics. A circular aperture on such a viewing system will generate a diffraction pattern so that a point source will not give a point image on the viewing screen. The individual light intensities from the images of two point sources are plotted in figure 1-9.

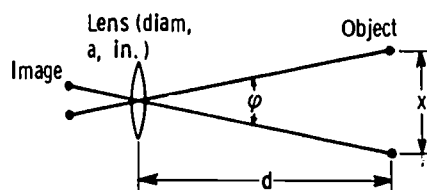
Clearly, if two images are closely spaced, the light patterns will blend so that they cannot be distinguished as separate. Conventionally, this closest spacing for resolution occurs when the central maximum intensity of the diffraction pattern of one point source falls at the first minimum intensity of the second point source. This gives a minimum angular resolution of

$$\varphi = 1.22 \frac{\lambda}{a} \quad (2)$$

where φ is the angular separation of the two point sources in radians, λ is the wavelength of the radiation, and a is the aperture diameter. As shown in the sketch below, this angle φ is also equal to the distance x between the two point sources divided by the distance d of the two sources from the observation station. Hence,

$$\varphi = 1.22 \frac{\lambda}{a} = \frac{x}{d} \quad (3)$$

and the quantity x approximates the uncertainty of position or definition of a viewed object.



By using equation (3), a 1-inch-diameter optical telescope mounted on a satellite 200 miles above the Earth can be used to resolve point light sources if they are more than 23 feet apart. With a 12-inch scope, the resolved distance is 1.9 feet. This resolved distance approximately represents the fuzziness of the boundaries of the object under observation. Thus, with a 12-inch scope, ships, roads, buildings, trains, and general map characteristics, including automobiles in parking lots, could be determined. A satellite equipped with a reasonable telescope (12-in. objective lens) probably could be used to detect, classify, and establish the locations of surface ships, military installations, and troop movements of an alien power without the aid of spies or decoding experts.

The question might be raised as to whether there is sufficient illumination for observing the Earth's surface from a satellite. During daytime, there is certainly ample illumination. The light-transmission coefficient through the entire atmosphere is approximately 85 percent at the zenith. Therefore, from a satellite, the Earth appears to be about six or seven times as bright as the full Moon. The brightness of an object viewed from the zenith through the entire atmosphere is about equivalent to that of an object 5.3 miles away along the surface of the Earth.

Useful observations of the Earth can be made with a manned satellite even at night. According to Russell (ref. 1), the detection of a point light source by the unaided human eye requires a radiant flux, from the light source, of at least 2.5×10^{-9} erg per second. (Radiant flux is the rate of flow of radiant energy.) A 1-watt light bulb with a 1-percent efficiency should, therefore, be observable from a satellite located at an altitude of 200 miles and equipped with a 12-inch-objective telescope. A photographic plate with an exposure time of 1 minute could probably detect a 60-watt light bulb.

It is a well known fact that the stars appear to twinkle while the planets do not. This twinkling effect is due to atmospheric turbulence and temperature gradients. These disturbances modify the index of refraction of the atmosphere and cause local bending of the light rays passing through it. Thus, the observed position of a star changes transiently with time, and this change causes the twinkling appearance. The position of a star as seen through the atmosphere is statistically uncertain by 1 to a few seconds of arc. Because the angular size of the planets is larger, the twinkling is not apparent, even though it is still present. Mars, for example, subtends an angle from Earth of about 17 seconds at closest approach. A pinpointed object on the rim of the Mars disk, or on the Moon for that matter, would have the same circle of confusion due to turbulence as does a star. The positional uncertainty of a satellite as viewed from the ground might be as much as 3 seconds of arc associated with atmospheric turbulence. The corresponding distance error Δx_g for a satellite at 200 miles, as seen from the ground, is about 15 feet.

The ability to locate an object on the ground from a satellite is much more precise

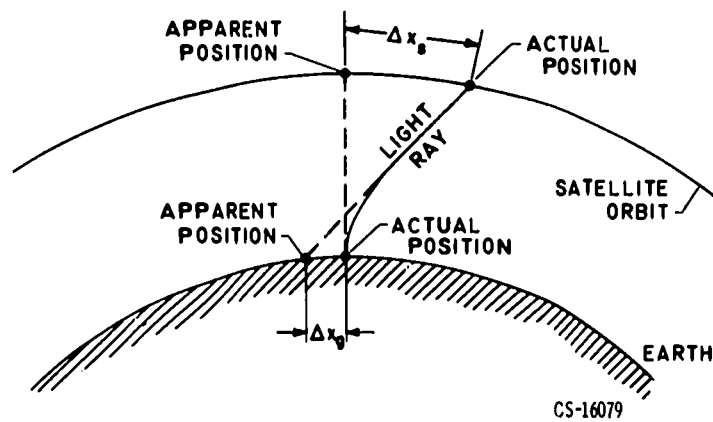


Figure 1-10. - Atmospheric shimmer.

than the ability to locate a satellite from the ground. This is shown in figure 1-10 by the relative sizes of the positional errors Δx_g and Δx_s . The index of refraction of a gas is related to its density, and the density of the atmosphere decreases exponentially with altitude. Hence, the air layers near the surface of the Earth (where the density of the air is high) produce the greatest bends on the light path. In figure 1-10, the same light path is traveling between the ground observer and the satellite astronaut, but each appears to see his object along the projected tangent to the local light path. The bending is great near the ground observer while hardly any bending occurs near the satellite. In fact, the ratio of the errors ($\Delta x_s / \Delta x_g$) can be shown to be about 45 to 1 for a 200-mile-altitude satellite. Thus, atmospheric shimmer causes an error Δx_g of only a few inches in the astronaut's observation of the ground. An objective lens with a diameter of up to 6 feet could be used for viewing the ground from a satellite at an altitude of 200 miles before the inherent optical resolution would be better than the resolution due to turbulence and atmospheric shimmer.

Since the orbital path of a satellite has considerable bearing on the ability of an astronaut to observe the ground, a brief discussion of orbits (fig. 1-11) might be of

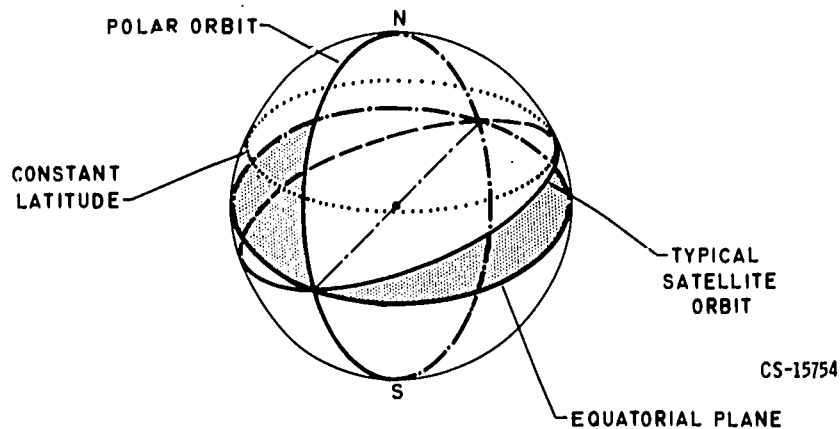


Figure 1-11. - Satellite orbits.

interest. If the satellite is launched from either pole, only a polar orbit can be established. In this case, the entire Earth comes under surveillance as it rotates under the satellite's orbit. Clearly, however, it is not possible to establish an equatorial orbit with a ballistic launch from the poles. In fact, the inclination of the orbital plane to the equator must be equal to or greater than the latitude of the launching site. Thus, only from the equator can all kinds of orbits, that is, equatorial, polar, etc., be established, unless midcourse thrusting is employed.

The position of the orbital plane of the satellite depends on the inhomogeneities of the Earth's gravitational field. The Earth is not a perfect sphere, so that the idealized variation of the gravitational attraction with the inverse square law is only approximately true. The actual Earth bulges at the equator; that is, it somewhat resembles a sphere with a belt around the equator. The gravitational pull of this belt is stronger on a satellite at the equator than at the poles. The Earth's bulge, therefore, influences the orbit of a satellite. The perturbations of this orbit may, in turn, be used to make geophysical measurements of the Earth's gravity. Such studies with the Vanguard I satellite led to the discovery of the pear-shaped Earth.

There are two important ways in which the equatorial bulge influences the orbit of a satellite (fig. 1-12). First, the bulge deflects the satellite toward the normal (perpendicular) to the equator each time the satellite crosses the equator. Thus, the plane of an eastwardly launched satellite rotates toward the west. The approximate rate of rotation, in degrees per day, is given by the equation

$$R = 8 \cos \alpha \quad (4)$$

where α is the inclination, in degrees, of the orbital plane to the equatorial plane.

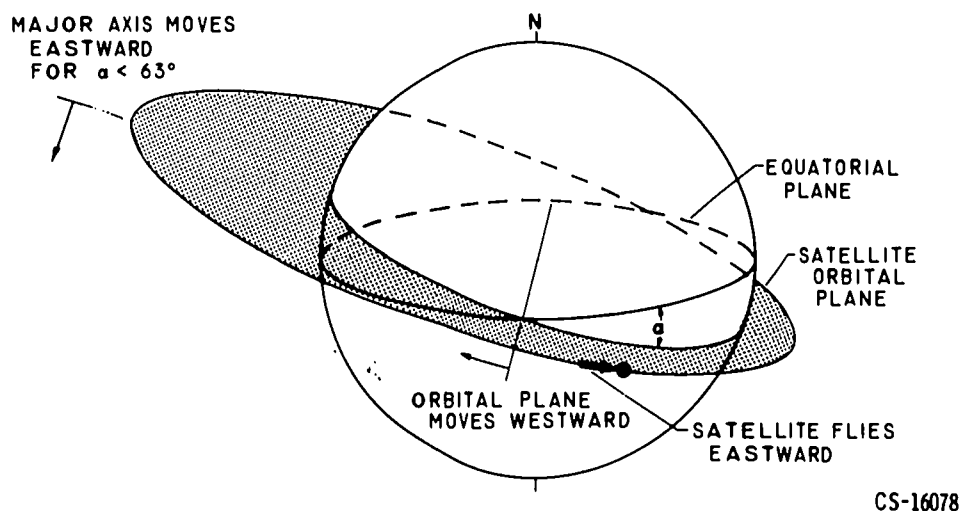


Figure 1-12. - Effect of Earth's equatorial bulge on satellite orbit. (Bulge not shown in this figure.)

Second, the bulge causes the satellite to speed up when it crosses the equator. This speedup, in turn, causes the major axis of the elliptical path to rotate in the plane of the orbit. The approximate rate of rotation, in degrees per day, is given by the equation

$$S = 4(5 \cos^2 \alpha - 1) \quad (5)$$

The direction of this rotation reverses above latitudes of approximately 63° . The plane angle, or inclination, of the early Russian satellites was approximately 63° . Thus, the perigee of the orbit remained over Russia, and data transmission was improved. The numbers in equations (4) and (5) are for a 200-mile-altitude satellite.

A satellite in orbit is always falling toward the Earth. Because of the Earth's curvature, however, the horizon keeps dropping so that the satellite never reaches the surface but continues to go around the Earth. A body in free fall, such as a satellite, experiences the phenomena associated with weightlessness.

The weightless environment is still of considerable worry to space scientists. The influence of weightlessness on man for extended periods of time might lead to deteriorations of muscular and bodily functions through lack of stimulation. The fuel in a rocket tank may settle at the top, the bottom, or the sides of the tank. Hence, venting of the tank may be as much of a problem as locating the fuel at the tank discharge port. A detailed discussion of weightlessness is presented in chapter 8.

The thermal environment in space depends greatly on location. Space has such a high vacuum (of the order of 10^{-16} millimeter of mercury or better) that only a few molecules of hydrogen are present in each cubic centimeter. Hence, the normal definition of temperature that depends on a statistical distribution of molecular or vibrational speeds probably has no meaning. Also, the heat transfer to or away from a spacecraft must be principally by radiation. Therefore, the temperature of space might be defined as that equilibrium temperature that a body would assume in absence of sunlight or planet light. This temperature for deep space is perhaps 3° to 4° K but may be as high as 20° K in portions of the Milky Way. The temperature of a body in solar space is determined by equating the energy absorption by the body from the solar and planet radiations to the energy reradiated to deep space and to any nearby objects. The radiation from a black body is proportional to the fourth power of the absolute temperature of the black body and of the environment surrounding it. This relation is shown by the equation

$$E = \sigma(T_1^4 - T_2^4) \quad (6)$$

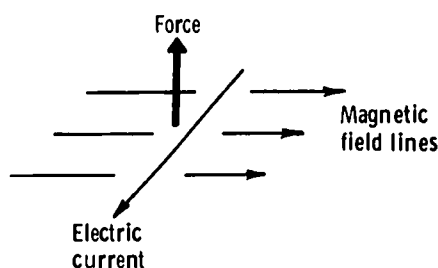
where E is the radiant emittance of the black body, σ is the Stefan-Boltzmann constant

of proportionality, T_1 is the absolute temperature of the black body, and T_2 is the absolute temperature of the environment surrounding the black body.

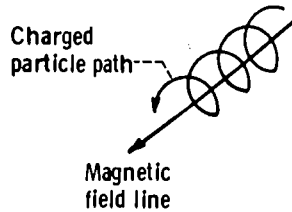
The energy received near the Earth from the Sun is 1.34 kilowatts per square meter. This energy is largely in the visible range. If this energy is absorbed by a spacecraft, the reradiation is largely in the infrared range. Since materials have different absorption and emissivity coefficients according to the wavelength of the radiation, the temperature of spacecraft may be controlled by selection of appropriate surface coatings. A coating with high absorptivity in the visible region and low emissivity in the infrared region has a higher equilibrium temperature than if the reverse is true. By combinations of stripes and selected coatings, spacecraft temperatures are usually adjusted to be near normal room temperatures. The coatings are quite sophisticated since they are tailored for particular orbital paths or missions. Mariner, for example, requires a different coating than do satellites near Earth. Even on near-Earth satellites, the coatings are altered if the orbital path is changed because of delays of a few days at launch.

A simple energy balance will indicate the variations of equilibrium temperature on a spacecraft in solar space. If we assume a sphere with sufficient conductivity to have uniform surface temperature, the black body solar energy absorbed will vary inversely as the square of the distance from the Sun. The energy radiated will be proportional to the fourth power of the surface temperature. Thus, the equilibrium temperature obtained by equating the absorbed and radiated energy varies inversely as the square root of the radial distance from the Sun.

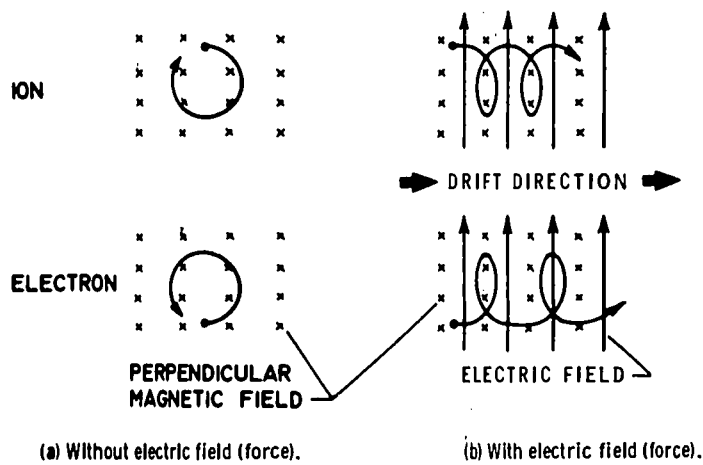
The Earth has a magnetic field which has an important influence on the near-Earth space environment. A charged particle moving through space acts like an electric current. An electric current in a magnetic field generates a force perpendicular to the direction of the current and of the magnetic field, as shown in the following sketch:



A charged particle moving parallel to the magnetic field is not affected by the field. However, a charged particle moving perpendicular to the field experiences a force which causes it to move around a field line in a circular path. If a charged particle approaches the magnetic field at some angle other than 90° , the particle will spiral along a field line as shown in the following sketch:



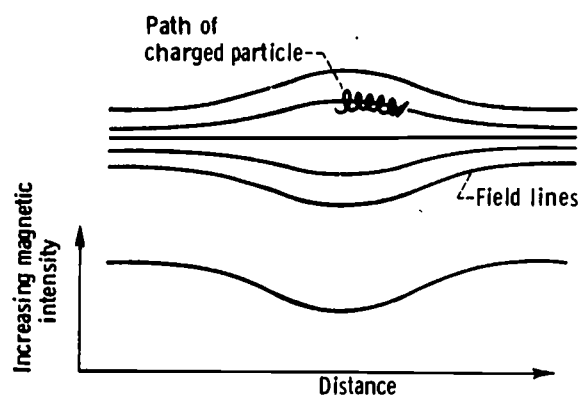
Any force on the charged particle in a constant direction normal to the magnetic field will cause the charged particle to travel alternately slower and faster while it is spiraling around the field line. Hence, the path radius of curvature will alternately increase and decrease. This will cause the particle to drift sideways in a direction perpendicular to the force and the field lines as shown in figure 1-13. Note that both positive and negative charges drift in the same direction.



CS-18299

Figure 1-13. - Charged-particle motions in magnetic and electric fields.

If the field is increasing in the direction of the spiral motion, then the radius of the path will decrease, and the converging field lines will produce a force to reflect the particle back in the direction from which it came (see following sketch). Thus, we could make magnetic mirrors to trap charged particles in the region between increasing magnetic fields.



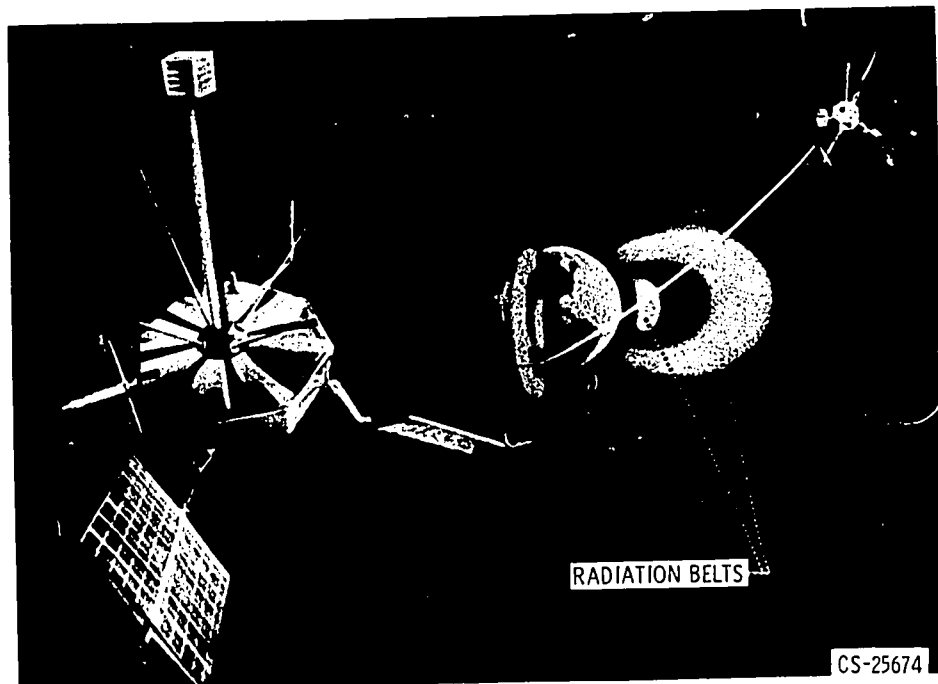


Figure 1-14. - Explorer XII satellite.

The Earth has a magnetic field surrounding it, and this field increases toward the poles. Hence, the Earth's magnetism forms a magnetic bottle to trap charged particles. These particles are spiraling around the magnetic field lines, bouncing back and forth along spiral paths from pole to magnetic pole. Simultaneously, there is a very small drift velocity in the circumferential direction associated with the gravitational field. Thus, the charged particles diffuse around the Earth to form the Van Allen belts. (A detailed discussion of the Van Allen belts is presented in ref. 2.) The Van Allen belts generally do not persist to the lower altitudes of Project Mercury space flights; if they did, the upper atmosphere would soon cause their decay. The belts are strongest in the regions between 1 and 10 Earth radii. Data from Explorer XII (fig. 1-14) reversed previous concepts of the belts; the entire region is actually a single system of charged particles instead of two distinct belts. These charged particles are trapped by the Earth's magnetic field.

The chief constituents of the Van Allen belts are electrons and slow-moving protons, and the quantities of each vary with altitude. At 2000 miles, the predominant particles are protons with energies of tens of millions of electron volts (10 MeV). This region has been modified by nuclear explosions. At 8000 miles, protons with only a fraction of an MeV predominate, and at 12 000 miles, protons with energies of 0.1 to 4 MeV and electrons with energies up to 2 MeV are blended. The exact source of the charged particles in these regions is still a matter of controversy. The formation of one new artificial belt, however, is well understood. In this one, a high-altitude nuclear explosion filled the region with electrons. The surprise associated with this one is that

the strength of the belt persisted much longer than originally estimated. It has knocked out the power supplies of several satellites. This degradation is due to damage to the solar cells.

The outer regions of the Van Allen belts contain large numbers of low-energy protons. These protons pose less of a radiation hazard than the high-energy electrons. The occupants of a space vehicle passing quickly through these regions on the way to the Moon or beyond would be in little danger from the protons but would need to be protected from the X-rays generated by impingement of electrons on the spacecraft components. On the other hand, the protons would pose a serious problem to the occupants of even a heavily shielded, electric-propulsion spacecraft or an orbiting laboratory if the residence time were 2 weeks or longer.

The most common unit for a radiation dose is the rem (roentgen equivalent man). The rem is that quantity of any type of ionizing radiation that, when absorbed in the human body, produces an effect equivalent to the absorption of 1 roentgen of X or gamma radiation at a given energy. The roentgen is the quantity of X or gamma radiation required to produce (in 1 cubic centimeter of dry air) ions carrying 1 electrostatic unit of positive or negative charge. Since man has a radiation exposure limit of 25 rem, a 2-week exposure time in the inner Van Allen belt would require a shield weight of approximately 140 grams per square centimeter (55 in. of water thickness). The normal background cosmic-ray intensity from all sources is about 0.65 rem per week. Thus, with a 25-rem exposure limit, an unshielded space traveler would reach his limit on radiation exposure from this source alone in about 38 weeks.

It should be pointed out that the Van Allen belts are not steady and unchanging. The belts have been modified by nuclear explosions, and they are also modified and distorted by the solar winds. During solar flares and intense sunspot activity, tongues of plasma (fig. 1-15) along with a trapped magnetic field are shot out toward the Earth. The geo-

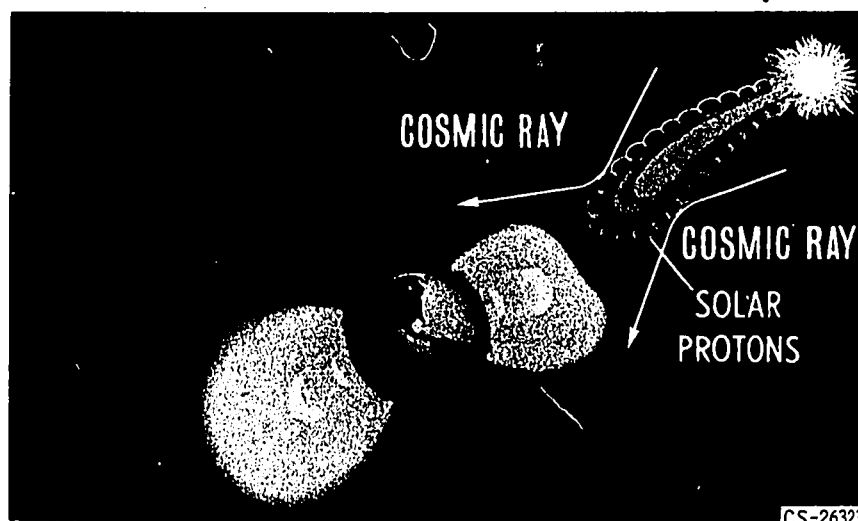
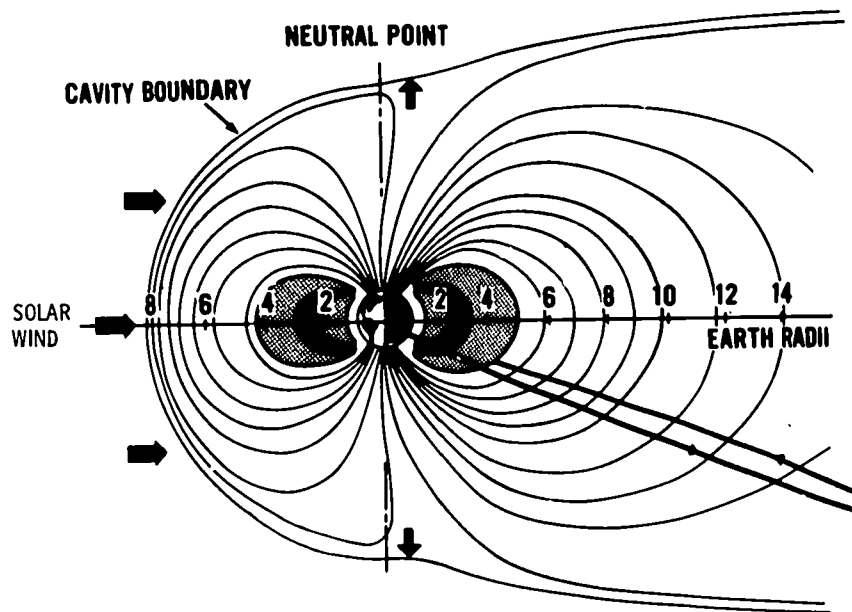


Figure 1-15. - Radiation belts and solar disturbance.



CS-26321

Figure 1-16. - Distortion of radiation belts by solar wind. Solar wind has flux of 10 protons per centimeter and velocity of 500 kilometers per second.

magnetic sphere of the Earth forms a shock wave in this plasma sheath; consequent distortions of the Van Allen belts occur as shown in figure 1-16. The edge of the geomagnetic sphere confined inside this shock wave and on the side of the Earth facing the Sun is at an altitude of some 30 000 to 40 000 miles.

Solar flares pose a serious threat of radiation to man. These flares eject high-energy particles, most of which are protons with energies ranging from less than 10 MeV to almost 50 BeV. The classification of solar flares is shown in table 1-I. The minor flares of classes I-, I, and II are not particularly troublesome, but the major flares of classes III and III+ are relatively serious. Sixty such major flares were recorded between 1956 and 1961; therefore, the average rate of occurrence is approximately once a month. Occasionally, giant solar flares larger than those of class III+ occur. Seven of these giant flares have been observed during the past 18 years.

Weight limitations may restrict the radiation shield of the Apollo spacecraft to be-

TABLE 1-I. - SOLAR-FLARE DATA

| Class | Fraction of visible hemisphere | Duration, min | Energy | Frequency of occurrence |
|-------|---|---------------|-------------|-------------------------|
| I- | 25×10^{-6} | 5 to 20 | ----- | } 2/hr |
| I | 100×10^{-6} to 250×10^{-6} | 4 to 43 | ----- | |
| II | 250×10^{-6} to 600×10^{-6} | 10 to 90 | ----- | |
| III | 600×10^{-6} to 1200×10^{-6} | 20 to 155 | 100 MeV | } 12/yr |
| III+ | $>1200 \times 10^{-6}$ | 50 to 430 | 1 to 40 BeV | |

tween 10 and 30 grams per square centimeter. Such a relatively thin shield would protect man for the short times he might spend in the Van Allen belts, and it would offer partial protection against minor and major solar flares. Thus, the greatest source of danger would be the unpredicted giant solar flares.

Almost all protons of energies greater than 100 to 200 MeV will pass through a 10- to 30-gram-per-square-centimeter shield. A class III+ solar flare has flux levels as high as 10^4 protons per square centimeter per second, and large numbers of these protons have energies greater than 100 to 200 MeV.

The energy loss mechanism (ionization and scattering) in thin shields is orderly and well understood. In thin shields, the protons collide only occasionally with a shield nucleus, and hence secondary radiations are unimportant. Future space flights of very long duration, however, will require thick shields. Then the secondary radiations arising from nuclear reactions in the radiation shield and spacecraft material will become important. In cascade reactions, a proton enters a heavy nucleus, which then disintegrates to a lighter nucleus and emits protons and neutrons. These, in turn, cause other disintegrations. In evaporation reactions, a proton enters a nucleus to form a radioactive atom. Such an atom might decay and emit a neutron, which could cause further reactions. As the shield thickness increases, the secondary radiations become increasingly more important relative to the primary ones.

The danger from giant solar flares results partly from the inability of Earth scientists to predict them. Some success has been obtained by first calculating the size of the shaded area (penumbra) surrounding each sunspot group (fig. 1-3, p. 3). (The size of the penumbra might be a measure of sunspot intensity.) The numbers obtained from these calculations are then used to predict the expected relative safety of a 4- to 7-day space flight as proposed for the Apollo program. Malitson (ref. 3) examined the results of such calculations and drew the following conclusions:

(1) If the established criterion for unsafe flight due to a sunspot group is a penumbral area larger than 1000 millionths of the solar surface, the usable flight time is reduced by 33 to 40 percent, and encounters with approximately half the number of giant solar flares are still possible. From the standpoint of safety, this criterion is obviously unsatisfactory.

(2) If a reduced penumbral area of 500 millionths of the solar surface is used as the criterion for unsafe flight, then the safe flight time is reduced to 20 to 35 percent of the actual usable flight time. This criterion would have allowed only one encounter with a giant solar flare during each of the years 1949 and 1950.

(3) During the year 1951, even if the criterion for unsafe flight had been a penumbral area larger than 300 millionths of the solar surface, two encounters with giant solar flares could have occurred.

These calculations clearly indicate that the present methods of predicting giant

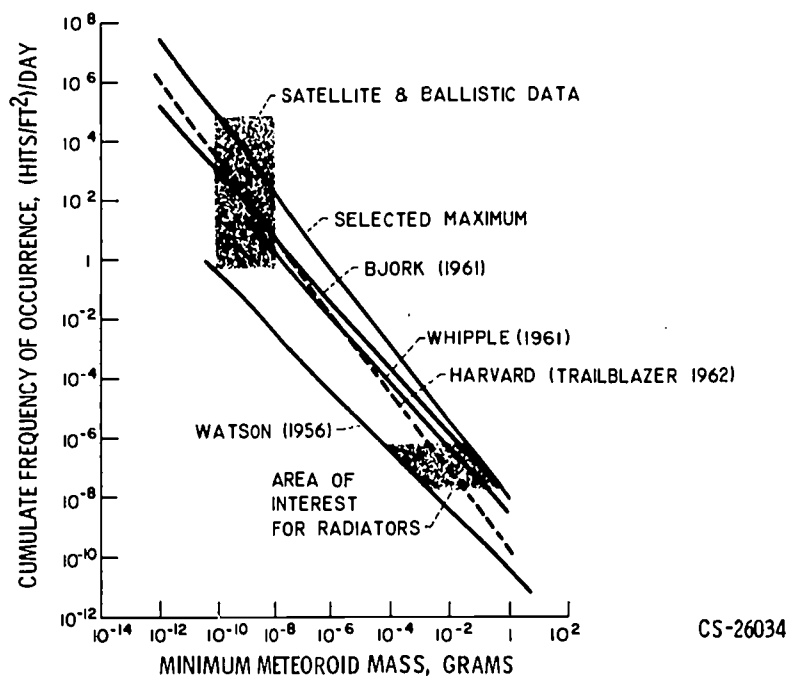


Figure 1-17. - Meteoroid mass-frequency distribution.

solar flares are inadequate. Therefore, these flares would be dangerous sources of radiation on extended-time manned missions to Mars and other planets.

Another source of danger to a spacecraft is the meteoroid. A meteoroid is any of the countless small bodies moving in the solar system. If the meteoroid passes with incandescence through the atmosphere, it is a meteor; if it reaches the surface of the Earth, then it becomes a meteorite. Meteoroids vary in both size and density. Some of them may be as light as snow, with a specific gravity of perhaps 0.15. The stony meteorites seen in museums have specific gravities of 2 to 3, while the specific gravities of the nickel-iron ones are about 7 or 8. The sizes of the meteoroids range from infinitesimal up to perhaps a few pounds or heavier. In Arizona there is a mile-wide crater which was formed by a meteorite. Obviously, a meteorite capable of producing such a change in the surface structure of the Earth must be very large.

Estimates of the mass-frequency distribution of meteoroids are shown in figure 1-17. The data for the curves are generally obtained by observers of meteor trails either visually or by means of radar. The curves in this figure show that particles which have a large mass have very low occurrence rates and, conversely, particles which have high occurrence rates have very little mass.

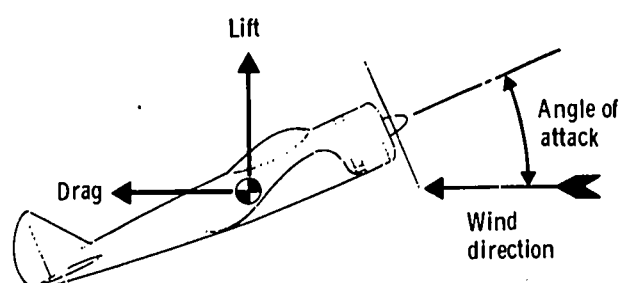
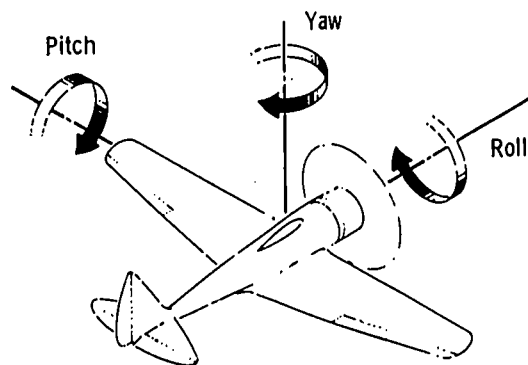
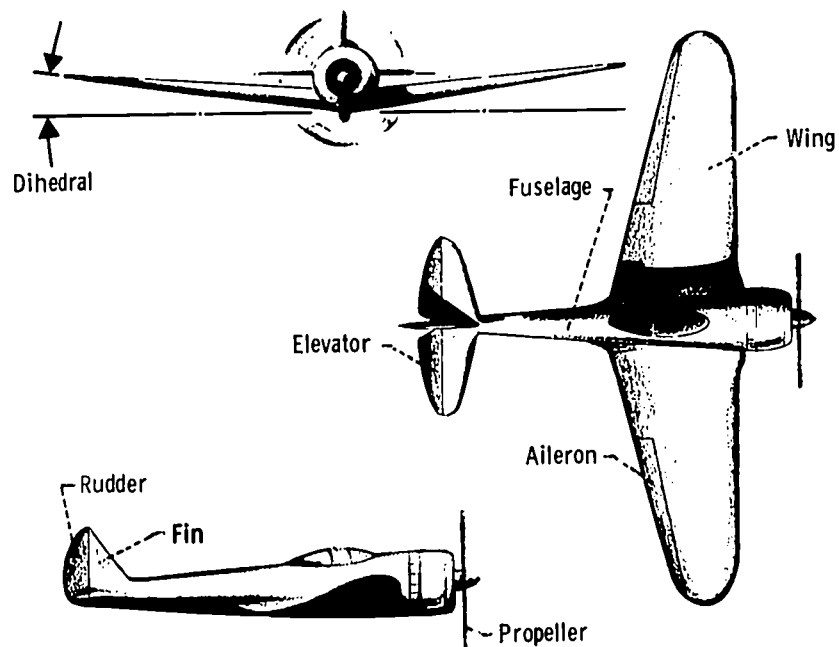
Figure 1-18 shows how the meteoroids are distributed in space. To an Earth observer, there are many more particles approaching the Earth from the leading hemisphere than from the trailing hemisphere as the Earth moves in orbit around the Sun. However, if these data are corrected for the speed of the Earth, then the results show that the majority of the particles are traveling in orbits around the Sun in the same

- 1954 Boeing-707 is tested: speed, 550 mph; range, 3500 miles; capacity, 150 passengers.
- 1959 First flight of North American X-15, built for hypersonic flight, eventually to approach Mach 7.
- 1962 X-15A, with Joseph Walker as pilot, reaches 4104 mph. Major Robert M. White climbs to 314,750 feet altitude in the X-15A.
- 1963 Lieutenant Colonel Robert A. Rushworth attains Mach 6.06 in the X-15A, causing craft's skin temperatures to rise above 1300^o F. The B-58 Hustler makes the longest supersonic flight in history (nonstop from Tokyo to London in 8 hours, 35 minutes, for an average speed of 938 mph).
- 1964 First test flight of the F-111A (TFX) variable-sweep-wing, tactical fighter, designed for maximum speed of Mach 2.5. The Lockheed A-11, or USAF YF-12A, a Mach 3 prototype fighter, is announced. (This plane was first flown secretly in 1963.)
- 1965 Design cruising speed of Mach 3 is attained for the first time by the XB-70A Valkyrie strategic bomber (North American) on its 17th flight, October 14.

APPENDIX B

AIRPLANE COMPONENTS AND TERMINOLOGY

The components of an airplane and the terminology used are defined in the following sketches:



BIBLIOGRAPHY

- Anon.: The American Heritage History of FLIGHT. American Heritage Publ. Co., Inc., 1962.
- Dryden, Hugh L.: Aerodynamics - Theory, Experiment, Application. Aeron. Eng. Rev., vol. 12, no. 12, Dec. 1953, pp. 88-95.
- Dryden, Hugh L.: A Half Century of Aeronautical Research. Proc. Am. Philosophical Soc., vol. 98, no. 2, Apr. 15, 1954, pp. 115-120.
- Gray, George W.: Frontiers of Flight, The Story of NACA Research. Alfred A. Knopf Publ., 1948.
- Morris, Lloyd; and Smith, Kendall: Ceiling Unlimited. The Macmillan Company, 1953.
- Shrader, Welman A.: Fifty Years of Flight. Eaton Manufacturing Co., 1953.
- Stever, H. Guyford; Haggerty, James J.; and the Editors of Life: Flight. Time, Inc., New York, 1965
- USAF Photo Package No. 1, Rev. May 1965.
- USAF Photo Package No. 2, reissued 1967, Historical Aircraft Photos.

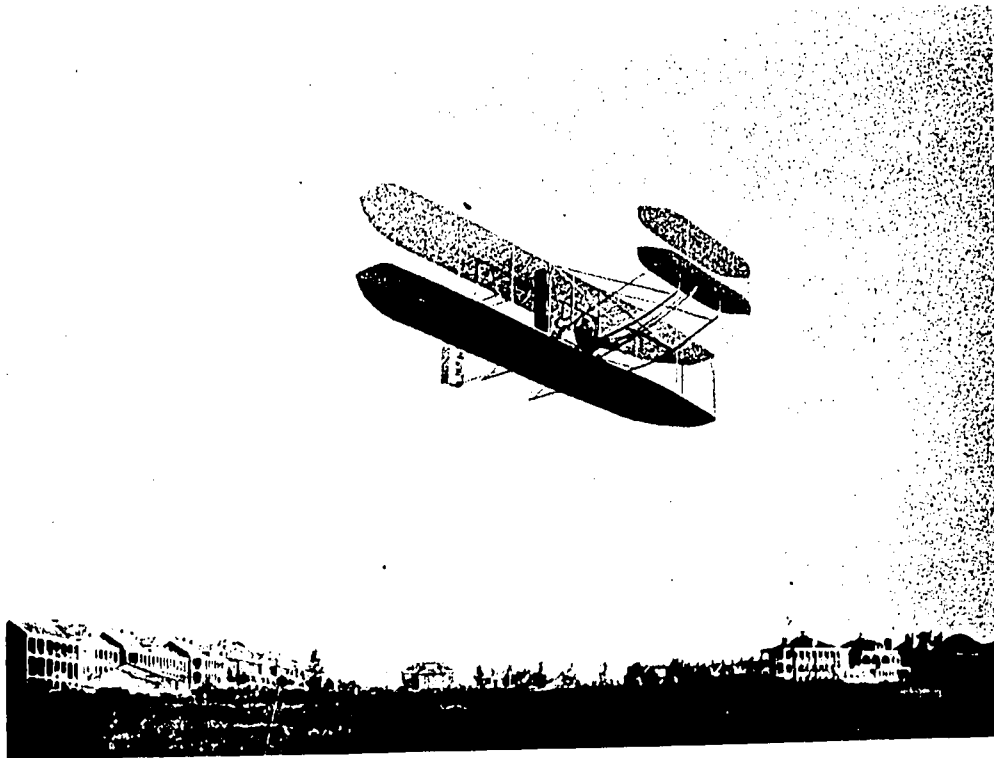


Figure 1-1. - Orville Wright circles Fort Myer, Va., during tests conducted for the War Department, in 1908. During these tests, he made the world's first flight of longer than 1 hour.



Figure 1-2. - Wilbur Wright's Flyer is moved into a "hangar" while curious military and civilian spectators watch.

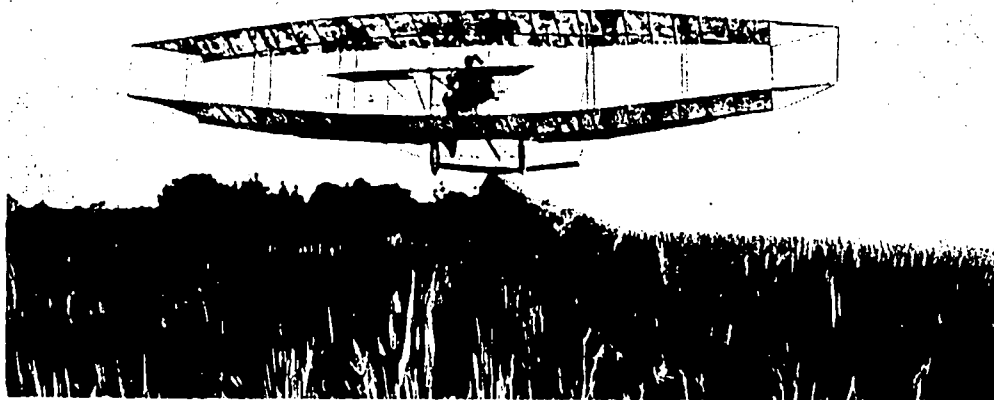


Figure 1-3. - Glenn Curtiss scored a dusty triumph when his "June Bug" made a 6000-foot flight in 1908.



Figure 1-4. - Early U. S. aviator prepares for a flight in a Curtiss military airplane in 1913. Powered by a four-cylinder engine mounted behind the pilot, these pusher-type airplanes proved too dangerous and were not accepted by the War Department after 1914.

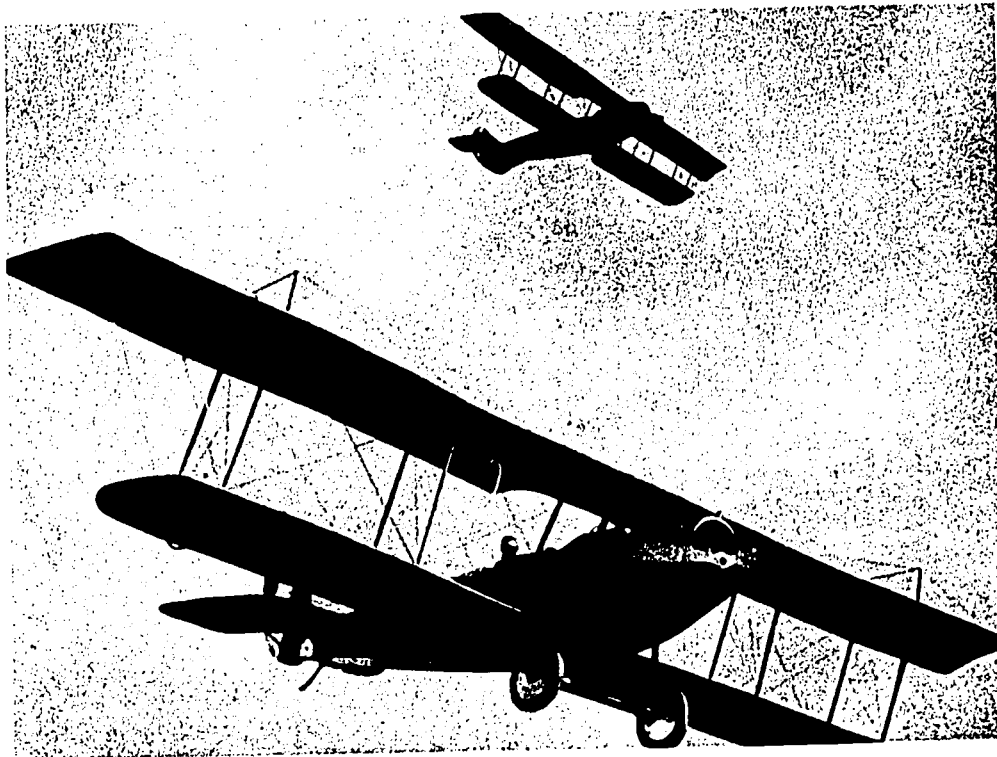


Figure 1-5. - World War I Curtiss JN-4's in formation. Although thousands of these airplanes were built during the war years, none took part in the air battles over France and Germany. Affectionately known as the "Jenny," this plane, flown by a generation of pilots, was the mainstay of the early barnstorming era.

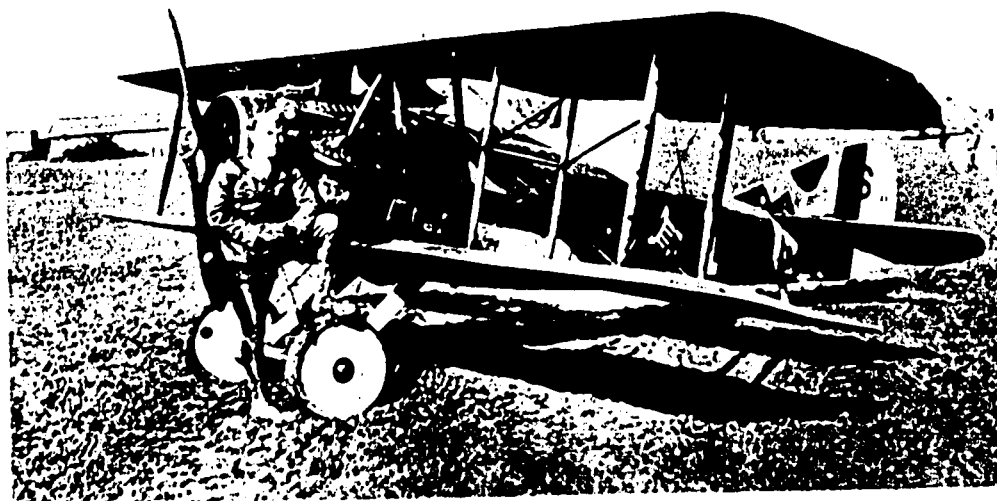


Figure 1-6. - U. S. ace of aces, Captain Eddie Rickenbacker, with his famous "Hat-in-the-Ring" Spad 13 of World War I fame. The Spad, one of the finest fighting machines developed during World War I, was the favorite airplane of American pilots. Built by the French, 893 of these machines were purchased by the United States.

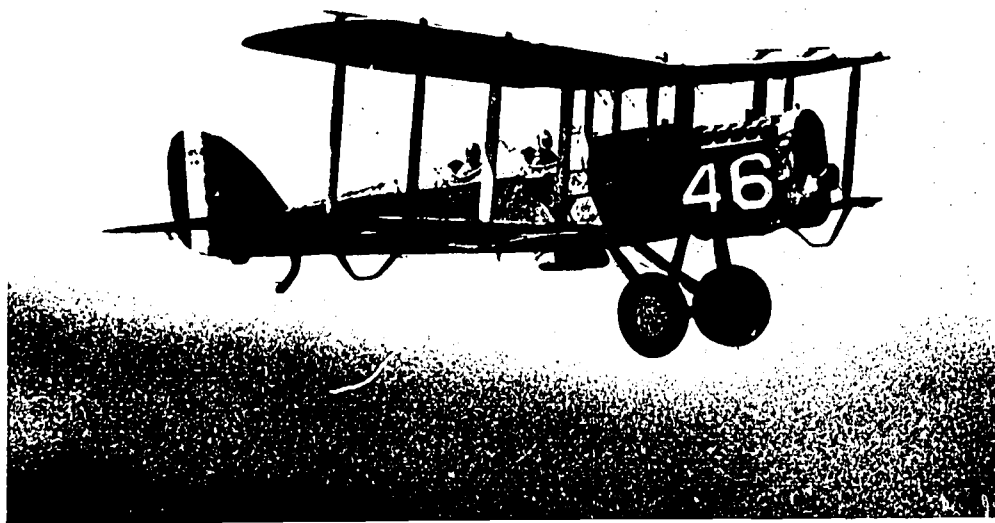


Figure 1-7. - The DeHavilland 4-B, post-war American modification of British-designed DeHavilland 4, which had been produced in the United States for use during World War I. American pilots used the original DeHavilland 4 for observation and bombing missions during 1918.

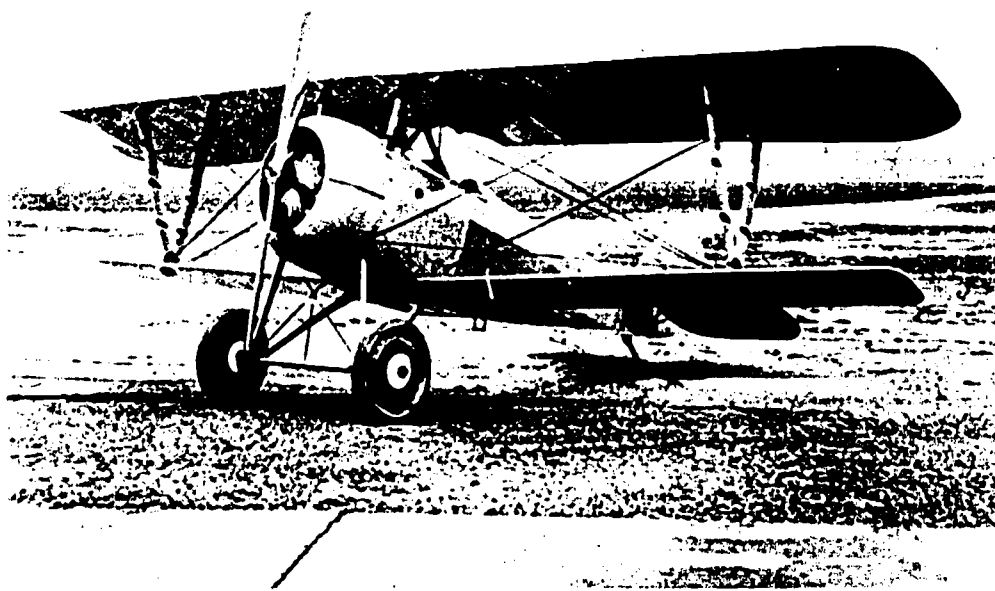


Figure 1-8. - The Nieuport 27, built by the French, was flown by many American pilots during World War I. Although it had the uncomfortable habit of shedding fabric from its top wing, many top-ranking aces built up their scores in this highly maneuverable little pursuit airplane. This was the plane that Captain Eddie Rickenbacker used in starting his string of victories.

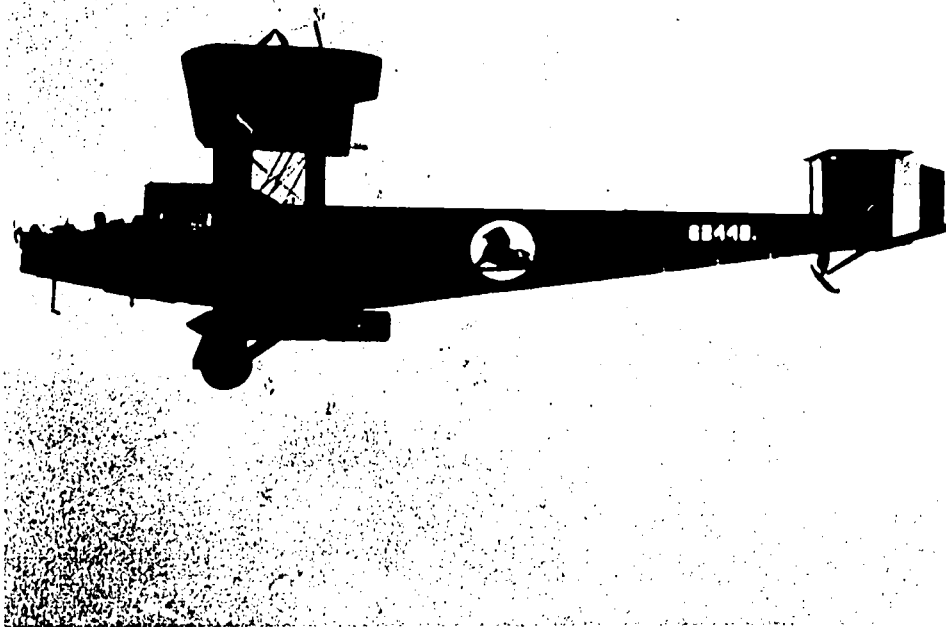


Figure 1-9. - Handley-Page bombers of British design were manufactured in the United States during World War I. With a gross weight of more than 14,000 pounds, this twin-engine aircraft was truly a "heavy" of its time. Air Marshall Hugh M. Trenchard organized British-built heavies like these into an Independent Strategic Bombardment Force for attacks against the German homeland.

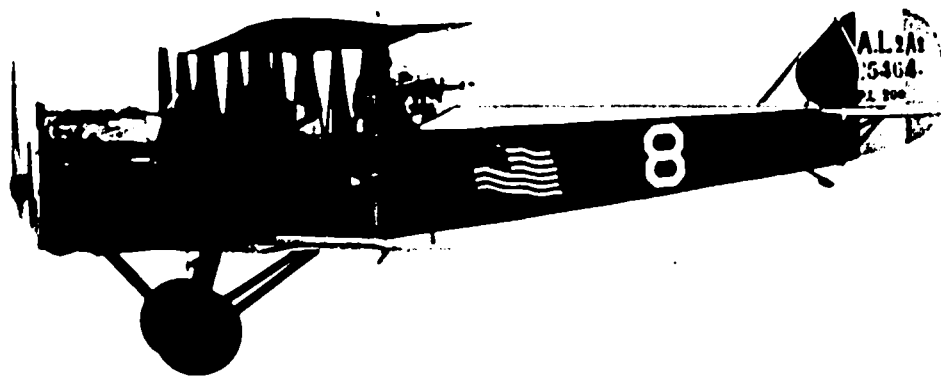


Figure 1-10. - The Salmson 2 A. 2 was a French-designed, two-place observation plane used by the American Expeditionary forces in World War I. The United States procured 705 of these planes for use in 10 A. E. F. Air Service observation squadrons serving in France. Powered by a 750-horsepower engine, the Salmson had a top speed of 116 miles per hour.

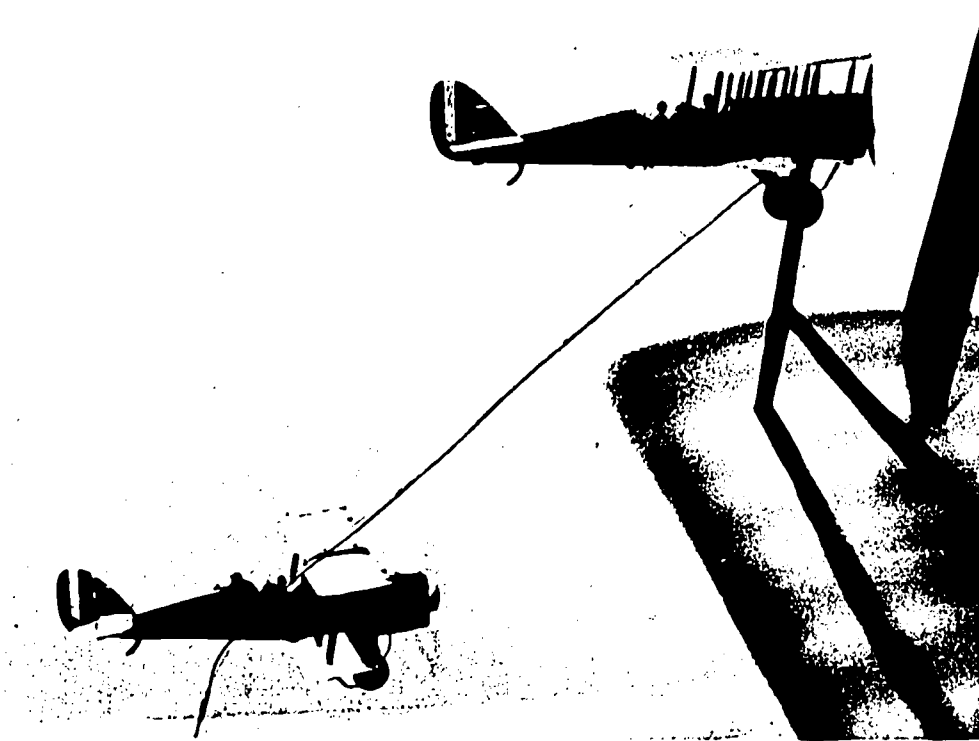


Figure 1-11. - Refueling tests using DeHavilland 4-B's were conducted by military aviators in 1923. These tests set the pattern for techniques that were to be so important in the development of aviation. As crude as the equipment was, an endurance record of 37 hours and 15 minutes was established by these pioneering pilots.

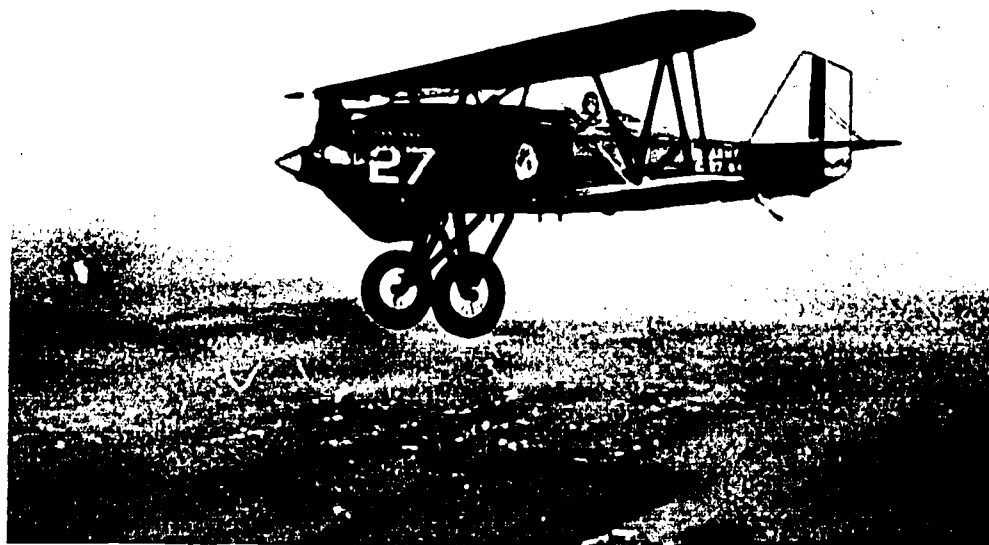


Figure 1-12. - The Curtiss Hawk P-1 flew from New York to San Francisco in 1924. The 2670-mile flight, made in 21 hours and 48 minutes, included five stops. This Hawk biplane was refined from the P-1 through the P-6.

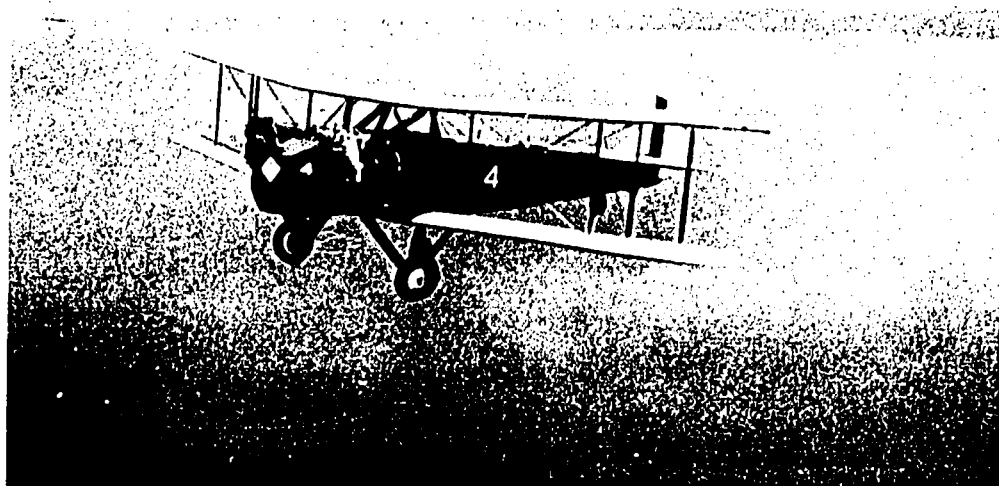


Figure 1-13. - The Keystone B-3, first of the "B" category bombers. Delivered to the newly established Army Air Corps, it had a 74-foot, 8-inch wing span and a gross weight of more than 12,950 pounds. The B-3 was powered by two 525-horsepower, air-cooled radial engines and had a crew of five.

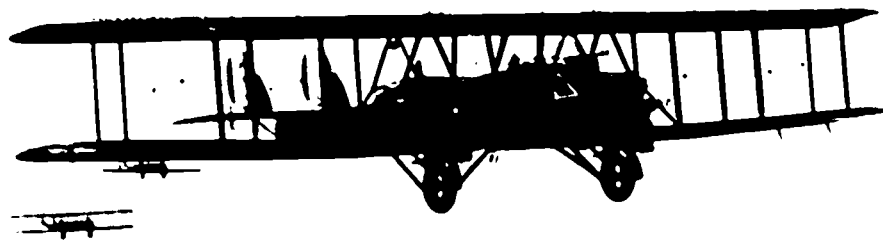


Figure 1-14. - "Mosquitoes to kill elephants" was said of General Billy Mitchell's Martin MB-2 bombers when he sent them against battleships. During tests conducted in 1921 and 1923, three war-prize German warships and two obsolete U. S. battleships were sunk by these aircraft.

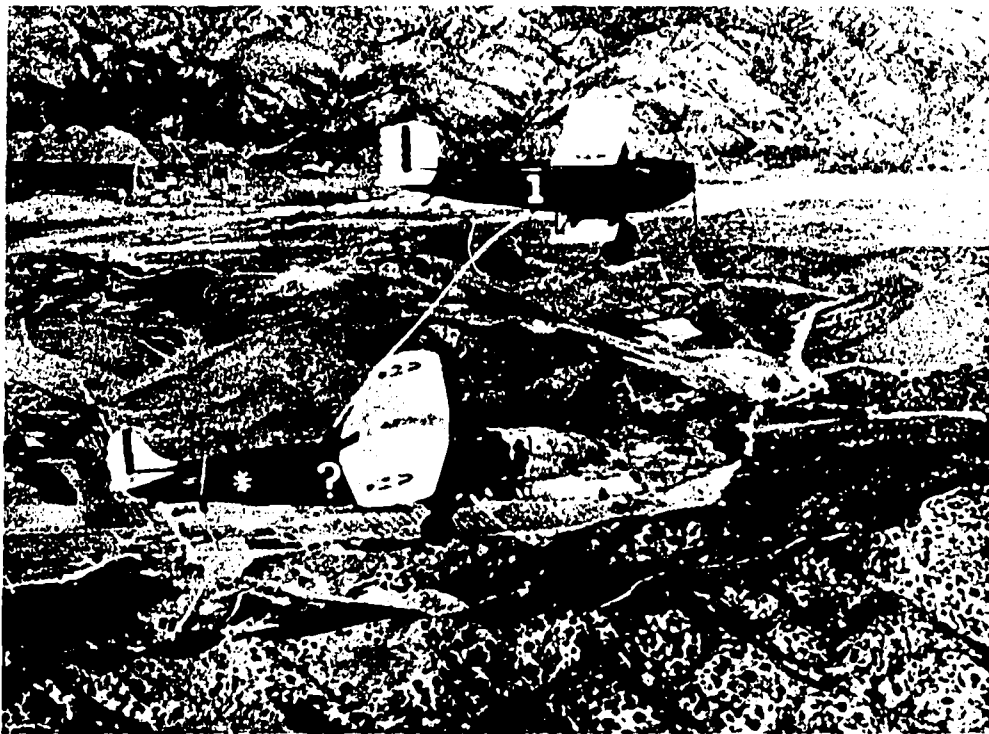


Figure 1-15. - The "Question Mark," a Fokker C-2, supplied more information on refueling techniques when it set an endurance record of almost 151 hours in 1929. Forty-three times during the historic flight the refueling plane hovered less than 20 feet over the appropriately named "Question Mark," passing down food, supplies, and more than 5000 gallons of gas.

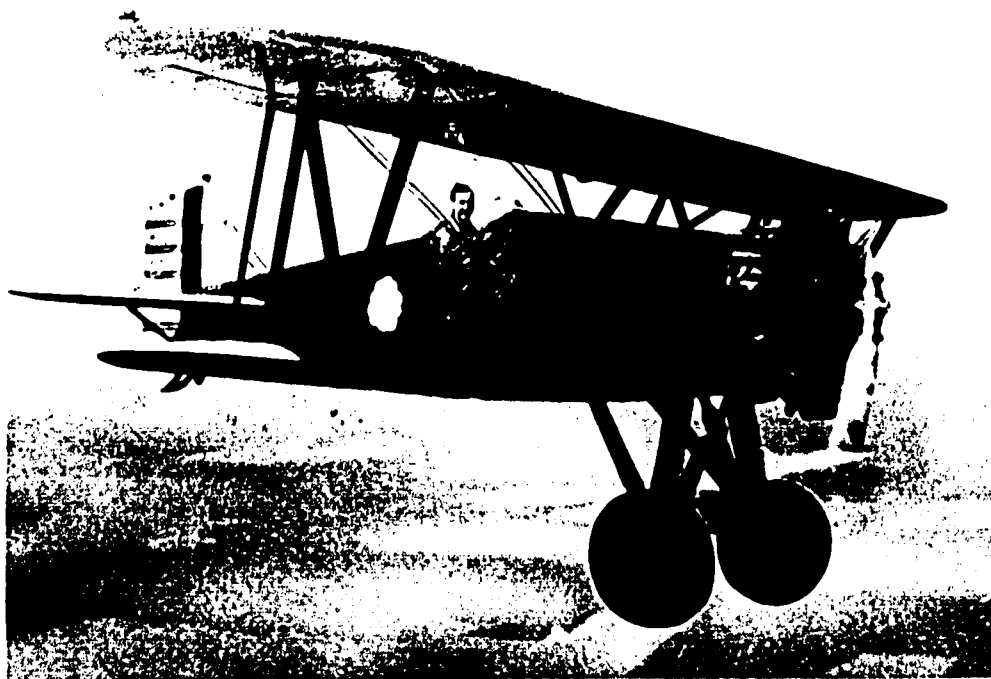


Figure 1-16. - The Boeing P-12 series pursuit aircraft was one of the finest biplane fighter aircraft ever designed. It was a highly maneuverable, sensitive plane. Grossing only 2700 pounds, this little pursuit aircraft, with its 450-horsepower engine and a skilled pilot at the controls, could loop on takeoff, a feat that attested to its outstanding design.

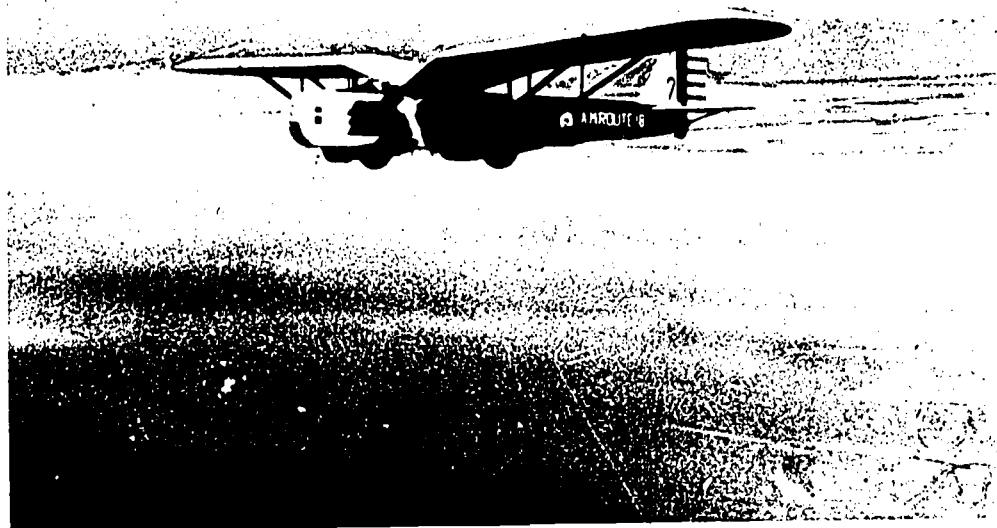


Figure 1-17. - The Douglas B-7, a transitional product of new bomber theories, still had the struts that typified the age of the biplane. Designed as a fast day-bomber, it had fabric-covered wings, an all-metal fuselage, metal control surfaces, and hydraulically operated, retractable landing gear. The B-7 flew mail over the Salt Lake City - Oakland route in early 1934 when the War Department was directed to take over all domestic airmail flights.



Figure 1-18. - The Curtiss P-6E was the most famous of the Hawk series of pursuit planes. One of the most beautiful biplane fighters ever built for the Air Corps, it was highly maneuverable and armed with two synchronized machineguns. Powered by a 600-horsepower liquid-cooled Curtiss engine turning a three-bladed propeller, this little fighter had a top speed of 197 miles per hour. A later model, the P-6F, was the first military aircraft to exceed 200 miles per hour in level flight.

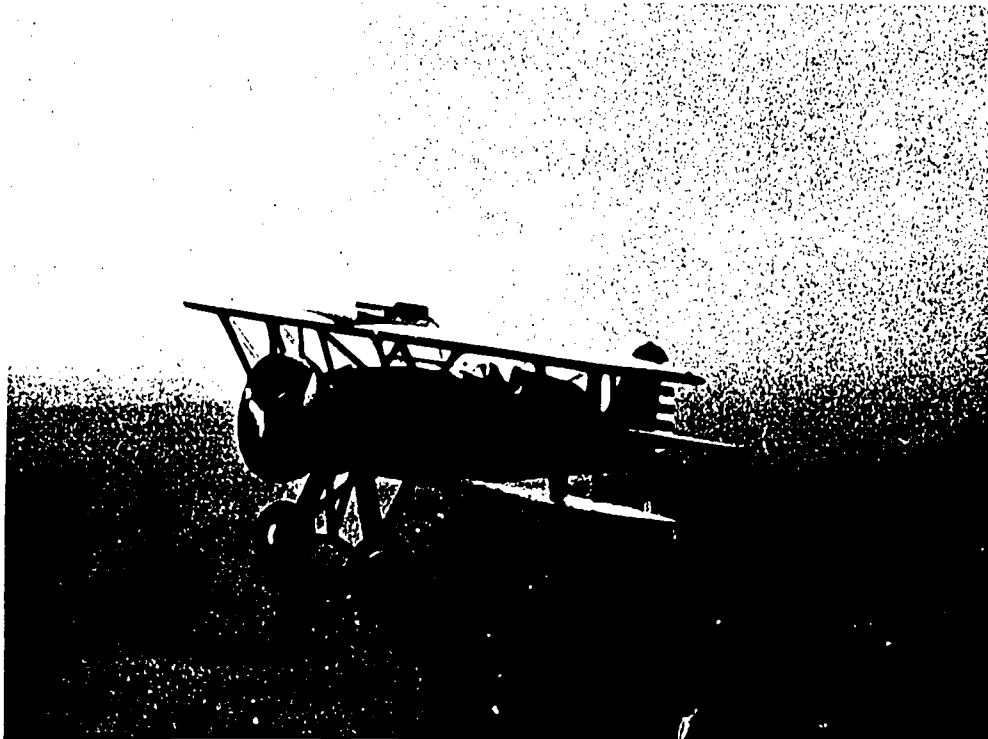


Figure 1-19. - The P-12E by Boeing was the first production-built Air Corps pursuit plane with an all-metal, monocoque fuselage. The P-12's had a long service life, serving with frontline squadrons from 1929 to 1936. In all, 366 of this series were produced; 110 of them were E models.



Figure 1-20. - A new aerodynamic concept was introduced when Boeing Aircraft Company produced the B-9, a low-wing, all-metal monoplane, in the 1930's. Earlier bomber aircraft, generally designed for multipurpose use, could not be as effective as one planned for a specific mission.

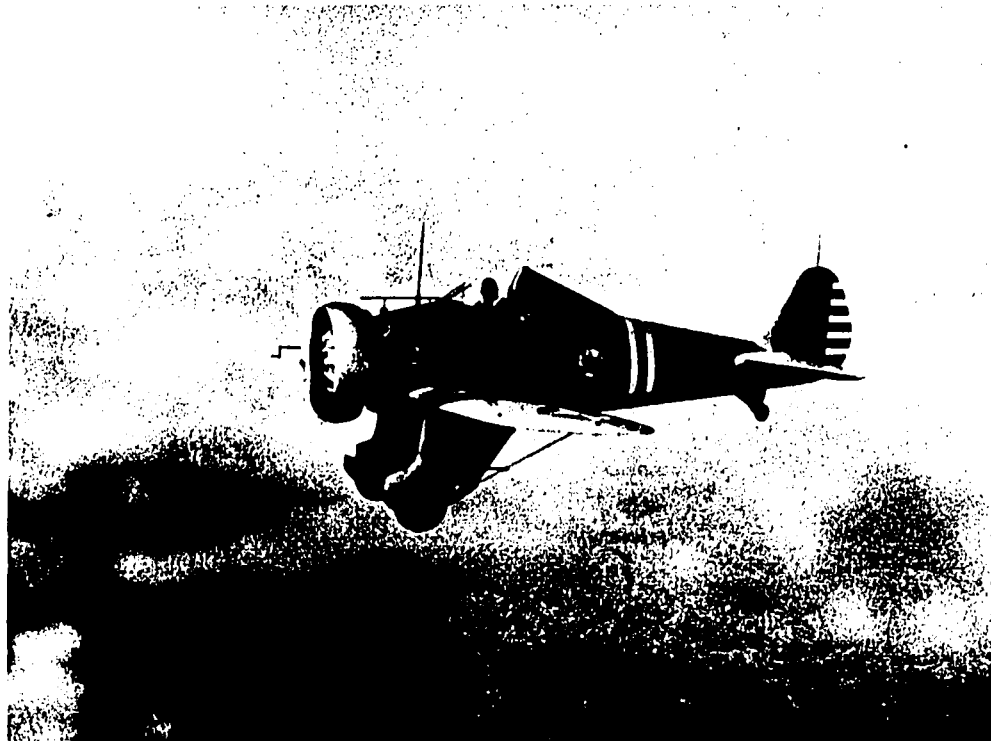


Figure 1-21. - The Boeing P-26 Peashooter, designed to meet the increasing performance of the new bombers, was the first all-metal, low-wing fighter delivered in numbers. During this period, many thought the pursuit ship obsolete. Bombers were becoming so much faster that it was difficult for fighters to keep up with them.

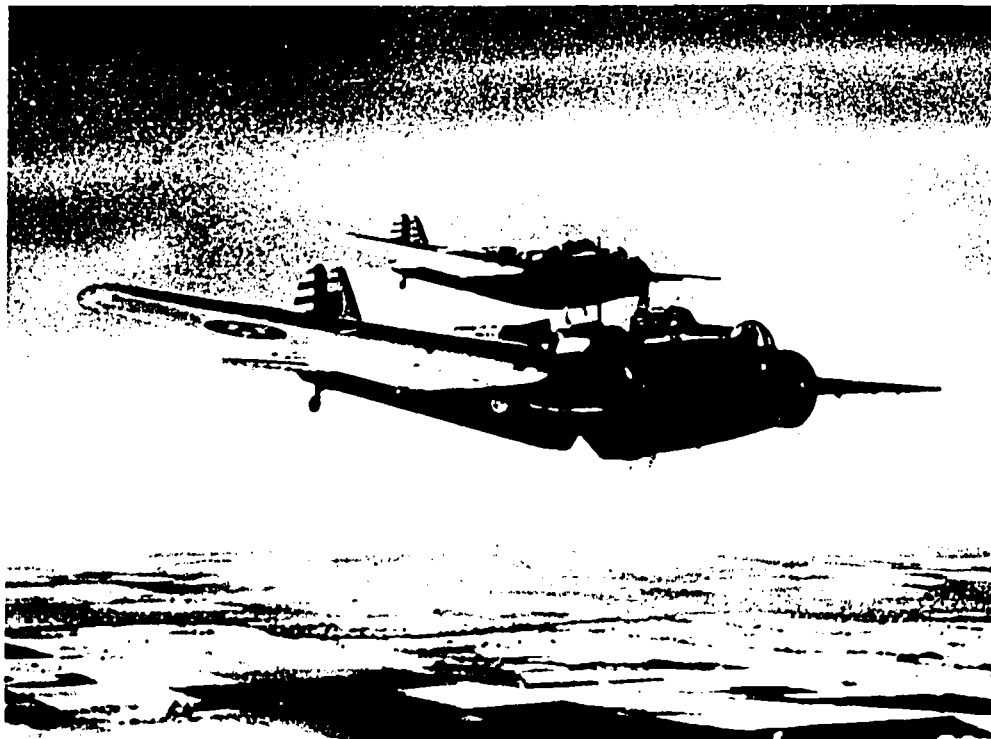


Figure 1-22. - A new generation of bombers was realized with the production of the Martin B-10. Featuring enclosed cockpits, a power-operated turret, retractable landing gear, and newly designed engine cowlings, it had a top speed of 212 miles per hour.



Figure 1-23. - In August 1934, Boeing began construction of the XB-17. First flown in July 1935, it led the way to one of the world's most famous series of bomber airplanes. Flying characteristics of this plane were outstanding for the time, establishing performance records that far outclassed most airplanes of the era. Accepted by the military in January 1937 as the YB-17 Flying Fortress, it had a top speed of 256 miles per hour, service ceiling of 30,600 feet, and a maximum range of 3320 miles.

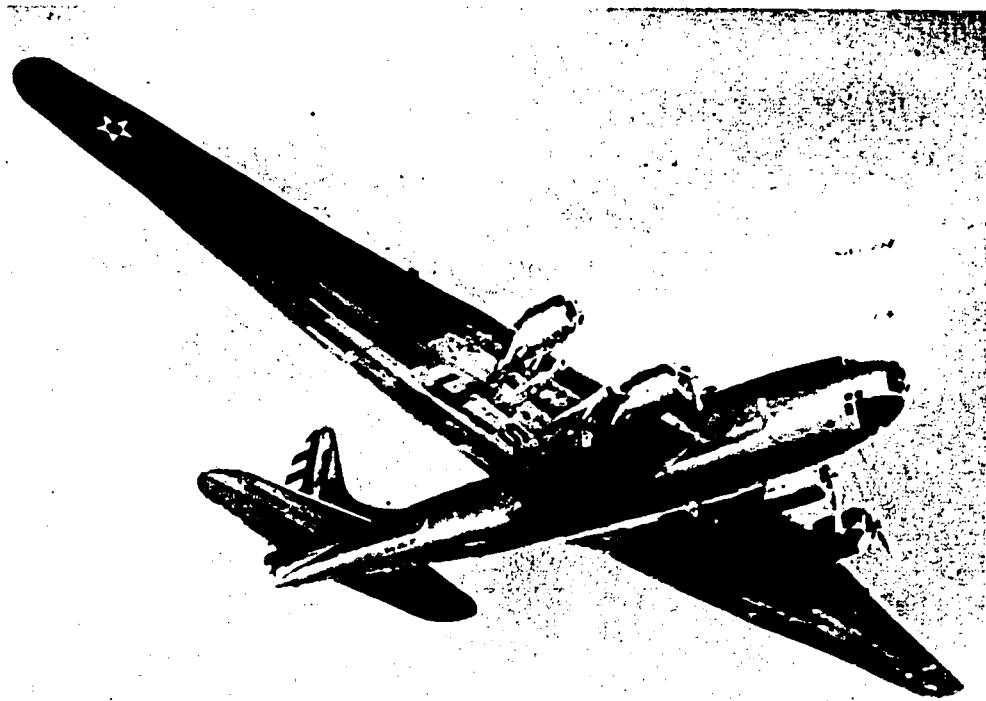


Figure 1-24. - The Douglas XB-19, conceived in 1935, first flew in 1941. The culmination of $6\frac{1}{2}$ years of engineering, this giant aircraft dwarfed all others of the time. It had a wing span of 212 feet, a 132-foot, 4-inch fuselage, 8-foot main tires, and a rudder 42 feet high. It had a range of 7710 miles with a fuel load of 10,400 gallons.

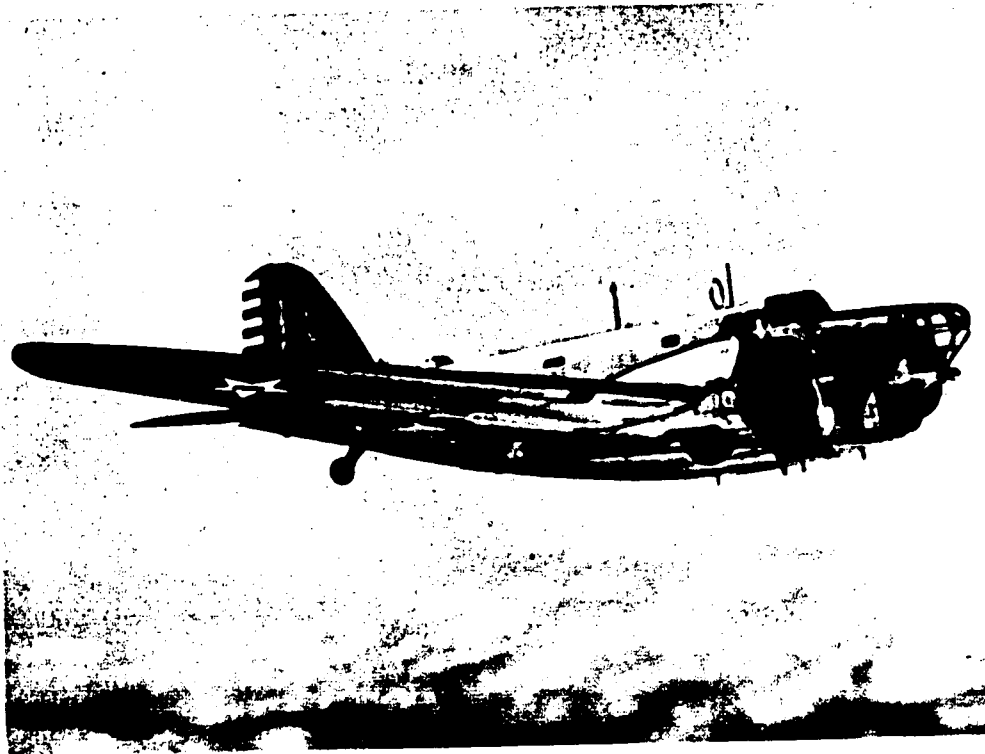


Figure 1-25. - Air Corps bomber competition of 1936 resulted in Douglas Aircraft Company getting an order for 177 B-18 Bolos. Quite similar in appearance to the famed DC-3 commercial airliner just coming off Douglas production lines, the Bolo was a very reliable airplane with good performance.



Figure 1-26. - The P-35 of Major Alexander DeSeversky's aircraft company (1936), a forerunner of future fighters, proved to be a wonderful airplane to fly. Almost 50 miles per hour faster than the P-26, its armament still did not make it the fighting machine pilots needed to keep up with bomber development.

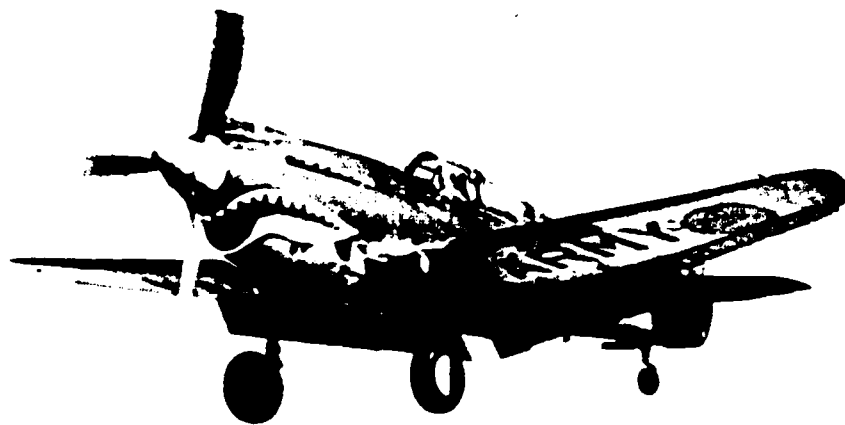


Figure I-27. - Hawk, Tomahawk, Kittyhawk, Warhawk were the official names given to the Curtiss P-40. Praised, abused, called excellent and inferior, this much-discussed World War II fighter saw action on every fighting front in the world. Always less maneuverable and slower than first-line German and Japanese adversaries, it proved far more rugged.

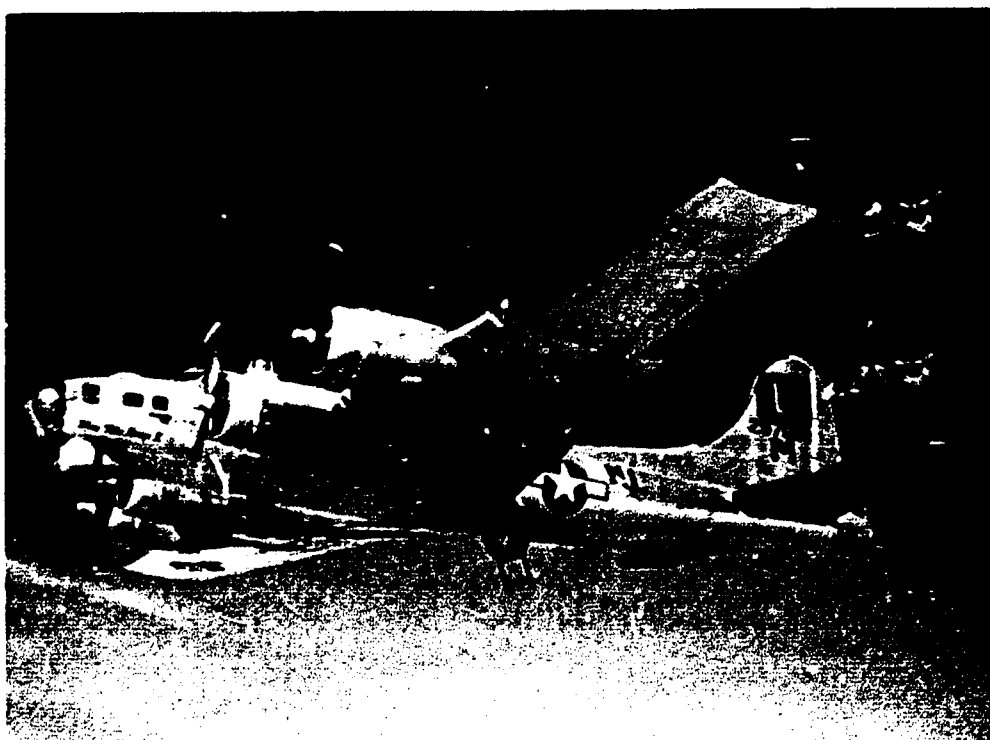


Figure I-28. - The World War II Flying Fortress (B-17), scourge of the skies over embattled Europe, no longer had the thin, graceful lines of its 1936 sister. Redesigned to take the war to the enemy, the slim rudder had given way to a broad dorsal fin that enclosed twin stinger 50-caliber machineguns in the tail. Top and belly turrets bulged from the fuselage, showing their ugly gun snouts. Airmen gunners stood at open side hatches with their 50's bearing on anything that came their way.

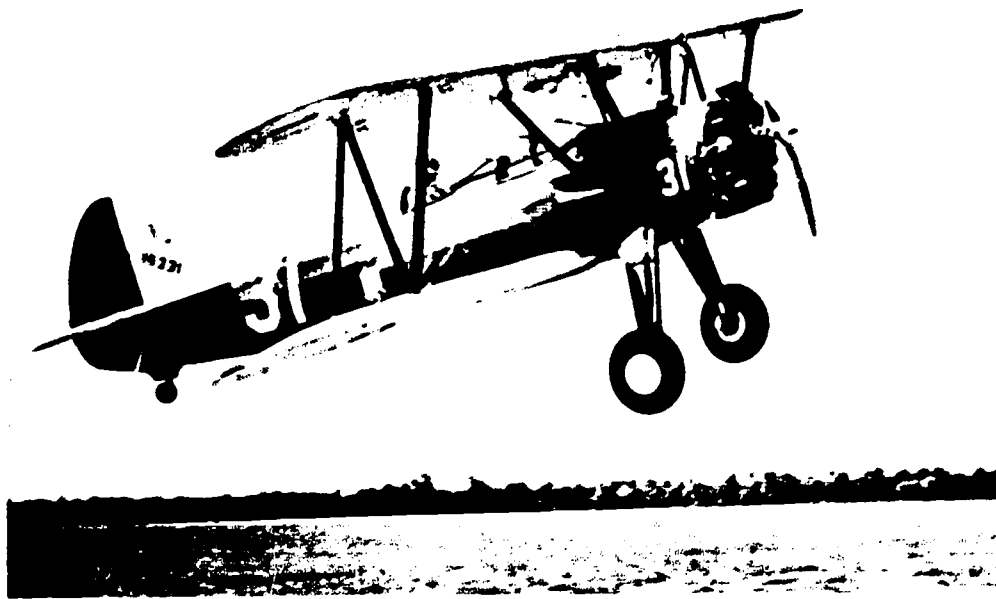


Figure I-29. - The Stearman PT-17 Kaydet was used for primary flight training prior to and during World War II by both the Air Force and the Navy. Equipped with a 220-horsepower engine, the two-place biplane had a top speed of 135 miles per hour.



Figure I-30. - The Vultee "Vibrator" (BT-13) was familiar to thousands of fledgling pilots going through basic flying training in the 1940's. The BT-13 was a heavier airplane than those flown in primary training, and its higher horsepower and pronounced torque provided trainees with the feel for the combat planes to come.

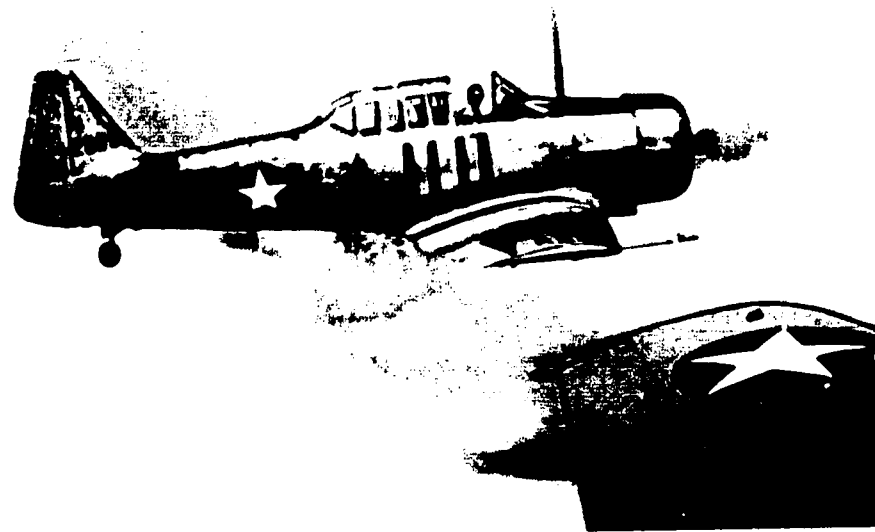


Figure 1-31. - Flown by more military pilots, worldwide, than any other aircraft, the North American AT-6 Texan had an unusually long service life. Produced as an advanced trainer in 1938, it was used in U. S. Air Force pilot schools until September 1956.

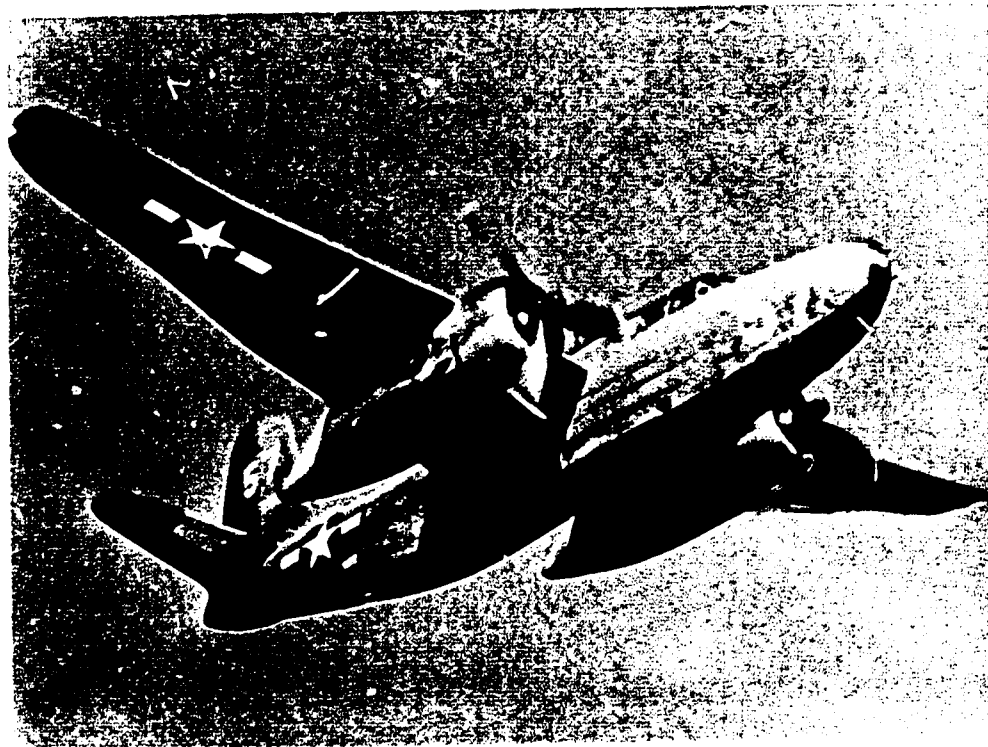


Figure 1-32. - The Douglas A-20 was developed from a bomber designed for the French in 1937 and first flown in 1938. Designated the Havoc by the Americans, early production models were delivered to the British, who renamed it the Boston.

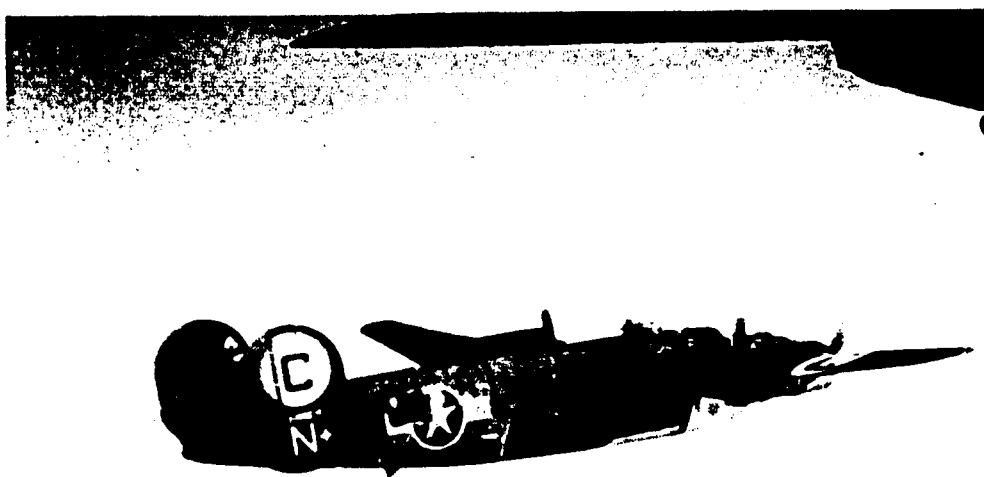


Figure 1-33. - The Convair B-24 Liberator is probably best remembered for its service in early raids on Nazi oil refineries at Ploesti, Rumania. Losses during the August 1, 1943, raid on Ploesti were extremely high. Of the 163 Liberators that reached the target, 54 were lost, and 144 airmen were killed or missing.



Figure 1-34. - The North American B-25 Mitchell bomber, named after General Billy Mitchell, saw combat in most World War II theaters. The most famous exploit of this versatile plane was unquestionably the carrier-based attack planned by the Air Corps and led by Lieutenant Colonel Jimmy Doolittle against the Japanese mainland early in the war.

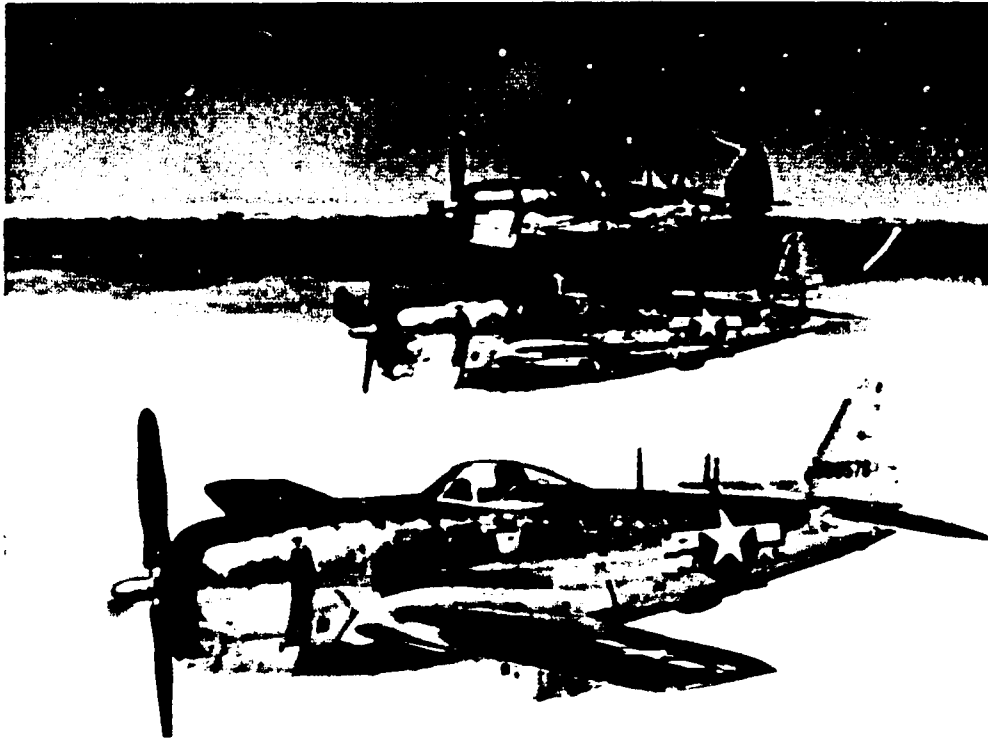


Figure 1-35. - "Juggernaut," or affectionately "Jug," was the name given to the rugged Republic P-47 Thunderbolt by its pilots. Twice as heavy as any single-engine fighter before it, the P-47 was the culmination of years of work by Major Alexander DeSeversky.

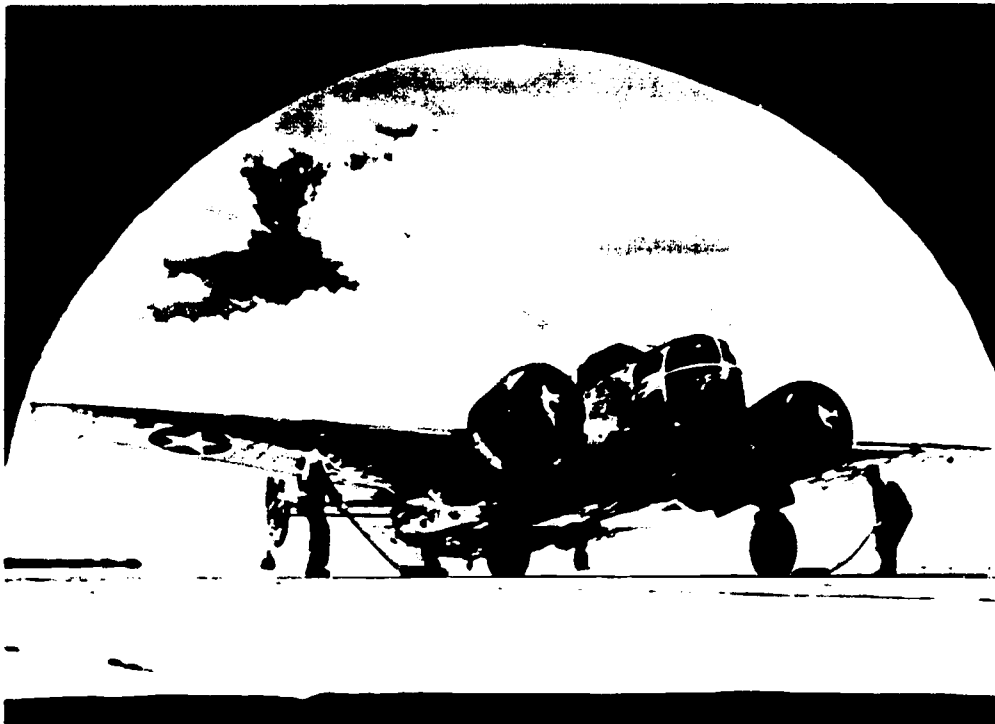


Figure 1-36. - In continuous production since 1937, the twin-tailed, model 18 Beech light commercial transport was adapted to navigator and bombardier training during World War II. As the Plexiglas-nosed Beech AT-11, it was a familiar classroom to the 45,000 World War II bombardier cadet graduates.



Figure 1-37. - DC-3, C-47, Dakota, and Skytrain were the official names of this world-famous Douglas-built cargo and passenger plane. To her crews, however, this lovable old bird was called the "Gooney." Large airline demands for this model and resultant production improvements led to the DC-3 in June 1936. This is the plane that became the workhorse of the Services during World War II.

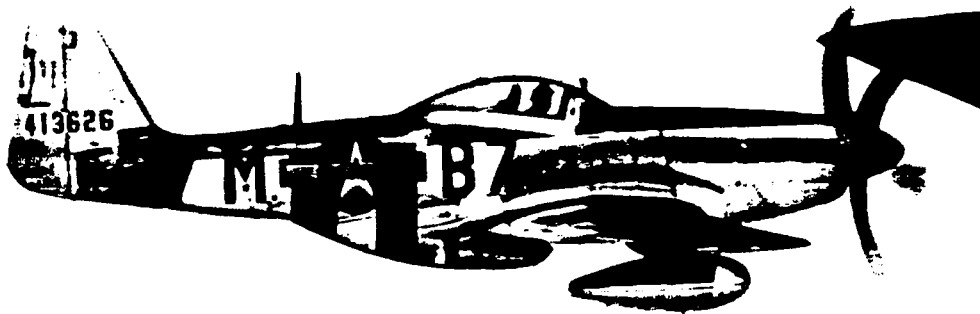


Figure 1-38. - The P-51 Mustang was originally designed for the Royal Air Force in 1940. With a deadline of 120 days for delivery, North American Aviation achieved the almost impossible, by producing the first model in 117 days. Called the best all-around American-built fighter of World War II, it was faster, more maneuverable, and most important, had a greater cruising range than any other fighter in the USAAF.



Figure 1-39. - The C-46 Commando, built by the Curtiss-Wright Corporation, first saw action late in World War II. With a capacity of 15,000 pounds, it was the largest twin-engine plane at the time. The Commando served in all theaters as a troop and cargo carrier, flying ambulance, and tow plane for gliders.

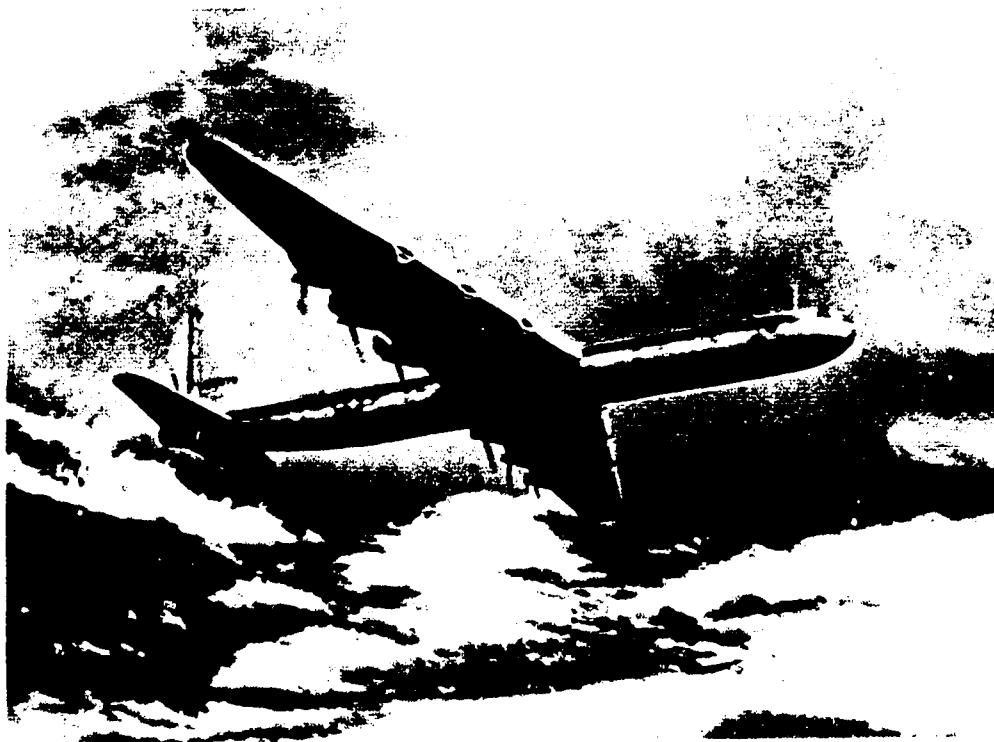


Figure 1-40. - The Consolidated B-36 Peacemaker was the biggest bomber, in size, to enter the Air Force inventory. Development began in 1941. It was not flown, however, until the fall of 1947. The Peacemaker lived up to its name in helping to deter general war for more than 10 years. The B-36 originally was powered by six turbopropeller, pusher engines. The "D" version, introduced in 1949, had four additional turbojet engines paired in pods, one under each wing. This ten-engine version had a top speed of 435 miles per hour, a ceiling of 45,000 feet, and a bomb load of 84,000 pounds.

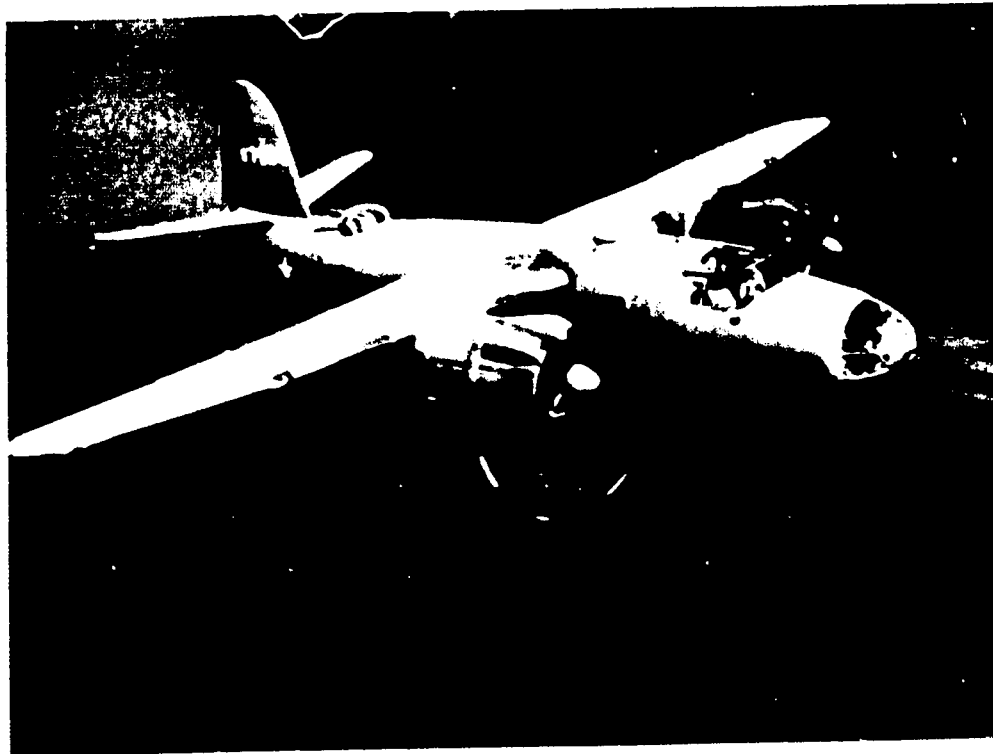


Figure 1-41. - Built by Martin, the B-26 Marauder amassed a credible combat record in Africa, Europe, and the Pacific during World War II. With its unusually high wing loading and a landing speed of 135 miles per hour, the Marauder was one of the most controversial airplanes of its time.

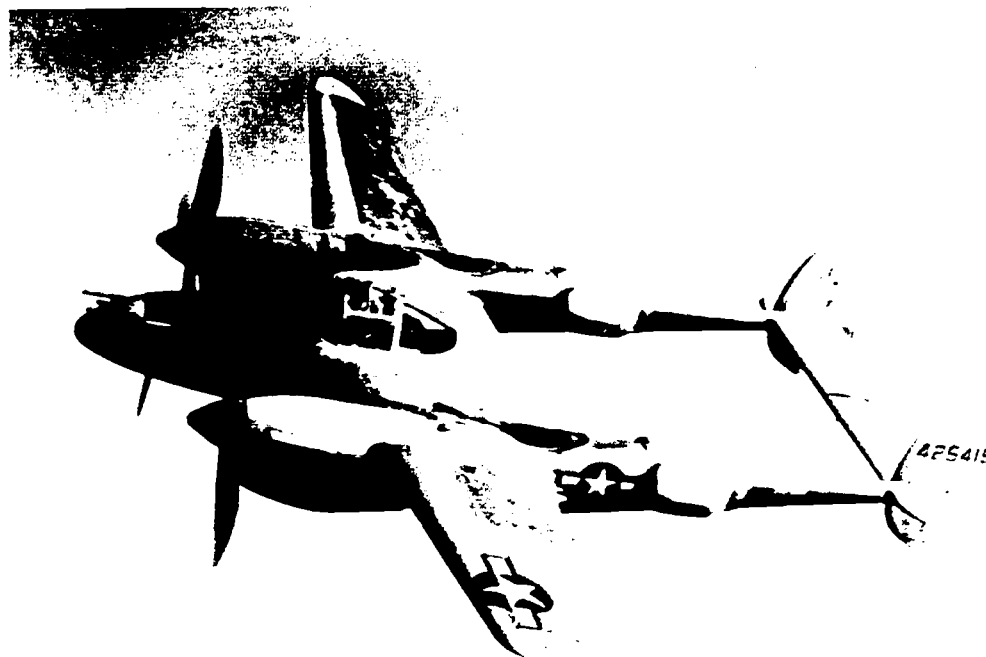


Figure 1-42. - Operational in 1942, the Lockheed P-38 Lightning was designed in 1937 and first flew in 1939. Known as the "Fork-Tailed Devil" by the Germans and Japanese, the Lightning piled up an impressive record in Europe and the Pacific. With hydraulic aileron boost and counterrotating propellers, it was a wonderful airplane to fly. A rapid roll, the ability to dive at extremely high speeds (up to 780 mph), and concentrated firepower made it a formidable adversary.

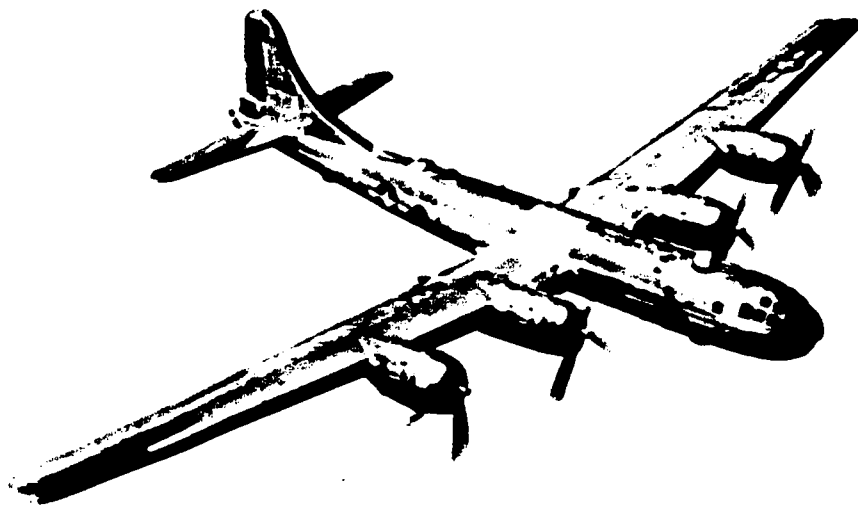


Figure 1-43. - The B-29 Superfortress, built by Boeing, has been called the weapon that won the war in the Pacific. Designed to carry large bomb loads long distances, it made possible the strategic bombardment that brought Japan near to collapse. It was a very sophisticated airplane with a pressurized cabin, highly advanced remote-control gun-firing system, and tremendous bomb capacity.



Figure 1-44. - The first jet aircraft produced for the USAAF and flown in October 1942 was the Bell XP-59A Airacomet (bottom). Powered by twin 2000-pound-thrust jets, this airplane was not as fast as the operational fighters of the time. The Bell P-63 Kingcobra (top) was propeller driven and had a 37-millimeter cannon in the nose.

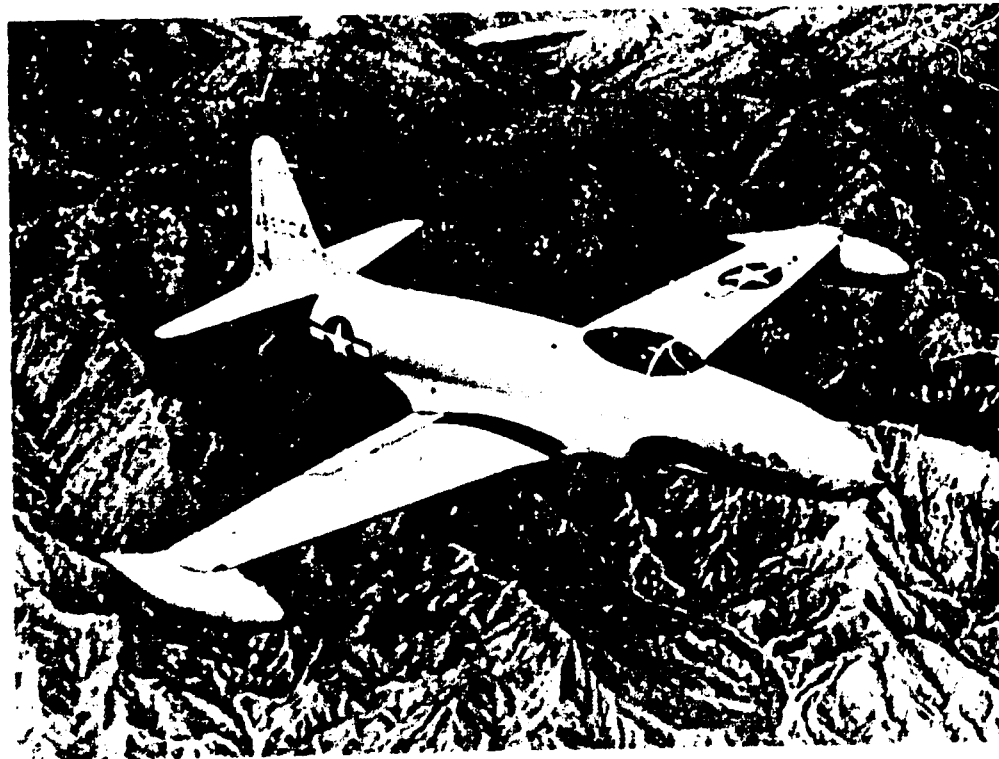


Figure 1-45. - Development of the jet-propelled Lockheed P-80 Shooting Star marked the dawn of the jet age. The Shooting Star, designed as an answer to the enemy jets appearing in the skies over Europe, was built in the record time of 143 days. The prototype of this jet flew on January 2, 1944.

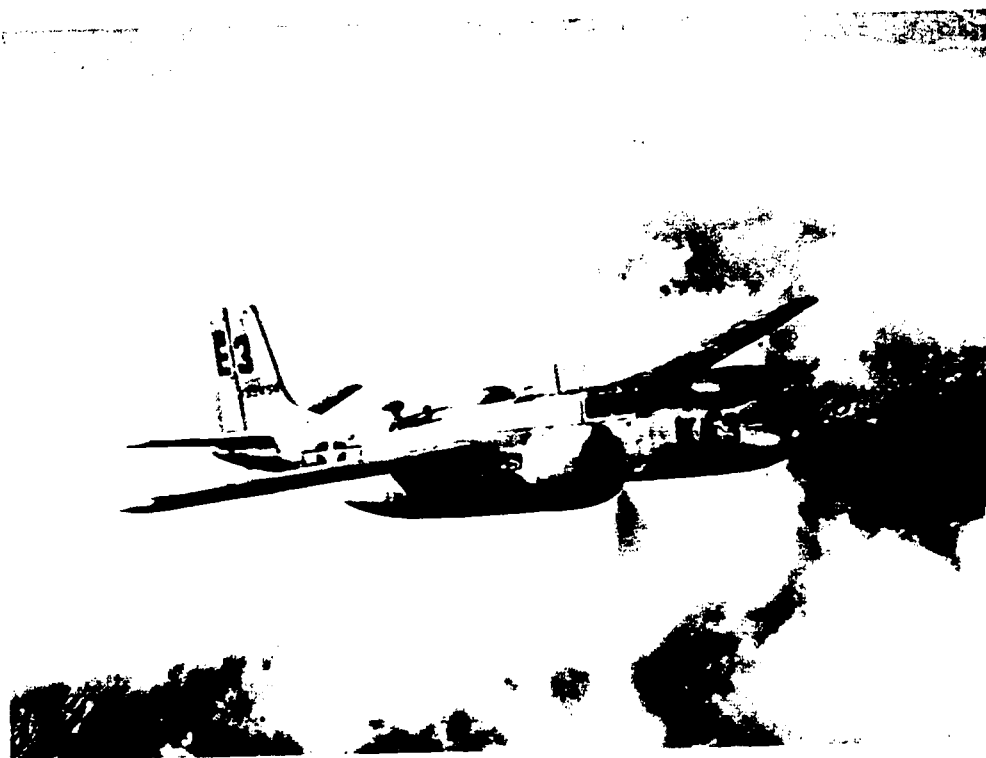


Figure 1-46. - The Douglas B-26 Invader is a tactical light bomber well suited for counter-guerrilla air action. The earliest models of the B-26 (then the A-26) saw service during the Battle of the Bulge in World War II. Extremely versatile, it has a speed of more than 350 miles per hour.

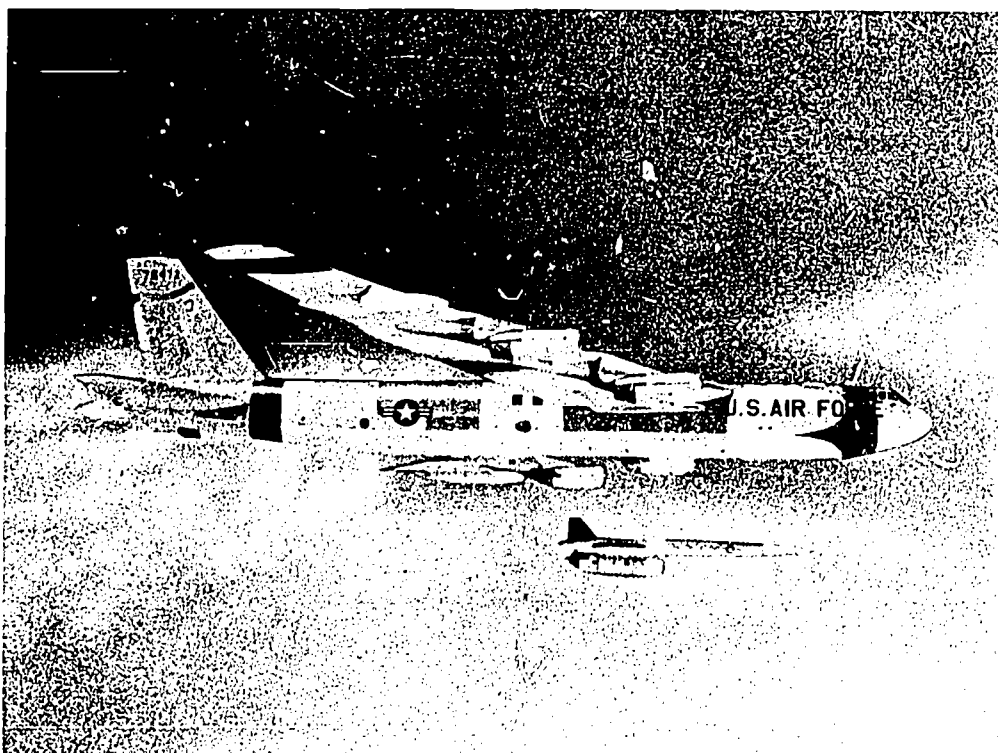


Figure 1-47. - Since 1955, the Boeing B-52 Stratofortress has been the Strategic Air Command's primary heavy bomber. It can carry two Hound Dog air-to-surface guided missiles. In 1957, three B-52's, using in-flight refueling, flew around the world, 24,325 miles, in 45 hours.

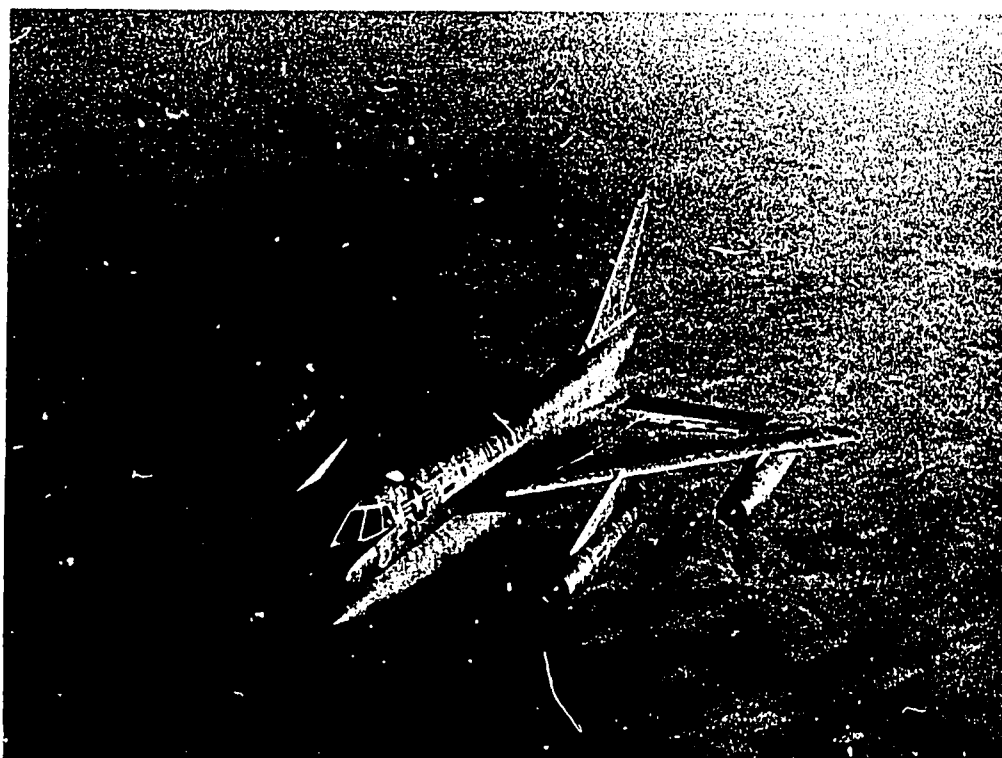


Figure 1-48. - The fastest bomber in the Strategic Air Command, the Convair B-58 Hustler has made the longest supersonic flight in history. In October 1963, a B-58 flew nonstop from Tokyo to London in 8 hours and 35 minutes, averaging 938 miles per hour. It carries its nuclear punch in a pod slung underneath.

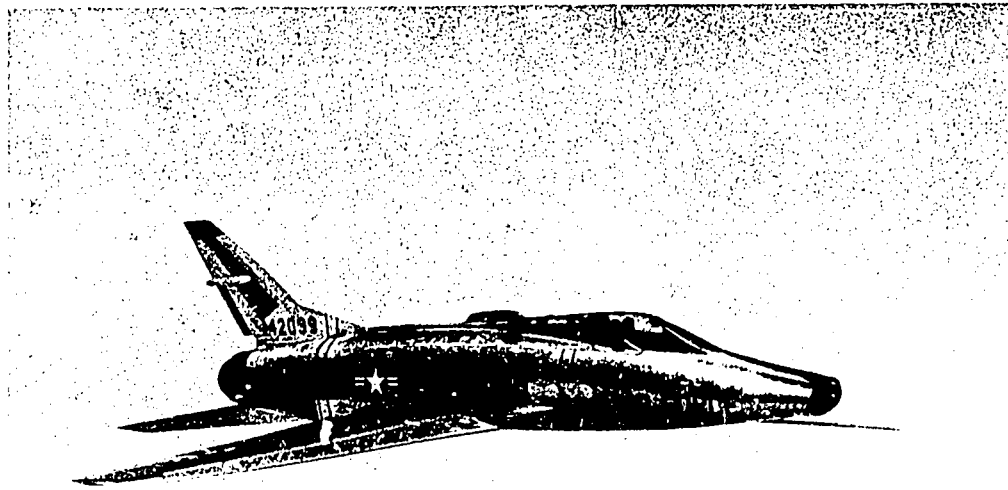


Figure 1-49. - The first USAF aircraft to fly supersonically in level flight, the North American F-100 Supersabre has been the workhorse of tactical air units. The first Supersabre was delivered to the Tactical Air Command in late 1954.

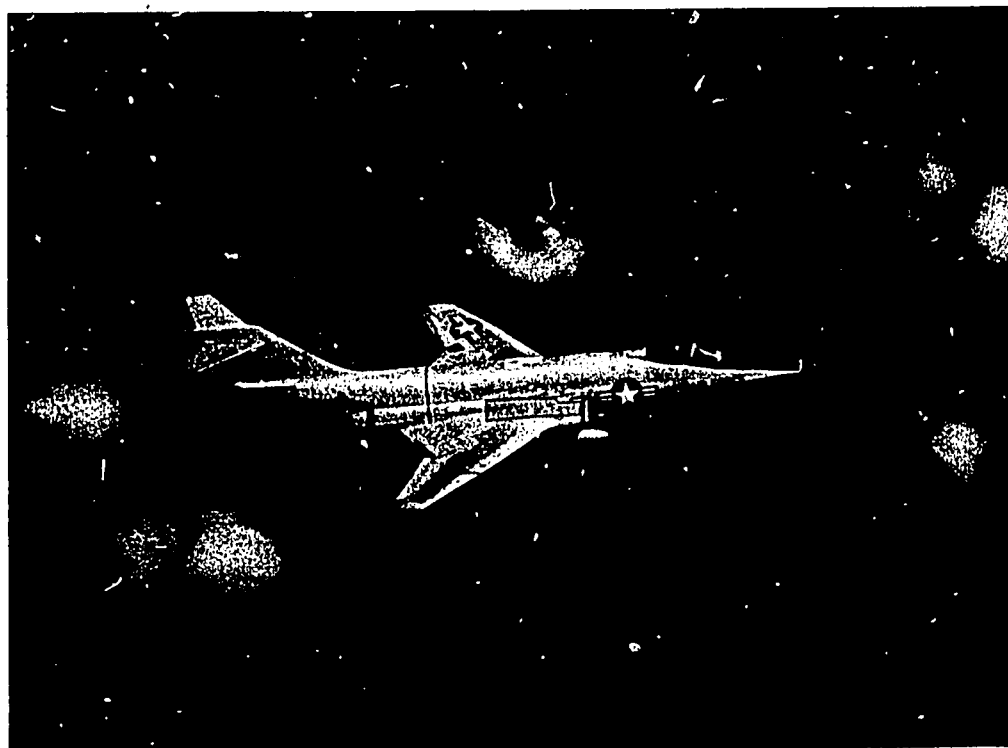


Figure 1-50. - The McDonnell RF-101 Voodoo was the USAF's first supersonic photoreconnaissance aircraft. From 45,000 feet, the Voodoo can photograph an area 217 miles long and 8 miles wide plus an area mosaic of 20,000 square miles.

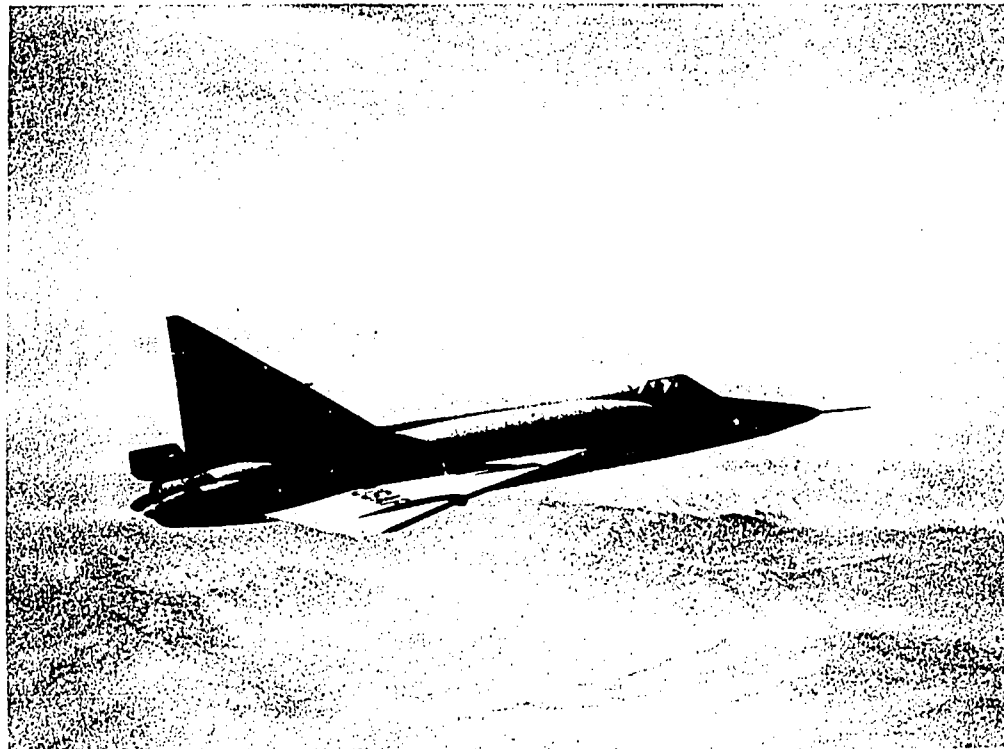


Figure 1-51. - The Convair F-102 Delta Dagger was the world's first supersonic all-weather jet interceptor. Flown first in 1953, it became operational in the Air Defense Command in 1956. It uses electronic "eyes" to locate hostile aircraft by day or night, in good or bad weather.

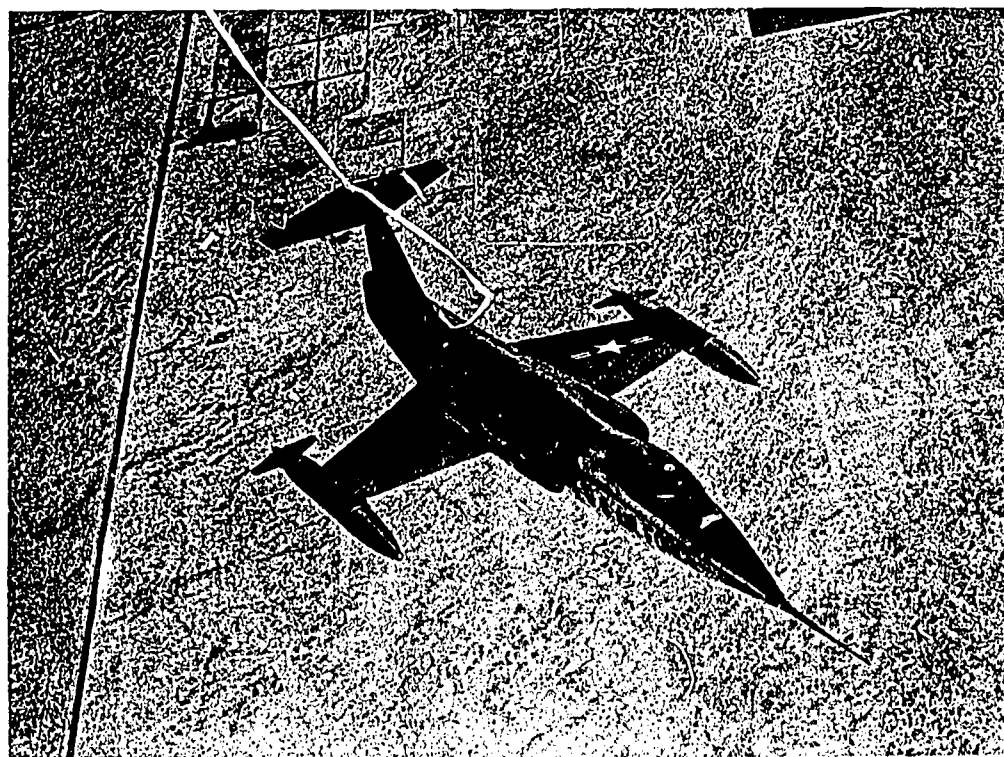


Figure 1-52. - The Lockheed F-104 Starfighter was designed as a supersonic air superiority fighter. It serves either as a tactical fighter or as a day-night interceptor.

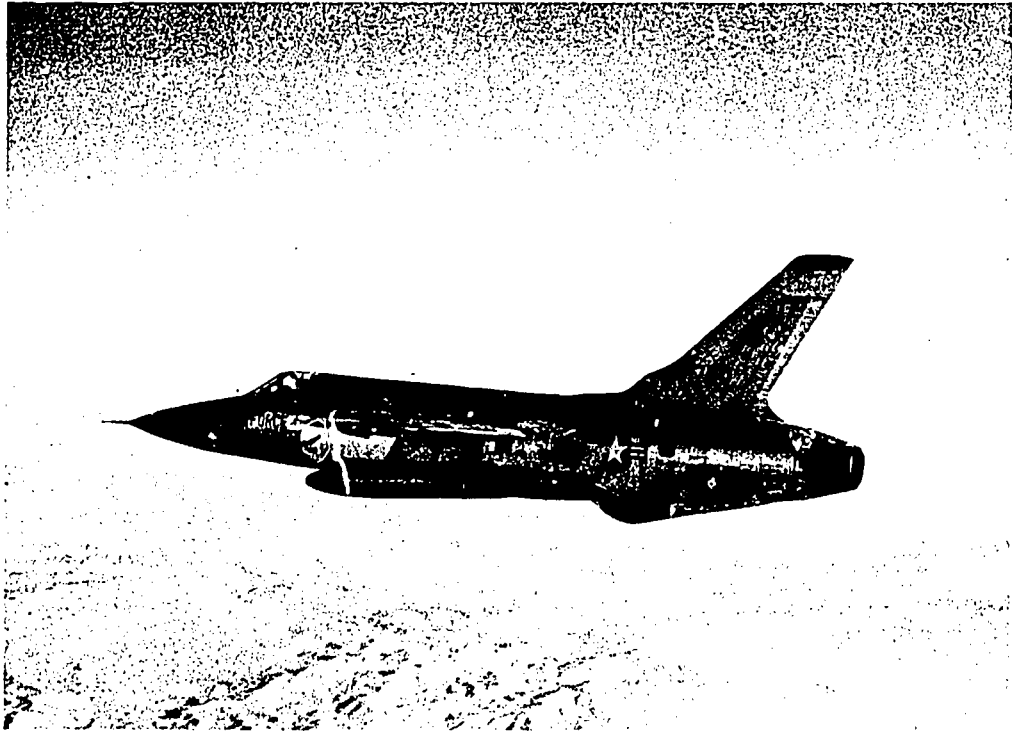


Figure 1-53. - The Republic F-105 Thunderchief is a 1400-mile-per-hour aircraft which can deliver 12,000 pounds of bombs. It also has a nuclear payload capability.



Figure 1-54. - The Convair F-106 Delta Dart's afterburning jet engine can push this all-weather interceptor to speeds of more than 1400 miles per hour and to altitudes above 50,000 feet.

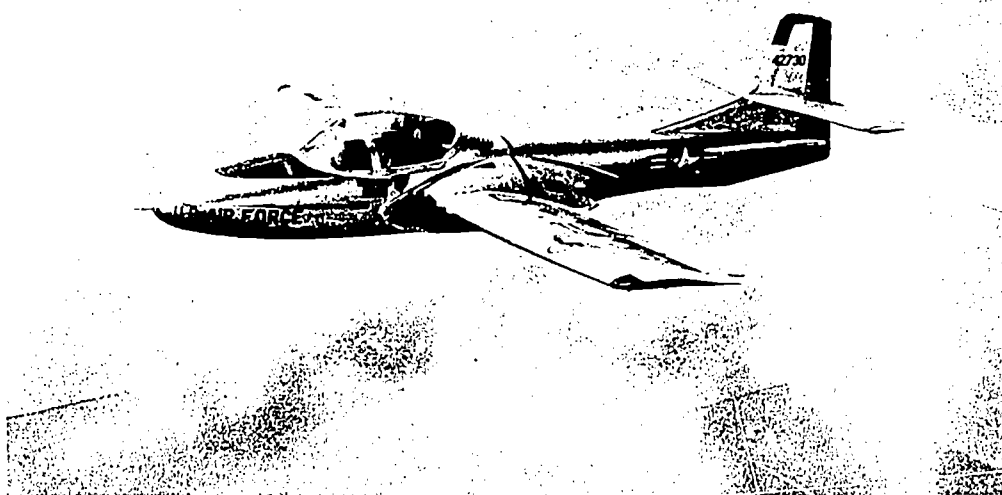


Figure 1-55. - The Cessna T-37 is a 350-mile-per-hour jet trainer.

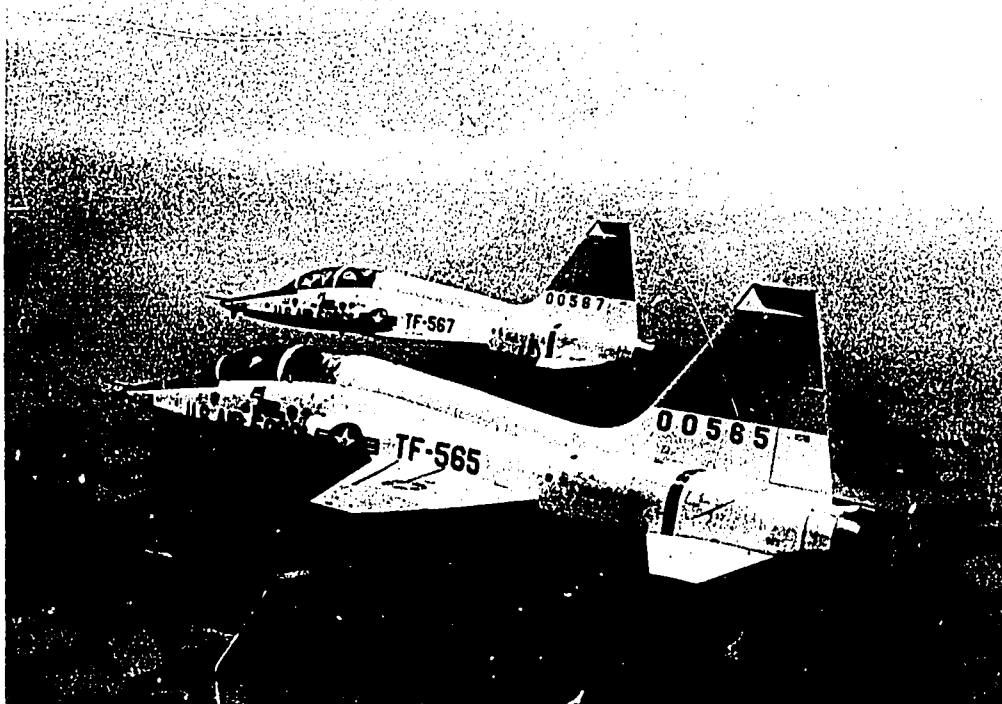


Figure 1-56. - The Northrop T-38 Talon is a basic, two-place, supersonic jet trainer capable of 850 miles per hour with a range beyond 1150 miles.

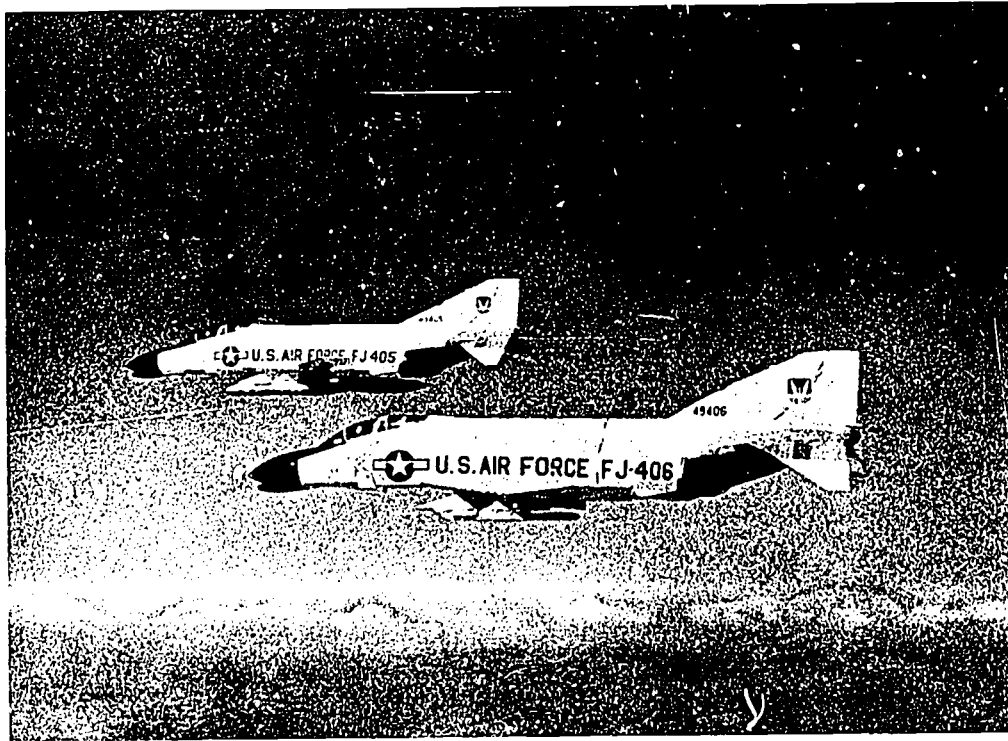


Figure 1-57. - McDonnell F-4C is capable of 1600 miles per hour. It has an all-weather bombing system for use in placing either conventional or nuclear bombs on target.

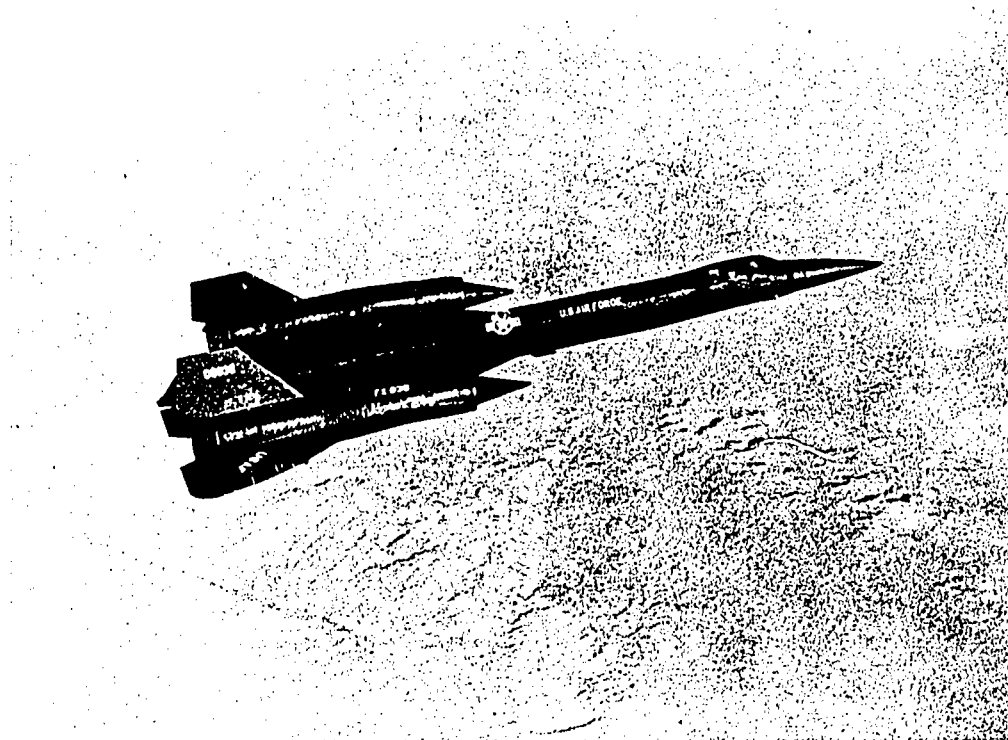


Figure 1-58. - The Lockheed YF-12A has been tested in sustained flight at more than 2000 miles per hour at altitudes above 70,000 feet.

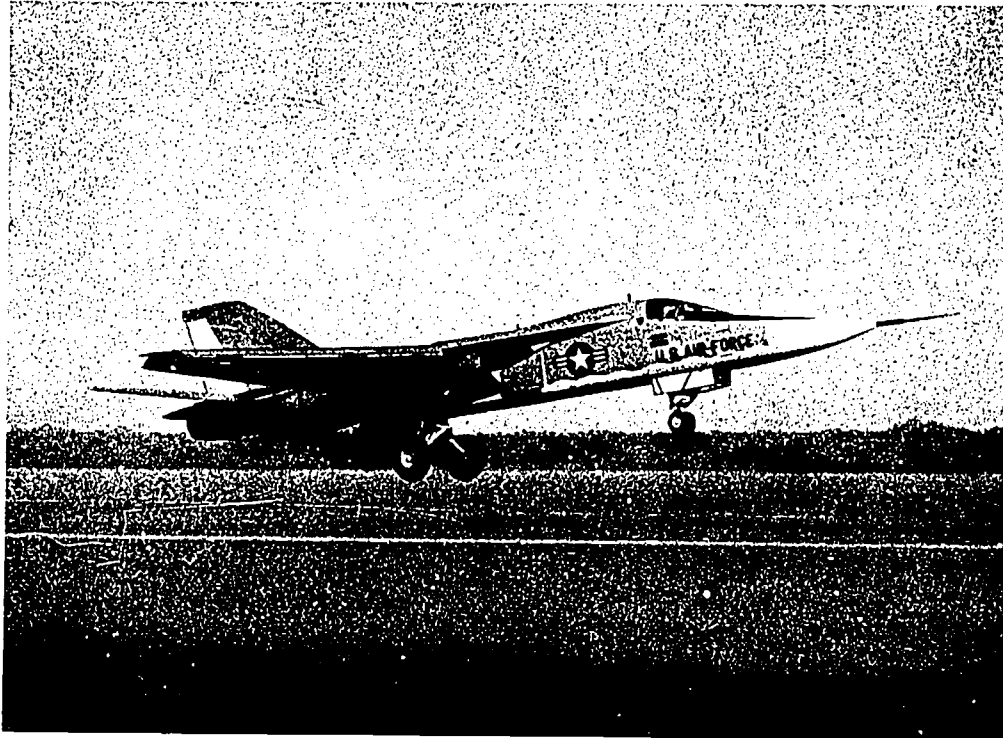


Figure 1-59. - The General Dynamics F-111A is a fighter with wings that can be extended or swept back sharply while in flight. A multipurpose aircraft, it can be used for counter-air, interdiction, close air support of ground forces, and reconnaissance missions.

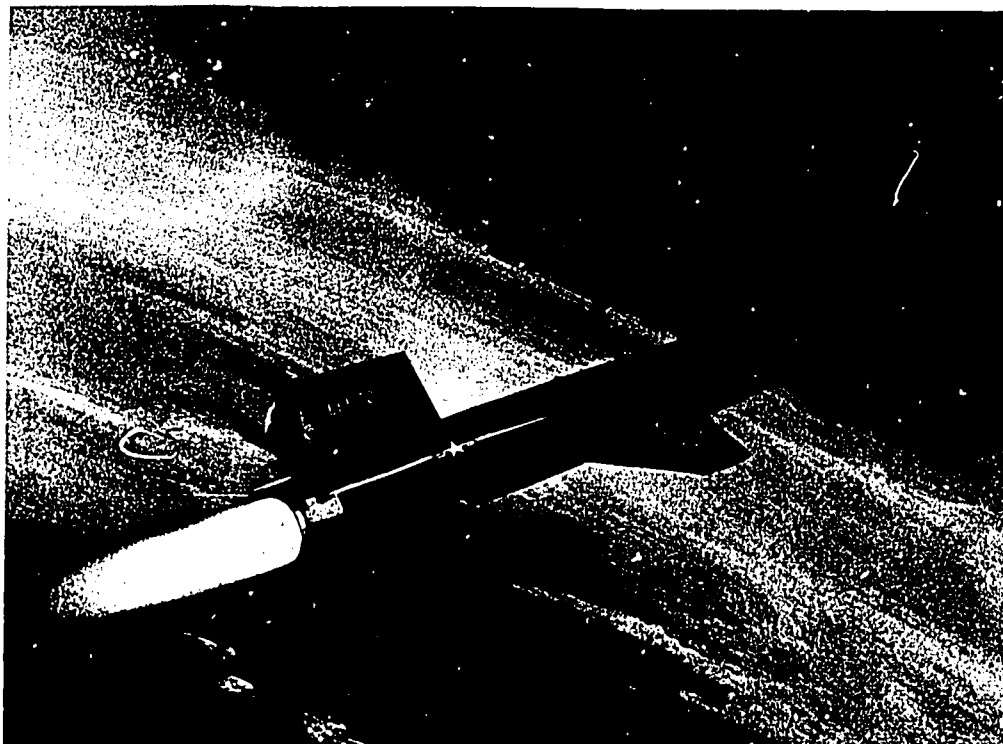


Figure 1-60. - More spacecraft than aircraft, the North American X-15 is the product of an experimental program jointly begun by the USAF, NASA, and the Navy to study aerodynamic, structural, and physical problems encountered during hypersonic flight and reentry.

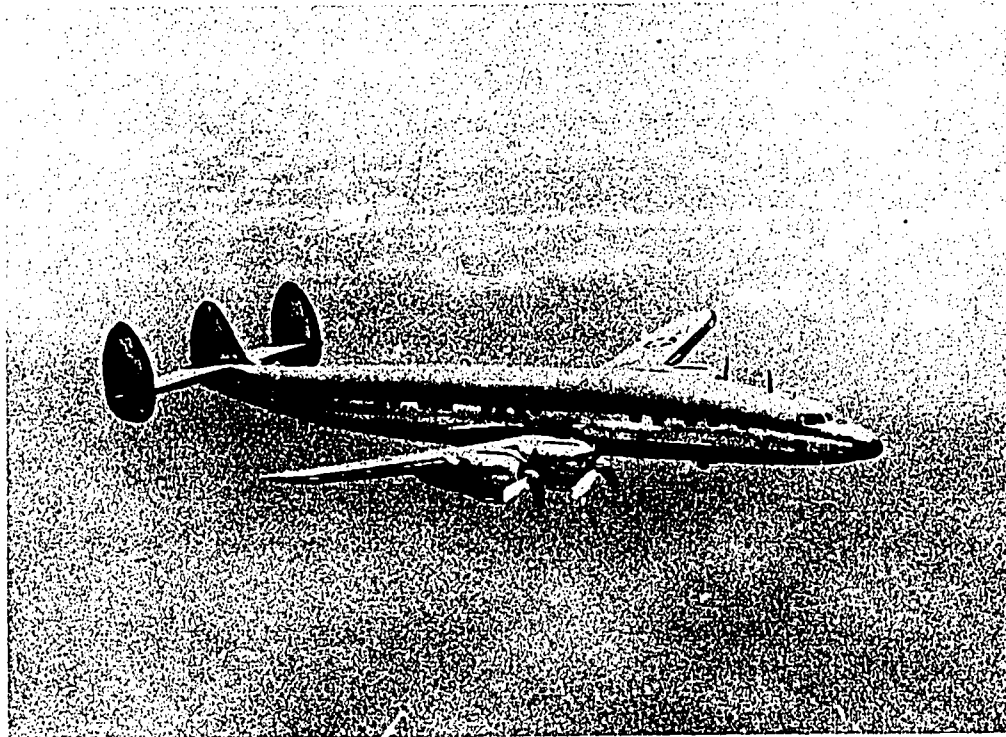


Figure 1-61. - The Lockheed C-121 Super Constellation is a four-engine transport with a cruising speed of about 300 miles per hour. It can fly more than 3500 miles nonstop.

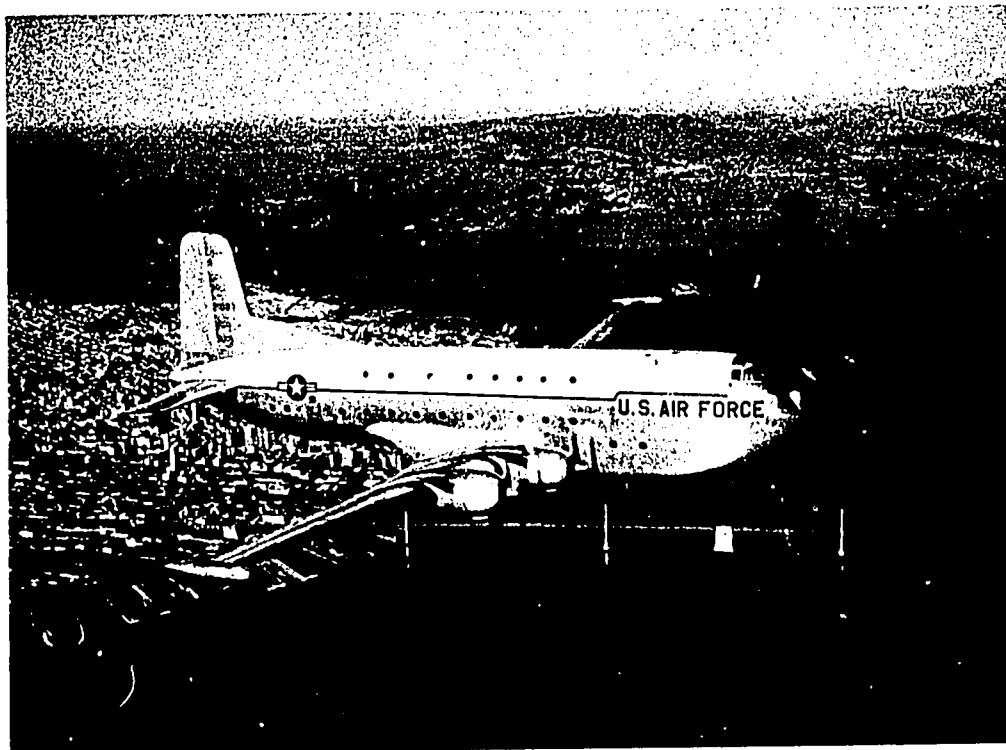


Figure 1-62. - The Douglas C-124 Globemaster can carry 50,000 pounds of cargo for more than 2300 miles.

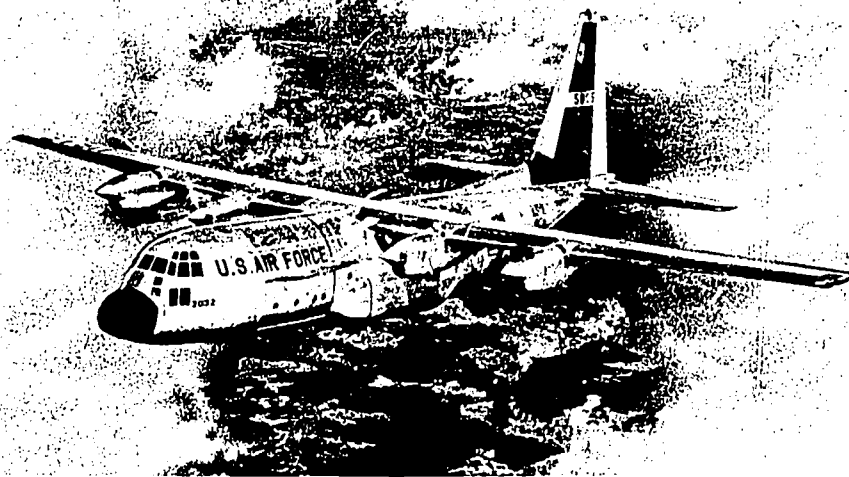


Figure 1-63. - The Lockheed C-130 Hercules has made the difficult military job of aerial resupply routine. It can transport 92 combat troops with full battle gear, 64 fully equipped paratroopers, or 74 litter patients and two medical attendants across the Atlantic nonstop.



Figure 1-64. - The Douglas C-133 Cargomaster, largest turboprop transport in the USAF inventory, made its first flight in 1956. It can airlift our operational intercontinental ballistic missiles at speeds up to 300 miles per hour.



Figure 1-65. - The jet-powered Boeing KC-135 Stratotanker first entered the USAF inventory in 1957. It functions as a "flying filling station" for jet bombers and fighters.

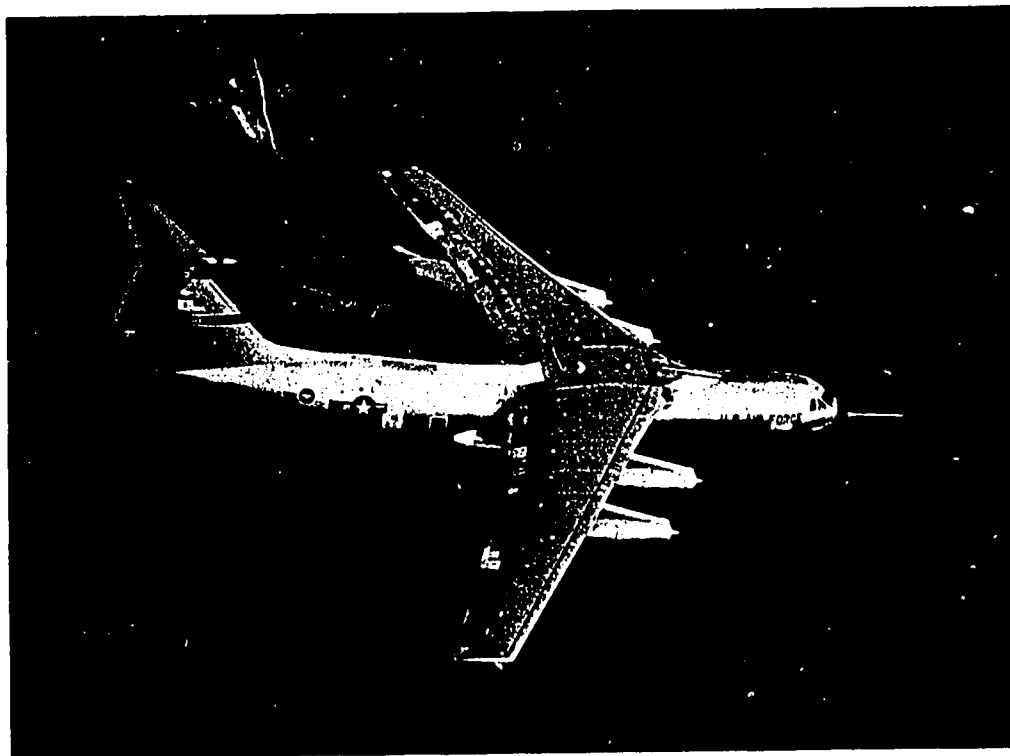


Figure 1-66. - Lockheed C-141A Starlifter has a 6547-cubic-foot cargo compartment with an automated cargo handling system.

07

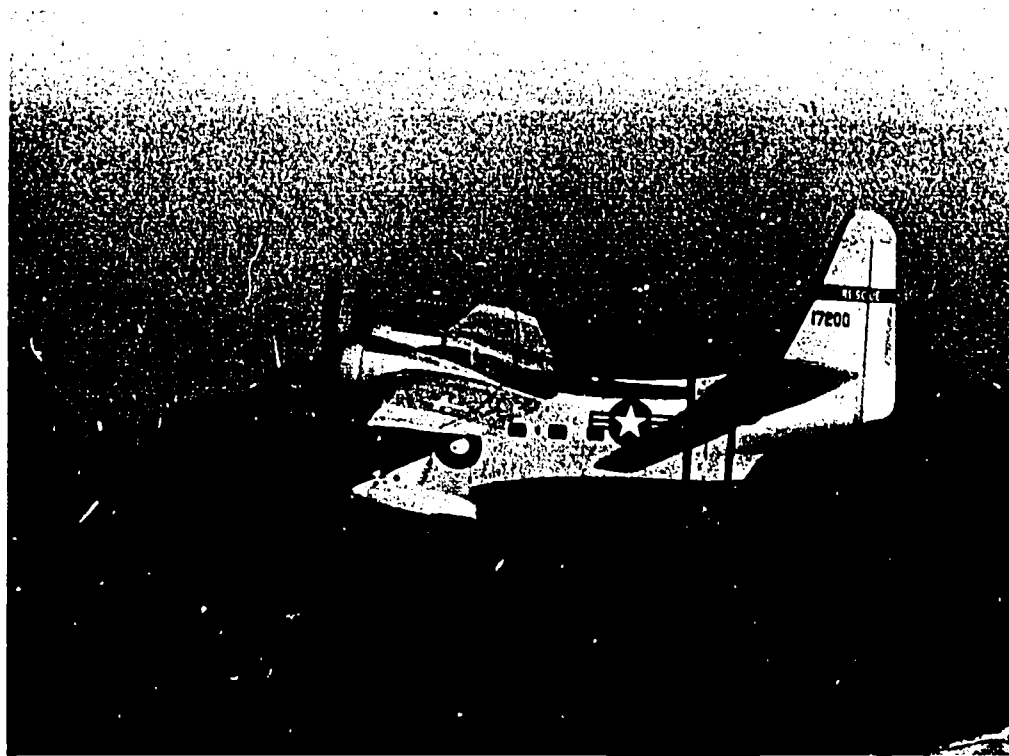


Figure 1-67. - The Grumman HU-16 Albatross is a twin-engine amphibian used by the Air Rescue Service. It first flew in 1947.

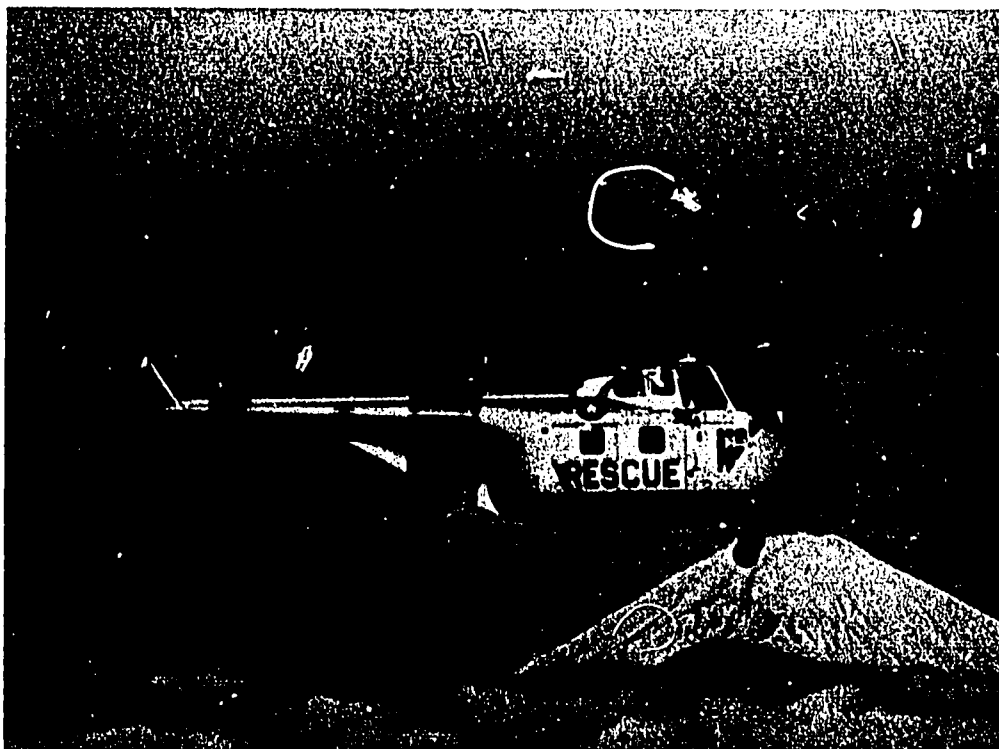


Figure 1-68. - The Sikorsky HH-19 Chickasaw is the original "whirlybird." It can fly at 70-mile-per-hour speeds over distances exceeding 300 miles.



Figure 1-69. - The Vertol CH-21 Workhorse can carry 20 fully equipped troops. It also serves as a flying ambulance able to evacuate 12 litter patients and a medical attendant from locations inaccessible to conventional aircraft.

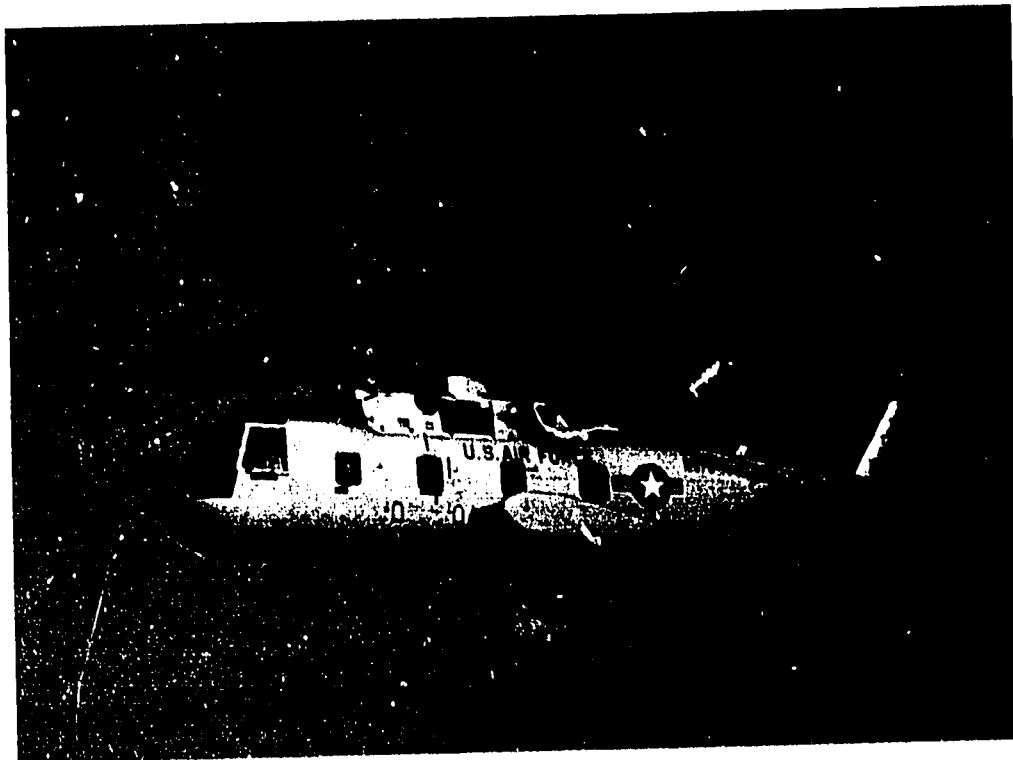


Figure 1-70. - The Sikorsky CH-3C is powered by twin turbine engines and has a hydraulically operated rear loading deck and a 5000 pound payload capacity. It is amphibious.

2. FLUID PROPERTIES PERTAINING TO AERODYNAMICS

Robert W. Graham*

Aeronautics is concerned with the flight of aircraft through the Earth's atmosphere. Aerodynamics, on the other hand, is a technical discipline dealing with the motion of air or any other gaseous fluid and with the forces acting on a body that is in motion relative to such a fluid. Thus, aerodynamics might include the study of air flowing through a jet engine, hot combustion gases flowing through the thrust chamber and nozzle of a rocket engine, air flowing over the outside surfaces of aircraft, and the reentry heating problems of spacecraft.

Some basic characteristics of airflow are discussed in this chapter. The relations of these flow characteristics to the lifting performance of a wing or the thrusting capability of an engine are explained in greater detail in subsequent chapters.

EARTH'S ATMOSPHERE

The discussion of the flow characteristics of air should begin with a brief explanation of the nature and composition of the Earth's atmosphere. Our atmosphere is composed principally of oxygen (21 percent by weight) and nitrogen (78 percent by weight). It also contains measurable quantities of 15 other elements or chemical compounds, including carbon dioxide, neon, hydrogen, methane, and ozone. The sum of all these constituents gives air a molecular weight of 28.964, which applies for the first 60 miles of altitude. This is generally within the range of altitude considered for flight applications. Above 60 miles, the composition of the atmosphere changes abruptly, as shown by the molecular weight distribution in figure 2-1.

Other properties of the atmosphere that are of interest include static temperature, static pressure, and density. These properties also vary with changing altitude. (The adjective "static" is used to modify "temperature" and "pressure" because these properties are measured with an instrument that is not moving with respect to the air.)

Figures 2-2 to 2-4 show the approximate distribution of the static temperature, static pressure, and density, up to an altitude of 200 miles. It is interesting to note that the

*Head, Experimental Section, Fundamental Heat Transfer Branch.

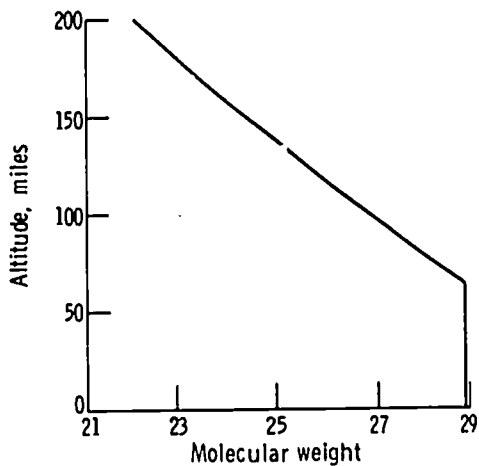


Figure 2-1. - Variation of molecular weight of air with altitude.

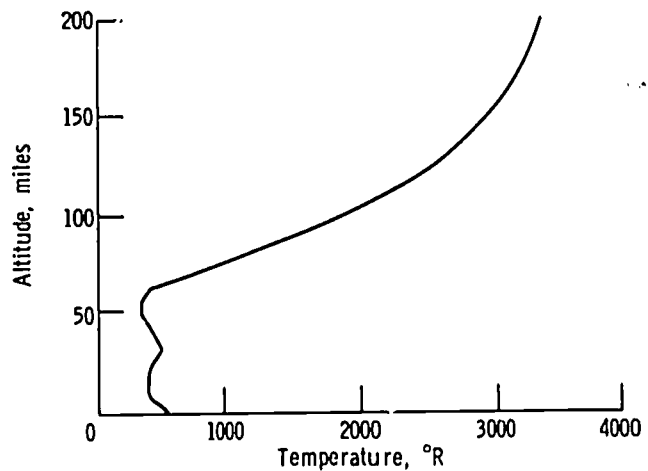


Figure 2-2. - Variation of atmospheric temperature with altitude.

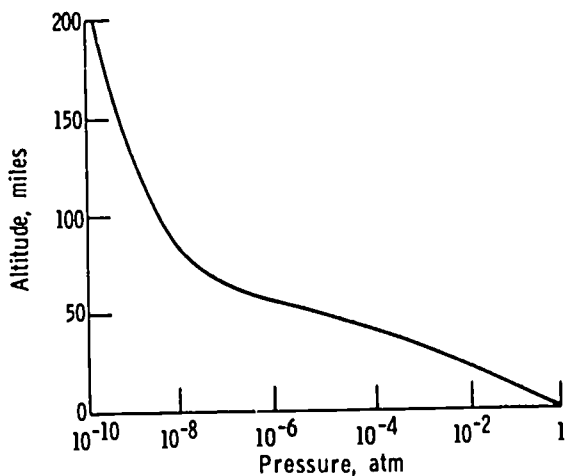


Figure 2-3. - Variation of atmospheric pressure with altitude.

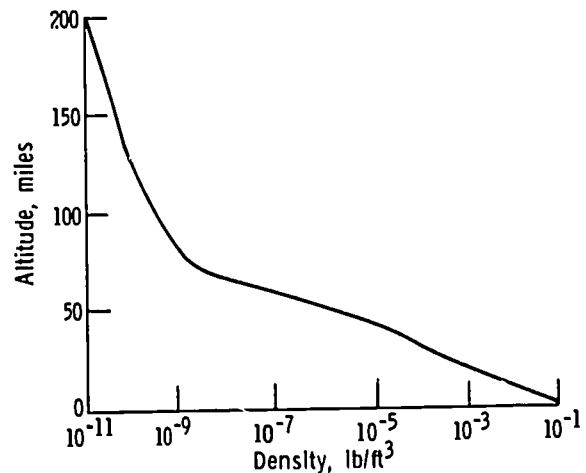


Figure 2-4. - Variation of atmospheric density with altitude.

temperature distribution goes through two reversals in trend before reaching a definite high-altitude trend of a rapidly increasing temperature.

Both density and pressure drop rapidly with increasing altitude in the lower altitudes (less than 60 miles). It appears that the drop in pressure has the greatest effect on the local density. (Density is also dependent upon temperature.)

Any consideration of a flight path over a range of altitude must take into account the rapid changes in the static properties of the atmosphere.

CHARACTERISTICS OF FLUIDS

Although air has its own properties as an atmosphere, it belongs to a general family of materials known as fluids. To be classed as a part of this family, air has to have cer-

tain generic traits of fluids. These traits are important in understanding flight and propulsion in the atmosphere.

Continuum Character

The first characteristic of a fluid is its continuum property. Although the spacing between atoms or molecules may be large, and there may be large voids in the fluid structure, the spacings are close enough so that a disturbance initiated at any point in the fluid is sensed by the neighboring molecules and can be transmitted far beyond the origin of the disturbance.

For instance, when water is being poured into a glass, all of the molecules sense the restraining effect of the glass. Likewise, all of the gas in a balloon senses the wall surrounding it. As a continuum, the fluid easily conforms to the shape of any vessel into which it is placed.

The continuum characteristic of a fluid enables it to transmit pressure and to conduct heat. Pressure and temperature result from the molecular-scale collisions of the fluid.

Compressibility

A simple fluid structure model may be thought of as a series of spheres connected by springlike forces. Such a model is sketched in figure 2-5. For liquids, the flexible bonds between the molecules are strong and stiff. As a result, the spacings between the molecules do not change appreciably. The fluid is said to be incompressible. Gases, on the other hand, have more flexible bonds, which enable the spacing to vary. This variable spacing is called compressibility. Compressibility is an important characteristic of air. For all gases, increased temperature spreads the spacing, and increased pressure tightens

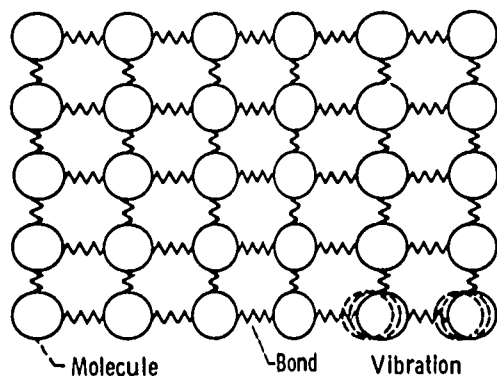


Figure 2-5. - Model of fluid structure.

the spacing. As is probably self-evident, the density of a gas is related to compressibility. For a given gas, the density is directly proportional to pressure and inversely proportional to temperature. This relation is known as the perfect gas law.

$$\rho = \frac{1}{R} \frac{P}{T}$$

where ρ is the density, P is the pressure, R is the gas constant, and T is the absolute temperature.

With a properly used general gas constant, the above simple equation applies to all gases over a broad range of conditions. If, from the preceding equation, the variation of the density of a gas for different temperatures and pressures is known, the compressibility of the gas can be computed. Suppose a gas is initially at density ρ_1 and by external compression it reaches a final density ρ_2 . In this compression, the pressure has changed from P_1 to P_2 . In equation form the compressibility is

$$\text{Compressibility} = \frac{\left(\frac{\text{Change in density}}{\text{Final density}} \right)}{\text{Change in pressure}} = \frac{\left(\frac{\rho_2 - \rho_1}{\rho_2} \right)}{P_2 - P_1}$$

Acoustic Velocity

It has been mentioned that a fluid has the capability of transmitting disturbances by its continuum property. The mechanism of transmission is a chain reaction of forced molecular collisions. These collisions produce small, local pressure changes in the fluid. The speed with which the disturbance travels depends on how quickly one molecule can reach an adjacent one. If the molecular spacing is large, the disturbed molecule has a relatively large distance to travel before transmitting its message. However, if the spacing is small, the message travels quickly. We learned earlier that the relative magnitude of the spacing determines the compressibility of the fluid. Thus, in highly compressible fluids (gases) these disturbances travel slower than in nearly incompressible fluids (liquids).

When a person is speaking, his voice is a disturbance to the air around him. The small pressure waves generated by the speaker's voice box are transmitted to the listener by the mechanism described previously. The velocity of transmission is the acoustic velocity. The acoustic velocity is the speed with which all small pressure disturbances travel in a fluid. The term "small" means that the disturbance is small compared with the average pressure of the fluid. Large disturbances, such as detonations, can travel

at velocities exceeding the acoustic velocity. In this case, the disturbance pressure may be many times greater than the original static pressure of the fluid. It has already been explained that the acoustic velocity is affected by the compressibility of the fluid. For small disturbances, the relation of the acoustic velocity to the compressibility and density of the fluid is given by the following equation:

$$\text{Acoustic velocity} \approx \sqrt{\frac{1}{(\text{Density})(\text{Compressibility})}}$$

Viscosity

In discussing the continuum characteristic of a fluid, it was mentioned that a fluid easily conforms to the shape of a surrounding vessel. In fact, this facility to conform to shapes is a distinguishing characteristic of fluids. While the molecules of a fluid arrange themselves easily, they do have a resistance to motion. This resistive force, which acts to prevent the motion of one fluid molecule on top of another, is called viscosity. Figure 2-6 is a diagram illustrating the viscous force between two fluid layers. An impor-

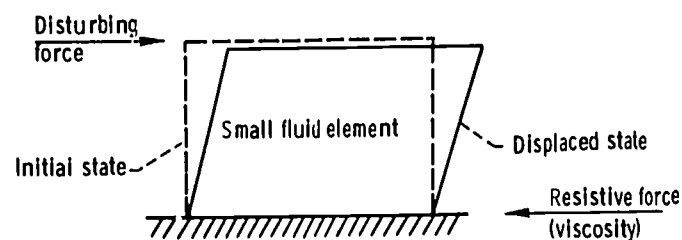


Figure 2-6. -Viscosity of a fluid.

tant extension of this concept occurs at the interface between a fluid and a solid wall. The resistive force between the fluid molecules and the wall material is known as viscous drag. Its magnitude depends on the fluid viscosity, the smoothness of the wall, and the velocity of the fluid motion (actually the square of the velocity). Viscous drag is very important in any fluid-flow situation, whether it is flow through an engine or flow over a wing.

CHARACTERISTICS OF FLUIDS IN MOTION

In the preceding discussion we dealt primarily with the static characteristics of fluids. The following discussion concerns the dynamic characteristics of fluids.

Total Pressure and Temperature

Static pressure and temperature result from random molecular motion. However, when a fluid is in motion, the molecules possess motion in the direction of flow as well as their inherent translational motion. Thus a temperature or pressure probe placed so that its sensing element is facing the flow will sense a higher temperature or pressure. Such measurements are referred to as total measurements, because the energy of directed fluid motion is included. They are indexes of the total energy possessed by a fluid in motion. The difference between total and static measurements is used to compute the velocity of fluid flow.

Mach Number

Mach number is the ratio of the fluid velocity to the local acoustic velocity of the fluid. Since acoustic velocity is inversely proportional to compressibility, Mach number is directly proportional to compressibility. This is the important meaning of Mach number to the aerodynamicist. A high Mach number means that in a flow process the density is subject to considerable change throughout the flow field.

Reynolds Number

Another important number in fluid mechanics is the Reynolds number. In this number, the momentum of the flow (product of density ρ times velocity V) is compared with the coefficient of viscosity μ .

$$Re = \frac{\rho V}{\mu} \cdot d$$

The Reynolds number Re is made dimensionless by the inclusion of a length dimension d . This length dimension can be a characteristic length, such as the flow-path length, the chord of a wing, or the diameter of a duct.

Reynolds number tells whether the momentum or viscous forces dominate the flow. A low Reynolds number signifies that the viscous forces are dominant; a high Reynolds number denotes that the momentum controls the flow and the fluid viscosity is less important.

Perhaps one of the most significant uses of Reynolds number is in the discrimination between laminar and turbulent flows, which are discussed in the following section.

Laminar and Turbulent Flows

At low Reynolds numbers, where viscosity is dominating, the flow of fluids can be described as layers, or lamina, of steady fluid streams which do not appear to mix as the flow progresses down the channel. The flow has the appearance of fluid fibers bundled in the channel. This type of flow is called laminar flow.

At a higher Reynolds number, the flow pattern changes into turbulent flow. The identifiable fluid layers, or fluid fibers, of laminar flow no longer exist. Instead, there is considerable mixing in the flow, through the action of eddies or vortices. These eddies give the flow a fluctuating, or nonsteady, characteristic, which can be measured. Figure 2-7

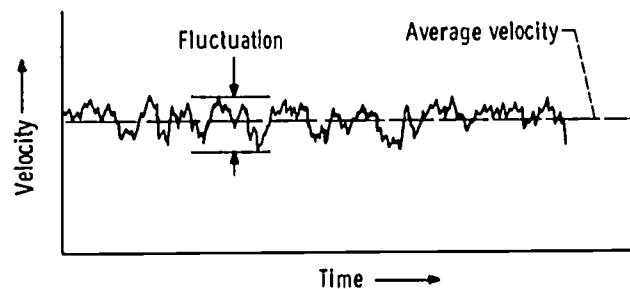


Figure 2-7, - Turbulent-flow velocity trace.

represents an actual velocity measurement of a turbulent flow. A sensitive instrument called a hot wire was placed at a fixed position in a flow channel and the flow was recorded over a time interval. Note from the figure that there is an average velocity, but the instantaneous level fluctuates around this average.

Turbulent flow is the most frequently encountered type in practical applications of flight and propulsion, and it is much more difficult to analyze than laminar flow.

Boundary Layer

In discussing the viscosity of fluids, it was mentioned that a very significant viscous effect occurs at the interface between a solid wall and a fluid. In fact, this frictional effect represents the chief resistance that the flow experiences. This friction is the drag of the airplane or the pressure loss in a pipe or channel.

Most of these frictional effects are absorbed by the fluid in a layer near the wall. The viscous effects in this region can be observed by measuring the local velocity distribution at various positions (distances) away from the wall. A velocity profile, such as shown in figure 2-8, results from such measurements. Note that the velocity decays

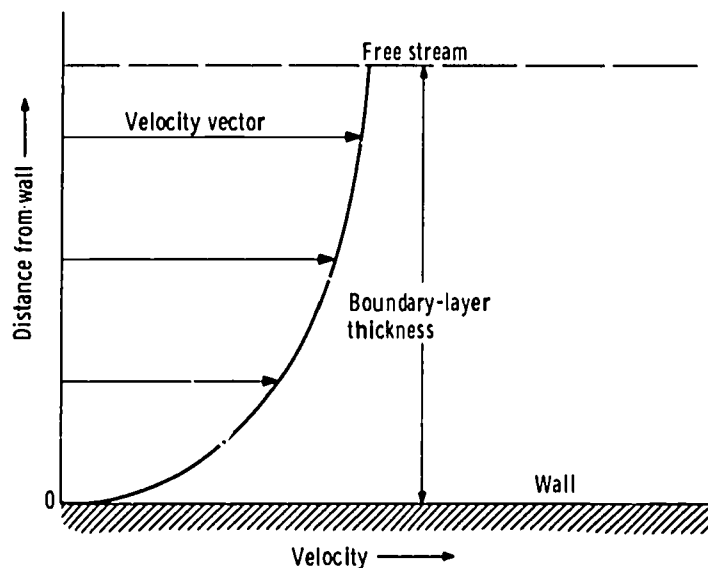


Figure 2-8. - Boundary-layer velocity profile.

to zero velocity at the wall. The thickness over which most of this velocity decay occurs is called a boundary layer. It represents the fluid thickness wherein the viscous qualities of the fluid are dominant. In most analytical procedures the boundary layer and the free stream (flow region outside the boundary layer) are treated separately. Different assumptions are applied in the analyses for each region. The presence of friction makes the boundary layer a very complicated region to analyze.

The boundary layer is also important in studies of heat transfer between the fluid and the wall. In aerodynamic heating, the fluid friction of the boundary layer is converted to heat at the wall. For instance, if all the kinetic energy of relative fluid motion is converted to heat within the boundary layer, an airplane flying at Mach 2 (at 100 000 ft altitude) may experience surface temperatures exceeding 300° F. At higher Mach numbers the heating can be very severe. Reentry vehicles from space missions develop surface temperatures which can vaporize metal. Consequently, cooling techniques, such as the use of ablative shields, are required to protect the vehicle.

BIBLIOGRAPHY

- Anon.: U. S. Standard Atmosphere, 1962. NASA, USAF, and U. S. Weather Bureau, Dec. 1962.
- Cowling, Thomas G.: *Molecules in Motion*. Harper & Brothers, 1960.
- Zucrow, Maurice J.: *Principles of Jet Propulsion and Gas Turbines*. John Wiley & Sons, Inc., 1948.

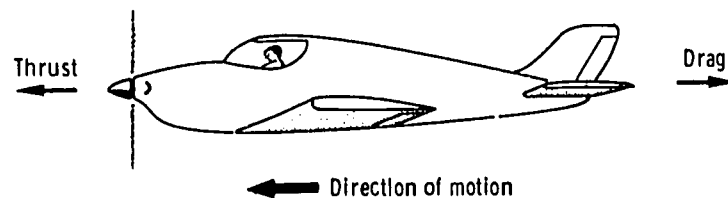
3. DRAG

Richard J. Weber*

When an object moves through the air, the air molecules are moved from their normal positions. When the molecules are disturbed, according to Newton's Third Law of Motion, they in turn react back on the object and exert aerodynamic forces. Sometimes there is a force perpendicular to the direction of motion; this is called lift and is discussed in chapter 4. Invariably, there is an additional force that acts parallel, but opposite, to the direction of motion; this retarding force is called drag.

Since the drag continually tends to slow down an airplane, a forward thrust must be provided by the engine(s) in order to keep flying (fig. 3-1(a)). The larger the thrust that is needed, the more fuel that is consumed. Calculating the drag of an airplane is, therefore, extremely important, since it affects how big the engines must be and how much fuel must be consumed.

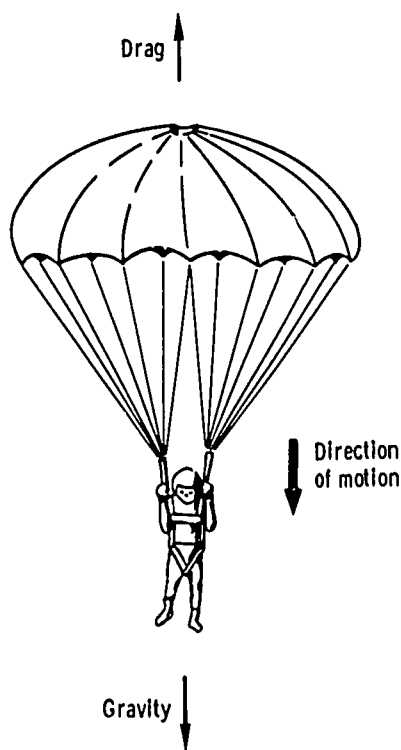
Drag is not always undesirable (fig. 3-1(b)). In fact, the same viscous effects which cause friction drag also make it possible to generate lift on a wing. That is, a perfect nonviscous fluid would not cling to or follow the contour of the wing surface. This clinging is called the Coanda effect and is necessary to obtain the flow deflection that results in lift. Hence, the existence of drag is essential to the production of lift. The relation of this Coanda effect to lift is discussed further in chapter 4.



(a) Detrimental drag.

Figure 3-1. - Effects of drag.

*Chief, Mission Analysis Branch.



(b) Beneficial drag.

Figure 3-1. - Concluded.

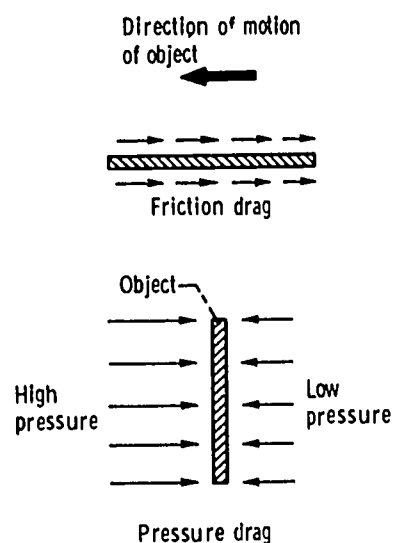


Figure 3-2. - Two kinds of drag on a moving object in a fluid.

It is convenient to classify drag in two different categories - friction drag and pressure drag - depending on how the drag force is exerted on the object (fig. 3-2). Friction drag is due to the stickiness of fluids. Even a smooth, flat plate tends to drag along fluid molecules, and this causes a retarding force. Pressure drag is caused by unequal pushing of the air on the front and back of an object. The pressure drag may be further classified as induced drag, which is related to the amount of lift, and wake drag, which is independent of lift. (Another way of classifying drag is in terms of whether or not it depends on lift. In this system of classification drag due to lift is the induced drag, and profile (or parasite) drag is the sum of friction and wake drags.)

Since induced drag is discussed in chapter 4, only friction and wake drags are discussed herein.

FRICION DRAG

As an object moves through the atmosphere, molecules of air tend to stick to the surface and be dragged along. To accelerate these molecules, a force is required, and the reaction force on the object is felt as friction drag. The sticking tendency of a fluid is

measured by its viscosity, as already mentioned in chapter 2. Air is not as viscous as liquids such as molasses, but friction drag is, nevertheless, the main type of drag for subsonic airplanes.

Friction drag of a gas is quite different from the solid friction to which we are more accustomed. When an automobile tire pushes against the ground, for example, solid friction produces a force that drives the car. The force is generated locally at the junction between the tire and the ground. It is fairly accurate to consider the force as due to the interlocking of microscopically small bumps on the two surfaces. This is true even if the tire is spinning or skidding relative to the ground, except then the little bumps tend to tear away from the main material.

However, when a solid object is placed in a gas stream, the gaseous friction generates a force not just at the surface of the object but over a finite distance from the surface, called the boundary layer (see chapter 2). At the outer edge of this layer, the gas molecules move at the full velocity of the gas stream; at the inner edge of the layer, the molecules hardly move at all (relative to the object). This gradual change in velocity through the layer causes a sliding or shearing motion that results in a drag force. The boundary layer may be likened to a deck of cards on a table. If the top card is slowly pushed sideways, it slides and moves the next card a little less, which, in turn, moves the next card even less, and so forth, until the bottom card is reached, which sticks to the table.

The magnitude of the friction drag depends on the physical properties of the gas (density and viscosity), the velocity of the gas stream (or of the object moving through the gas), and the surface, or "wetted," area of the object. For laminar boundary layers, which are expected at low values of the Reynolds number (see chapter 2), the friction drag is proportional to the velocity raised to the 1.5 power. For example, doubling the velocity increases the laminar drag by $2^{1.5}$, or 2.83 times.

As the velocity (and hence the Reynolds number) is increased more and more, the flow eventually becomes turbulent, and the friction drag jumps to a value perhaps 4 times higher. In this region the drag is roughly proportional to the velocity squared. Doubling the velocity now increases this new, high drag by 2^2 , or 4 times.

Obviously, the friction drag on an airplane can be reduced considerably if the laminar boundary layer can be prevented from becoming turbulent.

PRESSURE DRAG

When any object is standing still in the atmosphere, there is a pressure force (equal to 14.7 lb/in.² at sea level) pushing on it. Because the pressure is the same on all sides of the object, there is no net force in any particular direction. If the object is moving, however, pressure differences can develop.

Theoretically, in subsonic flight through an ideal nonviscous fluid, these pressure differences are nonexistent; that is, if the pressure gets higher on the front (or upstream) side of the object, it should get just as high on the back (or downstream) side. Thus, the net pressure force would be zero. This situation should apply to all objects, regardless of shape. Physically it requires that the flow of air, which divides in front of the object to go around it, should smoothly follow the shape of the object and join together again at the back of the object. In so doing, the pressure would be high at the front, decrease to a low value at the side, and rise again to the same high value at the back.

In actuality this smooth joining together at the back of the object does not happen; the reason for this is friction. The air in the boundary layer loses energy because of friction and cannot fight its way back to the same high pressure on the back side (just as a roller coaster cannot roll down one hill and then coast up to the same height on the next hill). As a result, a region of low-pressure "dead" air forms behind the object. The main flow of air separates from the object in order to pass around this "dead" space.

The ideal and the actual situations are illustrated in figure 3-3 for the case of a circular cylinder moving from right to left. The figure shows the direction of the air particles as they stream past the cylinder and graphs of the pressures exerted on the surface of the cylinder. In the ideal case the air fills in behind the cylinder just as smoothly as it divided in front. The corresponding pressure distribution is just as smooth. The pressure force is proportional to the area under the curve and is the same on the back side as on the front. No net force is generated.

In the actual case, the flow separates from the back of the cylinder, and the pressure is lower than it should be. The graph area for the front side is higher than for the back, so that there is a net force on the front of the cylinder pushing it backward, or downstream. This force is called the pressure drag and is added to the friction drag described

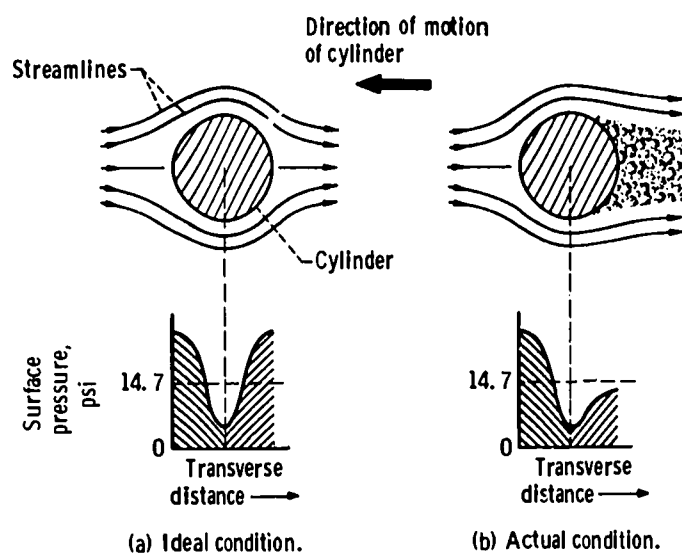


Figure 3-3. - Pressure drag on a circular cylinder.

earlier. (In subsonic flow, the pressure drag is really caused by the friction drag. In supersonic flow, however, the pressure drag becomes even larger and is caused by shock waves. This is discussed in chapter 11.)

For blunt shapes, the pressure drag can be very high. For example, the pressure drag on a cylinder is between 30 and 120 times (depending on Reynolds number) as high as the direct friction drag. Therefore, streamlining is an important consideration in aircraft design.

INTERFERENCE DRAG

Up to this point, we have discussed the drag of simple shapes (spheres, cylinders, flat plates, etc.) with nothing else near them. A complete airplane, of course, is not one of these simple shapes. However, in order to simplify the design and analysis of a new type of airplane, it is convenient to consider the airplane as being composed of many smaller, simpler shapes that are put together. Experimental and theoretical data have been accumulated on the drag of common simple shapes, such as wings or streamlined fuselages. The drag of the complete airplane can then be estimated by adding up the drags of the individual pieces. When this is done, it is usually discovered that the actual drag of the airplane is greater than the sum of the individual drags. This extra increment of drag is called interference drag. It exists because the individual drags are measured for isolated components. However, when the components are combined in an airplane, each one sets up disturbances in the airstream that affect the flow over the other components. These disturbances usually (not always) result in an increase in total drag.

As an example, suppose a small step is to be put on the side of a fighter airplane to help the pilot climb into the cockpit. When the step is tested by itself in a wind tunnel, it has a drag of 1 pound. However, if the step is installed on the plane in the corner between the wing and the fuselage, its drag is 6 pounds. The drag due to interference in this case is 5 pounds.

COMPRESSIBILITY DRAG

The preceding discussion is based on flight at fairly slow speeds (no more than a few hundred miles per hour). At these speeds the air can be considered to be incompressible; that is, the changes in velocity and pressure of the air flowing around the airplane do not change the density of the air. At higher speeds, density changes start to become important. The primary effects arise at flight speeds approaching the speed of sound. The reason for this is that as the airstream flows around the outside of the airplane, it is

forced to travel a longer, more circuitous path than if the airplane were not present. The longer path requires the air to move momentarily at a higher velocity than the flight speed, or the free-stream velocity. (The free stream is that stream of air flowing past the aircraft which is not affected by the aircraft.) Thus, as the flight speed approaches the speed of sound, the velocity of the airflow over the surfaces of the aircraft may become supersonic and form shock waves, which cause major increases in drag. This sudden drag rise is the reason why most airplanes (such as current passenger planes) do not fly faster than about 550 miles per hour. As more powerful jet engines are developed, however, it becomes more feasible to fly faster despite the high drag. Also, different shapes can be used to partly avoid the drag rise. As a result, military airplanes can now fly supersonically, and even commercial supersonic transports are being developed. The drag rise due to the presence of shock waves (i. e., compressibility drag) is a different type of pressure drag. Its characteristics are discussed in chapter 11.

METHODS OF DRAG REDUCTION

The following discussion concerns some of the various methods that can be used to

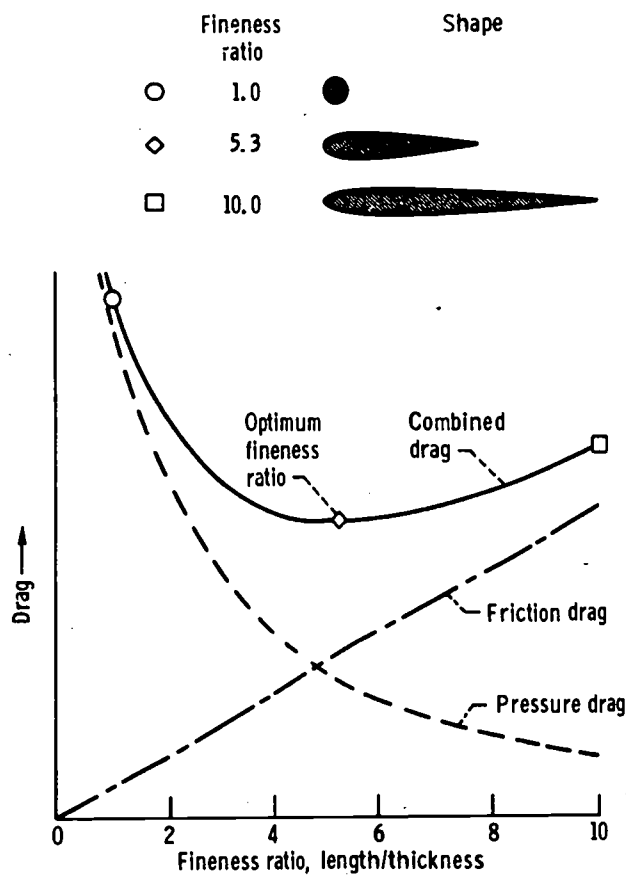


Figure 3-4. - Effect of streamlining.

reduce drag. It should be noted that at subsonic flight speeds all drag-reduction methods involve some form of boundary-layer control.

Because the pressure drag on a blunt shape can be intolerably high, it is necessary to shape the various parts of an airplane in the proper fashion to minimize drag. This is called streamlining, and its purpose is to enable the air to flow as smoothly as possible around the various parts of the airplane without separating on the back side. Generally this requires the use of well-rounded edges and long, slender shapes. (The relation between shape and airflow is discussed in more detail in chapter 4.)

The effectiveness of streamlining is shown in figure 3-4. For a constant thickness, as the length is increased, the pressure drag decreases. The process cannot be carried to extremes, however. More length increases the surface area of the object, which increases the friction drag. When the two drags are added together, it is found that there is an optimum fineness ratio (length divided by thickness) that yields minimum combined drag.

We might also include in the term "streamlining" the avoidance of abrupt bumps and roughness (such as protruding rivet heads). Each little rough spot contributes a bit of pressure drag. Since there could be many rivets and other protrusions on an airplane, the total increase in drag would be appreciable if roughness were not controlled. Even dirt and mud can cause noticeable penalties. The following table shows how small roughness affected the measured profile drag on one particular wing:

| Surface condition | Relative drag |
|--|---------------|
| Smooth and polished | 1.00 |
| Common service condition (with rivets, joints, camouflage paint) | 1.32 |
| Service condition with thin mud | 1.94 |
| Service condition with heavy mud | 2.78 |

Another reason for streamlining is that it is sometimes possible to control the pressure distribution around an object in such a fashion that the boundary layer is prevented or delayed from becoming turbulent. The corresponding reduction in friction drag can be very worthwhile. (Chapter 1 mentioned the application of this technique to the wings of the P-51 "Mustang" airplane of World War II.)

A method of reducing friction drag that is now being tried on some airplanes is the removal of some of the boundary layer before it can become turbulent. Figure 3-5 shows how this works. The top of the figure shows the cross section of an ordinary wing. The boundary layer always starts out thin and laminar. However, as distance from the leading

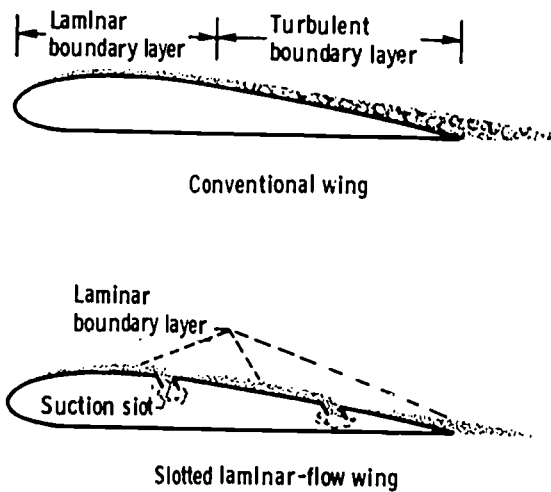


Figure 3-5. - Boundary-layer control by means of suction slots.

edge increases, the boundary layer gradually thickens. At some thickness the layer becomes unstable and the smooth flow breaks down and becomes turbulent. (A more general measure of boundary layer was introduced in chapter 2 in terms of the Reynolds number, which varies directly with distance.) To prevent this transition from laminar to turbulent flow, suction slots may be placed in the wings, as shown in the lower part of figure 3-5. The thick boundary layer is sucked away through the slot by means of a pump, so that the flow behind the slot starts all over again as if it were at the front of the wing. The slots are located at such intervals that the boundary layer is never long enough to become turbulent.

The friction drag on this slotted type of wing can be much lower than on the conventional wing. Some of the drawbacks are the power and weight needed to operate the pump and the tendency of the slots to become clogged with dirt.

An interesting method of drag reduction is the use of vortex generators, which are placed on the upper surfaces of the wings of some airplanes. Each generator is actually a little wing, only 1 or 2 inches long, sticking out into the airstream. Despite the previous statements about the importance of streamlining and avoiding roughness, the use of vortex generators actually reduces the total drag of the wing. The reason they work is that they mix some of the high-energy free-stream air into the low-energy boundary layer. (The behavior and effects of vortexes are explained in chapter 4.) The energized boundary layer is then more capable of following the wing surfaces near the trailing edge, so that separation is delayed or prevented. This prevention of separation is effective both in decreasing drag and increasing lift, especially at high angles of attack. Vortex generators cause some increase in friction drag, but this is outweighed by the greater reduction in pressure drag.

Other methods of controlling the boundary layer include the addition of high-energy air by blowing through reverse scoops and the use of mechanical means (discussed in

chapter 4) to turn the airflow. Most of these methods impose some penalties in the forms of increased complexity and weight.

SAMPLE CALCULATIONS OF DRAG EFFECTS

Detrimental Drag

For a better understanding of the detrimental effects of drag, it is helpful to calculate the effect of drag on the performance of an actual airplane. Because data happened to be available (ref. 1), let us consider the Messerschmitt Me-109. This was a small, propeller-driven fighter used by the Germans in World War II. Its weight was 6700 pounds, and it had a top speed of 380 miles per hour with a 1200 horsepower engine. The total drag at maximum speed was 1140 pounds. This was distributed among the various parts of the airplane as follows:

| Aircraft component | Percent of total drag |
|--------------------------------------|-----------------------|
| Wing (including surface roughness) | 38 |
| Fuselage (with roughness and canopy) | 14 |
| Tail surfaces (including roughness) | 7 |
| Engine and radiator installation | 23 |
| Extras (such as guns and tail wheel) | 11 |
| Induced drag | 7 |

(These values are taken from reference 1, which is probably the best source of information on all aspects of the subject of drag.) Another way of breaking down the total drag of this airplane is on the basis of friction and pressure drags:

| Type of drag | Percent of total drag |
|--|-----------------------|
| Skin-friction drag (smooth, turbulent) | 33 |
| Pressure drag due to surface roughness and imperfections | 15 |
| Pressure drag due to exposed parts (mostly engine) | 33 |
| Interference drag | 6 |
| Compressibility drag | 6 |
| Induced drag | 7 |

These percentages show that the Me-109 was actually a very poor aerodynamic design. The unavoidable portions of the drag are the friction drag (33 percent) and the induced drag (7 percent). Very good design could get rid of practically all of the remaining drag. Compared with a well-streamlined airplane, the Me-109 had an aerodynamic efficiency of only $33+7 = 40$ percent.

It is interesting to consider what would happen to the top speed if the efficiency were raised from 40 to 100 percent (i. e., if the efficiency were increased by a factor of 2.5). If the speed were not changed, the engine power required to overcome drag would decrease by the same factor; that is, only 480 of the available 1200 horsepower would be used. The speed of the airplane could now be increased until the power requirement increased by the factor of 2.5 and the full 1200 horsepower would again be utilized. Most of the drag would be turbulent skin friction, which, as has been mentioned previously, is proportional to the velocity squared. The power required to propel an airplane is proportional to the product of drag times velocity, hence to velocity cubed. This is equivalent to saying that the cube root of the power is proportional to the velocity. For our particular example then, if the power were to increase by a factor of 2.5, the speed could increase by a factor of $\sqrt[3]{2.5} = 1.36$. Thus, the new top speed would be $380 \times 1.36 = 516$ miles per hour.

Beneficial Drag

In a few situations, drag is useful. In some types of boats (with the old square-rigged or the modern spinnaker sails), drag is used for propulsion. Drag brakes are sometimes used on airplanes to slow them down. Parachutes also produce deceleration through drag.

The usefulness of the drag of a parachute can be illustrated by a comparison of the terminal velocities of a falling man with and without a parachute. Terminal velocity refers to the speed at which the drag force that retards the fall is equal to the gravitational pull downwards. This is then the maximum falling speed that can be reached.

As a first step, it is convenient to introduce the concept of aerodynamic coefficients. This is a way of expressing aerodynamic forces in nondimensional form, namely

$$C = \frac{F}{\frac{1}{2}\rho V^2 A}$$

where

07

- C coefficient of force
- F actual force
- ρ air density
- V velocity
- A some reference area

Since this chapter is concerned with drag forces, the drag coefficient C_D is defined as

$$C_D = \frac{\text{Drag}}{\frac{1}{2}\rho V^2 A}$$

The usefulness of this concept is that C_D tends to be nearly constant when changes are encountered in air density, velocity, or size of the object.

In the example of a falling man the upward drag force is set equal to the downward weight W ; thus

$$\text{Drag} = W$$

By using the definition of drag coefficient, the equation can be rewritten to obtain

$$\frac{1}{2}\rho V^2 A C_D = W$$

or

$$V_t = \sqrt{\frac{2W}{\rho A C_D}}$$

where V_t is the terminal velocity. A man-shaped object has a drag coefficient of about 1.0. An average value for the frontal area of a 180-pound man is about 5 square feet. Substituting these values in the equation (where $\rho = 0.0024$ slug/ft³ at sea level) yields

$$V_t = \sqrt{\frac{2 \times 180}{0.0024 \times 5 \times 1}} = 173 \text{ feet per second} = 118 \text{ miles per hour}$$

For comparison, a typical parachute has a drag coefficient of 1.6 and an area of 490 square feet. Substituting these values into the equation gives

$$V_t = \sqrt{\frac{2 \times 180}{0.0024 \times 490 \times 1.6}} = 14 \text{ feet per second}$$

REFERENCE

1. Hoerner, Sighard F.: *Fluid-Dynamic Drag*. Second ed., Midland Park, N. J., 1958.

4. AIRFOIL AND WING THEORY

Roger W. Luidens*

Herein we will concern ourselves with the wing or airfoil: its purpose, its working principles in terms of fundamental physical laws, and the design devices that can be used to give certain desired performance characteristics.

FORCES ON AN AIRPLANE

The function of a wing is best seen by examining the forces on an airplane in horizontal, unaccelerated flight (fig. 4-1). The airplane is pulled vertically downward by the attraction of gravity. This force is the weight W . If the airplane were unsupported, it would fall to the Earth. The purpose of the wing is to provide an upward lift L to support the airplane weight. In the process of providing lift, the wing also causes a drag D in the horizontal, downstream direction. This drag, as well as other drags, must be overcome by the engine thrust T .

An airplane designed for long-range cruising requires a highly efficient wing. The wing efficiency is measured by how much drag it produces while providing the lift to sup-

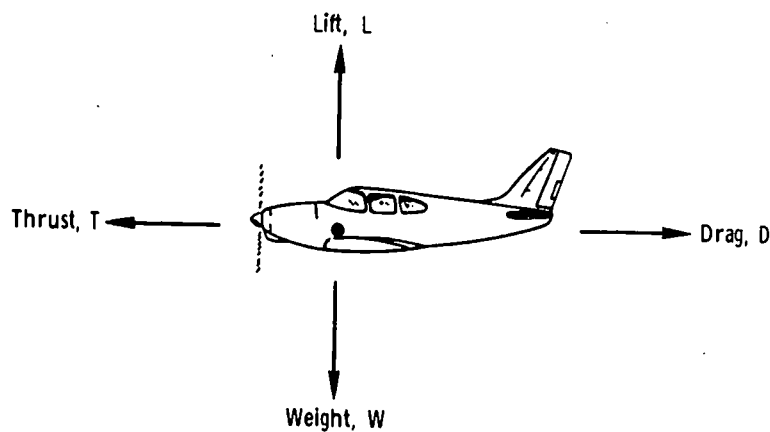


Figure 4-1. - Forces on an airplane.

*Chief, STOL Propulsion Branch.

port the airplane. This is expressed as the lift-to-drag ratio L/D . Thus, a high L/D indicates high efficiency.

For reasons of safety and ease of flying, slow takeoff and landing speeds are desirable. This requires a wing that provides adequate lift at slow speed. In the jargon of the aerodynamicist, this is a "high-lift" wing.

AIRPLANE FLIGHT TESTS VERSUS WIND-TUNNEL TESTS

To observe and study the airflow over a wing, it is obviously not practical to move alongside the airplane while it is in flight. It is more convenient to place the airplane in a wind tunnel, where it is held stationary while air is blown past it. It is important to understand that these two situations are equivalent. This is perhaps most easily rationalized by considering the example of a slow-flying airplane being observed by a man standing on the ground. If the airplane is flying at a speed of 30 miles per hour in still air, it passes the observer at a speed of 30 miles per hour. In other words, the airplane is moving at 30 miles per hour with respect to both the ground and the air. However, if this same airplane is flying against a 30-mile-per-hour headwind, then it is flying at 30 miles per hour through (with respect to) the air, but it is standing still with respect to the ground. In this case, the person on the ground can observe the airplane much more easily. If sidewalls were placed around the airplane and the 30-mile-per-hour headwind were continued, the airplane would be, in effect, in a wind tunnel. In considering the airflow, the important thing is the motion of the air relative to the airplane (or vice versa) and not the motion of the airplane relative to the ground. Thus, from the standpoint of aerodynamics, the wind-tunnel forces are the same as the flight forces. The remainder of the discussion, therefore, is based on the assumption of a stationary airplane with air moving past it.

BASIC PRINCIPLES OF LIFT

Wing lift is frequently explained in terms of Bernoulli's law (see chapter 5). In our analysis of the flow over a wing, however, we can utilize Newton's laws of motion to obtain a physical representation of the principles of lift.

Newton's Laws of Motion

Newton's Third Law of Motion states that for every action there is an equal and oppo-

site reaction. A familiar example of this law is the firing of a gun. Consider a single-shot pistol mounted on a theoretically weightless and frictionless roller skate, as shown in figure 4-2. (In this example, aerodynamic drag is also neglected.) When the gun is fired, the bullet, which has a mass m_1 , leaves the gun with a velocity v_1 . (The bullet mass, in slugs, is its weight at the Earth's surface, in pounds, divided by the acceleration due to gravity at the Earth's surface, in feet per second per second.) At the same

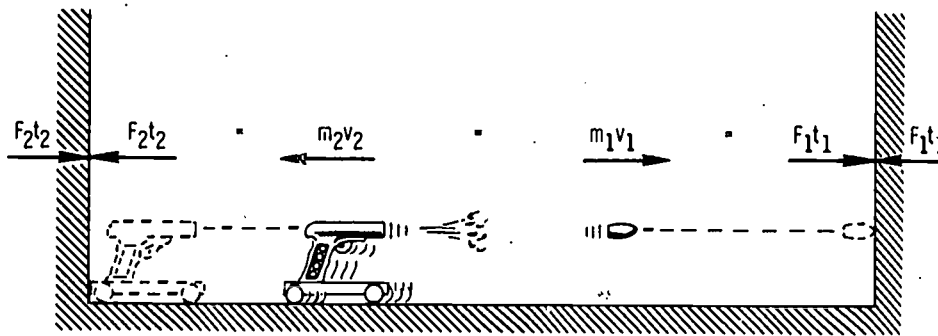


Figure 4-2. - Illustration of Newton's laws of motion.

time, the gun is "kicked" in the opposite direction. If the mass of the gun is m_2 , it moves backward at a velocity v_2 . The momentum of the bullet is m_1v_1 , and the reaction momentum of the gun is m_2v_2 ; according to Newton's law, these two momentums are equal. The bullet will hit the wall on the right with a force F_1 that exists for a short time t_1 . The gun will hit the wall on the left with a different force F_2 that exists for a different time t_2 . The kick that is received and counteracted by each wall is the product of the respective force and the length of time that the force exists. Therefore, the kick from the bullet that is received and counteracted by the right wall is F_1t_1 , and the kick from the gun at the left wall is F_2t_2 . This is the kick that a person feels in his hand if he is holding the gun when it is fired.

Newton's Second Law of Motion states that the rate of change of momentum of a body is proportional to the force acting on the body. This law can be represented by the equation $F = mv/t$, or $ft = mv$ (where mv is the momentum). Newton's First Law of Motion states that if a body in motion is not acted upon by an external force, its momentum remains constant. Thus, the application of Newton's laws of motion to the example of the gun shows that the kick of the gun against the left wall equals the momentum of the gun, which equals the momentum of the bullet, which equals the kick of the bullet against the right wall.

$$F_2t_2 = m_2v_2 = m_1v_1 = F_1t_1 \quad (1)$$

For the next example, a machinegun is used instead of the single-shot pistol. The bullets from this gun are fired into a bullet trap that is mounted to a wall by means of a spring-and-shock-absorber assembly, as shown in figure 4-3. (Springs and shock absorbers on a car are used to smooth out the many "kicks" from the road into an average force that is equal to and counteracts the weight of the car.) The bullet trap, by virtue of its mounting, converts the kicks from the individual bullets into an average force F that is

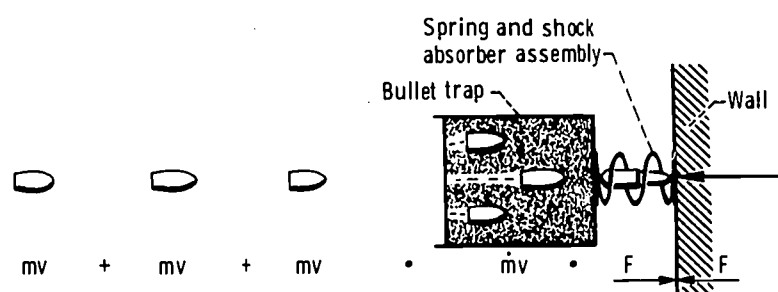


Figure 4-3. - Converting individual impulses to an average force.

received and counteracted by the wall. "Average force" in this context means a force that exists continuously in time and does not vary in magnitude. By this definition of average force, the total, or continuous, kick at the wall over a long period of time t must be Ft . The total "action" from a large number of bullets in the same length of time is the number of bullets n times the action per bullet. Equating the total action with the continuous kick, by Newton's laws of motion, yields

$$nmv = Ft \quad (2)$$

But the number of bullets n is equal to the number of bullets per second \dot{n} times the time t . Therefore, equation (2) can be written as

$$t\dot{n}mv = Ft \quad (3)$$

Since t occurs on both sides of the equation, it can be cancelled from both sides. Also, the number of bullets per second \dot{n} times the mass per bullet is just the mass flow per second \dot{m} . The average force on the wall from a stream of machinegun bullets is then the mass of bullets per second (the mass flow rate) times their velocity.

$$F = \dot{m}v \quad (4)$$

Figure 4-4 illustrates a series of examples, each of which gives the same average

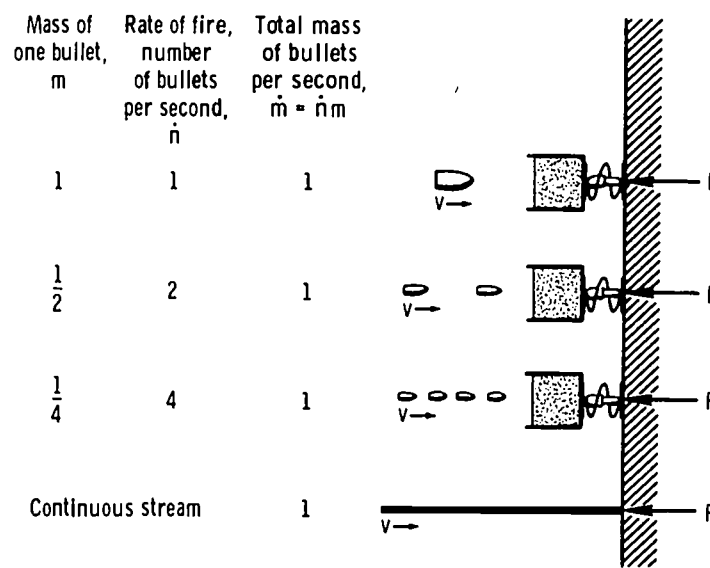


Figure 4-4. - Various mass flow systems producing same average force.

force F on the wall. As the number of bullets per second \dot{n} is increased, the mass m of each bullet is correspondingly decreased to maintain the same mass flow rate \dot{m} (see columns at left of fig. 4-4). The limit is a continuous flow of mass (similar to water out of a hose). For the example with the bullets, a bullet trap, spring, and shock absorber are needed to obtain the average force. However, this equipment would not be needed if the example were one of a continuous stream of mass.

Equation (4) is a general law that results from Newton's laws of motion. It is important to note that the force F acts along the same line as v .

Air Flow

Aerodynamics concerns the flow of air rather than bullets. Therefore, the next step towards understanding the lift of a wing is the application of equation (4) to a stream of air.

To determine the force of a stream of air by equation (4), the mass flow rate per unit time, \dot{m} , must first be known. If the airstream is flowing through a tube, as shown in

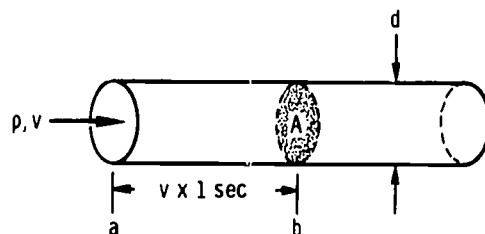


Figure 4-5. - Airstream in a tube.

figure 4-5, the mass flow rate is the mass flow past any point in the tube during some unit period of time, such as 1 second. Consider a particle of air that is at point a when timing is begun. At the end of 1 second, that particle of air is at some point b downstream from a. The distance between points a and b is determined by multiplying the flow velocity v by 1 second. Thus, the volume of air that passes point a during 1 second is obtained by multiplying the cross-sectional area of the tube A by the flow velocity of the air v by 1 second. The mass of this air (which is the mass flow rate per unit time, \dot{m}) is the density ρ multiplied by the volume flow per unit time, vA .

$$\dot{m} = \rho v A \quad (5)$$

For a sample calculation of mass flow rate, consider a tube being held out the window of a moving car so that the longitudinal axis of the tube coincides with the direction in which the car is traveling. The air density is obtained from a table of air density versus altitude above sea level. The velocity v of the air in the tube is the car velocity, obtained from the speedometer. The cross-sectional area of the tube is obtained by measuring the tube diameter d and then using the equation

$$A = \frac{\pi d^2}{4} \quad (6)$$

The preceding example of airflow in a straight tube was used only to determine the mass flow rate; there was no force, or lift, on the tube. However, airflow through a bent tube does produce a force on the tube.

Assume that the downstream end of the horizontal tube of the preceding example is bent downward at an angle β , as shown in figure 4-6. The upward force, or lift, L produced by the bent airstream can be calculated by equation (4). The mass flow rate \dot{m} has already been calculated by equation (5). The lift is caused by the flow velocity that is parallel but opposite in direction to the direction of the lift; this velocity is designated v_L . The flow exiting from the end of the bent tube has a velocity v and an angle β with

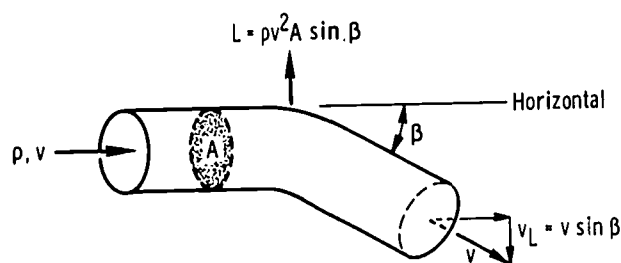


Figure 4-6. - Bent airstream generates lift.

respect to the horizontal plane. The vertical downward component of this velocity is $v \sin \beta$. Therefore, from equations (4) and (5), the lift L is given by

$$L = mv_L = (\rho v A)(v \sin \beta) = \rho v^2 A \sin \beta \quad (7)$$

For those who are unfamiliar with trigonometry, a brief explanation of trigonometric functions should be useful at this point. Trigonometry is the mathematical study of the relations between component parts of triangles. In any triangle, if three of the parts (angles and sides) are known, including at least one side, the other three parts can be

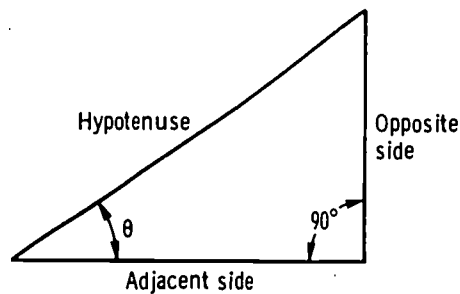


Figure 4-7. - Right-angled triangle as it applies to definitions of trigonometric functions.

determined by using trigonometric functions. These functions are simply ratios of sides of a right-angled triangle, shown in figure 4-7. The most commonly used functions (sine, cosine, and tangent) are defined as follows:

$$\sin \theta = \frac{\text{Side opposite } \theta}{\text{Hypotenuse}}$$

$$\cos \theta = \frac{\text{Side adjacent to } \theta}{\text{Hypotenuse}}$$

$$\tan \theta = \frac{\text{Side opposite } \theta}{\text{Side adjacent to } \theta}$$

where the hypotenuse is the side opposite the right angle (90°). These functions depend only on the angle θ , because if this angle and the right angle are maintained constant, an increase in any side of the triangle requires a proportionate increase in the other sides. Because all sides of the triangle increase or decrease proportionately, the ratios of sides (i. e., the functions) remain constant. Therefore, the trigonometric functions vary only when the angle θ is varied.

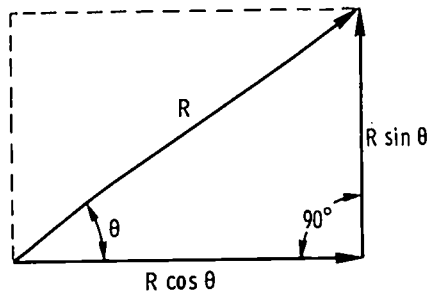


Figure 4-8. - Vector relations.

Trigonometric functions are useful in vector considerations. (A vector is any quantity that has both magnitude and direction, such as force, velocity, acceleration, and displacement.) In many problems it is useful to replace a single vector by two or more vectors equivalent to it, or vice versa. The equivalent two or more vectors are called components of the original vector, which, conversely, is called the resultant of the components. For example, a vector R (resultant) along the hypotenuse at an angle θ from the adjacent side is equivalent to, or can be resolved into, a component $R \cos \theta$ along the side adjacent to θ and a component $R \sin \theta$ along the side opposite θ , as shown in figure 4-8. The vectors are represented by arrows. The length of the arrow is proportional to the magnitude of the vector, and the direction of the arrow is the direction of the vector. It should be noted that the resultant vector R represents the diagonal, and the component vectors represent two adjacent sides of a rectangle. These two component vectors may be drawn so as to form any one of the four corners (right angles) of the rectangle. However, the component vectors must have the correct directions; that is, the arrows representing the component vectors must point away from the tail and/or toward the head of the arrow representing the resultant vector.

Velocity is a vector because it has magnitude (speed) and direction. Therefore, the velocity v of the airstream bent downward at an angle β from the horizontal, as shown in figure 4-6, can be resolved into a horizontal component $v \cos \beta$ in the direction of the original flow and a vertical downward component $v \sin \beta$.

Lift on a Wing

A first approximation of the lift on a wing can be obtained by relating the airflow over a wing to the airstream in a tube (fig. 4-9). In the figure, the wing is shown by the solid lines. For illustrative purposes, let us assume that the effective stream tube of air affected by the wing is a tube with a diameter that is equal to the wingspan b . Therefore, in equation (7),

$$A = \frac{\pi b^2}{4}$$

Substituting this term into equation (7) yields the following equation for wing lift:

$$L = \rho v^2 \frac{\pi b^2}{4} \sin \beta \quad (8)$$

For small angles of attack, the angle β at which the flow is bent in the imaginary tube is just the wing angle of attack α .

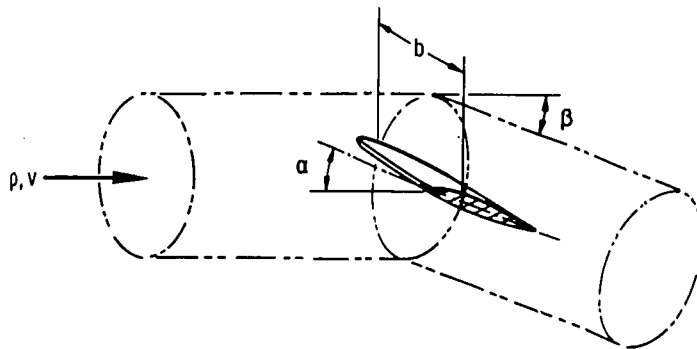


Figure 4-9. - Imaginary stream tube of air affected by wing.

It must be emphasized that equation (8) provides only an approximation of the lift; however, the equation does take into account most of the factors affecting lift. A more precise analysis of wing lift would show that equation (8) should be multiplied by the term $4/[2 + (b^2/S)]$, where b^2/S is the aspect ratio of the wing, which is discussed later in this chapter.

Coanda Effect

In the preceding development of the wing-lift theory, it was implied that separate particles, such as bullets, would lead to the same result as a continuous fluid, such as water or air. In the examples of the bullets and the flow in a tube, this was true. But, in other instances, fluids do have different properties from those of particles.

The theory of the preceding section that the flow over a wing can be approximated by the flow in a tube is dependent on a fluid property called the Coanda effect. This effect is best illustrated by the following simple experiment. If sand is poured on the upper right side of a cylinder, as shown in figure 4-10(a), the grains of sand bounce to the right. If water is poured on the upper right side of the cylinder (fig. 4-10(b)), the water

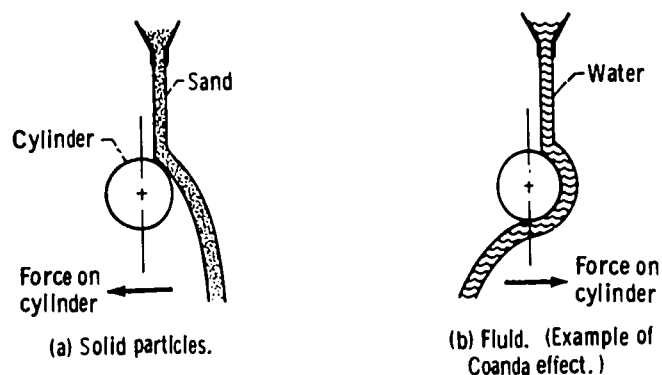


Figure 4-10. - Difference between paths of solid particles and fluid around a curved surface.

clings to the surface of the cylinder, so that it leaves the cylinder at the lower side and flows toward the left. This tendency of fluids to cling to surfaces over which they flow is the Coanda effect. The grains of sand, obviously, do not cling to the surface. Because of the Coanda effect, the airflow over a wing tends to cling to the surface of the wing and is, therefore, turned by the wing. It should be noted that this tendency of a fluid to cling to a surface is limited; that is, the fluid eventually breaks away from the surface, as shown in figure 4-10(b).

If equation (7) were applied to the two examples of figure 4-10, the sand would produce a component of force to the left on the cylinder because the grains of sand bounce to the right; the water would produce a component of force to the right on the cylinder because the water leaves the cylinder to the left.

HIGH LIFT

The preceding discussion dealt with the basic principles of lift. These principles will now be applied to the problem of generating high lift.

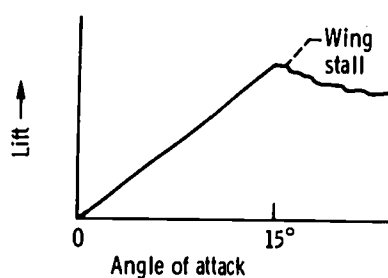
One of the principal requirements for high lift is at landing, because it permits a slower landing, which is easier and safer. (An airplane also requires high lift for improved maneuverability at high altitudes.) At landing, the lift still should be only equal to the airplane weight. Therefore, to the aerodynamicist the term "high lift" signifies the ability of an aircraft to fly slowly or to change direction rapidly at high altitude. From equation (8) it is obvious that if the lift L is too high (i. e., greater than the airplane weight), it can be reduced by decreasing the velocity v . Thus, achieving a high lift at a specified velocity is equivalent to achieving a lower velocity at a specified lift. For landing, flight at low velocity with the lift equal to the airplane weight is desirable. The present discussion considers the subject of lift from the standpoint of the aerodynamicist; that is, the discussion concerns high lift at a specified velocity.

The variables that affect lift are contained in equation (8). For the purpose of this

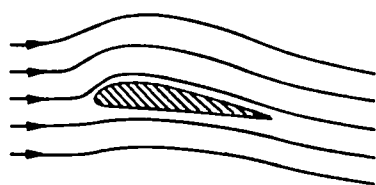
discussion, let us assume that three of these variables are fixed. The air density ρ is determined by the altitude of the airport at which the airplane is landing or by the altitude at which the airplane is maneuvering. The velocity v is assumed to be some specified value. The wingspan b is determined by the configuration of the airplane. Even if these three variables are fixed, high lift can still be obtained by means of flow turning.

Equation (8) includes the term $\sin \beta$, where β is the angle through which the flow is turned. According to equation (8), the lift should increase as the flow-turn angle β is increased up to the limit of 90° , where $\sin \beta$ reaches its maximum value of 1. In practice, for small angles of less than 15° , the flow-turn angle β (and the lift) can be increased by merely increasing the angle of attack α (fig. 4-11(a)). As the angle of attack is increased up to 15° , the airflow remains attached to the surface of the wing (Coanda effect) and is turned by it (fig. 4-11(b)); thus, the flow-turn angle β is the same as the angle of attack α . However, if the angle of attack is increased above 15° , the lift does not increase any more; instead, it drops a little and then remains fairly constant for higher angles of attack. The reason for this is that when the angle of attack is greater than 15° , the airflow separates from the upper surface of the wing and is no longer turned by it (fig. 4-11(c)). In this case, the flow-turn angle β is no longer the same as the angle of attack α . This condition of flow separation, which is analogous to the water breaking away from the surface of the cylinder in figure 4-10(b), is called wing stall. (In a liquid, such as water, this separation phenomenon is referred to as cavitation.)

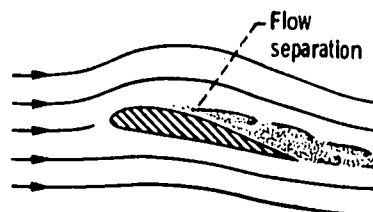
Obviously, the principle of turning the airflow through a large angle to obtain high lift is difficult to put into practice because of the problem of getting the flow to turn. Some attempted solutions to this problem are the so-called "high-lift devices" discussed in the next section.



(a) Lift as function of angle of attack.



(b) Angle of attack less than 15° . Attached airflow; complete flow turning.



(c) Angle of attack greater than 15° . Separated airflow; partial flow turning.

Figure 4-11. - Effect of angle of attack on lift and airflow.

HIGH-LIFT DEVICES

The high-lift devices used to improve flow turning are actually antistall or antiseperation devices. A measure of the success of such a device in preventing flow separation, or in turning the flow, is the maximum lift produced by the wing to which the device is applied. The maximum lift is expressed as a dimensionless coefficient $C_{L, \max}$. The various devices are compared in terms of this parameter.

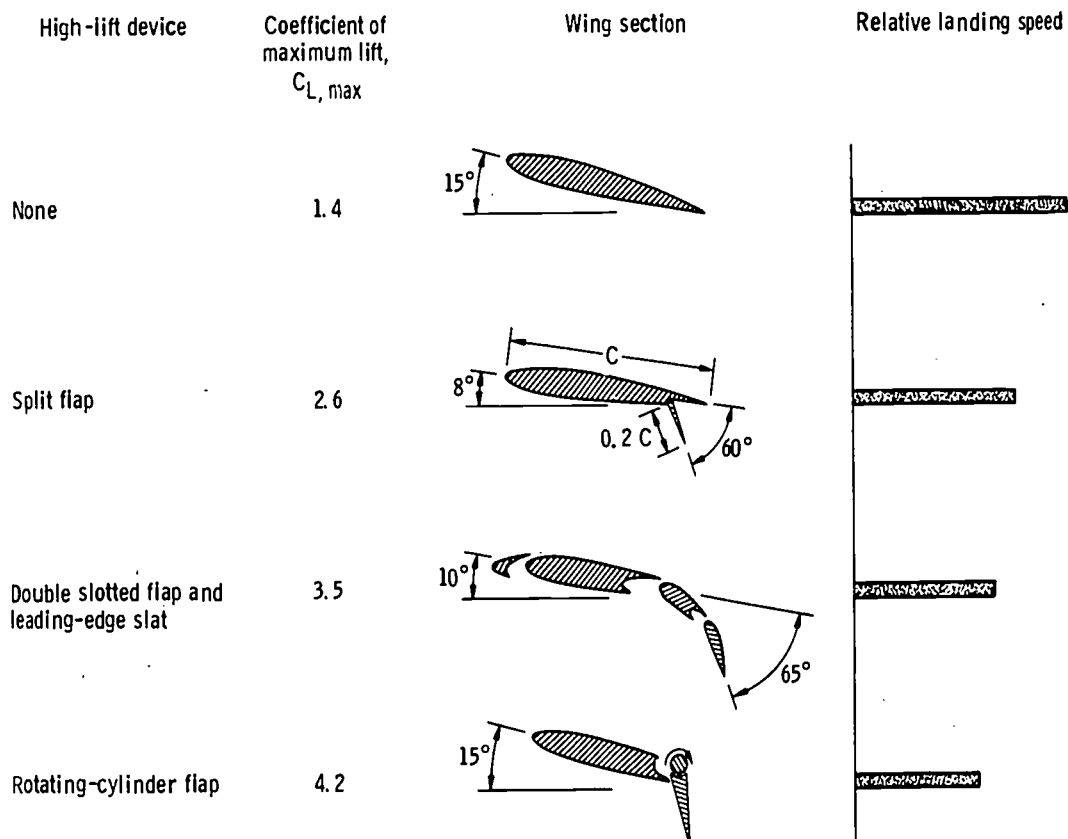


Figure 4-12. - High-lift devices.

Wing stall can occur abruptly, as when the flow separates from the leading edge, or it can occur gradually, as when the flow separation spreads forward from the trailing edge. Therefore, there are leading-edge and trailing-edge high-lift devices. Figure 4-12 shows several types of high-lift devices and their effectiveness in terms of $C_{L, \max}$. The $C_{L, \max}$ increases from approximately 1.4 for a plain wing to approximately 4.2 for a wing with a rotating-cylinder flap.

The effect of a rotating cylinder, one of the high-lift devices, is illustrated in figure 4-13. Because of the Coanda effect, the flow of water is turned a certain amount even if the cylinder is stationary (fig. 4-13(a)). If the cylinder is rotating in the direction of flow, the attachment is increased and the flow is turned through a greater angle (fig. 4-13(b)). This is exactly the way a rotating cylinder works when it is applied to the wing

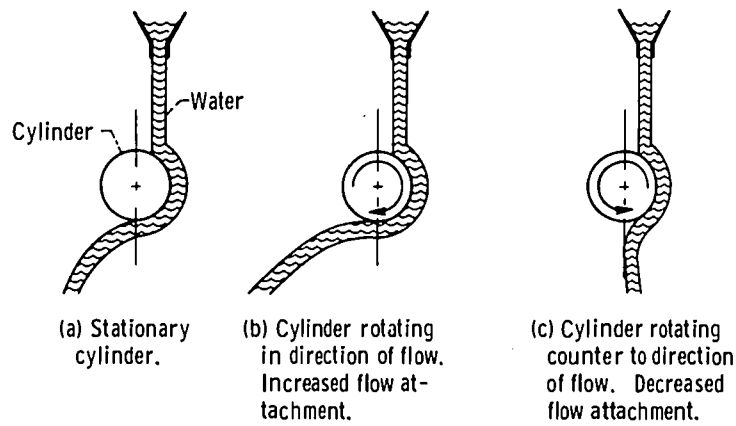


Figure 4-13. - Effect of rotating cylinder on flow attachment.

of an airplane. Of course, if the cylinder is rotating counter to the direction of flow, separation occurs sooner and the flow is turned less (fig. 4-13(c)).

DRAG AND EFFICIENCY

The preceding discussion of high lift did not deal with the subject of wing drag. To learn why a wing of finite span causes drag and to understand wing efficiency, the flow around a wing must be examined in more detail than was done in the preceding discussion.

Local Flow Over a Finite Wing

When a wing is producing lift, the pressures on the bottom of the wing are higher than those on the top. Any fluid tends to flow from an area of high pressure to one of low pressure. Therefore, the air tends to flow from the bottom to the top of the wing, as indicated by the upward arrows at the leading and trailing edges in figure 4-14. To understand what actually happens to this upward flow of air, it is helpful to consider again the example of water flowing around a cylinder, as shown in figure 4-15. The flow readily

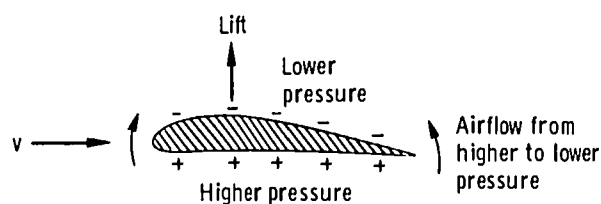


Figure 4-14. - Pressures on lifting wing.

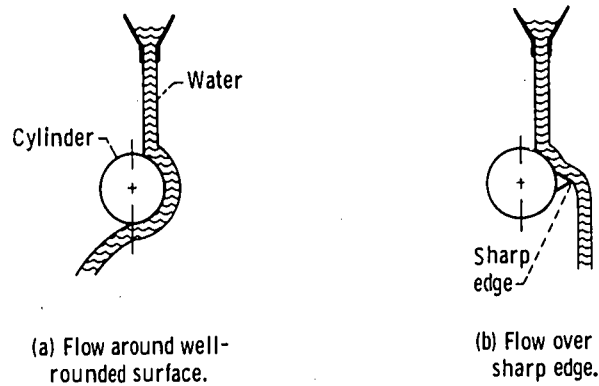


Figure 4-15. - Effect of sharp edge on flow attachment.

follows a smooth, well-rounded surface (fig. 4-15(a)), but it cannot follow the surface around a sharp corner or over a sharp edge (fig. 4-15(b)). Therefore, the leading edge is made round and the trailing edge sharp, so that air from the bottom of the wing will flow up around the leading edge but not around the trailing edge (fig. 4-16). This upward flow around the leading edge causes the streamlines ahead of the wing to rise up to meet the wing, as shown in figure 4-16. The overall effect of the wing-section shape is that it turns the airflow so that the air leaves the wing in a downward direction; thus, the wing produces a lifting force.

The higher pressures on the bottom of a lifting wing also cause air to flow up around the wingtips, as shown in figure 4-17. In this case, the airflow pivots up and around the wingtip in a circular pattern (viewed from the front), with the tip of the wing in the center of the circle. This is called a vortex flow.

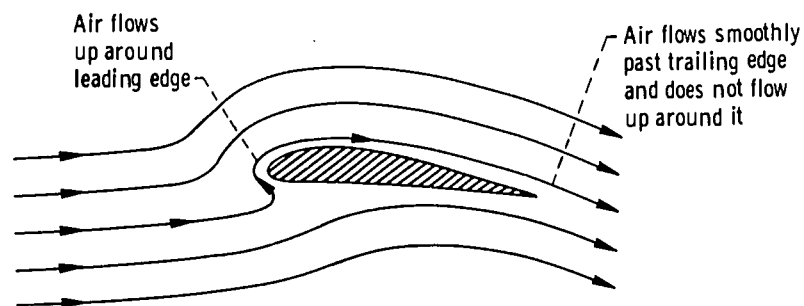


Figure 4-16. - Flow induced by pressures on lifting wing.

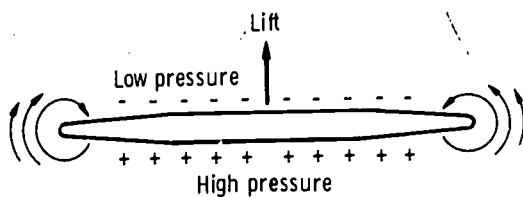


Figure 4-17. - Front view of lifting wing showing vortex flows around wing tips.

Vortex Flow

There are many common examples of vortices: tornadoes, hurricanes, dust devils, water spouts, the flow down the bathtub drain, the flow around a canoe paddle during a stroke, smoke rings, the flow around the tips of a lifting airplane wing. The twist in the exhaust flow from a moving car, especially a car with twin exhausts, looks much like the pattern shown in figure 4-17.

Vortex flow is characterized by velocities that are higher at the center than at the outer edges of the vortex (fig. 4-18). A simple experiment for observing the wingtip vortex and the velocity distribution in a vortex is shown in figure 4-19. At the tip of a wing, three paddle wheels of different diameters are mounted on an axis that is aligned with the free-stream direction. Each paddle wheel is free to rotate independently of the others. The paddle blades are aligned with the free stream direction, so that if there were no disturbance to the free-stream flow, the blades would remain aligned with the flow and the paddle wheels would not rotate. However, in their position behind the wingtip, the paddle blades will tend to align themselves with the local flow, which is changed from the free-

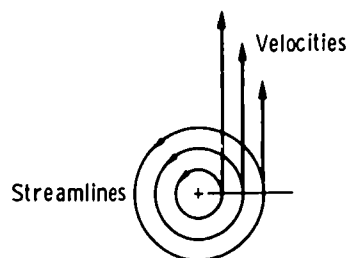


Figure 4-18. - Velocity distribution in a vortex.

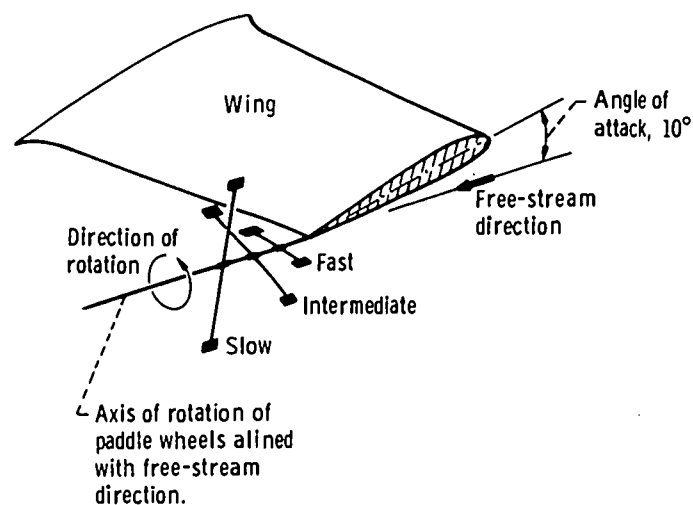


Figure 4-19. - Experiment illustrating wingtip vortex flow.

stream direction by the effect of the wing at its angle of attack. The movement of the paddle blades in alining themselves with the local flow causes the paddle wheels to rotate. Therefore, the rotation of the paddle wheels is an indication of the vorticity of the local flow downstream of the wingtip. This experiment will also show that the smallest-diameter paddle wheel rotates the fastest and the largest-diameter wheel rotates the slowest. This is consistent with the previous description of the velocity distribution in a vortex (fig. 4-18). This experiment can be performed with a model wing mounted to the side of an automobile so that the forward motion of the automobile generates the free-stream velocity relative to the wing.

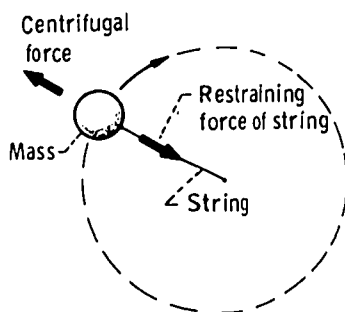


Figure 4-20. - Centrifugal force.

Centrifugal force, illustrated in figure 4-20, is a familiar phenomenon which acts on any body, or mass, that is being constrained to travel along a curved path. The air in a vortex has mass and is, therefore, subject to centrifugal force. However, a force that is caused by the pressure variation in a vortex prevents the air from being thrown out of the vortex by the centrifugal force. The pressures in a vortex are low at the center and high at the outside. This pressure variation creates an inward force (air tends to flow from high to low pressure) that counteracts the centrifugal force. Thus, the force due to the pressure variation serves the same purpose as does the string in the example of figure 4-20.

Since a vortex has low pressure in the center, the end of the vortex cannot be open to the higher-pressure outside air, because this higher-pressure air tends to flow into the center and break up the vortex by eliminating the pressure force which counters the centrifugal force. Thus, as shown in figure 4-21, vortices are closed loops (such as a smoke ring), or they terminate at the fluid boundary (as a tornado terminates on the ground).

The vortices from the wingtips extend rearward and join a lateral vortex that is shed from the trailing edge of the wing when the wing speed is changed, as when the speed is increased at takeoff. These joined vortices and the wing form a closed-loop pattern similar to that of a smoke ring.

The direction of the wingtip vortex flow (fig. 4-22) is such that these vortices exert

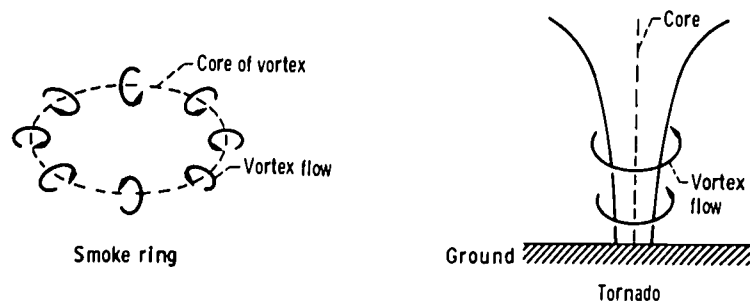


Figure 4-21. - Vortexes are closed loops or terminate at the boundary of the fluid.

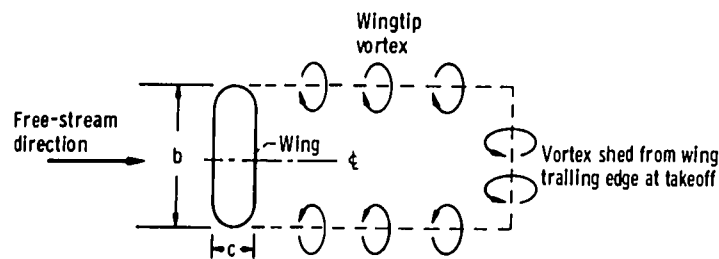


Figure 4-22. - Top view of wing and vortex pattern.

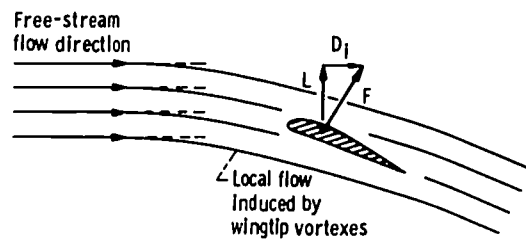


Figure 4-23. - Effect of wingtip vortexes.

a downward force on the local airflow about the wing, as shown in figure 4-23. It has already been explained and shown (figs. 4-18 and 4-19) that the velocity is greatest near the center of a vortex. Therefore, the downward flow (and force) of a wingtip vortex is greatest at the center of the vortex. To minimize the downward effect of the wingtip vortexes on the local airflow about the wing, the vortexes should be moved as far apart as possible; that is, the wingspan b should be large in comparison with the wing chord c . The ratio of the wingspan to the mean aerodynamic chord \bar{c} (or the ratio of wingspan squared to wing area S) is called the wing aspect ratio AR .

$$AR = \frac{b}{\bar{c}} = \frac{b^2}{S} \quad (9)$$

Induced Drag

As shown in figure 4-23, the downward influence of the wingtip vortices extends even ahead of the wing, so the wing operates in a downflow. Even though the force F on the wing is perpendicular to the local flow, this force now has a component parallel to the free-stream direction; this component is the induced drag D_i . The induced drag is proportional to the lift L . The downflow at the wing, which is related to the wing aspect ratio AR , is also proportional to the lift L . The drag due to lift, or induced drag, is actually given by the following equation:

$$D_i = \frac{L^2}{\pi AR}$$

The induced drag is only one of the drags on an airplane; other drags are discussed in chapter 3.

The previous description of flow, illustrated in figure 4-16, seems to conflict with the present description, illustrated in figure 4-23. Actually, both descriptions are correct. The two flows exist simultaneously and are superimposed on each other as shown in figure 4-24.

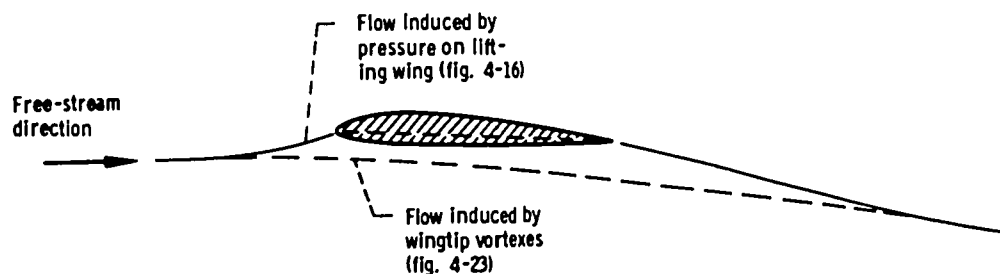
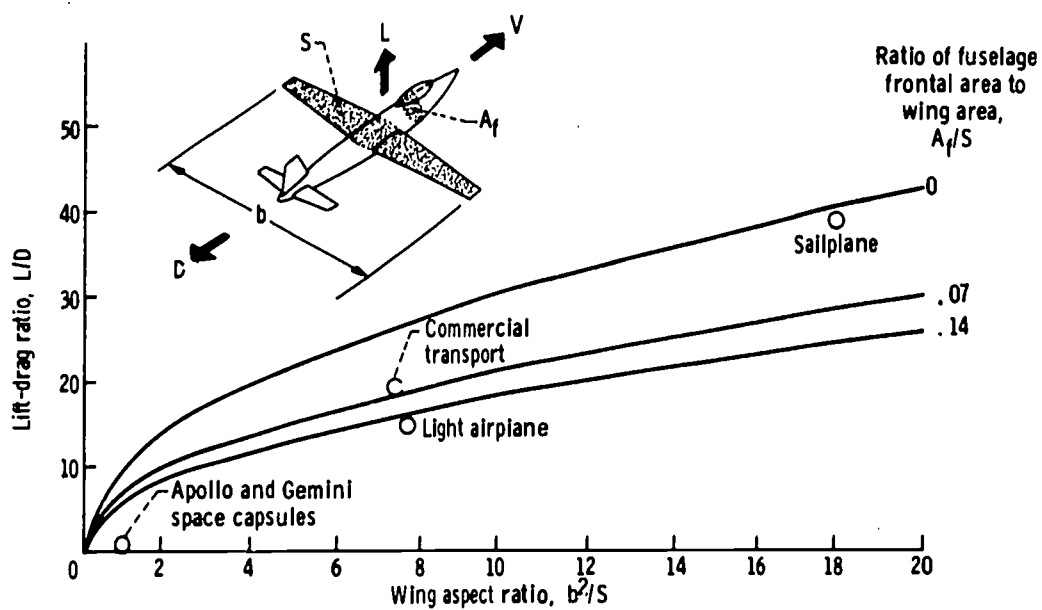


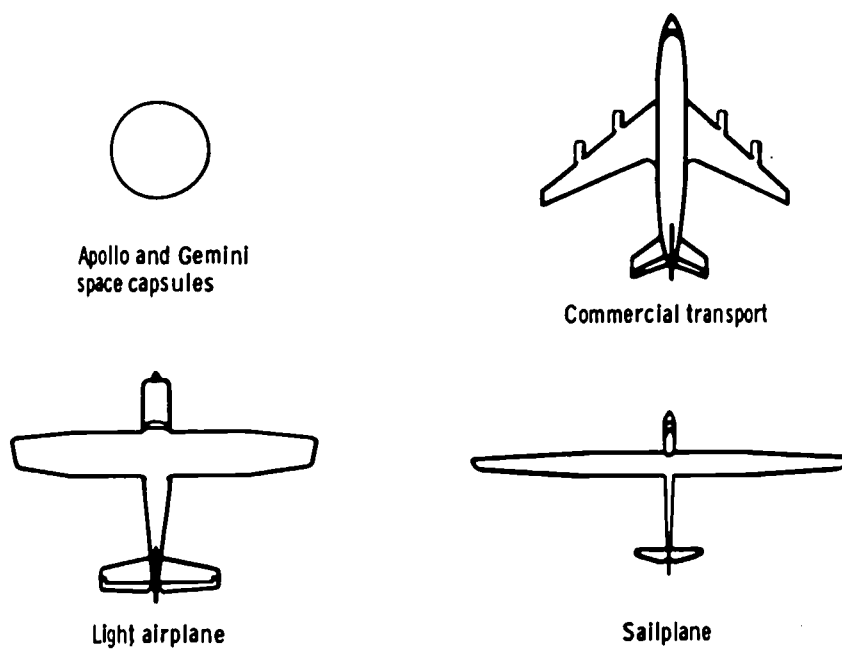
Figure 4-24. - Airflow about lifting finite wing.

Lift-To-Drag Ratio

The aerodynamic efficiency of a wing (or airplane) is measured by its lift-to-drag ratio L/D ; that is, the efficiency is measured by how much drag a wing causes while providing a specified lift. At the subsonic speeds being considered in the present discussion, the wing aspect ratio has a most important effect on wing efficiency, as shown in figure 4-25(a). In general, a high wing aspect ratio leads to a high airplane lift-to-drag ratio. What aspect ratio is selected depends on the design objective. (Plan views of various design configurations are shown in fig. 4-25(b).) The four-place light airplane indicated in the figure is designed for a range of about 1000 miles and to be cheap. The commercial



(a) Effect of wing aspect ratio and fuselage size on aircraft lift-drag ratio.



(b) Aircraft plan views.

Figure 4-25. - Aircraft lift-drag ratios.

transport is designed for a range of about 3000 miles and to make money for the airlines. The sailplane is designed to glide a long distance. The Apollo and Gemini space capsules (which travel in the atmosphere at hypersonic and supersonic speeds, as well as at subsonic speeds) are designed aerodynamically to provide only limited control over the landing accuracy on return from orbit (i.e., ability to land in a target area with a diameter of perhaps 50 miles).

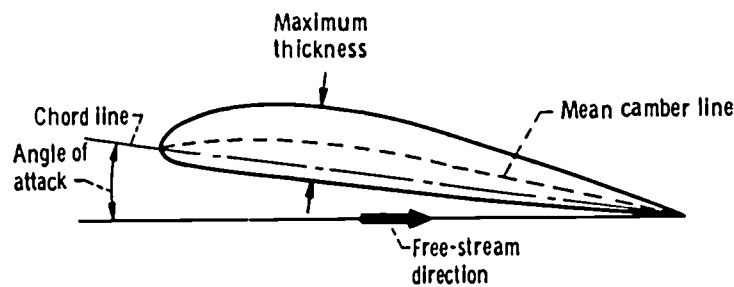
GLOSSARY

aerodynamic center. A point in a cross section of an airfoil, on the aerodynamic chord, about which the pitching moment remains practically constant with nearly all changes in angle of attack. This point is usually located a distance of approximately 25 percent of the mean aerodynamic chord back from the leading edge. This is the point where lift can be considered to be concentrated.

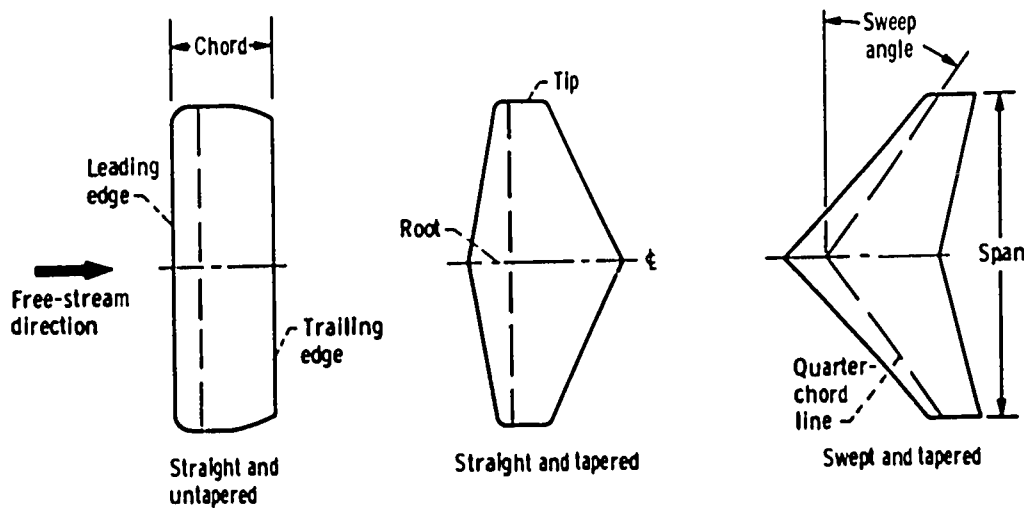
angle of attack. The angle between the chord line and the free-stream direction (fig. 4-26(a)).

aspect ratio. The ratio of the square of the span of an airfoil to the total airfoil area, or the ratio of the span to the mean geometric chord.

camber. The curvature of the mean line, or centerline, of an airfoil profile (section) relative to the chord line.



(a) Wing cross section.



(b) Wing planforms.

Figure 4-26. - Airfoil and wing terminology.

chord. The straight line joining the leading and trailing edges of an airfoil or joining the ends of the mean line (or mean camber line) of an airfoil profile. The length of that part of the chord line intercepted by the extremities of the leading and trailing edges of an airfoil section (fig. 4-26(b)).

chord line. A straight line through the centers of curvature of the leading and trailing edges of an airfoil section. This line is generally used as a reference line from which the ordinates and angles of an airfoil are measured (fig. 4-26(a)).

free stream. The stream of fluid outside the region affected by a body in the fluid.

leading edge. The forward edge of an airfoil or wing. The edge that normally meets the air first (fig. 4-26(b)).

maximum thickness. The maximum dimension of an airfoil or wing measured perpendicular to the chord line and usually occurring at the quarter-chord line (fig. 4-26(a)).

mean aerodynamic chord. Approximately the same as the mean geometric chord.

mean camber line. The mean line, or centerline, of an airfoil profile; that is, the line midway between the upper and lower surfaces of an airfoil (fig. 4-26(a)).

mean geometric chord. The average chord length of an airfoil, obtained by dividing the planform area of the airfoil by the span.

moment. A tendency to cause rotation about a point or axis, as of an airplane about its center of gravity; the measure of this tendency, equal to the product of the force and the perpendicular distance between the point or axis of rotation and the line of action of the force.

pitching moment. A moment about a lateral axis of an airfoil or aircraft.

planform area. The area within the outline of an object as viewed from the top. With respect to an airfoil or a wing, it is the area within the outline of the projection of the airfoil or wing on the plane of its chords (fig. 4-26(b)).

quarter-chord line. The line through the quarter-chord points of an airfoil (fig. 4-26(b)).

quarter-chord point. The point on the chord line at one quarter of the chord length behind the leading edge.

root. The base or inner end of an airfoil, wing, or blade (fig. 4-26(b)).

span. The dimension of an airfoil or a wing from tip to tip, measured in a straight line (fig. 4-26(b)).

sweep. The slant (forward or rearward) of a wing or airfoil, or of a reference line in an airfoil, with respect to a plane that is perpendicular to the longitudinal axis of the aircraft (fig. 4-26(b)).

sweep angle. The angle between a reference line, usually the quarter-chord line, of an airfoil or wing and a plane that is perpendicular to the longitudinal axis of the aircraft (fig. 4-26(b)).

sweepback. The backward slant from root to tip of an airfoil or wing, or of some reference line of an airfoil (fig. 4-26(b)).

taper. A gradual reduction, from root to tip, of either the chord length or thickness of an airfoil or wing (fig. 4-26(b)).

taper ratio. The ratio of the tip chord length of an airfoil to the root chord length.

tip. The outermost extremity of an airfoil or wing (fig. 4-26(b)).

trailing edge. The rear edge of an airfoil or wing. The edge over which the airflow normally passes last (fig. 4-26(b)).

twist. A variation of the angle of attack of an airfoil from root to tip.

washout. A permanent twist (or warp) given a wing such that the angle of attack decreases from the root to the tip of an airfoil.

5. PROPELLER THEORY

Earle O. Boyer*

An aircraft propeller may be considered as an engine-driven screw. The blades of the propeller correspond to the threads of a screw. As a propeller rotates, the blades "bite," or slice, into the air in a manner similar to the way the threads of a wood screw, for example, slice into the wood. (Some European engineers and aerodynamicists call an aircraft propeller an "airscrew.") Thus, in its rotation, the propeller reacts with the surrounding fluid to produce an axial force, or thrust.

This chapter concerns specifically the aircraft propeller, but the basic principles discussed herein are also applicable to rotors and fans. This discussion is intended to provide merely some basic understanding of the theory and principles of a propeller rather than to provide a comprehensive knowledge of the subject. (Technical expressions pertaining to propellers are defined in the GLOSSARY at the end of this chapter.)

It is important to realize that even in this age of jet aircraft, rockets, nuclear power, and space exploration the propeller still serves a vital function in both civilian and military aviation. The reason for this is that currently the piston engine and propeller are a more efficient and more economical power plant than the jet engine for low flying speeds. That is, at low speeds the piston engine uses less fuel than the jet engine to develop a given thrust. Also, the piston engine is currently cheaper than the jet engine. Therefore, the piston engine and propeller are commonly used to power small private airplanes, agricultural airplanes, military spotter airplanes, and bush-flying airplanes. Propellers are proving useful, too, in the field of V/STOL aircraft (see chapter 10).

PRINCIPLES OF PROPELLER THRUST

Let us now concern ourselves with some of the basic principles by which a propeller actually produces thrust. In this discussion, aerodynamic lift and propeller thrust are explained in terms of Bernoulli's law. (In chapter 4, lift was explained in terms of Newton's laws of motion.)

* Aerospace Engineer and Pilot, Aircraft Operations Branch.

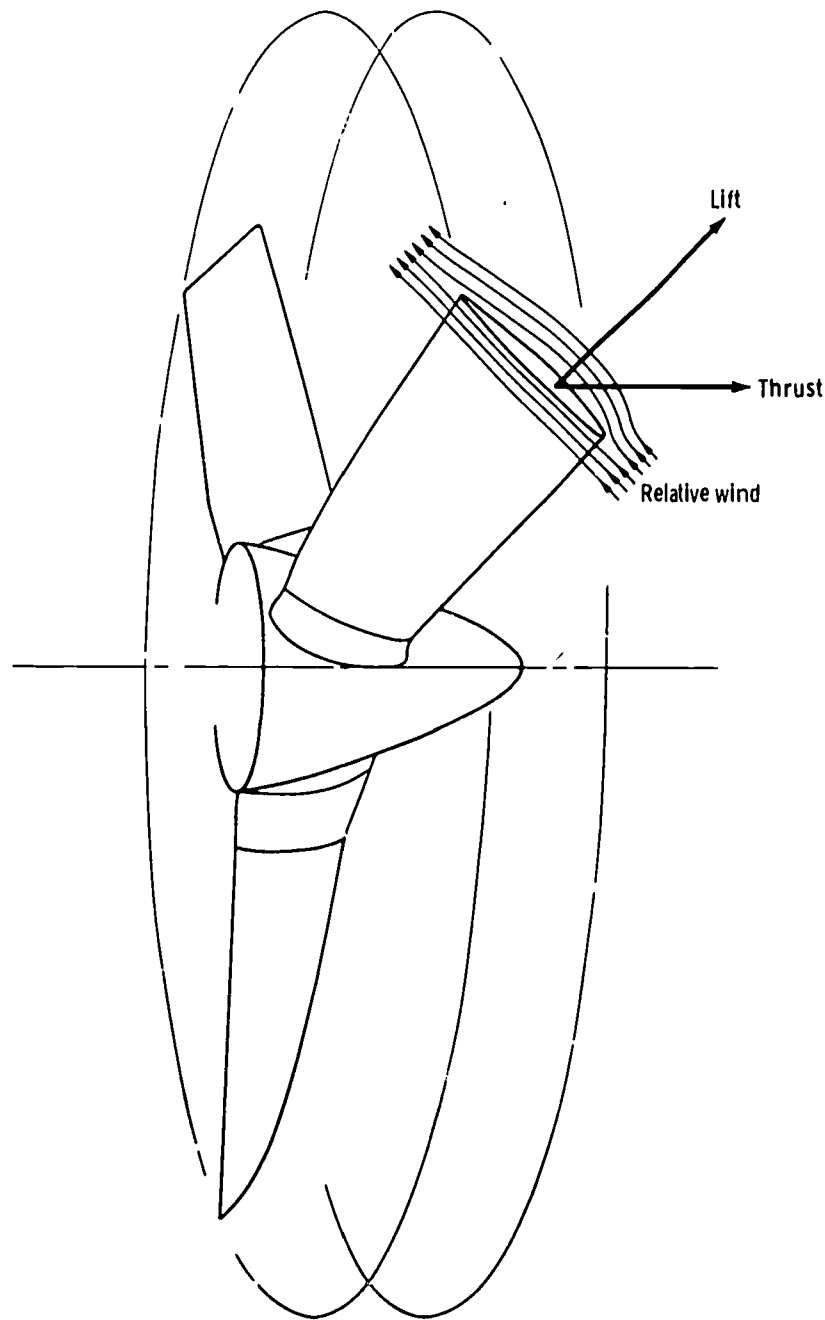


Figure 5-1. - Propeller blade considered as an airfoil rotating in the vertical plane.

A propeller blade is an airfoil (similar to a wing) set to rotate in the vertical plane (fig. 5-1). Thus, the blade may be considered as "lifting" the airplane forward, as the wing lifts it upward. Figure 5-2 shows the basic forces (lift and drag) generated by an airfoil. The upward lift that is generated is the net result of the pressure distribution over the airfoil (fig. 5-3(a)). One of the factors governing the pressure pattern over an airfoil is the velocity of the air flowing over the surface (fig. 5-3(b)).

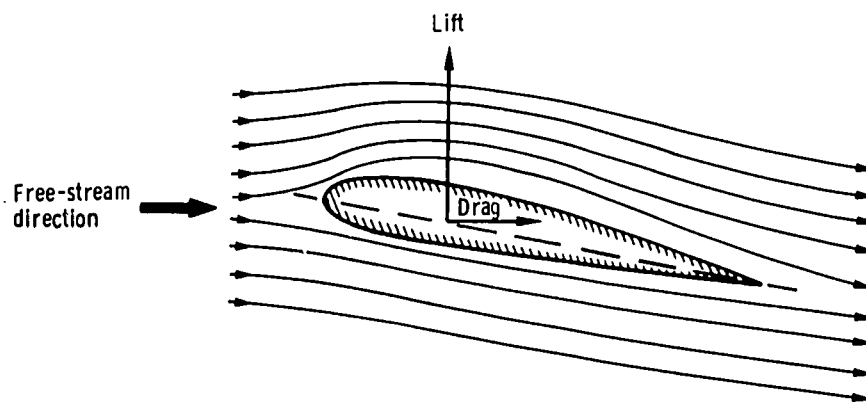


Figure 5-2. - Basic forces generated by an airfoil in an airstream.

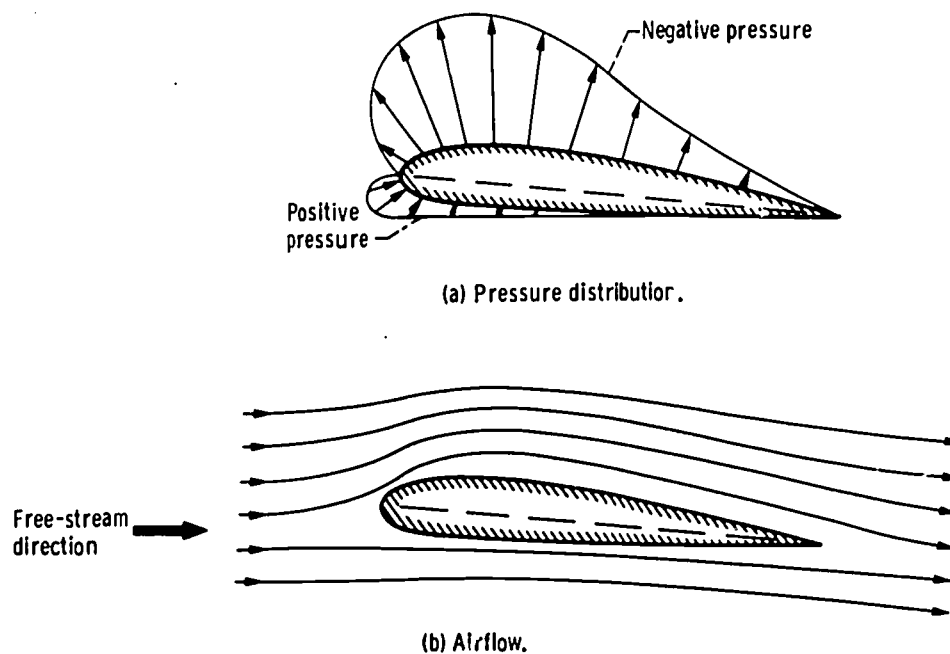


Figure 5-3. - Interrelation of pressure distribution and local airflow velocity over an airfoil.

Bernoulli's Law

The relation between velocity and pressure is given in Bernoulli's law, which states that in a flow of incompressible fluid the sum of the static pressure and the dynamic pressure along a streamline is constant if gravity and frictional effects are disregarded. (For calculations involving low subsonic flow velocities, air may be considered to be incompressible.) The equation for Bernoulli's law is

$$P = p + \frac{1}{2} \rho V^2 = \text{Constant}$$

where P is the total pressure, p is the static pressure, and $\frac{1}{2} \rho V^2$ is the dynamic-pressure term, wherein ρ is the fluid density and V is the flow velocity. From Bernoulli's law it follows that where there is a velocity increase (dynamic-pressure increase) in a fluid flow, there must be a corresponding pressure decrease (i. e., a static-pressure decrease). Figure 5-4 illustrates Bernoulli's law as it applies to airflow within

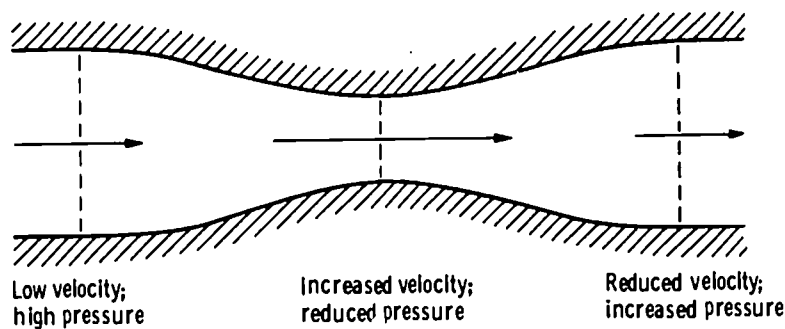


Figure 5-4. - Bernoulli's law applied to airflow within a venturi.

a venturi. At the venturi inlet, the velocity is relatively low and the static pressure is relatively high. In the throat region of the venturi, where the velocity increases, the pressure decreases in accordance with Bernoulli's law. (The principle of flow acceleration in a venturi is discussed in chapters 6 and 7.) Finally, at the venturi exit the velocity decreases and, therefore, the pressure increases.

Perhaps Bernoulli's law is more easily understood if it is considered as representing a special form of the principle of the conservation of energy, illustrated in figure 5-5. The total mechanical energy of the rolling ball shown in this figure corresponds to the total pressure of the fluid flow of Bernoulli's law, the potential energy corresponds to the static pressure, and the kinetic energy corresponds to the dynamic pressure. Thus, the total mechanical energy of the ball is the sum of its potential energy and its kinetic

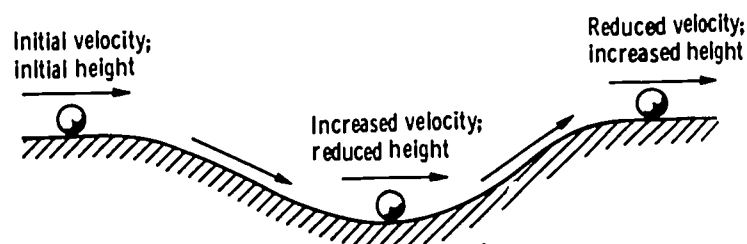


Figure 5-5. - Principle of conservation of energy. (Velocity represents kinetic energy; height represents potential energy.)

energy. If the ball is assumed to roll without friction, the total mechanical energy remains constant (conservation of energy) regardless of the relative magnitudes of the potential and kinetic energies.

As the ball rolls along a level surface at a constant velocity, the potential and kinetic energies are both constant. When the ball starts to roll down a slope, the velocity and kinetic energy begin to increase, and the height and potential energy begin to decrease. At the bottom of the slope, the velocity and kinetic energy are maximum, and the height and potential energy are minimum (or zero). The bottom of the slope of this example corresponds to the venturi throat of the previous discussion, where the flow velocity (dynamic pressure) is maximum and the static pressure is minimum. As the ball rolls up the next slope, the velocity (kinetic energy) decreases, and the height (potential energy) increases. Throughout these changes in the potential and kinetic energies, the total mechanical energy of the ball remains constant, just as the total pressure of the fluid flow in Bernoulli's law remains constant.

Airflow Over Airfoil Surfaces

Of course, Bernoulli's law alone does not explain the lift of an airfoil. Because of the profile of an airfoil and the angle of attack, the air that flows over the top surface of an airfoil must follow a longer, more indirect path (see fig. 5-3(b)) than does the air that flows along the bottom surface. (On a propeller blade, the "top" surface is the upstream face, or camber face, and the "bottom" surface is the downstream face, or thrust face.) The air that flows along the longer path must speed up so that behind the airfoil it can rejoin the stream of air flowing along the shorter path. Therefore, according to Bernoulli's law, the pressure on the top surface of the airfoil becomes lower than the pressure on the bottom surface. This pressure difference is the basis of the lift of an airfoil (or the thrust of a propeller blade). In fact, the lift of an airfoil is directly proportional to the dynamic pressure of the airflow, which is a function of the velocity (dynamic pressure = $\frac{1}{2}(\text{density})(\text{velocity})^2$).

The velocity of the local airflow relative to the surface, particularly the top surface, of an airfoil (therefore, the lift or thrust of the airfoil) depends on the profile, or shape, of the airfoil, the angle of attack, and the velocity with which the airfoil meets the air-stream (i. e., the relative-wind velocity).

Airfoil Profile and Angle of Attack

The profile and the angle of attack of an airfoil determine how much the air flowing

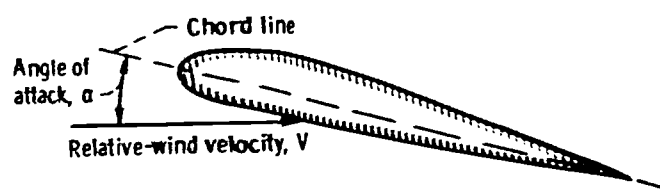
over the top surface of the airfoil must detour from the path of the air flowing along the bottom surface. The extent of this detour, in turn, determines the increase in the velocity of the local airflow along the top surface over the velocity of the local airflow along the bottom surface.

The effective profile of a wing can be changed during flight by the use of certain types of flaps. The profile of a propeller blade, however, cannot be changed during operation.

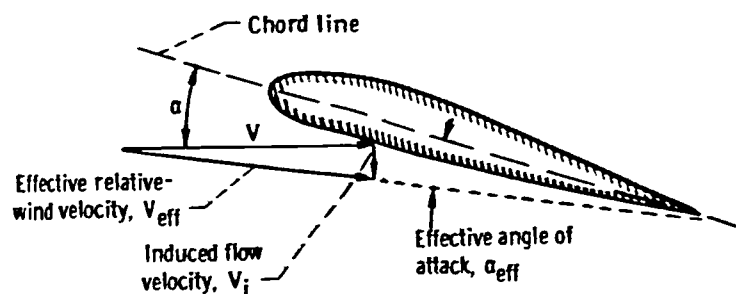
The angle of attack of an airfoil is the acute angle between the chord line of the airfoil and the direction of the relative wind. On most aircraft the wing is mounted immovably to the fuselage. Therefore, the wing angle of attack of an aircraft in flight is normally changed by changing the pitch attitude of the aircraft. (On some aircraft the leading edge of the wing can be raised and lowered to change the wing angle of incidence and, therefore, the wing angle of attack. The wing angle of incidence is the acute angle between the wing chord line and the longitudinal axis of the aircraft.) The angle of attack of a propeller blade can be changed by changing the rotational speed (rpm) of the propeller, the forward velocity of the aircraft, or the pitch of the propeller blade.

Relative Wind

For a simplified analysis of a wing, the velocity of the relative wind may be assumed to be the forward velocity V of the aircraft (fig. 5-6(a)). For a more precise analysis,



(a) Induced flow (downwash) velocity not included.



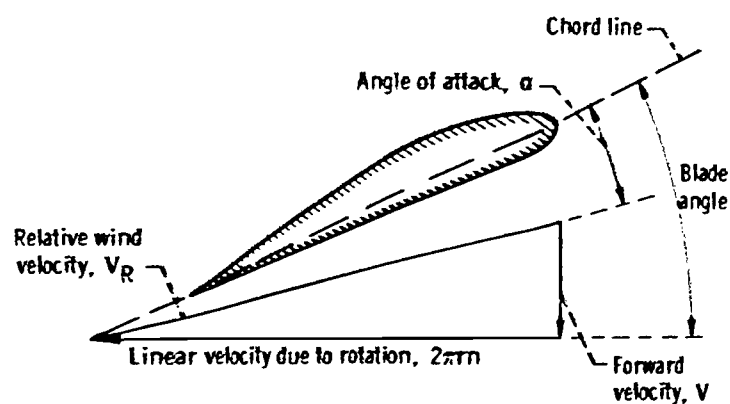
(b) Induced flow (downwash) velocity included.

Figure 5-6. - Relative wind velocity for a wing.

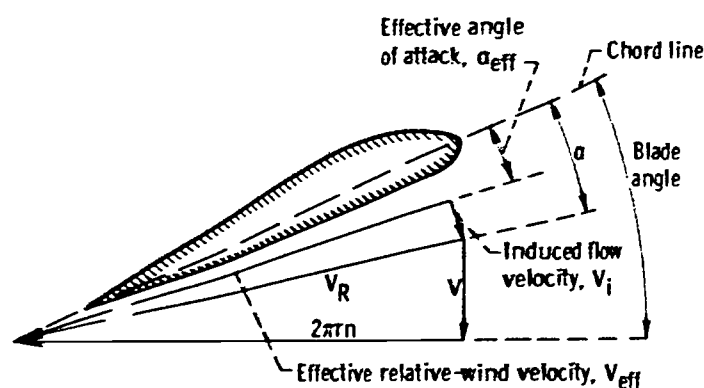
however, the velocity of the induced flow (downwash) due to the tip vortex (discussed in chapter 4) must also be considered. Thus, the actual effective relative-wind velocity V_{eff} (fig. 5-6(b)) is the resultant of the forward velocity V and the induced-flow velocity V_i . (The resolution of vector quantities, such as velocities, is discussed in chapter 4.)

The relative wind of a propeller blade is more complex than that of a wing, because a propeller has rotational motion as well as forward motion. For a simplified analysis, the relative-wind velocity at any segment of a propeller blade (fig. 5-7(a)) may be assumed to be the resultant velocity V_R of the forward velocity V and the linear velocity $2\pi rn$ due to rotation. (In the term for the velocity due to rotation, r is the radius from the axis of rotation to the blade segment, and n is the rotational speed.) For a more precise analysis of a propeller blade, just as for a wing, the induced-flow velocity must be taken into account. Therefore, the actual effective relative-wind velocity V_{eff} (fig. 5-7(b)) for any segment of a propeller blade is the resultant of the forward velocity V , the linear velocity due to rotation $2\pi rn$, and the induced-flow velocity V_i .

The linear velocity $2\pi rn$ in the plane of rotation is much less at the blade root than



(a) Induced flow velocity not included.



(b) Induced flow velocity included.

Figure 5-7. - Relative-wind velocity for a propeller blade.

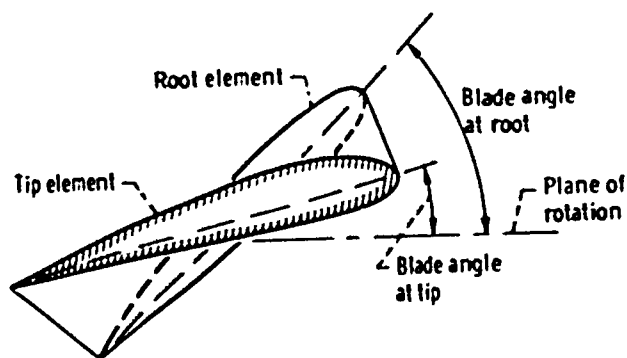


Figure 5-8. - Blade twist.

at the blade tip. Therefore, the relative wind at the root sections is almost parallel to the axis of rotation, while at the tip it is nearly perpendicular to this axis. To obtain an efficient angle of attack at all points along the blade, the blade is twisted (fig. 5-8) so that the blade angle at the root is large, while at the tip the angle is quite small.

The rotational speed of a propeller (and therefore the relative wind) is normally limited by the blade-tip speed's approaching the speed of sound. As this limit is approached, high tip losses occur. Tip loss is the loss of lift at the tip of an airfoil because of the tip vortex (discussed in chapter 4). Also, when the blade tip approaches sonic velocity, shock waves can cause severe vibrations, which, in turn, can damage or destroy the propeller. (The cause and the effects of shock waves are discussed in chapter 11.)

Lift and Drag - Thrust and Torque

On an aircraft wing, the relative wind produces a force vector R which can be resolved into components perpendicular and parallel to the relative wind (fig. 5-9); the perpendicular component is lift, and the parallel component is drag. On a propeller blade, the force vector R produced by the relative wind is resolved into components perpendi-

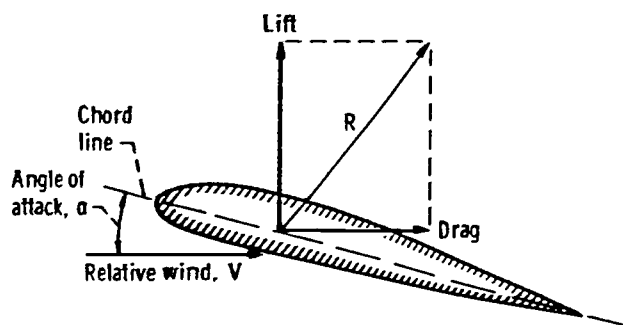


Figure 5-9. - Resolution of the total aerodynamic force acting on a wing into lift and drag components.

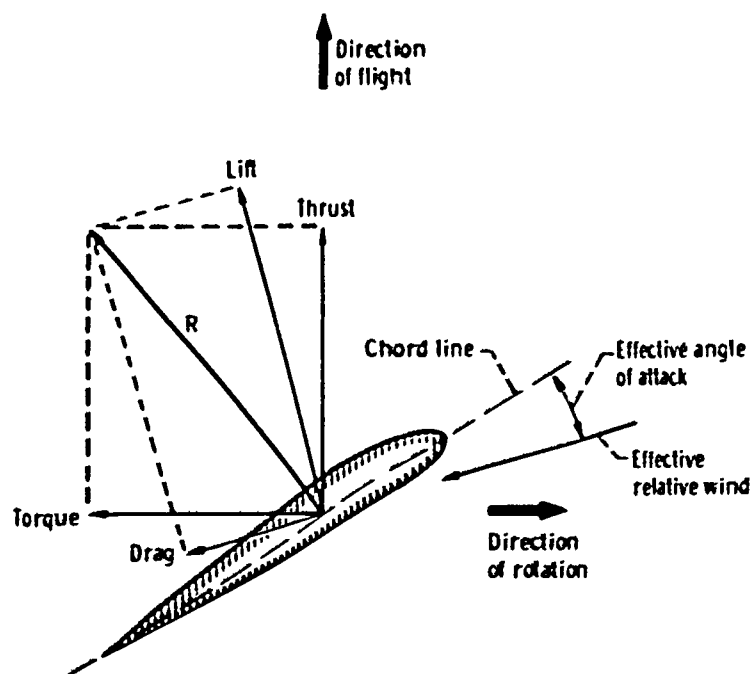


Figure 5-10. - Resolution of the total aerodynamic force acting on a propeller blade into thrust and torque components.

cular and parallel to the plane of rotation (fig. 5-10); the perpendicular component is thrust, which propels the aircraft forward, and the parallel component is torque, which counteracts the engine torque. (Note that fig. 5-10 also shows the lift and drag for the propeller blade.)

Aerodynamic Efficiency

The efficiency of a wing is measured by its lift-to-drag ratio (discussed in chapter 4). It was explained earlier that lift is a function of the angle of attack. However, drag is also a function of the angle of attack. (Drag increases with increasing angle of attack.) Therefore, the most efficient angle of attack for a given wing is that angle which provides the maximum lift-to-drag ratio. Since the effect of the relative wind on a propeller blade is resolved into thrust and torque components, the efficiency of a propeller is measured by the ratio of the thrust power produced by the propeller to the torque power supplied by the engine. Thus, the most efficient angle of attack for a given propeller blade is the angle at which this ratio is maximum.

At a constant rotational speed (rpm), the most efficient, or desirable, angle of attack can be maintained by varying the blade pitch to compensate for the effects of variations in the forward velocity. However, variations in the forward velocity (and in the angle of attack) affect not only the efficiency of the propeller but also the load on the engine. That is, a change in the angle of attack causes a change in the engine torque power required to

turn the propeller. This variation in the load, in turn, causes a variation in the rpm. It is usually desirable to operate an aircraft engine at some specific rpm that will provide the required power at a satisfactory rate of fuel consumption with a safe margin of engine reliability. Therefore, the blade pitch of a controllable-pitch propeller is normally varied to maintain a specific rpm for most efficient engine operation rather than to maintain a specific angle of attack for most efficient propeller operation. However, a propeller is always matched to the engine to provide maximum thrust from the available engine power. Thus, by varying the blade pitch it is possible to maintain an efficient engine speed, without seriously degrading the aerodynamic efficiency of the propeller as its angle of attack is changed.

THEORETICAL PERFORMANCE OF A PROPELLER

So far, we have explained the principles by which a propeller blade or blade segment produces thrust. Now we shall briefly consider the three commonly used theories for calculating the total thrust of the entire propeller.

Momentum Theory

A propeller produces thrust by slicing into the air and accelerating it rearward in a long slipstream. As the propeller forces the air mass rearward, a reaction force (thrust) is produced in the forward direction, in accordance with Newton's laws of motion. The more air the propeller pushes back each second, the greater is the thrust.

The momentum theory assumes that a rotating propeller is composed of an infinite number of blades and can, therefore, be replaced physically by an actuator disk. This actuator disk is assumed to be capable of producing a uniform change in velocity (in the axial direction) of the air stream passing through it, without any air losses at the periphery of the disk (i. e., at the blade tips). Furthermore, the air being accelerated through the disk is assumed to be a perfect, incompressible, nonviscous fluid. The airstream flowing through the disk is assumed to be irrotational. Thus, the energy of the flow in front of and behind the disk (but not through the disk itself) is considered constant, with no energy lost because of rotation.

As the air stream approaches the face of the disk, the velocity increases from the original free-stream velocity, and the pressure decreases from the original free-stream pressure. The velocity continues to increase as the flow passes through the disk. However, the pressure at the disk suddenly increases by twice the amount that it had decreased in front of the disk. Thus, as the flow leaves the disk, the pressure is higher

than the free-stream pressure. Downstream of the disk, the pressure decreases again to the free stream value, while the velocity increases. According to the momentum theory, one-half the velocity increase occurs in front of the disk and one-half behind the disk. (Note that Bernoulli's law does not hold for flow through the disk, but it does hold for the flow in front of and behind the disk.)

The momentum theory is useful for illustrating the type of flow produced by a propeller, and it can be used to calculate the maximum theoretical thrust of a propeller. However, this theory is of limited use in propeller design work, because it does not account for energy lost in slip-stream rotation, profile drag losses, losses due to nonuniform thrust along the blade, blade-interference losses, and losses due to increased drag and changes in flow at speeds where air becomes compressible.

Blade-Element Theory

The blade-element theory for calculating the performance of a propeller is more accurate than the momentum theory, because it takes into account the rotational speed, blade twist, blade airfoil section, and number of blades.

This theory considers any element of a propeller blade as a small wing and assumes that each element acts independent of the other elements. This theory further assumes that the induced-flow velocity for each, or any, element is the same as for a wing of a given aspect ratio (usually 6).

First, the thrust and torque for individual elements (with the assumed induced flow velocity) are calculated. Then, these thrust and torque values obtained for individual elements are summed (added together) to obtain the total thrust and the total torque for the entire propeller.

Although the blade-element theory is useful for preliminary calculations, it is still not sufficiently precise, because it merely assumes a certain induced-flow velocity and it ignores tip losses and blade interference losses.

Vortex Theory

In principle, the vortex theory is very similar to the blade-element theory. However, with the vortex theory the induced-flow velocity for each blade element is actually calculated, rather than assumed to be the same as produced by a wing of aspect ratio 6.

The calculated thrust and torque values obtained with the vortex theory closely approximate the actual values, even though this theory also ignores tip losses and blade-interference losses. More exact theories, which account for these losses, have been developed, but these theories are beyond the scope of this chapter.

TYPES OF PROPELLERS

A propeller is commonly classified according to its means of pitch control, its configuration, or its location on the engine. These general bases for classification result in many specific types of propellers. The following are just a few of these types.

The fixed-pitch propeller is one that has a certain built-in blade pitch, or blade angle, which cannot be changed. The principal advantages of this type of propeller are simple construction (usually a single piece of wood or aluminum), low weight, and low cost. The main disadvantage of this type is that it is designed to provide maximum efficiency at only one specific operating condition.

The adjustable-pitch propeller is one whose blade angle may be varied only while the propeller is at rest. Thus, this propeller may be adjusted (on the ground) to provide maximum efficiency at any one specific operating condition.

A controllable-pitch propeller is one whose blade angle may be changed by remote control from the cockpit while the propeller is rotating. This enables the pilot to select the most efficient blade angles for the various operating conditions during the flight. In the simplest versions of this type of propeller, the blade angle is changed by mechanical means, such as a simple lever arrangement. In the more elaborate versions, the blade angle is changed by electrical and/or hydraulic means.

An automatic propeller is one that incorporates a control mechanism which automatically adjusts the blade angle for maximum efficiency for the varying operating conditions during flight. Various electrical, hydraulic, and mechanical devices are used to change the blade angle, or pitch angle, but all these devices depend on a centrifugal governor for primary control. The governor senses any changes in the engine speed and causes the pitch-changing mechanism to change the blade angle accordingly.

A feathering propeller is a controllable-pitch propeller whose blades can be rotated about their root-to-tip axes so that the blade chords can be oriented approximately parallel to the thrust axis or to the direction of airflow (blade angle approximately 90°). Feather-

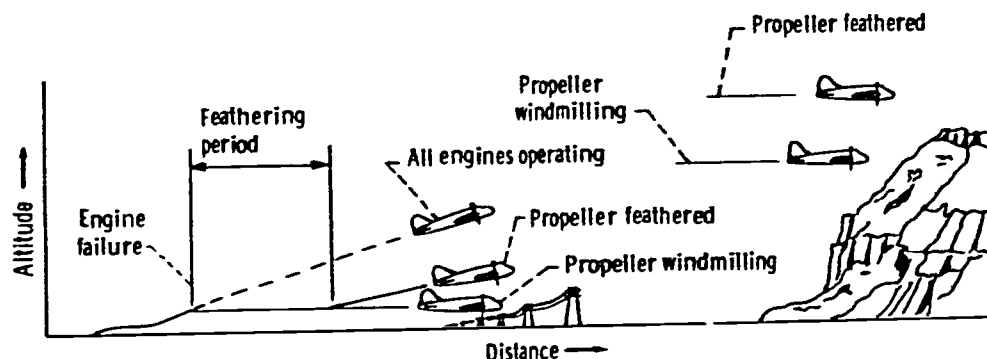


Figure 5-11. - Effect of propeller feathering on performance of multiengine aircraft with one engine inoperative.

ing the propeller of an inoperative engine prevents the propeller from windmilling and minimizes its drag. Thus, on a multiengine aircraft, feathering the propeller helps the aircraft to maintain a specific flight condition with the remaining operative engines (fig. 5-11) and reduces the asymmetric thrust.

A reversible-pitch propeller is a controllable-pitch propeller whose pitch, or blade angle, can be changed (during rotation) from positive to negative values so as to provide reverse thrust. This reverse thrust is used primarily to slow down the aircraft during the landing roll, thereby reducing the landing roll and the brake wear. Reverse thrust can also be used during a dive to prevent the airplane from exceeding the maximum speed that its structure can withstand safely.

A contrarotating propeller consists of two propellers mounted on concentric shafts, having a common drive, and rotating in opposite directions. A contrarotating propeller can absorb (and convert to thrust) more engine power than can a single propeller. Therefore, contrarotating propellers are used on engines that produce more power than can be absorbed by single propellers. The contrarotating propeller also provides some aerodynamic advantages over the single propeller. The slipstream from a single propeller rotates. This rotating slipstream strikes the surfaces of the aircraft from various angles and thereby increases the drag. Furthermore, the rotation of the propeller in one direction causes the airplane to tend to rotate in the opposite direction (torque reaction), thereby creating a control problem. With a contrarotating propeller both of these problems are eliminated, because the slipstream flows in a straight line and the torque reaction is neutralized. The main disadvantages of the contrarotating propeller are increased weight and complexity.

GLOSSARY

airfoil. An aerodynamic surface (such as an airplane wing or a propeller blade) designed to provide a useful reaction force when in motion relative to the surrounding air.

airfoil section. A cross section of an airfoil taken perpendicular to the span axis or root-to-tip axis of the airfoil. Also, the form or shape of an airfoil section.

angle of attack. The acute angle between the airfoil-section chord line and the relative wind velocity, measured in a plane perpendicular to the span axis or the root-to-tip axis of the airfoil.

blade (propeller). The thrust-producing and major torque-absorbing component of a propeller. It may be constructed integrally with a propeller hub, or it may be assembled in a propeller hub.

blade angle. The acute angle between the blade airfoil-section chord line and the plane of rotation.

blade axis. The root-to-tip axis about which the individual blade may rotate to change pitch.

blade element. A segment of a blade between two blade sections that are an infinitesimal distance apart.

blade root. That portion of the blade nearest the hub.

blade tip. The outermost extremity of the blade; the portion of the blade farthest from the hub.

chord. The straight line joining the leading and trailing edges of an airfoil; the length of that part of the chord line intercepted by the extremities of the leading and trailing edges of an airfoil section.

chord line. A straight line through the centers of curvature of the leading and trailing edges of an airfoil section. This line is generally used as the reference line from which the angles of the airfoil are measured.

disk area. The area of a circle having the same diameter as a given propeller.

induced flow. Flow drawn into a propeller disk by the vortex system of the propeller; the downwash on the top surface of an airfoil produced by the tip vortex.

thrust (propeller). That component of the total aerodynamic force acting on a propeller which is parallel to the axis of rotation. Positive thrust is in the direction of flight.

tip loss. A loss of lift or thrust at the tip of an airfoil due to the tip vortex.

tip speed. The linear speed of the blade tip of a propeller.

windmilling. The forced rotation of a propeller by the action of air flow through the disc area, which occurs when engine power is cut off suddenly.

BIBLIOGRAPHY

- Anon.: Aircraft Propeller Handbook. Bul. ANC-9, Departments of Air Force, Navy, and Commerce, 1956.
- Cargnino, Lawrence T.; and Karvinen, Clifford H.: Aircraft Propulsion Powerplants. Third ed., Educational Publishers, Inc., 1962.
- Glauert, Hermann: The Elements of Aerofoil and Airscrew Theory. Second ed., Cambridge University Press, 1948.
- Hurt, H. H., Jr.: Aerodynamics for Naval Aviators. Office of the Chief of Naval Operations, Aviation Training Division, 1960.
- Jones, Bradley: Elements of Practical Aerodynamics. Third ed., John Wiley & Sons, Inc., 1942.
- Nikolsky, Alexander A.: Helicopter Analysis. John Wiley & Sons, Inc., 1951.

6. AIRCRAFT PROPULSION

Robert W. Koenig*

The development of aircraft propulsion and the attendant technological advances have been a result of the interaction between economic and military needs. The history of aircraft propulsion began in the 15th century when screw propellers were first envisioned by Leonardo da Vinci. However, the actual need for a propeller did not arise until an engine was devised to drive it. The first successful mechanical flight of a piloted airplane (Wilbur and Orville Wright - 1903) used a screw propeller with a reciprocating engine for power. This type of system still serves well when flight speeds of less than approximately 350 miles per hour are suitable. When man sought to fly at higher speeds (originally for military reasons), a lighter and smaller power plant became essential. The jet engine answered this need. The world's first jet-propelled airplane was flown by the Germans in 1939. It is interesting to note that there was no incentive for developing a jet engine until the art of airplane design had advanced enough to make high-speed flight practical. As a matter of fact, the jet is not particularly attractive for low-speed flight. The propeller provided an essential first step without which we almost certainly would not have developed airplanes at all.

The first successful aircraft propulsion device was a steam engine designed by Henry Gifford; this engine powered a propeller for a dirigible balloon in 1851. Many different propulsion schemes have been used since then, but this chapter concerns only current aircraft propulsion systems and those of the near future. The engines considered are for use only in the atmosphere. They use the oxygen from this atmosphere (air) to combine with fuel for combustion. These engines are classified as airbreathing engines. Experimental aircraft exist that use rocket engines for propulsion (e.g., the X-15). Such an engine carries its own oxygen supply. However, this type of engine will not be considered herein.

INTERNAL-COMBUSTION, RECIPROCATING ENGINE

Four-Stroke Cycle of Operation

The reciprocating engine was originally the primary power source used to drive a

*Aerospace Engineer. Mission Analysis Branch.

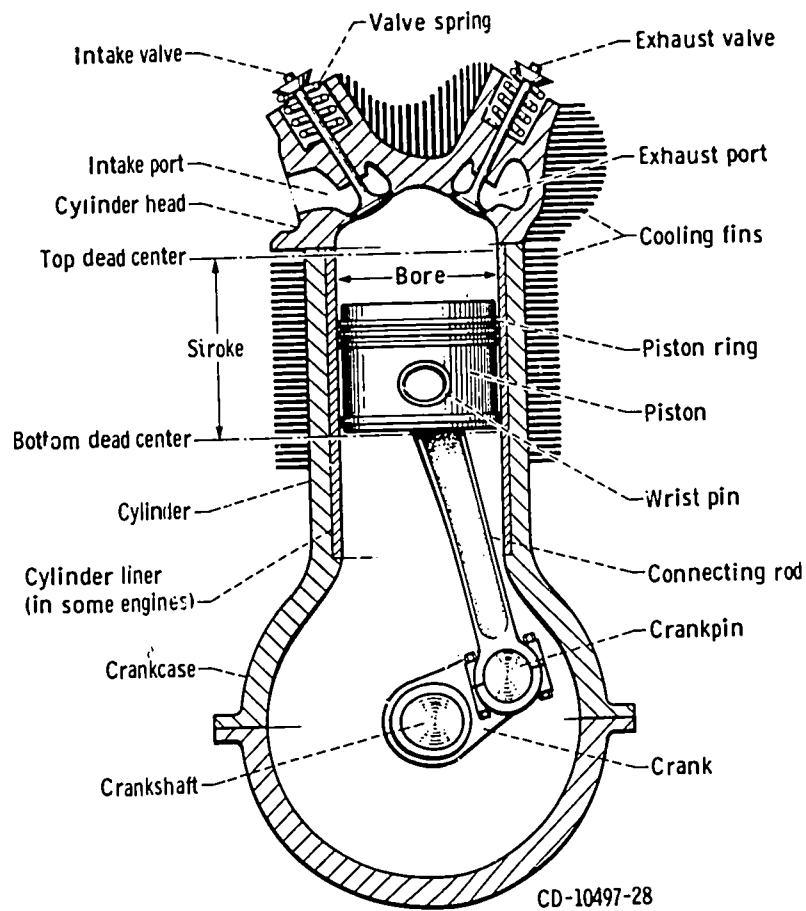


Figure 6-1. - Nomenclature of air-cooled, internal-combustion, reciprocating engine.

propeller. An internal-combustion, reciprocating engine has one or more cylinders in which the combustion of fuel takes place. Some of the principal parts and nomenclature of an air-cooled engine are shown in figure 6-1.

In general, a machine of any kind performing its function repeats over and over again a series of operations. The order in which these operations are performed is fixed, and all parts of the machine return to their original positions at the end of each series. One complete series of this kind is called a cycle.

Most reciprocating engines operate on what is known as a four-stroke cycle; that is, each cylinder requires four strokes of its piston, or two revolutions of the crankshaft, to complete the normal series of operations. There is also a two-stroke cycle, which is normally associated with smaller engines. This cycle is discussed later in the chapter, in the section on model-airplane engines.

The first four-stroke cycle, internal-combustion engine was built by Dr. N. A. Otto, a German, in 1876. Thus, the four-stroke cycle is also called the Otto cycle.

Figure 6-2 illustrates the four strokes (intake, compression, power, and exhaust) of the Otto cycle. The volume swept by the piston during one stroke is called the displacement volume of the cylinder. The volume remaining above the piston at top dead center is called the clearance volume.

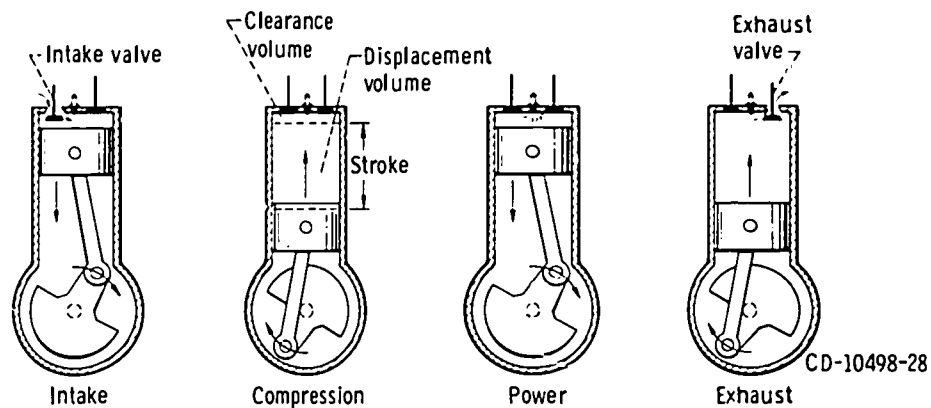


Figure 6-2. - Four-stroke cycle of operation of internal-combustion engine.

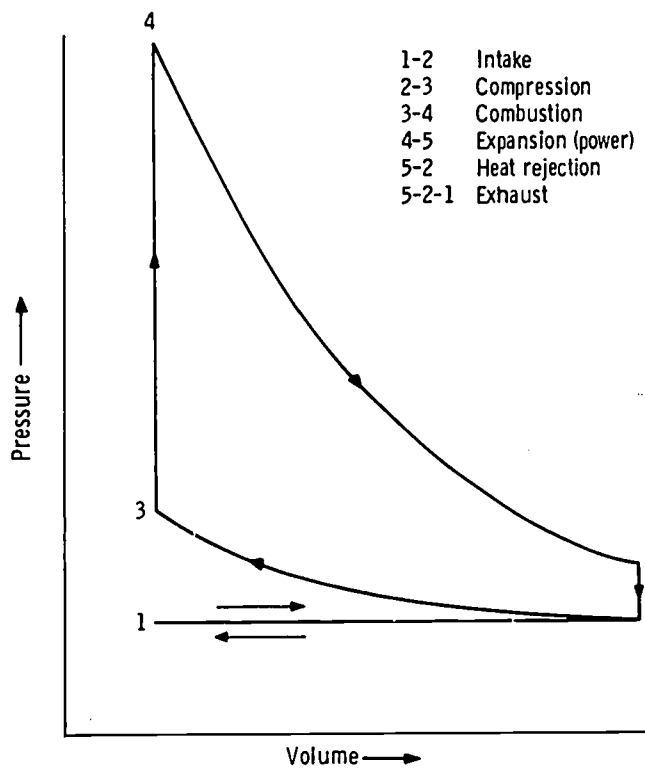


Figure 6-3. - Idealized pressure-volume diagram for cylinder of four-stroke-cycle (Otto cycle) engine.

Figure 6-3 shows a typical pressure-volume diagram for the gas in the cylinder of a four-stroke-cycle engine. The cycle starts with the intake stroke, when the piston is at top dead center (point 1 in fig. 6-3). The intake valve is open, the exhaust valve is closed, and the motion of the piston toward the bottom of the cylinder draws a mixture of fuel and air into the cylinder (line 1-2 in fig. 6-3). When the piston approaches the bottom, the intake valve closes.

The compression stroke (line 2-3) takes place with both valves closed while the piston returns to top dead center. During this stroke, the pressure in the cylinder rises

$$\eta_t = \frac{\text{Work output}}{\text{Fuel-energy input}} \quad (1)$$

$$= \frac{W}{e_c \times w_f} \quad (2)$$

where

W work

e_c chemical energy per pound of fuel

w_f pounds of fuel

The output and input may be measured over any convenient interval such as 1 cycle or 1 minute. Both output and input energies must be expressed in the same kind of units, since η_t is a number without units.

Power Calculations

Power is the rate of doing work. It is generally useless to do a certain amount of work unless it can be done within a reasonable length of time. When work is done at a rate of 33 000 foot-pounds per minute, the quantity of power being produced is known as 1 horsepower. Therefore,

$$\text{hp} = \frac{W/\text{min}}{33\,000} \quad (3)$$

From equation (2),

$$W = w_f \times e_c \times \eta_t \times J \quad (4)$$

where J is the mechanical equivalent of heat (a conversion factor) and has a value of 778 foot-pounds per Btu. Then,

$$\text{hp} = \frac{(w_f/\text{min}) J \times e_c \times \eta_t}{33\,000} \quad (5)$$

The power of an engine depends on the rate at which chemical energy is supplied to the engine (Btu/min) and on the efficiency (η_t) with which the chemical energy supplied is

converted into work output.

The power of an engine can be calculated by first determining the mean effective pressure within a cylinder. This mean effective pressure, in turn, can be determined from the pressure-volume diagram, as will be explained later.

The effective pressure acting against the piston face (top of piston) at any instant during the power stroke is the difference between the downward pressure on the piston face and the upward pressure on the bottom of the piston. This effective pressure varies throughout the power stroke. The average of this effective pressure is called the mean effective pressure (mep).

Work, which is the transfer of energy, is produced when the point of application of a force moves along the line of action of the force. The quantity of work is the product of the force F and the linear displacement L of its point of application in the line of action.

$$W = F \times L \quad (6)$$

The force F is the force (lb) on the piston face. This force is the product of the mean effective pressure mep (lb/in.²) and the area of the piston face A_p (in.²).

$$F = \text{mep} \times A_p \quad (7)$$

The distance L in the work equation is the distance (in.) that the piston travels in the cylinder during one full stroke. Therefore, the work produced in one cylinder during one cycle is given by the equation

$$W = \text{mep} \times A_p \times L \quad (\text{in.} \cdot \text{lb}) \quad (8)$$

But the product of the piston-face area A_p and the stroke L is the displacement volume V_d of the cylinder.

$$V_d = A_p \times L \quad (9)$$

Therefore,

$$W = \text{mep} \times V_d \quad (\text{in.} \cdot \text{lb}) \quad (10)$$

or

$$\text{mep} = \frac{W}{V_d} \quad (11)$$

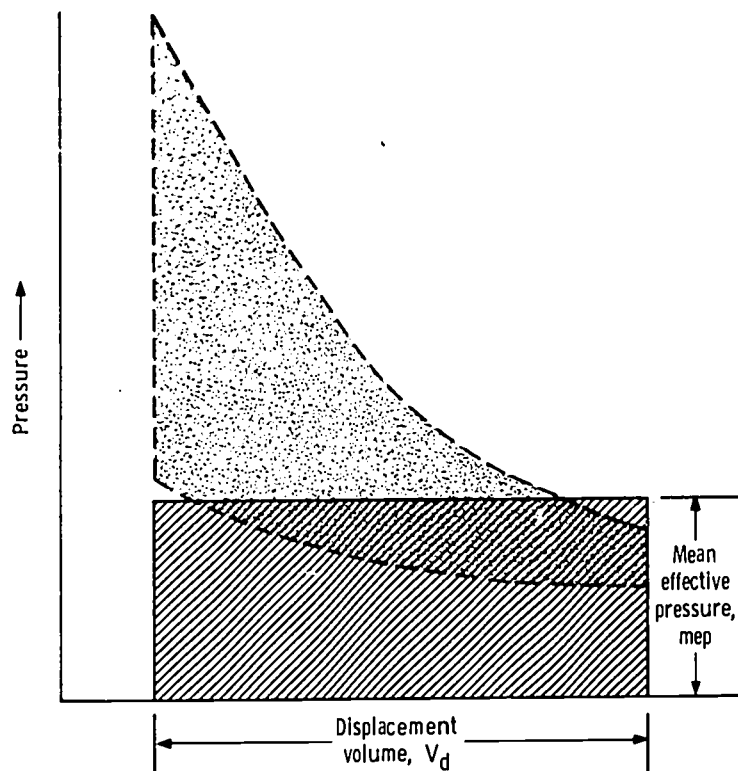


Figure 6-4. - Relation of mean effective pressure to pressure-volume diagram. (Area of rectangle is equal to area within pressure-volume diagram.)

Figure 6-4 illustrates the relation of the mean effective pressure to the pressure-volume diagram. The rectangle in the figure is a simplification of the pressure-volume diagram. The area of the rectangle is the same as the area enclosed within 2-3-4-5-2 in figure 6-3, and the length of the base of the rectangle (displacement volume) is equal to the line 1-2 in figure 6-3. Therefore, the height of the rectangle is the average pressure, or the mean effective pressure.

It has already been shown that the work produced in an engine cylinder during one cycle is the product of the mean effective pressure and the displacement volume. Thus, the area of the rectangle ($mep \times V_d$) or the area of the pressure-volume diagram represents the work of the cylinder. The mean effective pressure, therefore, can be determined by dividing the area of the pressure-volume diagram by the displacement volume.

As shown in figure 6-5, the pressure-volume diagram of an actual engine cycle is somewhat different from that of the ideal Otto cycle. For the ideal cycle, the work of the cylinder is represented by the area within the dashed line 2-3-4-5-2 in figure 6-5. For an actual cycle, the net useful work is represented by the net positive area of the pressure-volume diagram. The net positive area is the positive area within the solid line 2-3-4-5-2 minus the negative area within the solid line 1-2-1. The positive area represents the total work produced in the cylinder. The negative area represents the work required to draw the fuel-and-air mixture into the cylinder (intake) and to discharge

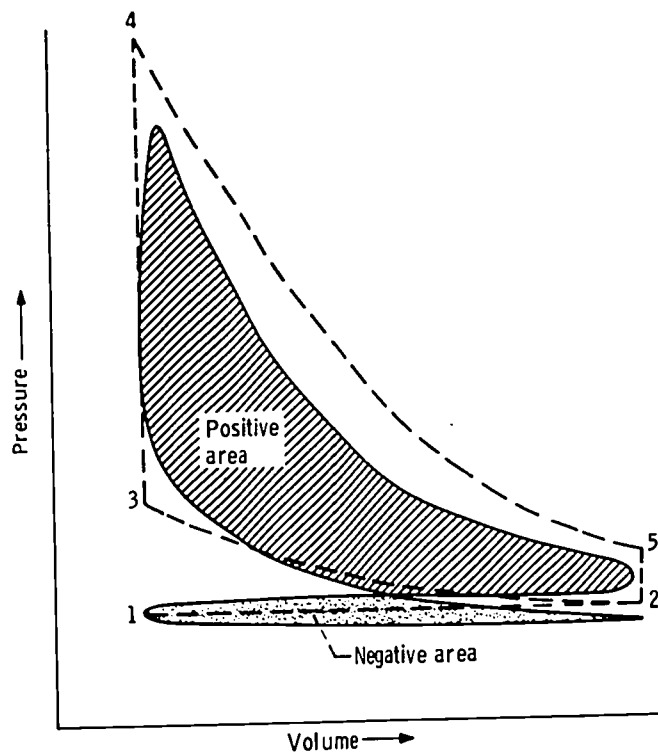


Figure 6-5. - Comparison of pressure-volume diagrams of ideal and actual Otto cycles. (Positive area of diagram of actual cycle represents total work produced in cylinder; negative area represents work expended in drawing fuel-air mixture into cylinder and in discharging exhaust gases from cylinder.)

the products of combustion from the cylinder (exhaust). Thus, for an actual cycle, the mean effective pressure is obtained by dividing the net positive area of the pressure-volume diagram by the displacement volume.

The equation for horsepower was presented earlier in this chapter.

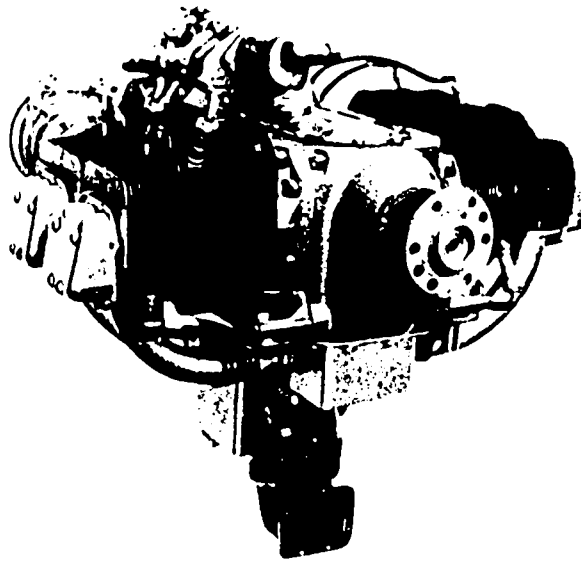
$$\text{hp} = \frac{W/\text{mir.}}{33\,000} \quad (3)$$

From equation (10), the total work produced by the engine W_E in 1 minute is

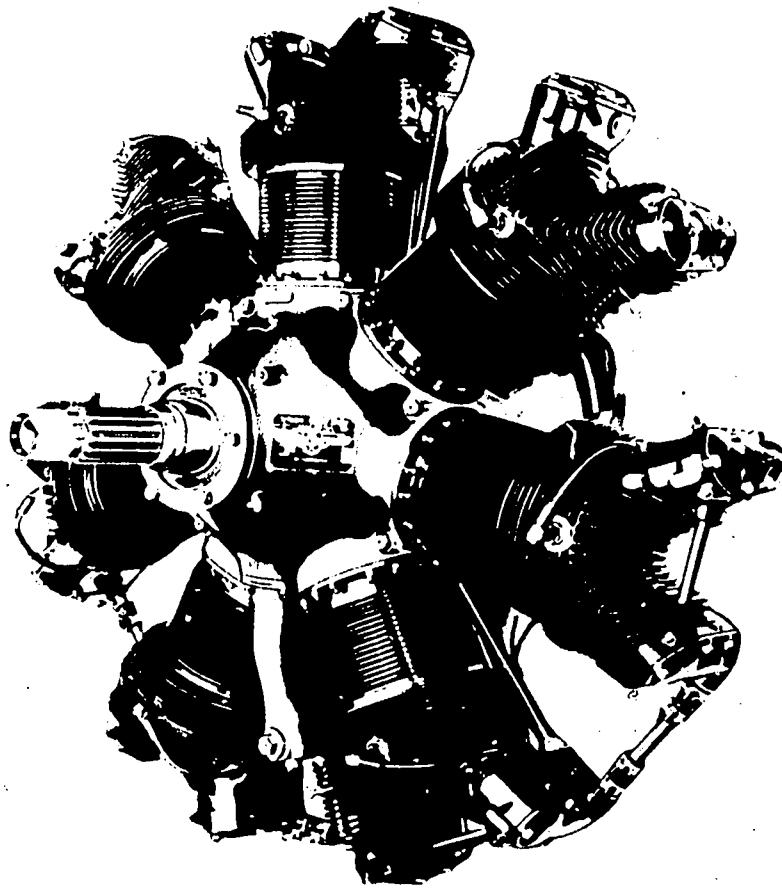
$$\frac{W_E}{\text{min}} = \text{mep} \times V_d \times \text{cpm} \times n \quad (12)$$

where cpm is the number of cycles per minute, and n is the number of cylinders. The horsepower of the engine hp_E is then given by the equation

$$\text{hp}_E = \frac{\text{mep} \times V_d \times \text{cpm} \times n}{33\,000 \times 12} \quad (13)$$



(a) Opposed-cylinder engine (4 cylinders, air cooled).



(b) Radial engine (7 cylinders, air cooled).

Figure 6-6. - Reciprocating engines.

where 12 is the factor for converting the denominator from foot-pounds to inch-pounds. This conversion is necessary because the numerator is in inch-pounds (see eqs. (8) and (10)).

Engine Types

Reciprocating engines are commonly classified according to their cylinder arrangements. An in-line engine has its cylinders arranged in a straight line parallel to the crankshaft. Such a line, or row, of cylinders is called a bank. A V-engine has two, a Y-engine has three, and an X-engine has four banks of cylinders so arranged that they resemble, in an end view of the engine, the respective letter. An opposed-cylinder engine (fig. 6-6(a)) has two banks of cylinders on opposite sides (180° apart) of the crankshaft. In this configuration, the axes of the cylinders are usually in the horizontal plane. A radial engine (fig. 6-6(b)) has its cylinders arranged radially around the crankshaft, like the spokes of a wheel. The radial engine is the most popular reciprocating engine for aircraft, because it has a relatively short, stiff crankshaft and a compact crankcase. The frontal area of the radial engine is relatively large, however. Small in-line engines are usually air-cooled, and large in-line engines are usually water-cooled. Radial engines are almost always air-cooled.

JET ENGINES

Gas-Turbine Engines

A gas-turbine engine is essentially a compressor-combustor-turbine combination which provides a net useful shaft-torque output and/or a useful supply of hot, high-pressure exhaust gases. The method used to harness the shaft torque and/or the energy of the exhaust gases to provide thrust determines whether the gas-turbine engine is a turbojet, turbofan, or turboprop engine.

Brayton cycle of operation. - The gas-turbine engine operates on a thermodynamic cycle known as the Brayton cycle. In the ideal Brayton cycle, air is compressed, heated at constant pressure, expanded, and finally cooled at constant pressure. Actually, the cooling phase is an open part of the cycle; that is, the hot air is exhausted, and a fresh charge of cool air is drawn in to be compressed.

Figure 6-7 is an idealized pressure-volume diagram of a gas-turbine engine. This figure illustrates the Brayton cycle of operation and the interrelation of the compressor work and the turbine work of the engine. In the ideal cycle, air enters the compressor at atmospheric pressure (line 1-2 in fig. 6-7), is compressed (line 2-3), and is discharged into the combustor (line 3-4). The area within 1-2-3-4-1 represents the work consumed in the compression (i. e., the work required to drive the compressor). In the combustor,

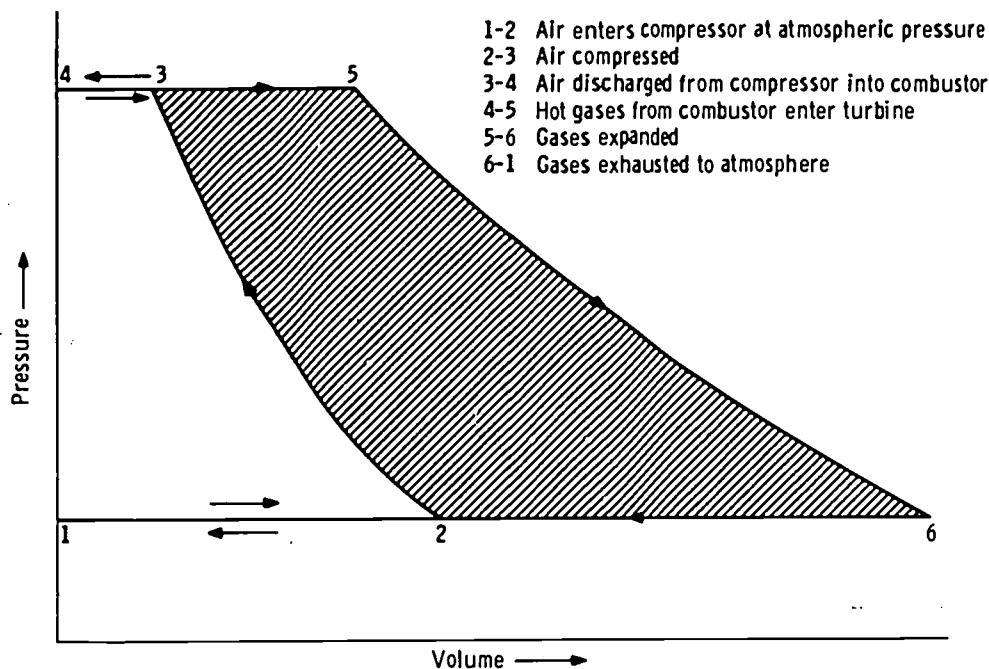
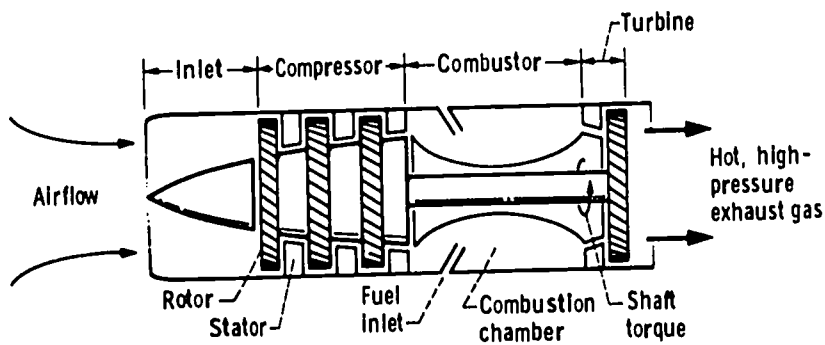


Figure 6-7. - Idealized pressure-volume diagram for Brayton cycle of operation of gas-turbine engine. (Shaded area represents net useful work output of engine.)

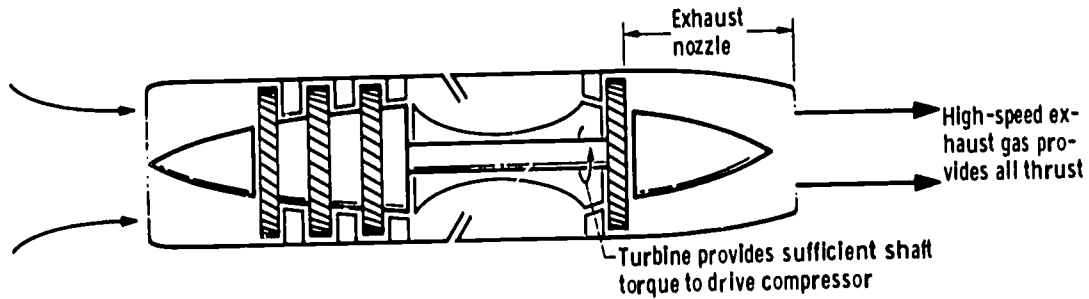
the air is mixed with fuel, and the mixture is burned at constant pressure. During this constant-pressure heating, the original volume of air entering the combustor (line 3-4) becomes a larger volume of hot combustion gases that enters the turbine (line 4-5). This increase in volume of the working gas during combustion enables an ideal turbine to produce more work than an ideal compressor consumes. Next, the hot combustion gases are expanded (line 5-6) to ambient pressure. The gases may be nearly fully expanded in the turbine to produce shaft power, or they may be partially expanded in the turbine, to produce some shaft power, and partially in an exhaust nozzle to produce a high-velocity exhaust stream. After expansion, the gases are exhausted to the atmosphere (line 6-1) at ambient pressure. This total cycle of operation is continuous, so that fresh air is continuously entering the engine while exhaust gases are continuously being discharged.

The total work produced by the engine is represented by the area 4-5-6-1-4 in figure 6-7. The work required by the compressor is represented by the area 1-2-3-4-1. Therefore, the net useful work output of the engine is represented by the area 2-3-5-6-2.

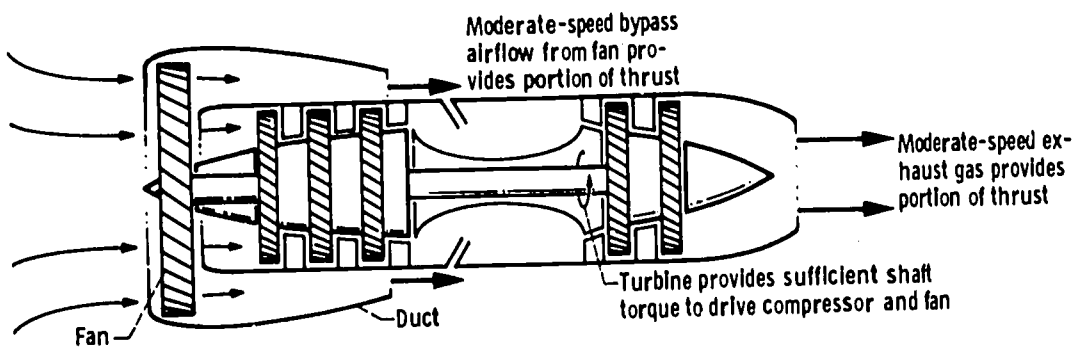
A schematic diagram of a basic gas-turbine engine is shown in figure 6-8(a). The compressor is essentially a gas pump and is generally classified as either a centrifugal-flow or an axial-flow compressor. The present discussion concerns only axial-flow compressors. The axial-flow compressor is made up of a multiplicity of stages. Each stage consists of a rotating element (rotor) and a stationary element (stator). Each element is circular and has blades mounted radially on its periphery. The gas flows through these stages in a generally axial direction, and the pressure of the gas rises in each stage.



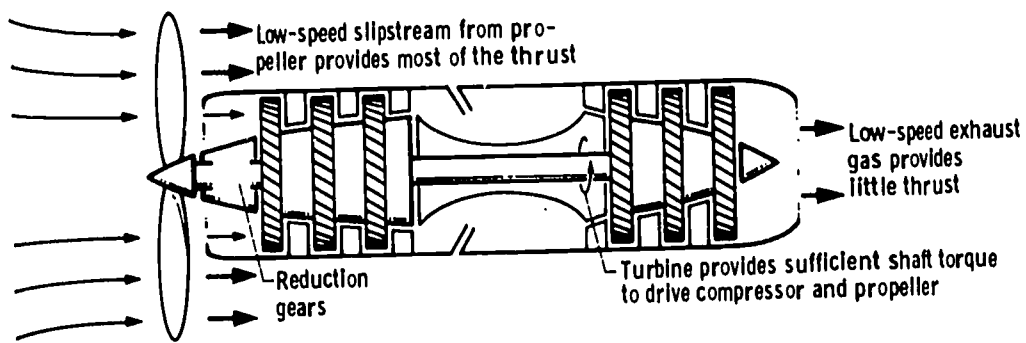
(a) Basic gas-turbine engine.



(b) Turbojet engine.



(c) Turbofan engine.



(d) Turbopropeller engine.

Figure 6-8. - Schematic diagrams of gas-turbine engines.

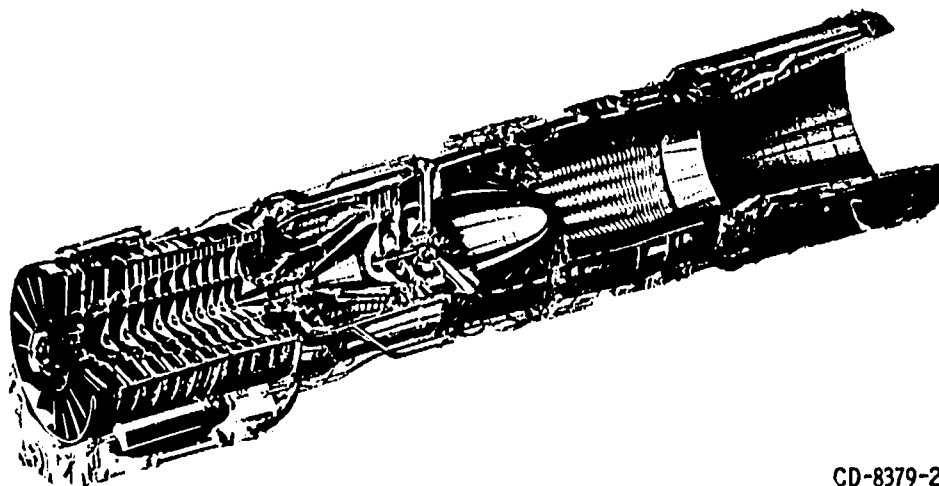
The rotor blades increase both the velocity and the pressure of the gas. The stator blades reduce the velocity of the gas and thereby convert its kinetic energy into pressure. The high-pressure gas from the compressor is mixed with fuel (kerosene or gasoline) and burned in the combustor. The high-pressure, high-temperature gas is then expanded through the turbine, which drives the compressor and provides a net useful shaft power. In certain types of gas turbine engine, the gas is further expanded through a nozzle to provide a high-velocity exhaust stream.

Turbojet engine. - In a turbojet engine, shown schematically in figure 6-8(b), the gases are partially expanded in the turbine only to provide sufficient shaft power to drive the compressor and accessories. The turbojet engine achieves its thrust by expanding and accelerating the hot gas in a nozzle (i. e., by imparting high momentum to a fluid).

Turbofan engine. - The turbofan (or bypass) engine (fig. 6-8(c)) is a turbojet that has a fan as an additional compressor, along with a duct for the cold air which bypasses the basic gas-turbine engine. To drive the fan, an additional turbine is required, wherein the gas from the combustor is further expanded. Thus, lower velocity exists in the nozzle, since the gas has less available energy to be converted to velocity. However, the large fan enables the engine to draw in more air. Thus, the turbofan engine produces thrust by a combination of high airflow and moderate exhaust velocities.

Turbopropeller engine. - The turbopropeller engine (fig. 6-8(d)) has a propeller driven by a substantially enlarged turbine by means of gears. Nearly all the available gas energy is used in the turbine to drive the propeller. The airflow that the propeller accelerates produces nearly all the thrust for this engine type, with very little nozzle expansion occurring for additional thrust.

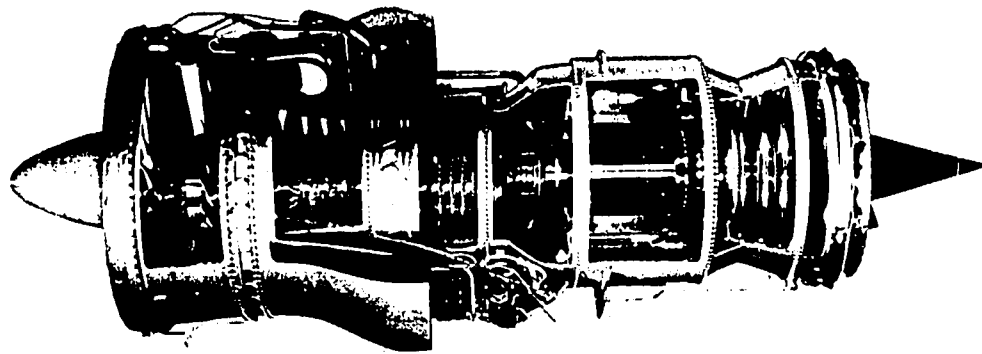
Obviously, all these engines are adaptations of the basic gas-turbine engine. Some examples of these various types of gas-turbine engines are shown in figure 6-9.



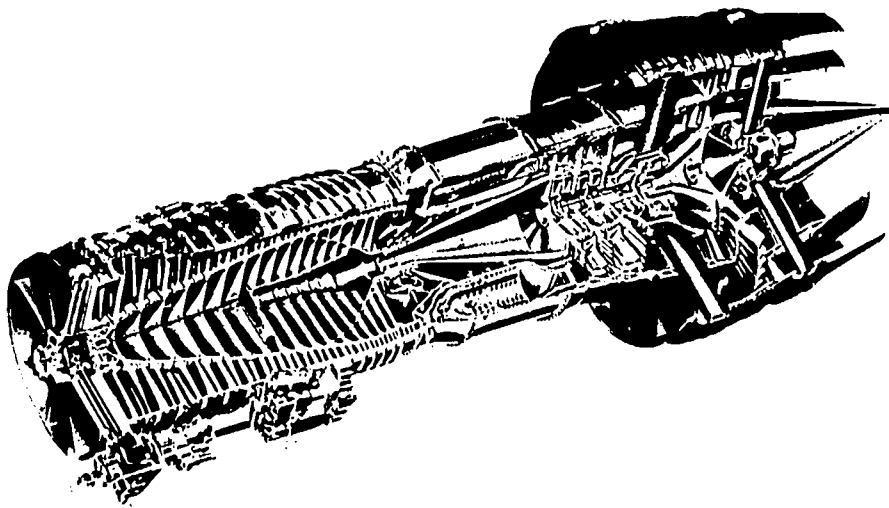
CD-8379-28

(a) Turbojet engine with afterburner. (General Electric YJ93-GE3.)

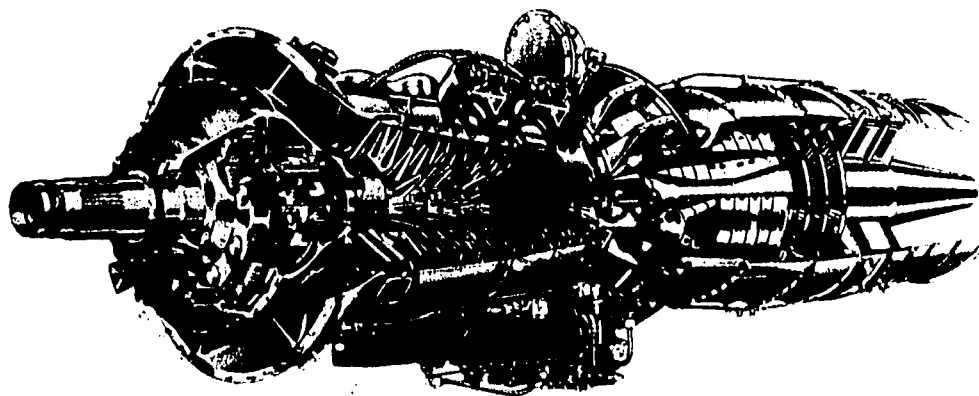
Figure 6-9. - Cutaway views of typical gas-turbine engines.



(b) Turbofan engine with forward fan. (Pratt & Whitney JT3D-3B.)



(c) Turbofan engine with aft fan. (General Electric CJ805-23B.)

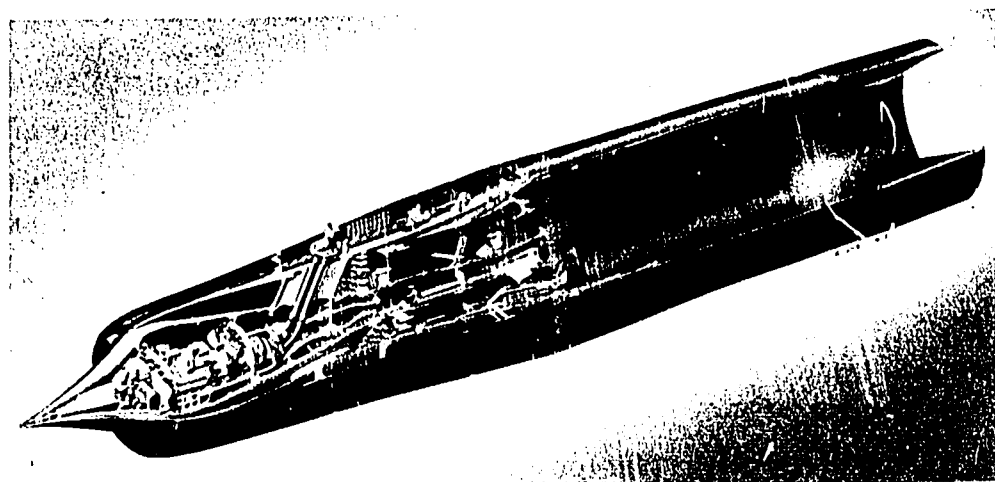
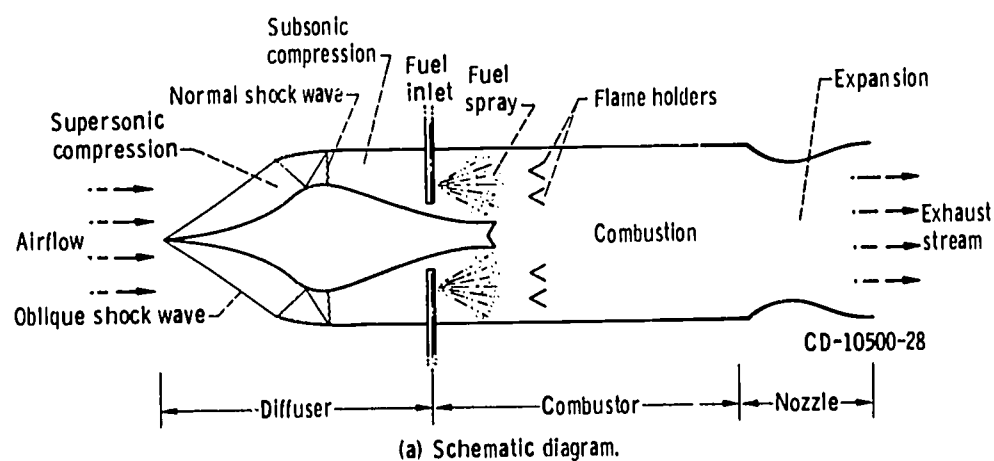


(d) Turbopropeller engine. (Pratt & Whitney T34-P-9W.)

Figure 6-9. - Concluded.

Ramjet Engines

The ramjet (fig. 6-10) is the simplest of all airbreathing engines; it consists of a diffuser, a combustion chamber, and an exhaust nozzle. In the diffuser, the pressure rises as the incoming air is decelerated from flight speed to a relatively low speed (Mach 0.1 to 0.3) before it enters the combustion chamber. The air entering the diffuser is compressed by the ramming action caused by the engine's high forward speed. The air is then mixed with fuel and burned in the combustion chamber. The hot combustion gases are then expelled through the nozzle. Since the incoming air is decelerated to such a low speed, a ramjet can operate at subsonic speeds, but it cannot operate under static conditions (i. e., it cannot develop takeoff thrust). The increased pressure rise occurring in the diffuser at increased flight speeds renders the ramjet more suitable for supersonic flight.



(b) Cutaway view. (Courtesy of Marquardt Corp.)

Figure 6-10. - Ramjet engine.

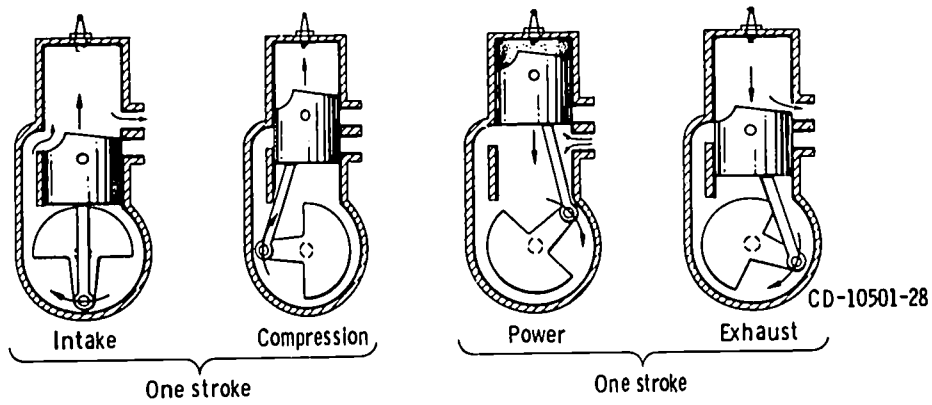


Figure 6-11 - Two-stroke cycle of operation of internal-combustion engine.

First, by creating a partial vacuum in the crankcase, the mixture (fuel and air) is sucked into the crankcase through a special port. Second, vaporized fuel mixture previously forced upward through the bypass passage to the space above the piston is now greatly compressed and ignited. During the resulting power stroke the downward-moving piston uncovers the exhaust port to allow exhaust gases to blow out, and it uncovers the intake port at the upper end of the bypass to allow fresh fuel mixture to push its way into the

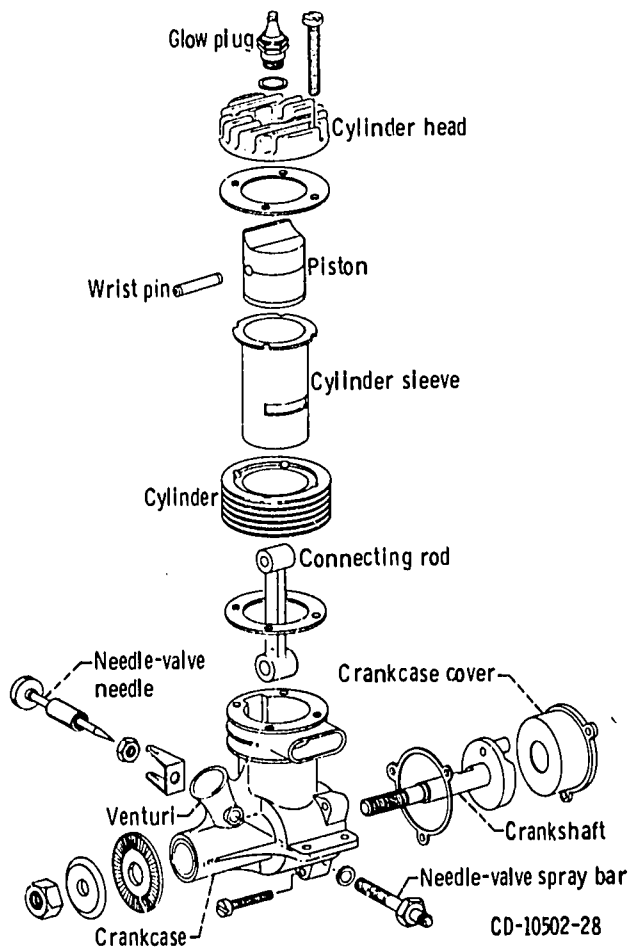


Figure 6-12 - Model-airplane engine.

cylinder. Then, as the piston moves upward again, it covers the exhaust port opening and the bypass intake port, thereby trapping the fuel charge in the combustion chamber. It is interesting to note that vaporized fuel mixture actually fills the crankcase of the two-stroke-cycle engine.

Even though most model airplane engines are of the two-stroke-cycle type, considerable differences may be found between engines of different manufacturers and even between different engines of the same manufacturer. These differences may or may not be obvious and/or significant. Figure 6-12 shows an exploded view of a typical model engine and its nomenclature.

Fuel Systems

One way of classifying model-airplane engines is according to the method used to introduce the fuel mixture into the cylinder. In the two-stroke cycle, for the downward-moving piston to drive the vaporized fuel mixture up through the bypass into the combustion chamber, the crankcase must be sealed. Yet, for the mixture to get into the crankcase in the first place, an opening must be provided. Thus, some means is necessary to close off this opening or port when the piston travels downward and to open it when the piston moves upward.

The simplest and most popular porting system is the shaft valve. This system is characterized by the location of the venturi, or air intake, at the lower front of the cylinder. The crankshaft is bored out from the rear, so that it is hollow, or tubular, for most of its length. At the point where the axis of the venturi crosses the crankshaft, there is a hole through the wall of the crankshaft to the central bore. This hole is radially positioned so that it coincides with the venturi opening at precisely the right time during each cycle to allow the fuel and air mixture to pass from the venturi through the crankshaft into the crankcase. Furthermore, the size of this hole in the wall of the crankshaft determines how long during each revolution of the crankshaft, or each cycle, the mixture can enter the crankcase.

The second most popular intake porting method is the rear rotary valve. In this system, the venturi attaches to the rear crankcase cover and extends outward to the rear, usually in a horizontal position. Inside the crankcase, an accurately machined disk of metal faces up snugly to the smooth inside face of the rear crankcase cover plate. This disk is rotated by an extension of the crankshaft. Cut through the disk is an elongated, arc-shaped opening concentric with the circumference of the disk. The placement and length of this slot as it passes over the opening from the venturi are designed to allow the vaporized fuel mixture to enter the engine at the proper time. The slot determines when and how long the fuel may enter the crankcase during each cycle.



A highly efficient porting system, but one that imposes very exacting design and manufacturing requirements, is the reed-valve system. In this design a thin strip of appropriate metal covers and uncovers an intake port in the rear crankcase cover plate in response to variations in crankcase pressure during each cycle.

Regardless of what method is used to introduce the mixture into the cylinder, a carburetion system is needed to supply the correct amount of the proper mixture of fuel and air to the cylinder. The typical model airplane engine has a very simple carburetor consisting of a venturi and a needle valve, which extends across the throat (i. e., the narrowest portion) of the venturi.

A venturi is a convergent-divergent (wasp-waisted) passage in which the pressure energy of the airstream entering the wide end of the passage is converted into kinetic energy by the acceleration of the airstream through the narrow part of the passage. The model-airplane engine venturi is designed, in length and cross section, to supply the proper amount of air to the engine and to provide maximum acceleration of the air as it passes the needle valve.

In the model-airplane engine, the action of the piston creates a vacuum in the crankcase. Because of this vacuum, air from outside the engine is drawn into the crankcase through the venturi. In other words, the higher pressure outside the engine pushes air into the crankcase. The air enters the wide end of the venturi at some particular flow rate. (Flow rate is the quantity of air passing a given point in the passage per unit of time.) If the pressure difference between the outside and inside of the crankcase remains constant, the pressure will continue to push air into and through the venturi at a constant flow rate. As the cross-sectional area of the converging passage becomes smaller, fewer molecules of air can pass through the reduced area simultaneously. (This holds true only at subsonic velocities, where air is considered to be incompressible.) Therefore, each molecule passing through the constriction must speed up to allow the same number of molecules that enter the wide end of the venturi per unit of time to pass through the constricted part in the same unit of time.

According to Bernoulli's law (see chapter 5), as the velocity of the airflow in the throat of the venturi increases, the pressure decreases. This reduced pressure, as well as the vacuum in the crankcase, causes fuel to be drawn out of the needle valve and mixed with the air in the venturi.

The needle valve is used to set the fuel flow to obtain the desired air-fuel mixture ratio. The needle valve is basically a tube with a tapering rod that fits inside it. The tube (called the spray bar) is mounted across the throat of the venturi. One or two holes are drilled in the wall of the spray bar where it crosses the venturi throat. The fuel line from the tank is connected to one end of the spray bar, and the tapering rod (called the needle, or pin) is inserted in the other end. The end of the spray bar and a portion of the needle are threaded to provide a means of adjusting the position of the needle in the

spray bar. As the needle is screwed inward or outward, a different portion (thicker or thinner) of the tapered needle is located over the hole in the wall of the spray bar. Thus, the obstruction in the path of the fuel is varied.

The venturi-and-needle-valve combination is simple and highly effective, but, since it lacks the float-and-valve system of more elaborate carburetors, it cannot compensate for the changing fuel requirements of the engine during operation. Normally, the needle valve is set before the plane takes off and the setting cannot be changed during flight. However, an engine may be equipped with a pivoted butterfly valve to alter the amount of air entering through the venturi, a double needle valve to alter the amount of fuel entering the crankcase, and a pivoted cover over the exhaust to alter the back pressure in the cylinder. These three devices are usually interconnected to operate simultaneously, and they provide at least two distinct power settings, for high-speed and low-speed operation.

Ignition Systems

Model-airplane engines may be classified according to their ignition systems. Three systems are commonly used to ignite the fuel charge in the cylinder.

The most popular system is the glow-plug system, which has the advantages of simplicity and lightness. The glow plug is similar in appearance to a spark plug, but instead of having two electrodes, it has a small filament. This filament is heated from an outside source (the booster battery) while the engine is being started. Once the engine is running properly, the booster leads are removed, and the glow plug maintains sufficient heat to continue igniting the fuel under compression. The fuel is specially blended to ensure easy ignition and to provide proper lubrication.

Less popular is the spark ignition system, which uses an ordinary spark plug, together with a spark coil, condenser, batteries, switch, and wiring, all of which must be carried inside the plane. A set of contacts, or points, is contained in a housing, usually at the front of the engine, on the shaft. These points make and break contact by means of a cam on the shaft, which separates the points when the lobe, or bump, of the cam comes by once every revolution. By means of a spark coil and condenser, a high-tension current is shot to the spark plug when the points separate. (The collapse of the magnetic field when the points separate produces a high-voltage inductive "kick".) Inside the combustion chamber, an intense spark jumps across the narrow gap formed by the two electrodes of the plug and ignites the fuel charge. This system uses a mixture of gasoline (usually white gas) and SAE No. 70 oil, mixed either two or three parts gasoline to one of oil.

One advantage of this spark ignition system is that the spark may be advanced or retarded to govern the engine speed. Another advantage is the relatively low cost of the fuel. A disadvantage is that the weight of all the extra gear requires a plane large enough

to carry the extra load, and it handicaps the performance of the plane. For this reason, the spark ignition system is used only on relatively large engines.

The third ignition system is compression ignition, or the diesel system. In this case, a special fuel ignites by itself when quickly and greatly compressed. Such a fuel consists of ether, oil, and kerosene, usually in equal parts. However, there are many mixture variations, such as 50 percent ether and 50 percent diesel truck fuel. Compressing the fuel mixture to the point of ignition requires a much higher compression ratio than is required with other ignition systems. Therefore, a diesel engine must be stronger and is usually heavier than an equivalent glow-plug or spark-ignition engine. This extra weight is a handicap in a model airplane. In a diesel engine, the compression ratio required for starting is often different from that required for continuous running. Even while the engine is running, the compression ratio must sometimes be varied because of fuel mixture, excessive fuel introduced into the engine by choking or priming, temperature, etc. The compression ratio in a model diesel engine is varied by means of an adjustable conrapiston that fits inside the cylinder at the cylinder head. A T-shaped lever that is connected to the conrapiston extends out through the cylinder head. By turning the lever the conrapiston can be screwed further into or out of the cylinder. This way the volume of the cylinder is decreased or increased, and the compression ratio is increased or decreased. Normally, the conrapiston is adjusted until the particular fuel mixture ignites easily for starting, and then it is readjusted, if necessary, for high-speed running.

Controls

As discussed in the preceding sections, all model engines are equipped with some control devices that affect the performance. The glow-plug engine has a needle valve that controls the fuel and air mixture and, thereby, the speed. The needle valve can be adjusted while the engine is operating, but normally it cannot be adjusted in flight. However, some glow-plug engines are equipped with special venturis, needle valves, and exhausts that can be adjusted during flight for high-speed and low-speed operation. These devices were discussed earlier. The ignition timing of the glow-plug engine cannot be adjusted, because the filament of the plug glows continuously during operation. However, a minor degree of control over the timing is possible by selecting a plug that glows strongly, for early ignition, or a plug that glows weakly, for late ignition. Similar results can be achieved by choosing a fuel that ignites more easily or less easily. Obviously, adjustments cannot be made by these indirect means of control while the engine is operating.

The spark-ignition model engine has the same fuel-mixture control (needle valve) as does the glow-plug engine, but its ignition timing can also be advanced or retarded to suit

the operating requirement. With this system the ignition timing can be adjusted while the engine is operating.

The diesel model engine has a needle valve for control of the fuel mixture. The ignition timing of the diesel engine is controlled by means of the adjustable contrapiston, which was described earlier. This contrapiston can be adjusted while the engine is operating, but it cannot be adjusted in flight.

Displacement Volume

In addition to being classified according to its intake porting and its ignition system, a model airplane engine may also be classified according to its size. The size is based on piston displacement, which is the volume displaced by the piston in a cylinder in a single stroke. The displacement volume is the product of the piston travel, or stroke, and the cross-sectional area of the cylinder. The engine classes based on size are given in the following table:

| Class | Displacement, in. ³ |
|-----------------|-----------------------------------|
| $\frac{1}{2}$ A | 0.000 to 0.050 |
| A | .051 to .200 |
| B | .201 to .300 |
| C | .301 to .650 |

BIBLIOGRAPHY

- Anon.: Aviation Week and Space Technology, vol. 86, no. 10, Mar. 6, 1967, pp. 191-196.
- Durham, Franklin P.: Aircraft Jet Powerplants. Prentice-Hall, Inc., 1951.
- Hesse, Walter J.; and Mumford, Nicholas V. S., Jr.: Jet Propulsion for Aerospace Applications. Pitman Publishing Corp., 1964.
- Rogowski, Augustus R.: Elements of Internal Combustion Engines. McGraw-Hill Book Co., Inc., 1953.
- Wilkinson, Paul H.: Aircraft Engines of the World 1964/1965. Paul H. Wilkinson, Washington, D.C.

7. GAS-TURBINE JET ENGINES

Jack B. Esgar*

Within the last 15 years, the jet engine has almost completely replaced the reciprocating (piston) engine as a power plant for high-performance, high-speed aircraft. The two main reasons for this change are (1) the propeller used with reciprocating engines becomes inefficient as the velocity of the propeller tip relative to the airstream exceeds sonic velocity, and (2) the power output for a given engine weight for turbine engines is much greater than for reciprocating engines. As a practical limitation, propeller-driven airplanes are limited to flight Mach numbers of about 0.6 (450 mph) or less. Maximum efficient cruise speeds for propeller-driven aircraft are of the order of 300 miles per hour. Commercial jet aircraft cruise efficiently at speeds in excess of 600 miles per hour, and some military aircraft cruise at about 2000 miles per hour. The U.S. supersonic transport, now under development, will be powered by gas-turbine jet engines and will cruise at almost 1800 miles per hour. The main purpose of the jet engine, therefore, is to enable aircraft to fly efficiently at the high speeds demanded by both military and civilian aviation.

Through the development of the modern airplane powered by jet engines, practically any place in the United States is within 4 hours' flying time, and Europe is only 8 hours away by commercial transportation. It is even possible for the traveler to leave the United States in the morning and land in the Orient before sundown. When supersonic transports become operational, these flying times will be cut by as much as two-thirds.

The term "jet engine" is a generic term that can refer to a wide variety of power plants, including turbojet and turbofan engines for powering conventional aircraft, rocket engines for launching space vehicles, and ramjet engines for powering future hypersonic aircraft. In this chapter, however, the term "jet engine" refers to gas-turbine jet engines, such as turbojets and turbofans. Some of the principles discussed, however, are equally applicable to other types of jet engines.

*Assistant Chief, Airbreathing Engines Division.

THRUST AND POWER COMPARISONS BETWEEN RECIPROCATING AND JET ENGINES

Conventionally, a reciprocating engine is rated by the horsepower it delivers at the propeller shaft, and a jet engine is rated by the amount of jet thrust it generates. For a 100-percent efficient conversion, horsepower and thrust can be related by the following equation:

$$\text{Horsepower} = \frac{(\text{Thrust})(\text{Flight speed})}{550}$$

where the thrust is in pounds, the flight speed is in feet per second, and 550 is the factor for converting foot-pounds per second to horsepower. At constant altitude and subsonic velocity, a gas-turbine jet engine develops nearly constant thrust over a wide range of velocities. It can be seen from the above equation that the faster an airplane flies, the more horsepower a jet engine will develop. A reciprocating engine, on the other hand, develops essentially constant power for a given altitude over a range of flight velocities. Thus, the thrust from a reciprocating engine is high at low velocities, but decreases as velocity increases. According to the equation, the thrust of a reciprocating engine should be infinite at zero velocity. Actually, the thrust is limited by the propeller. A conventional aircraft propeller has a thrust limit of approximately 3.5 pounds of thrust per horsepower.

Figure 7-1 presents a comparison of thrust and horsepower outputs of three actual engines (R-4360, JT8D, and GE4), for speeds up to 600 miles per hour at sea level.

The R-4360 is a radial, reciprocating engine built by Pratt & Whitney Aircraft. It is the largest and most powerful aircraft reciprocating engine built. The maximum power at the propeller shaft is 3500 horsepower. The engine weighs approximately 3500 pounds.

The JT8D is a turbofan jet engine used extensively in commercial aircraft such as the Boeing 727 and 737 and the McDonnell Douglas DC-9. The engine, built by Pratt & Whitney Aircraft, has a maximum thrust of 14 000 pounds and weighs approximately 3100 pounds.

The GE4 is a turbojet engine under development by the General Electric Company to power the U.S. supersonic transport. It will have a maximum thrust of about 67 000 pounds and will weigh about 11 000 pounds. At cruise altitude of 65 000 feet and cruise speed of about 1800 miles per hour, the thrust will be reduced to about 15 000 pounds as a result of the rarified air at that altitude.

The R-4360 and the JT8D are approximately the same weight (actually the JT8D is lighter) but the jet engine has greater thrust at all flight speeds and is able to fly at higher speeds. At 300 miles per hour the thrust of the R-4360 has dropped to about one-third of that of the JT8D. The horsepower per pound of engine weight developed by the reciprocating engine is

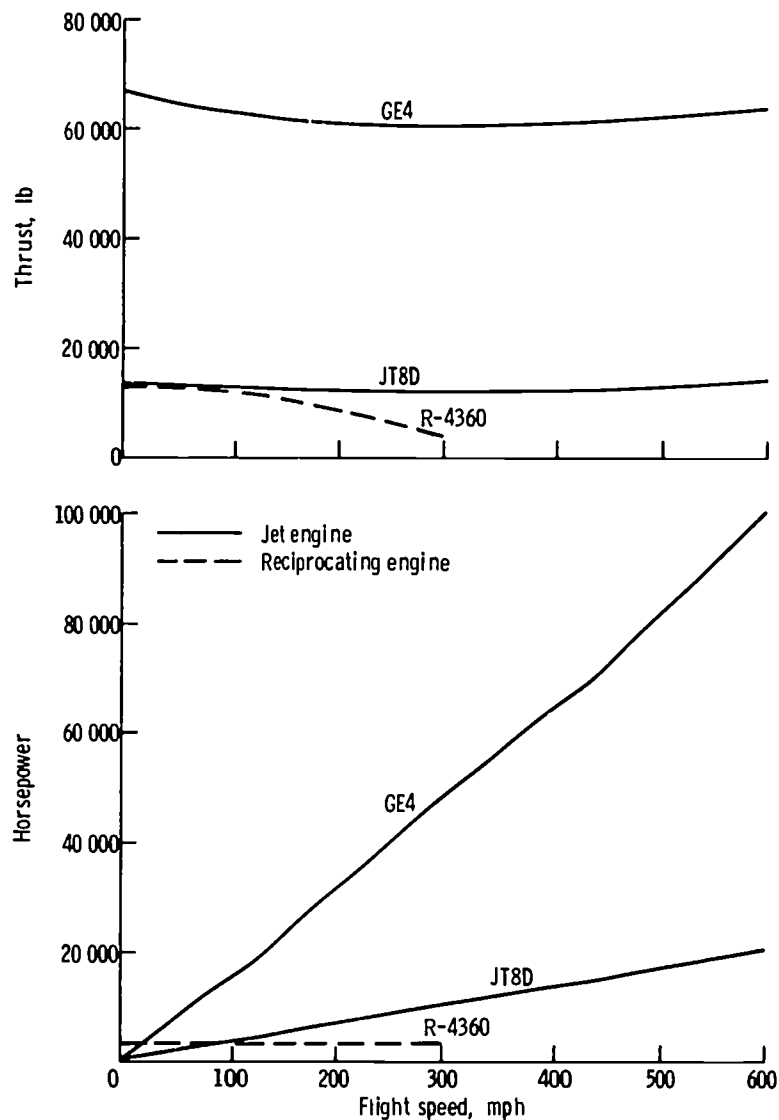


Figure 7-1. - Thrust and horsepower comparisons of reciprocating and jet aircraft engines at sea level.

cating engine remains constant at about 1 horsepower per pound at all flight speeds, but at 600 miles per hour the JT8D jet engine develops almost 7 horsepower per pound. The bigger and more powerful GE4 jet engine develops over 9 horsepower per pound at 600 miles per hour at sea level.

All engines have some limiting flight speed. The practical speed limit for the reciprocating engine is between 300 and 400 miles per hour, because of the low propeller efficiency at high speeds and the steady loss in thrust as speed increases. Jet engines such as the JT8D are primarily subsonic engines. This subsonic limit is imposed by the temperature of the air entering the engine. The GE4, on the other hand, is designed for higher temperatures by using higher temperature materials and cooling in strategic areas. At flight speeds of Mach 2.7 (approximately 1800 mph), at which the U.S. supersonic transport will cruise, the air entering the engine will be approximately 500° F as a result of air compression in the inlet.

At this flight speed and at high altitude, the engine thrust of the GE4 will be approximately the same as that of the JT8D flying subsonically at sea level, but because of the high supersonic cruise velocity, the GE4 will develop about $3\frac{1}{2}$ times as much power as the JT8D does subsonically.

JET-ENGINE THRUST

The thrust of the jet engine is similar to that produced by a toy balloon when it is blown up and released so that the air can escape. Many people think that this thrust results from the escaping air pushing on the air outside of the balloon. This is not a true explanation. The thrust would also occur in a vacuum. To understand the mechanism of this thrust consider figure 7-2. Figure 7-2(a) shows an inflated balloon with the opening

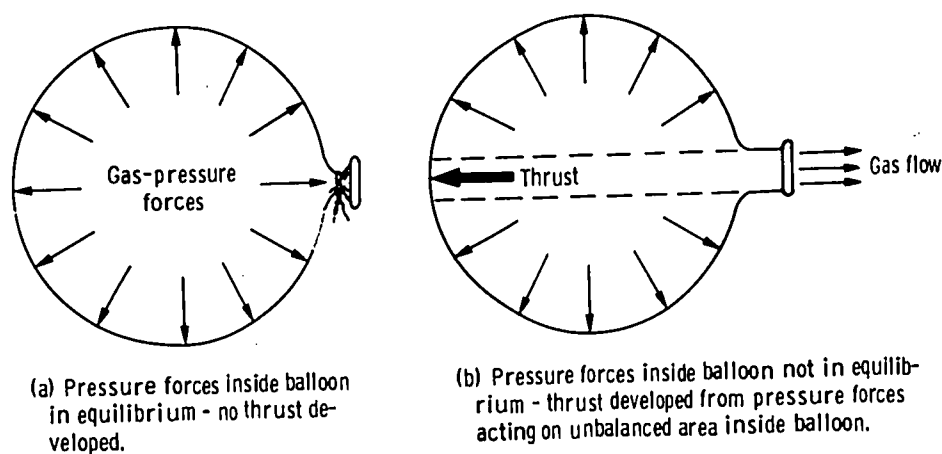


Figure 7-2. - Jet thrust from toy balloon.

shut. On the inside of the balloon the gas pressure forces act equally in all directions. As a result, the balloon is in equilibrium; that is, there are no forces causing the balloon to move. Figure 7-2(b) shows the inflated balloon with an opening through which the gas can escape. Now, unequal pressures are acting on the inside of the balloon. At the balloon opening there is no surface for the pressure to act against, but directly opposite the opening the pressure is pushing against the inside of the balloon. As a result, the balloon is accelerated in the direction shown.

In the example of the toy balloon, the thrust is equal to the product of the pressure difference between the inside and outside of the balloon and the net unbalanced area inside the balloon against which the internal pressure acts. This thrust is also equal to the change in momentum per unit time of the gas as it leaves the balloon. Momentum per unit time is the product of mass flow rate (weight flow rate divided by a gravitational constant g) and the velocity. Since the initial velocity of the gas inside the balloon is zero,

gas. Therefore a jet engine must be capable of pumping the air entering the engine to a high pressure, heating it to a high temperature, and then expanding it through an exhaust nozzle to a high velocity. Five major engine components are required to generate this high-temperature, high-velocity exhaust-gas stream to produce thrust in the jet engine. These components are the engine inlet, the compressor, the combustor, the turbine, and the exhaust nozzle. For some applications, additional components, such as a fan or an afterburner, are added to provide greater thrust.

FUNCTIONS OF ENGINE COMPONENTS

Figure 7-3 shows cutaway and exploded views of a turbojet engine. Figure 7-4 illustrates schematically the main components of turbojet engines for subsonic and supersonic flight.

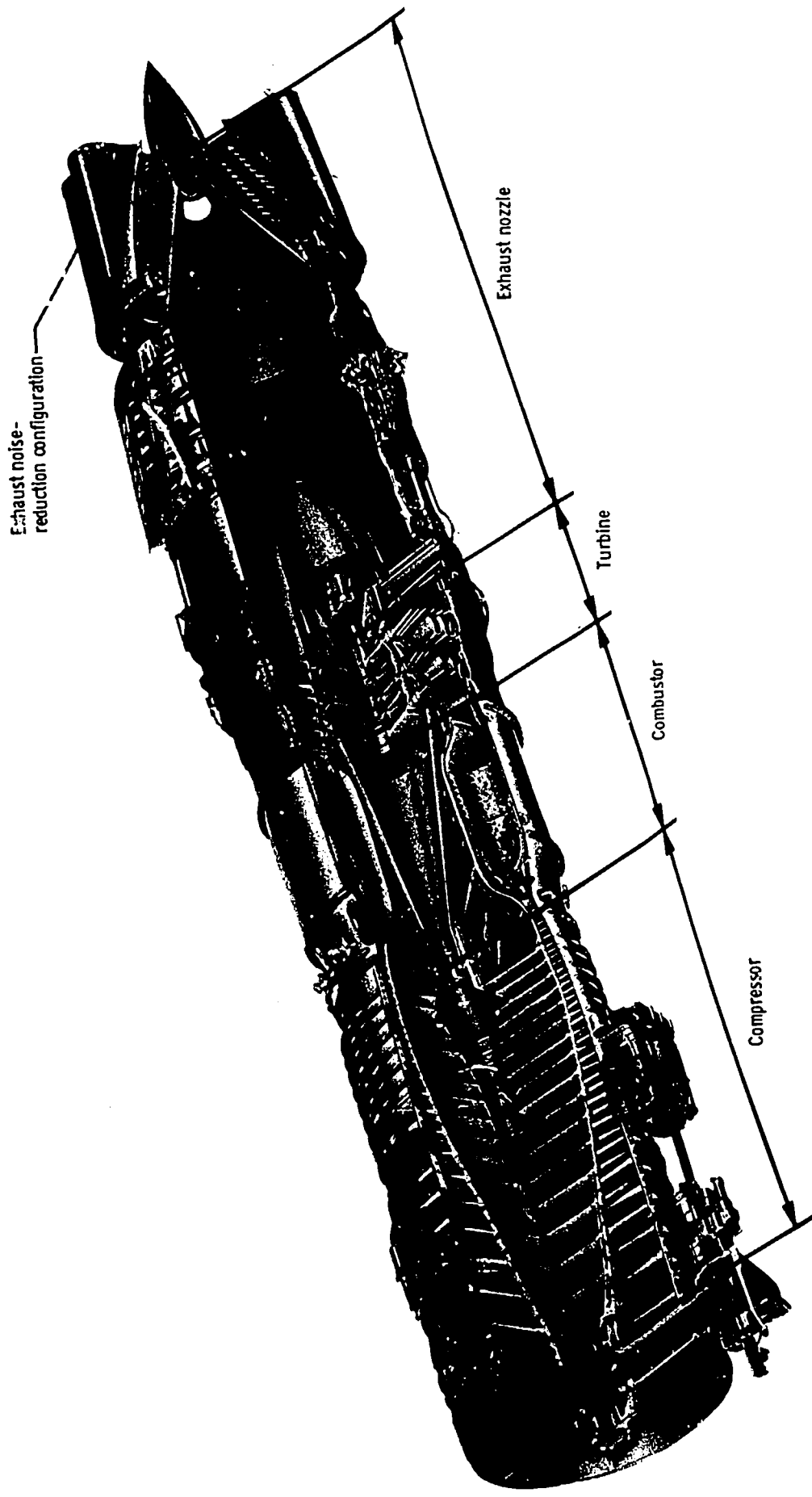
The inlet collects ram air and directs it towards the engine compressor. A certain amount of air compression occurs in the inlet. For subsonic flight, this compression is low, but it can become quite high at supersonic flight.

The engine compressor, which can be considered similar to a series of fans mounted on a single shaft, further compresses the air to pressures of from 4 to about 25 times the pressure at the compressor entrance. The amount of air compression in the compressor is dependent primarily on the engine design, but it is also influenced by engine speed and flight conditions.

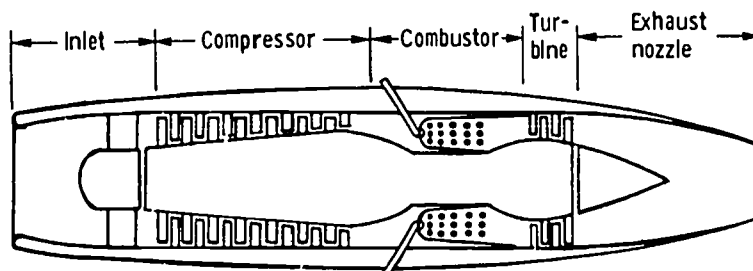
After the air leaves the compressor, energy must be added to it in the combustor. The combustor in some ways resembles a blowtorch. Fuel is burned in the air stream to increase the temperature to a level of from 1500° F to 2500° F, depending on the engine design. At 1500° F, metal glows with a bright yellow color, and at 2500° F, many metals melt. It is, therefore, obvious that special materials are required in the hot portion of the engine. For combustor outlet temperatures above 1800° F, sophisticated cooling methods are required for engine parts downstream of the combustor.

The purpose of the turbine is to supply power to drive the compressor. As shown in figure 7-4, the compressor and turbine are mounted on a single shaft or assembly. The turbine is similar in operation to the windmills used in the Western prairies or in Holland to pump water. The hot gases passing through the turbine rotate the turbine wheel, which in turn rotates the compressor.

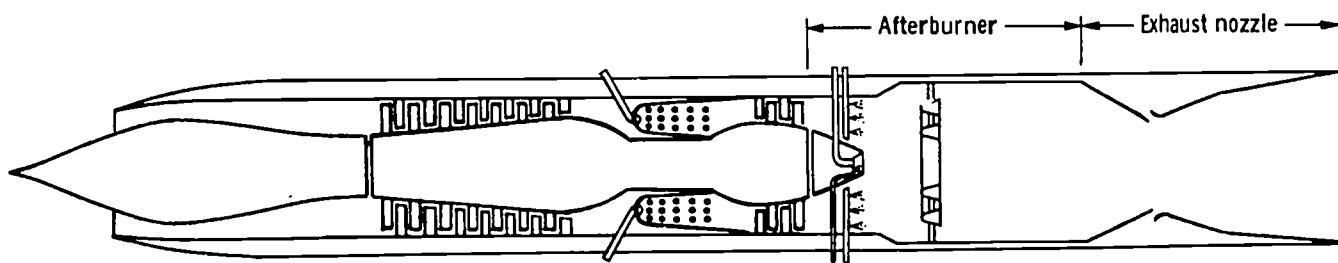
After leaving the turbine, the hot gases are expanded through the exhaust nozzle to a high velocity to create engine thrust. In the case of the supersonic-flight engine, shown in figure 7-4(b), it is often desirable to increase the thrust level of the engine by further increasing the temperature, and consequently the velocity, of the exhaust gases. The temperature level of the gases leaving the combustor must not exceed the temperature that the turbine blading can withstand. Therefore, to obtain higher exhaust-gas tempera-



(a) Cutaway view of engine.
Figure 7-3. - General Electric CJ 805-3B turbojet engine.



(a) Subsonic-flight engine.



(b) Supersonic-flight engine.

Figure 7-4. - Schematic illustrations of turbojet engines.

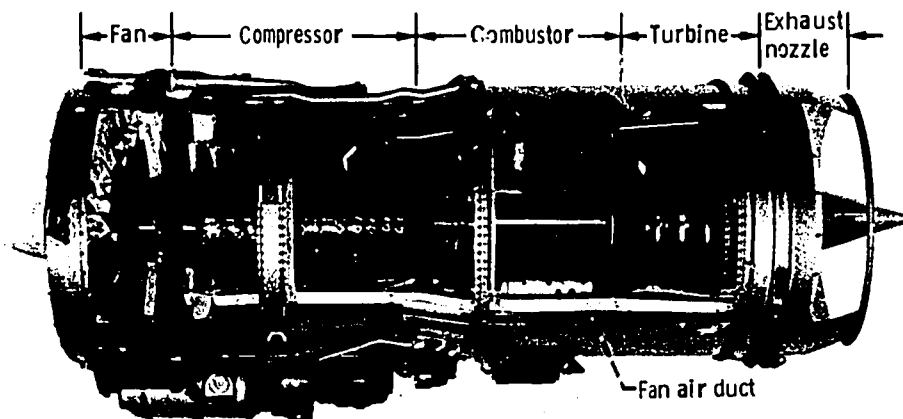


Figure 7-5. - Pratt & Whitney JT8D-1 turbofan engine.

tures, it is necessary to use an afterburner. Fuel is burned in the afterburner in a manner somewhat similar to that in the combustor, and the gas temperature level is raised to as high as 3800° F. This temperature is near the maximum attainable by burning kerosene-type fuels in air. Afterburners are used in military aircraft primarily to obtain bursts of power for relatively short periods of time during takeoff, to achieve high accelerations, or to achieve supersonic flight. For supersonic-cruise aircraft the afterburners are required for takeoff and for accelerating through the transonic speed range (near Mach number of 1.0). Afterburning temperature during cruise is usually lower

than required for takeoff and transonic acceleration.

Turbofan engines, such as shown in figure 7-5, are used in aircraft that are designed to cruise at subsonic speeds. In this type of jet engine, part of the fan airflow bypasses the "core" engine, which consists of the compressor, combustor, and turbine. The amount of air that is bypassed may vary from about one-half to eight times the airflow through the core engine, depending on the engine design.

A turbofan engine has a reduced jet velocity because the average temperature of the jet is reduced - the lower jet velocity improves engine efficiency. Thrust per pound of airflow is also reduced as jet velocity decreases. A turbofan engine compensates for this lower thrust per pound of airflow by having an increased airflow, relative to that of a turbojet, from the bypass air. The net effect is improved efficiency for a turbofan engine with equal or greater thrust for a given core-engine size.

The various engine components that have been mentioned above will now be discussed in greater detail.

ENGINE INLET

Some people do not consider the inlet as part of the jet engine. They consider the front face of the compressor as being the front of the engine. Actually, in terms of an overall powerplant system, the inlet is an important component of the jet engine. In fact, in a supersonic-flight engine most of the air compression occurs within the inlet. Because of the importance of the inlet, and because it is often less well understood than other engine components, we will discuss this component in somewhat greater detail than the others.

During flight, the airplane is moving at a high velocity relative to the ambient air. At high flight speeds (above 300 mph) the air going into the compressor must flow at a velocity slower than the airplane speed in order to maintain efficient compressor operation. As a result, the air must be slowed down in the inlet. As the air slows down, the pressure increases. (The phenomenon was examined in the discussion of drag in chapter 3.) What actually happens in the inlet is that the energy of the air molecules is converted from velocity (or kinetic) energy to pressure (or potential) energy. (The principle of this energy conversion is stated in Bernoulli's law, which is discussed in chapter 5.) The efficiency of an inlet is measured by how much of the total kinetic energy it converts to pressure energy. The amount of pressure that can be generated within an inlet becomes quite high at high flight speeds, as shown in figure 7-6. If all the velocity energy of the air at a flight Mach number of 3 (about 2000 mph) were converted to pressure energy, the pressure would be increased across the inlet by a factor of 37. This pressure rise would be greater than the pressure rise across compressors of current turbojet engines.

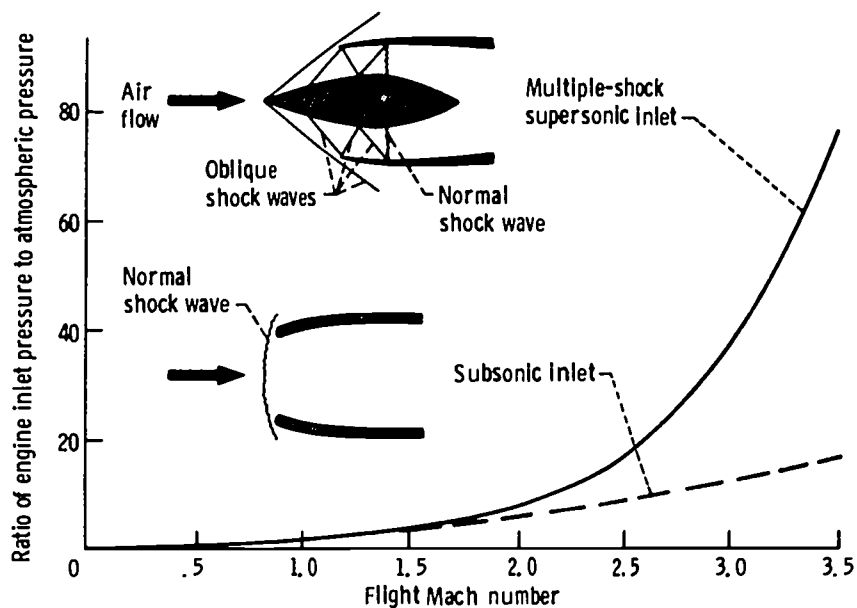


Figure 7-6. - Air compression in engine inlets.

Diffusion and Acceleration

An inlet is basically a diffuser. Therefore, a brief explanation of the diffusion and acceleration processes in subsonic and supersonic flow may be helpful at this point. A diffuser (or inlet) decreases the flow velocity and increases the pressure. A nozzle increases the flow velocity and decreases the pressure. In subsonic flow, a diverging channel acts as a diffuser, and a converging channel acts as a nozzle. In supersonic flow, a converging channel acts as a diffuser, and a diverging channel acts as a nozzle. To understand how diffusers and nozzles work, let us start out by considering a venturi (fig. 7-7) similar to that in the carburetor of an automobile. In the venturi, with subsonic flow at the inlet, the air velocity must increase as the air flows through a converging channel (nozzle section in fig. 7-7) to the throat. The driving force required to accelerate the air molecules is a reduced pressure in the direction of flow (downstream). The

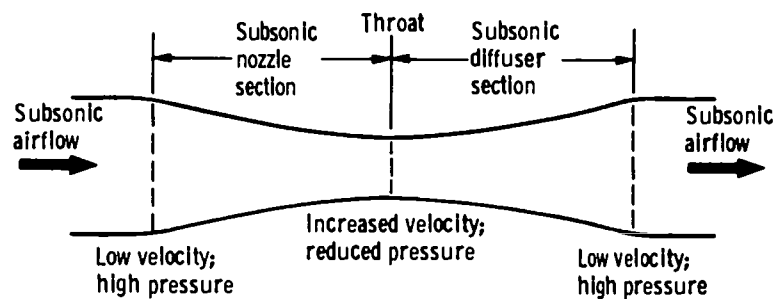


Figure 7-7. - Venturi. (Accelerates subsonic flow to higher subsonic velocities and thereby reduces pressure. Maximum velocity and minimum pressure occur at throat.)

maximum velocity occurs at the venturi throat, where the cross-sectional area is a minimum.

The diffuser section of the venturi acts in a manner opposite to that of the nozzle section. As the cross-sectional area of the passage expands, or diverges, the flow velocity decreases and the pressure increases. The velocity and pressure at the exit of the diffuser section can be almost the same as at the venturi inlet (nozzle-section inlet).

By reducing the pressure at the exit of the diffuser section of the venturi, the pressure is further reduced at the venturi throat, and the velocity increases until, finally, sonic velocity is obtained at the throat. Pressure waves are propagated at the speed of sound; therefore, once sonic velocity is obtained at the throat, pressure waves generated in the diffuser-section exit can no longer be propagated upstream through the throat. As a result, the pressure at the throat cannot be further lowered by reducing pressure in the diffuser section, and the throat velocity cannot be increased above sonic velocity.

The preceding discussion has shown that with subsonic flow a diffuser is a divergent channel, that the diffuser acts in a manner opposite to a subsonic nozzle, that the maximum velocity possible in a convergent nozzle is the velocity of sound, and that this maximum velocity occurs at the minimum cross-sectional area (throat). Obviously, supersonic flow cannot be obtained in a nozzle by further decreasing the flow area. If this were done, a new throat would be formed and sonic velocity would occur at the new throat. Keeping the downstream channel area the same as the throat would keep the flow

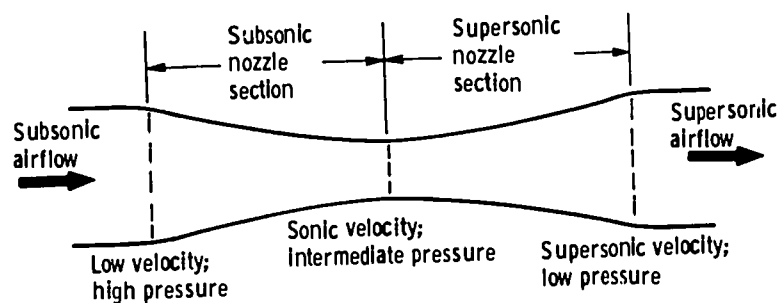


Figure 7-8. - Supersonic nozzle. (Accelerates subsonic flow to supersonic velocities if exit pressure is lowered sufficiently.)

near sonic. Therefore, if supersonic flow is to be obtained, the only approach possible is to increase the flow area downstream of the throat. The resulting nozzle configuration for supersonic flow (fig. 7-8) is similar to a venturi. With this configuration, supersonic flow can be obtained downstream of the throat if the exit pressure of the convergent-divergent nozzle is reduced to a value of about one-half of the inlet pressure, or less.

As pointed out in the discussion of the venturi, a diffuser acts in a manner opposite to a nozzle. Therefore, if we want to reduce the velocity of a supersonic airstream, and also obtain an increase in pressure, the supersonic diffuser (fig. 7-9) would first have a

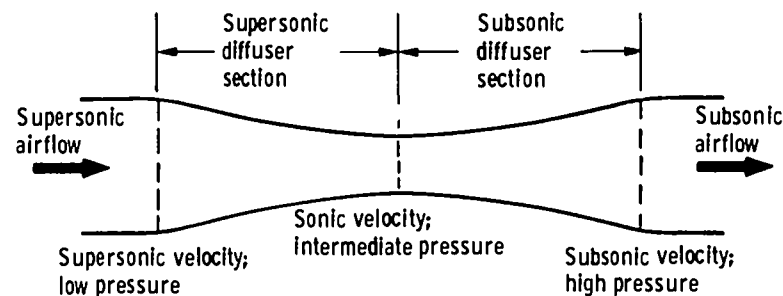


Figure 7-9. - Supersonic diffuser. (Decelerates supersonic flow to subsonic velocities and thereby generates high pressure.)

convergent section to decrease the supersonic velocity to sonic at the throat, and then the diffuser would have a divergent section to further decrease the air velocity subsonically. (Note that the diffuser configuration is also similar to venturi.)

A diffuser with a fixed geometry, as illustrated in figure 7-9, is a schematic, simplified illustration. Variable geometry or an air bleed is required to get a supersonic diffuser with large internal compression "started" or to get it to operate over a range of inlet Mach numbers (or over a range of flight speeds). The ratio of the throat area to the diffuser inlet area must be different for each inlet Mach number, otherwise a normal shock wave (described in the next section) will not stabilize in the diffuser throat. The flow velocity drops from supersonic to subsonic across this shock wave. If the normal shock wave is located in the supersonic region of the diffuser, where the flow has not yet been decelerated to near sonic velocity, large pressure losses may result. In order to "start" a supersonic diffuser with internal area contraction or to get the normal shock wave located at the throat requires that either (1) the diffuser geometry be variable to open up the throat area at low inlet Mach numbers to get the normal shock wave properly located, and then to decrease the throat area as the inlet Mach number increases, or (2) some air be bled out of the diffuser ahead of the throat at the lower inlet Mach numbers (this approach simulates a change in flow area). Additional and more detailed information on flow in inlets is presented in chapter 11.

Subsonic and Supersonic Inlets

At subsonic speeds the function of the inlet is not so much to compress the air as it is to reduce drag by streamlining the nacelle and to direct the inlet air to the compressor face. Inlets for subsonic and supersonic flight are quite different. This difference can be seen in the schematics of the two inlets shown in figure 7-6. The subsonic inlet concept is simple. The inlet is a divergent channel with entrance lips that are rounded to provide an efficient flow field at subsonic speeds. In contrast, the supersonic inlet lips

are sharp, and the inlet is a relatively complicated device.

The supersonic inlet must be capable of efficient operation at both subsonic and supersonic flight speeds. Let us first consider its operation at supersonic flight speed. The airflow channel must first be converged in a manner similar to that described for supersonic diffusers. Part of this convergence and supersonic flow deceleration can be accomplished external to the inlet lips through the use of shock (or compression) waves generated by a contoured centerbody that projects out ahead of the inlet lips, and part of the convergence is inside the inlet. (See multiple-shock inlet in fig. 7-6.) Shock waves and their characteristics are described in chapter 11. As air is decelerated from supersonic to sonic or subsonic velocity, shock waves are formed. A shock wave is a pressure wave across which there is a discontinuity (sudden change) in pressure and velocity. Shock waves can be either efficient or inefficient methods of converting velocity energy to pressure energy. An oblique shock wave, which forms at an angle to the local airflow direction, results in only a relatively small air-velocity reduction. The flow behind the shock wave remains supersonic, but at a reduced Mach number. Oblique shock waves are efficient converters of velocity to pressure, and they can be generated on centerbody surfaces with small successive inclinations to the airflow direction, as shown in figure 7-6.

A normal shock wave at high supersonic speeds is a particularly inefficient method of converting velocity to pressure. A normal shock is one which has its shock front perpendicular to the direction of flow. The air decelerates very abruptly from supersonic to subsonic velocity as it passes through a normal shock wave.

In a well-designed inlet the supersonic airflow is first slowed down through a series of oblique shock waves until the supersonic Mach number is near 1, and then a normal shock occurs near the inlet throat. The inlet then has a divergent section for deceleration of the subsonic airflow downstream of the throat and the normal shock wave. The subsonic airflow is then decelerated to a Mach number of about 0.4 (about 300 mph) at the compressor face.

Figure 7-6 also illustrates why it is necessary to use the complicated supersonic inlet configurations when flying at high supersonic speeds. The figure shows both the ideal compression (if there were no pressure losses) from a multiple-shock supersonic inlet and the compression from a subsonic inlet that provides only a normal shock at the inlet entrance. Up to a flight Mach number of about 1.5, the two inlets are equally satisfactory. But at Mach 3, for example, the pressure recovered from the supersonic inlet is over three times as high as that recovered from a subsonic inlet.

During subsonic flight with a supersonic inlet, the inlet geometry must be changed for efficient operation. By collapsing the centerbody or moving it backward, the amount of flow contraction in the supersonic inlet is reduced, and this permits the inlet to be used at subsonic speeds. Intermediate centerbody positions are usually required at supersonic flight velocities below the maximum velocity for which the inlet is designed.

Matching of Inlet Airflow Capacity to Engine Airflow Requirement

Another problem that is encountered with supersonic inlets results from the airflow supply characteristics of the inlet being different from the engine requirements. The inlet size is usually chosen so that it will supply the proper amount of air to the engine at a selected flight Mach number. Figure 7-10 illustrates an example in which the inlet and engine airflow characteristics are matched at a Mach number of 3. The quantity of air entering the inlet at this Mach number is exactly the amount of air that would be contained

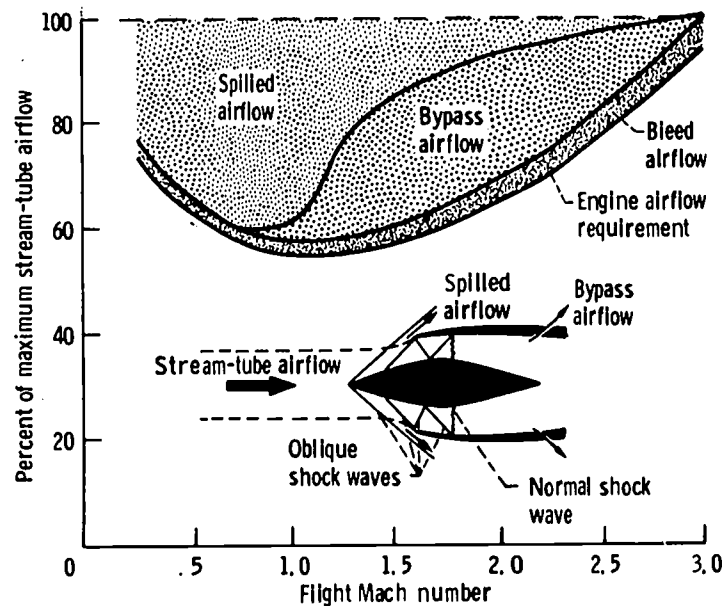


Figure 7-10. - Matching of inlet airflow to engine airflow requirements.

within a "stream tube" of the same diameter as the engine inlet. A stream tube is an imaginary tube of free-stream air containing the air that will pass through the engine. The maximum stream-tube airflow, referred to in the ordinate of figure 7-10, is the airflow that would occur if the stream-tube diameter were equal to the engine inlet diameter. When the diameter of the stream tube of air required by the engine is less than the inlet diameter, air from in front of the inlet must be spilled by shock deflection over the inlet lips, and air is bypassed out of the inlet as illustrated in figure 7-10. This spilled and bypassed air causes increased drag on the engine installation and is undesirable. Part of the research conducted on inlets and on engines is to provide methods of reducing and minimizing these drags in order to improve overall airplane performance. The bleed airflow is air that is bled from the throat region of the inlet to prevent separation of the boundary layer from the walls of the inlet and the centerbody. Bleed ports are located both in the walls of the inlet and in the surface of the centerbody.

COMPRESSOR

As stated previously, the purpose of the compressor is to compress the air leaving the engine inlet to a pressure that is from 4 to about 25 times as high as the pressure at the exit of the engine inlet. The pressure rise is dependent upon many things, including the purpose for which the engine is designed and the flight operating conditions. Modern engines are being designed for much higher pressures than were the engines of a few years ago.

Most engines utilize the axial-flow compressor, such as illustrated in figures 7-3, 7-4, and 7-5. A compressor of this type consists of many stages of rotating and stationary rows of airfoil-shaped blades. From the compressor inlet to the compressor exit the blades become progressively shorter (fig. 7-3), because a smaller flow area is required as the air becomes compressed. Compression of this air requires that work be done on it. This work raises both the pressure and the temperature of the air. The power required to drive the compressor is supplied by the turbine, which will be described later.

The manner in which the air is compressed can be explained with the help of figure 7-11. This figure shows three rows of compressor blades: the inlet guide vanes, the rotor blades, and the stator blades. The inlet guide vanes are used only at the entrance to the compressor. The purpose of these vanes is to turn the air to a favorable entrance angle before it enters the first compressor rotor. In some engines the inlet guide vanes

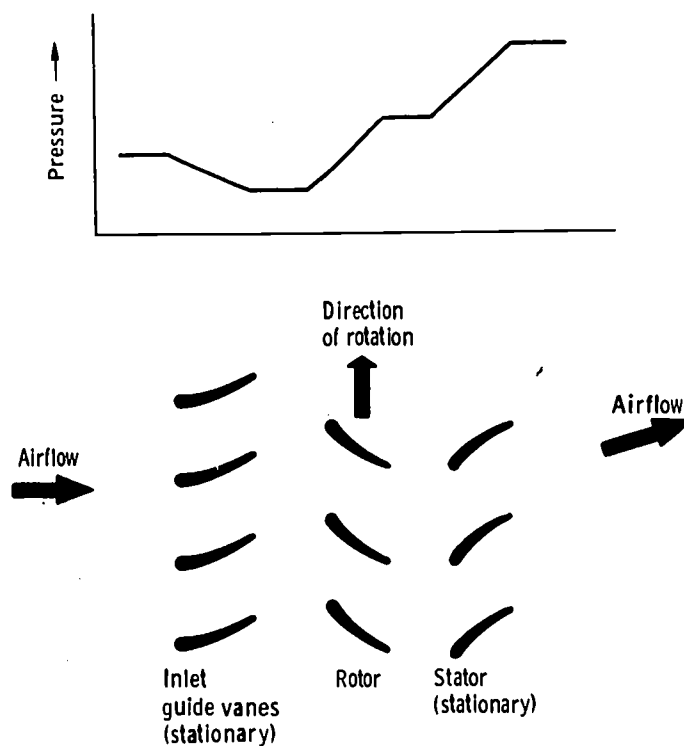


Figure 7-11. - Compressor operation.

Whereas there is an increase in the pressure and temperature of the air across the compressor, there is a reduction in the pressure and temperature of the gases across the turbine. To ensure that the pressure drop across the turbine will be less than the pressure rise across the compressor (in order to have enough power to drive the compressor and have pressure left for creating thrust in the exhaust nozzle), it is necessary to add energy to the air leaving the compressor. This energy addition is provided in the combustor in the form of thermal energy. The combustor heats the air entering the turbine to temperatures ranging from about 1500°F to well over 2000°F , depending upon the engine design. The combustor will be discussed later.

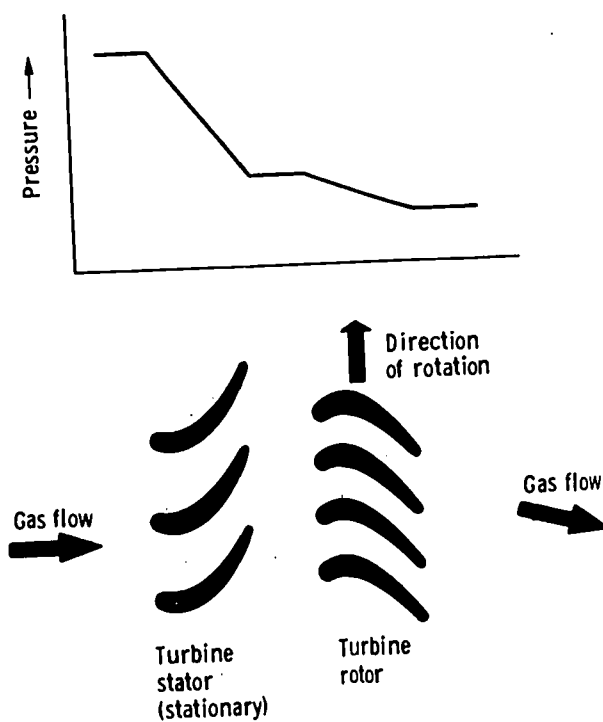


Figure 7-12. - Turbine operation.

The operation of the turbine is illustrated in figure 7-12. The gas leaving the combustor enters the turbine stator at a Mach number of about 0.4 or less. The stator turns the gas to provide a favorable entrance angle to the rotor blades. Furthermore, adjacent stator blades provide converging passages (see fig. 7-12) in which the gas velocity is increased to about Mach 1 at the exit of the stator. The gas pressure decreases in the stator as the velocity increases (a conversion of potential energy to kinetic energy). At a gas temperature of 2000°F , the gas velocity at Mach 1 is over 1600 miles per hour. This high-velocity gas then impinges on the turbine rotor blades and forces them to rotate in a manner similar to that of a windmill. The gas leaving the turbine rotor is at a velocity much lower than that entering the rotor. A large portion of the kinetic energy of the gas has, therefore, been transferred to the rotor in the form of mechanical energy to

provide the power to drive the compressor. The turbine is usually made up of several stages of stator and rotor blades. Modern engines have from two to eight turbine stages.

Most of the current gas-turbine engines have turbine-inlet gas temperatures of 1700° F or less. There are high-temperature turbine blade materials available that can withstand these temperatures. For future engines, however, the trend is toward increasing this turbine-inlet gas temperature in order to provide more power, or thrust, with a given engine size. To enable them to operate at these higher temperatures, the turbine blades must be cooled. This cooling is accomplished by ducting some of the air from the compressor through passages within the turbine blades. Since the air from the compressor is at a lower temperature than the hot gases entering the turbine, the turbine blade temperatures can thus be reduced. Research is currently being conducted to develop cooling concepts and blade materials that will permit operation at higher turbine inlet temperatures.

COMBUSTOR

The purpose of the combustor is to add thermal energy (heat) to the air leaving the compressor. Without this added energy, the turbine would be incapable of driving the compressor.

The combustor consists of four different sections, or zones, as shown in figure 7-13. The first section is the diffuser, in which the air velocity leaving the compressor is reduced to a level that permits efficient burning. The second section is the combustion zone. In this zone, a portion of the air (less than half) is mixed with fuel sprayed into the air by the fuel nozzle. This fuel and air mixture is burned, and the temperature of the gas is raised to between 3000° and 4000° F.

Stable combustion is possible only within these temperature limits for the combustion zone. Since this temperature is too high for the turbine to withstand, it must be reduced.

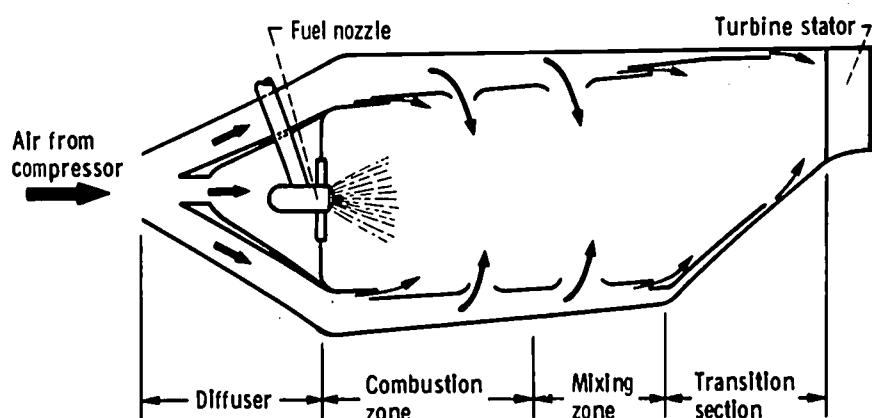


Figure 7-13. - Cross section of annular combustor.

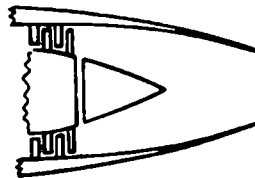
The operation of the afterburner is relatively simple and somewhat different from that of the combustor. Burning takes place in a gas stream that has already been heated by the engine combustors and from which some of the oxygen has already been consumed. In some turbofan applications, the fan air is ducted in with the exhaust gases leaving the turbine and this may also be heated in the afterburner. An afterburner nearly always has a pilot burner (shown in fig. 7-14) with an igniter, such as a spark plug, to light the pilot burner. This pilot burner provides an ignition source for the rest of the afterburner. Fuel is sprayed into the main gas stream from fuel spray bars, as illustrated in the figure. A series of flameholders is located a few inches downstream of the spray bars. These flameholders are usually gutter-shaped rings that provide turbulence in the gas stream and provide regions of lower gas velocity, where the burning can take place. Burning cannot take place in high-velocity gas streams at the temperatures encountered in afterburner inlets. Therefore, all of the burning occurs downstream in the turbulent wakes of the flameholders. The temperature of the gas in the afterburner may reach as high as 3800° F, which is far above the melting point of materials used in afterburner or exhaust-nozzle construction. These parts are kept from melting by controlling the temperature profile of the gases leaving the afterburner. The outer annular area of the gas coming into the afterburner does not enter into the combustion process and is not heated to high temperatures. This provides an insulating layer of cooler gas between the afterburner and exhaust-nozzle structures and the hot core gas in the afterburner. In addition, these structures are usually further cooled by ram air or air that is bled from the inlet and that bypasses the engine.

EXHAUST NOZZLE

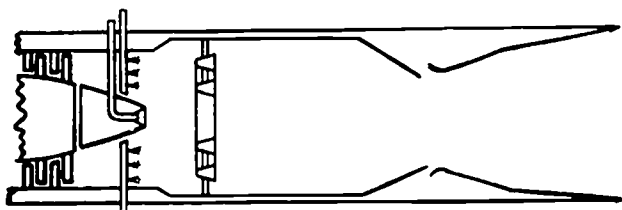
As discussed earlier, in the section entitled JET-ENGINE THRUST, the thrust from the exhaust nozzle is proportional to the amount of gas flowing through the nozzle and to the exhaust velocity. The purpose of the exhaust nozzle, therefore, is to accelerate the gases leaving the engine to as high a velocity as possible.

The exhaust nozzle for a subsonic engine is much simpler than one for a supersonic engine. For subsonic flight, a fixed-area convergent exhaust nozzle (shown in figs. 7-4(a) and 7-15(a)) can be used. In a subsonic engine, the pressure of the gases within the exhaust nozzle is only high enough to accelerate the gases leaving the nozzle to a speed of about Mach 1 or slightly higher. For this gas pressure, a convergent nozzle is satisfactory.

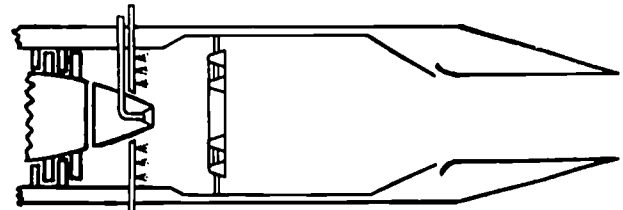
When an afterburner is used, it is necessary to vary the diameter of the exhaust nozzle. With the afterburner in operation, the gases in the nozzle are heated to a higher temperature and their volume increases; therefore, the exhaust nozzle area must be increased during periods of afterburning.



(a) Fixed-area nozzle for subsonic-flight engine.



Convergent-divergent configuration for supersonic exhaust velocity



Convergent configuration for sonic exhaust velocity

(b) Afterburner and variable-area nozzle for supersonic-flight engine.

Figure 7-15. - Exhaust-nozzle configurations.

For supersonic flight, the pressure within the exhaust nozzle is much higher than at subsonic flight speeds, because of the added compression that is obtained in the engine inlet. This higher pressure in the exhaust nozzle permits accelerating the gases to velocities much higher than sonic. This acceleration of the gases to supersonic speeds requires both convergent and divergent sections within the exhaust nozzle, as illustrated in figure 7-15(b). The requirement for convergent and divergent passages to obtain supersonic velocities was discussed in the section titled Diffusion and Acceleration.

Since supersonic airplanes must also be able to fly at subsonic speeds, the exhaust nozzle must be variable not only in area but also in shape. Figure 7-15(b) illustrates the variation that must be made in the nozzle configuration between supersonic and subsonic flight.

ENERGY CONVERSION IN JET ENGINE

The discussion thus far has described the operation of the various engine components. It is of interest to consider the entire engine as being made up of a series of energy converters. The more efficiently the components are able to convert between various forms of energy, the more thrust the engine will produce from a given amount of fuel burned. The following energy conversions are performed in the engine:

The inlet converts kinetic energy (velocity) of the entering air to potential energy (pressure) and thermal energy (heat - the air is also heated during the pressure rise). The pressure created acts on portions of the inlet to provide forward thrust, and pressure is also required in the turbine and exhaust nozzle.

The compressor converts mechanical energy (power) to potential energy (pressure) and thermal energy (heat).

The combustor provides most of the thermal energy (heat) to the gas ahead of the turbine by a conversion of the chemical energy in the fuel.

The turbine creates the mechanical energy (power) to drive the compressor by conversion of the potential energy (pressure) and thermal energy (heat) from the gases entering the turbine.

The afterburner converts chemical energy to thermal energy in the gases ahead of the exhaust nozzle.

The exhaust nozzle converts potential energy (pressure) and thermal energy (heat) to kinetic energy (velocity) to produce the remaining thrust output of the engine.

The amount of thrust depends on the size of the engine (the amount of air it can handle), the pressure rise of the air in the engine, the temperature of the exhaust gases, and the efficiency with which all of the engine components can convert energy from one form to another.

8. AIRCRAFT STRUCTURES AND MATERIALS

Robert H. Johns*

We will develop the story of aircraft structures and materials more or less from a historical perspective, beginning with a discussion of wood, piano-wire, and fabric construction, and ending with a brief discussion of supersonic aircraft. Although this includes the entire history of manned powered flight, it has all taken place in the relatively short time since the turn of the century.

Considering only the current inventory of craft for manned flight, the spectrum runs from fabric-covered gliders and small private planes to high-performance military aircraft and huge transports. In addition, there are airships, helicopters, V/STOL craft, and even capsules and lifting bodies for manned space flight and Earth reentry. It is readily apparent that a wide variety of aircraft structural problems can be encountered. They range in complexity from the routine to those requiring highly complex electronic computers for their solution. New problems continue to arise as the state of the art of aircraft design, manufacture, and performance continues to progress at a very rapid pace.

STRUCTURES OF WOOD, PIANO WIRE, AND FABRIC

Obviously, one of the primary considerations in the design of aircraft structures is light weight. This is most apparent when considering gliders. The first successful airplanes were very similar in construction to the gliders of the day. The airplane which the Wright brothers used to make the first successful manned powered flight in 1903 is shown in figure 8-1. The basic materials of construction were wood, piano wire, and fabric. It was most desirable to use the piano wire wherever possible, because it provided the most strength for the least weight. However, the wire could carry only tensile loads; therefore, wood was used to carry compressive and bending loads. The fabric carried no loads but simply served to give the desired shape to various parts of the airplane.

The basic forces which must be considered in designing an airplane are (1) gravity

*Head, Structures Analysis Section.

164/165

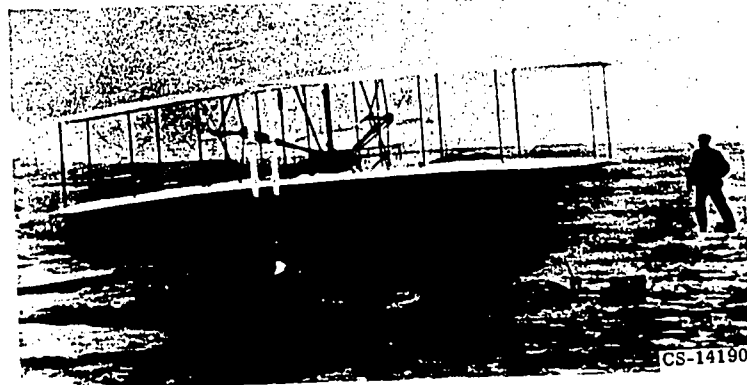


Figure 8-1. - Wright brothers' airplane (1903).

forces, (2) lift forces, (3) drag loads, (4) thrust or propulsive forces, (5) maneuvering loads, and (6) landing loads. In level flight at constant speed, the gravity forces are balanced by the lift forces and the drag forces are equal and opposite to the propulsive thrust.

Wings

Figure 8-2 clearly shows the struts and wires by which loads (forces) were transferred between major components of early airplanes. The earliest airplanes generally had two

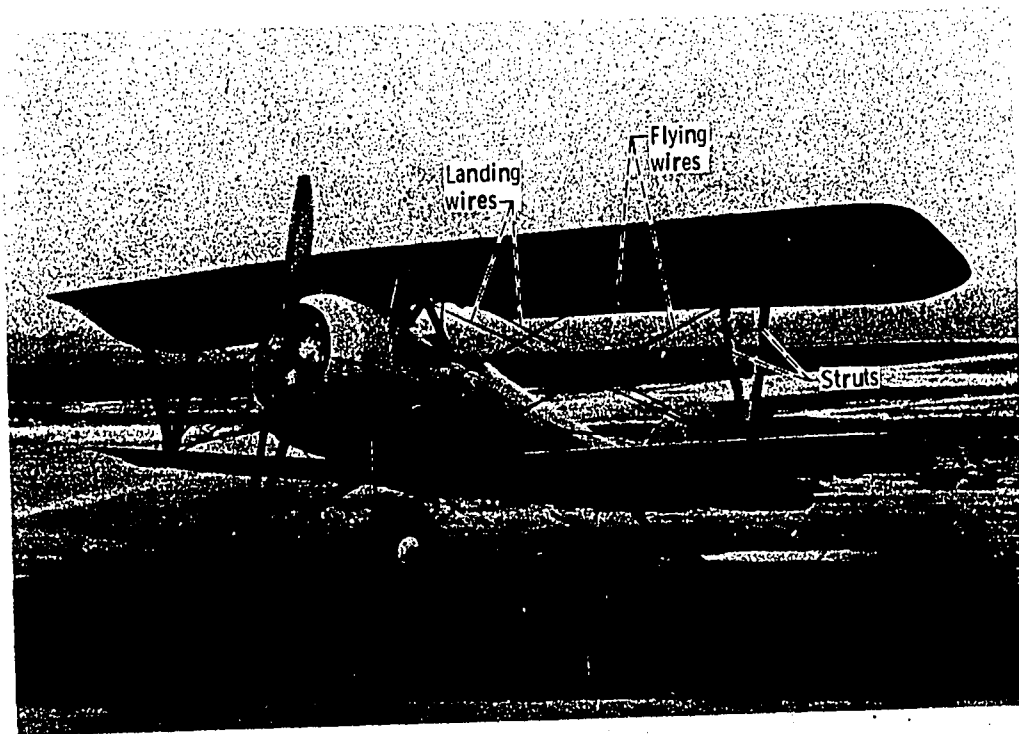


Figure 8-2. - Nieuport 27 biplane.

major lifting surfaces, or wings, and were thus called biplanes. Most of the weight (or gravity force) was in the fuselage, where the engine and passengers were located. The lifting forces, which resist the gravity forces and maintain the airplane aloft, come mainly from the wings. Thus, the lifting forces acting on the wings must be transmitted to the center of gravity (the point through which the resultant of the gravity forces can be assumed to act), which is in the fuselage area. These lifting forces acting on the wings were transmitted to the fuselage through struts and wires between the wing surfaces, as well as through wooden beams, or spars, within the wing cross sections.

When in flight, the lifting forces on the wings are acting upward. The lifting forces on the lower wing are resisted by compressive forces in the outer struts (see fig. 8-2), as well as directly by the fuselage. The compressive loads in the outer struts and the lifting forces on the outer portions of the upper wing are resisted by tensile forces in the flying wires. The lift on the inner portion of the upper wing is transmitted to the fuselage by tensile forces in the inboard, or cabane, struts. Drag forces acting on the wings are transmitted to the fuselage by the spars and internal bracing and wires within the wing cross section.

When the airplane is on the ground or touching down upon landing, the gravity and inertial forces acting on the wings are downward. The inertial forces result from a change in the sinking speed, or the vertical downward component of the velocity of the aircraft. This reduction in the vertical velocity is a negative acceleration, or a deceleration, which produces downward inertial forces throughout the airplane. According to Newton's Second Law of Motion ($F = ma$), the inertial forces are distributed as the product of the local mass and acceleration. The upper wing forces are transmitted in compression through the struts. The forces from the outboard portions of the lower wing and from the outboard struts are resisted by tensile forces in the landing wires; these

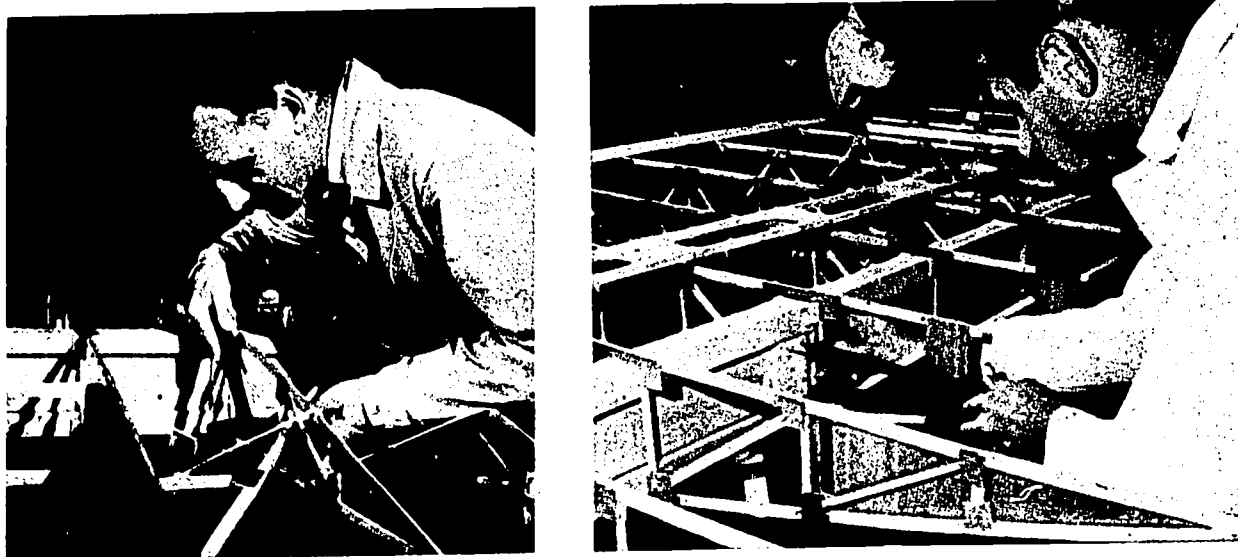


Figure 8-3. - Early wing construction. (Reprinted from Ryan Reporter, July/Aug. 1967, with their permission.)

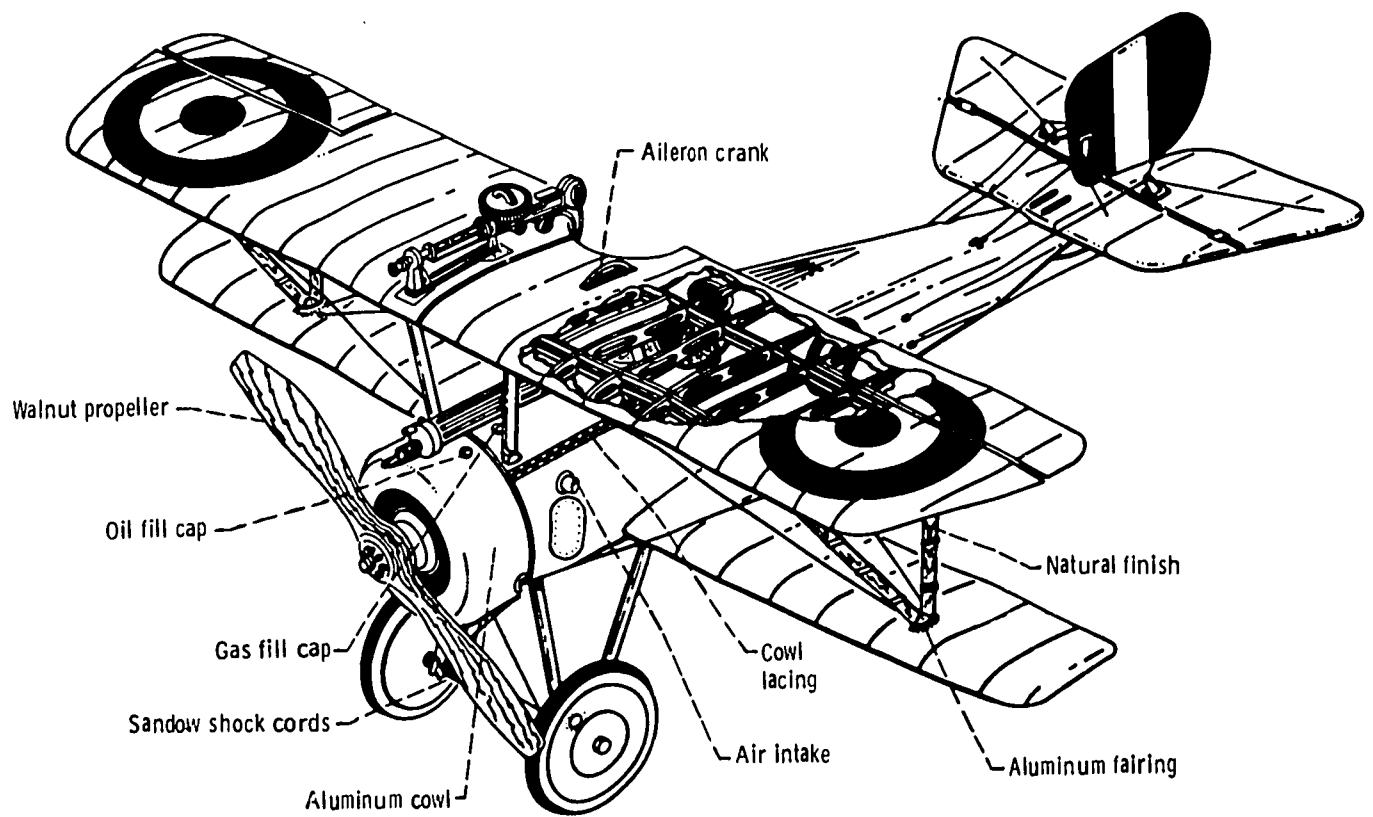
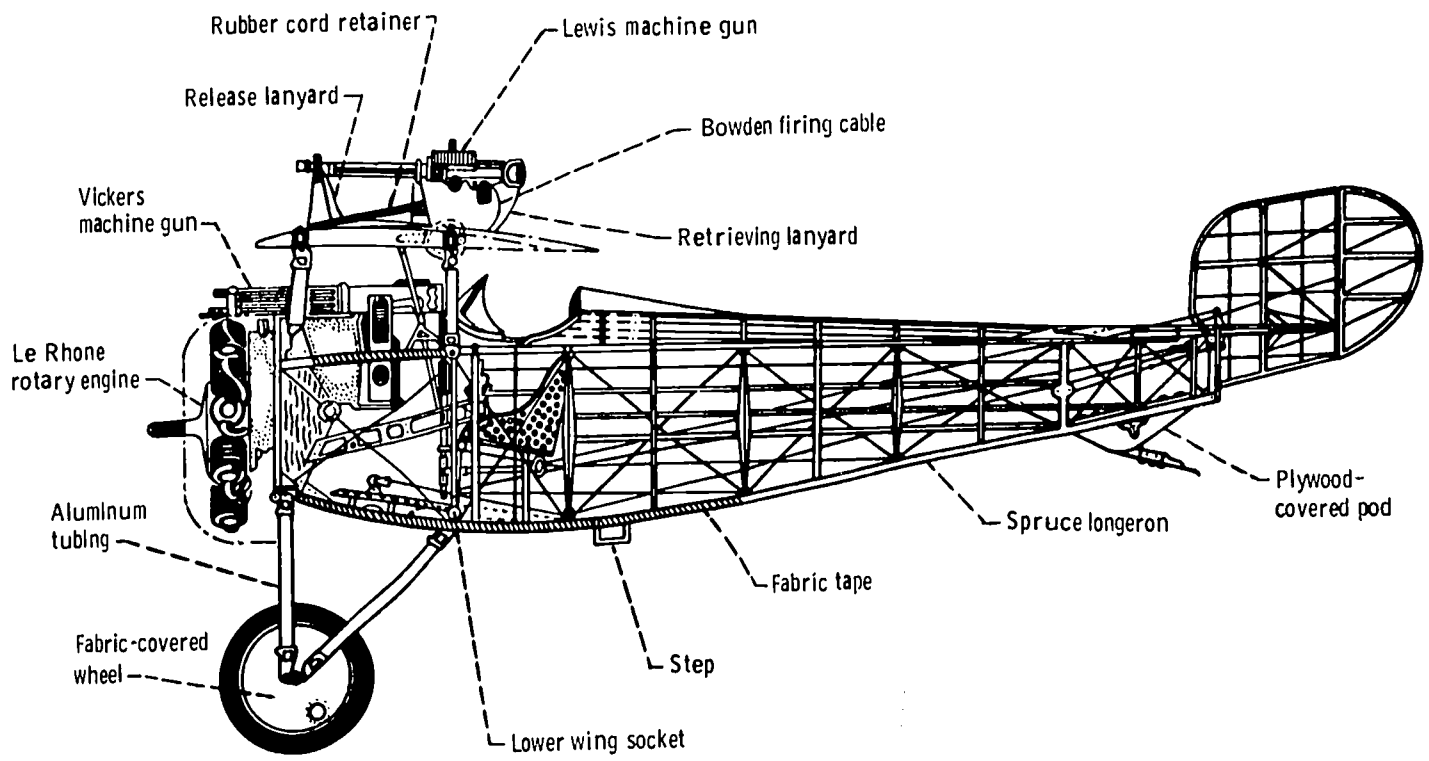


Figure 8-4. - Nieuport 17C.1 Scout biplane (1915).

tensile forces are transmitted to the fuselage as compression in the inboard struts.

An example of early wing construction is shown in figure 8-3. These photographs were taken during the construction of the "Spirit of St. Louis II," a replica built to commemorate the 40th anniversary of Charles A. Lindbergh's solo flight across the Atlantic in the original "Spirit of St. Louis." The materials used were wood, high-strength wire, and fabric. The photographs show the two main spars and the truss-type structure and wire bracing between the spars.

Fuselage

One example of early fuselage construction is shown in figure 8-4. The structure was basically rectangular in cross section with vertical and horizontal trusses made of wood and wire. The side trusses provided strength and stiffness to carry small lift loads from the tail and to carry forces from the horizontal control surfaces. In addition, loads from the tail skid or wheel were transmitted through the sides. Top and bottom trusses supported loads from the vertical stabilizer and rudder and provided torsional strength and stiffness for the fuselage.

METAL SKIN AND TUBULAR TRUSSES

Metal Structures

As the knowledge of airplane flight loads and structural design progressed, the biplane gradually gave way to the monoplane, such as shown in figure 8-5. Wing construc-



Figure 8-5. - Early high-wing monoplane with semicantilever wing. (Photo from J. W. Galer collection.)

tion had improved sufficiently to permit the outboard portions of the wings to be cantilevered with the lift forces now being carried as bending loads by the structure within the cross section of the wing. This method of support is in marked contrast to carrying the loads through compression struts and tension wires between lifting surfaces and the fuselage. The single wing was more efficient than the double wing. It also eliminated much of the drag associated with the external wires and struts between the two lifting surfaces. However, struts were still necessary to carry the large lifting forces and bending loads near the fuselage.

Eventually, metals began to play a larger role in aircraft construction. An evolutionary change in materials was made in the 1920's when the Ford Trimotor (fig. 8-6)

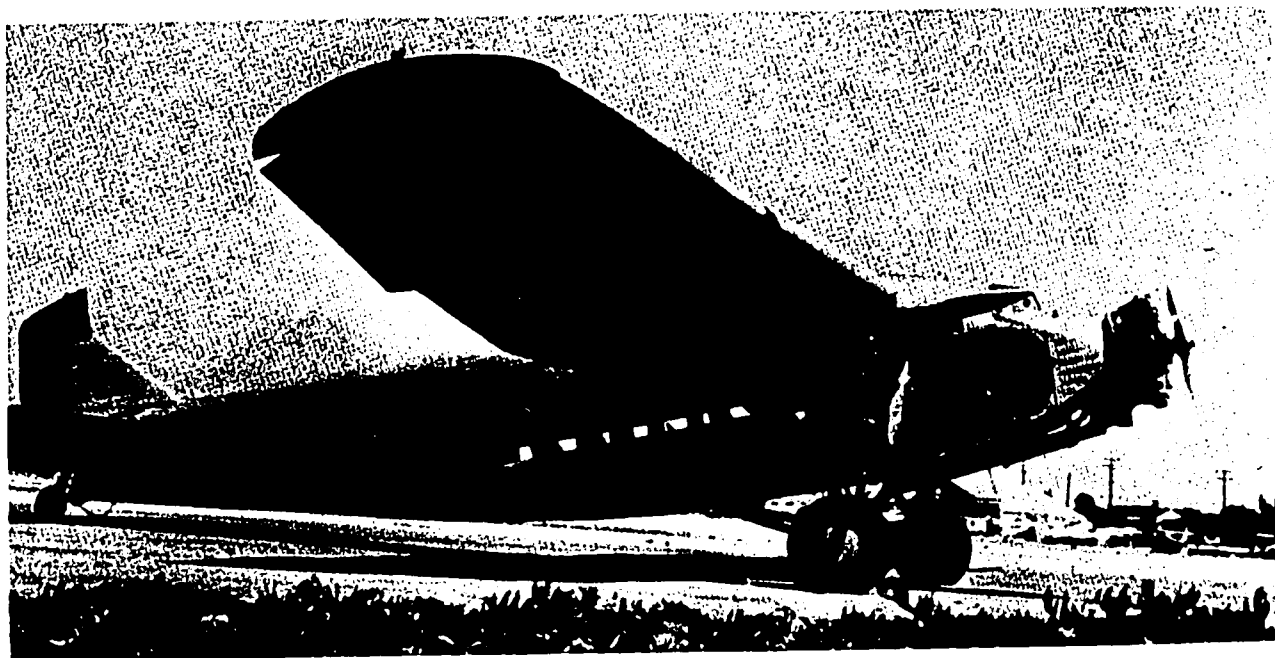


Figure 8-6. - Ford Trimotor, with tubular truss structure and corrugated metal skin. (Courtesy of Island Airlines.)

appeared with a corrugated metal skin covering a metal truss framework. The structure was still not very efficient, however, because most of the loads were carried by relatively heavy welded steel tubing rather than by the skin.

Figure 8-7 shows again details of the construction of the "Spirit of St. Louis II." The many longitudinal stringers apparent in the picture were simply to give aerodynamic shape to the fabric covering. Structural loads were carried by a welded metal truss, which can be seen inside the wooden stringers.

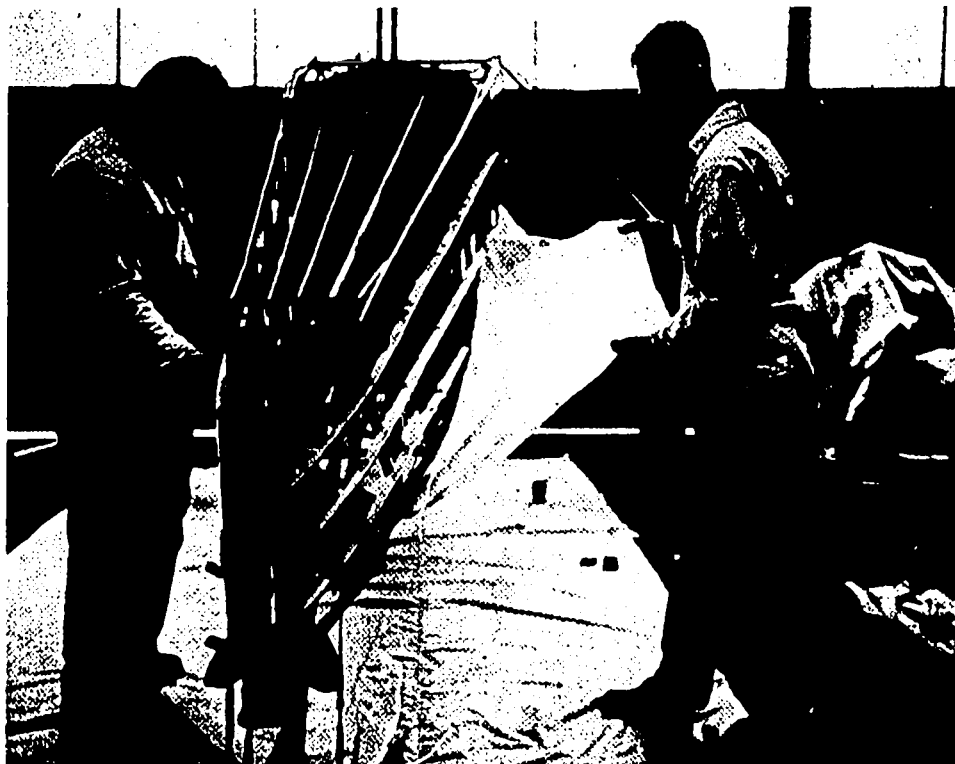


Figure 8-7. - Early fuselage construction. (Reprinted from Ryan Reporter, July/Aug. 1967, with their permission.)

Stressed Skin

The high drag and inefficient load-carrying properties of corrugated metal coverings, the relatively heavy construction of welded tubular trusses, the need for increased compartment space for passengers, and the development of strong aluminum alloys led to the introduction of stressed-skin shell, or "monocoque," structures.

Even prior to World War I, laminated wood (plywood) and metal were being tried in place of the fabric covering on parts of some airplanes. A thin wood fuselage was made by gluing together thin layers of wood on a mold. The smooth wood fuselage was usually stiffened by circular or oval ring frames and longitudinal stiffeners. The wooden shell carried most of the loads and provided a relatively smooth aerodynamic surface with reduced drag. The first such fuselage appeared in France in 1912. This type of construction with a load-carrying shell, or skin, is called "monocoque" after the name of the first model. Literally translated, the word "monocoque" means "single shell."

The use of stressed skin led to the development of thick wing profiles of tapered design, which resulted in a strong cantilever construction with no external bracing (fig. 8-8). The elimination of struts and wires increased the aerodynamic efficiency of the airplane. The thick monoplane wings permitted mounting engines on them and retracting the landing gear into them in flight to reduce the drag further. It also became possible to mount the

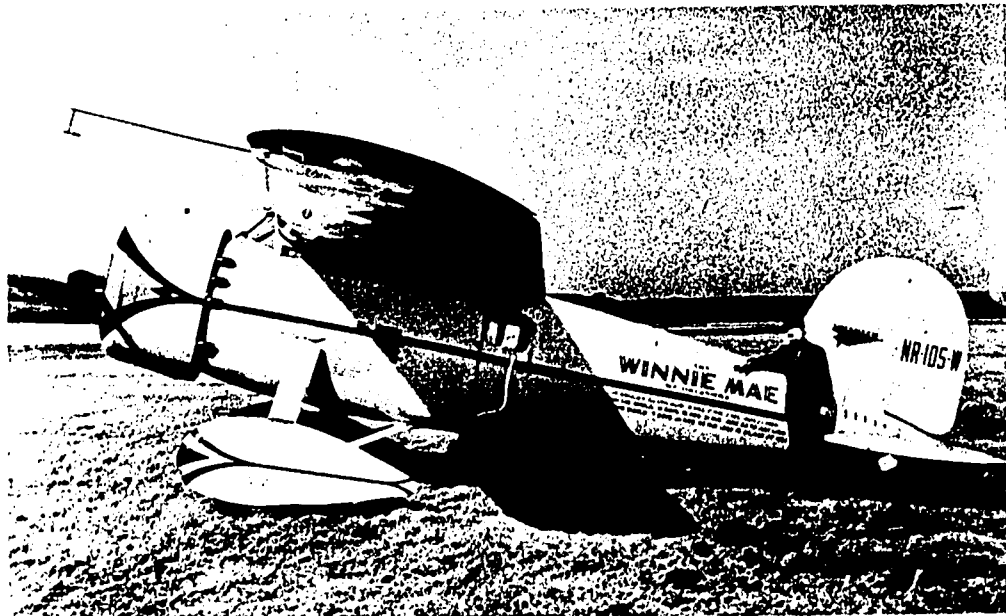


Figure 8-8. - Early monoplane with full-cantilever wing. (Photo from J. W. Caler collection.)

fuel tanks in the wings near the engines and thus free more space in the fuselage for passengers and cargo. The weight of the fuel and engines on the wings counteracted some of the lifting forces and thereby decreased the bending moments at the wing roots. The culmination of these advances was the Douglas DC-3 transport (fig. 8-9), which appeared in the mid-1930's.

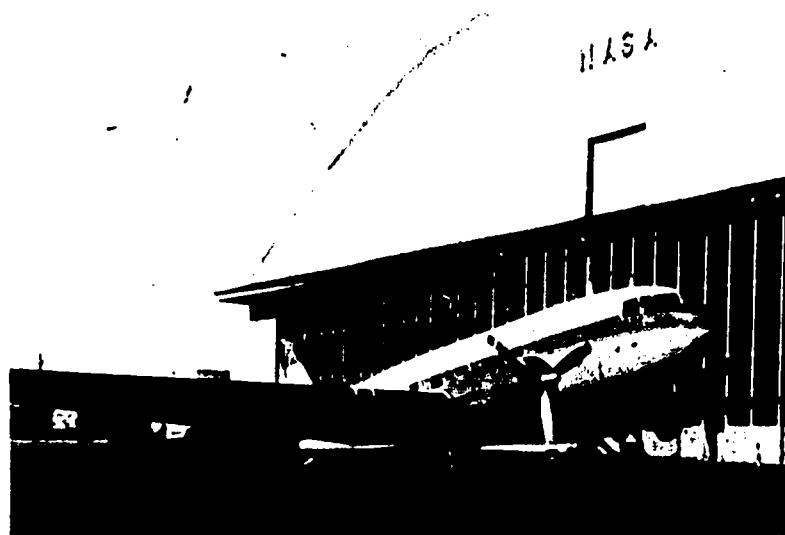


Figure 8-9. - Douglas DC-3 transport.

SEMIMONOCOQUE STRUCTURES

Stiffening

Most elements of today's aircraft structures are made from sheet metal. High-strength thin sheet is very efficient in transmitting tensile loads. However, when called upon to support compressive or shear loads, the thin sheet must be stiffened by ribs, formers, stringers, and longerons to prevent or minimize buckling. If no stiffening members are used, the sheet is designed to carry all the load, and the construction is called "monocoque," or "full monocoque," which means "single shell," as was mentioned previously. A shell thick enough to support all loads would usually be too heavy. Therefore, formers and stringers are used to stiffen the thin skin sufficiently to carry all loads in a lightweight structure. Such stiffened shells are called "semimonocoque" structures.

A typical example of the stiffening used in the semimonocoque structure of an airplane is shown in figure 8-10. This skeletal structure is covered with thin sheet aluminum, which then acts as a stressed skin and is a major load-carrying element of the aircraft. The skin is riveted or spot-welded to the frame. Although not apparent in this illustration, some of the longitudinal structural members are usually much thicker than others. In addition to being stiffeners, they are major load-carrying elements of the primary structure and are called "longerons." Likewise, some of the formers are much heavier than others that serve simply as stiffeners for the skin. They may be closed or nearly closed by webs with reinforced openings in them. Such partitions are called "bulkheads," and may serve to isolate certain parts of the fuselage from others for purposes of pressurization, heating, minimizing noise transmission, fire and smoke protection, or simply to provide surface area on which to mount equipment.

Large concentrated loads, such as those transmitted from the tail surfaces or landing gear, are distributed to the fuselage through fittings on the longerons and bulkheads. Similarly, concentrated loads on the wings, such as engines, rockets, bombs, and droppable fuel tanks, are carried through fittings attached to the main spars in the wings.

Cutouts or access holes must be provided in many areas of the aircraft to permit access to locations within the fuselage. In designing the airframe, the locations and spacing of longerons and bulkheads must be compatible with the locations of major openings such as passenger-access, landing-gear, bomb-bay, and cargo-bay doors. The longerons and bulkheads frequently reinforce the openings and provide alternate load paths for the forces which must be redistributed around the openings. Figure 8-10 illustrates some of these considerations.

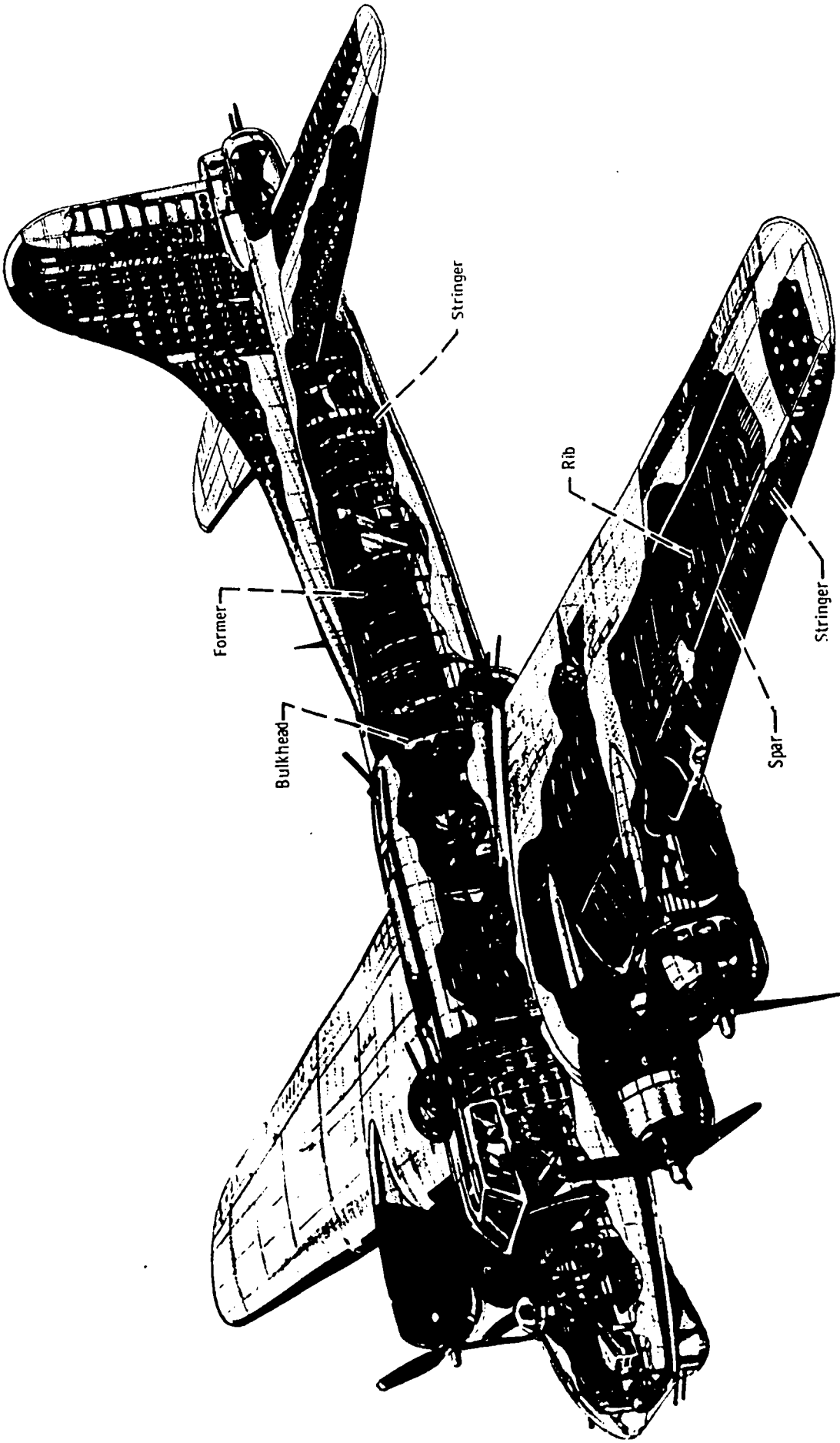


Figure 8-10. - Semimonocoque structure of Boeing B-17G bomber. (Taken from Flying, Jan. 1945, with permission of Aviation Division of Ziff-Davis Publishing Co.)

Pressurized Cabins

Commercial-transport design improved rapidly in the 1930's and 1940's. Along with increased range and altitude capability came the need for passenger-compartment pressurization. Airplanes such as the DC-6 routinely operated at 20 000 feet altitude, where the atmospheric pressure is less than half that at sea level. Passenger comfort and health required that the cabin be pressurized to an equivalent altitude of 7000 or 8000 feet. Thus, the pressure differential across the cabin wall could be as much as 5 to 6 pounds per square inch. Today's commercial jet transports fly at altitudes of about 40 000 feet, with a pressure differential of 8 to 10 pounds per square inch across the cabin wall.

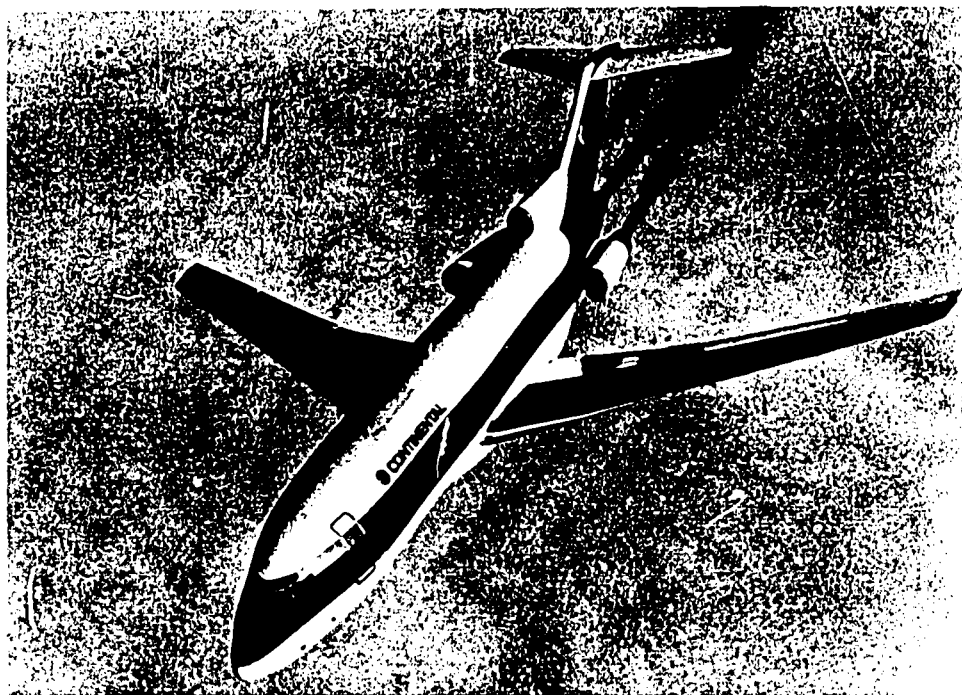


Figure 8-11. - Boeing 727 jet transport. (Reprinted from Aviation Week & Space Technology, Oct. 30, 1967, with their permission.)

Most current commercial jet aircraft are much larger than their predecessors with piston engines. In many respects, these jet aircraft are also quite different in appearance, with swept-back wings, T-shaped tails, and engines mounted directly on the fuselage and at the aft end of the airplane, as shown in figure 8-11. The basic structure, however, is still of aluminum, stressed-skin, semimonocoque construction not unlike the DC-3 of the 1930's.

Thin Wings

Supersonic flight has become possible with the advent of the jet engine. The aerodynamics of such high-speed flight make very thin wings highly desirable. New types of wing structures have been designed to provide the strength and stiffness for such thin wings. Large portions of the outer skin and internal stiffening are machined or forged as an integral structure. This type of construction avoids the forming and riveting together of many smaller pieces and provides a reduction in weight and an increase in the internal volume available for fuel storage. However, the wings of high-performance military aircraft are so thin that some fuel must be carried in the fuselage, and, in many cases, in external droppable tanks under the wings. The trend toward very thin wings has also forced the designer to locate the main landing gear so that it can be retracted into the fuselage rather than into the wings.

MATERIAL AND STRESS CONSIDERATIONS

Ultimate Strength

Until about the 1930's the basic structural requirement was simply that the structure have sufficient strength to support the loads without failing and that it be relatively light. Essentially this meant determining the loads and providing sufficient cross-sectional area so that the stress (load divided by area) did not exceed the ultimate strength of the material.

The most common measure of the ability of a material to provide high strength with minimum weight is its strength-to-density ratio. As the name implies, this is the ratio of the tensile strength of a material to its density (weight per unit volume). The higher the strength and the lower the density of a material, the higher is its strength-to-density ratio and, therefore, its ability to provide minimum-weight structures. However, most high-strength aircraft structural materials, such as aluminum, titanium, magnesium, and stainless steel, have about the same strength-to-density ratio at room temperature. Therefore, other factors usually control the selection of these materials for structural applications. Some of these factors are cost, availability, fabricability, corrosion resistance, fracture toughness (related to impact or notch sensitivity), fatigue strength, service temperature, and creep strength.

Fabricability

Since steel has about the same strength-to-density ratio as aluminum, a logical question is why more steel is not used in airframes. A major reason has to do with minimum gage (thickness) for handling and fabrication. Steel is about three times as strong and three times as dense as aluminum. Consequently, even though they can theoretically carry equal loads with equal weight structure, the steel sheet would be only one-third the thickness of the aluminum. This is undesirable for two reasons. First, the thickness of steel required might be only a few thousandths of an inch. This could produce handling problems during manufacture and increase the manufacturing costs, because such parts can become bent or damaged accidentally more easily than the much thicker aluminum. Also, the possibility of accidentally denting or puncturing the skin of the aircraft is greater.

A second, and more important, reason for using aluminum instead of steel has to do with increased buckling strength to resist compression or shear loads. This will be discussed more thoroughly in the following section on Buckling.

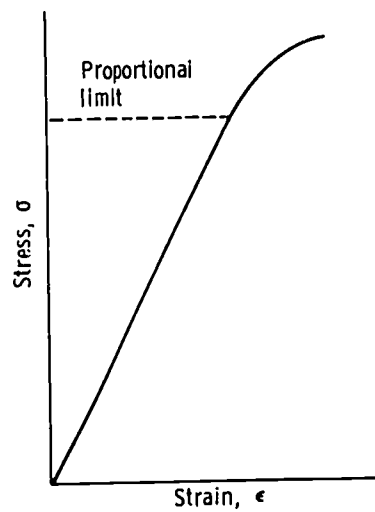
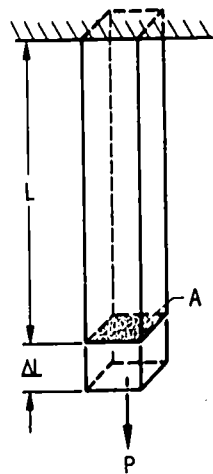
Magnesium has been used in airframe construction but only to a limited extent. It is not normally used, because it is relatively hard to work. Forming magnesium sheet into parts such as channels and angles must be done hot and under controlled conditions. Magnesium is also less corrosion resistant than is aluminum.

Buckling

Less than half of the material in the airframe is selected on the basis of tensile or ultimate strength. Over half of the material is chosen on the basis of buckling considerations. When relatively thin sheets or sections are subjected to compressive or shear stresses, they may buckle or wrinkle at stresses considerably below the yield or ultimate strength of the material. The buckling strength is a function of the geometry of the part, the edge support (or fixity), and the modulus of elasticity (or stiffness) of the material; it is not a function of the tensile strength of the material.

The modulus of elasticity is a material constant relating the deformation to the load on a structural component. Referring to figure 8-12, consider a simple bar with constant cross-sectional area A under the action of a tensile load P . The stress σ , which is a measure of the load intensity on the structure, is defined as the ratio of the load to the cross-sectional area, or

$$\sigma = \frac{P}{A}$$



$$\text{Stress} = \frac{\text{Load}}{\text{Area}}$$

$$\sigma = \frac{P}{A}$$

$$\text{Strain} = \frac{\text{Change in length}}{\text{Original length}}$$

$$\epsilon = \frac{\Delta L}{L}$$

$$\text{Modulus of elasticity} = \frac{\text{Stress}}{\text{Strain}}$$

$$E = \frac{\sigma}{\epsilon}$$

Figure 8-12. - Stress, strain, and modulus of elasticity.

If the load is measured in pounds and the area in square inches, the units of stress are pounds per square inch (psi).

Any body subjected to a stress also undergoes a deformation. If the bar in figure 8-12 has initial length L , it will lengthen some amount ΔL under the action of the stress σ . The strain ϵ is defined as the ratio of the change in length to the original length, or

$$\epsilon = \frac{\Delta L}{L}$$

As can be seen, the strain is dimensionless and, therefore, has the same value irrespective of the system of units being used.

A typical plot of stress versus strain is shown in figure 8-12. Up to some value of stress called the proportional limit, stress is usually linearly proportional to strain; that is, the ratio of stress to strain is a constant. This constant of proportionality E is called the modulus of elasticity, or "Young's modulus," and is defined by the equation

$$E = \frac{\sigma}{\epsilon}$$

Since strain is dimensionless, the units of the modulus of elasticity E are the same as for stress, namely, pounds per square inch.

As mentioned previously, the buckling strength is a function of the geometry, edge support conditions, and the modulus of elasticity. For a given structural design, the buckling strength (or critical compressive stress σ_{cr}) of the sheet is proportional to the product of the modulus of elasticity and the thickness squared.

$$\sigma_{cr} \propto Et^2$$

As was also mentioned previously, steel and aluminum structures theoretically can be designed to carry the same loads in tension with the same weight. This is because the steel would be only one-third the thickness of the aluminum, since it is about three times as strong. Since the density of steel (0.3 lb/in.^3) is three times that of aluminum (0.1 lb/in.^3), the weights would be the same. However, the modulus of elasticity of steel is also three times that of aluminum ($30\,000\,000 \text{ lb/in.}^2$ for steel and $10\,000\,000 \text{ lb/in.}^2$ for aluminum). Therefore, from the preceding equation, the buckling strength of a steel panel will be only one-third that of an equal weight aluminum panel, because the buckling strength is proportional to thickness squared. (In contrast, the tensile strength is proportional to thickness to the first power.) Consequently, since most of an aircraft structure is designed on the basis of buckling, aluminum airframes are lighter in weight than those designed of steel for subsonic and some supersonic applications. Material selection for supersonic application will be discussed in the section titled THERMAL BARRIER.

Fatigue

Not only must the aircraft structure be designed to carry the maximum load, but it must also be designed to carry the loads repeatedly. A structure may fail if a given load is applied to it many times even though the stresses are low compared with the failure stress which can be obtained under a single cycle of loading. This phenomenon is called metal fatigue. The smaller the maximum stress, the larger will be the number of times the load can be applied without producing a fatigue failure, as shown in figure 8-13. For most materials there is a stress below which an infinitely large number of cycles can be applied without failure. This stress is called the endurance limit or fatigue limit.

One of the primary sources of stress which must be considered in designing against fatigue failure is gust loading. The wings, in particular, may flex many times in response to vertical gust loading during a single flight of the aircraft. Today's jets, flying at 35 000 to 40 000 feet altitude, are above most of the weather and thus are subjected to fewer cycles of gust loading than piston-engine airplanes, which fly at 15 000 to 20 000 feet altitude.

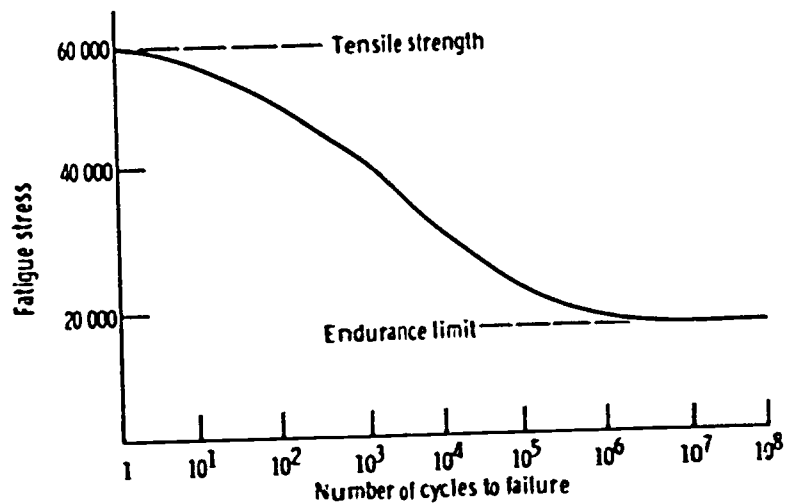


Figure 8-13. - Typical curve of fatigue stress as function of number of cycles to failure.

Pressurization of the passenger compartment produces stresses which are cyclic but occur only once per flight. However, this pressurization was found to be the cause of two disastrous disintegrations at high altitude of the British de Havilland Comet I. This airplane, which was one of the earliest high-altitude jet transports, entered service in 1952. The accidents, which occurred in 1954, were attributed to metal fatigue in the passenger compartment. A test cabin had been statically subjected to twice the expected pressure differential without difficulty. The same cabin was then run through a series of fatigue tests with no failure. However, it was learned later that the high-pressure static test had produced local plastic flow in the material around the windows, which changed the stress pattern produced in the fatigue tests. The fatigue life of the test cabin was thus unknowingly increased beyond that of the production cabins, which were never subjected to such a high-pressure static test.

AEROELASTICITY

The term "aeroelasticity" refers to the mutual interaction between aerodynamic forces and the elastic response of the structure. If the aircraft structure were perfectly rigid, there would be no aeroelastic problems. However, modern aircraft structures are very flexible and therefore must undergo a thorough aeroelastic analysis. This flexibility is vividly illustrated in figure 8-14, which shows the tip of a B-52 wing being deflected upward 22 feet from the undeflected position during a static test of the structure.

Aerodynamic forces produce structural deformations which may, in turn, produce additional aerodynamic forces. Such interactions may be damped out to stable equilibrium, or they may diverge and result in the destruction of the aircraft. One of the most

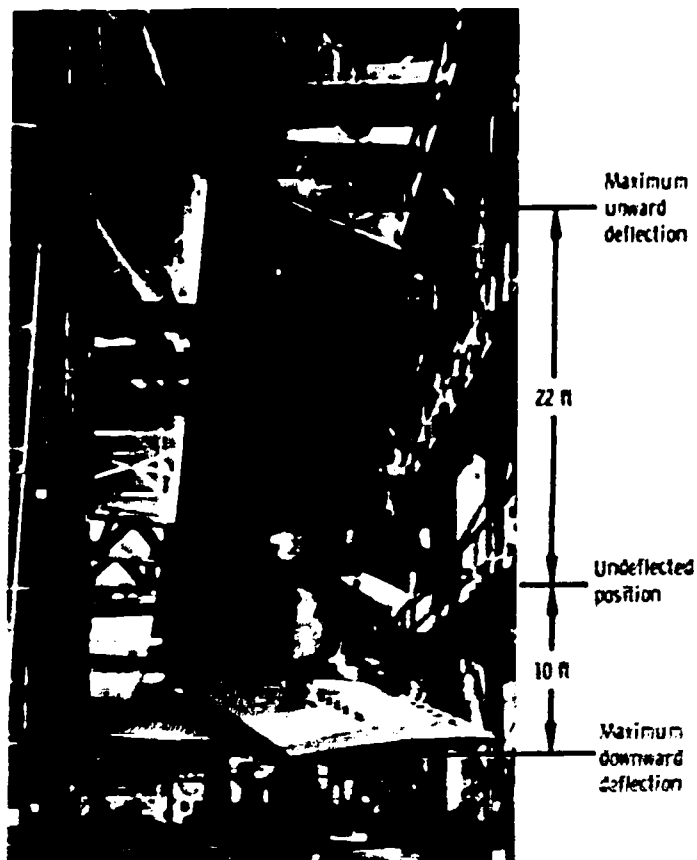


Figure 8-14. - Static test of flexibility of wing of B-52 aircraft. (Taken from "Principles of Aeroelasticity" by Raymond L. Bisplinghoff and Holt Ashley, with permission of John Wiley & Sons, Inc., Pub. 1)

complex aeroelastic phenomena is called flutter. Flutter is a dynamic instability which occurs at a critical speed called the flutter speed and results from the elasticity of the structure.

A simple example of aerodynamic flutter is the waving motion of a flag. Another example is the behavior of tree leaves, which oscillate as the air load varies between their upper and lower surfaces. Airplane wings, stabilizers, and control surfaces will flutter mildly at certain air speeds but fail violently if the flutter speed is exceeded. It is thus necessary that the flutter speed of all structural components susceptible to this phenomenon be above the maximum flight speed of the aircraft.

Flutter affects aircraft structural design most in requiring high torsional stiffness of the wings. In some instances, wing skin thickness has been dictated by aeroelastic considerations. Mass balancing the control surfaces with respect to the hinge line is also done to minimize flutter.

Another aeroelastic phenomenon which must be considered when designing the aircraft structure is called buffeting. Buffeting is a transient vibration, or shaking, of a structural component, produced by an unsteady airflow with rather powerful impulses. These impulses usually come from wakes or vortexes behind wings, nacelles, or objects

carried under the wings, such as fuel tanks, bombs, or even landing gear. Buffeting can occur at low or high speed and can be mild or catastrophic in nature. Mild buffeting at low speed can be beneficial in that it may warn the pilot that he is at a very high angle of attack attitude and about to stall or lose lift. Severe buffeting can result from interaction between the frequency of the aerodynamic pulses and the natural frequency of a structure, such as a tail surface. This could lead to metal fatigue over a period of time or to sudden collapse of the structure if the stiffness, strength, and damping are insufficient.

THERMAL BARRIER

Just a few years ago, engineers referred to the sonic barrier when discussing technical problems anticipated for future aircraft. As is well known, the term "supersonic" refers to speeds greater than the speed of sound (about 670 miles per hour at sea level; also called Mach 1). Hypersonic speeds are greater than five times the speed of sound, or Mach 5. Today some military aircraft fly at supersonic speeds under cruise conditions. Commercial transports are being built today to fly at almost three times the speed of sound. Obviously, the so-called sonic barrier has been overcome.

Today the thermal barrier appears formidable when considering future airplanes for supersonic and hypersonic flight. The thermal barrier refers to the structural and material problems resulting from very high temperatures being encountered both in the airframe and in the engine. Skin temperatures, especially on the leading edges of wings and tail surfaces, become very high as a result of aerodynamic heating as the air molecules collide with the airframe at very high speed. A typical plot of skin temperature as a function of Mach number is given in figure 8-15.

Aluminum retains most of its strength up to about 300° F and falls off quite rapidly above about 400° F, as shown in figure 8-16. Thus, figures 8-15 and 8-16 show why the

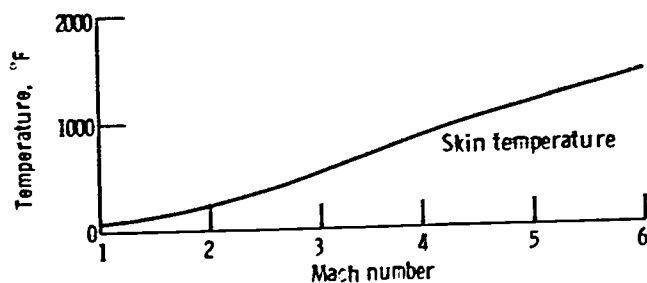


Figure 8-15. - Typical skin temperature as function of Mach number.

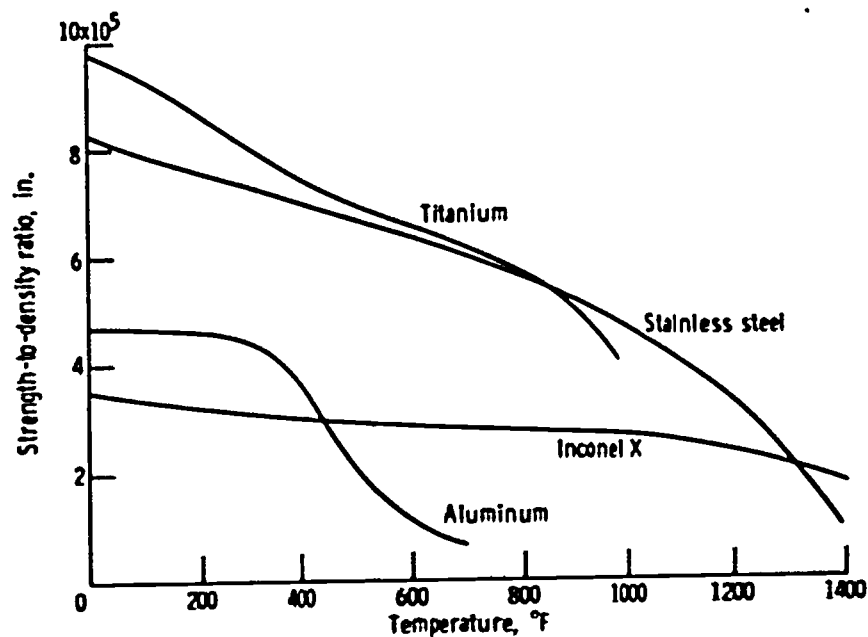


Figure 8-16. - Material strength-to-density ratio as function of temperature.

British-French Concorde, which is an aluminum airplane, is being designed to fly at Mach 2.2. This is about the upper limit of speed and temperature for an aluminum airframe. The United States supersonic transport (SST) will fly at Mach 2.7, or about 1800 miles per hour. The U.S. SST will be built of a titanium alloy to withstand skin temperatures in excess of 500° F.

At speeds in excess of Mach 3, or 2000 miles per hour, skin temperatures exceed 700° or 800° F, which is about the upper limit of usefulness for titanium. Therefore, materials such as stainless steel or Inconel must be used. The experimental X-15 airplane has flown at speeds as high as Mach 6.06 (4104 mph) and up to 354 200 feet (67 miles) altitude. It has an Inconel X skin which has withstood repeated flights that have heated large areas of the structure to a cherry-red 1300° F.

At high temperatures, other problems in addition to those involving material strength are encountered. As discussed earlier, over half of the aircraft structure is critical from the standpoint of buckling strength, which is directly proportional to the modulus of elasticity, or stiffness, of the material. Unfortunately, the modulus of elasticity, and therefore the buckling strength, decreases with increasing temperature. Another problem area involves thermal stresses that are induced because of the differences in temperature and, therefore, the differences in free thermal expansion in adjacent areas of the structure. These thermal stresses must be superimposed on the other stresses when designing the structure.

At high temperatures, materials creep and deform under long-time loading. There is an upper limit on the amount of creep a material can withstand, or the time it can be stressed to a given level; this limit is called the creep-rupture life of the material. Since

the SST is being designed for a life greater than 10 years or 30 000 to 50 000 hours of flying time, creep might be a significant problem. Thermal distortions and creep also affect the aerodynamic properties of the lifting surfaces. These may influence the performance of the airplane, particularly during a maneuver condition.

CONCLUDING REMARKS

This chapter has covered some aspects of the historical development of the modern aircraft structure and the technical advances which permitted its rapid evolution. Some of the ways in which material behavior influences structural design and ways in which aircraft performance may influence material selection have been discussed briefly. Of necessity, the discussion has been general and cursory. Helicopters and V/STOL airplanes were not considered. Lifting bodies for reentry from orbital or space flights and hypersonic airplanes were also omitted from the discussion. As these new types of craft are being developed and tested, aircraft structures and materials are also continually being changed and improved to meet the new requirements.

BIBLIOGRAPHY

- Bisplinghoff, R. L. : The Supersonic Transport. *Scientific American*, vol. 210, no. 6, June 1964, pp. 25-35.
- Bisplinghoff, Raymond L. ; and Ashley, Holt: *Principles of Aeroelasticity*. John Wiley & Sons. Inc. , 1962.
- Bruhn. E. F. : *Analysis and Design of Flight Vehicle Structures*. Tri-State Offset Co. , 1965.
- Corning, Gerald: *Supersonic and Subsonic Airplane Design*. Second ed. , Edwards Bros. , Inc. , 1960.
- Heldenfels, Richard R. : *Frontiers of Flight Structures*. *Aeronautics and Astronautics*. Nicholas John Hoff and Walter Guido Vincenti, eds. , Pergamon Press, 1960, pp. 29-51.
- Heldenfels, R. R. : *Structural Prospects for Hypersonic Air Vehicles*. *Aerospace Proceedings 1966*. Vol. 1. Joan Bradbrooke, Joan Bruce, and R. R. Dexter, eds. , Macmillan and Co. , 1967, pp. 561-583.
- Hoff, Nicholas J. : *Thin Shells in Aerospace Structures*. *Astronautics and Aeronautics*, vol. 5, no. 2, Feb. 1967, pp. 26-45.

Hunsaker, Jerome C.: A Half Century of Aeronautical Development. Proc. Am. Phil. Soc., vol. 98, no. 2, Apr. 1954, pp. 121-130.

Nayler, J. L.; and Ower, E.: Aviation: Its Technical Development. Dufour Editions, 1965.

Stack, John: The Supersonic Transport. Int. Sci. Tech., no. 22, Oct. 1963, pp. 50-54, 56, 58, 61.

9. AIRCRAFT STABILITY AND CONTROL

Clifford C. Crabs*

The stability and control characteristics of an airplane determine its ability to fly smoothly at a constant attitude and air speed, to recover from the effects of atmospheric disturbances, and to respond adequately to the control of the pilot. Stability is the tendency of an object (in our case, an airplane) to remain in a state of equilibrium. An object is in a state of equilibrium when the sum of all the forces and the sum of all the moments acting on it are equal to zero (i. e. , when all forces and all moments are in balance). Thus, an object that is in a state of equilibrium experiences no acceleration in any direction. An airplane that is in a steady flight condition (equilibrium) will remain in this condition until the balance of forces or moments is disturbed by some force. Disturbing forces can be caused, for example, by changes in weight, weight distribution, engine thrust, surface shape, surface area, or flight attitude. Such changes may be accidental (e. g. , a wind gust disturbing the airplane), or they may be deliberate (e. g. , the pilot moving a control surface).

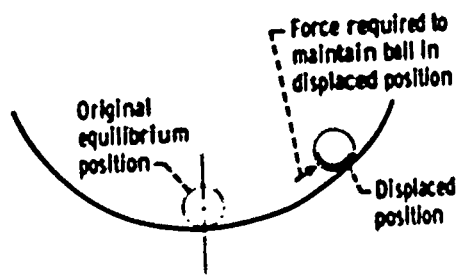
MECHANICAL STABILITY

Mechanical stability is the property that causes an object to develop forces opposing any influence that disturbs the object from its equilibrium position or motion. Mechanical stability has two components: static stability and dynamic stability. Static stability is the property whereby an object that is disturbed from a state of equilibrium develops restoring forces or moments that counteract the disturbance and tend to start the object back towards equilibrium. Dynamic stability is the property whereby the oscillations set up by the restoring forces or moments of a statically stable object that is disturbed from equilibrium are damped. Mechanical stability (both static and dynamic) may be classified as positive, neutral, or negative.

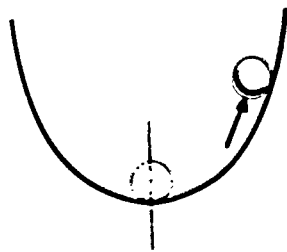
Static Stability

With positive static stability, an object that is disturbed from a state of equilibrium

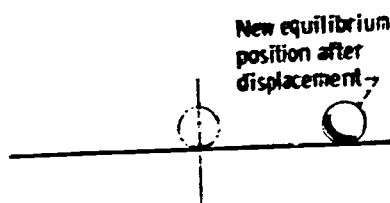
* Aerospace Engineer and Pilot, Aircraft Operations Branch.



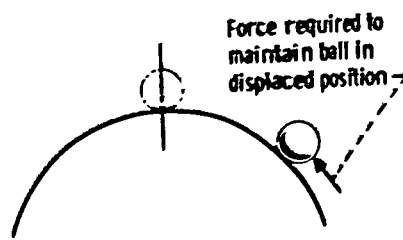
(a) Positive.



(b) More positive.



(c) Neutral.



(d) Negative.

Figure 2-1. - Static stability.

tends to return to the original condition. With neutral static stability the object tends to remain in a state of equilibrium, but when the object is disturbed, it may come to rest in a new state of equilibrium. In other words, after the disturbance the object tends neither to return to the original state nor to move further away from it. With negative static stability (static instability), the object is unstable. When the object is disturbed, it tends to continue to move further away from the original state, even after the initial disturbance.

A simple analogy for static stability is a ball resting on various curved and flat surfaces. Figure 9-1(a) illustrates positive static stability. If the ball in this example is displaced from its equilibrium position at the bottom of the curve, it tends to resist the displacement. When the disturbing force is removed and the ball is released in the displaced position, it tends to return to its original equilibrium position at the bottom of the curve.

Figure 9-1(b) illustrates a greater degree of positive static stability. In this example the behavior of the ball is similar to that of the previous example. However, the ball now has a greater tendency to return to its original equilibrium position, because the slope of the curved surface is steeper. Therefore, a greater force is required to displace the ball from its equilibrium position.

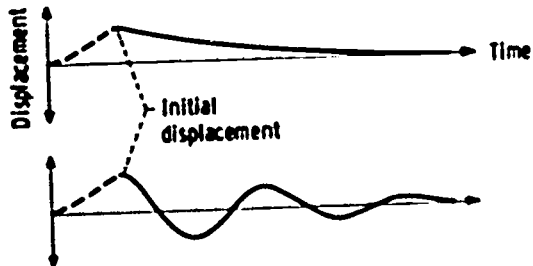
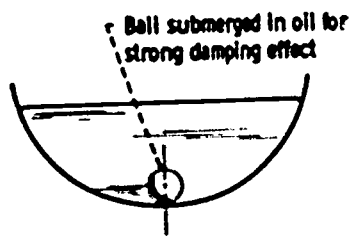
Neutral static stability is illustrated in figure 9-1(c). In this example, when the ball is displaced, it has no tendency to return to its original equilibrium position. Therefore, the ball can be displaced by a smaller force than that required to displace the ball with positive stability. When the disturbing force is removed, the ball does not tend to return to its original equilibrium position but assumes equilibrium in the displaced position.

Figure 9-1(d) shows an example of negative static stability (or instability). In this case, the ball is very easily displaced from its equilibrium position. Once the ball is displaced, it continues or tends to continue to move farther away from its equilibrium position, even after the initial disturbance is removed.

The restoring forces or moments developed by an object with positive static stability tend to cause the object to oscillate about its equilibrium position. For example, if the ball in figure 9-1(a) is displaced from its equilibrium position to some point up the slope and is released, it tends to roll back down the slope toward its equilibrium position. If there is no force to slow down the ball, its momentum will cause it to roll through the equilibrium position and up the opposite slope. Then the ball will tend to return down the slope, through the equilibrium position, and back up the original slope. Thus, an oscillation is set up. Dynamic stability concerns the damping (i. e., the displacement-time history) of such oscillations.

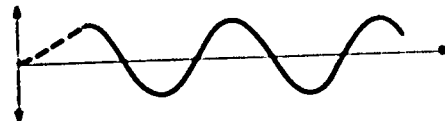
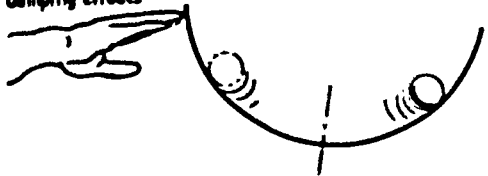
Dynamic Stability

An object that has positive static stability also has either positive, neutral, or nega-



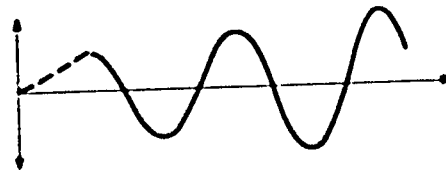
(a) Positive dynamic stability - positive static stability.

Rocking force sufficient to counteract damping effects

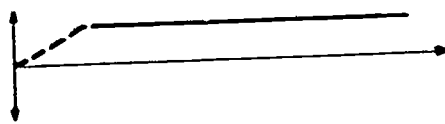


(b) Neutral dynamic stability - positive static stability.

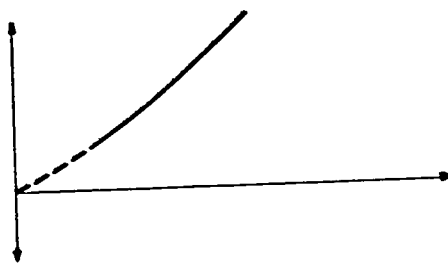
Rocking force greater than damping effects



(c) Negative dynamic stability - positive static stability.



(d) No dynamic stability characteristics - neutral static stability.



(e) Negative dynamic stability - negative static stability.

Figure 9-2. - Examples and displacement-time histories of dynamic stability and interrelation of static and dynamic stabilities.

tive dynamic stability. When an object with positive dynamic stability is disturbed from a state of equilibrium, the oscillations set up by the restoring forces or moments are damped, and the object gradually returns to its original state of equilibrium. With neutral dynamic stability, the oscillations of the object neither increase nor decrease in magnitude. With negative dynamic stability (dynamic instability), the oscillations of the object increase in magnitude.

Figure 9-2 shows examples of dynamic stability and curves of displacement as a function of time. Positive dynamic stability is illustrated in figure 9-2(a). In this example, the oil provides a damping effect. Thus, if the ball is displaced from its equilibrium position and is released, it returns to, and eventually comes to rest in, its original equilibrium position. The displacement-time curve shows that the ball may return to equilibrium either in a single motion (simple subsidence) or in a series of damped oscillations whose amplitude decreases with time.

Neutral dynamic stability is shown in figure 9-2(b). In this example, either the system is assumed to be frictionless or an outside force is applied to the system (e. g., to rock the concave surface) that is exactly equal to and counteracts the damping forces of the system. Under either of these conditions, the ball rolls the same distance up each slope on every oscillation. The displacement-time curve shows that the amplitude of the oscillations remains constant with time.

Figure 9-2(c) illustrates negative dynamic stability (dynamic instability). In this example, if an outside force is applied to the system that counteracts and exceeds the damping forces, the ball will roll farther up the slope with each oscillation. The displacement-time curve shows the amplitude of the oscillations increasing with time.

With neutral static stability (fig. 9-2(d)), an object does not display any dynamic stability characteristics.

An object with negative static stability (fig. 9-2(e)) has negative dynamic stability.

AERODYNAMIC STABILITY

The aerodynamic stability of an airplane in flight is a form of mechanical stability. An airplane has three components of stability (lateral, longitudinal, and directional), based on its three stability axes (roll, pitch, and yaw), about which it may rotate. These axes (fig. 9-3) are mutually perpendicular and usually intersect at the center of gravity of the airplane. The roll axis is the longitudinal axis about which the airplane rotates when it is inclined laterally (i. e., banked). The pitch axis is the lateral axis about which the airplane rotates when its nose is raised or lowered relative to the tail, as when the airplane is shifted into a climbing or diving attitude. The yaw axis is the normal axis (perpendicular to the plane of the other two axes) about which the airplane rotates when

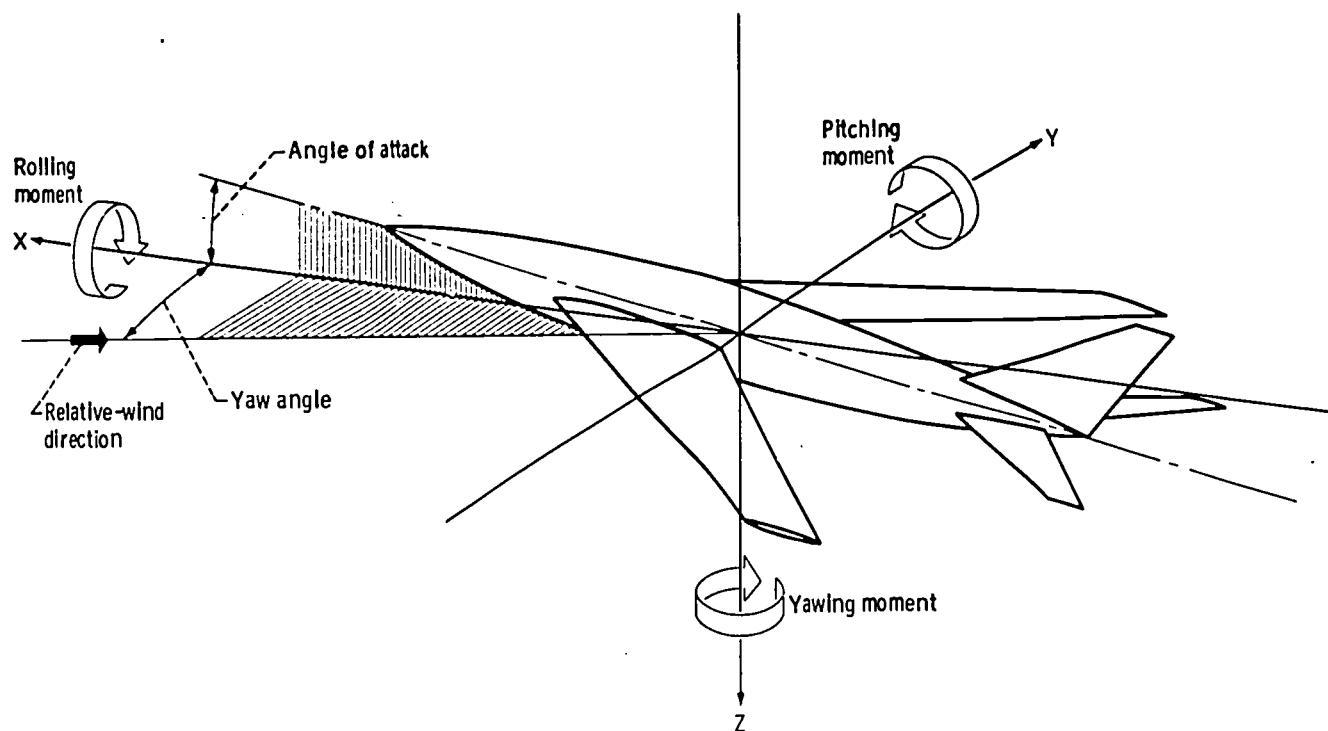


Figure 9-3. - Stability axes. (Arrows indicate conventional positive directions of axes and moments.)

the nose of the airplane is pointed in a new direction to the right or left of the original direction.

An airplane in flight has three degrees of freedom relative to each of its stability axes. (A degree of freedom is one of a limited number of ways in which a point or a body may move or a dynamic system may change.) The three degrees of freedom are angular displacement (rotation) about the axis, linear displacement along the axis, and change of velocity along the axis. Any actual change or displacement of the airplane generally involves a combination of motions and velocity changes relative to all three stability axes.

Of the three previously mentioned components of aerodynamic stability, longitudinal stability pertains to pitching motions, vertical displacements, fore-and-aft displacements, and changes in forward or vertical velocities. Lateral stability refers to rolling motions, lateral displacements (sideslip), and changes in lateral velocity. Directional stability pertains to yawing motions.

Because of its complexity, the overall subject of airplane stability cannot be explained thoroughly in this chapter. Therefore, the following brief and limited discussion is devoted to only static longitudinal stability, and specifically to pitching motions.

Longitudinal Stability

The behavior of an airplane in each component of its stability is similar to the be-

havior of the ball in the preceding examples. Thus, if an airplane with positive static and positive dynamic longitudinal stability is displaced from a level-flight attitude, it returns to and eventually resumes the original attitude. With positive static and neutral dynamic stability, an airplane tends to return to the original attitude but does not resume that attitude. Instead, the airplane overshoots the original attitude and begins an oscillatory pitching motion of constant amplitude. With positive static and negative dynamic stability, an airplane tends to return to the original level-flight attitude, but it begins an oscillatory pitching motion of increasing amplitude.

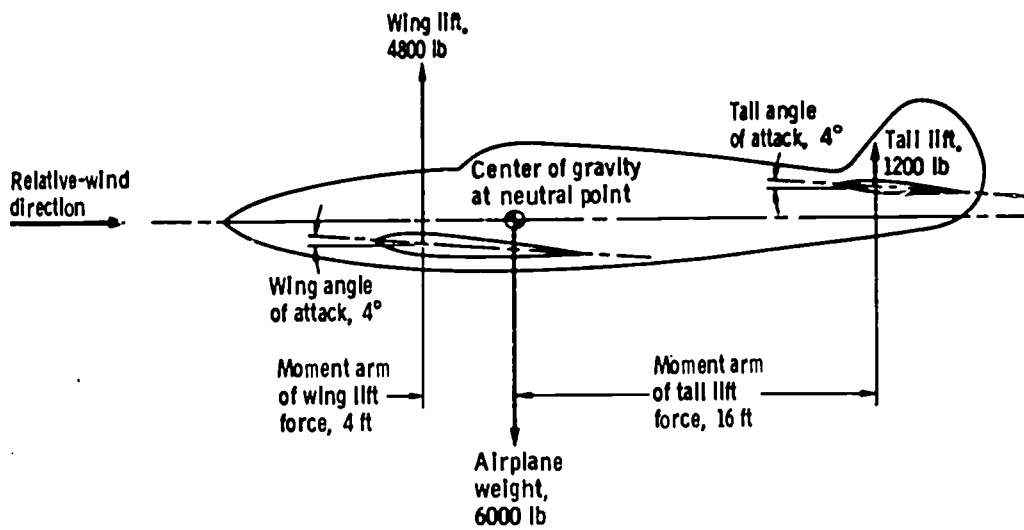
With neutral static longitudinal stability, an airplane tends to maintain any pitch attitude (climbing or diving attitude) to which it is displaced. When an airplane with negative static longitudinal stability (static longitudinal instability) is displaced from a level-flight attitude, it tends to continue to diverge ever farther from the original attitude.

Effect of Location of Center of Gravity on Stability

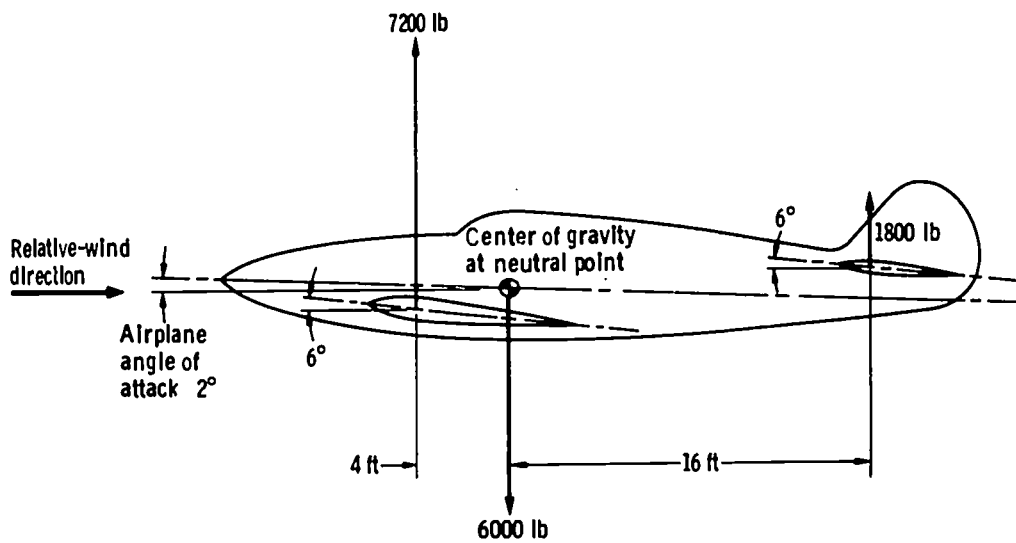
One of the factors that affect the static, longitudinal stability of an airplane is the location of the center of gravity relative to the neutral point of the airplane. The neutral point is that point about which the pitching moment of the airplane remains constant, even when the angle of attack of the airplane is changed. In other words, the neutral point is the aerodynamic center of the entire airplane.

When the center of gravity of an airplane is located at the neutral point (fig. 9-4), the airplane possesses neutral, static, longitudinal stability. Figure 9-4(a) shows a neutrally stable, example airplane in an equilibrium, level-flight attitude. The total lift produced by the wing (4800 lb) and the horizontal tail (1200 lb) equals the airplane weight (6000 lb). The nose-up pitching moment produced by the wing ($4800 \text{ lb} \times 4 \text{ ft} = 19\,200 \text{ lb-ft}$) is equal to the nose-down pitching moment produced by the tail ($1200 \text{ lb} \times 16 \text{ ft} = 19\,200 \text{ lb-ft}$). The center of gravity is located at the neutral point. The wing and the horizontal tail have equal angles of incidence (4°). This condition of equal angles of incidence is called "zero angular difference." Any airplane whose center of gravity is located at the neutral point must have zero angular difference to achieve equilibrium.

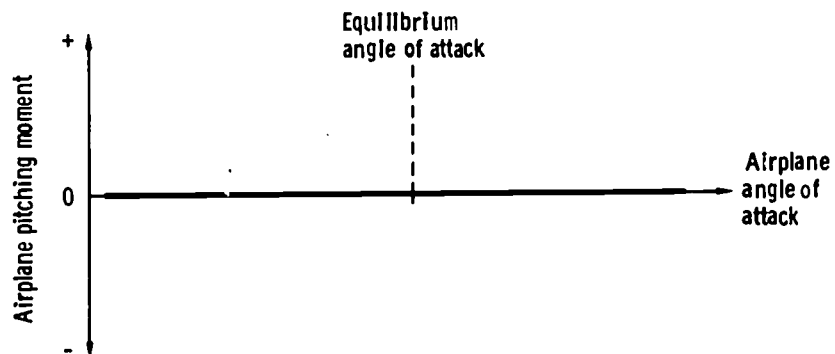
The angle of incidence of an airfoil is the angle between the chord of the airfoil and the longitudinal axis of the airplane. The angle of attack of an airfoil is the angle between the chord of the airfoil and the direction of the relative wind at the airfoil. For this example airplane in the level-flight attitude, the relative-wind direction for both the wing and the horizontal tail is assumed to be parallel to the longitudinal axis of the airplane. Therefore, in the level-flight attitude, the incidence angles of the wing and the horizontal tail are also their angles of attack. However, when the example airplane is disturbed



(a) Airplane in initial, equilibrium, level-flight attitude.



(b) Airplane in displaced, nose-up attitude.



(c) Airplane pitching-moment curve. (Nose-up moment is positive; nose-down moment is negative.)

Figure 9-4. - Forces acting on example airplane with neutral, static, longitudinal stability.

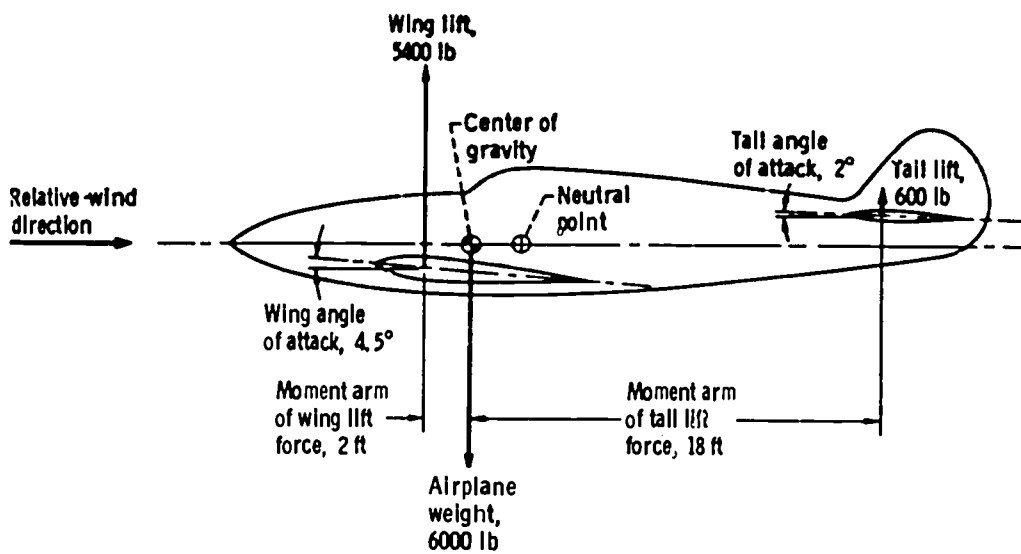
from the level-flight attitude, the angles of attack change, whereas the incidence angles remain unchanged.

When this airplane is pitched upward or downward from its initial, equilibrium, level-flight attitude, it maintains neutral stability. Figure 9-4(b) shows the airplane in a new, upwardly displaced attitude. The airplane angle of attack has been increased by 2° . Therefore, the angles of attack of both the wing and the horizontal tail have increased by 50 percent (from 4° to 6°). Since the lift of an airfoil is a linear function of its angle of attack, the wing lift has increased from 4800 pounds to 7200 pounds, and the tail lift has increased from 1200 pounds to 1800 pounds. However, the nose-up pitching moment produced by the wing ($7200 \text{ lb} \times 4 \text{ ft} = 28\,800 \text{ lb-ft}$) is still equal to the nose-down pitching moment produced by the tail ($1800 \text{ lb} \times 16 \text{ ft} = 28\,800 \text{ lb-ft}$), so that the resultant pitching moment of the airplane is zero. Therefore, when this airplane is displaced from its initial, equilibrium, level-flight attitude, it tends to remain in the new, displaced attitude. Thus, the airplane displays neutral, static, longitudinal stability.

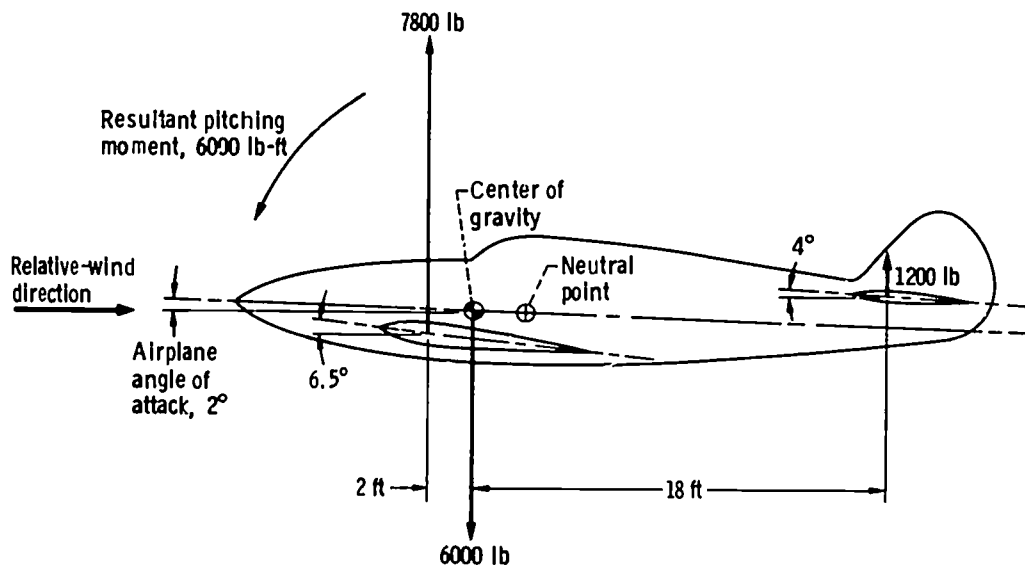
Figure 9-4(c) shows an example curve of the pitching moment as a function of angle of attack for an airplane with neutral stability. The slope of the curve is zero. This indicates that when the airplane angle of attack is varied, the resultant pitching moment of the airplane remains zero.

If the center of gravity of an airplane is located ahead of the neutral point, the airplane possesses positive, static, longitudinal stability. Figure 9-5(a) shows the example airplane again in an equilibrium, level-flight attitude. The total lift produced by the wing (5400 lb) and the horizontal tail (600 lb) is equal to the airplane weight (6000 lb). The nose-up pitching moment produced by the wing ($5400 \text{ lb} \times 2 \text{ ft} = 10\,800 \text{ lb-ft}$) is equal to the nose-down pitching moment produced by the horizontal tail ($600 \text{ lb} \times 18 \text{ ft} = 10\,800 \text{ lb-ft}$).

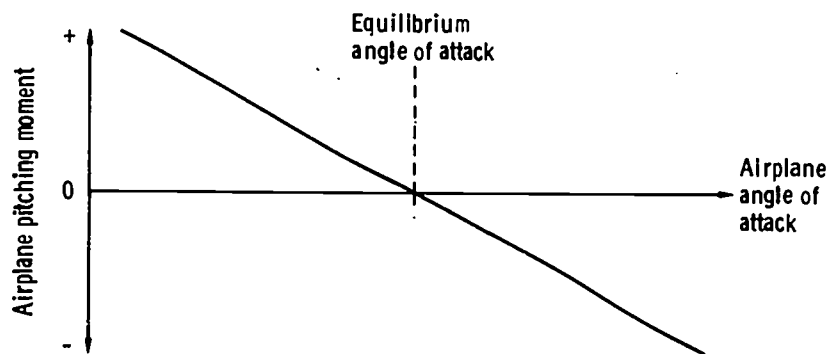
Since the center of gravity has been moved forward of the neutral point, the moment arm of the wing lift force has decreased (from 4 ft to 2 ft), while that of the tail lift force has increased (from 16 ft to 18 ft). Therefore, to achieve equilibrium in the level-flight attitude, the lift force of the wing has been increased (from 4800 lb to 5400 lb), and that of the tail has been decreased (from 1200 lb to 600 lb). These changes in the lift forces have been accomplished by increasing the wing angle of attack and decreasing the tail angle of attack. As mentioned previously, the angles of attack of the wing and tail of this example airplane in the level-flight attitude are assumed to be the same as their incidence angles. So, the incidence angle of the wing has been increased (from 4° to 4.5°), and that of the tail has been decreased (from 4° to 2°). Therefore, the incidence angle of the wing is now greater than that of the tail. This condition is called "positive angular difference." Any airplane whose center of gravity is moved forward of the neutral point, but whose wing and tail surface areas remain unchanged, must have positive angular difference to achieve equilibrium.



(a) Airplane in initial, equilibrium, level-flight attitude.



(b) Airplane in displaced, nose-up attitude.



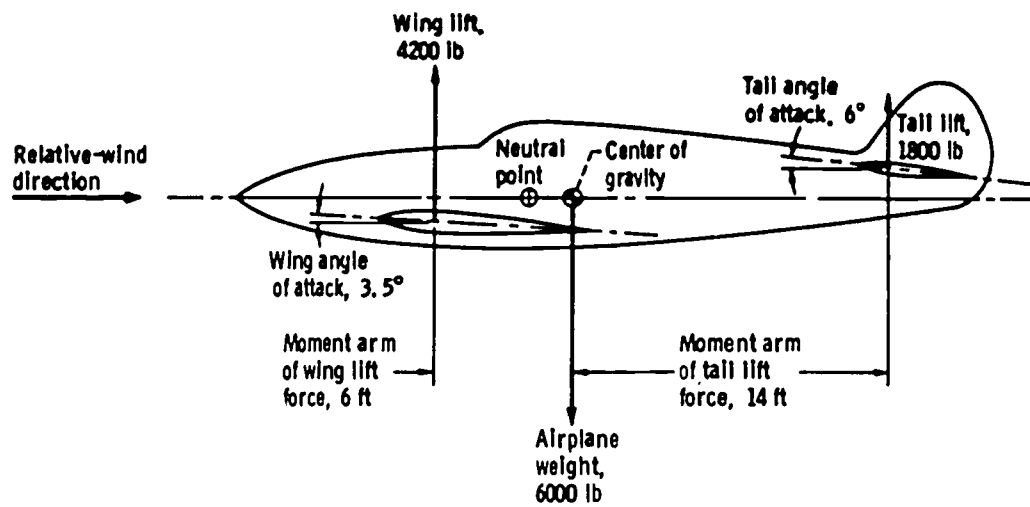
(c) Airplane pitching-moment curve. (Nose-up moment is positive; nose-down moment is negative.)

Figure 9-5. - Forces and resultant pitching moment acting on example airplane with positive, static, longitudinal stability.

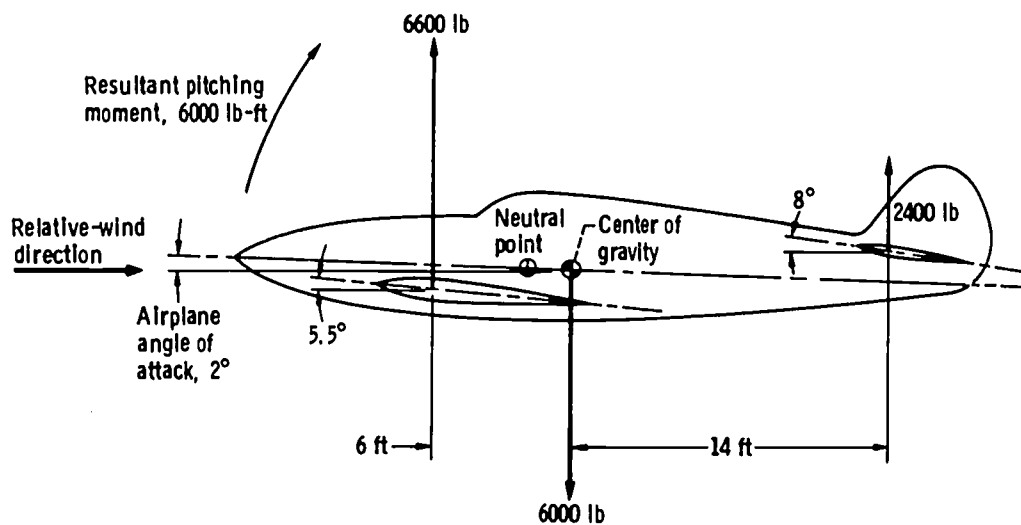
When this airplane is pitched upward or downward from its initial, equilibrium, level-flight attitude, it displays positive stability. Figure 9-5(b) shows the airplane in a new, upwardly displaced attitude. The airplane angle of attack has been increased by 2° . Since the wing and the horizontal tail are attached to the fuselage, their angles of attack have also increased by 2° . However, because of the initial, positive angular difference, the wing and tail angles of attack have increased by different percentages. The wing angle of attack has increased by approximately 44.4 percent (from 4.5° to 6.5°), and the tail angle of attack has increased by 100 percent (from 2° to 4°). The lift forces produced by the wing and the horizontal tail have also increased by these percentages. Therefore, the nose-up pitching moment produced by the wing ($7800 \text{ lb} \times 2 \text{ ft} = 15\,600 \text{ lb-ft}$) is now less than the nose-down pitching moment produced by the horizontal tail ($1200 \text{ lb} \times 18 \text{ ft} = 21\,600 \text{ lb-ft}$). Thus, the airplane has developed a resultant, nose-down pitching moment (6000 lb-ft) that is opposite in direction to the initial, nose-up displacement. This resultant moment tends to return the airplane to its initial, equilibrium attitude. Therefore, this airplane displays positive, static, longitudinal stability.

Figure 9-5(c) shows an example curve of the resultant pitching moment as a function of angle of attack for a stable airplane. For angles of attack smaller than the equilibrium angle of attack (i. e., when the airplane is pitched downward from its equilibrium attitude), the pitching moment is positive (nose-up). At the equilibrium angle of attack, the pitching moment is zero. For angles of attack greater than the equilibrium angle of attack (i. e., when the airplane is pitched upward from its equilibrium attitude), the pitching moment is negative (nose-down). Thus, figure 9-5(c) shows that for a longitudinally stable airplane, the pitching-moment curve has a negative slope. The degree of stability is indicated by the slope, or steepness, of the curve.

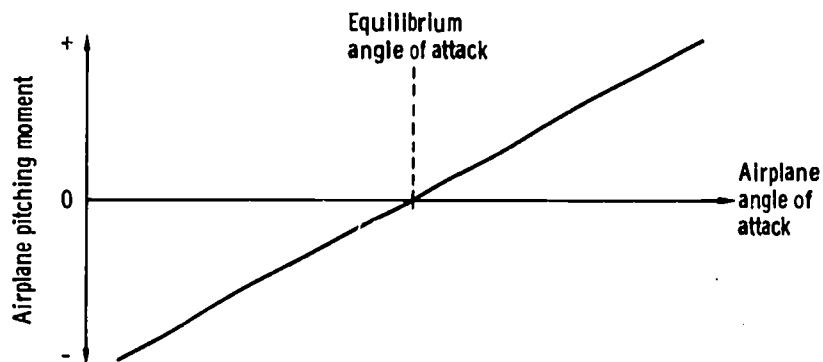
When the center of gravity of an airplane is located behind the neutral point, the airplane possesses negative, static, longitudinal stability. Figure 9-6(a) shows the example airplane again in an equilibrium, level-flight attitude. The total lift provided by the wing (4200 lb) and the tail (1800 lb) is equal to the airplane weight (6000 lb). Also, the nose-up pitching moment produced by the wing ($4200 \text{ lb} \times 6 \text{ ft} = 25\,200 \text{ lb-ft}$) is equal to the nose-down pitching moment produced by the horizontal tail ($1800 \text{ lb} \times 14 \text{ ft} = 25\,200 \text{ lb-ft}$). However, the center of gravity is now located behind the neutral point. For this unstable configuration, the relative lengths of the moment arms of the wing and tail lift forces are such that equilibrium in any specific pitch attitude can be achieved only if the incidence angle of the wing is less than that of the tail. This condition is called "negative angular difference." Any airplane whose center of gravity is moved rearward of the neutral point, but whose wing and tail surface areas remain unchanged, must have negative angular difference to achieve equilibrium. For the example airplane of figure 9-6(a), the wing incidence angle is 3.5° , and the tail incidence angle is 6° . (It should be remembered that for our example airplane in the level-flight attitude, the angles of attack are



(a) Airplane in initial, equilibrium, level-flight attitude.



(b) Airplane in displaced, nose-up attitude.



(c) Airplane pitching-moment curve. (Nose-up moment is positive; nose-down moment is negative.)

Figure 9-6. - Forces and resultant pitching moment acting on example airplane with negative, static, longitudinal stability.

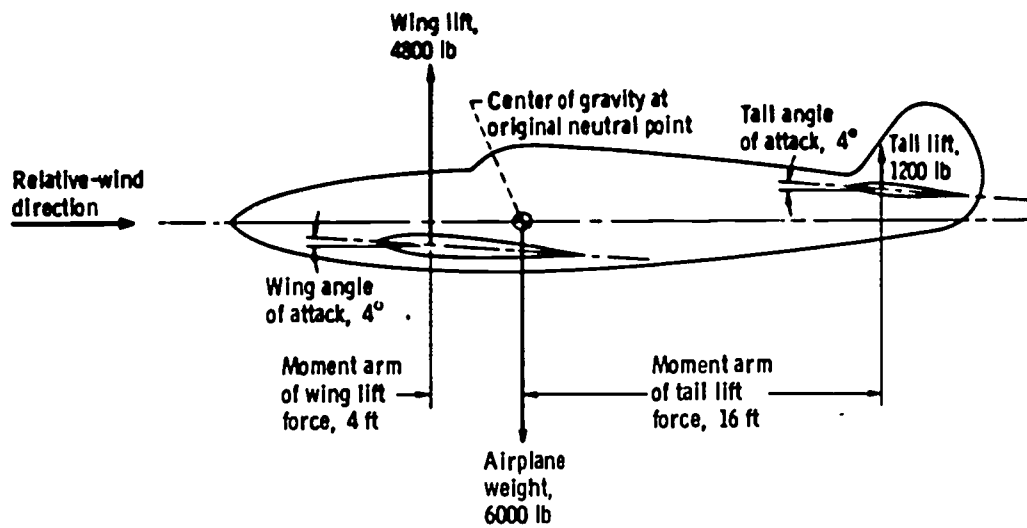
assumed to be the same as the incidence angles.)

When this airplane is pitched upward or downward from its equilibrium attitude, it displays negative stability. Figure 9-6(b) shows the example airplane in an upwardly displaced attitude. The airplane angle of attack has been increased by 2° . Thus, the wing angle of attack has increased by approximately 57 percent (from 3.5° to 5.5°), and the tail angle of attack has increased by approximately 33 percent (from 6° to 8°). The wing and tail lift forces have increased by these same percentages. Therefore, the nose-up pitching moment produced by the wing ($6600 \text{ lb} \times 6 \text{ ft} = 39\,600 \text{ lb-ft}$) is now greater than the nose-down pitching moment produced by the tail ($2400 \text{ lb} \times 14 \text{ ft} = 33\,600 \text{ lb-ft}$). Thus, the airplane has developed a resultant, nose-up pitching moment (6000 lb-ft) in the same direction as the initial, nose-up displacement. This resultant pitching moment tends to cause the airplane to continue to diverge farther from the initial, equilibrium, level-flight attitude. Thus, this airplane displays negative, static, longitudinal stability.

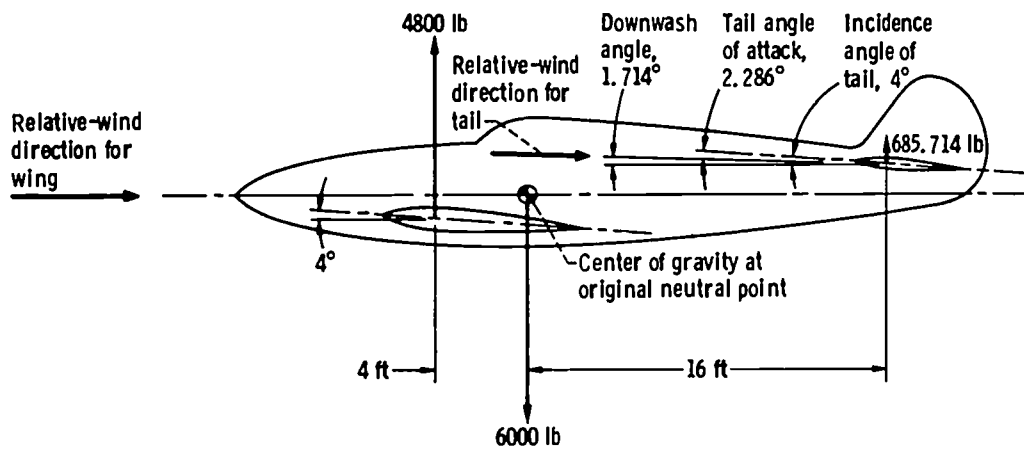
Figure 9-6(c) shows an example curve of the resultant pitching moment as a function of angle of attack for an unstable airplane. For angles of attack smaller than the equilibrium angle of attack (i. e., when the airplane is pitched downward from its equilibrium attitude), the pitching moment is negative (nose-down). At the equilibrium angle of attack, the pitching moment is zero. For angles of attack greater than the equilibrium angle of attack (i. e., when the airplane is pitched upward from its equilibrium attitude), the pitching moment is positive (nose-up). Thus, figure 9-6(c) shows that for a longitudinally unstable airplane, the pitching-moment curve has a positive slope. The degree of instability is indicated by the slope, or steepness, of the curve.

To simplify the preceding discussion of stability, the relative-wind direction was assumed to be the same for the wing and the horizontal tail. However, the horizontal tail of an actual airplane in flight generally operates in the downwash created by the wing. The local airflow past the wing is turned downward by it (see chapter 4), so that the local relative-wind direction at the horizontal tail is different from that at the wing. The downwash from the wing reduces the angle of attack of the tail and thereby affects the longitudinal stability of the airplane. Essentially, the effect of downwash on the horizontal tail necessitates shifting the neutral point (and center of gravity) to a more forward location to maintain the longitudinal stability of the airplane.

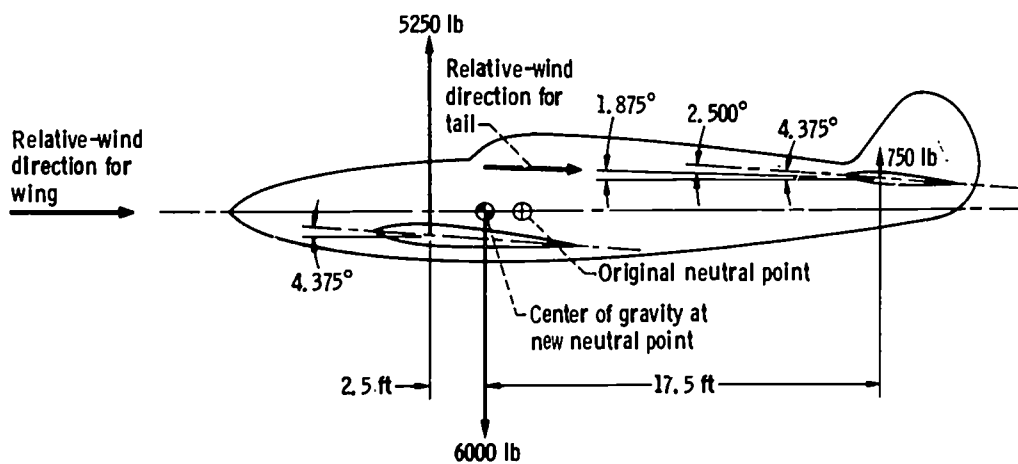
Figure 9-7(a) shows the neutrally stable, example airplane in an equilibrium, level-flight attitude, without any downwash. (This is the same example airplane as the one shown in fig. 9-4(a).) The total lift produced by the wing and the horizontal tail equals the airplane weight. The nose-up pitching moment produced by the wing is equal to the nose-down pitching moment produced by the tail. The center of gravity is located at the neutral point. The wing and the horizontal tail have equal angles of incidence (i. e., zero angular difference). Also, in the level-flight attitude, the relative wind direction is again assumed to be parallel to the longitudinal axis of the airplane. Thus, in the level-flight



(a) Neutrally stable airplane in equilibrium, level-flight attitude, without downwash.

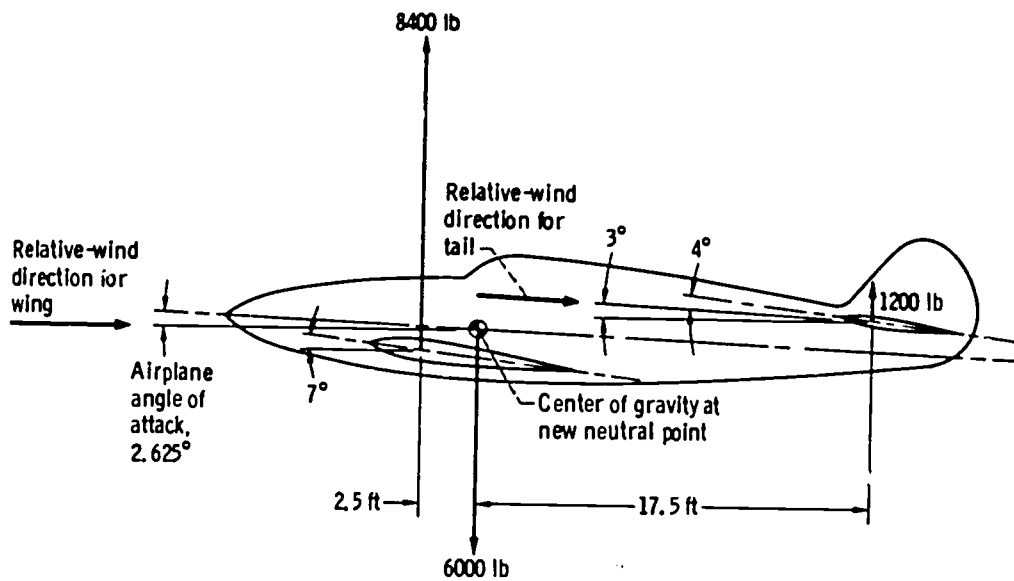


(b) Airplane, with downwash, in level-flight attitude, but no longer in equilibrium nor neutrally stable.



(c) Airplane modified to achieve neutral stability and equilibrium in level-flight attitude.

Figure 9-7. - Effect of downwash from wing on stability and on location of neutral point of example airplane.



(d) Airplane in displaced, nose-up attitude.

Figure 9-7. - Concluded.

attitude, the incidence angles of the wing and tail are also their angles of attack.

It has been shown previously that if this airplane is pitched upward or downward from its initial, equilibrium, level-flight attitude, it maintains neutral stability.

Figure 9-7(b) shows the same example airplane, still in a level-flight attitude, but with the horizontal tail now operating in the downwash created by the wing. The size of the downwash angle at the horizontal tail depends on the wing angle of attack and the configuration of the airplane. For a given airplane configuration, the ratio of the downwash angle to the wing angle of attack remains fairly constant with changes in the wing angle of attack. The numerical value of this ratio depends on certain design characteristics, such as the horizontal and vertical distances between the wing and the horizontal tail, the surface area of the wing, the aspect ratio of the wing, etc. For the example airplane of figure 9-7(b), the value of the ratio is arbitrarily assumed to be 0.4285. This means that for any given angle of attack, the downwash angle at the horizontal tail is equal to the wing angle of attack multiplied by 0.4285.

To be neutrally stable, an airplane must have zero angular difference, regardless of whether or not the downwash effects are taken into consideration. Therefore, in figure 9-7(b), the incidence angle of the wing is still equal to that of the tail. Since the relative-wind direction for the wing is still parallel to the longitudinal axis of the airplane, the angle of attack of the wing is still the same as its incidence angle (4°). However, the downwash angle at the horizontal tail ($4^\circ \times 0.4285 = 1.714^\circ$) has reduced the angle of attack of the horizontal tail from 4° to 2.286° . This reduction in the angle of attack has decreased the lift force produced by the tail from 1200 pounds to 685.714

pounds. Therefore, the example airplane is no longer in equilibrium nor neutrally stable. The total lift produced by the wing (4800 lb) and the horizontal tail (685.714 lb) is now less than the airplane weight (6000 lb). The nose-up pitching moment produced by the wing ($4800 \text{ lb} \times 4 \text{ ft} = 19\,200 \text{ lb-ft}$) is now greater than the nose-down pitching moment produced by the horizontal tail ($685.714 \text{ lb} \times 16 \text{ ft} = 10\,971.424 \text{ lb-ft}$).

This airplane can be restored to a neutrally stable, equilibrium, level-flight condition by first shifting the neutral point and center of gravity forward and then increasing the wing and tail lift forces. First, to restore neutral stability, the neutral point must be moved forward sufficiently to again equalize the nose-up and nose-down pitching moments. For neutral stability, the center of gravity must be located at this new neutral point. Next, to restore equilibrium, the wing and tail lift forces must be increased sufficiently to again equalize the total lift and the airplane weight. These lift forces must be increased by equal percentages at the wing and tail, so as not to destroy the equality of the nose-up and nose-down pitching moments. This change in the lift forces can be accomplished either by increasing equally the wing and tail angles of incidence or by increasing the airplane angle of attack.

Figure 9-7(c) shows the example airplane modified to reach neutral stability and equilibrium in the level-flight attitude. The neutral point has been moved forward, so that the nose-up and nose-down pitching moments are again equal. This new neutral point is valid for the wing and tail lift forces (4800 lb and 685.714 lb) shown in figure 9-7(b), as well as for the new lift forces shown in this figure. The center of gravity is now located at this new neutral point.

The wing and tail lift forces have both been increased by 9.375 percent, so that the total lift produced by the wing (5250 lb) and the tail (750 lb) is again equal to the airplane weight (6000 lb). These changes in the lift forces have been accomplished by increasing the incidence angles of both the wing and the tail by 9.375 percent, from 4° to 4.375° . Thus, the wing angle of attack, which, in this example, is assumed to be the same as the wing incidence angle, has also increased by 9.375 percent. This increase in wing angle of attack, in turn, has produced a 9.375-percent increase (from 1.714° to 1.875°) in the downwash angle. Since, in this example, the wing and tail angles of incidence are equal, the tail angle of attack is equal to the wing angle of attack (4.375°) minus the downwash angle (1.875°). Therefore, the tail angle of attack has also increased by 9.375 percent, from 2.286° to 2.500° .

When this airplane is pitched upward or downward from its level-flight attitude, it displays neutral, static, longitudinal stability. Figure 9-7(d) shows the airplane in a new, upwardly displaced attitude. The wing and tail lift forces have both increased, but the nose-up and nose-down pitching moments are still equal. Therefore, the airplane is still neutrally stable.

The preceding examples have shown only the effect of the center-of-gravity location

on the longitudinal stability of an airplane. However, many other factors affect longitudinal, lateral, or directional stability. The following are some of those factors: location and size of stabilizer; location and size of fin; location of wing; wing dihedral; wing sweepback; location of center of pressure; location of aerodynamic center; power loading; wing loading; location of thrust line; location of propeller(s); location of jet-engine inlet(s); location of jet-engine exhaust(s); and flight Mach number.

Effect of Stability on Controllability

Stability in an airplane is always desirable, but not necessarily in the maximum possible degree. Stability has a direct effect on controllability. The controllability of an airplane determines the ease of operating its controls and/or its responsiveness to the controls. Excessive stability reduces maneuverability and renders the airplane stiff, or heavy, to the controls. Too little stability (approaching neutral stability) renders the airplane too sensitive and too responsive to the controls, reduces the control feel received by the pilot, and increases the risk of overcontrol by the pilot. Therefore, the design of any airplane must achieve a satisfactory balance, or compromise, between stability and controllability.

AIRPLANE CONTROL

Control Surfaces

An airplane is controlled by means of various movable surfaces, or airfoils, attached to the wings and tail. When these control surfaces are deflected by the pilot, the aerodynamic forces on the airplane are changed and, therefore, the attitude or direction of the airplane is changed.

The primary control surfaces, shown in figure 9-8, are the elevator, the rudder, and the ailerons. The elevator, which is usually hinged to the rear of the stabilizer, controls pitch. The rudder, which is normally hinged to the rear of the fin, controls yaw. The ailerons, one on each wing, provide roll control. They are located at the trailing edges of the wings and are so connected that when one is deflected upward, the other deflects downward. Simple climbing and diving maneuvers (pitch) can be accomplished by merely deflecting the elevator. But most other maneuvers, including banks (roll) and turns (yaw), require that the pilot coordinate the deflections of two or all three primary control surfaces.

On some airplanes a single control surface serves the combined functions of the ele-

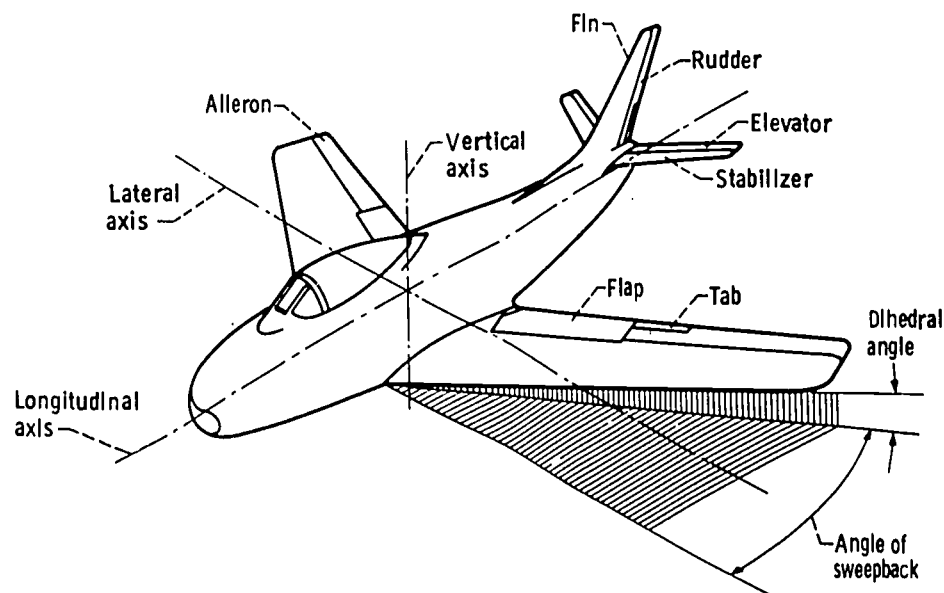


Figure 9-8. - Elements of stability and control.

vator and the ailerons or of the elevator and rudder. Sometimes, an entirely movable horizontal tail surface is used instead of the fixed stabilizer and movable elevator arrangement. Also, an entirely movable vertical tail may be used instead of the fixed fin and movable rudder arrangement.

The secondary control surfaces are tabs, flaps, and spoilers. Tabs are used for balancing and trimming the primary control surfaces, as will be discussed later in the chapter. Flaps have many variations and many uses. Most commonly they are hinged, pivoted, or sliding surfaces located at the rear of the wings and deflected or extended downward to increase the wing lift, especially at takeoff and landing. Spoilers are usually hinged or sliding surfaces mounted on the wings and/or the fuselage. They are used to slow down the airplane by increasing the drag when they are extended.

Hinge Moment of Control Surface

The forces required to move the control surfaces must be of a magnitude tolerable to the pilot. When the pilot deflects a control surface, the pressure distribution resulting from the airflow over the surface creates a moment about the hinge axis. This hinge moment causes the control surface to resist deflection and tend to rotate about its hinge axis back to its undeflected position. Therefore, to maintain the control surface at any given deflection, the pilot must apply, through the controls, an equal and opposite moment to the surface.

The magnitude of the control-surface hinge moment (and, therefore, the magnitude

of the control-stick force required to deflect the surface) increases with the size and speed of the airplane. The stick force increases as the cube of the increase in size and as the square of the increase in speed. For example, if the size of the airplane is doubled, the force required to move a control surface (at any given flight speed) becomes 2^3 , or 8, times as great. If the speed of an airplane is doubled, the stick force (for any given airplane size) becomes 2^2 , or 4, times as great. Therefore, on large and/or fast airplanes, various techniques are used to reduce the stick force to a reasonable level.

Aerodynamic Balances

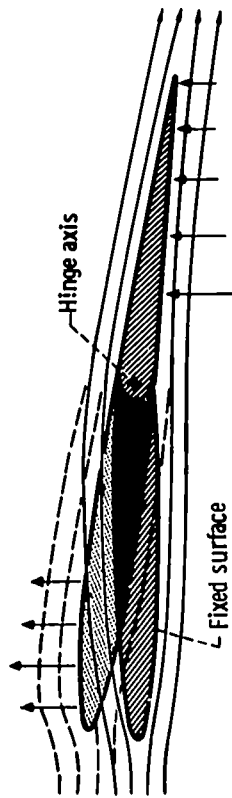
One technique for reducing the hinge moment and stick force is to change the pressure distribution about the hinge axis of the control surface by means of some type of aerodynamic balance.

A control surface may have an overhang balance, as shown in figure 9-9(a). For this balance the hinge axis is offset rearward from the leading edge of the control surface. When the control surface is deflected, the pressures on the area ahead of the hinge axis create moments about the hinge axis that are opposite to those produced by the pressures on the area behind the axis. Thus, the net hinge moment of the control surface is reduced.

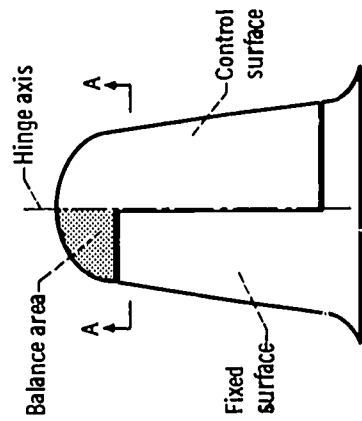
The horn balance, shown in figure 9-9(b), is similar to the overhang balance, but its balance area is concentrated at one portion of the span of the control surface. When the control surface is deflected, the pressures acting on the balance area (horn area) produce moments that assist the pilot.

The internal balance, shown in figure 9-9(c), consists of an overhang, or balance area, extending forward of the hinge axis of the control surface into a chamber within the contour of the fixed airfoil. The chamber is vented to the ambient upper and lower surface pressures at one chordwise point. Thus, the balancing air pressures are free to act on the enclosed overhang. Within the chamber, the leading edge of the overhang (or balance area) may be sealed by a flexible partition to the forward wall of the chamber. The sealed internal balance is more effective than the unsealed one.

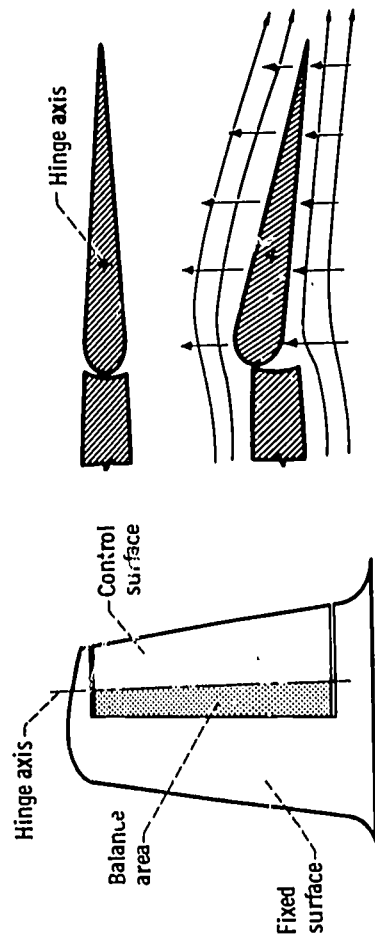
Another type of aerodynamic balance consists of making the trailing edge of the control surface wedge shaped, or beveled, as illustrated in figure 9-9(d). A deflection of the control surface by the pilot causes the bevel on the deflection side of the trailing edge to protrude into the airstream. Then the airstream, which must move faster in going around the bevel, induces a lower pressure on that side of the trailing edge. This tends to pull the control surface in the deflected direction.



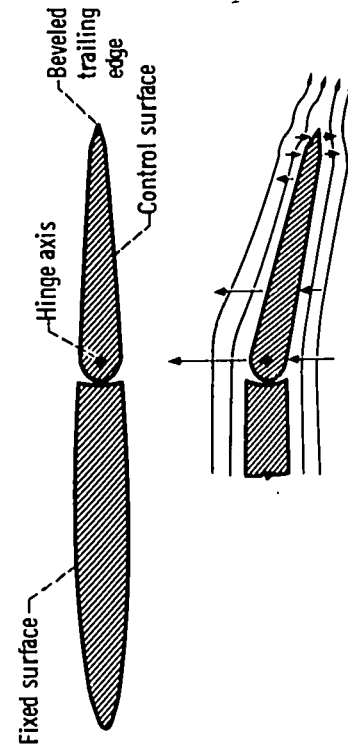
Section A-A



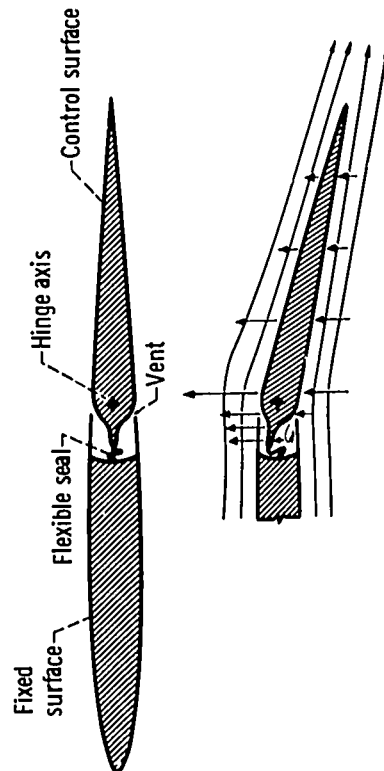
(b) Horn balance.



(a) Overhang balance.



(d) Beveled trailing edge balance.



(c) Sealed internal balance.

Figure 9-9. - Aerodynamic balances for control surfaces.

Tabs

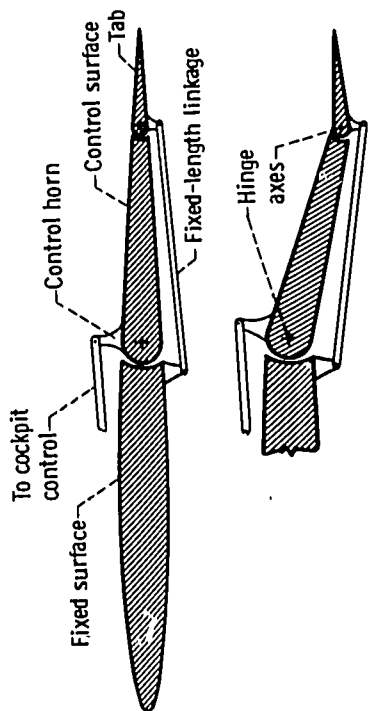
A common and effective method of reducing an excessive control-stick force is by the use of a secondary control surface called a tab. This device is a hinged, auxiliary airfoil built into the trailing edge of the control surface. The purpose of the tab is to change the pressure distribution on the control surface near the trailing edge, thereby changing the hinge moment of the control surface. In a strict sense, a tab is really just another form of aerodynamic balance, but the two are commonly treated separately. A tab is extremely versatile, since it can be linked so as to decrease the stick force, trim the airplane, or increase the stick force.

The lagging tab (fig. 9-10(a)) is so linked that when the control surface is deflected by the pilot, the tab deflects in the opposite direction, thereby producing a force which helps to move the control surface. Since the lagging tab is intended merely to help move the control surface, the system must be designed so that the moment produced by the force on the tab is smaller than the hinge moment of the control surface.

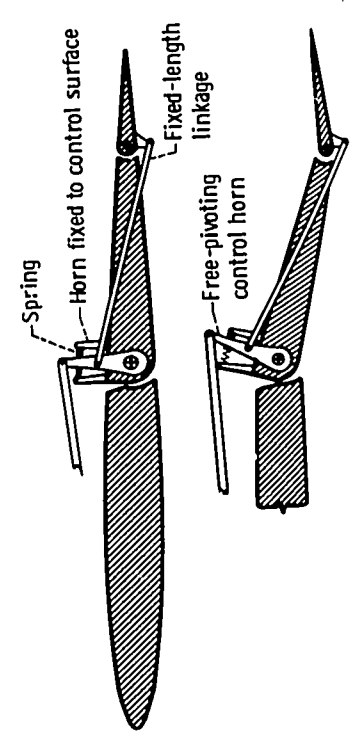
The servo tab (fig. 9-10(b)) is linked directly to the cockpit controls. The pilot deflects the tab, which then causes the control surface to be deflected in the opposite direction by the aerodynamic forces acting on the tab. Since the servo tab must provide all the force necessary to move the control surface, the system must be designed so that the moment produced by the force on the tab is larger than the hinge moment of the control surface.

The spring tab (fig. 9-10(c)) is actuated by a spring-loaded mechanism that causes it to supply a fixed percentage of the force required to move the control surface. The action and use of the spring tab are similar to those of the servo tab. However, the springs incorporated in the control system allow the tab to supply only a part, rather than all, of the force required to move the control surface. Some of the stick force is always transmitted through the springs directly to the control surface. As the hinge moment of the control surface increases, the deformation of the springs also increases. This, in turn, causes the linkage to increase the deflection of the tab. The amount of force supplied by the tab depends on the spring rates. Obviously, if the springs are infinitely weak (equivalent to no springs at all), the tab behaves as a servo tab. If the springs are infinitely stiff (equivalent to a rigid rod), the tab does not deflect at all. By preloading the springs, the deflection of the tab can be delayed until a predetermined control force is achieved.

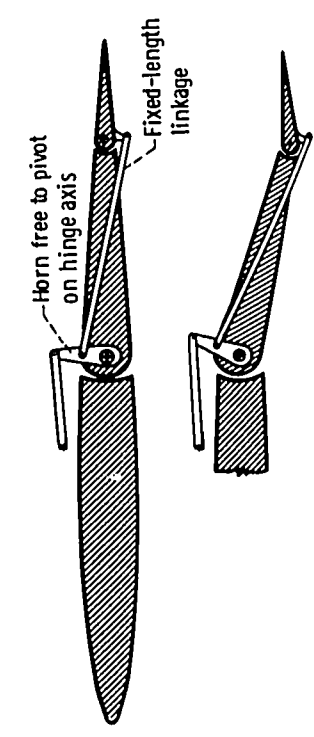
At times it is necessary to hold a control surface in a deflected position to keep the airplane in the desired flight attitude, or trim. Obviously, it would be both inconvenient and tiring for a pilot to apply a constant stick force for long periods of time. Therefore, a trim tab (fig. 9-10(d)) is normally used to keep the control surface deflected. An adjustable linkage allows the pilot to set the tab at the proper angle to reduce the hinge moment of the control surface to zero for any desired flight condition. In other words, the trim



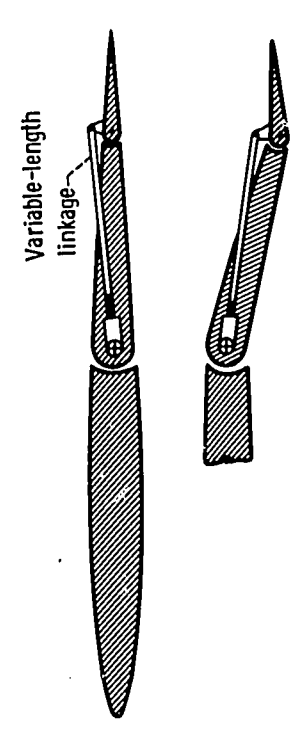
(a) Lagging tab.



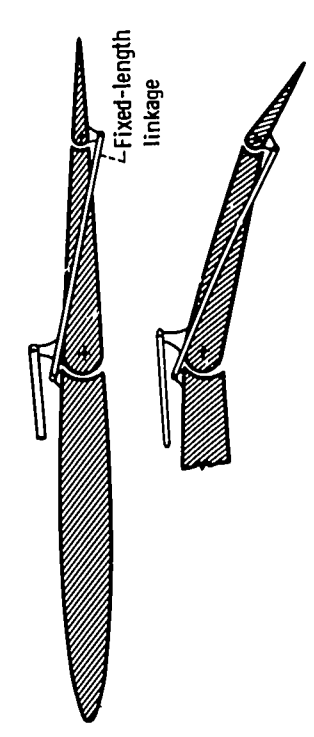
(c) Spring tab.



(b) Servo tab.



(d) Trim tab.



(e) Leading tab.

Figure 9-10. - Tabs used as balances on control surfaces.

tab is set to keep the control surface deflected so that the airplane will maintain the desired flight attitude.

In all these methods of balancing a part of the control force to assist the pilot, there is the danger of providing too much assistance. With too much balancing, a slight movement of the controls may call into play excessively large forces that might overcontrol the airplane. Also, too much balancing reduces the feel that the pilot receives from the controls and thereby impairs his judgement. Thus he may unwittingly overcontrol the airplane. Because of these dangers, the various balancing schemes (including aerodynamic balances) must be designed to leave a sufficient amount of control feel to the pilot. Furthermore, the control feel must be progressive; that is, the control feel must become heavier with increasing deflection of the control surface.

Because of the importance of control feel to the pilot, it is sometimes necessary to increase the stick force. One way to do this is to use a leading tab (fig. 9-10(e)), which serves to increase the hinge moment of the control surface. The leading tab is so linked that when the control surface is deflected the tab deflects in the same direction, thereby adding to the hinge moment.

Mechanical Boost Systems for Control Actuation

On an airplane flying through the transonic speed zone, any type of aerodynamic hinge-moment-reducing device (aerodynamic balance or tab) may perform erratically while mixed subsonic and supersonic flow exists on the control surface. Therefore, on

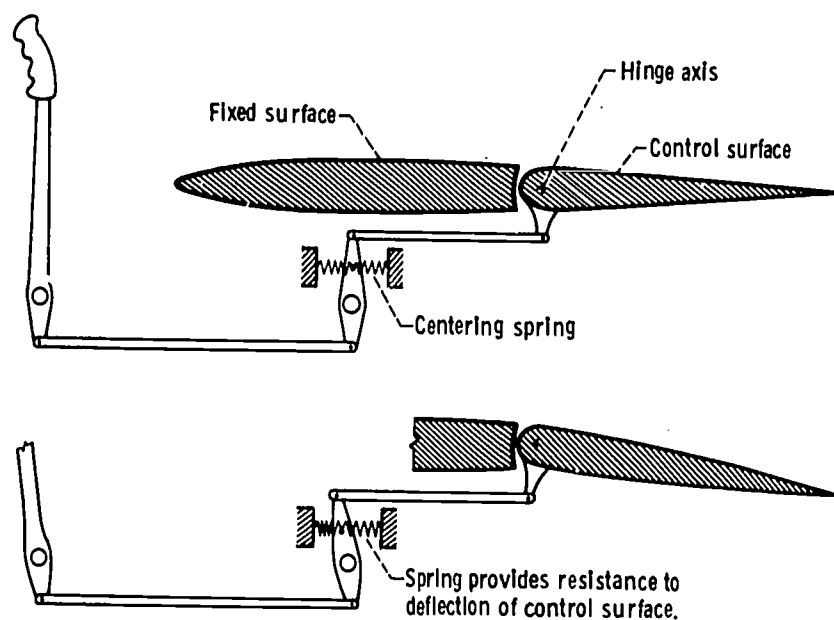


Figure 9-11. - Control stick centering spring used to increase control feel.

some airplanes mechanical systems are used to assist the pilot. Two basic types of mechanical control-actuation systems are in use: the power-boost system and the power-operated system.

In the power-boost system, a mechanical actuator is connected parallel to the direct mechanical linkage between the cockpit and the control surface. Thus the mechanical actuator supplies only part of the force required to move the surface, and the pilot still receives control feel through the direct linkage.

In the power-operated system, the control surface is moved entirely by the mechanical actuator, which, in turn, is controlled by the pilot. With this system, the entire force required to move the control surface is supplied by the mechanical actuator, and none of the hinge moment is fed back to the cockpit controls. Therefore, some sort of artificial feel system must be built into the controls to provide the pilot with the necessary control feel, or resistance. This artificial feel may be provided by a spring system on the controls, as shown in figure 9-11.

BIBLIOGRAPHY

- Anon.: Stability and Control Manual. FTC-T1H-64-2004, USAF Aerospace Research Pilot School.
- Hurt, H. H., Jr.: Aerodynamics for Naval Aviators. Navweps 00-80T-80, Office of the Chief of Naval Operations, Aviation Training Div., 1960.
- Kershner, Wm. K.: The Private Pilot's Flight Manual. Second ed., Iowa State University Press, 1963.
- Perkins, Courtland D.; and Hage, Robert E.: Airplane Performance Stability and Control. John Wiley & Sons, Inc., 1949.
- Seckel, Edward: Stability and Control of Airplanes and Helicopters. Academic Press, 1964.

10. V/STOL AIRCRAFT

Seymour Lieblein*

Air and ground traffic congestion is a growing problem for commercial aviation. The growth of aviation is creating increased demands on airspace. Some of the major airports are inadequate for handling the increased air traffic. Thus, aircraft are spending more and more time on taxiways, waiting to take off, or in holding patterns on the approaches to the airports, waiting to land. The growth of the automotive industry is creating increased congestion on the highways between city centers and airports, between suburban centers and airports, and between cities. Because of these delays in the air and on the ground, the total travel time for the airline passenger is actually increasing.

Air service could be improved and total travel time could be reduced if there were aircraft that could provide short-haul service between city centers, between city centers and major airports, and between major airports. Such aircraft would have to be able to take off and land either vertically or on very short runways and to maneuver (in flight) in confined areas.

Of course, we already have an aircraft that can do this - the helicopter. The usefulness of the helicopter has been demonstrated in military operations, for rescue work in times of disaster, and also for hauling materials and assisting in putting large structures together. However, the helicopter is limited in what it can do - it cannot fly very fast or very far. Therefore, we are looking for something that bridges the gap between the relatively small and slow helicopter and the large, speedy jet transport. This takes us into the realm of the V/STOL's (Vertical/Short Take-Off and Landing), which are aircraft that can take off or land vertically or with a relatively short ground run.

NEED FOR V/STOL AIRCRAFT

V/STOL aircraft can play an important role in both civilian and military aviation. Therefore, aircraft companies and various government agencies, such as the National Aeronautics and Space Administration, the Department of Transportation, the Federal Aviation Agency, the Department of Commerce, and the Department of Defense, are currently conducting studies on civilian and military V/STOL aircraft concepts and applications.

* Chief, VTOL Propulsion Branch.

Today, around our large cities, the effects of increased congestion on the ground and in the air are clearly evident to those who travel. For example, the total travel time (ground and air) between downtown New York City and downtown Washington, D. C., increased from 125 minutes in 1948 to 167 minutes in 1963, despite the fact that airplane flight speeds increased considerably during this period. The increases in travel time result from delays both in the air and on the ground.

Conventional airports must be located on the fringes of cities, because of the need for land and the problem of noise. Thus, as the cities grow larger, the airports will be farther away from the centers of towns, and the ground travel time will increase even more in the future. Also, both the cost and the availability of land limit the number of conventional large airports that are economically feasible. Obviously, then, there is little that can be done to reduce door-to-door trip times with conventional takeoff and landing aircraft.

V/STOL aircraft could solve some of these problems, since their short or vertical takeoff and landing characteristics would enable them to operate from small landing fields (or existing heliports) located closer to the ultimate destinations, and thus reduce the travel time on the ground. Also, such craft could operate at flight speeds approaching those of conventional jets, make their final approaches in the less congested airspace (e.g., at altitudes under 1500 ft), and provide further time savings in the air as well.

The various functions that V/STOL aircraft can provide the civilian community of the near future are shown in figure 10-2, which illustrates anticipated air operations in a seaboard metropolis. First, large transcontinental jets like the Boeing 747 and the

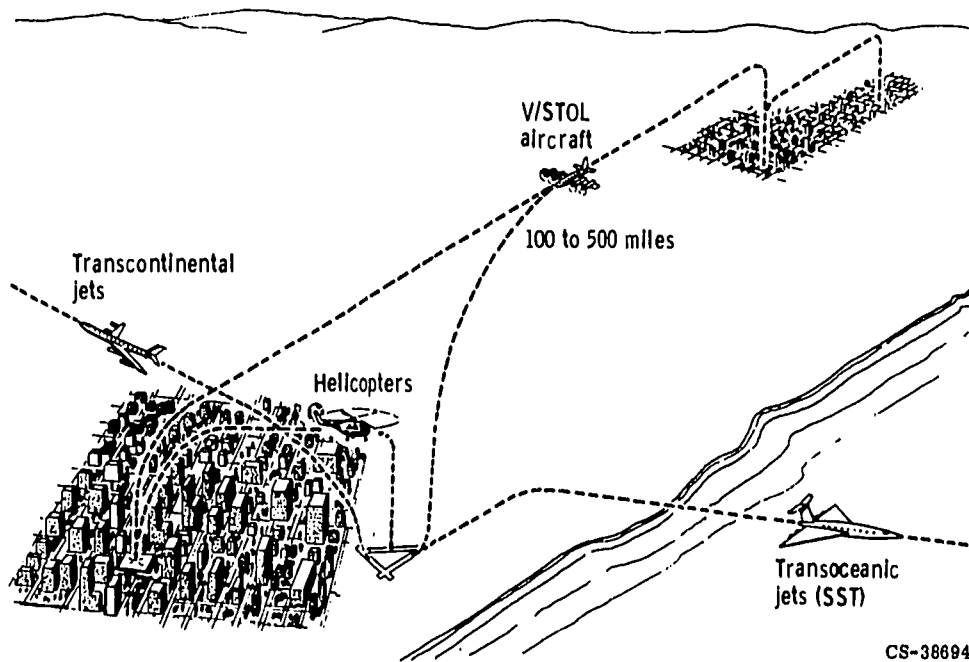


Figure 10-2. - Function of V/STOL aircraft in commercial air service.

Supersonic Transport (SST) will continue to operate from the existing major airfields for these long-range trips. The V/STOL aircraft will provide service for trips from around 100 to 500 miles at speeds approaching those of conventional jets. The V/STOL routes will be between city centers or from city centers to outlying airports as feeder operations for the long-range flights. Also, V/STOL aircraft will provide service between various points within a large city (around-the-town service). In short, the V/STOL aircraft will provide a vital link in a system of speedy, integrated air service that will meet the needs of an expanding, mobile population. As shown in the figure, helicopters will continue to serve for very short trips around town.

At this point, one may ask why helicopters are not used for all VTOL operations. The reason is that current helicopters do not have the speed and range capabilities of the V/STOL aircraft. This is illustrated in figure 10-3, which shows the cruising-speed and

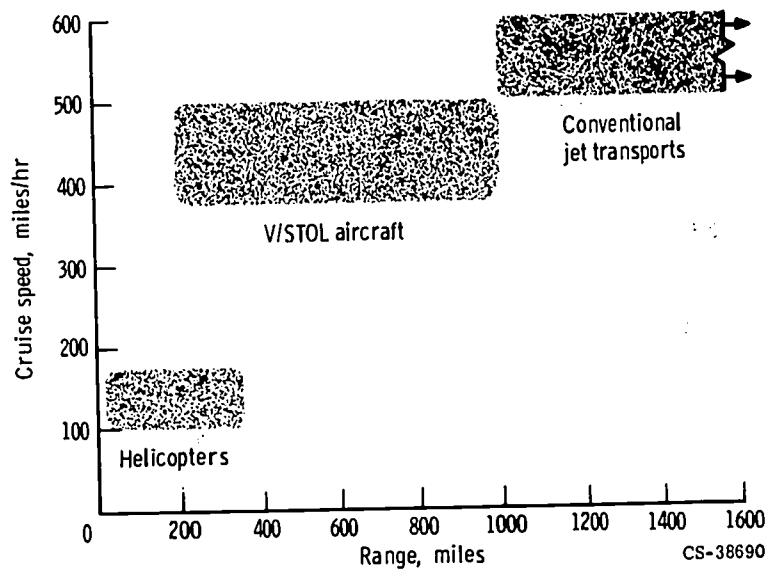


Figure 10-3. - Speed and range capabilities of helicopters, V/STOL aircraft, and conventional jet transports.

range capabilities of the three major types of aircraft: current helicopters, V/STOL aircraft, and conventional jet aircraft. The speed of the current helicopter is restricted by the large drag and performance limitations of the rotor blades, and the low range is due to low fuel capacity. As shown in the figure, the V/STOL aircraft can function over a longer range and at higher cruise speed than the helicopter. Thus, the V/STOL aircraft can bridge the gap between the helicopter and the long-range jet.

Suitable sites for V/STOL airports can be found even in congested cities. Obviously, the selection of an airport site will be governed by considerations of cost, availability of space, and acceptable noise levels. Also, air traffic considerations dictate that the airports within the city use natural flight-approach corridors as much as possible. Hence,

1980

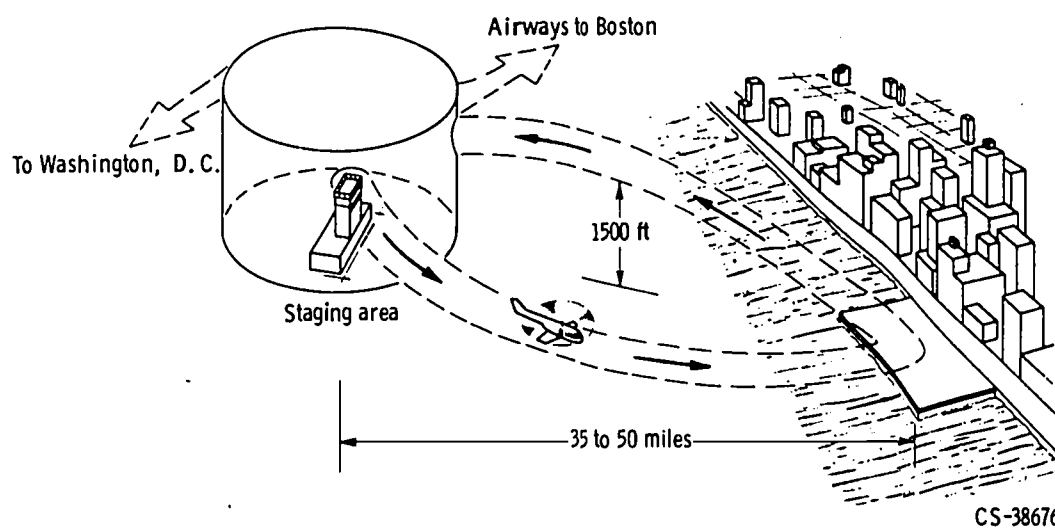


Figure 10-4. - V/STOL air traffic into and out of a large city.

V/STOL airports are expected to be located along rivers, along the shores of large bodies of water, along transportation rights of way, or in "wasteland" areas within the city that are unsuitable for housing or industry. For example, figure 10-4 illustrates a proposed location for an airport along the Hudson River that could serve the mid-Manhattan area of New York. The V/STOL landing pad could be located along the riverfront, with runways no longer than about 1000 feet, and could be built over the roofs of existing waterfront buildings or, better yet, over unused piers. As shown in the figure, the inbound and outbound V/STOL flights would be controlled from a staging area about 35 to 50 miles from the downtown airport. A 1500-foot ceiling would be observed by V/STOL aircraft flying between the staging area and the downtown airport in order to stay below the already congested traffic lanes for conventional aircraft flights.

Airports for V/STOL aircraft should also be located near convenient parking and

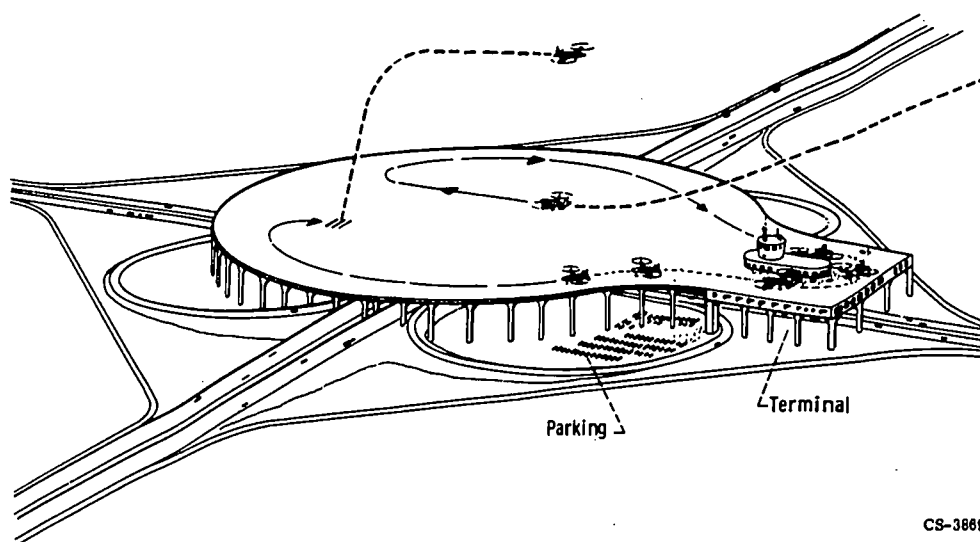


Figure 10-5. - V/STOL airport located over highway cloverleaf.

ground transportation facilities to reduce ground time as well as air time between ultimate destinations. Thus, such airports might be located over large cloverleaf intersections as shown in figure 10-5. The parking areas would be on the ground level under the airport, and the passenger terminal would be immediately beneath the flight deck. The entire airport structure might be about 1500 feet long and about 1000 feet wide. Approach and departure paths would be to and from the central areas of the pad, and the taxiways would be routed along the outer perimeter of the field.

Military Applications

In the past, the major portion of the direct financial support from the Government for the development of V/STOL aircraft has been provided for military applications. The major military uses of V/STOL aircraft are shown in figure 10-6. The foremost application is in the transport function. The long-range transport of supplies and equipment would be provided by heavy transport aircraft such as the Lockheed C-141 (now in service) or the Lockheed C-5A (currently under flight test). The V/STOL transport aircraft would pick up the supplies at the overseas base and deliver them close to the forward area at some remote location. These V/STOL aircraft could use relatively small airstrips that would require minimum preparation. Thus, fast, efficient, large-scale

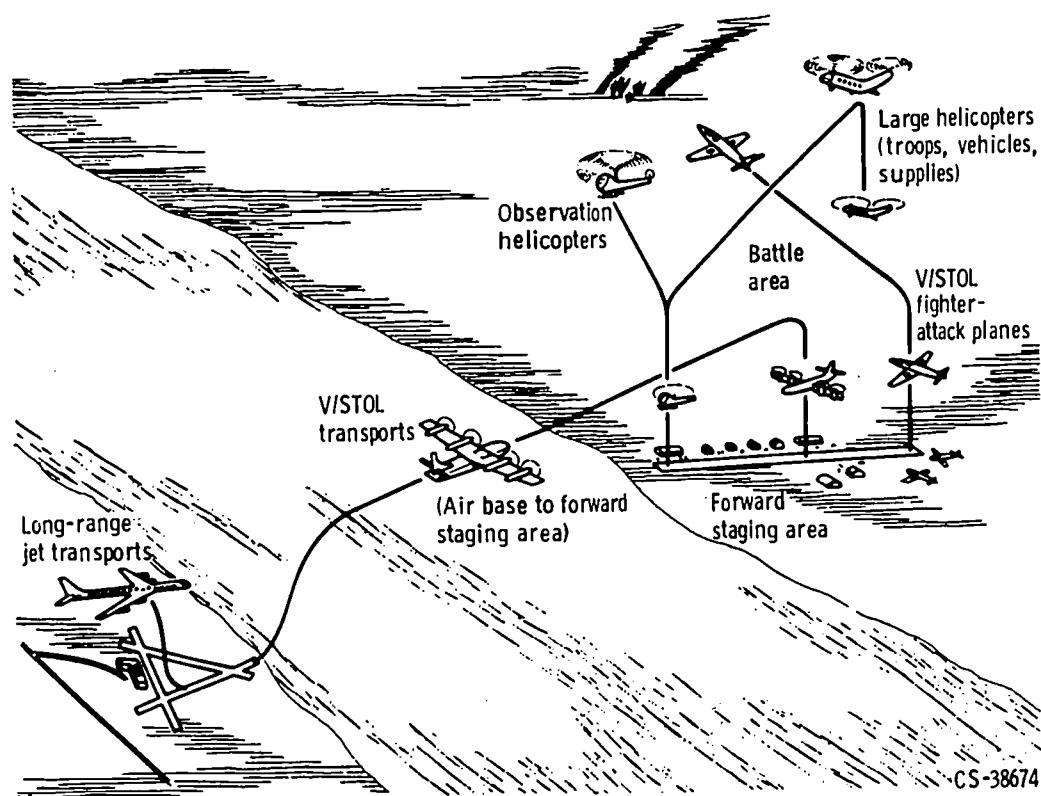


Figure 10-6. - Military functions of V/STOL aircraft.

logistical support (delivery of troops or supplies) could be provided close to the front lines, and this support could keep up with the mobility of the ground forces.

Another military requirement is for V/STOL tactical fighters or ground support aircraft. The operating requirement most critical here is the ability to function from small, unprepared or quickly prepared airstrips. In this way, the fighters can provide maximum support and flexibility and also be sufficiently widely dispersed to make the entire fighter squadron less vulnerable to massive attack and loss of airplanes and runways. In this concept, the V/STOL transport aircraft would provide the necessary supplies for the fighter planes, as well as for the troops. Other important military missions for V/STOL aircraft would be rescue service and antisubmarine warfare.

BASIC CONCEPTS

Figure 10-7 compares the takeoff runs required by three classes of aircraft. A Conventional Take-Off and Landing (CTOL) aircraft is one that requires a long run of about 4000 feet, or more, to take off. A Short Take-Off and Landing (STOL) aircraft is defined as one that requires a takeoff run of 500 to 2000 feet. A Vertical Take-Off and Landing (VTOL) aircraft obviously requires no takeoff run. The combined term V/STOL is used to refer to both VTOL and STOL aircraft as a class, as differentiated from the conventional, or CTOL, aircraft.

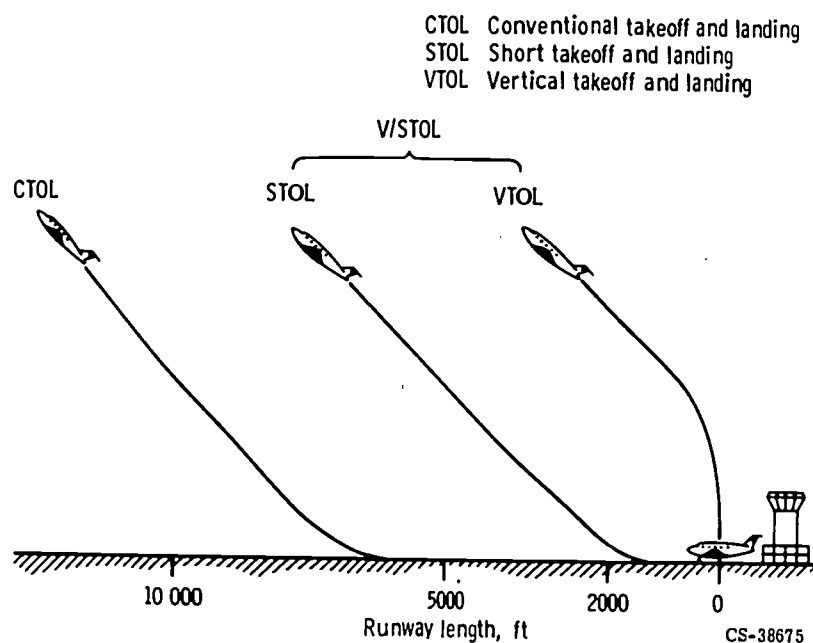


Figure 10-7. - Comparison of takeoff runs of CTOL and V/STOL aircraft.

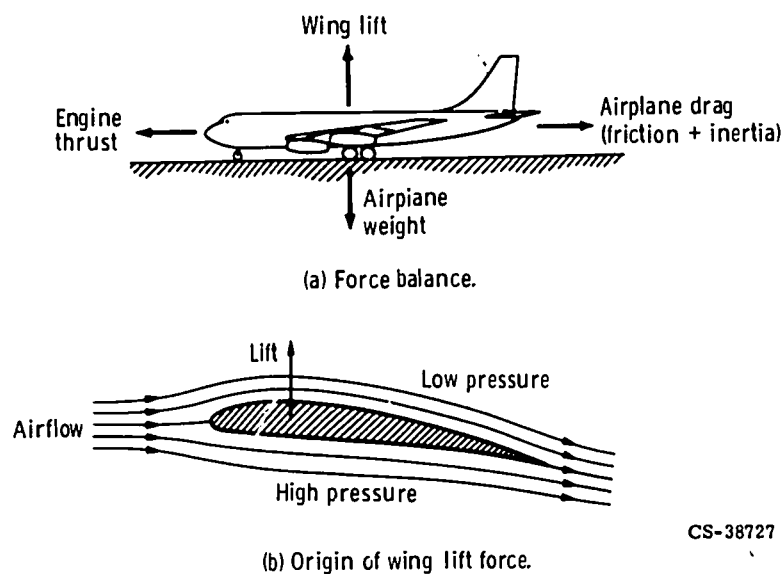


Figure 10-3. - Forces acting on airplane during takeoff run.

Figure 10-8(a) is a quick refresher on the four major forces acting on an airplane as it proceeds down the runway to take off: (1) the airplane weight, which tends to keep it on the ground; (2) the thrust of the engine, which propels the airplane forward; (3) the drag of the airplane, which resists the forward motion; and (4) the upward lift force generated by the wings.

Wing lift is generated because the airflow over the wing creates regions of high and low pressure, as shown in figure 10-8(b). (The principles of lift generation are discussed in chapters 4 and 5.) The pressure difference between the upper and lower surfaces of the wing results in a net upward lift force. This wing lift force is zero at zero flight speed and increases with the square of the forward speed according to the relation

$$L = C_L S \frac{\rho V^2}{2g} \quad (1)$$

where

L lift force, lb

C_L wing lift coefficient determined by the geometry of the wing and its angle of attack

S wing planform area, ft²

ρ air density, lb/ft³

V flight velocity, ft/sec

g acceleration due to gravity, 32.2 ft/sec²

Thus, as the airplane accelerates down the runway, it eventually reaches a forward speed at which the generated wing lift force becomes equal to the airplane weight, and the plane can lift off. Specifically, then, the takeoff condition is

$$L = W \quad (2)$$

where W is the gross weight of the airplane.

STOL Aircraft

From the lift equation we see that the wing lift force can be increased by increasing the lift coefficient. Greater lift coefficients can be obtained if the wings create a greater downward deflection of the air that flows around the wing. Thus, to attain a greater lift coefficient, the wing can be designed with a large flap system, as shown in figure 10-9. The flaps are extended during takeoff to increase the lift coefficient. Thus, the wing lift necessary to balance aircraft weight can then be achieved at a lower forward speed, and consequently, with a shorter runway length. After takeoff, the flaps are retracted to their normal (or cruise) position, as shown by the dotted outline.

However, there is one big problem with such a flap. If we try to deflect the air too much, the air flowing over the upper surface cannot negotiate the curve, so to speak, and separates from the wing surface. (Flow turning and flow separation are discussed in chapter 4.) When this happens, there is a large loss in lift. The boundary layer separates from the surface because the air molecules close to the surface are slowed by friction and form a "dead air" space. The main flow of air must then separate from the surface to

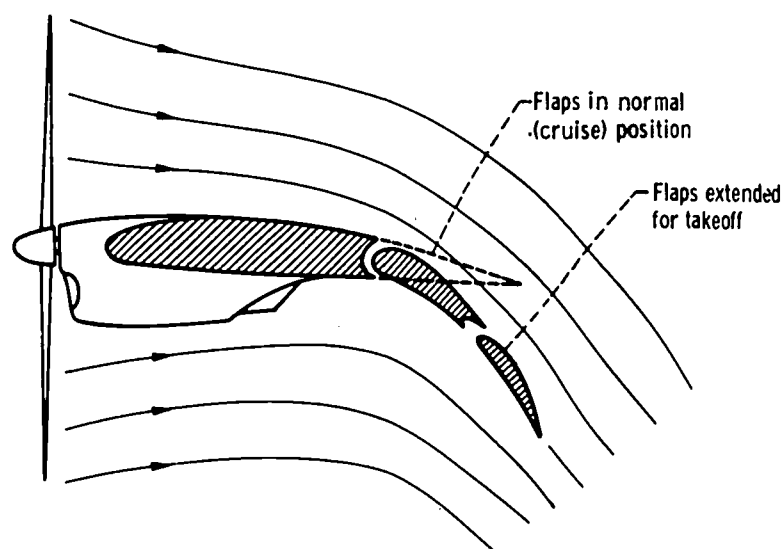


Figure 10-9. - Flaps used to increase lift of STOL aircraft.

CS-38703

pass around this "dead" air. Flow separation can be prevented by adding energy to the boundary layer, so that the molecules will not slow down sufficiently to form a "dead" space.

Some of the ways of energizing the boundary layer for STOL airplanes are shown in figure 10-10.

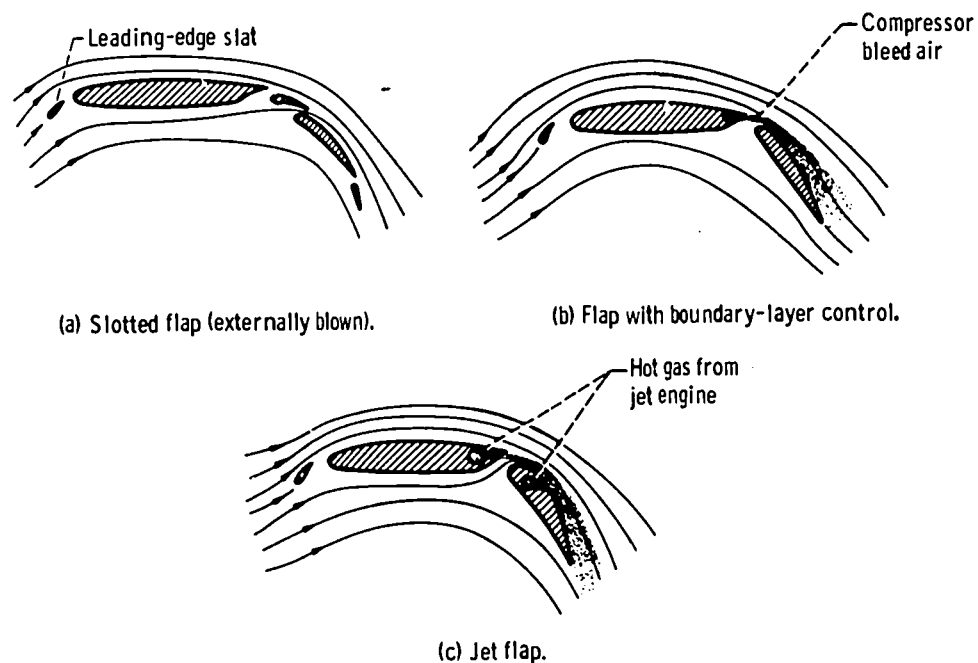


Figure 10-10. - High-lift devices for STOL aircraft.

CS-38710

The wing flap can be slotted, as shown in figure 10-10(a), so that the airflow from the jet engines or propellers can be made to blow through the slots, thus energizing, or speeding up, the boundary layer on the surfaces. High-pressure air can be bled off from the engine compressor and injected along the leading edge of the flap, as shown in figure 10-10(b), thereby energizing the boundary layer. Part of the jet-engine exhaust can be piped through ducts in the wing and flap to blow down as a sheet of jets over the upper surface of the flap, as shown in figure 10-10(c). The large amounts of airflow used in this jet-flap scheme not only energize the boundary layer but also contribute a sizable vertical component of thrust.

All the high-lift schemes shown in figure 10-10 also incorporate leading-edge slats to increase the wing lift coefficient further. The slats increase the lift by increasing the effective curvature of the airfoil.

Another approach that can be used to generate high lift at low forward speeds is to reduce the amount of lift that has to be generated by the wings. This is accomplished either by adding auxiliary engines to provide vertical thrust or by deflecting the exhaust

of the main engines so that there is a vertical downward component of thrust. In this case, the wing lift required for takeoff (total lift = weight) will be

$$L_w = W - T_e \sin \beta \quad (3)$$

where

L_w required wing lift, lb

W gross weight of airplane, lb

T_e engine thrust, lb

β angle of direction of engine exhaust with respect to the horizontal

Thus, the increase in wing lift coefficient C_L required to produce the necessary wing lift at takeoff (eq. (1)) will be reduced compared to the previous cases. For conventional engines with horizontal exhaust, $\beta = 0$, and the lift equation is equation (2).

The use of a vertical thrust component during takeoff is being considered for STOL airplanes, because it can provide for a better design with respect to airplane stability and overall performance than a design which uses only wing lift with very high values of C_L . A vertical thrust component during the takeoff can be obtained by changing the orientation of the axis of the engines or by using deflectors, such as vanes, to deflect the exhausts of the horizontally mounted engines.

VTOL Aircraft

The situation for a vertical takeoff is illustrated in figure 10-11. In a vertical take-

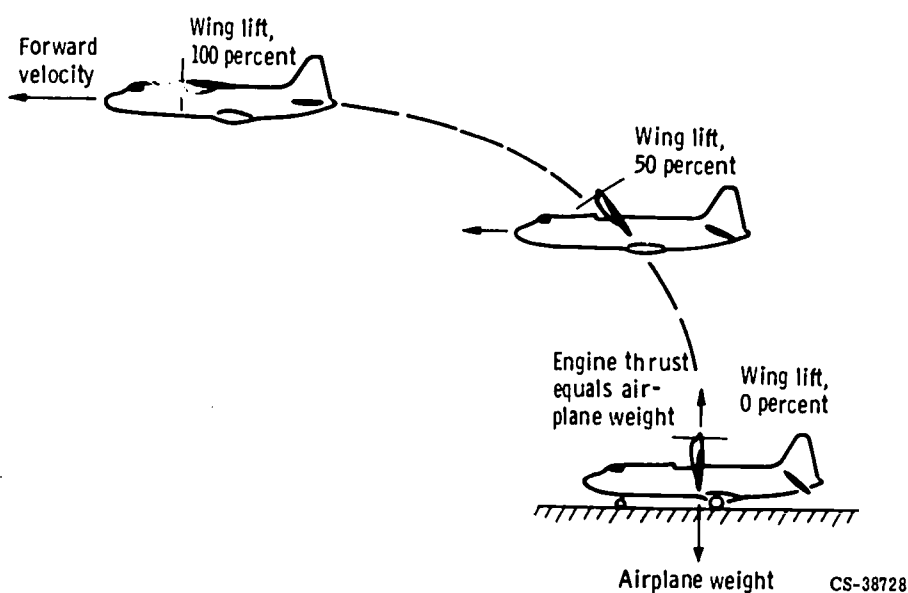


Figure 10-11. - Vertical takeoff.

227

off, the engine thrust is used directly to generate the entire lifting force, since there is no forward speed to generate wing lift. The figure shows a turboprop airplane in which the wing and engine have been rotated 90° to provide a vertical propeller thrust. (This is just one of several schemes that will be discussed later.) As the airplane rises, the wing is rotated toward the horizontal, so that a forward thrust component is obtained. This causes the airplane to accelerate in the forward direction and start to develop wing lift. After complete transition to the horizontal position, all the thrust is in the forward direction, and the airplane flies away in the normal cruise mode. For vertical landings, the reverse of the process is used.

In addition to differences in takeoff characteristics, VTOL aircraft also differ markedly from CTOL airplanes in the attitude-control devices required for takeoff and landing. To be more explicit here, it may be helpful to review how a CTOL airplane is controlled for maneuvers or for stable flight. The control methods for CTOL airplanes operate on the principle of aerodynamic control; that is, local surfaces are used to deflect the oncoming airstream and thus change the direction of the resultant force vector. Now, to turn a conventional airplane (fig. 10-12) to the left or right, the rudder is deflected left or right; this is called yaw control. To cause the plane to nose up or nose down, the elevators are deflected up or down; this is called pitch control. Finally, to raise one wing and lower the other, the ailerons near the wing tips are deflected in the opposite directions; this is referred to as roll control. (Airplane control is discussed in greater detail in chapter 9.)

Since a VTOL aircraft has no forward flight speed during takeoff or landing, it cannot be controlled during those phases of flight by the methods used on CTOL airplanes. Therefore, some other means of control must be provided for the VTOL aircraft. Two methods of control that can be used are: (1) modulation, or differential variation, of the

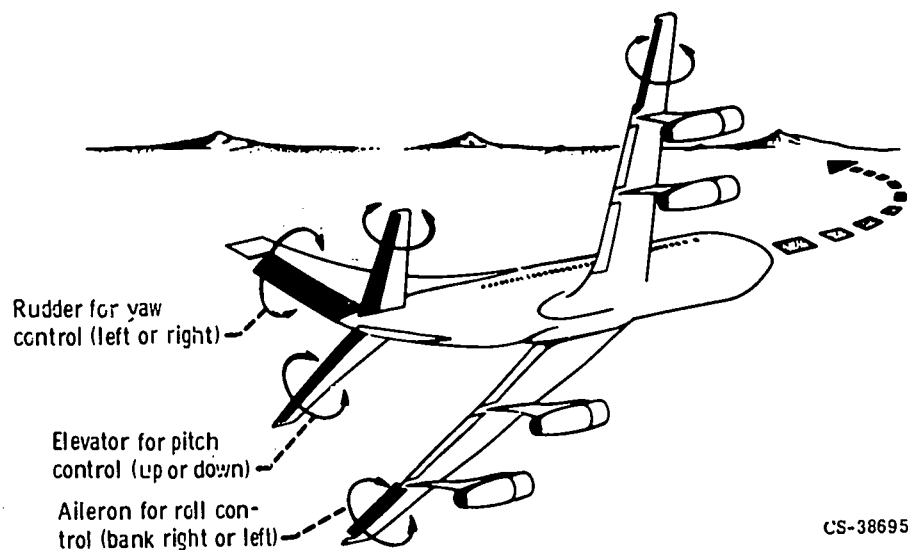


Figure 10-12. - Control methods for CTOL aircraft.

CS-38695

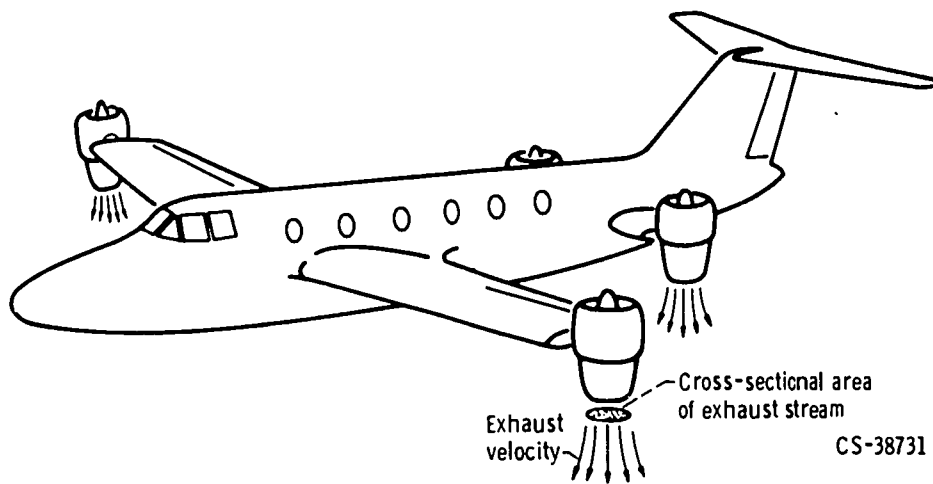


Figure 10-13. - VTOL aircraft control by modulation of the thrust of individual lifting engines.

thrust of the individual lifting engines, or (2) use of auxiliary thrust devices added specifically for control purposes. In some cases a combination of the two methods is used.

The thrust-modulation method of control is illustrated in figure 10-13. This figure shows an example VTOL airplane that has jet lifting engines on the wing tips and on each side of the fuselage near the tail. To nose up or nose down the airplane, the thrust from the two front engines can be varied with respect to the thrust from the two rear engines. Similarly, to roll the airplane from side to side, the thrust on each side of the plane can be varied. Finally, yaw control can be achieved by tilting the wing tip engines in opposite directions laterally.

The use of auxiliary thrust devices for control of a VTOL aircraft is illustrated in figure 10-14, which shows an example tilt-wing airplane. Nose-up and nose-down maneu-

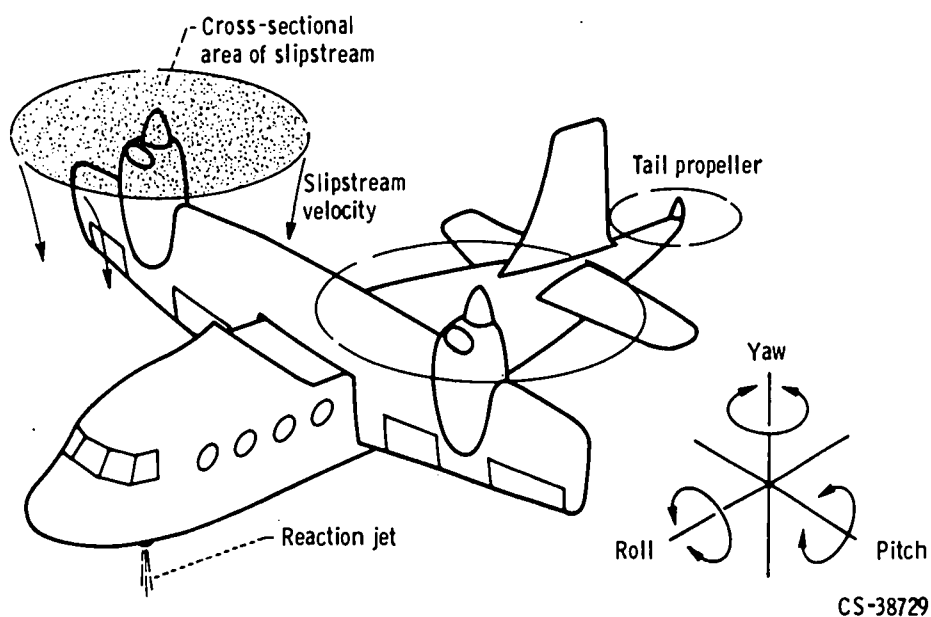


Figure 10-14. - Control of VTOL aircraft by a combination of thrust modulation of the lift engines and auxiliary thrust devices (reaction jet and tail propeller).

vers of the example airplane can be controlled either by the high-velocity jet of air ducted downward under the nose of the airplane, which tends to lift the nose, or by the small propeller in the tail, which tends to lift the tail end. These are called auxiliary control devices because they are not part of the main lifting-engine system, which, in the figure shown, consists of two wing propellers. Reaction jets, such as the one in the nose of the airplane, can also be used on the wing tips for roll and yaw control, but these are not illustrated in this figure.

Figures 10-13 and 10-14 also illustrate some fundamental terms that will be used later in this chapter. Thrust is the propelling force (in pounds) produced by the propulsion system. During vertical takeoff (no forward speed), the thrust equals the air flow rate generated by the propulsion system multiplied by the exhaust velocity of a jet engine or the slipstream velocity of a propeller, rotor, or ducted fan. The exhaust velocity is the velocity at which the exhaust gas is discharged from the jet engine, as indicated by the arrows in figure 10-13. The slipstream velocity is the velocity of the stream of air driven aft or down by the propeller, rotor, or fan, as indicated by the arrows in figure 10-14.

A significant yardstick for comparing the overall performance of various types of V/STOL aircraft propulsion systems, as will be discussed later, is the disk loading. This parameter is obtained by dividing the thrust (lb) of the engine by the cross-sectional area (ft²) of the exhaust stream or of the slipstream. The cross-sectional area of the exhaust stream is the exit area of the exhaust nozzle of the jet engine, as shown in figure 10-13. The cross-sectional area of the slipstream is the disk area, or swept area, of the propeller or rotor, as shown in figure 10-14, or it is the exit area of the duct surrounding the fan. In general, disk loading and exhaust, or slipstream, velocity are interrelated so that when one is low, the other is also low. Specifically, the disk loading is proportional to the exhaust, or slipstream, velocity squared. This relation between disk loading and velocity squared is derived as follows:

$$\text{Disk loading} = \frac{\text{Thrust}}{\text{Area}}$$

$$\text{Thrust} = \text{Mass} \times \text{Velocity}$$

$$\text{Mass} = \text{Density} \times \text{Area} \times \text{Velocity}$$

Thus,

$$\frac{\text{Thrust}}{\text{Area}} = \frac{\text{Density} \times \text{Area} \times \text{Velocity} \times \text{Velocity}}{\text{Area}}$$

$$= \text{Density} \times (\text{Velocity})^2$$

With density generally constant,

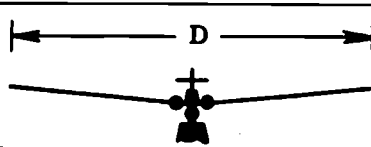
$$\text{Disk loading} \propto (\text{Velocity})^2$$

AIRCRAFT TYPES

Many research V/STOL aircraft have been built and tested in the United States and abroad in the past 15 years, but only one, a British VTOL fighter, has reached operational status. In general, all these aircraft have been different, particularly in the systems used to achieve vertical or short takeoff. Before considering specific V/STOL designs, let us examine the systems used to produce the lift for takeoff or landing.

The four basic devices used to produce thrust for V/STOL aircraft are the rotor, the propeller, the ducted fan, and the jet engine. Table 10-I lists the relative diameter, the

TABLE 10-I. - LIFT-PRODUCING DEVICES FOR VTOL AIRCRAFT

| Thrust device | Relative diameter, D | Disk loading, lb/ft ² | Slipstream velocity, mph |
|---|----------------------|----------------------------------|--------------------------|
| Rotor  | 15 | 6 to 10 | 40 to 80 |
| Propeller  | 5 | 10 to 90 | 90 to 200 |
| Ducted fan  | 3 | 90 to 800 | 200 to 500 |
| Turbojet  | 1 | 900 to 10 000 | 900 to 1600 |

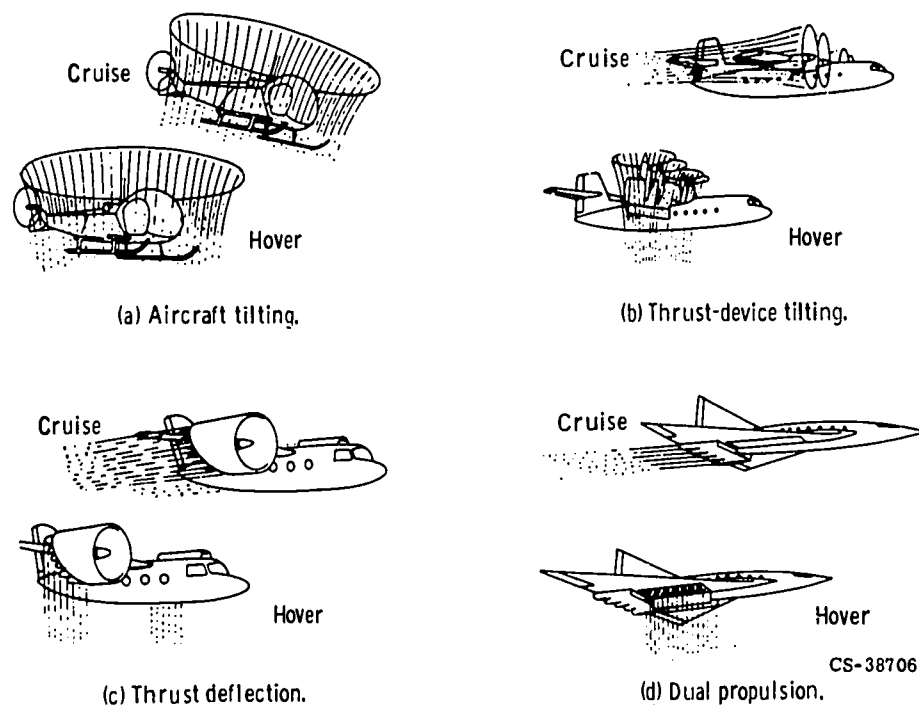


Figure 10-15. - Flight-mode conversion techniques.

typical value of disk loading, and the slipstream velocity of each device.

In addition to these four basic thrust-producing devices, there are four basic methods for directing the thrust in the proper direction for vertical or horizontal flight. These methods, shown in figure 10-15, are aircraft tilting, thrust-device tilting, thrust deflection, and dual propulsion. The figure shows the aircraft in both the hover and cruise mode for each category.

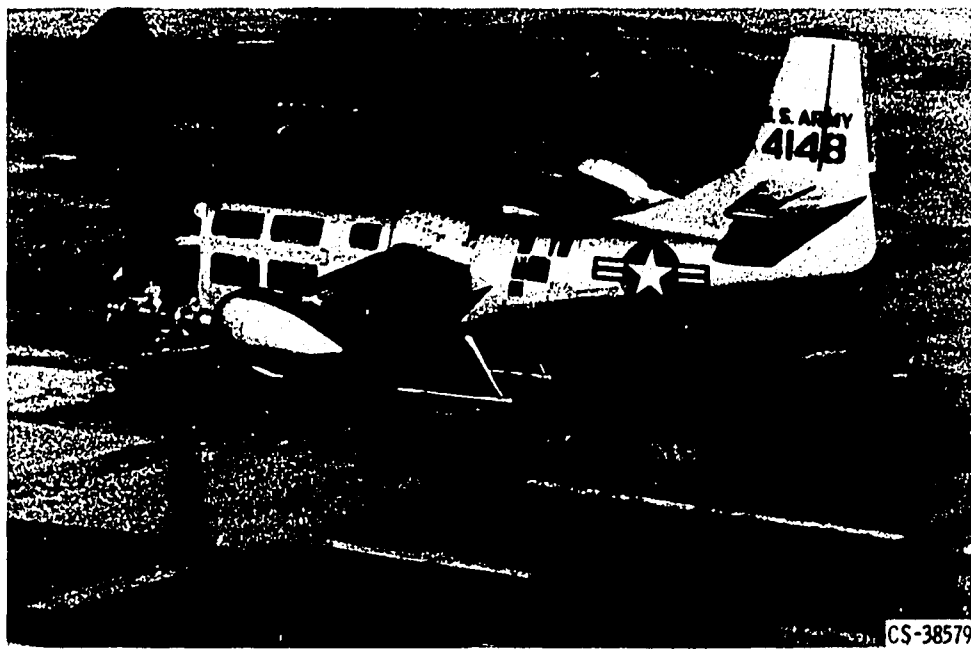
V/STOL aircraft with practically all possible combinations of the thrust-producing devices (table 10-I) and the thrust-directing techniques (fig. 10-15) have been built and flown, with varying degrees of success. Examples of a few of the more successful types will now be given.

Figure 10-16 shows a tilt-rotor VTOL aircraft in the hover and cruise modes. This is the Bell XV-3 convertiplane, which uses two 23-foot-diameter tilting rotors mounted on the wing tips. The rotors can be turned through slightly more than 90° and are driven by shafts and gears from an engine located in the fuselage. Attitude control in hovering flight is the same as for a helicopter. In the event of engine failure in cruise flight, the rotors can be turned to the hover position for an autorotation landing. The aircraft has been flown at speeds up to 180 miles per hour. More modern versions of this aircraft type are being considered for observation, reconnaissance, and rescue missions.

Figure 10-17 shows the Fairey Rotodyne, which was designed by the British as a civilian transport to carry about 60 passengers. This aircraft is a compound helicopter that uses a single 109-foot-diameter rotor for vertical flight and twin propellers for cruise. Two turboshaft engines drive the propellers in cruise and also power auxiliary



Hovering



Cruising

Figure 10-16. - Bell XV-3, tilt-rotor convertiplane.

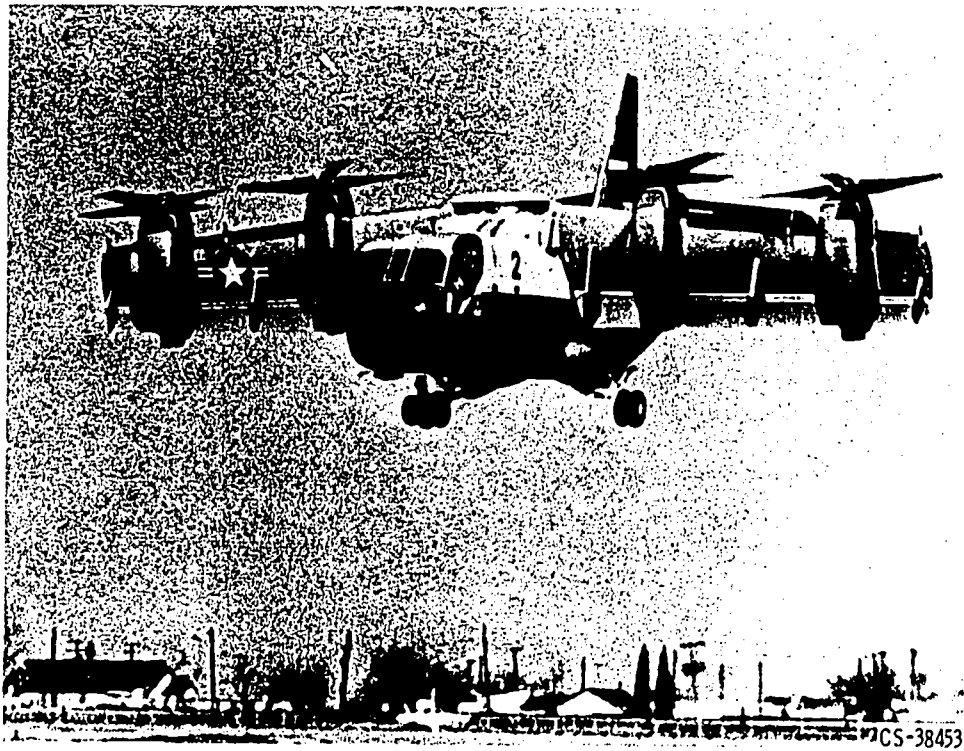


CS-38682

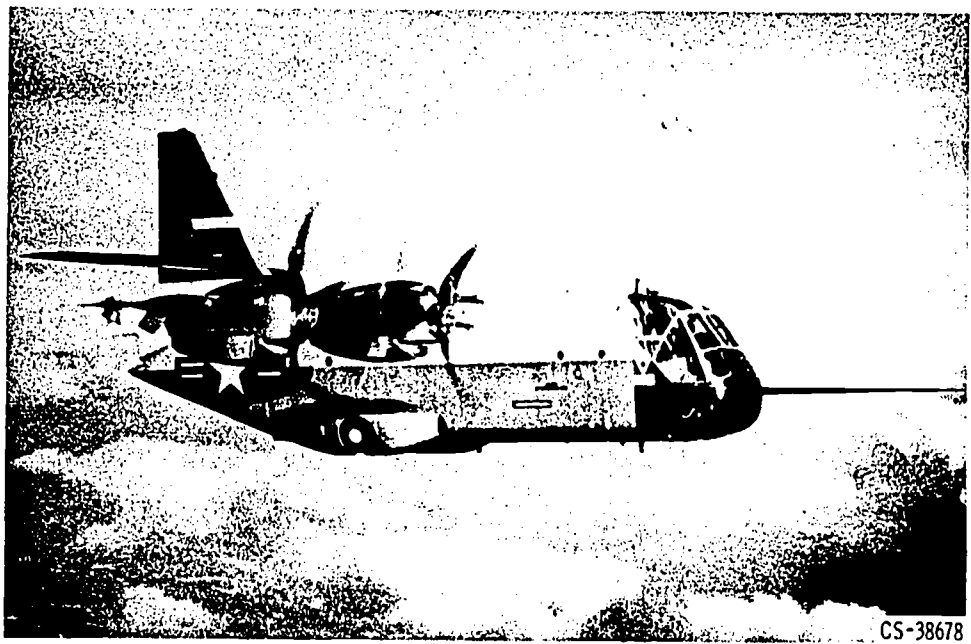
Figure 10-17. - Fairey Rotodyne, compound helicopter.

compressors which provide compressed air to drive the rotor by pressure jets on the rotor tips. During cruise, some of the power is removed from the rotor; that is, the rotor is unloaded. Unloading the rotor reduces the drag and allows a higher cruise speed (in this case, around 200 mph). More recent U.S. designs for this type of aircraft have incorporated concepts in which the rotor is stopped and folded back or stopped and retracted into the fuselage during cruise flight. The purpose of these techniques is to reduce or eliminate the rotor drag and thereby increase the cruise speed capability, in some cases up to 350 miles per hour.

Figure 10-18 illustrates a tilt-wing type of VTOL aircraft. This is the Ling-Temco-Vought XC-142A, which was designed as a military transport. The tilting wing carries four turboshaft engines in separate nacelles. Each engine drives a four-bladed propeller about 16 feet in diameter. The engines and propellers are interconnected by shafts and clutches to provide for symmetrical thrust distribution if one engine fails. The wing is tiltable through 100° from the horizontal, so that the aircraft can hover in a tail wind or fly backwards. The wing is equipped with a large trailing-edge flap and a leading-edge slat, which are programmed (synchronized) with the wing-tilt angle to increase the lift and prevent stall during transition flight. Yaw control during hover is obtained by ailerons in the propeller slipstream. Pitch control is by a horizontal rotor located behind the tail. Roll control is obtained by differential pitch on the propellers. Cruise speed at sea level is about 300 miles per hour, with a range of about 400 nautical miles. At the present time, the XC-142 is being flown to determine the operational suitability of this type of VTOL aircraft for military transport service. Aircraft of this type are also being seriously considered for civilian transport use.

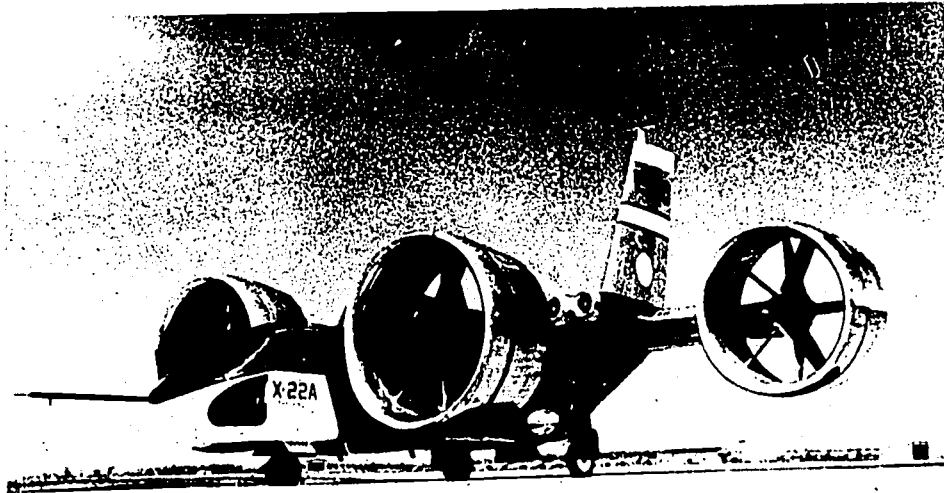


Hovering



Cruising

Figure 10-18. - Ling-Temco-Vought XC-142A, tilt-wing VTOL aircraft.



CS-38456

Figure 10-19. - Bell X-22A, tilting-ducted-propeller VTOL aircraft.

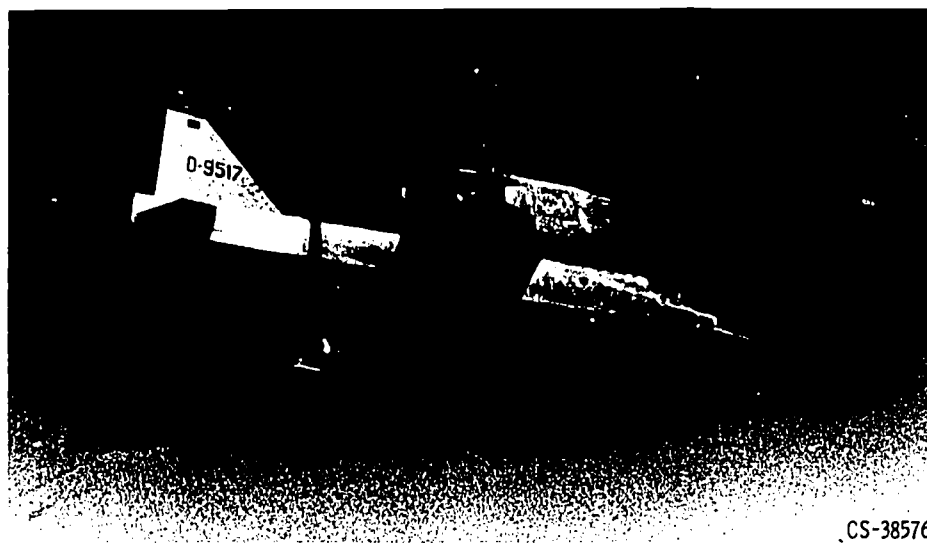
Figure 10-19 shows the Bell X-22A. This VTOL aircraft has a propulsion system consisting of four tilting, ducted propellers. It is primarily a research aircraft that is being used to determine the feasibility of this type of VTOL aircraft for military and civilian transport use. Vertical flight is obtained by rotating the ducted propellers to the vertical position. To translate from hovering to cruise flight, the ducts are slowly rotated forward. In cruise flight, lift is supplied by the stubby fore and aft wings and the surfaces of the ducts themselves. Attitude control in both hover and cruise flight is obtained by differential thrust from the propellers and by deflection of the propeller slipstream by movable vanes in the duct exits. Power is provided by four turboshaft engines located on the inboard section of the aft wing. Here again, the engines and propellers are all interconnected. Design cruise speed is 290 miles per hour.

Figure 10-20 shows the EWR-Sud VJ101C, a West Germany fighter aircraft which utilizes a mixed class of VTOL propulsion systems. It has dual propulsion and thrust tilting. The aircraft has six turbojet engines, two for lift only and four for lift and cruise. The lift engines are mounted in the forward part of the fuselage. The four lift-cruise engines are in pairs in tilting pods at the wing tips. This triangular arrangement of the engines allows the use of thrust modulation for pitch and roll control in hovering flight. Yaw control is obtained by tilting the wing-tip pods slightly from the vertical in opposite directions. The aircraft has been flown at speeds slightly over Mach 1.

A transport version using lift engines in fixed pods at the ends of the wings is also being tested by the West Germans. This airplane is called the Dornier Do-31. It has four lift engines in each wing pod and two cruise engines in conventional nacelles under the wings.



Hovering



Cruising

Figure 10-20. - EWR-Sud VJ101C, thrust-tilting, dual-propulsion VTOL fighter. (Courtesy of Interavia.)

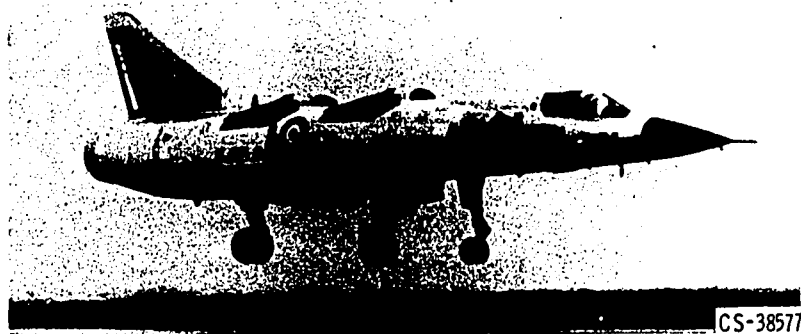


Figure 10-21. - Hawker-Siddeley P1127 Harrier, thrust-deflection type VTOL strike/reconnaissance aircraft.

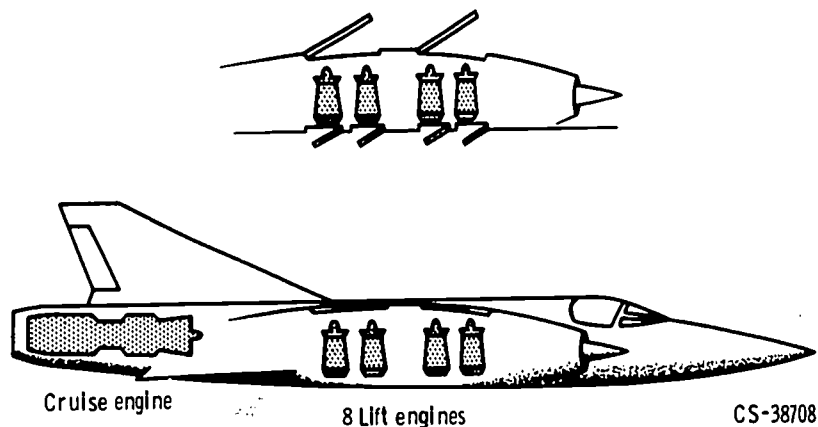
Figure 10-21 shows the British Hawker-Siddeley P1127 Harrier. This is a thrust-deflection-type VTOL aircraft. A single large turbofan engine is located in the center of the fuselage. The engine discharges its air through two nozzles on each side of the fuselage: one ahead and the other behind the center of gravity. Fan discharge air exhausts through the front nozzles, and the hot gases exhaust through the rear nozzles. All four nozzles are fitted with turning vanes, and the nozzles are rotatable, so that the engine thrust can be directed either downward for vertical flight or rearward for horizontal flight. Attitude control in low-speed flight is by means of reaction jets located at the nose, tail, and wing tips. These reaction jets are fed by compressed air from the engine. The aircraft is designed for transonic flight. The first operational squadron of these strike/reconnaissance aircraft has been formed.

Figure 10-22(a) shows the Dassault Mirage 3V aircraft. This is a French high-speed fighter with VTOL capability. It is a dual-propulsion aircraft with separate engines for lift and for cruise. The layout of the engines in the aircraft is shown in figure 10-22(b). A single cruise engine is located in the tail of the aircraft. Eight turbojet lift engines are located in tandem pairs in the central portion of the fuselage. Air for the lift engines enters the four scoops on the top of the fuselage and exits through doors on the bottom. Attitude control in hover is by reaction jets located at the nose, tail, and under each wing tip. These jets are powered by air from the lift engines.

A more recent dual-propulsion aircraft design was evolved for the proposed V/STOL fighter that was to have been developed jointly by the United States, West Germany, and Great Britain. This aircraft design called for a single cruise engine in the rear, and two



(a) Aircraft in hover mode.

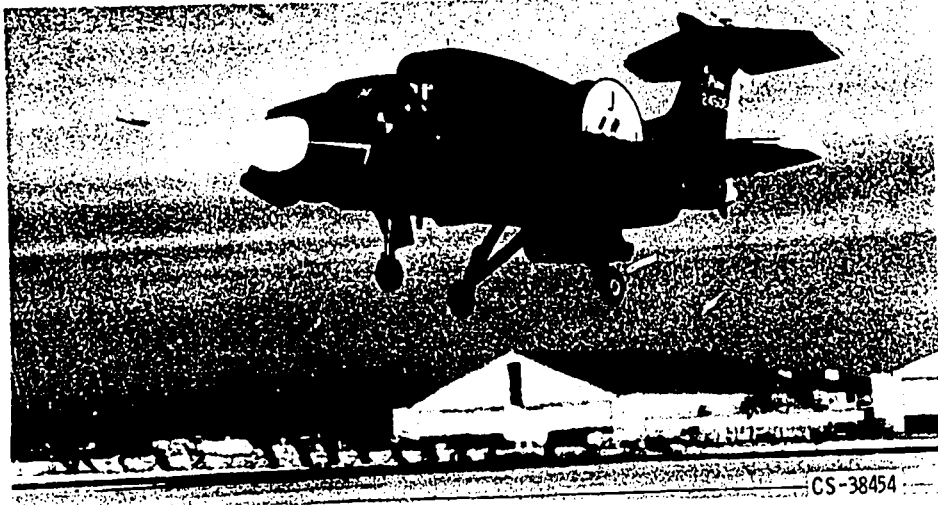


(b) Schematic of dual propulsion system.

Figure 10-22. - Dassault Mirage 3V, dual propulsion VTOL fighter.

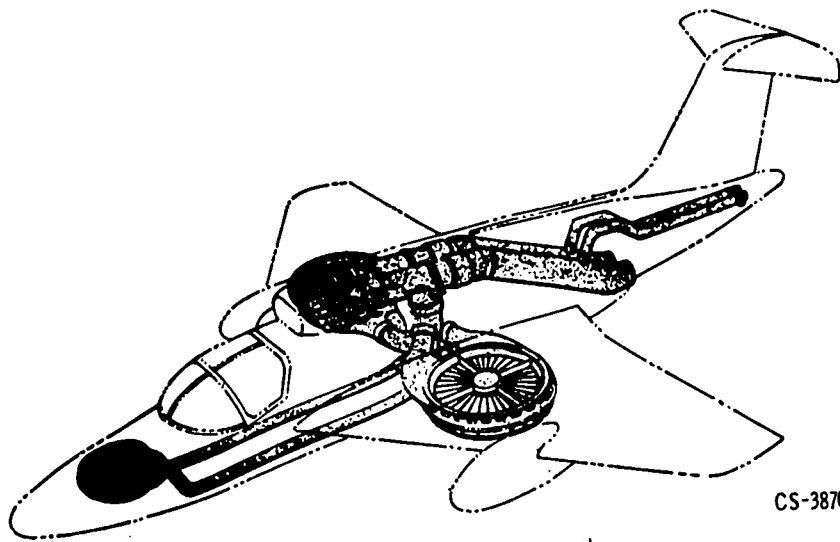
direct-lift engines, on each side of the fuselage, that would swing out (like landing gears do) when needed for takeoff or landing. The cruise engine was designed with an exhaust deflector, so that downward thrust could also be obtained from this engine during lift-off. This project, which has just recently been cancelled, was to have been a joint effort in which the U. S. and West Germany were to build the airplane, and the U. S. and Great Britain were to build the engines.

Figure 10-23(a) shows the Ryan XV-5A semi-dual-propulsion VTOL airplane developed for the U. S. Army. A schematic of the propulsion system for this airplane is shown in 10-23(b). Lift thrust is provided by a ducted fan in each wing. These two fans are powered by two turbojet engines located in the top of the fuselage. Cruise thrust is obtained from these same engines. During hover, exhaust gas from the turbojet engine is diverted by a valve to a turbine located on the fan tips, as shown in figure 10-23(c). These tip-turbine fans approximately triple the basic thrust of the jet engines. Each fan is about 5 feet in diameter and is covered during cruise flight by doors on top of the wing and by span-wise louvers underneath the wing. During vertical flight, the doors and louvers are opened fully. In transition, the exit louvers are moved to deflect the airflow backwards. This gives the aircraft a forward acceleration. When minimum speed for



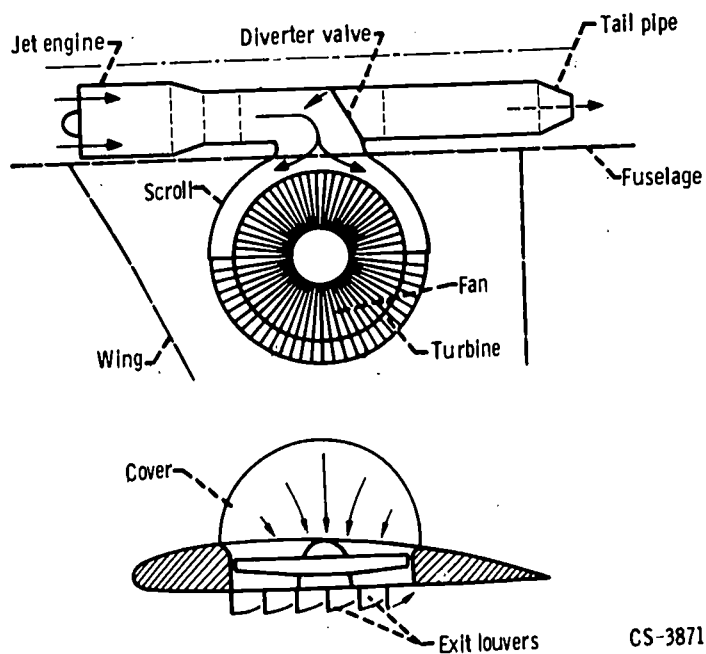
CS-38454

(a) Aircraft in hover mode.



CS-38705

(b) Propulsion-system arrangement.



CS-38712

(c) Schematic of propulsion-system elements.

Figure 10-23. - Ryan XV-5A, semi-dual-propulsion VTOL aircraft.

wing-supported flight is reached, the engine exhaust gases are diverted (by means of the valve shown in fig. 10-23(c)) from the fans to conventional jet nozzles under the rear of the fuselage, shown in figure 10-23(b). In hovering, pitch control is obtained by an additional fan in the fuselage nose, and by reaction jets in the tail. Yaw control is by differential movement of the louvers on the fan exits. Roll control is by differential thrust of the wing fans. To provide for symmetrical thrust during an engine failure, the turbojet engines and fan turbines are interconnected. The cruise speed of this airplane is approximately Mach 0.7. The aircraft currently is being flight tested.

TECHNICAL PROBLEMS

In spite of the many V/STOL aircraft that have been and are being designed and built, very few have become operational. One reason for this is that the design and operation of V/STOL aircraft present many problems that have not yet been solved completely satisfactorily. In the following discussion, the principal technical problems pertaining to V/STOL aircraft are summarized briefly and are compared with the problems of CTOL aircraft. The discussion deals primarily with VTOL aircraft, but all items mentioned also apply to STOL aircraft, although to a lesser degree.

Thrust Requirements

One important difference between V/STOL and CTOL aircraft is in their engine propulsion requirements. For conventional jet aircraft, the ratio of engine thrust to aircraft gross weight is about 0.25 to 0.35; that is, a 100 000-pound aircraft would require jet engines that produce around 25 000 to 35 000 pounds of thrust. In contrast, the theoretical minimum basic propulsion thrust for a VTOL aircraft is the thrust required for a vertical takeoff. This means that the ratio of lift thrust to gross weight must be at least 1.0. However, the actual design value of thrust must be even greater than the weight of the aircraft, because of other considerations that will be discussed later. This increased thrust requirement complicates the design of an aircraft. For example, powering a jet airliner such as the Boeing 707 for vertical takeoff would require that it be fitted with at least 12 jet engines instead of four, or that its four engines be doubled in size.

For STOL aircraft, the required thrust-to-weight ratios range between about 0.35 and 0.8, depending on the type of propulsion system and the runway length allowed.

The earlier discussion (in the section titled BASIC CONCEPTS) explained that during takeoff and landing, when the VTOL aircraft has zero or low forward flight speed, the control surfaces do not generate lift or control forces. Therefore, the propulsion system of a VTOL aircraft must also supply control forces to regulate the stability and attitude of the aircraft. (STOL aircraft do not generally require auxiliary control systems.) Some

of the methods by which control forces are obtained were described earlier, in the section titled AIRCRAFT TYPES. For VTOL aircraft, the ratio of required control-thrust power to aircraft weight might range from about 0.1 to 0.2, depending on the configuration. These required values of thrust, just for the control of VTOL aircraft at low speeds, are about half as much as the total propulsive thrust required for today's jet transports. The need for such powerful control systems stems partly from a lack of aircraft stability in hovering near the ground and partly from the requirement that VTOL aircraft be able to maneuver precisely within small or confined areas in turbulent wind conditions. This maneuvering capability demands a rapid control response (approx. 0.1 or 0.2 sec). Therefore, much thrust is needed to meet these control requirements. However, many different control systems are possible, and their exact thrust requirements depend greatly on the total design of the aircraft. Consequently, there is considerable uncertainty among designers concerning the amount of control thrust that is absolutely necessary.

In addition to the control-thrust requirements, the related problems of maintaining sufficient thrust and control in the event of an engine, or thrust-device, failure must also be considered. The thrust problem stems from the fact that during takeoff, landing, or hovering the VTOL aircraft depends entirely on the engine power for lift. Thus, the failure of an engine or thrust device could be disastrous. A brute-force solution to this problem is the use of many thrusters and many engines, where each engine is oversized so that it is capable of producing excess power. Thus, if one engine fails, the others can produce sufficient excess power to compensate for the lost thrust of the failed engine. For example, if jet engines are used to provide thrust directly, the amount of excess thrust that each engine must be capable of producing depends on the number of engines used; as the number of engines increases, the excess thrust capability required from each engine decreases. For a VTOL aircraft, when two engines are used, each engine must be capable of producing 100 percent excess thrust. With four engines, the excess thrust required from each engine is about 34 percent, and with eight engines it is about 15 percent. In comparison, the excess thrust capability required for each engine of a four-engine CTOL aircraft is only about 10 percent.

When one engine fails, increased power can also be obtained from the remaining engines by overspeeding them. However, this procedure is undesirable, because it can severely damage the oversped engines.

The control problem is that the failure of one engine of a multiengine VTOL aircraft could cause the aircraft to flip over, because of the unbalanced thrust. A solution to this problem is to cross-connect all of the engines by either ducting or shafting, depending on the type of propulsion system. For example, figure 10-24 shows the cross-shafting system used on the Ling-Temco-Vought XC-142A, the tilt-wing turboprop aircraft shown in figure 10-18. A clutch located between each propeller and engine automatically disengages the failed engine. The reduced total power is then redistributed through the cross-

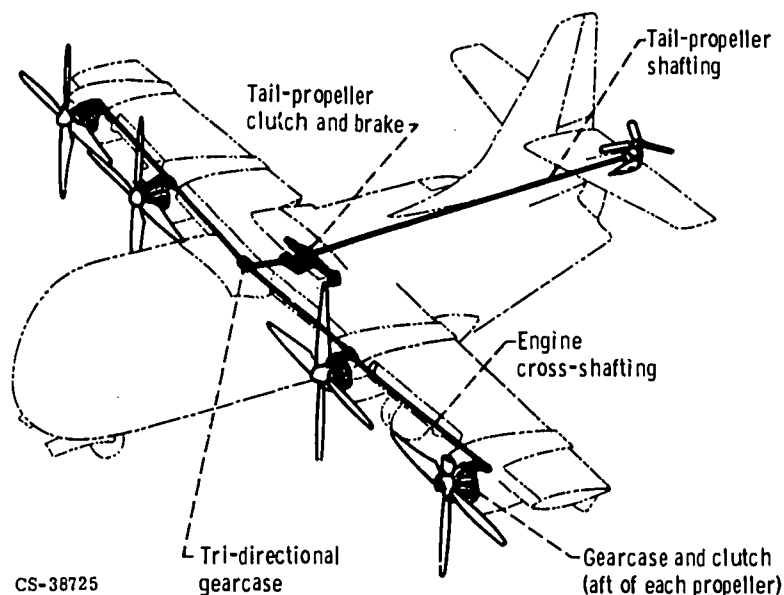


Figure 10-24. - Engines cross-connected for safety in the event of failure of one engine.

shafting system so that equal power is delivered to each of the four main propellers. A reduced power flow also goes to the tail propeller. Obviously, this is a complex arrangement.

The engine- or thruster-failure problem during takeoff or landing is also important for STOL aircraft. However, the tendency of the aircraft to upset because of unbalanced thrust is not as severe, since the STOL airplane is supported completely or mostly by the lift of the wings (lift tends to remain uniformly distributed when an engine fails).

To satisfy the three previously mentioned thrust requirements (lift-off thrust, control thrust, and excess thrust for engine failure) for VTOL aircraft, the ratio of total thrust to aircraft weight must be about 1.15 to 1.3, depending on the overall configuration of the aircraft.

For STOL, as mentioned previously, the required thrust-to-weight ratios are from 0.35 to 0.8. The propulsion system of a V/STOL aircraft will therefore be heavier than for a comparable CTOL plane. For example, for the same size airplane, the propulsion system is only around 6 percent of the total weight for CTOL, but this increases to 12 to 18 percent for STOL, and to 20 to 32 percent for VTOL.

When considered on the basis of the same mission, V/STOL aircraft will certainly be heavier and more costly than comparable CTOL aircraft. In fact, studies indicate that for the same payload (passenger or cargo) capacity, a VTOL transport will be around 50 percent heavier than a CTOL transport and cost about 50 percent more to operate. A breakdown of the relative weights of these two types of aircraft is presented in figure 10-25.

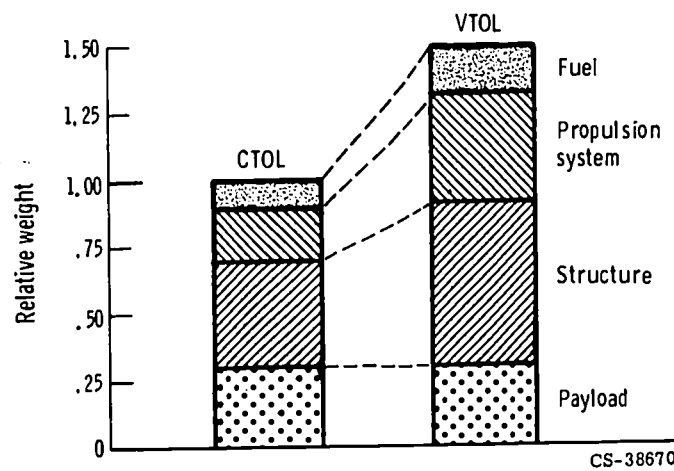


Figure 10-25. - Weight comparison of typical VTOL and CTOL transports with same payload, range, and cruise speed capabilities.

Power Matching

The fact that relatively large amounts of power are required for takeoff with V/STOL aircraft creates a problem for the cruise condition. V/STOL aircraft, especially subsonic configurations, have far more installed power than is necessary to sustain normal cruise flight. For example, if the overall lift-to-drag (L/D) of the airplane in cruise is 10, then the required cruise thrust is only 0.1 of the airplane weight (thrust = drag). However, the installed thrust required for vertical takeoff could be around 1.2 times the airplane weight. Thus, a reduction in thrust to around 8 percent of the takeoff value is required for cruise. Current propulsion systems cannot operate over such a wide range of power output. This is called power mismatch.

Several approaches are taken to ease this "mismatch" problem. In all cases, the powerplants can be designed to give wide ranges of power (e.g., by using variable-geometry components). Using high-bypass-ratio fan engines also helps, since power output falls off rapidly with flight speed for this type of system.

However, these steps may not be sufficient, especially for VTOL. In many cases, it will be necessary to shut down some of the engines during cruise flight, or to use two completely separate systems - one for takeoff and landing, and the other for cruise flight. Examples of this approach to the mismatch problem are the previously discussed EWR-Sud VJ101C aircraft (fig. 10-20) and the Dassault Mirage 3V (fig. 10-22).

Noise

One great obstacle to successful V/STOL operations, especially commercial operations, is noise. The basic reasons for this are that V/STOL operations will bring air-

craft much closer to the populous areas of cities and these aircraft will have far more powerful engines than those used on current CTOL airplanes. It is easy to see, therefore, that aircraft noisiness will be a very important consideration in the evaluation of V/STOL systems.

Aircraft noise is measured in terms of a factor called PNdB, which stands for "perceived noise level in decibels." Noise is basically a succession of pressure waves that are propagated from a generating source (like the aircraft engine). The intensity of the noise (amplitude of the pressure wave) is measured in terms of decibels of the sound pressure with respect to some reference level. Noise is usually propagated over a range of frequencies from about 20 to 10 000 cycles per second. (For rating purposes, sound pressure is usually divided into eight frequency ranges, called octave bands.) Sound of a given intensity can be very annoying if generated at certain frequencies, and less annoying at other frequencies. The perceived noise level of a given sound is numerically equal to the sound pressure level of a reference sound that is judged by listeners to have the same perceived noisiness as the given sound, the reference sound being a band of random noise 1 octave in width centered on 1000 cycles per second.

The PNdB noise rating is an attempt to weigh the sound pressure level (intensity) value to account for the effects of different frequencies. It was originated about 8 years ago from a study of people's reaction to the noise from turbojet and turboprop commercial aircraft operating from the New York City airports. It was found that frequencies in the range from 600 to 4800 cycles per second were most annoying. Thus, the PNdB rating gives relatively more weight to the mid-frequency range of sounds. However, noise prediction is a very complex and difficult procedure, because there are many noise sources and influencing factors involved (such as duration, atmospheric conditions, and the variation in tolerance among different people). Considerable effort is currently underway to improve our ability to rate and predict noisiness and to take these factors into account in a rational manner.

The principal sources of noise in a jet aircraft are the hot gas exhaust from the jet engine and the high-speed rotor blades of the engine compressor. The roar of a jet plane as it takes off is from the exhaust jet, while the whine that is heard when a plane is landing is from the compressor. Propellers and rotors are the principal noisemakers in turboprop planes and helicopters. A rough rule of thumb is that the loudness (intensity) of the noise of an airplane depends on the disk loading (slipstream velocity) of its thrust device, where the higher the disk loading, the louder the noise.

A gross comparison of the predicted noise levels for various types of V/STOL aircraft currently under study is shown in figure 10-26. The figure shows predicted values of PNdB heard at 400 feet either to the side or below a VTOL aircraft of 75 000 pounds gross weight at full power setting. Values are plotted against disk loading, and the various types of thrust devices that were mentioned earlier are located on this scale. Also

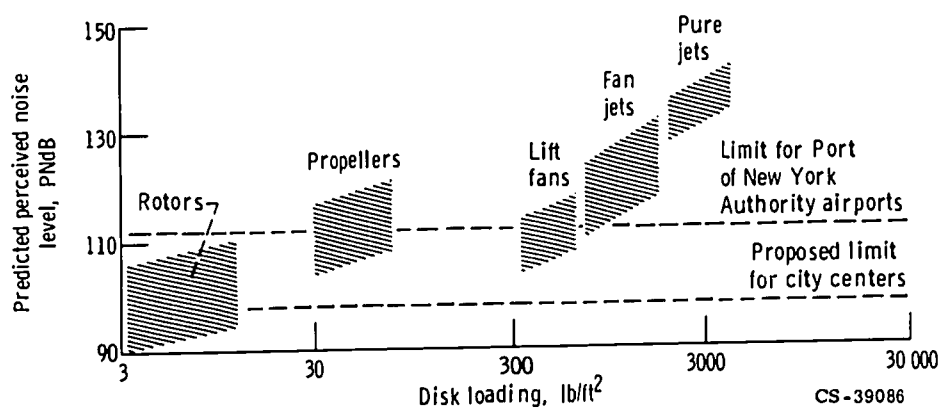


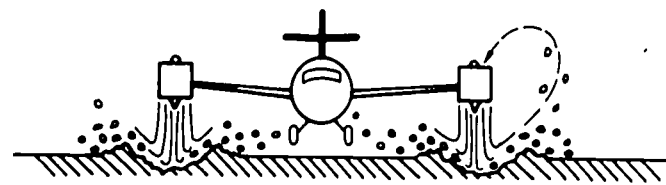
Figure 10-26. - Predicted noise level as function of disk loading for various types of V/STOL thrust devices. Powerplant at full power setting; gross weight of aircraft, 75 000 pounds; distance of aircraft from noise detector, 400 feet. (For comparison purposes, the following are some typical perceived noise levels in decibels: residential area (daytime), 50 to 60; city traffic (daytime), 80 to 90; train at 100 feet, 90 to 100; boiler shop, 125 to 135.)

shown in the figure are two tentative noise limits (indicated by dashed lines). The limit of 112 PNdB is in effect for Port of New York Authority airports (Kennedy, LaGuardia, and Newark). The lower limit of 98 PNdB has been proposed for V/STOL operations from city-center areas. The proposed limit for V/STOL operations is lower because the noise duration would be longer with the slower V/STOL flight speeds near airports and because the airports would be located in or near highly populous areas. The figure indicates that pure jets are completely unacceptable. Fan jets (turbofans), which have drastically reduced slipstream velocities, are a basic improvement, but not enough. With this type of engine the overall PNdB remains high because of the predominant compressor fan noise. In terms of the PNdB, propellers seem to be reasonably good and rotors seem best. However, the character of the noise of these thrust devices is different from that of the jet engines. The noise of rotors, in particular, includes fluctuations (or beats) that can be objectionable. This rotor noise is sometimes referred to as banging. It is quite intense and of relatively low frequency. The PNdB rating as it is now determined does not account for this rotor noise. Therefore, the actual sound of a rotor is worse than is indicated by the noise rating.

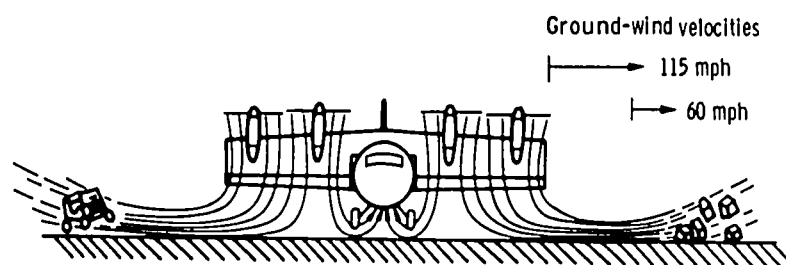
Obviously, the noise levels of proposed V/STOL aircraft will have to be reduced, but this will be difficult and expensive.

Downwash Effects

With a VTOL aircraft, high slipstream or exhaust velocities can cause trouble when the discharge from the thrust device is directed downward. Some of the effects of a high-velocity downwash are illustrated in figure 10-27. For example, when a jet-powered



(a) Ground erosion.



(b) Ground winds.

CS-36672

Figure 10-27. - Downwash effects of hovering VTOL aircraft.

aircraft is hovering over unprepared ground (fig. 10-27(a)), the exhaust streams from the jet engines can quickly start blasting sizable holes in the earth. Pieces of debris can be recirculated up and into the engine inlet and also can be thrown up against the landing gear and fuselage. Ground erosion increases with increasing exhaust velocities. Figure 10-27(b) shows a typical turboprop-powered tilt-wing aircraft hovering over a paved runway. The slipstream is turned by the pavement, and the horizontal winds created can be 60 miles per hour even 60 feet away from the aircraft. Such winds can cause damage to objects near the aircraft. The fact that VTOL aircraft are expected to operate from small, confined landing areas makes the ground-wind problem even more serious.

Another aspect of these ground winds is that they can create either positive or negative pressures under the aircraft, depending on the aircraft configuration. With some configurations, the propeller slipstreams or the jet exhaust streams may collide after impinging on the ground surface and flow vertically upward against the bottom of the aircraft (fig. 10-27(b)). This upward flow produces a local positive pressure, or boosting effect.

For airplanes with wings in the normal horizontal position, the high-velocity exhaust of a vertically mounted or deflected jet will drag some of the surrounding air along with it (this phenomenon is called air entrainment). This creates a pronounced airflow toward the jet along the undersurface of the wing or the fuselage. This flow, in turn, reduces the pressures on the surface and results in a negative lift, or downward suction. These positive and negative ground effects contribute to the instability and control problems mentioned earlier.

Another operational problem related to downwash velocity with jet or fan thrusters is that hot exhaust gases may recirculate and enter the drive engines, thereby decreasing

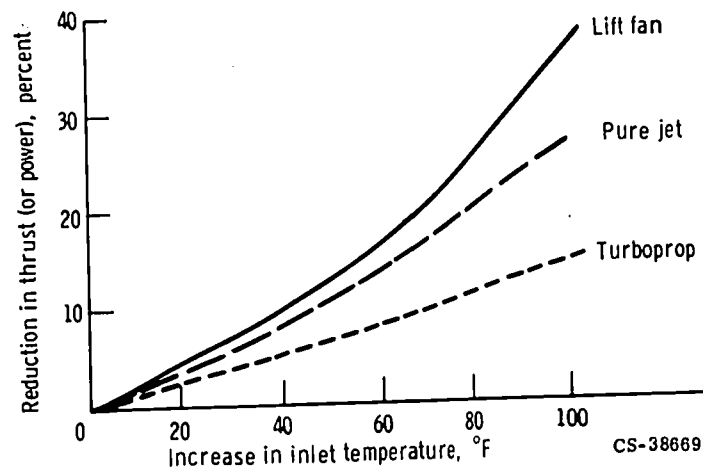


Figure 10-28. - Reduction in engine thrust or power with increase in inlet temperature.

their thrust. Figure 10-28 shows that an inlet temperature increase of only 40° F can cause a 10-percent reduction in thrust in some powerplants. Such a reduction in thrust can seriously affect the performance of a VTOL aircraft. The relative positions of the curves for the three propulsion types shown in the figure are not precise for all engines. They merely show a general trend, based on manufacturers' engine specifications.

Powerplant Selection

A difficult problem confronting V/STOL aircraft designers is the selection of the propulsion system for the aircraft. Of the various propulsion systems (jet, fan, propeller, or rotor) that can be used for V/STOL aircraft, none is clearly far superior to the others. Each system has its advantages and disadvantages. How any given propulsion system compares with other systems depends on the type of aircraft under consideration and the mission it is intended to accomplish. There is an extremely close inter-relationship between aircraft configuration and propulsion system, and both have to be considered together when the airplane is designed. This is far more important with V/STOL aircraft than with CTOL aircraft.

However, the principal requirements and desired characteristics of any propulsion system include light weight, small volume, low noise output, low cost, good engine-failure safety, low fuel consumption, small downwash effects, and best match between takeoff and cruise power. Some of these qualities are conflicting by nature. Therefore, any propulsion-system design is a compromise in which some desirable characteristics are sacrificed in order to obtain those characteristics that are essential to the particular application. For example, for a military aircraft, the compromise might be in favor of powerplant performance at the expense of noise and cost. However, for a civilian transport, the compromises may have to be in favor of low noise and low cost.

Recent studies based on current powerplant technology have indicated that VTOL aircraft operation may be up to 50 percent more expensive than CTOL aircraft operation. Most of this cost difference is a result of the relatively greater power requirement of a VTOL aircraft. Considerable effort will therefore be required to improve the characteristics of V/STOL propulsion systems so that they can result in more financially as well as technically attractive aircraft.

NASA PROGRAMS

NASA is strongly interested and actively involved in research on V/STOL aircraft. This phase of aeronautical research is receiving increased emphasis in the three major NASA research centers - Langley, Ames, and Lewis. The Langley and Ames Centers are primarily concerned with overall aircraft aerodynamics and design and with actual flight operations. Their tests are conducted on large-scale airplane models in wind tunnels and on full-size test aircraft.

Here at Lewis the emphasis is on research on propulsion systems and propulsion-airframe integration. Currently, studies are being made of promising propulsion systems for STOL and VTOL aircraft. We are trying to get a better picture of the relative design and performance characteristics of the propulsion systems, as well as their problem areas. The objective is to select systems (powerplants and thrust devices) for further experimental evaluation. Current emphasis is on high-bypass-ratio fans for both STOL and VTOL propulsion. Various design and operating problems are being defined, and means for solving them are being devised. We are also devising and studying various attractive airplane configurations for VTOL and STOL transports.

11. SUPERSONIC AERODYNAMICS

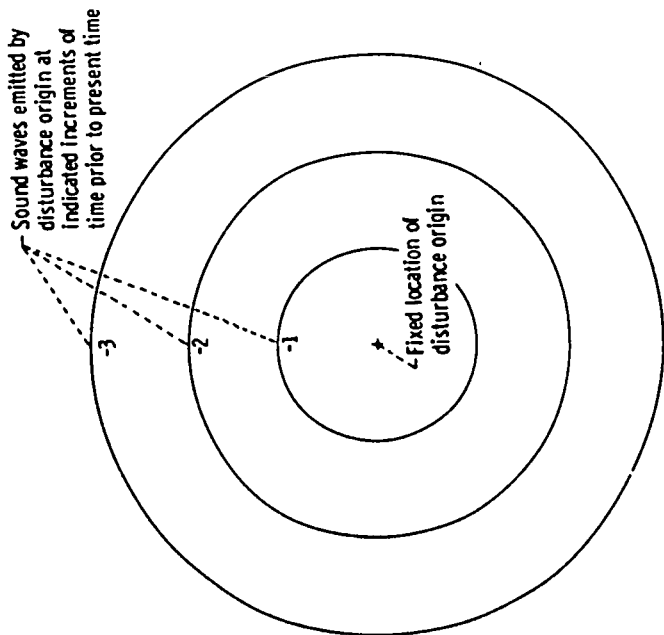
David N. Bowditch*

To introduce supersonic aerodynamics, let us first consider what characterizes supersonic flow. "Supersonic" obviously refers to speeds faster than the speed of sound, or the sonic velocity. A sound wave is a wave with a very small pressure rise across it. When you speak, you form sound waves that travel through the air to someone who senses and interprets the waves as words. These same sound waves speed ahead of a subsonic airplane and start the air moving around its body and wings. However, at supersonic speeds, these sound waves can no longer reach ahead of the airplane and prepare the air to flow smoothly around its parts. The sound waves coalesce to form discrete shock waves with large pressure rises across them. As the aircraft travels faster than the speed of sound, these shock waves are attached to the pointed or sharp (low-angle) surfaces of the aircraft and abruptly deflect, or push, the air around the surfaces of the aircraft. These shock waves, more than any other feature, characterize supersonic flow.

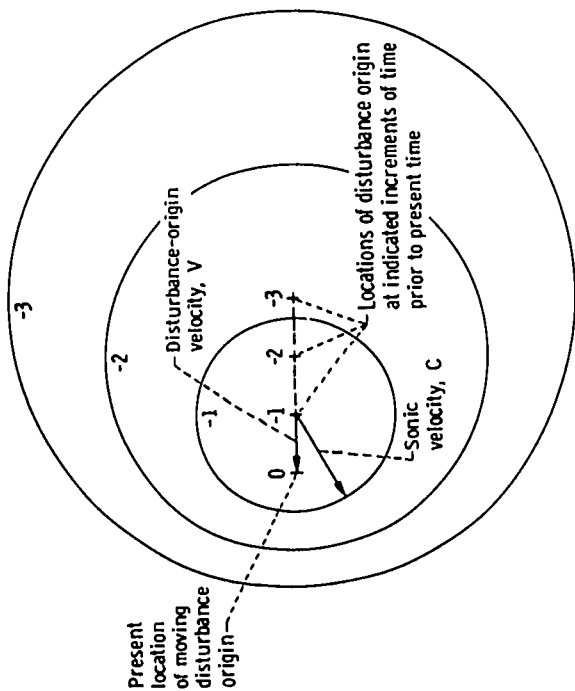
FLOW REGIMES

The characteristics of four flow regimes covering the subsonic through supersonic range are depicted in figure 11-1. In the figure, the point 0 represents the present location of the disturbance, and the points -1, -2, and -3 represent the locations of the disturbance at one, two, and three units of time previously. The circles look like ripples in a pond, caused by a pebble dropped at the disturbance origin. However, in the three-dimensional atmosphere, the circles represent spherical sound waves propagating in all directions at the speed of sound. For zero disturbance-origin velocity, the sound waves form concentric circles about the disturbance (fig. 11-1(a)). When the disturbance-origin velocity V is greater than zero but less than the speed of sound C , the sound waves still propagate ahead of the moving origin (fig. 11-1(b)). However, when the disturbance-origin velocity equals the speed of sound ($V/C = 1$), there is a zone of silence ahead of the disturbance origin that is unaffected by the disturbance (fig. 11-1(c)). At supersonic velocity ($V/C > 1$), the disturbance origin continually outruns the earlier sound waves

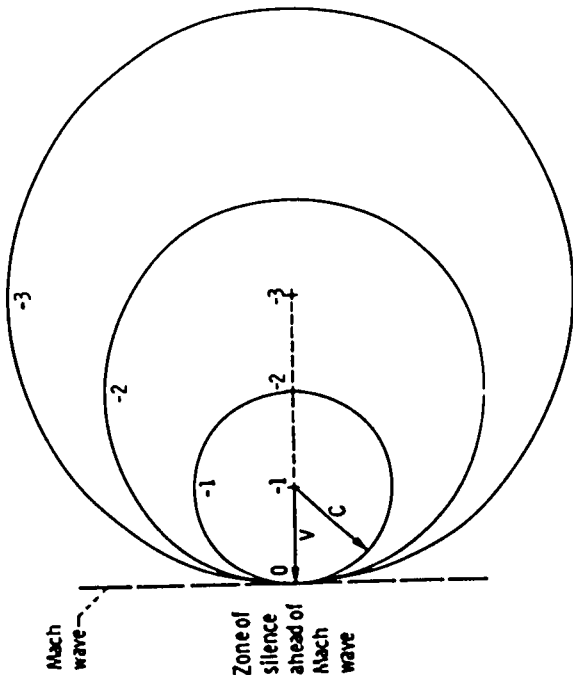
*Chief, Propulsion Aerodynamics Branch.



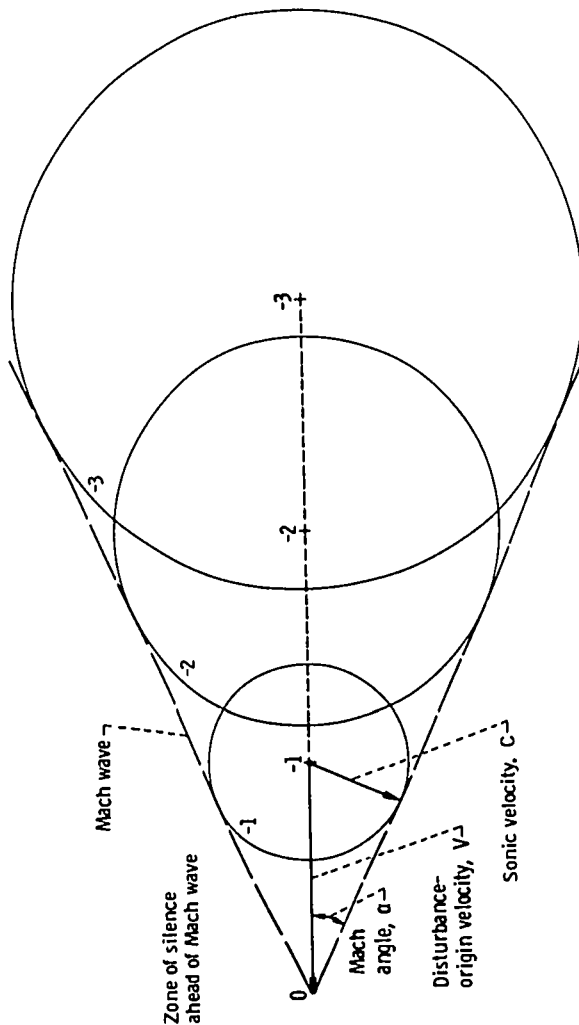
(a) Zero disturbance-velocity ($V/C = 0$).



(b) Subsonic disturbance-velocity ($V/C < 1$).



(c) Transonic disturbance-velocity ($V/C \approx 1$).



(d) Supersonic disturbance-velocity ($V/C > 1$).

Figure 11-1. - Pressure fields produced by a point disturbance origin moving at various constant velocities.

(fig. 11-1(d)). Thus, the spherical waves propagating from previous points along the path of the origin form a cone behind the moving disturbance origin. The half angle of the cone, called the Mach angle α , is given by the equation

$$\alpha = \arcsin \frac{C}{V} = \arcsin \frac{1}{M}$$

where C is the sonic velocity, V is the disturbance-origin velocity, and M is the Mach number.

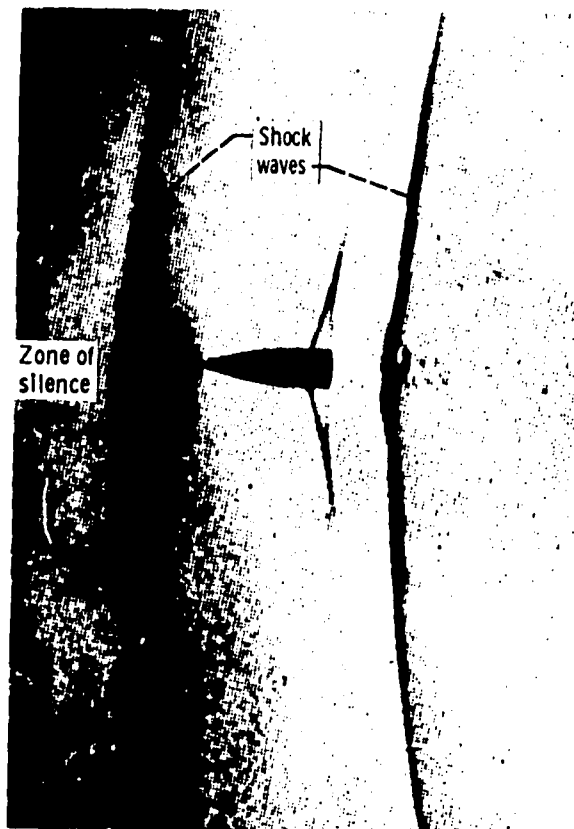
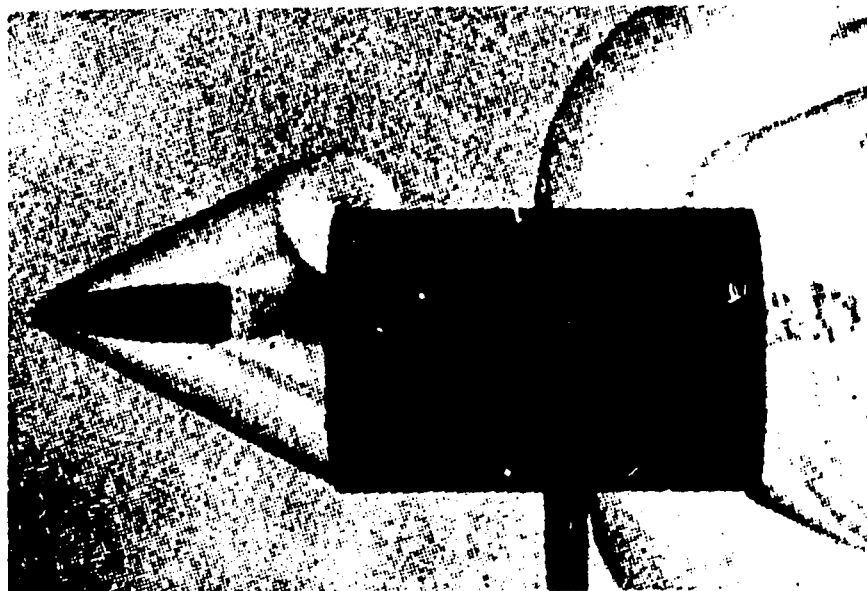


Figure 11-2 - Schlieren photograph of bullet traveling at transonic speed. (From Ackeret and reprinted from "The Dynamics and Thermodynamics of Compressible Fluid Flow," by Ascher H. Shapiro, with permission of the Ronald Press Co.)

Figure 11-2 is a schlieren photograph of a bullet traveling at transonic speed. The shock waves are nearly perpendicular to the direction of the bullet. The "zone of silence," discussed previously, is ahead of the bow wave of the bullet. Figure 11-3 shows two bullets traveling at supersonic speeds through short cylindrical tubes. The tubes restrict the wave travel. As the bullet emerges from the tube (fig. 11-3(a)) or as it passes by a circumferential slot in the tube (fig. 11-3(b)), the spherical nature of the



(a) Shadowgraph of bullet passing through single tube.



(b) Schlieren photograph of bullet passing through several short tubes in series.

Figure 11-3. - Photographs of supersonic bullets passing through cylindrical tubes, showing Mach cones and spherically spreading wave fronts. (From Ackeret and reprinted from "The Dynamics and Thermodynamics of Compressible Fluid Flow," by Ascher H. Shapiro, with permission of the Ronald Press Co.)

sound wave front is clearly evident. The relatively small Mach angles of the shock waves indicate that these bullets are traveling at high supersonic velocities.

ONE-DIMENSIONAL, ISENTROPIC FLOW

Supersonic flow conditions can be achieved either by accelerating the air past an object to supersonic speeds (as in a wind tunnel) or by moving an object through the air at supersonic speeds. Figure 11-4 is a schlieren photograph of supersonic flow through a

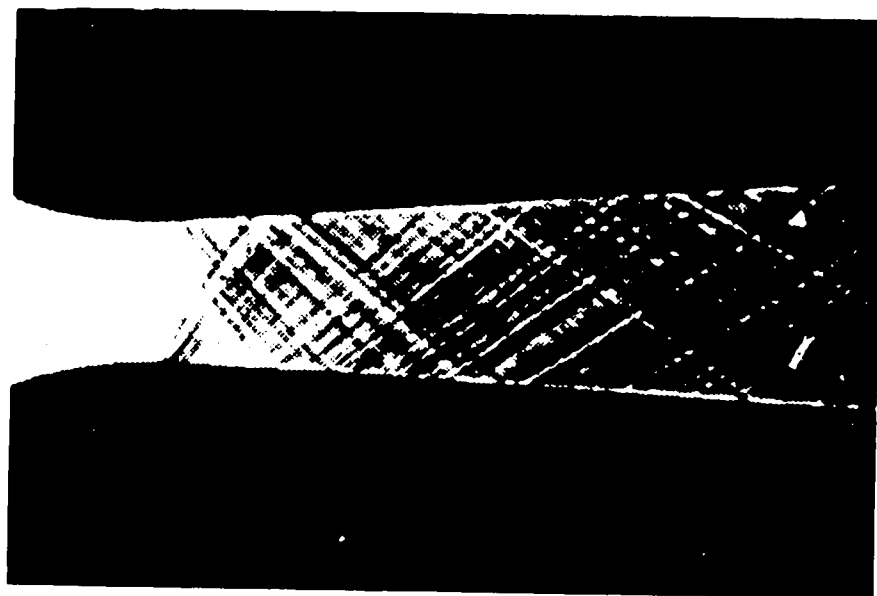


Figure 11-4. - Schlieren photograph of supersonic flow through a nozzle. (From Busemann and reprinted from "The Dynamics and Thermodynamics of Compressible Fluid Flow," by Ascher H. Shapiro, with permission of the Ronald Press Co.)

nozzle. Upstream of the nozzle throat the flow is subsonic. This is indicated by the absence of shock waves. Downstream of the throat the flow is supersonic and attains progressively higher Mach numbers, as indicated by the decreasing angles between the shock waves and the local wall of the nozzle.

The study of flow properties in a nozzle can be simplified by assuming that the flow is one-dimensional and isentropic. These assumptions make it possible to determine the average flow properties at any station in the nozzle. "One-dimensional" means that the flow is assumed to be uniform across the duct at any axial station in the nozzle. The term

"isentropic" specifies two characteristics of the flow: first, there is no heat transfer out of or into the flow (the walls are thermally insulated); second, any conversion of the energy of the random motion of the gas molecules to some other form of energy or work is 100 percent efficient. Pressure and temperature are measures of this random energy.

In order to investigate some of the properties of supersonic flow, we can relate the pressure p , density ρ , temperature T , and flow area A of the gas flowing in a duct to its velocity V , or Mach number M . This requires some basic equations relating the flow properties at any two stations in the duct. The following are the basic relations for the flow properties at any two stations in an isentropic, one-dimensional flow.

Continuity equation (conservation of mass):

$$(\text{Mass flow})_1 = (\text{Mass flow})_2$$

or

$$(\rho VA)_1 = (\rho VA)_2$$

Energy equation (conservation of energy):

$$(\text{Energy flow})_1 = (\text{Energy flow})_2$$

Isentropic relation:

$$\frac{P_1}{P_2} = \left(\frac{\rho_1}{\rho_2} \right)^k$$

Perfect gas relation:

$$p = \rho RT$$

The continuity equation states that the mass flow at station 1 must equal the mass flow at station 2. This assumes that the duct has no leaks. The mass flow is the product of the density ρ , the velocity V , and the local duct area A . Since no energy or work is allowed to leave the duct, the energy equation states that the energy at stations 1 and 2 must be equal. This energy is the sum of the kinetic energy of the flowing gas, which is proportional to ρV^2 , and the energy in the random motion of the gas molecules. The energy equation does not state that either the kinetic or the random energies are equal at

stations 1 and 2, but only that their sums are equal at the two stations. Therefore, this permits conversion of random energy into the directed kinetic energy associated with the gas velocity. Since 100-percent conversion efficiency has been assumed, the isentropic relation between pressure and density can be used. The perfect gas relation relates the pressure, density, and temperature of the gas by utilizing a constant R , which is a property of the gas mixture.

For ratios of pressure, temperature, density, and duct area between stations 1 and 2 in terms of Mach number, we calculate the property variations shown in figure 11-5. The pressure, temperature, and density variations with Mach number are presented as ratios of the local values to their values at the point of zero Mach number (i. e., stagnation point). This is accomplished by letting station 1 correspond to a Mach number of zero and presenting the ratios of the local conditions at station 2 to the zero-Mach-number conditions at station 1. Since the duct area is infinite for zero Mach number, the area variation is presented in the form of the ratio of the local duct area A to the area A^* at the point in the duct where the flow speed is Mach 1.0. The velocity variation is presented in a similar manner.

Figure 11-5 shows that the cross-sectional area of the duct is minimum at Mach 1.0 (where flow velocity is sonic). This is in agreement with figure 11-4, which showed that the change from subsonic to supersonic flow occurs at the throat. Therefore, achieving supersonic flow in a duct requires that the duct first converge to a minimum area, or throat, and then diverge downstream of the throat. The velocity becomes sonic at Mach 1, and then asymptotically approaches a value of about 2.5 times that speed at very high Mach numbers. This velocity represents all the random molecular energy converted to directed gas velocity. The static pressure is about 50 percent of its stagnation value at Mach 1.0 and drops precipitously thereafter, reaching one-tenth of its stagnation value at Mach 2.1 and one-hundredth at about Mach 3.5. This means that if the stagnation pressure of air entering a nozzle is 15 pounds per square inch, the wall static pressure is only 0.15 pound per square inch at the point in the nozzle where the flow speed is Mach 3.5. It also means that an airplane flying at Mach 3.5 at low altitude, where the atmospheric static pressure is 15 pounds per square inch, could collect air at a stagnation pressure of 1500 pounds per square inch for an engine if the inlet were 100 percent efficient. Figure 11-5 shows that the temperature ratio also drops quickly with Mach number. Thus, if an aircraft is flying at Mach 3.5 through air that has a static temperature of 520° Rankine (60° F), the total temperature of the air striking the surfaces of the aircraft is 1800° R ($520^{\circ} \div 0.29$). If the airplane speed were Mach 6.7, the total temperature would be 5200° R, hotter than the inside of a jet-engine afterburner. This is the heat barrier.

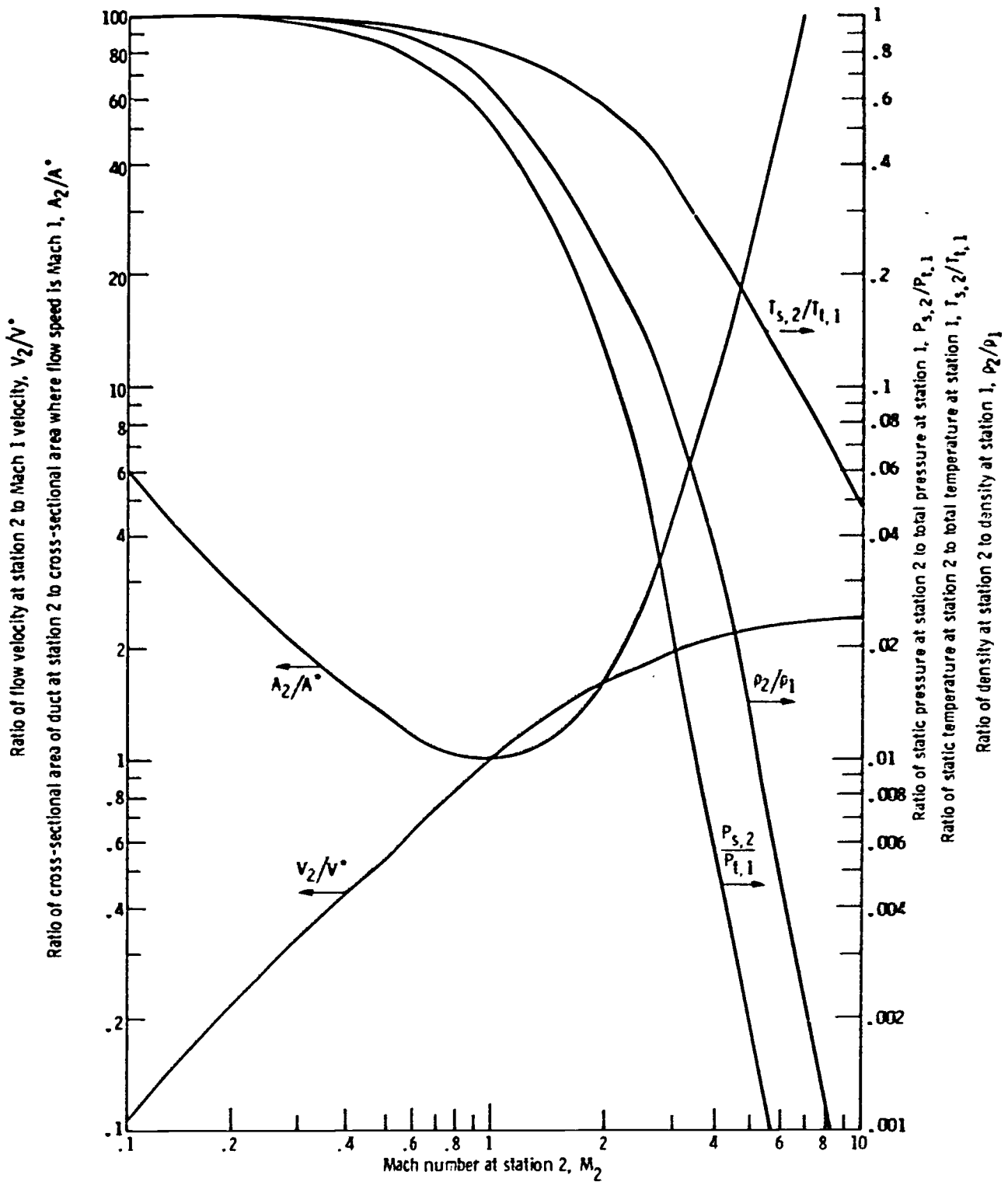


Figure 11-5. - Variation of temperature, density, pressure, area, and velocity ratios with Mach number for isentropic, one-dimensional flow. (Stagnation conditions are assumed to exist at station 1; station 2 is downstream of station 1.)

NORMAL SHOCK WAVE

The following discussion concerns shock waves. The simplest is the normal shock wave (fig. 11-6). Across such a shock wave, the static pressure ratio can be very large. The thickness of a normal shock wave is only about 0.00001 inch. Statistically, this is the average distance an air molecule travels before it collides with another. In supersonic flow, the shock wave produces an abrupt discontinuity in pressure and velocity across it.

The interior detail of the normal shock wave is very complex. To avoid the

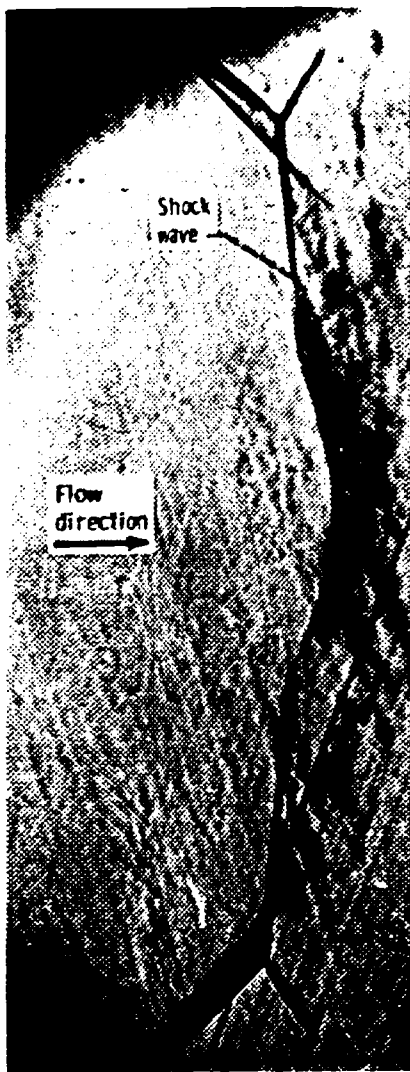
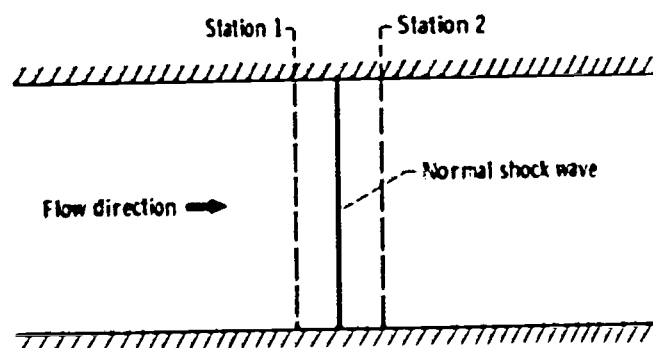


Figure 11-6. - Schlieren photograph of normal shock wave in supersonic wind tunnel. (Courtesy of Massachusetts Institute of Technology Gas Turbine Laboratory.)

necessity of dealing with the complex internal shock processes, the flow is considered at stations a short distance on either side of the shock wave, as shown in the sketch below.



Determining the flow properties across the shock wave again requires some basic relations. The previously discussed continuity equation, energy equation, and perfect gas relation are again applicable. However, the energy-conversion process across the shock wave is no longer 100 percent efficient. Therefore, a new equation is needed to replace the previously used isentropic relation. This necessary new equation is the momentum equation.

$$(\text{Pressure force})_1 + (\text{Momentum flux})_1 = (\text{Pressure force})_2 + (\text{Momentum flux})_2$$

where the momentum flux equals mass flow rate times velocity.

The momentum equation is derived from Newton's Second Law of Motion (Force = Mass \times Acceleration). The force is provided by the pressure difference across the shock wave. This force decelerates the flow from a very high velocity upstream of the shock wave to a lower velocity downstream of the shock wave.

Figure 11-7 presents the variation of ratios of pressure, temperature, and other flow parameters across the normal shock wave. Here we see that the downstream Mach number M_2 is always subsonic, becoming smaller as the upstream (initial) Mach number M_1 increases. From the static pressure ratio $P_{s,2}/P_{s,1}$ it can be seen that a normal shock wave with a very small static pressure ratio travels at Mach 1.0. However, increases in pressure ratio increase the speed of the shock wave. A pressure ratio of 10 is required for Mach 3.0, and a pressure ratio of almost 100 is required for Mach 9. The stagnation pressure behind the normal shock $P_{t,2}$ decreases drastically as Mach number is increased. Recovery of this stagnation pressure is one measure of efficiency. Thus, a high-Mach-number normal shock wave has a low stagnation pressure downstream and a corresponding low efficiency. These normal-shock-wave equations hold for a fixed-position normal shock wave terminating supersonic flow in a duct,

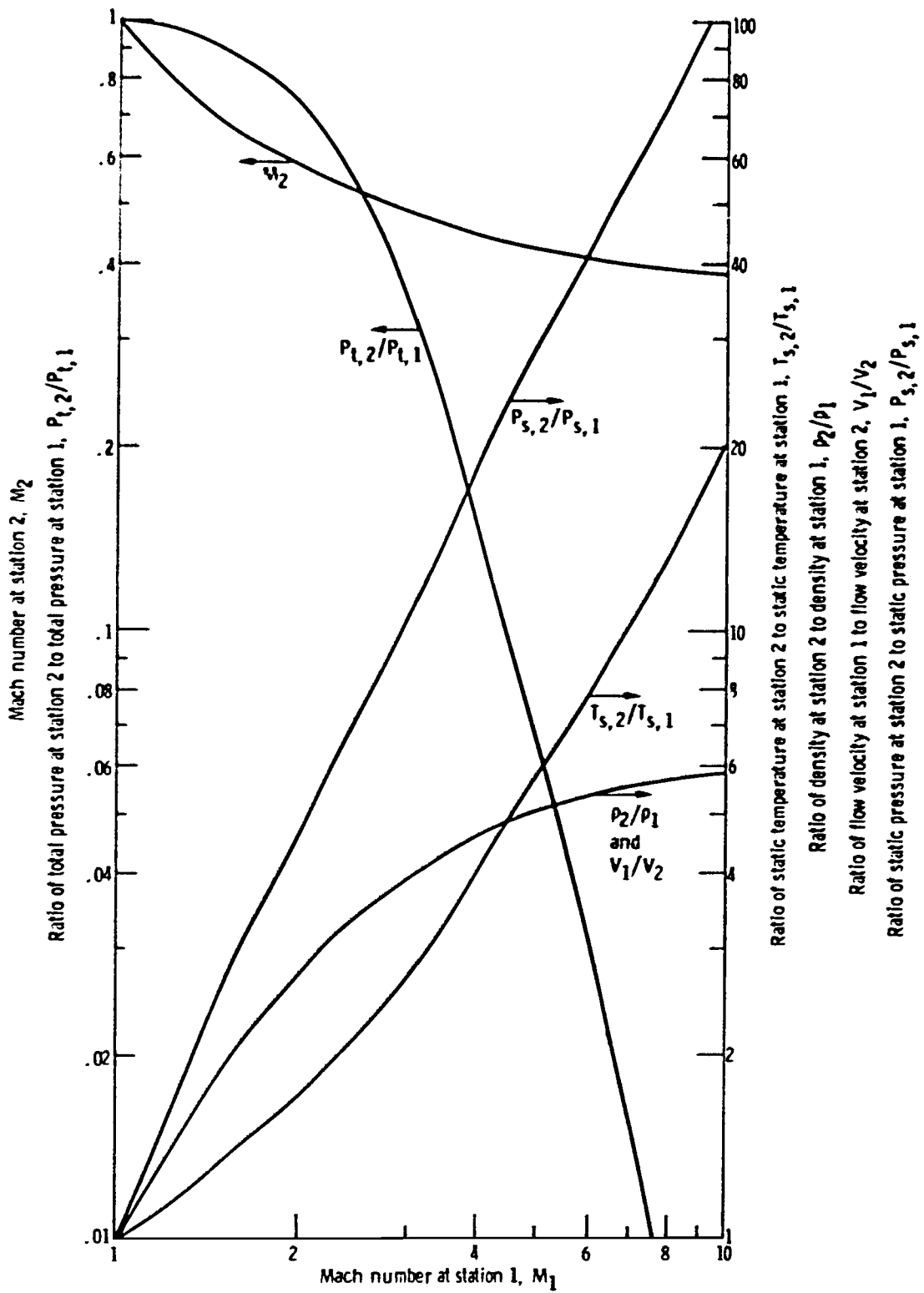


Figure 11-7. - Variation of downstream Mach number and ratios of total pressure, static pressure, static temperature, density, and velocity with upstream Mach number for flow across normal shock wave. (Station 1 is upstream and station 2 is downstream of shock wave.)

for a normal shock wave in front of a supersonic airplane nose, and for a blast wave from an explosion.

OBLIQUE SHOCK WAVE

So far, only flow in one dimension has been considered. This approach permits determining only average conditions and does not consider the details of how the flow travels from one station to another. To do that requires considering at least two dimensions. In the earlier discussion the air was always assumed to be flowing in the same axial direction. In the case of the oblique shock wave, the flow is turned an angle δ from the initial axial direction, as shown in figure 11-8. This then requires considering flow in more than one direction. The pressure rise across an oblique shock wave can be very small for small turning angles or very large for large turning angles and high Mach numbers.

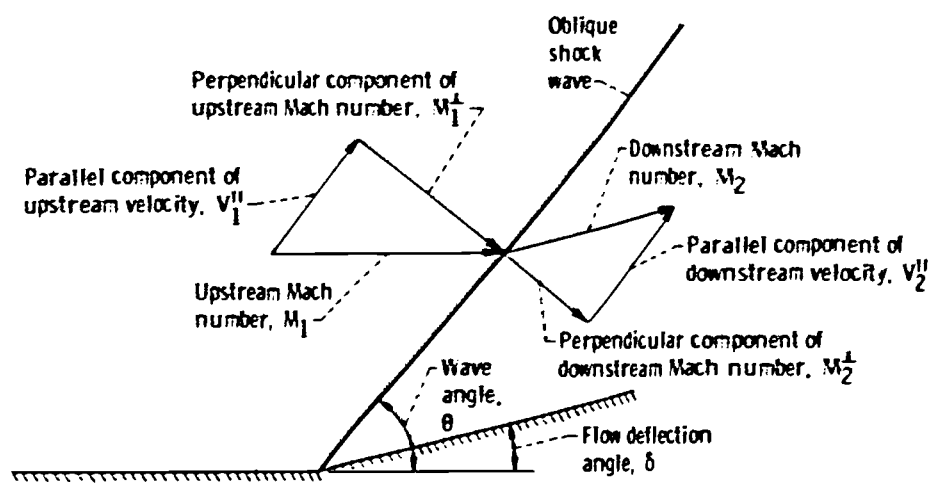


Figure 11-8. - Flow field across two-dimensional oblique shock wave for flow deflection angle of δ degrees.

The pressure force is perpendicular to the wave, so any flow velocity changes must be restricted to this same direction. This means that the velocity V^\parallel parallel with the oblique shock is unchanged in traveling across the shock wave. By considering the Mach number component perpendicular to the shock wave, we find that the relation between M_1^\perp and M_2^\perp is the same as for a normal shock wave. Therefore, if the initial Mach

number M_1 and the wave angle θ are known, it is possible to determine V'' and M_2^1 , which define the flow deflection angle δ . Normally, the known quantities are M_1 and δ , and tables and graphs are available (ref. 1) to solve the problem without iteration.

Oblique shock waves vary from Mach waves whose normal Mach number is 1 and whose pressure rise is extremely small to waves with large turning angles and large pressure rises. The downstream Mach number M_2 is normally supersonic. Beyond the turning angle δ , where M_2 becomes 1, the oblique shock wave will detach from the turn and move upstream. It is impossible to obtain a low subsonic velocity behind an oblique shock wave. Therefore, the turning angle in an oblique shock wave is limited, and this maximum turning angle increases with Mach number.

PRANDTL-MEYER FLOW

The final type of flow to be considered is two-dimensional isentropic flow, shown in figure 11-9. The changes across shock waves in supersonic flow are very abrupt and

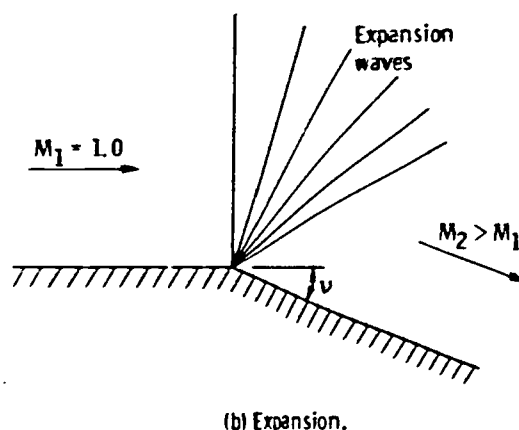
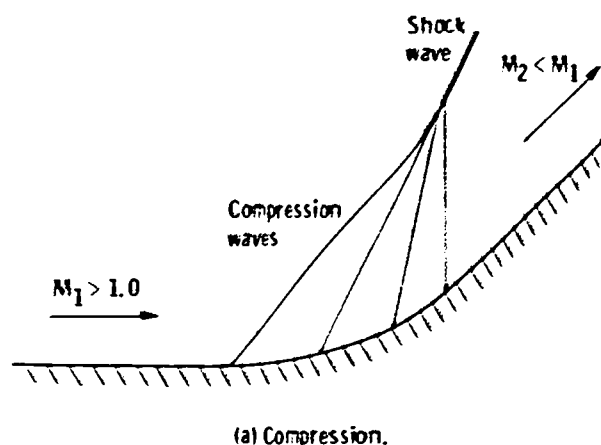


Figure 11-9. - Two-dimensional, isentropic, Prandtl-Meyer flow.

inefficient. However, gradual changes in supersonic flow can be made with 100 percent efficiency by means of a Prandtl-Meyer flow. In this type of flow, an infinite number of extremely weak sound waves are used to compress or expand and turn the flow.

For compression, the wall is turned gradually into the flow (fig. 11-9(a)), thereby creating a series of waves which turn and compress the flow. Wave angles steepen as the Mach number decreases, and the waves eventually coalesce into a single shock wave. For supersonic expansion, the wall is turned away from the flow (fig. 11-9(b)), thereby increasing the flow area in the duct and increasing the supersonic Mach number. As the Mach number increases, the wave angles become lower, and the expansion waves spread out in a fan and never coalesce as they do for a compression. Therefore, most expansions in supersonic flow are 100 percent efficient. For supersonic compression, however, the wall curvature (fig. 11-9(a)) must be carefully designed to prevent the compression waves from coalescing into a strong, highly inefficient shock wave.

For a Prandtl-Meyer expansion of a sonic flow, $M_1 = 1.0$ (fig. 11-9(b)), any specific expansion to an angle ν produces some specific Mach number M_2 downstream of the expansion. The relation between Mach number and the Prandtl-Meyer angle ν is shown in figure 11-10 (where $\nu = 0$ for Mach 1.0).

Since expansion or compression in a Prandtl-Meyer flow is 100 percent efficient, figure 11-10 can be used to determine Mach number or angle for either expansion or compression. Prandtl-Meyer relations can be used to describe and define the stream-

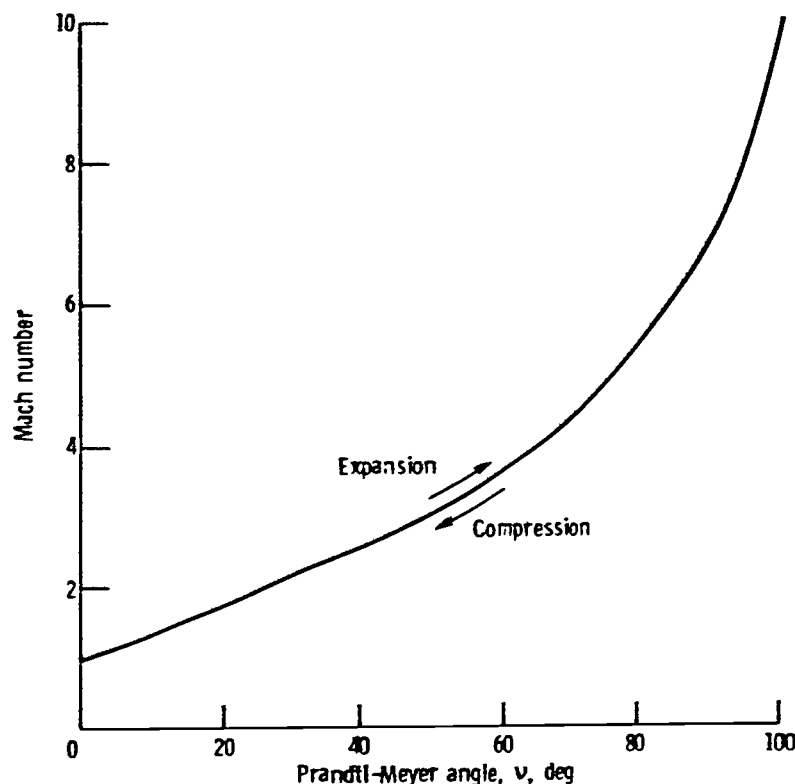


Figure 11-10. - Variation of Mach number with Prandtl-Meyer angle.

lines of flow expanding or turning around a sharp corner. For expansion, the resulting Mach number or the necessary angle can be determined by following the curve upward from the point representing the initial flow conditions to the point representing the final conditions. For compression, the Mach number or the angle can be determined by following the curve downward. For example, if the initial flow is at Mach 2.0 ($\nu = 27^\circ$) and the flow is expanded through an angle of 23° , the final Mach number will be 3.0 ($\nu = 27^\circ + 23^\circ = 50^\circ$). If the initial flow is at Mach 2.0 ($\nu = 27^\circ$) and the flow is compressed by an angle of 13° , the final Mach number will be 1.5 ($\nu = 27^\circ - 13^\circ = 14^\circ$).

CONCLUDING REMARKS

When the speed of an object is so high that sound waves, or extremely weak pressure waves, can no longer propagate ahead of the object, the flow is supersonic. To deflect the flow around a body at supersonic speeds, shock waves with a finite pressure rise across them are required. These waves can travel faster than sound, and their velocity increases as the pressure ratio across them increases. In general, expansion in supersonic flow is 100 percent efficient. Supersonic compression can be 100 percent efficient if it is done gradually. But the weak compression waves tend to coalesce into strong shock waves, which become inefficient.

REFERENCE

1. Ames Research Staff: Equations, Tables, and Charts for Compressible Flow. NACA Rep. 1135, 1953.

12. SUPERSONIC AIRCRAFT

James F. Dugan, Jr. *

To introduce supersonic aircraft, we will begin with current commercial jet aircraft and consider why they do not fly faster than about Mach 0.8. We will learn that the reason lies in an airflow phenomenon called transonic drag rise. We will see that shock waves, which are normally associated with speeds greater than Mach 1, are the cause of this transonic drag rise.

Next, we will consider an early military supersonic airplane that attempted to overcome the transonic drag rise and almost failed. We will learn that area ruling, or shaping the fuselage to resemble a Coke bottle, actually salvaged the airplane and was responsible for the F-102's going into production. This and other advances in supersonic aerodynamics and advances in high-thrust, low-weight jet engines led first to military airplanes that flew faster than Mach 2 and eventually to an operational reconnaissance airplane that flies faster than Mach 3.

These advances in military supersonic aircraft paved the way for the current effort to bring a commercial supersonic airplane into being. We will consider briefly the supersonic transports of the Russians, the British-French team, and the Americans. Finally, we will consider sonic boom: what it is, why it is such a problem, and how the sonic-boom problem is being handled in the proposed first generation of supersonic transports.

TRANSONIC DRAG RISE

The current subsonic commercial airplanes cruise at about Mach 0.8. Flying faster is attractive to the passenger, since it shortens his travel time. Flying faster is also attractive to the airlines, since it enables them to use their expensive airplanes more effectively and thus make more money. However, the cruise speed is limited to about Mach 0.8 by the sharp increase in airplane drag as Mach 1.0 is approached.

This drag increase is illustrated in figure 12-1, not for a complete airplane, but for a wing with a circular-arc airfoil. However, all wetted surfaces of the aircraft exhibit

*Head, Propulsion Section, Advanced Systems Division.

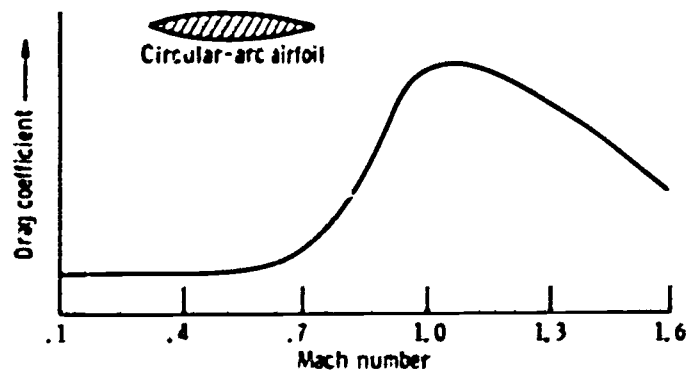


Figure 12-1. - Transonic pressure-drag rise of wing with circular-arc airfoil.

the trend of a high rise in drag as Mach 1.0 is approached. The peak drag occurs at, or just past, Mach 1.0. At higher speeds, drag decreases again, but not to the low levels characteristic of subsonic speed.

These changes in drag near Mach 1 are related to the formation of shock waves. These shock waves are shown in figure 12-2. Consider first the airflow over the wing when the airplane is flying at Mach 0.7. The local speed at the airfoil midspan can reach Mach 1.0, so that standing shock waves form above and below the airfoil and cause an increase in drag. When the airplane flies somewhat faster than Mach 1.0, a bow wave exists upstream of the airfoil leading edge and a pair of oblique shock waves exist at the trailing edge. With such a flow, drag is at maximum. At faster airplane speeds, like Mach 1.3, pairs of oblique shock waves are attached to the leading and trailing edges. Drag is below the maximum value, but still high because of the pressures induced on the wing surface by the oblique shock waves.

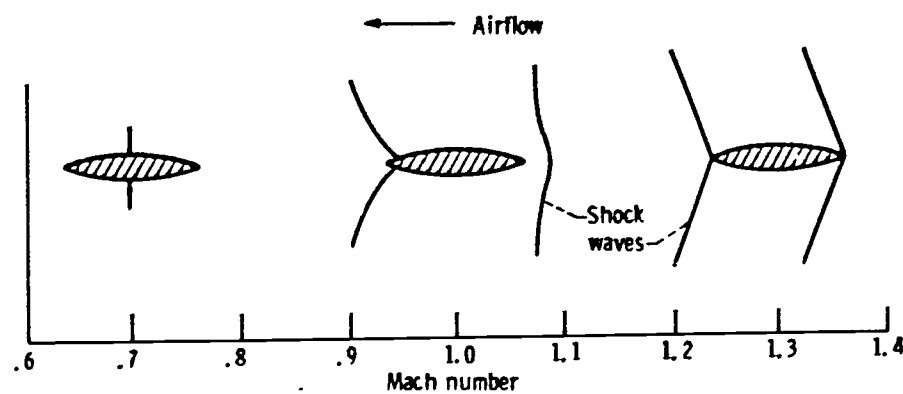


Figure 12-2. - Evolution of shock waves.

AREA RULE

The world's first supersonic all-weather interceptor, the Convair F-102 Delta Dagger, is shown in figure 12-3. In an attempt to meet the U.S. Air Force requirement for a supersonic interceptor, Convair scaled up an earlier configuration with a pure delta-wing planform. Early flight tests showed that even with a high-thrust turbojet engine this aircraft could not achieve supersonic speeds, because of high drag. The whole program was on the verge of being cancelled, but it was rescued by the application of the area-rule theory to the design of the aircraft.

This important theory was developed and verified by Richard Whitcomb, of the NASA Langley Research Center. Simply stated, the rule says that minimum supersonic drag is obtained when the individual airplane components (such as wing, tail, and fuselage) are configured so that a plot of cross-sectional area of the total airplane versus distance along the longitudinal axis of the airplane results in a smooth curve. This usually results in a "Coke-bottle" shape for the fuselage.

When Convair applied this area-rule theory to the F-102, they not only redesigned the fuselage to get the right Coke-bottle shape but also added bulges aft of the wing on each side of the tail pipe to give better area-rule distribution. The bulges can be seen in figure 12-3. These major modifications allowed the airplane to fly supersonically. The F-102 became operational in 1956, and a large number went into service with the U.S. Air Force.

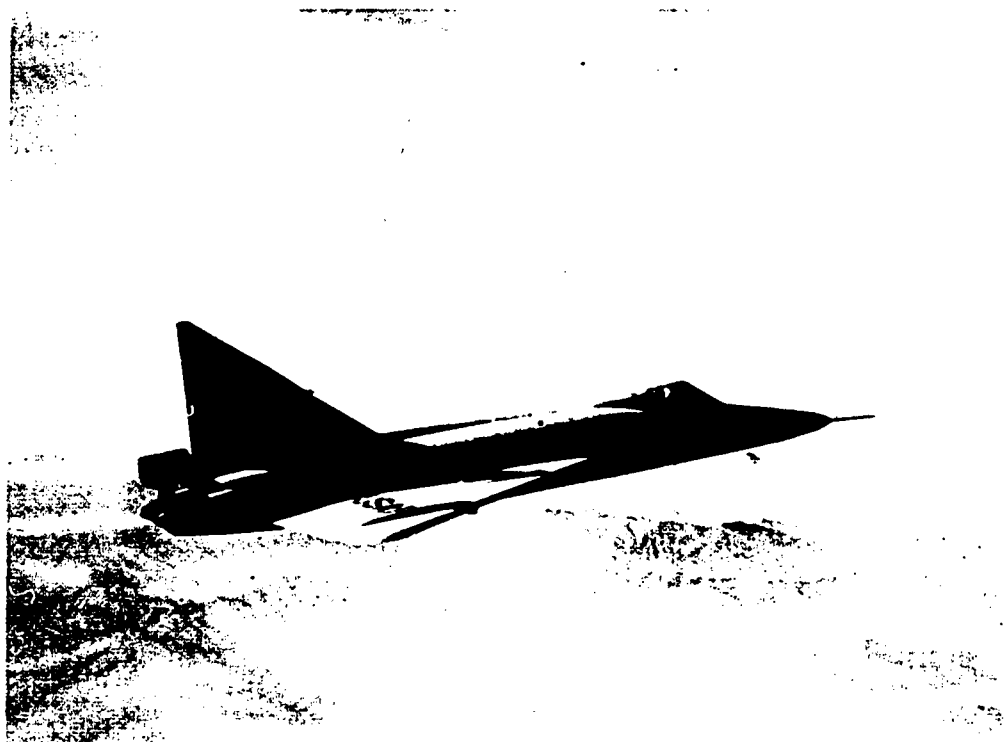


Figure 12-3. - Convair F-102 Delta Dagger Interceptor.

The area rule affects the pressure drag (not friction drag) and applies only at transonic and supersonic speeds. The cross-sectional area of the aircraft is obtained from imaginary slices cut through the aircraft, crosswise to its longitudinal axis. These area slices are inclined to the relative-wind direction at an angle equal to the Mach angle, because the wetted surface of the aircraft behaves as if it were subjected to a flow having the magnitude and direction of the velocity component normal to the Mach line. For aircraft speeds only slightly above sonic speed (e.g., Mach 1.2), the Mach angle is approximately 90° ; therefore, the cross-sectional slices are taken approximately normal to the relative-wind direction. As the aircraft speed increases, the Mach angle decreases, and the area slices are inclined to the relative-wind direction.

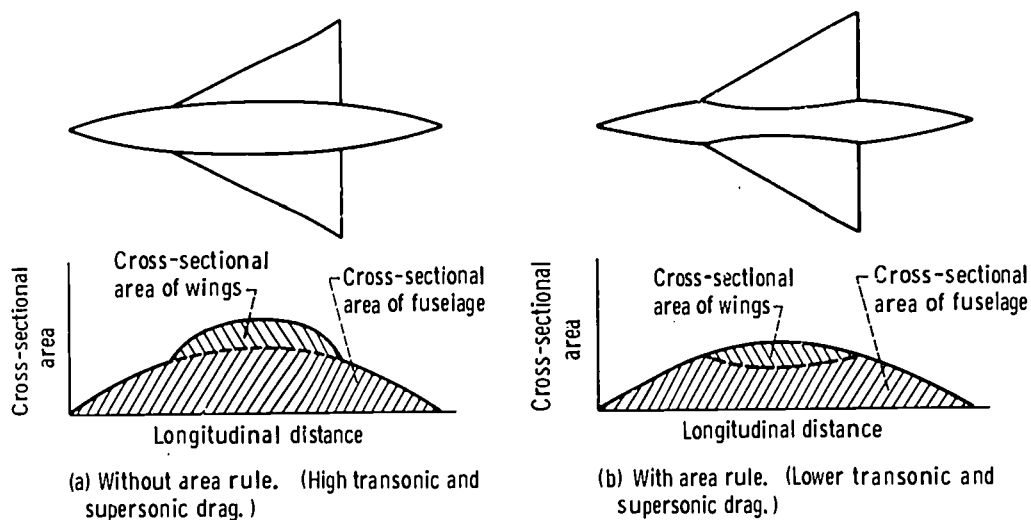


Figure 12-4. - Application of area rule to aircraft configuration.

Figure 12-4(a) shows a simplified airplane consisting of a streamlined fuselage and a delta wing. If cross-sectional area is plotted against length for this airplane, a bulge appears in the curve. This bulge represents the cross-sectional area of the wing. Since the area variation with length is not a smooth curve, the pressure drag of this airplane at transonic and supersonic speeds is high. Figure 12-4(b) shows a similar airplane, but with a fuselage that is narrowed where the wing is joined to it. The variation of cross-sectional area with length for this airplane is smooth. Therefore, the pressure drag of this airplane at transonic and supersonic speeds is lower than that of the previous example.

Figure 12-5 shows how this reduction in drag comes about. The pressure field produced by supersonic flow over the wing alone is shown in figure 12-5(a). The compressive turning of the supersonic flow by the forward-facing surfaces of the wing produces above-ambient pressures, indicated by "plus" signs. Expansion of the flow over the

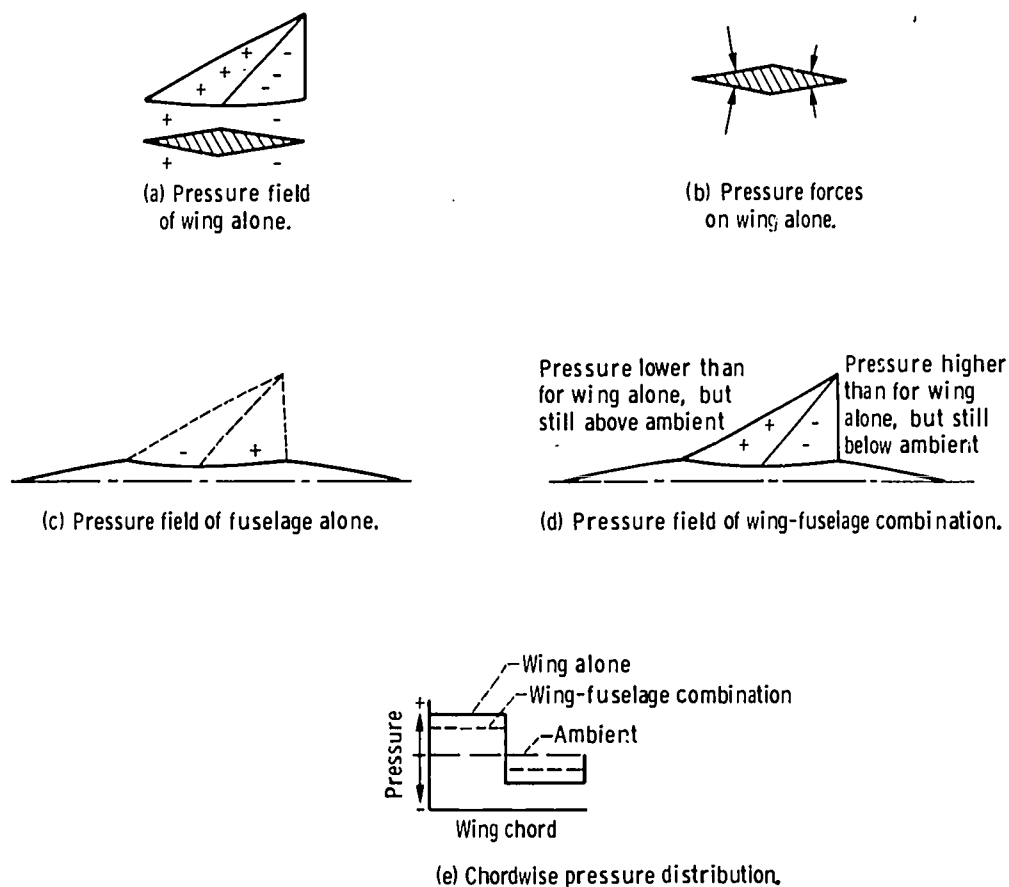


Figure 12-5. - Favorable pressure interference to reduce wing drag.

aft-facing surfaces produces below-ambient pressures, indicated by "minus" signs. (Compression and expansion of supersonic flow are discussed in chapter 11.)

Figure 12-5(b) shows the pressure forces acting on the wing surfaces. When these forces are summed in the lift and drag directions, the resultant lift force is zero, but there is a resultant drag force. Obviously, if the difference between the pressure forces on the forward-facing surfaces and those on the aft-facing surfaces were reduced, the resultant drag would also be reduced.

The indented fuselage alone is shown in figure 12-5(c). At the leading edge of the indentation, the supersonic flow expands around the corner and produces below-ambient pressures (minus signs) over the forward half of the indentation. The compressive turning of the supersonic flow over the rear half of the indentation produces above-ambient pressures (plus signs).

When the wing and fuselage are joined, their pressure fields combine. Thus, for the wing-fuselage combination (fig. 12-5(d)) the pressures on the forward-facing surfaces of the wing are lower and the pressures on the aft-facing surfaces are higher than for the wing alone. The pressure distribution along a wing chord line is shown in figure 12-5(e). The solid curve is for the wing alone and indicates a pressure above ambient (+) acting on the forward-facing wing surfaces and a pressure below ambient (-) on

the aft-facing wing surfaces. The dashed curve in the figure is for the wing-fuselage combination. The low pressures contributed by the forward half of the fuselage indentation have lowered the pressures on the front half of the wing. The high pressures contributed by the rear half of the fuselage indentation have raised the pressures on the rear half of the wing. Therefore, the difference between the pressures on the front half and those on the rear half of the wing is reduced, and the resultant drag force on the wing is also reduced.

In this simplified explanation of the area rule, we have only considered the effect of the rule on the pressure drag of the wing. However, in the design of an actual airplane, the area rule is applied so as to reduce the overall pressure drag of the entire airplane.

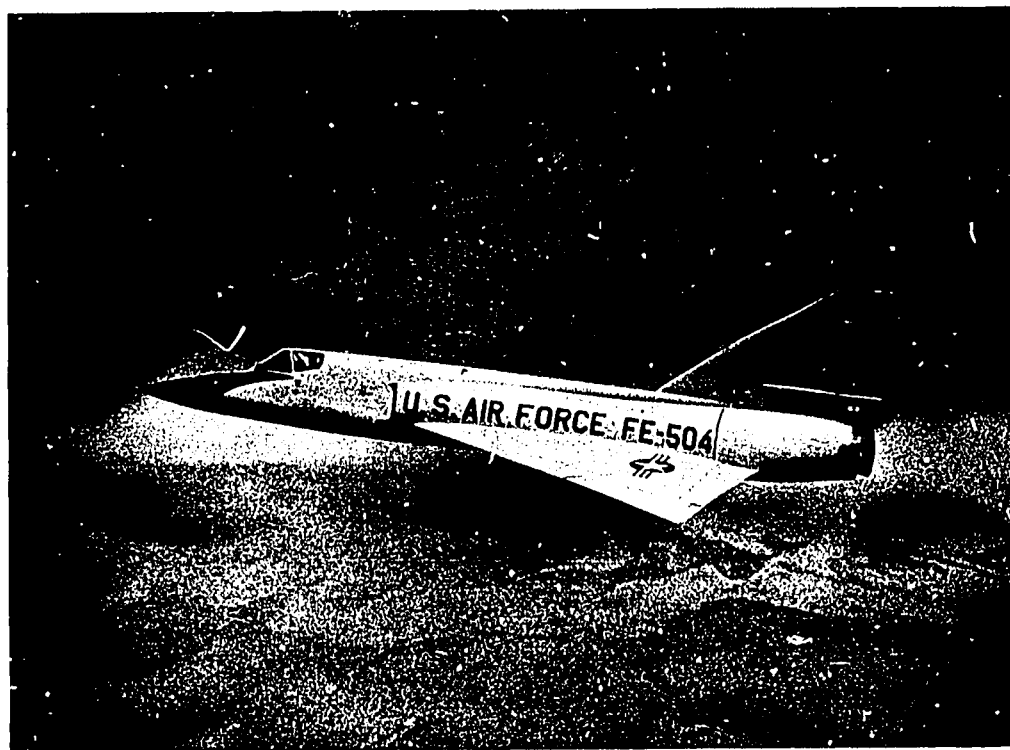


Figure 12-6. - Convair F-106 Delta Dart interceptor.

The Convair F-106 Delta Dart, the successor to the F-102, is shown in figure 12-6. The fuselage of the F-106 is enlarged, and the area rule is incorporated in a much more subtle manner. The prominent bulges on the aft fuselage have disappeared. The engine intakes are much larger than those on the F-102 and are located farther aft, near the wing root. To meet engine airflow requirements efficiently, the intakes must incorporate variable geometry to cover the greater speed range of the airplane. The top speed of the F-106 is Mach 2.3, while that of the F-102 is Mach 1.25. The F-106 became operational in 1959, but today it is still the backbone of the USAF Air Defense Command.

ADVANCED MILITARY AIRCRAFT

A much publicized and very controversial new airplane is shown in figure 12-7. It was known as the TFX during the time when its future and who was to build it were being hotly debated. It is now known as the F-111 and is built by General Dynamics. Designed for a top speed of Mach 2.5, the F-111 is to be used for a variety of roles, such as tactical strikes, interception, reconnaissance, and strategic bombing. To achieve this

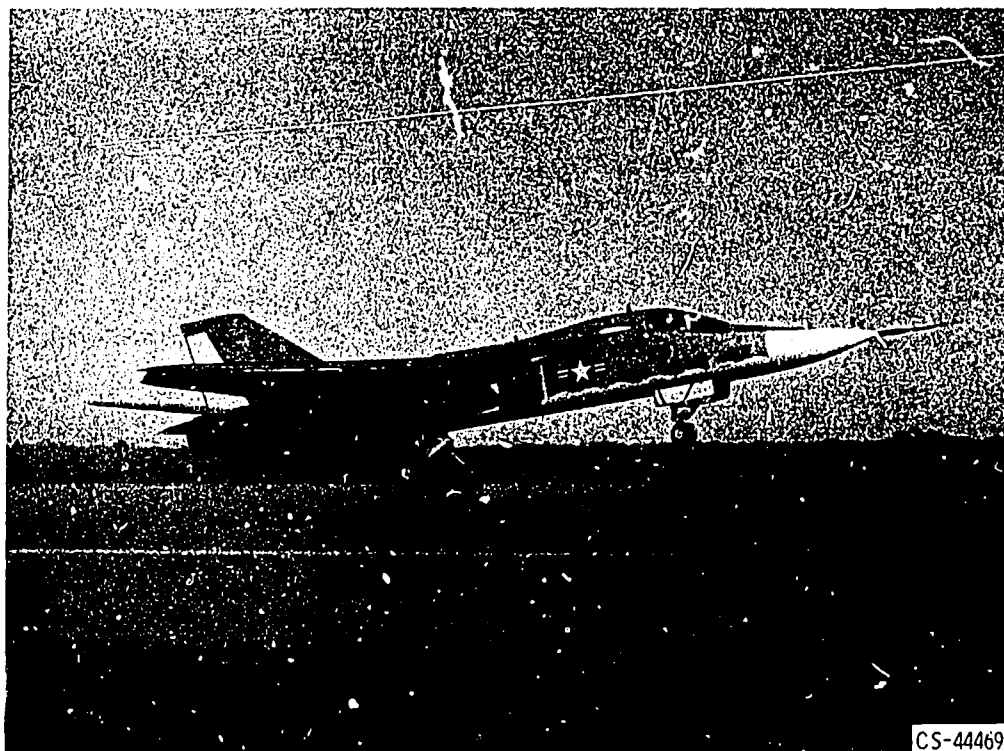


Figure 12-7. - General Dynamics F-111A fighter.

multimission capability, the F-111 makes use of a movable wing, the sweep angle of which can be varied. On supersonic missions, the sweep is great, and the airplane resembles the F-106 of figure 12-6. On subsonic missions and during takeoff and landing, the sweep of the F-111's wing is moderate.

The United States has achieved sustained Mach 3 flight with three airplanes: the North American XB-70, the Lockheed YF-12, and the Lockheed SR-71. The XB-70, shown in figure 12-8, was originally slated for a strategic bombing role. When the airplane is cruising at high Mach numbers, the shock waves arising from the large wedge-shaped engine box beneath the airplane create high pressures, or lifting forces, on the bottom surface of the wing. This was the first airplane designed to exploit the principle of interference, or compression, lift.

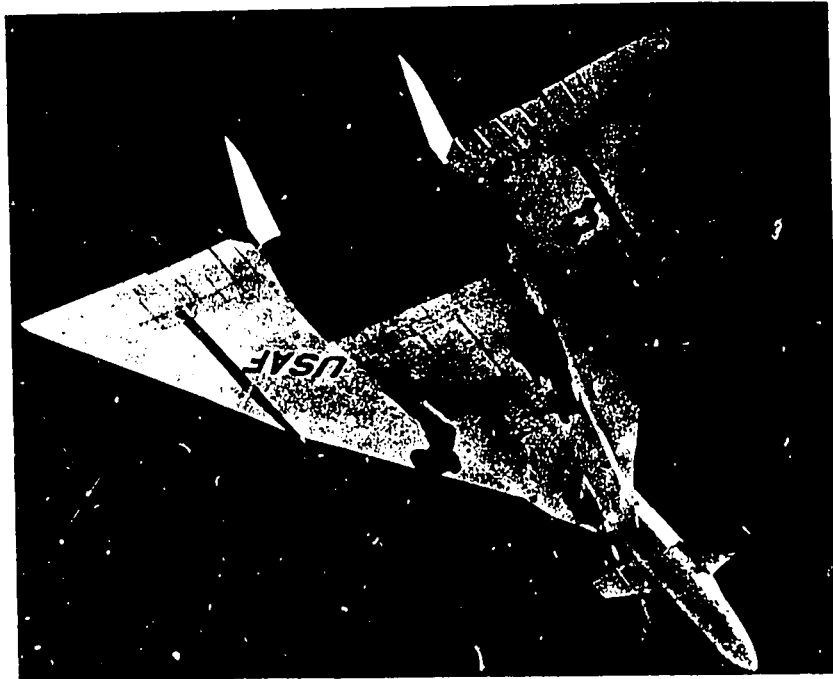


Figure 12-8. - North American XB-70. (Reprinted from Shell Aviation News, No. 318, 1964, with their permission.)

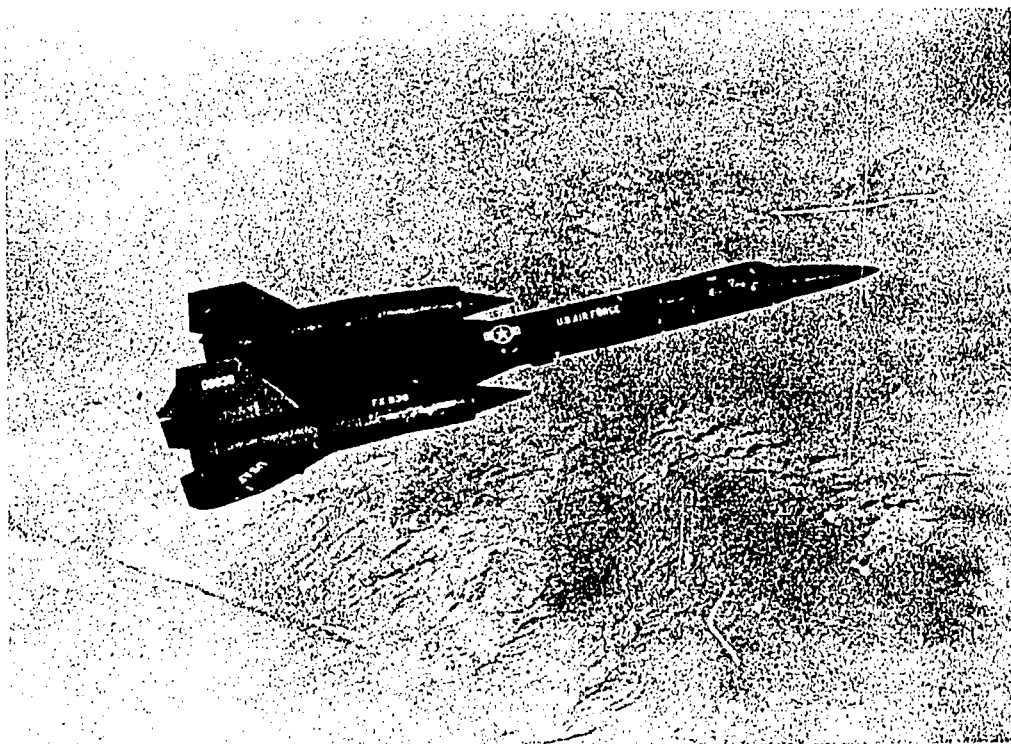


Figure 12-9. - Lockheed YF-12A.

The YF-12A, shown in figure 12-9, is a prototype Mach 3 interceptor. It had the most secret development of any airplane in American history, with the exception of its subsonic predecessor, the U-2. As an advanced experimental jet aircraft, the YF-12 has been tested in sustained flight at more than 2000 miles per hour and at altitudes in excess of 70 000 feet. Its structure is primarily titanium, to withstand the very high environmental temperatures associated with Mach 3 flight.

The SR-71, which resembles the YF-12, is a strategic reconnaissance version of the YF-12. Its nose fairing is different, and the fuselage is longer. The SR-71 has gone into service with the Strategic Air Command. It is equipped with the most advanced observational equipment in the world, which enables it to cover with its reconnaissance "eyes" an area of 60 000 square miles in one hour.

PROPOSED COMMERCIAL AIRCRAFT

Although supersonic airplanes have been in military service for many years, they have not yet been introduced into commercial service. However, three commercial supersonic transports are under development - the Tupolev Tu-144 (Russian), the BAC-Sud Concorde (British-French), and the Boeing supersonic transport (American). Before discussing these airplanes, we will consider why commercial supersonic aircraft are of interest. To the passenger, there is the attraction of much shorter flight times. For example, the supersonic-transport flight time from Chicago to London (4000 statute miles) would be about $2\frac{1}{2}$ hours, as compared to about $8\frac{1}{2}$ hours for the advanced subsonic transports. The airlines and airplane builders are, of course, motivated by the profit potential, which is greatly influenced by currently proven technology in aerodynamics, structures, and propulsion.

Consider first the status of technology in supersonic aerodynamics. Although techniques like the application of the area rule help keep supersonic drag down, the attainable lift-to-drag ratio (aerodynamic efficiency) at supersonic speeds is much lower than that at subsonic speeds, as indicated in figure 12-10. The lift-to-drag ratio is high around Mach 0.8 but drops sharply in the region around Mach 1, because of the onset of shock losses. After the steep drop, the lift-to-drag ratio tends to level off, but continues to decrease gradually as cruise speed increases. This trend is discouraging, but not hopeless, because airplane performance is affected by other factors.

Range is an important consideration in the evaluation of airplane performance. The equation for airplane range is

$$\text{Range} \approx k \frac{L}{D} \frac{M}{\text{sfc}} \log \frac{w_g}{w_s + w_p}$$

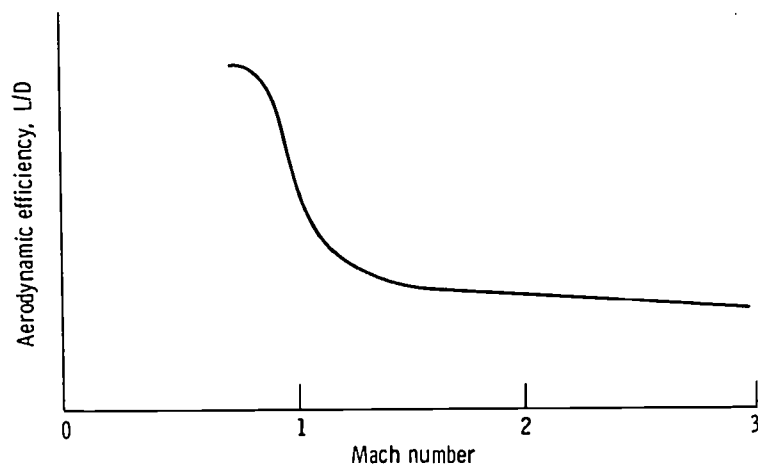


Figure 12-10. - Variation of aerodynamic efficiency with Mach number.

where

k constant

L lift

D drag

M Mach number

sfc specific fuel consumption (amount of fuel used per hour per pound of thrust)

w_g gross weight of airplane

w_s structural weight of airplane

w_p payload weight

The ratio of Mach number to engine specific fuel consumption M/sfc is a measure of engine efficiency. If w_g , w_s , and w_p are fixed, the airplane range will increase as the product of aerodynamic efficiency L/D and engine efficiency M/sfc increases. Fortunately, the efficiency of a gas-turbine engine increases with cruise speed, as shown in figure 12-11. (The curves in fig. 12-11 are intended to show only the general trends of the efficiency variations with Mach number. The curves do not reflect the relative levels, or the relative values, of the three efficiencies.)

The variation of lift-to-drag ratio, or aerodynamic efficiency, with Mach number is repeated in this figure. The overall-efficiency curve represents simply the product of aerodynamic efficiency and engine efficiency. Overall efficiency is high at Mach 0.8, the speed at which current jet transports operate. The efficiency drops at around Mach 1 and then begins to climb. Beyond Mach 2, the overall airplane efficiency is approaching the level attained by current subsonic jets. The choice of a specific cruise Mach number above 2 is largely dependent on the structural materials used for the airframe.

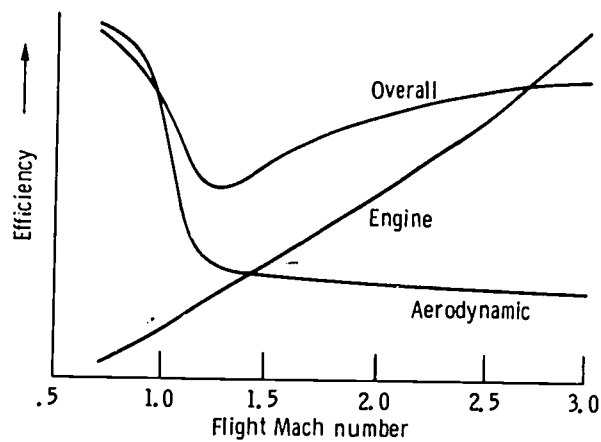


Figure 12-11. - Variation of aerodynamic, engine, and overall efficiencies with flight Mach number. (The curves show only the general trends of the efficiency variations with Mach number and do not reflect the relative levels of the three efficiencies.)

Figure 12-12 shows the variation of structural efficiency with Mach number for titanium and aluminum. The structural efficiency is measured by the ratio of the tensile strength of the material to its density. High ratios result in lightweight structures, which can provide higher airplane performance in terms of longer range or greater payload (in accordance with the range equation). The current subsonic jets that operate at about Mach 0.8 use aluminum as the primary airframe structural material. Aluminum can be used at higher speeds, but somewhat beyond Mach 2 the structural efficiency decreases rapidly to an unacceptably low level. The structural efficiency of titanium is

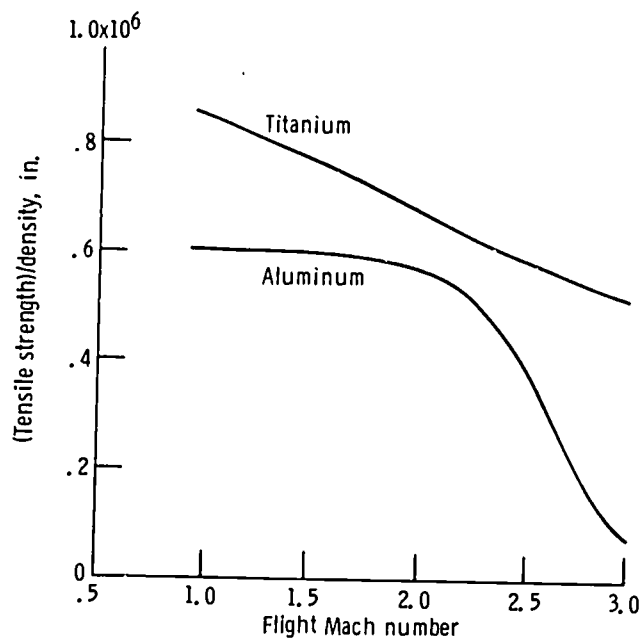


Figure 12-12. - Variation of structural efficiency ((tensile strength)/density) of titanium and aluminum with flight Mach number (speed).

appreciably higher than that of aluminum. Therefore, titanium seems to be a desirable structural material even for subsonic airplanes. However, the technology of using titanium is relatively new.

The Russian supersonic transport (fig. 12-13) is designed for a cruise Mach number of 2.35, and its prime structural material is aluminum. The British-French supersonic transport (fig. 12-14) also uses aluminum as the structural material and is designed for a cruise Mach number of 2.2. The American supersonic transport (fig. 12-15) is being designed for a cruise Mach number of 2.7, and titanium will be used as its prime structural material.



Figure 12-13. - Russian supersonic transport, Tupolev Tu-144. (Reprinted from Life, March 14, 1969, with their permission.)

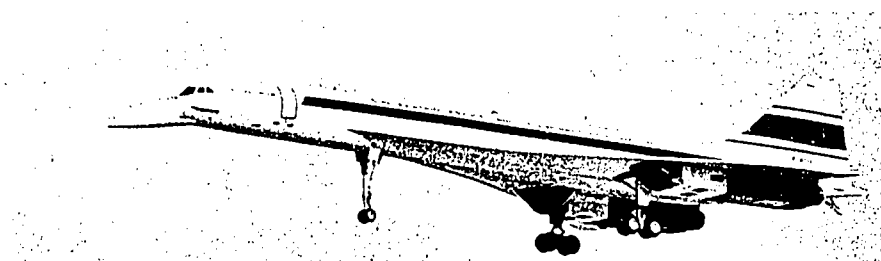


Figure 12-14. - British-French supersonic transport, BAC-Sud Concorde. (Taken from Aviation Week & Space Technology, March 17, 1969, with their permission.)

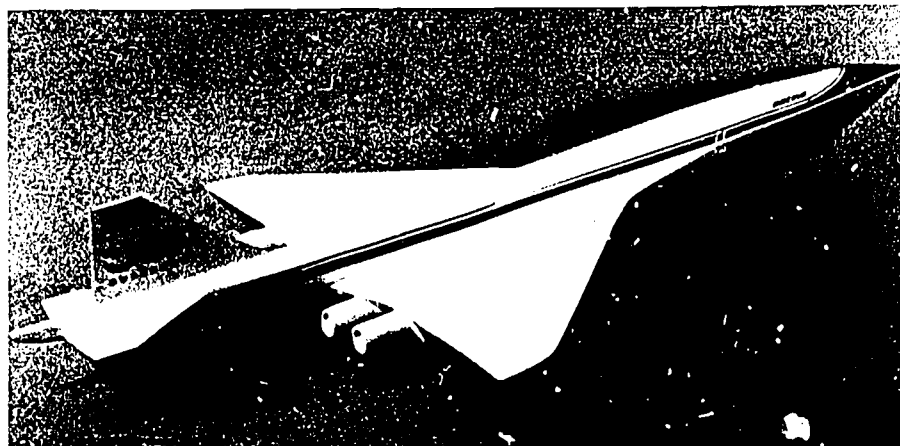


Figure 12-15. - Model of proposed American supersonic transport, Boeing design. (Reprinted from Interavia, January 1969, with their permission.)

SONIC BOOM

Whenever an airplane is flying at supersonic speed, shock waves are attached to the airplane and extend all the way to the Earth's surface, where they are reflected upward toward the sky (fig. 12-16). The variation in air pressure, shown at the bottom of the figure, indicates that there is an abrupt rise in pressure (overpressure) above ambient when the first shock wave passes. Then the pressure decreases to a value below ambient. When the trailing shock wave passes, there is a second abrupt pressure rise back to ambient. Sometimes a double boom can be heard, but generally the wave length and the time increment are so short that only a single boom is heard. The magnitude of the boom is described by quoting the change in pressure or overpressure, in pounds per square foot.

The relation of sonic boom level to probable public reaction is shown in table 12-I. Sonic booms in the range of 0.2 to 1.0 pound per square foot overpressure sound like distant thunder and would probably be acceptable. To achieve such a level of sonic boom, the gross weight of the airplane (and, hence, lift) would have to be low and the altitude for supersonic operation high. Low weight and high altitude both reduce sonic-boom intensity. Estimates based on current airframe and engine technologies indicate that a supersonic transport compatible with a sonic-boom level of 0.8 pound per square foot would have to be so small that it could carry only one or two dozen passengers. The passengers might be satisfied and the people on the ground might not object to the boom,

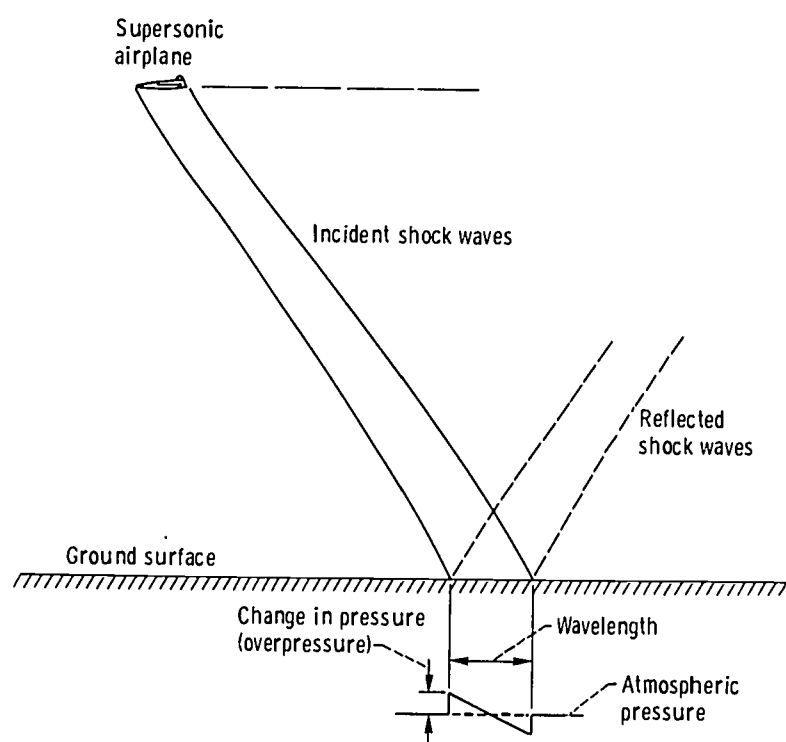


Figure 12-16. - Sonic boom of a supersonic airplane.

TABLE 12-1. - SONIC-BOOM GROUND EFFECTS

| Sonic-boom overpressure at ground level, lb/ft ² | Property damage | Comparable sound | Public reaction |
|---|--|----------------------------------|---------------------|
| 0.2 to 1.0 | No damage | Distant thunder | Probably acceptable |
| 1.5 to 2.0 | No damage to ground structures | Loud thunder | Not acceptable |
| 2.5 to 3.0 | Possible damage to windows and plaster | Close-range thunder or explosion | Intolerable |

but the airlines would not be able to make any money. Large supersonic airplanes, carrying hundreds of passengers, are required if the airlines are to make a reasonable profit.

The supersonic transports being planned will give rise to sonic booms in the upper range of values. Furthermore, atmospheric conditions, which cannot be controlled, can magnify sonic booms. Therefore, boom levels of 3.0 pounds per square foot and above can be anticipated during a certain number of flights. Booms of this magnitude are intolerable and can damage windows and plaster. Because of this sonic-boom problem, the first generation of supersonic transports is scheduled to service only the prime trans-oceanic routes. Thus, for the time being, the problem will only be sidestepped rather than solved.

13. MEASUREMENTS IN AERONAUTICAL RESEARCH

Clarence C. Gettelman*

From measurements of pressure, temperature, mass flow rate, and thrust, the performance of an aircraft, an airfoil, an engine, a compressor, or a turbine can be determined. To describe the performance of a wing, compressor or turbine blade, we are interested in the lift and drag under conditions of use. We must also know the velocity or Mach number of an aircraft or air in a wind tunnel. We may want to know the Reynolds number (ratio of the inertia force of the fluid to the viscous force of the fluid). The significances of these and other characteristics are discussed in preceding chapters. Let us examine these characteristics and how they are obtained from measured quantities.

The velocity of a fluid with respect to a body in the fluid is determined by measuring the pressure due to the motion of the fluid. This pressure, designated ΔP , is the difference between the total pressure P_t and the static pressure P_s . (These three pressures are discussed in greater detail in the next section.)

$$\Delta P = P_t - P_s \quad (\text{lb/ft}^2) \quad (1)$$

For an incompressible fluid, the pressure due to the motion of the fluid is

$$\Delta P = \frac{1}{2} \rho V^2 \quad (2)$$

where

ρ mass density of fluid, w/g, $\text{lb-sec}^2/\text{ft}^4$

w specific weight of fluid, lb/ft^3

g acceleration due to gravity, ft/sec^2

V velocity of fluid flow, ft/sec

The mass density ρ for a gas (e. g., air) is a function of static pressure and static temperature according to the equation

*Chief, Instrument Systems Research Branch.

$$\rho = \frac{P_s}{gRT_s} \quad (3)$$

where

R specific gas constant, (ft-lb)/(lb)(°R) (for air, 53.3)

T_s static temperature, °R

Equations (1) to (3) can be combined and solved for velocity V in terms of measurable quantities (ΔP, P_s, and T_s) and constants (g and R).

$$V = \sqrt{\frac{2\Delta P T_s}{P_s}} \cdot \sqrt{g} \cdot \sqrt{R} \quad (4)$$

For an incompressible fluid, the pressure ΔP due to the motion of the fluid is described by equation (2). For a compressible fluid, ΔP includes the compressibility effects and is described by the equation

$$\Delta P = \frac{1}{2} \rho V^2 \left(1 + \frac{M^2}{4} + \frac{2-k}{24} M^4 \dots \right) \quad (5)$$

where

M Mach number (dimensionless)

k $\frac{\text{Specific heat at constant pressure}}{\text{Specific heat at constant volume}}$ (dimensionless)

Air behaves as an incompressible fluid at low subsonic speeds and as a compressible fluid at high sonic and supersonic speeds. For example, at Mach 0.2 (subsonic speed) the compressibility effects increase the ΔP of air only about 1 percent above that of an incompressible fluid. Since the compressibility effects are so small, air may be considered as an incompressible fluid at low subsonic speeds. At Mach 1 (sonic speed), however, the compressibility effects increase the ΔP of air about 25 percent above that of an incompressible fluid. Therefore, at high sonic and supersonic speeds, air must be considered as a compressible fluid.

The preceding discussion has explained how two variables (velocity V and density ρ), which are not measured directly, can be determined from measurements of the pressure due to the motion of the fluid ΔP, the static pressure P_s, and the static temperature T_s.

Other variables, such as lift coefficient, drag coefficient, Reynolds number, and Mach number, are also not measured directly but are calculated from measurements of pressure, temperature, force, etc. Some of the devices used to make these measurements are discussed in the following sections.

PRESSURE

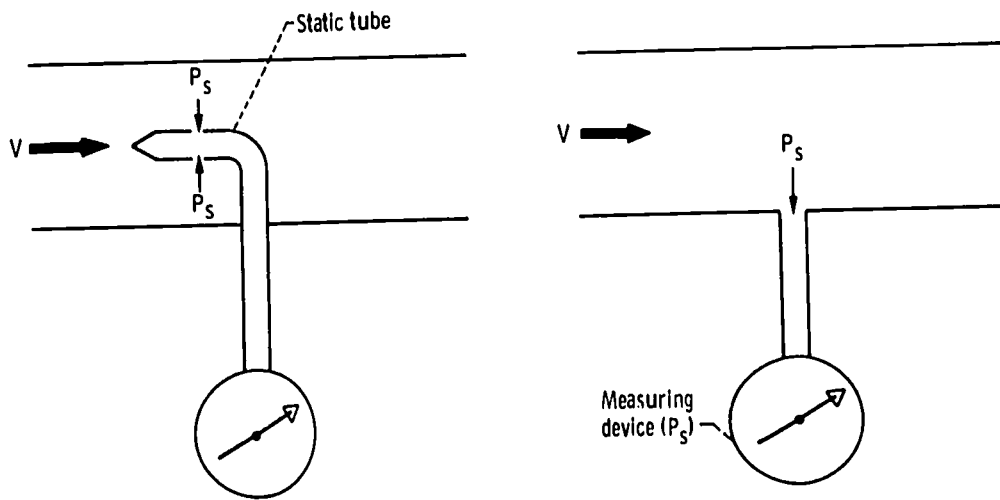
Sensing Devices

A moving fluid exhibits three kinds of pressure: static pressure P_s , total pressure P_t , and pressure due to the motion of the fluid ΔP . Before any of these pressures can be measured, some sensing device is required that will isolate and detect only that particular pressure which is to be measured. A pressure-sensing device is basically just a tube that is oriented in such a way that it senses one particular kind of pressure.

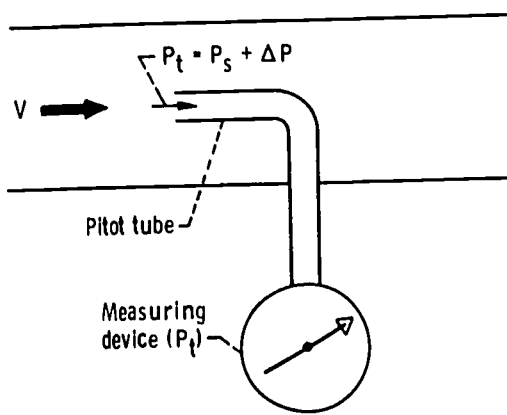
Static tube. - Static pressure P_s is the force per unit area that a fluid exerts on a surface that is at rest relative to the fluid. This pressure is due to the random motion of the fluid molecules. The static pressure of a flowing fluid is sensed by means of a static tube (fig. 13-1(a)). The tube is arranged so that the opening is facing perpendicular to the flow direction and is flush with a surface along which the fluid is flowing (i. e., a surface that is parallel with the direction of flow). Thus, the opening of the tube is oriented so that it is not subjected to impact or suction effects from the moving fluid. In effect, then, the static tube is at rest relative to the fluid and, therefore, senses only static pressure.

Pitot tube. - Total pressure P_t is the force per unit area that is exerted on a surface which is placed in the path of the flow (and perpendicular to the flow direction) so that it halts the flow. This pressure is due to both the inherent random motion of the fluid molecules and the ordered motion of the molecules in the direction of flow. Thus, total pressure P_t is the sum of the static pressure P_s and the pressure due to the motion of the fluid. Total pressure is sensed by means of a pitot tube (fig. 13-1(b)). This tube is arranged so that the open end of the tube protrudes into the fluid stream, and the opening faces upstream. Thus, the opening of the tube senses the pressure produced by the impact of the fluid stream against it.

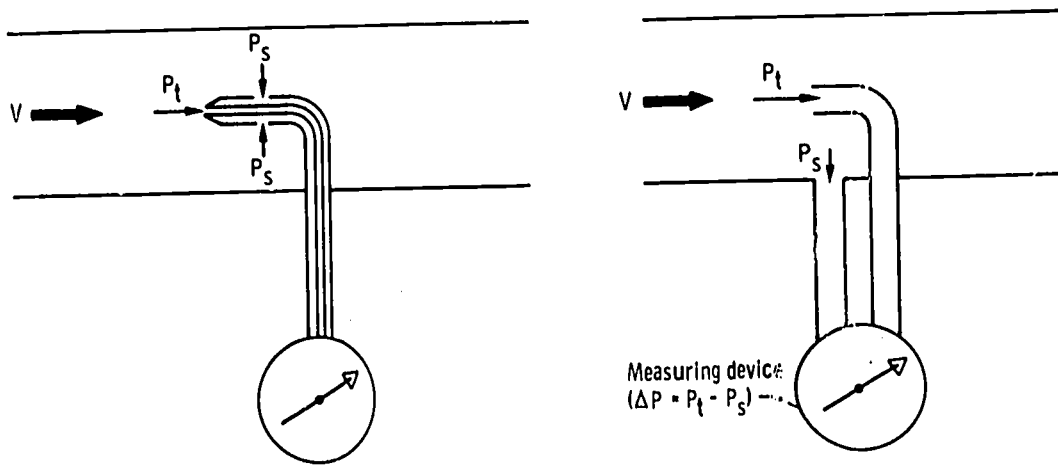
Pitot-static tube. - The pressure due to the motion of the fluid ΔP is the difference between the total pressure P_t and the static pressure P_s . This ΔP is obtained by means of a pitot-static tube (fig. 13-1(c)). This device does not actually sense ΔP . Instead, it simultaneously senses total pressure and static pressure. The difference between these two pressures can then be determined with the use of an appropriate measuring device.



(a) Static tubes.



(b) Pitot tube.



(c) Pitot-static tubes.

Figure 13-1. - Pressure-sensing devices.

Measuring Devices

The pressures of stationary and/or flowing fluids are normally measured with some type of pressure gage, such as a liquid-level manometer or a diaphragm pressure gage. A liquid-level manometer measures pressures of fluids by balancing the pressure against a column (in a tube) of a liquid that does not mix with the fluid whose pressure is being measured. A diaphragm pressure gage balances the pressure of the fluid against the elastic force of a spring or an elastic diaphragm. Both of these types of pressure gage can be designed to measure either differential pressure (i. e., the difference between two pressures) or absolute pressure (i. e., the pressure relative to zero pressure). For measuring the pressures of a flowing fluid, the pressure gage is used in combination with one of the pressure-sensing devices described in the preceding section.

Liquid-level manometer. - Figure 13-2 shows a liquid-level manometer designed to measure differential pressure (e. g., the pressure due to the motion of a fluid, ΔP). The two legs of the U-tube are subjected to two pressures P_1 and P_2 . If the two pressures are equal, the liquid level is the same in the two legs of the tube, as shown in figure 13-2(a). If the two pressures are different (e. g., $P_1 > P_2$), the difference between them ($P_1 - P_2$) causes the liquid in the tube to be displaced (fig. 13-2(b)) so that the liquid level is higher in that leg of the tube which has the lower pressure P_2 . The height of the liquid column is the vertical distance between the liquid levels in the two legs of the tube. The

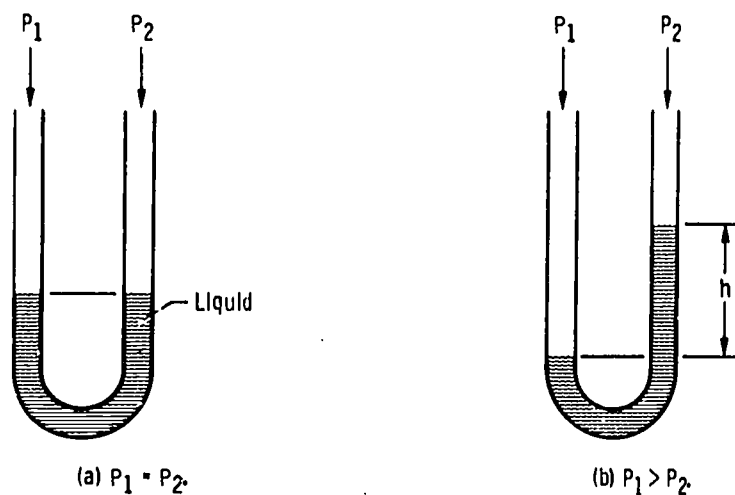


Figure 13-2. - Liquid-level manometer for measuring differential pressure.

basic equation for calculating the pressure indicated by a liquid-level manometer is

$$P_m = P_1 - P_2 = wh \quad (6)$$

where

P_m pressure difference indicated by manometer, lb/ft^2

P_1, P_2 pressures in the two legs of the tube

w specific weight of liquid, lb/ft^3

h height of liquid column, ft

Figure 13-3 shows a liquid-level manometer designed to measure absolute pressure (e. g., atmospheric pressure). In this instrument, one leg of the U-tube is sealed and evacuated to zero pressure P_2 . Thus, since P_2 is zero, the pressure indicated by the manometer ($P_1 - P_2$) is simply the absolute pressure P_1 .

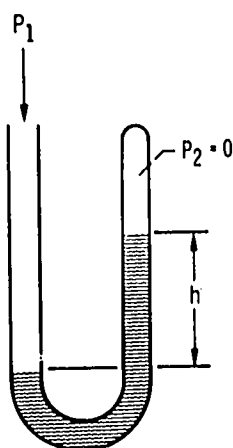


Figure 13-3. - Liquid-level manometer for measuring absolute pressure.

For any given pressure P_m indicated by a manometer, the magnitude of the displacement of the liquid (i. e., the liquid column height) depends on the specific weight of the liquid. The two liquids normally used are water and mercury, and pressure can be expressed as feet (or inches) of water or mercury. The specific weight of water is 62.4 pounds per cubic foot, while that of mercury is 846 pounds per cubic foot. Therefore, a column of water produced by a given P_m is 13.5 times as high as a column of mercury produced by the same P_m . Obviously, the greater the displacement of the liquid per unit of pressure, the easier it is to detect and measure small pressures. Therefore, a manometer that uses water is 13.5 times as sensitive as one that uses mercury.



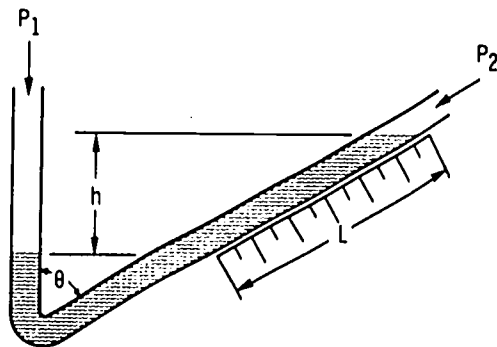


Figure 13-4. - Configuration for increasing sensitivity of liquid-level manometer.

Another method of increasing the sensitivity of a liquid-level manometer is illustrated in figure 13-4. Here the instrument is arranged so that the liquid is displaced at some angle θ relative to the vertical direction. Thus, the length of displacement L along the scale is an amplification of the height of the column h . The relation between h and L is given by the equation

$$h = L \cos \theta \quad (7)$$

Obviously, when θ is zero (i. e., when both legs of U-tube are vertical), cosine θ is 1, and L equals h . But as θ approaches 90° , cosine θ approaches zero, and L becomes larger than h .

Diaphragm pressure gage. - Figure 13-5 shows a diaphragm pressure gage designed to measure differential pressure. This instrument measures pressure by the deflection of an elastic diaphragm or spring element instead of a liquid. When the two pressures P_1 and P_2 are equal, the diaphragm is undeflected (fig. 13-5(a)). When the two pressures are different (e. g., $P_1 > P_2$), the differential pressure ($P_1 - P_2$) causes the diaphragm to deflect (fig. 13-5(b)) towards the chamber that has the lower pressure P_2 .

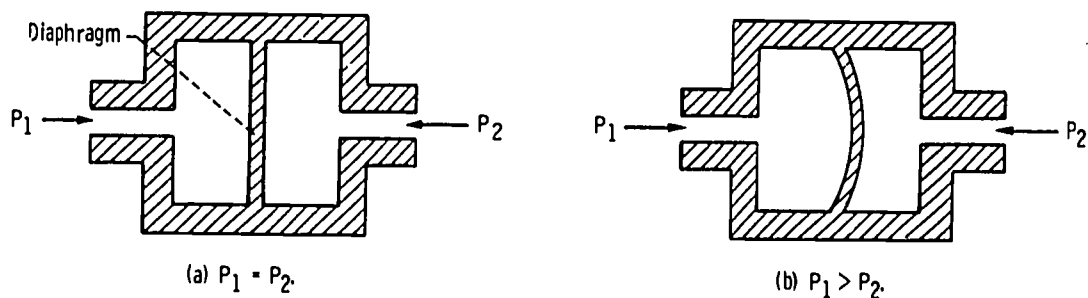


Figure 13-5. - Diaphragm pressure gage for measuring differential pressure.

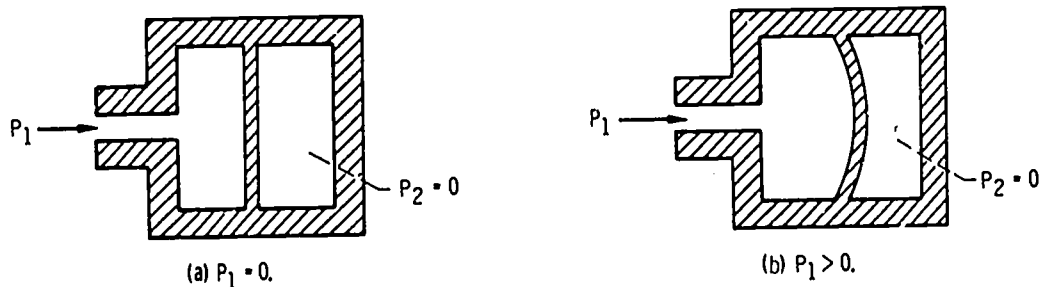


Figure 13-6. - Diaphragm pressure gage for measuring absolute pressure.

Figure 13-6 shows a diaphragm pressure gage designed to measure absolute pressure. In this instrument, one chamber is evacuated to zero pressure P_2 and sealed. Therefore, the pressure indicated by the deflection of the diaphragm ($P_1 - P_2$) is simply an absolute pressure P_1 .

Pressure can be determined from the deflection of the diaphragm of a pressure gage only if the instrument is properly calibrated against a liquid-level manometer or against some other pressure standard, and if the deflection can be measured accurately. Since the total range of deflection of the diaphragm is relatively small, the deflection is difficult to measure accurately by means of a scale. Therefore, the deflection of the diaphragm is commonly measured by means of a strain gage.

Strain Gage

A strain gage is a highly sensitive deflection-measuring device. It is not a pressure-measuring device, but it is used in some pressure gages to measure the deflection of the diaphragm. Then, the pressure that produces the deflection is determined from this measurement. Strain gages have many other applications, some of which are discussed later in this chapter.

A strain gage is basically a thin wire mounted on a surface in such a way that any deflection of the surface either stretches or compresses the wire. A current is passed through the wire and the resistance of the wire is measured to determine the deflection of the surface. The principle of the strain gage is that the resistance R of any given wire is directly proportional to its length L and inversely proportional to its cross-sectional area A .

$$R \propto \frac{L}{A} \quad (8)$$

If the wire is stretched, its length increases and its cross-sectional area decreases;

therefore, the resistance of the wire increases. If the wire is compressed, the effects are the opposite. Thus, the resistance of the wire is a measure of its deformation and of the deflection of the surface on which it is mounted.

Figure 13-7 shows how strain gages can be used to measure the deflection of the diaphragm in a pressure gage. Strain gages are bonded to both sides of the diaphragm. When the pressures P_1 and P_2 are equal and the diaphragm is undeflected (fig. 13-7(a)), the strain gages R_1 and R_2 have equal resistances. When the two pressures are un-

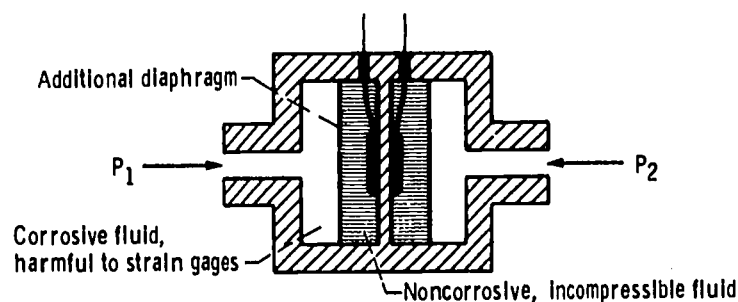
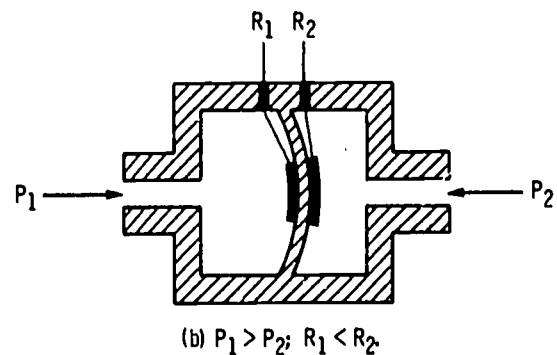
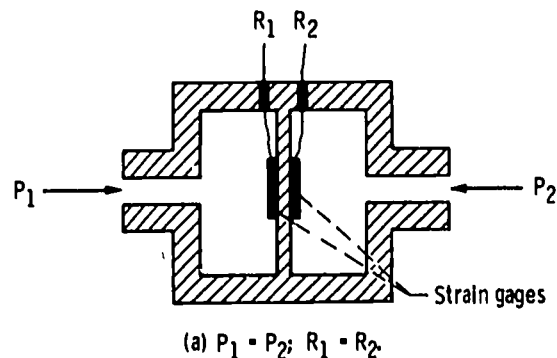
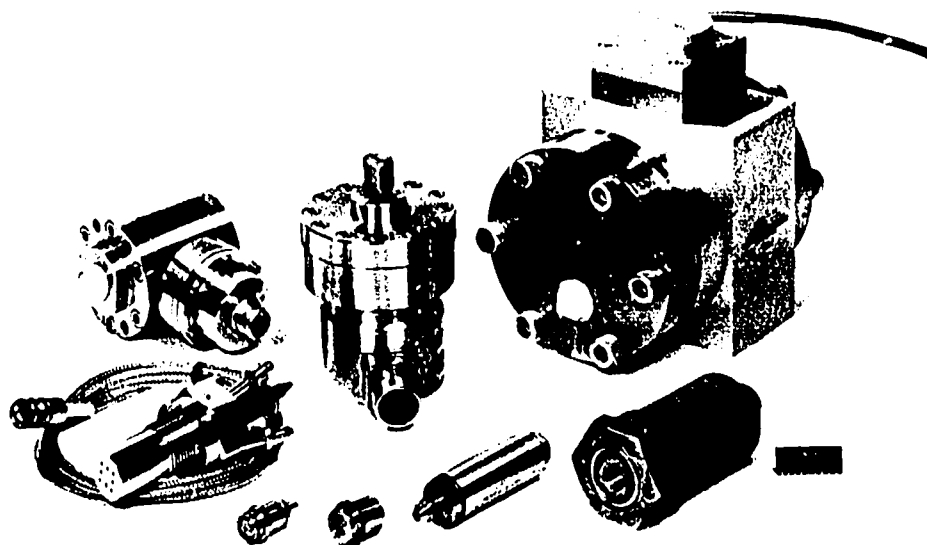


Figure 13-7. - Use of strain gages to measure deflection of diaphragm of pressure gage.

equal, the deflection of the diaphragm compresses one strain gage and stretches the other (fig. 13-7(b)). The resulting changes in the resistances of the strain gages indicate the extent of the deflection and, therefore, the magnitude of the pressure being measured. For pressure measurements of corrosive fluids, the strain gages can be protected by immersion in an incompressible, noncorrosive fluid contained within additional diaphragms, as shown in figure 13-7(c).

A few examples of commercially available diaphragm pressure gages equipped with strain gages are shown in figure 13-8. Many other pressure-measuring devices are available, and they range in price from about \$1 to about \$500. The price depends largely on the accuracy of the pressure gage.



CS-32134

Figure 13-8. - Examples of commercially available diaphragm pressure gages equipped with strain gages.

THRUST

The essential element of most thrust-measuring devices is a spring. When the spring is subjected to a thrust force, the deflection of the spring is a measure of the thrust. A good thrust-measuring spring is one that consistently deflects the same amount each time it is subjected to the same thrust force. Furthermore, the spring must maintain this consistency, or accuracy, over a reasonable range of temperatures.

A schematic diagram of a thrust-measuring spring is shown in figure 13-9. The solid line represents the outline of the spring before it is subjected to a force. When a thrust force F is applied to the spring in the compressive direction, the length of the spring decreases and the width increases, as indicated by the dashed line in the figure.

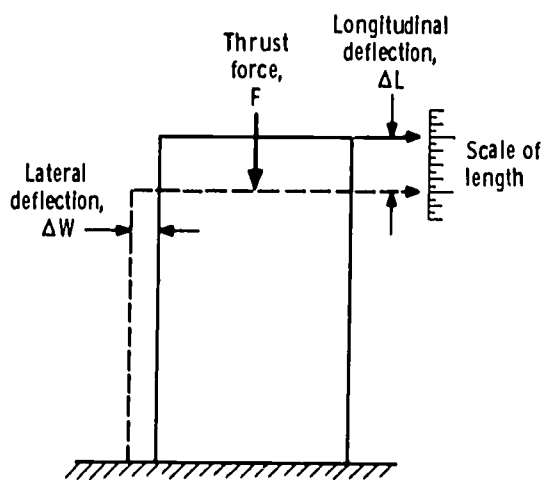


Figure 13-9. - Schematic diagram showing deformation of thrust-measuring spring under compressive load (thrust force).

However, the changes in length and width are not equal. The ratio of the change in width ΔW to the change in length ΔL is a material property known as Poisson's ratio μ .

$$\mu = \frac{\Delta W}{\Delta L} \quad (9)$$

This ratio is constant (within certain limits) for a given material. For most metals, the value of μ is about 0.3. This simply means that when the length of the spring decreases by 10 units, the width increases by 3 units.

For a good-quality spring (determined principally by the material), the longitudinal and lateral deflections are both proportional to the thrust force, even though the deflections are not equal in magnitude. Therefore, the thrust forces can be determined from the deflections (longitudinal and/or lateral) of the spring.

A relatively easy and accurate way to measure the spring deflections is by means of strain gages, which were discussed in the preceding section. Normally, four strain gages are mounted on the spring - two for measuring longitudinal deflections, and two for lateral deflections. The four strain gages are arranged (electrically) in a Wheatstone bridge circuit, as shown in figure 13-10. The resistances R_1 , R_2 , R_3 , and R_4 represent the four strain gages. Longitudinal deflection is indicated by R_1 and R_2 , and lateral deflection by R_3 and R_4 . Thus, when a force compresses the spring, strain gages R_1 and R_2 shorten and their resistances decrease, while R_3 and R_4 lengthen and their resistances increase. The difference in resistances indicates the extent of the deformation of the spring and, therefore, the magnitude of the force.

Some examples of the many commercially available thrust-measuring devices (thrust cells) for various thrust limits are shown in figure 13-11.

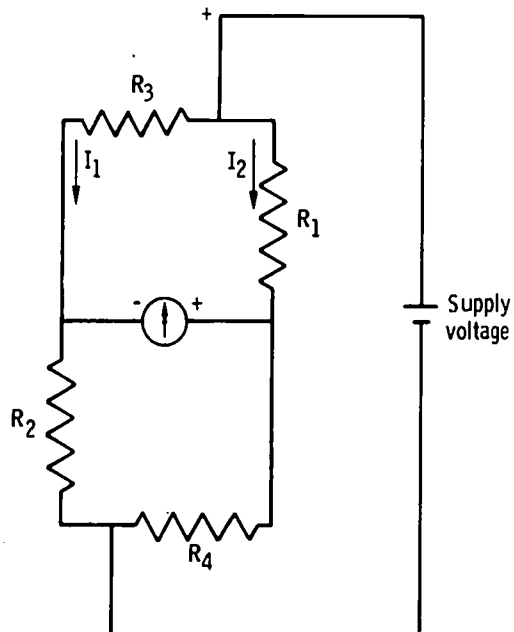
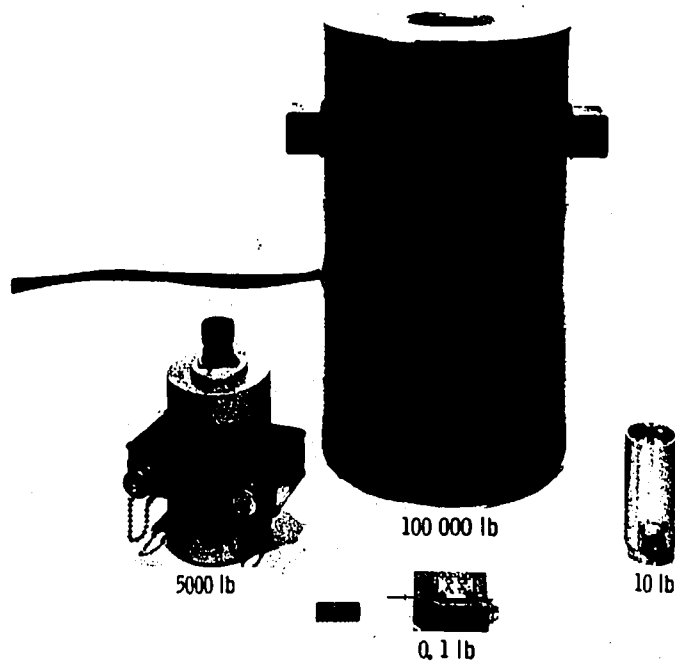


Figure 13-10. - Schematic diagram of Wheatstone bridge circuit arrangement of strain gages used to measure deflection of thrust-measuring spring. (Longitudinal deflections of spring are indicated by resistances of strain gages R_1 and R_2 ; lateral deflections indicated by R_3 and R_4 .)



C-69844

Figure 13-11. - Examples of commercially available thrust-measuring devices (thrust cells).

TEMPERATURE

Temperature is a measure of the intensity of heat, and heat is a form of energy resulting from the motions of the molecules or atoms of a substance (fluid or solid).

The temperature of a substance may be sensed by immersing a body (i. e., the sensor) in the substance or by placing it in contact with the substance. The temperature attained by the sensor relative to the temperature of the substance is a function of both the heat transfer from the substance to the sensor and the heat losses from the sensor. Therefore, the temperature of the sensor may not be exactly the same as that of the substance whose temperature is being measured.

If the substance is a flowing fluid, it has a static temperature and a total temperature. Static temperature refers to the heat due to the random motions of the molecules or atoms. Total temperature refers to the heat due to both the random motions of the molecules or atoms and the ordered motion in the direction of flow. Therefore, for static temperature measurements, the sensor must move with the fluid, so that the sensor and the fluid are motionless relative to each other. For total temperature measurements, a stationary sensor is placed in the flow in such a way that the flow is stopped by the sensor. Thus, the kinetic effect of the flow is included in the temperature measurement.

Two devices commonly used to measure temperature are the thermocouple and the resistance thermometer. Of the two, the thermocouple is the simpler device. The resistance thermometer is more complex, larger, more expensive, and more sensitive.

Thermocouple

A thermocouple (fig. 13-12) consists essentially of two electrical conductors of dissimilar metals welded together at one end, with the free ends connected to an electrical measuring instrument. The junction of the two conductors is placed at the point where the temperature T_1 is to be measured. The ends that are connected to the instrument are at a known reference temperature T_2 . The difference in temperature between T_1 and T_2 produces an electromotive force. Since T_2 is held constant, the electro-

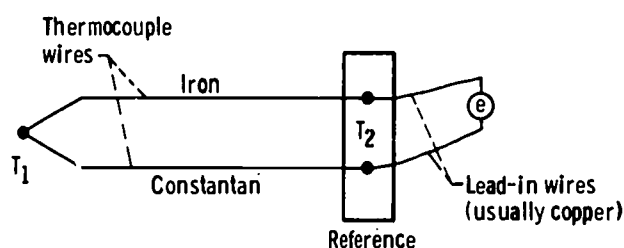


Figure 13-12. - Schematic diagram of thermocouple.

motive force is a function of the temperature T_1 . Thus, the voltage e measured by the instrument is an indication of the temperature T_1 . The voltage-measuring instrument must be highly sensitive because the voltage produced in the thermocouple is only about 0.00002 volt per degree Fahrenheit.

National Bureau of Standards Circular 561 lists temperature as a function of voltage for the following standard combinations of conductors used in thermocouples:

Chromel - Alumel
Chromel - Constantan
Copper - Constantan
Iron - Constantan
Platinum-13 percent rhodium - platinum

Specific pairs of metals are chosen on the bases of their physical and electrical properties at various temperature levels, as well as on the basis of cost.

Resistance Thermometer

The basis of the resistance thermometer is the fact that the resistance of materials varies with temperature. Thus, if a given piece of material, such as a length of wire, is properly calibrated (resistance as function of temperature), it can be used as a thermometer. The temperature is determined by measuring the resistance of the material.

The material used in the resistance thermometer depends on the temperatures to be measured and the accuracy required. For temperatures above 20° K (temperature of liquid hydrogen), metals are used, because their resistance increases with increasing temperature. The best metal is platinum, because it is obtainable in a highly pure form and because the variation of its resistance with temperature is very nearly linear. Thus, a platinum sensor provides a high degree of accuracy. Where less accuracy is satisfactory, nickel may be used. The metal, in the form of wire, is wound into a compact spiral and is enclosed in a suitable protective housing. Care must be taken to avoid straining the wire, for this would alter its resistance.

The resistance of the wire is measured with a Wheatstone bridge circuit similar to the one used to measure the resistances of the strain gages in a thrust cell (fig. 13-10). In this case, however, three of the resistances are known and fixed, and the fourth resistance is the one that is being measured.

At temperatures below 20° K, the variation of the resistance of metals with temperature becomes so small that the thermometer loses its sensitivity. However, the resistance of materials known as semiconductors, such as carbon or germanium, increases

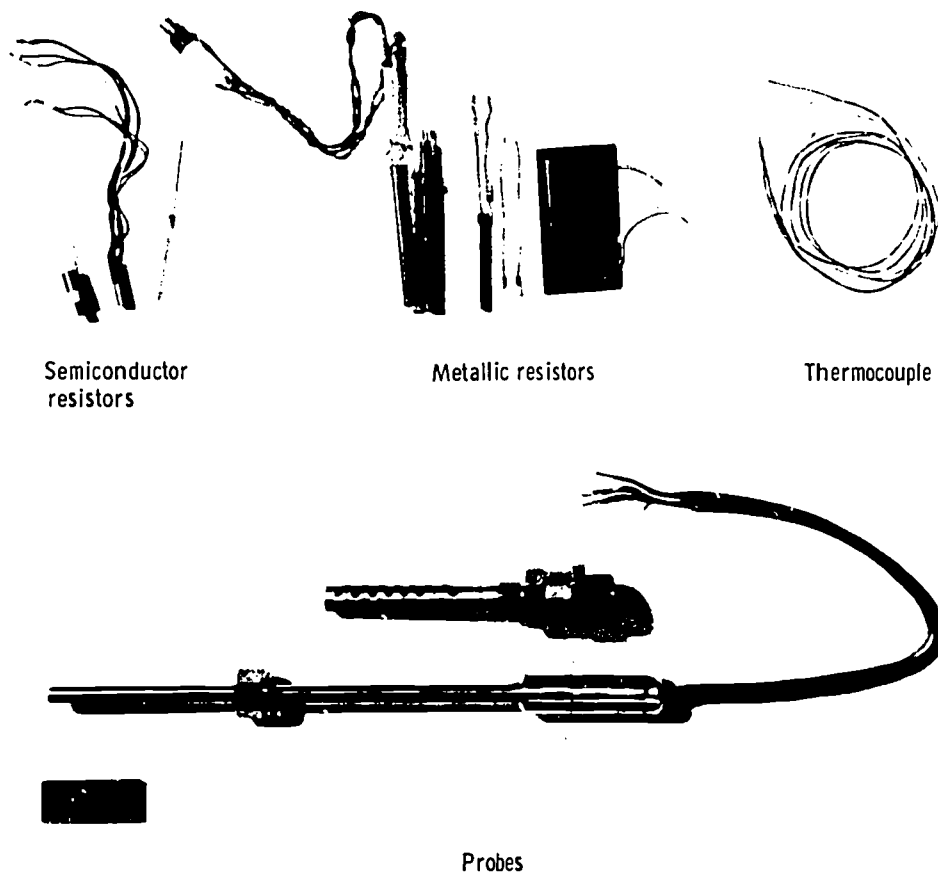


Figure 13-13. - Typical examples of temperature-sensing devices.

as the temperature decreases. Therefore, at temperatures below 20° K, semiconductor materials are used in resistance thermometers.

Some typical examples of temperature-sensing devices are shown in figure 13-13.

VOLUME FLOW RATE

Volume flowmeters, in general, are of two basic types, based on the method by which they measure the flow rate.

One type of flowmeter measures flow rate by repeatedly filling and emptying a known volume and counting the time rate of this action. Various forms of this type of meter are in common use, because they are reliable and relatively inexpensive. Common examples are the nutating-disk meters used to measure water in the home and gasoline at the filling station.

The other basic type of flowmeter determines the volume flow rate from the kinetic energy of the flowing fluid. The discussion at the beginning of this chapter explained how the velocity of a flowing fluid can be determined by equation (4) from certain measurable quantities that include the pressure due to the motion of the fluid. Volume flow rate, in turn, can be determined from the flow velocity by the equation

$$\dot{v} = AV_{ave} \quad (10)$$

where

\dot{v} volume flow rate, ft³/sec

A cross-sectional area of flow channel, ft²

V_{ave} average flow velocity, ft/sec

The velocity of a fluid generally varies from a maximum at the center of the flow channel to zero at the walls. Thus, the average flow velocity, required for equation (10), can be obtained from pressure measurements taken at various distances from the walls of the flow channel. This is an accurate but time-consuming process. However, the

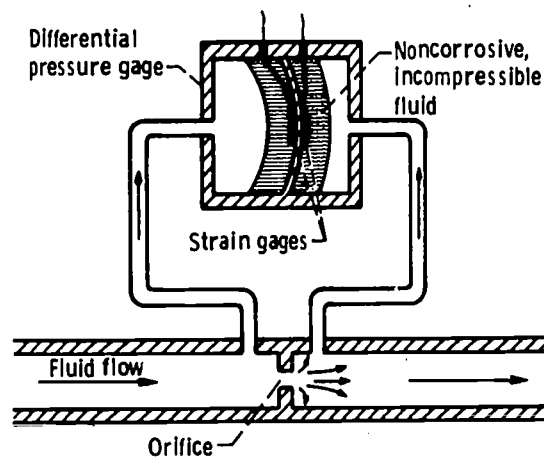


Figure 13-14. - Orifice flowmeter installation.

volume flow rate of an incompressible fluid of known density can be determined from a single pressure measurement. The pressure-measuring arrangement is shown in figure 13-14. A nozzle or orifice is placed in the flow channel, and the difference in static pressure between the upstream and downstream sides is measured with a differential pressure gage. The magnitude of this pressure difference is a function of the flow velocity through the nozzle or orifice. The flow velocity is calculated from this measured pressure differential and is used in the following equation to obtain volume flow rate.

$$\dot{v} = C_d AV \quad (11)$$

where

C_d nozzle or orifice discharge coefficient (dimensionless)

A cross-sectional area of nozzle or orifice, ft^2

V flow velocity, ft/sec

The discharge coefficient C_d is a correction factor that is determined by calibrating the nozzle or orifice. The value of C_d is normally about 0.98 for a nozzle and about 0.6 for an orifice. The coefficient is higher for a nozzle than for an orifice, because the nozzle produces a smoother flow than does the orifice.

Another device which determines volume flow rate from the kinetic energy of the flowing fluid is the turbine flowmeter. In this type of meter, the kinetic energy of the fluid turns a lightly loaded turbine. The load on the turbine is only bearing friction and the small amount of power required to measure the rotational speed of the turbine. The turbine blades are made of magnetic material. As the blades pass a coil-magnet combination, they generate electrical pulses. Thus, the time rate of pulses is a measure of the rotational speed of the turbine. The turbine flowmeter is calibrated (usually with water), and the calibration is expressed as pulses per gallon. Some typical turbine flowmeters, as well as a cutaway view of one, are shown in figure 13-15.

The preceding discussion has described several methods of measuring volume flow rate. In most instances, however, the quantity of primary interest is mass flow rate (lb/sec). The mass flow rate is obtained by multiplying the volume flow rate by the fluid density, which is measured independently.

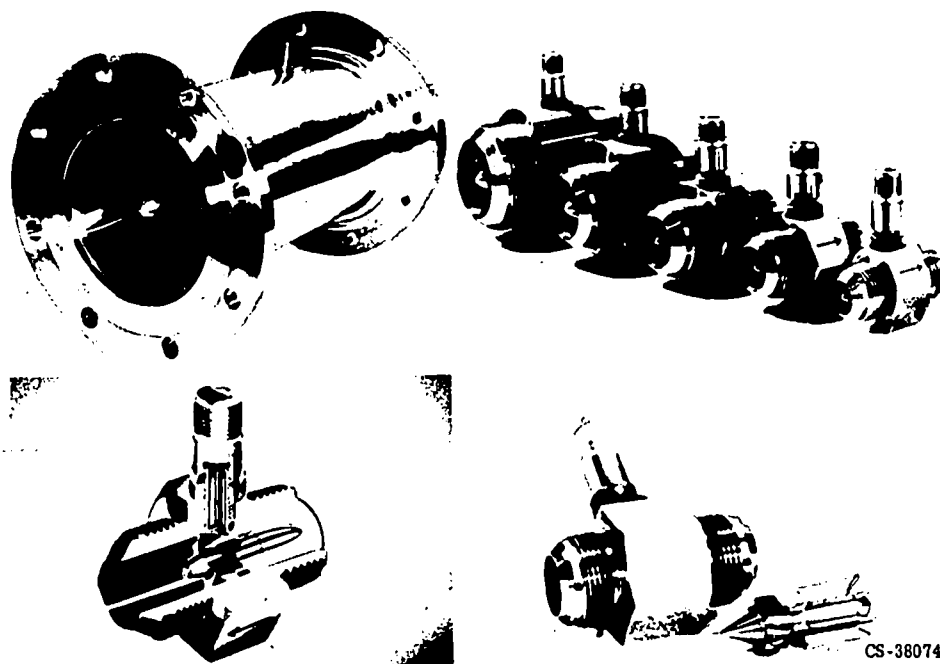


Figure 13-15. - Examples of commercially available turbine flowmeters.

CONCLUDING REMARKS

The measuring devices discussed in this chapter change some measured variable, such as temperature, to an electrical quantity, such as voltage. This is an essential requirement with modern data systems. Very few data are recorded manually. In fact, data should be recorded on a system, such as a digital tape-recording system, which enables the data to be entered in a computer.

BIBLIOGRAPHY

- Binder, Raymond C.: Fluid Mechanics. Fourth ed., Prentice-Hall, Inc., 1962.
- Cook, Nathan H.; and Rabinowicz, Ernest: Physical Measurement and Analysis. Addison-Wesley Publ. Co., 1963.
- Doebelin, Ernest O.: Measurement Systems: Application and Design. McGraw-Hill Book Co., Inc., 1966.
- Stout, Melville B.: Basic Electrical Measurements. Prentice-Hall, Inc., 1950.

14. WIND TUNNELS

Leonard E. Stitt*

Wind tunnels are ground facilities for aerodynamic testing of aircraft, missiles, propulsion systems, or their components under simulated flight conditions. The concept of a wind tunnel is rather simple: instead of the object flying through the air at the desired test speed and attitude, it is supported in the test attitude within the wind tunnel, and the air flows past the object at the test speed. The resulting forces of interaction between the object and the airflow are identical in both cases. In a wind tunnel, both the airstream and the attitude of the test model can be controlled by the engineer while all essential information is collected. Obviously, many scale models of a particular configuration can be evaluated in wind-tunnel tests at a relatively small cost, compared to the cost of designing, fabricating, and flight testing a full-scale prototype. Configuration changes can be made rapidly, and a final design can be arrived at that has a reasonable chance of success when the prototype is finally flown. The usefulness of wind tunnels in providing good aerodynamic design information has been demonstrated many times during the past 50 years, both in the United States and abroad.

Wind tunnels have been in use for many years; in fact, they were already in use prior to the first powered flight of the airplane in 1903. An estimated 1000 wind tunnels have been built throughout the world, and about 250 of these have been built in the United States. These wind tunnels range from simple, low-cost, low-speed tunnels used for testing subscale models to highly complex and expensive tunnels used for testing full-scale hardware at supersonic speeds. An example of the latter is the 10- by 10-Foot Supersonic Wind Tunnel at the NASA Lewis Research Center. This tunnel was built in the early 1950's, at a cost of \$35 million, to study the aero-thermodynamic problems of propulsion systems.

WIND-TUNNEL DESIGN CONSIDERATIONS

Wind tunnels exist in a wide variety of shapes and sizes depending on cost, speed range, power requirement, purpose, etc. One tunnel design parameter of particular

*Head, Exhaust Systems Section.

TABLE 14-I. - CLASSIFICATION OF WIND
TUNNELS ACCORDING TO SPEED OF
AIRFLOW IN TEST SECTION

| Tunnel class | Free-stream Mach-number ^a range |
|--------------|--|
| Low speed | 0 to 0.5 |
| High speed | 0.5 to 0.9 |
| Transonic | 0.7 to 1.4 |
| Supersonic | 1.4 to 5.0 |
| Hypersonic | >5.0 |

$$^a \text{Mach number} = \frac{\text{Local stream velocity}}{\text{Local velocity of sound}}$$

interest is the velocity of the airflow. In practice, wind tunnels can be classified according to their speed ranges, as shown in table 14-I. Some wind tunnels are restricted to one speed, while others operate over a wide range of speeds. For example, the 8-by 6-Foot Supersonic Wind Tunnel at the Lewis Research Center can operate at speeds ranging from about Mach 0.4 to Mach 2.0. Obviously, such a tunnel is quite useful to the engineer for evaluating a particular configuration over a wide range of flight conditions with only one installation. This versatility must, of course, be weighed against the initial cost and complexity of constructing and operating such a wind tunnel. A few key items that should be considered when designing a wind tunnel are discussed in the following sections.

Wind-Tunnel Types

The two general types of wind tunnels are the open-circuit and the closed-circuit types, shown in figure 14-1.

Open-circuit tunnel. - The open-circuit tunnel (fig. 14-1(a)) is the simpler of the two types and is the one normally used in most schools and universities for demonstration purposes and for laboratory instruction. (An example of this type of tunnel at Lewis is the low-speed tunnel used by the Lewis Aerospace Explorers and described in chapter 17.) Airflow is drawn through the test section by a suitable motor and propeller (or fan) arrangement. An airflow of good quality (low turbulence) is assured in the test area through the use of inlet screens and the proper contouring of the contraction cone. Large contraction ratios are useful in obtaining smooth flow in the test section. Typical contraction ratios (ratio of inlet area to test-section area) range from 7 to 14. The University of Notre Dame has recently used contraction ratios as high as 100 in developing a super-

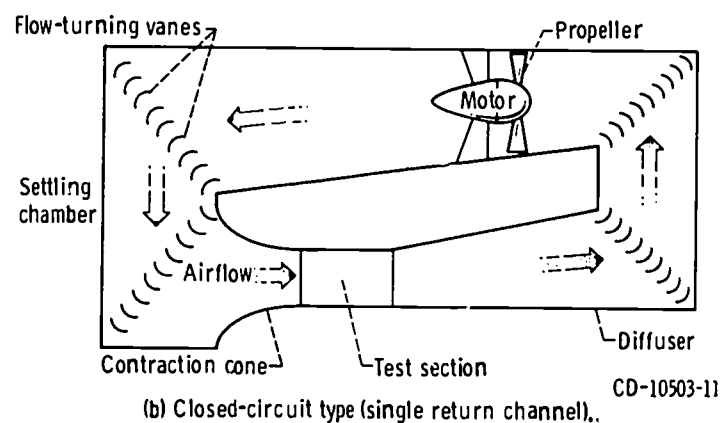
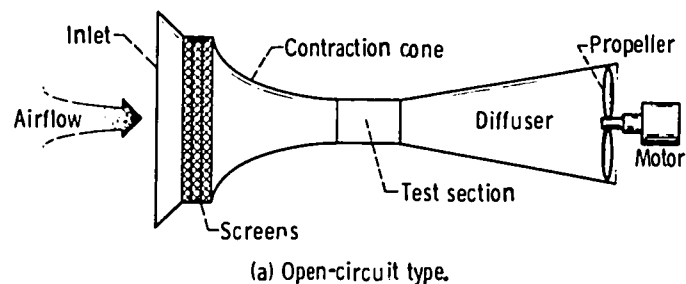


Figure 14-1. - Wind-tunnel types and nomenclature.

sonic smoke tunnel (ref. 1). The test section normally includes windows and appropriate illumination for viewing the model. Downstream of the test section, a diffuser is used to slow the airflow ahead of the propeller to a velocity at which the propeller operates efficiently. The area is increased as rapidly as possible without incurring flow separation from the diffuser walls. Diffuser expansion angles vary from about 6° to 12° , depending on the shape of the cross section. Safety screens can be added downstream of the test section to protect the propeller in case of model failure.

Closed-circuit tunnel. - The closed-circuit tunnel (fig. 14-1(b)) can be more efficient from the standpoint of the power requirement, but it requires more physical space and is more expensive to fabricate than the simple open-circuit tunnel. The closed-circuit tunnel is usually rectangular, and turning vanes are provided to turn the flow efficiently around the 90° bends. The closed-circuit tunnel also features the usual contraction cone and low-expansion-angle diffuser. A settling chamber is also included to reduce the flow turbulence at the entrance to the contraction cone. The test section can be of a variety of cross-sectional shapes, such as square, rectangular, octagonal, circular, elliptical, etc. The test section may be enclosed by walls, or it may be open (no walls) to facilitate access to the test model. A single return channel (fig. 14-1(b)) or two return channels may be used. With two return channels, the test section is normally located in the center between the two parallel channels. A suitable motor and propeller are required for each return channel.

Power Requirement

One of the main parameters that the wind-tunnel designer must consider is the power required to operate the tunnel. This power requirement may be computed by the following equation:

$$\text{BHP} = \frac{qAV}{\eta ER550}$$

where

BHP brake horsepower of motor

q dynamic pressure of airflow in test section, lb/ft²

A cross-sectional area of test section, ft²

V velocity of airflow in test section, ft/sec

η power transmission efficiency (a measure of power performance of fan-motor combination, relating power input to pumping power)

ER energy ratio of wind tunnel (a measure of aerodynamic efficiency of wind tunnel) and 550 is the factor for converting foot-pounds per second to horsepower.

For small, open-circuit wind tunnels, the energy ratio usually has a value between 1.5 and 2.5; a highly efficient open-circuit tunnel may have an energy ratio of 3.5. A closed-circuit wind tunnel with an enclosed test section may have an energy ratio between 3 and 7.

Since the dynamic pressure q is equal to $\frac{1}{2}\rho V^2$, the equation for horsepower can be rewritten in the following form:

$$\text{BHP} = \frac{1}{2} \frac{\rho AV^3}{\eta ER550}$$

where ρ is the air density in the wind tunnel, in slugs per cubic foot (1 slug = 32.2 lb-ft/sec²). It is obvious from this equation that the velocity of the airflow is the most influential variable affecting the power requirement of a wind tunnel. Therefore, from a power standpoint, the wind-tunnel designer is faced with a problem. He wants a large test section and a high-speed airflow, but both of these features require high horsepower. Therefore, the general design procedure is to select the desired airflow velocity range and then to determine the largest test-section area that is compatible with the available power.

The following sample calculations for two greatly different wind tunnels show the ef-

fects of tunnel variables on the horsepower requirements.

Tunnel used by Lewis Aerospace Explorers:

$$\begin{aligned} \text{BHP} &= \frac{1}{2} \frac{\rho AV^3}{\eta ER550} \\ &= \frac{1}{2} \frac{(0.002378)(4.16)(75)^3}{(0.75)(2.0)(550)} \\ &= 2.53 \end{aligned}$$

10- by 10-Foot Supersonic Wind Tunnel at Lewis:

$$\begin{aligned} \text{BHP} &= \frac{1}{2} \frac{\rho AV^3}{\eta ER550} \\ &= \frac{1}{2} \frac{(0.0001)(100)(3400)^3}{(0.75)(2.0)(550)} \\ &= 238\ 206 \end{aligned}$$

This power is supplied by seven electric motors rated at 37 500 horsepower each. This facility (highest-powered wind tunnel in United States) requires about 200 megawatts of electrical power at full load, at a cost of approximately \$1400 per hour. Because of the large power requirement, this facility operates primarily at night, when the power requirements of the community are minimum. At night, the electricity required to operate the wind tunnel is readily available at reduced cost from the local electric company.

The availability and cost of electrical power, as well as the initial and operating costs of the tunnel, influence the choice between intermittent and continuous operation.

Intermittent operation. - An intermittent wind tunnel is an open-circuit type that may be either a blowdown tunnel or an indraft tunnel. The blowdown tunnel (fig. 14-2(a)) has a large pressurized tank upstream of the test section. When the tank is opened, the compressed air from it blows through the test section. The indraft tunnel (fig. 14-2(b)) has a large vacuum tank downstream of the test section. When the evacuated tank is opened, its vacuum draws air through the test section.

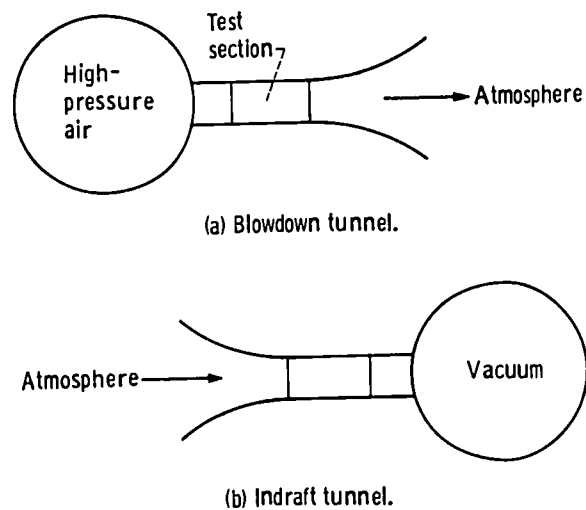


Figure 14-2. - Intermittent wind tunnels.

The main disadvantage of an intermittent tunnel is that it provides an airflow of only a brief duration before the tank must again be pressurized or evacuated. Therefore, testing time is limited, and special instrumentation must be used to obtain data. Changing model variables during the short test period is also an operational problem. With suitable control systems, the model attitude can be pre-programmed to vary automatically during the test.

Continuous operation. - Continuous operation, which is provided by either open-circuit or closed-circuit tunnels, such as those shown in figure 14-1, is more advantageous from the standpoint of test time. However, it is more costly from a power consideration.

Speed Variability Requirement

One useful feature of a subsonic wind tunnel is that the flow velocity in the test section can be varied by increasing or decreasing the propeller speed within the limits of available power or propeller design. The flow velocity can be increased in this manner until the local flow velocity equals the speed of sound (Mach 1). When this condition occurs, the tunnel is said to be "choked."

The flow velocity achieves Mach 1 at the minimum cross-sectional area (throat) of the tunnel. The only way to obtain a flow velocity greater than Mach 1 is to expand the flow by increasing the flow area downstream of the throat. (The acceleration of an airflow to supersonic velocities is discussed in greater detail in chapters 7 and 11.) The flow Mach number (velocity) downstream of the throat is rigidly determined by the ratio of the local cross-sectional area A to the throat cross-sectional area A^* . This relation between area ratio and Mach number has an important bearing on wind-tunnel design. A supersonic wind tunnel with a fixed area ratio A/A^* can provide only one specific flow

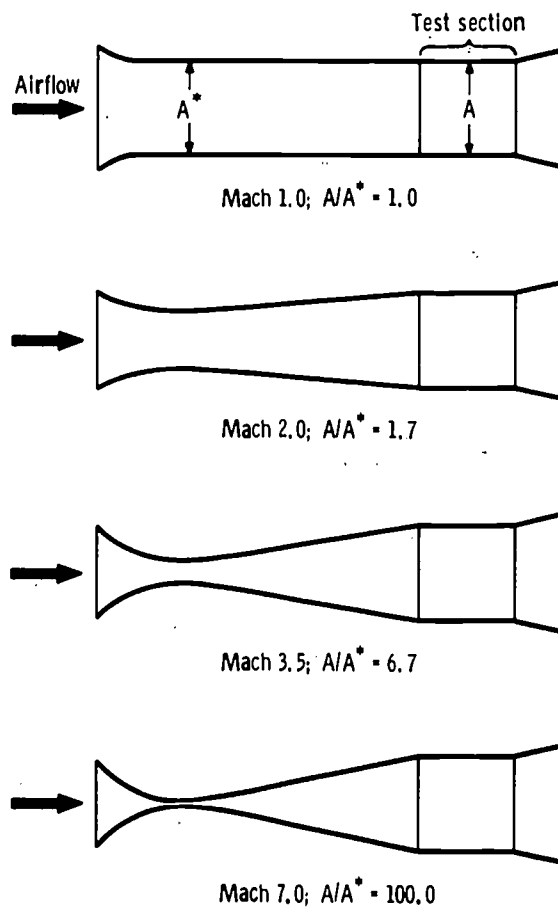


Figure 14-3. - Area variation required for supersonic wind tunnel.

Mach number in the test section. Thus, if the flow Mach number in the test section is to be variable, the tunnel must be equipped with some means of physically varying the area ratio A/A^* . For example, if the cross-sectional area of the test section is fixed, as shown in figure 14-3, the throat area must be increased by a factor of 100 to vary the test-section Mach number from 1.0 to 7.0. The 8- by 6-foot and 10- by 10-foot tunnels at Lewis use flexible nozzles to change both the throat area and the wall contour between the throat and the test section to provide variable Mach number capability. The 1- by 1-Foot Variable Mach Number Wind Tunnel at Lewis features a fixed test-section area and replaceable nozzle "blocks" with various throat areas to provide testing over a range of discrete Mach numbers up to Mach 5.0.

WIND-TUNNEL CALIBRATION

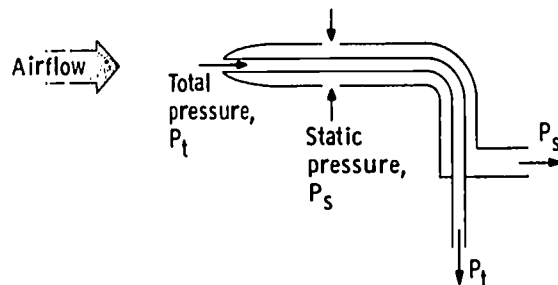
After a wind tunnel has been designed and fabricated, the quality of the airflow in the test section must be determined before the tunnel is used for testing. The flow characteristics that must be determined include the speed and direction of the local flow and the

thickness of the boundary layer along the walls.

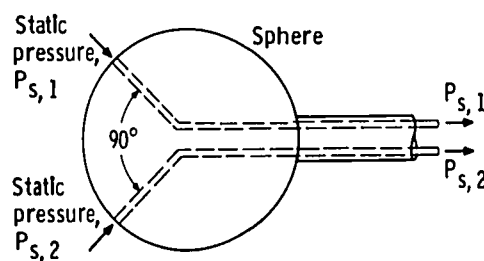
The speed of the airflow can be calculated from measurements of the density ρ , the static pressure P_s , and the total pressure P_t of the airflow. These properties, as well as methods of sensing and measuring them and the method of calculating velocity from them, are discussed in chapter 13. For wind-tunnel calibration, these properties are measured with calibration instruments (figs. 14-4 and 14-5) that are adaptations of the basic instruments discussed in chapter 13 and are tailored to the airflow speed range of interest.

Flow angularity, or direction, is usually determined by measuring static pressures or static and total pressures on opposite sides of a symmetrical object that can be aligned with the local flow direction or with the wind-tunnel centerline.

In a subsonic wind tunnel, the static and total pressures used to calculate the speed of the airflow usually are determined simultaneously with a pitot-static tube (fig. 14-4(a)).



(a) Pitot-static tube, for measuring flow speed.



(b) Yawmeter, for measuring flow angularity.

Figure 14-4. - Calibration devices for subsonic wind tunnels.

The pitot tube senses total pressure P_t , and the static tube senses static pressure P_s . Local flow angularity in a subsonic wind tunnel is usually determined with a yawmeter of the type shown in figure 14-4(b). This instrument is basically a sphere with two static-pressure orifices located 90° apart in its surface. The sphere is pitched in the tunnel until the static pressures at the two orifices are equal, and the angularity of the yawmeter (or flow direction) is then recorded. In this manner, flow angularities in any preselected plane can be measured by proper orientation of the yawmeter.

Both the speed and the direction of the airflow can be determined by means of a cali-

19. NUCLEAR ROCKETS

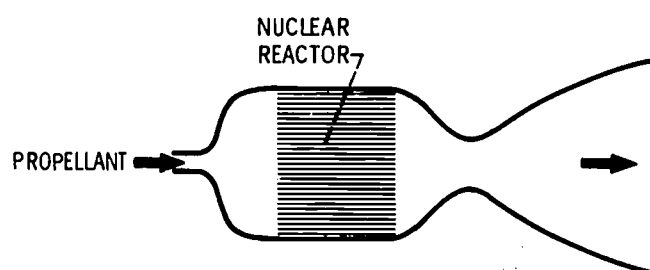
A. F. Lietzke*

Future interplanetary missions will require extremely heavy vehicles if chemical rockets are to be used for propulsion. Nuclear rockets have the performance potential to reduce the required weight for these advanced missions.

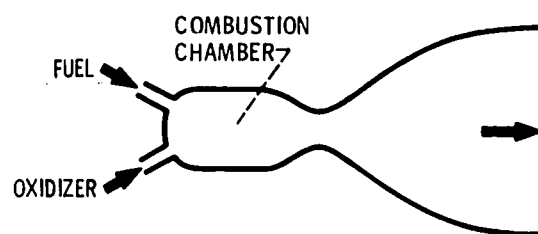
This chapter describes a nuclear rocket, how it functions, its limitations, and expected performance. The difference between chemical and nuclear rockets is illustrated. It is assumed that the reader is familiar with the general fundamentals of rockets. Therefore, only those aspects peculiar to nuclear rockets are emphasized herein.

A nuclear rocket, shown schematically in figure 19-1(a) uses a nuclear reactor to heat a propellant and a nozzle to accelerate the propellant.

The difference between a nuclear rocket and a chemical rocket can be seen by comparing figures 19-1(a) and (b). While the heat energy in a chemical rocket comes from burning the fuel with an oxidizer in a combustion chamber, the heat energy in a nuclear rocket comes from a nuclear reaction; the nuclear reactor (discussed later) replaces the combustion chamber. Moreover, the nuclear rocket uses a single propellant which does



(a) Nuclear rocket engine.



(b) Chemical rocket engine.

Figure 19-1. - Schematic diagrams of nuclear and chemical rocket engines.

*Chief, Reactor Components Branch.

not react chemically, whereas the chemical rocket requires two propellants - a fuel and an oxidizer.

Therefore, the propellant for a nuclear rocket is not restricted to one which reacts chemically and may be selected on the basis of other properties. This fact leads to the advantage of a nuclear rocket.

The nuclear rocket and the chemical rocket both use a convergent-divergent nozzle to accelerate the propellant and so convert thermal energy to kinetic energy. From our knowledge of the flow process in the nozzle (chapter 2), the ideal exhaust velocity can be expressed by the following equation:

$$V_e = \sqrt{\frac{99\,400\gamma T_i}{(\gamma - 1)m} \left[1 - \left(\frac{P_e}{P_i} \right)^{(\gamma-1)/\gamma} \right]}$$

where

- V_e ideal exhaust velocity
- γ ratio of specific heats of the propellant
- T_i propellant temperature at the nozzle inlet
- m propellant molecular weight
- P_e propellant pressure at the nozzle exit
- P_i propellant pressure at the nozzle inlet

If all of the factors in this equation are constant except T_i and m , then the ideal exhaust velocity is proportional to the square root of propellant temperature T_i and inversely proportional to the square root of the molecular weight m :

$$V_e \propto \sqrt{\frac{T_i}{m}}$$

The specific impulse I_{sp} is related to the exhaust velocity V according to the following equation (see chapter 2):

$$I_{sp} = \frac{V}{g}$$

where g is the acceleration due to gravity. Therefore,

$$I_{sp} \propto \sqrt{\frac{T_i}{m}}$$

Thus, I_{sp} increases as T_i increases and also I_{sp} increases as m decreases. The temperature T_i attainable in solid-core nuclear rockets is actually lower than the temperature in chemical engines. The advantage of the nuclear rocket over the chemical rocket results from the propellant selected. Because the nuclear rocket engine does not require a relatively high molecular weight oxidizer, the best propellant available can be selected, the one with the lowest molecular weight, pure hydrogen. Hydrogen H_2 has a molecular weight of 2 as compared with a value of 18 for one of the best chemical propellants, hydrogen-oxygen.

The materials of which a nuclear rocket can be constructed will limit the hydrogen temperature T_i to less than $6000^{\circ} R$ or a specific impulse of approximately 1000 pounds of thrust per pound of hydrogen flow per second. This specific impulse is over twice that of the best chemical propellants (see chapter 7).

As mentioned previously, the nuclear reactor replaces the combustion chamber or the "chemical reactor" in the chemical rocket. The operating principles of the nuclear reactor are based on the interactions between neutrons and atomic nuclei. Atomic nuclei consist of two kinds of primary particles, protons and neutrons. An atom consists of a nucleus surrounded by much smaller particles called electrons.

The chemical nature of an element depends on the number of electrons in orbit about the nucleus. This number of electrons is equal to the number of protons in the nucleus. Therefore, the chemical behavior depends on the atomic number of the element (atomic number = number of protons). Atomic numbers range from 1 for hydrogen to 92 for uranium.

The nuclear nature of an element depends on the conditions of the nucleus. The nucleus is made up of protons and neutrons. Atoms of a given element can exist with different numbers of neutrons in the nucleus. These different species of the same element are called isotopes of the element. Although the chemical properties of these isotopes are identical, their nuclear properties may be entirely different. Therefore, it is important to distinguish between isotopes of a given element. This can be done through the use of the atomic mass number, or simply mass number (mass number = number of protons plus number of neutrons). Thus, each isotope, instead of having a new name, is identified by writing the mass number after the chemical element or symbol. For example, the uranium isotope with a mass number of 235 is written as uranium-235 or U^{235} .

As neutrons pass through matter, they collide with atomic nuclei. The collisions cause various interactions between the colliding neutrons and nuclei. These interactions

can be divided into three types: scattering, parasitic capture, and fission interactions.

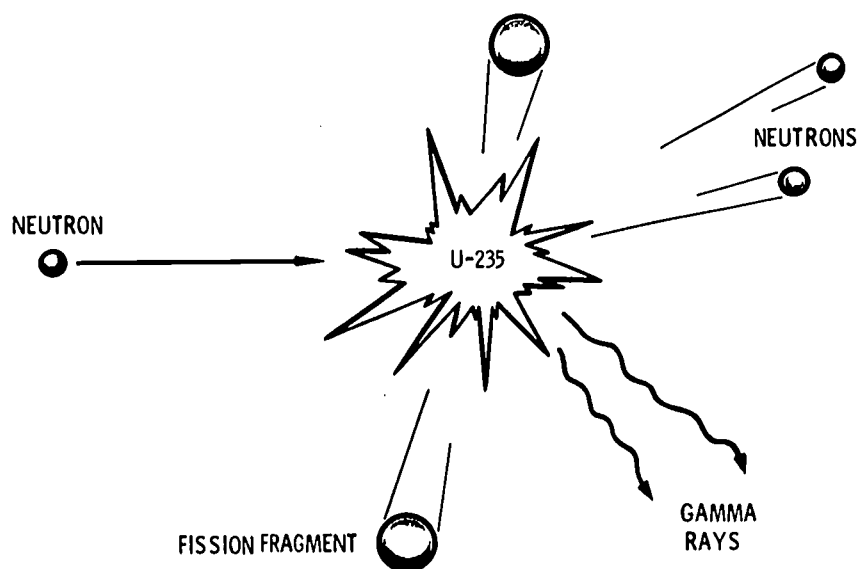
Scattering interactions result from those collisions which disrupt the neutron from its path. During such collisions the neutron transfers some or all of its energy to the nucleus but a neutron remains free after the interaction.

Parasitic capture reactions result from those collisions in which the neutron enters the nucleus and remains absorbed in the nucleus. When this happens, other subatomic particles and/or radiation are released from the compound nucleus.

Nuclear fission reactions result from those collisions in which neutron capture causes the nucleus to break up, with a release of a large amount of energy. The fission process is illustrated in figure 19-2. The nucleus is broken into two primary fission fragments (elements of lower atomic number than the original nucleus), neutrons, and gamma radiation (high energy X-rays). Most of the energy from the fission process appears as kinetic energy of the fission fragments moving at high speed. The new neutrons are also ejected at high speed. The latter are available to cause more fissions and offer the possibility of maintaining a chain reaction.

The various interactions can be summarized as follows. Each collision between a neutron and a nucleus will result in scattering and slowing down of the neutron, neutron capture, or nuclear fission. Most reactions produce damaging radiation requiring a protection or shield. Which of these interactions occur and the probability of each depend on the type of nucleus involved and the neutron energy.

Although essentially all of the elements can take part in scattering and parasitic capture of neutrons, the probability of such interactions occurring varies greatly from one element to another. On the other hand, only the heaviest elements will fission as a result of neutron collision. Of these heavy elements, uranium and plutonium are of pri-



CS-14406

Figure 19-2. - Nuclear fission process.

mary interest. The possibility of fission, however, depends on the particular isotope and the neutron energy. Considering uranium, for example, slow and fast neutrons will fission uranium-233 and uranium-235, whereas only fast neutrons will fission uranium-238. The probability of fission is greatest with uranium-233 and uranium-235; therefore, these isotopes are most desirable for nuclear reactors. Unfortunately, uranium appears in nature in the following isotopic proportions:

| Isotope | Percent in nature |
|-------------|-------------------|
| Uranium-234 | 0.006 |
| Uranium-235 | .712 |
| Uranium-238 | 99.282 |

Plutonium and uranium-233 are essentially nonexistent in nature. Consequently, most current nuclear reactors utilize uranium-235 which has been separated from the other isotopes of uranium in the gaseous diffusion plants at Oak Ridge, Tennessee; Paducah, Kentucky; or Portsmouth, Ohio.

The interactions of neutrons with nuclei are studied by means of the concept of nuclear cross sections. The cross section for a reaction may be defined as a measure of the probability of that reaction taking place under prescribed conditions. It is a property of a material and is a function of the energy of the incident neutron. A typical curve illustrating this variation with neutron energy is shown in figure 19-3.

At low energy (slow neutrons) the probability of reaction (cross section) is inversely proportional to the neutron velocity. This can be thought of as the cross section being proportional to the time the neutron is in the vicinity of the nucleus.

In the intermediate energy range, the cross section curve typically has peaks at certain energies, and this portion of the curve is called the resonance region.

At high energies, the cross section decreases steadily as the energy increases, and finally it approaches the geometrical cross section of the nucleus.

As a result of the interactions of neutrons with nuclei, a nuclear reactor can be designed which for steady state requires the following neutron balance:

$$\text{Production} = \text{Absorption} + \text{Leakage}$$

The fission of a uranium-235 nucleus by reaction with a low energy neutron produces an average of 2.5 neutrons. (The number of neutrons produced is not an integer because some fissions produce 2 neutrons and some fissions produce 3 neutrons.) If an average

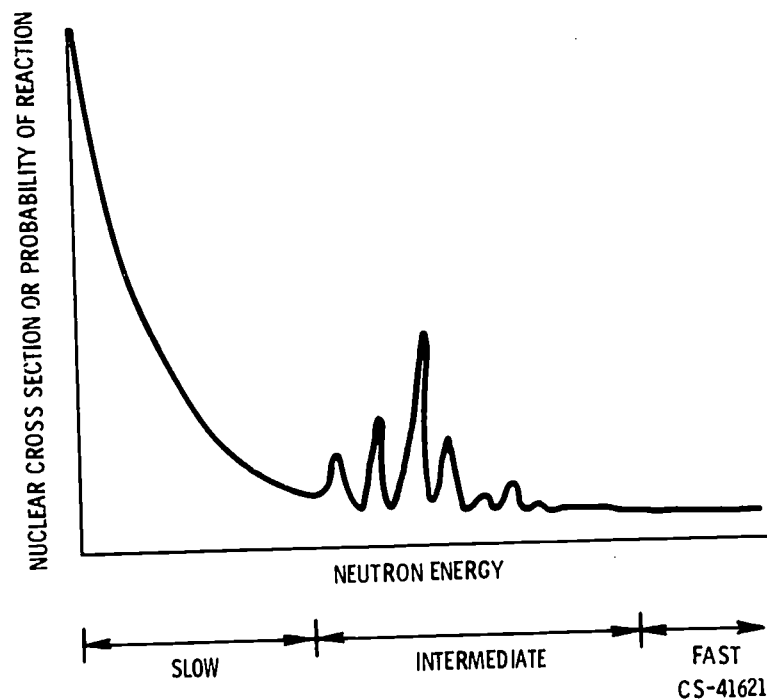


Figure 19-3. - Typical variation of nuclear cross section with neutron energy.

of one of these neutrons interacts to produce another fission before it is absorbed in parasitic capture or leaks (escapes) from the reactor, then a self-sustaining chain reaction results and nuclear energy will continue to be generated. This critical condition can be achieved most easily by restricting the materials of the reactor to fissionable materials and materials that have low parasitic capture cross sections and also by limiting the leakage from the reactor. The manner in which this critical condition is achieved determines the reactor type.

Merely increasing the number of nuclear fuel atoms (uranium-235) increases the probability of the neutrons hitting a fuel atom. The assembly of an amount of fuel necessary to achieve the critical condition results in a fast reactor, so-called because there is no neutron scattering or moderating material incorporated to slow down the neutrons and all the fissions must result from capture of fast neutrons. Because the cross section for fission is relatively low at these high energies, this type of reactor requires a large amount of nuclear fuel.

Leakage of neutrons from the reactor can be decreased by the addition of a material that scatters the neutrons but does not capture them to any appreciable extent. This material, in effect, increases the probability of fission capture by increasing the number of passes a neutron makes through the reactor. It is usual practice to select a low-atomic-weight element for this material in order to make it more effective in slowing down neutrons and thus increasing the fission cross section of the fuel. Such a reactor is called a moderated reactor. If enough of this moderating material is utilized to slow down the

neutrons to be in thermal equilibrium with the material, most of the fissions will occur as a result of capture of thermal neutrons. This is a special case of a moderated reactor called a thermal reactor.

Scattering material may also be used to surround the fuel and decrease the leakage by reflecting the neutrons back into the fuel of the reactor. This technique may be used for both the fast and moderated reactors.

When the concept of nuclear cross section (discussed earlier) is used, the interaction rate of neutrons with nuclei is given by

$$\text{Rate of interaction per cubic centimeter} = N\sigma nv$$

where

N number of target nuclei per cubic centimeter

σ nuclear cross section, $\text{cm}^2/\text{nucleus}$

n neutron density, neutrons/ cm^3

v neutron velocity, cm/sec

The rate of energy release, or the power of the reactor, is then given by

$$\text{Power per cubic centimeter} = E_f N \sigma_f nv$$

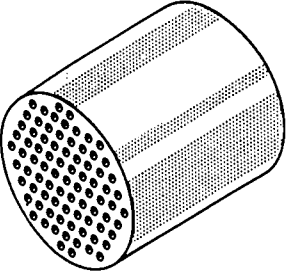
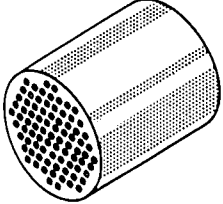
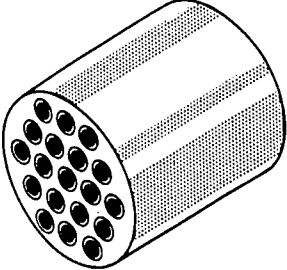
where E_f is the energy per fission and σ_f is the fission cross section of the fuel nuclei. Inasmuch as nuclear reactions are independent of the direction of neutron motion, it is usual to refer to neutron flux rather than neutron current. The product nv is called neutron flux, and this concept of flux can be applied to neutrons moving in random fashion.

A reactor can generate any power. The desired power is obtained merely by controlling the neutron population n . The neutron population, in turn, can be controlled by regulating (a) production (inserting or withdrawing fuel), (b) absorption (inserting or withdrawing material of high parasitic capture cross section), or (c) leakage (moving a reflector toward or away from the reactor).

The energy from the fission process is mainly in the form of kinetic energy of the fission products which is converted to heat energy as these products are stopped by the material of the reactor. The power of a reactor is limited only by the capability for removing this heat. In a nuclear reactor of a rocket the heat is transferred to the propellant, and provision must be made to allow passage of the propellant through the reactor.

Some of the reactor types and the materials which have been considered for nuclear rockets are listed in table 19-I. Two thermal reactors and one fast reactor are listed.

TABLE 19-I. - NUCLEAR ROCKET REACTORS AND MATERIALS

| Reactor type | Configuration | Moderating material | Fuel-bearing material |
|----------------------------|---|---|---|
| Thermal (homogeneous) |  | Graphite Beryllium oxide | Coated graphite |
| Fast |  | None | Tungsten Molybdenum Zirconium carbide |
| Thermal (heterogeneous) |  | Water Heavy water Beryllium Beryllium oxide Metallic hydrides | Tungsten Molybdenum Coated graphite |

The thermal homogeneous reactor has nuclear fuel dispersed throughout the moderating material and can be visualized as a large block with a number of cooling passages for propellant flow. The fission energy heats the block and this heat is transferred to the propellant as it flows through the holes in the block. Since heat transfer can only occur from a hotter to a cooler substance, the block must be at a higher temperature than the propellant. As shown previously, propellant temperature should be as high as possible. The fuel-bearing material for this reactor, therefore, must not only be a lightweight element but must also have high temperature capability. This dual requirement limits the choice to the two materials shown in the figure, graphite (carbon) and beryllium oxide. Of these two materials, graphite has the higher temperature capability and is preferred. Graphite reacts chemically with hydrogen, however, and must be coated with some other refractory material for protection. Because graphite is not one of the best moderating materials, substantial quantities are required to slow the neutrons and the reactor is necessarily large, even for low power levels. Beryllium allows a smaller reactor, but one that must operate at lower temperatures.

The fast reactor contains no moderating material. The low fission cross sections at the high neutron velocity prevailing must be compensated for by greatly increasing the

quantity of fuel. While the fission cross section is low at the high energy of the neutrons, the parasitic capture cross section for other materials is also low for the same reason. Any refractory material may therefore be considered for the fuel bearing material of a fast reactor with but little regard for nuclear properties. Refractory materials such as tungsten, molybdenum, and metallic carbides may be used. The high uranium concentrations required for the fast reactor compromise the high temperature capabilities of these materials because uranium compounds have melting points considerably lower than those of the fuel bearing materials.

The heterogeneous thermal reactor separates the moderator material from the fuel-bearing material. This separation permits independent cooling of the moderator, allowing it to run at much lower temperatures than the hot fuel element heat transfer surfaces. Water, heavy water, beryllium, and beryllium oxide may be considered for the moderator. The fuel-bearing material can be any of the best refractory materials such as tungsten or graphite but must be a low neutron absorbing material as well. If tungsten were to be used, it should be enriched with tungsten-184 because the other isotopes of tungsten are high neutron absorbers.

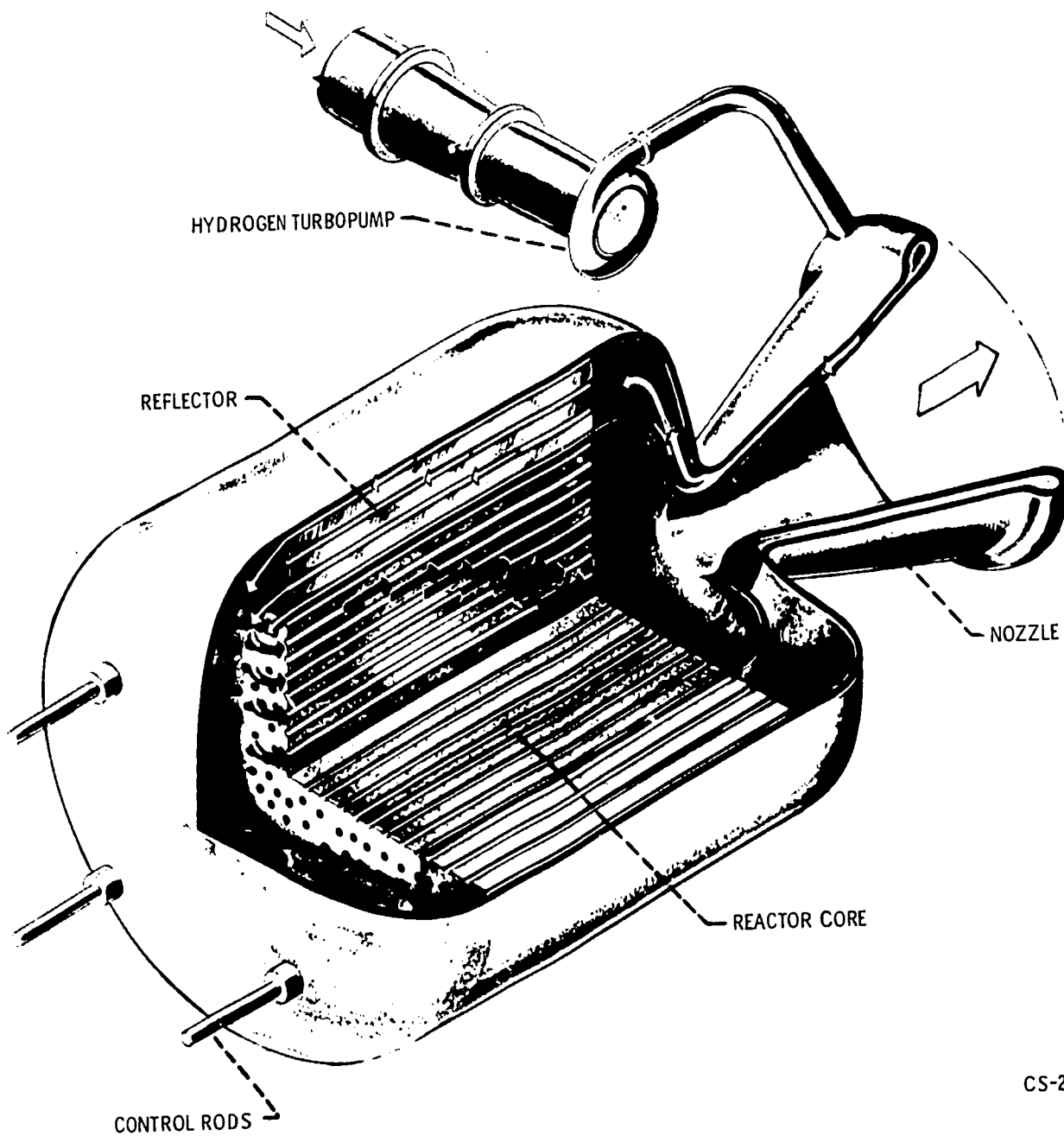
Reactors are employed in nuclear rockets in the manner illustrated in figure 19-4. This figure shows the propellant flow path. Liquid hydrogen is pumped from a storage tank through the nozzle walls and the reflector to cool these components. The hydrogen then flows through the reactor, where it is heated to a high temperature, and finally out the nozzle to produce thrust.

Power to drive the pump is supplied by a turbine which can be at one of several locations. Figure 19-5 shows an engine system using what is called a bleed turbine driven by hot hydrogen bled off the main hydrogen stream at the nozzle inlet. This bleed flow exhausts through auxiliary nozzles. Only a small percentage of the total flow is required to drive the turbine. Except for this bleed flow, the hydrogen flow path is the same as in figure 19-4.

Calculated weights of rocket engines employing the three reactor types of table 19-I are shown in figure 19-6. To these weights must be added the weight of shielding required to protect the cargo or crew from nuclear radiation. The minimum weights are of the order of a few thousand pounds; they cannot be made lighter, even if the thrust is zero. Consequently, a small scale working model is out of the question. An actual nuclear rocket engine is currently being developed under joint sponsorship of the AEC and NASA. A photograph of this engine under test is shown in figure 19-7.

The weight associated with the nuclear reactor and its radiation shield results in nuclear rocket engines being heavier than chemical rocket engines. Therefore, nuclear rockets offer better performance only when the engine weight is small relative to the propellant weight. In such cases, the higher specific impulse reduces the weight of pro-

pellant more than enough to compensate for the heavier engine. Therefore, high-energy missions (for example, interplanetary flight) can be accomplished with nuclear rocket vehicles that weigh considerably less than chemically powered vehicles.



CS-22804

Figure 19-4. - Propellant flow path through nuclear rocket.

314

314

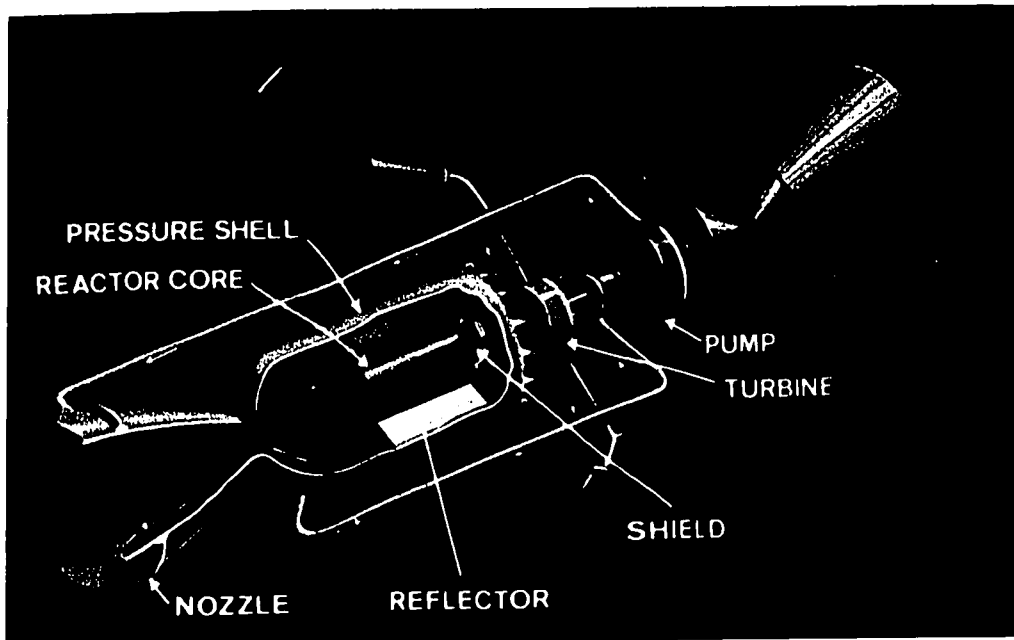


Figure 19-5. - Nuclear rocket engine.

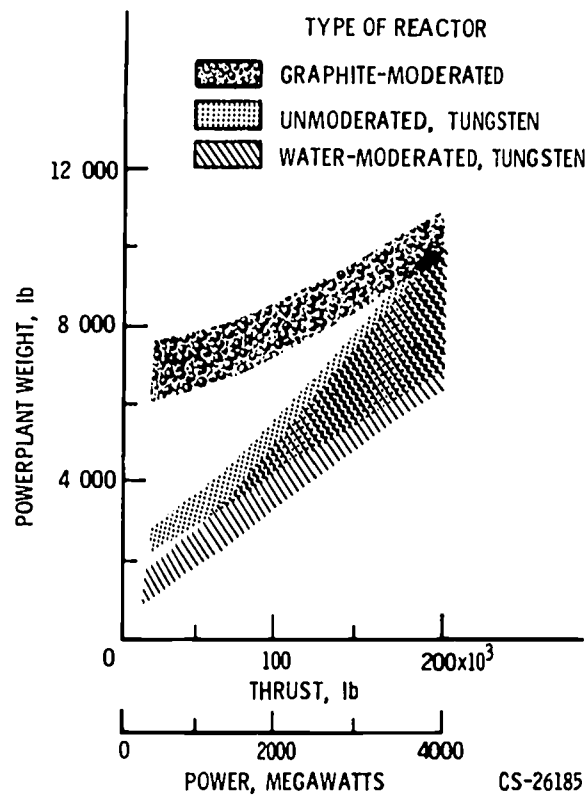


Figure 19-6. - Nuclear rocket powerplant weight.

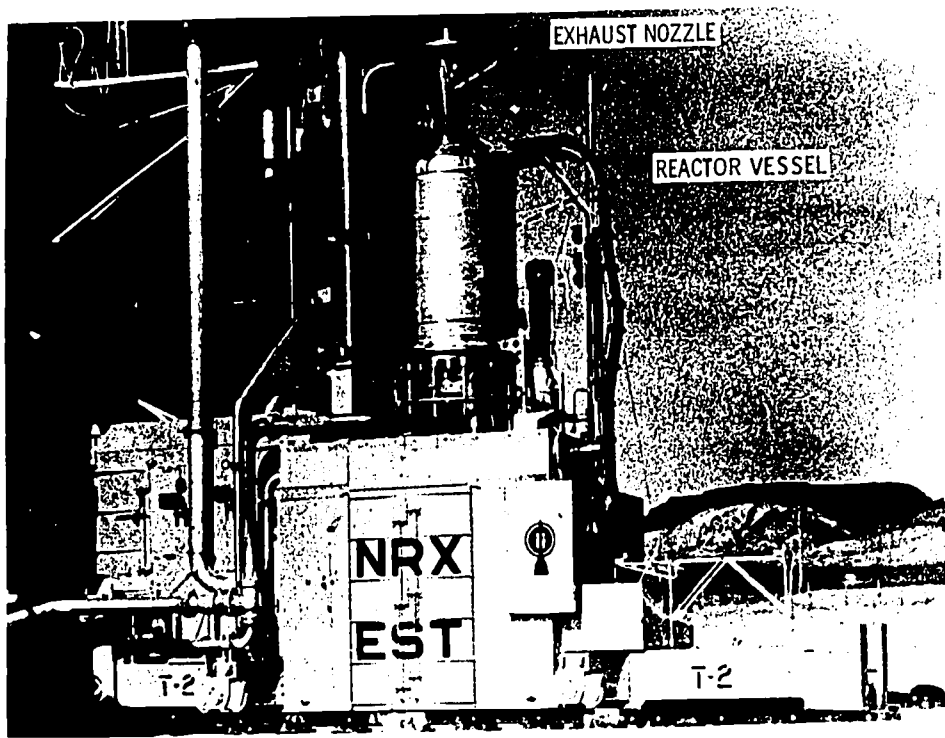


Figure 19-7. - Nuclear rocket engine under test.

20. ELECTRIC PROPULSION

Harold Kaufman*

The chemical rocket has a high propellant consumption because it has a low exhaust velocity. Because the relation between propellant consumption and exhaust velocity is not easily seen, some explanation is required. An important quantity in rocket space flight is the total impulse. This quantity is simply the rocket thrust multiplied by the thrusting time:

$$\text{Total impulse} = (\text{Thrust})(\text{Thrusting time})$$

In general, the longer the distance a rocket must travel or the faster must be its trip, the higher the total impulse must be. Thrusting time can be measured directly, but thrust itself can be calculated from

$$\text{Thrust} = (\text{Propellant flow rate})(\text{Exhaust velocity})$$

which may be introduced into the first equation as follows:

$$\text{Total impulse} = (\text{Propellant flow rate})(\text{Exhaust velocity})(\text{Thrusting time})$$

But, since propellant flow rate multiplied by thrusting time equals propellant mass, the first equation can now be simplified to describe total impulse as

$$\text{Total impulse} = (\text{Propellant mass})(\text{Exhaust velocity})$$

For a particular space flight, a certain total impulse is required. If the exhaust velocity is low, the propellant mass must be high. The chemical rocket has a low exhaust velocity and, therefore, needs a great amount of propellant.

The reason why chemical rockets have a limited exhaust velocity is because all chemical propellants have a fixed energy per pound (i. e., heat of combustion). Since the chemical combustion process can release only so much energy per pound, the exhaust velocity is limited to about 4000 meters per second. Fortunately, several other concepts of rocket propulsion systems promise much higher exhaust velocities. If these concepts can

*Assistant Chief, Electromagnetic Propulsion Division.



Figure 20-1. - Dr. Robert H. Goddard, American rocket pioneer.



Figure 20-2. - Professor Hermann Oberth, German rocket pioneer.

be made practical, high propellant mass would be unnecessary and heavy payloads could be carried on long-distance, fast, space flights.

Dr. Robert H. Goddard (fig. 20-1), the famous American rocket pioneer, realized that chemical rockets were limited in exhaust velocity. In 1906 he wrote that this limitation in rocket exhaust velocity might be overcome if electrically charged particles could be used instead of burnt gases. Dr. Goddard's idea of using electrically charged particles as a rocket exhaust was in essence the birth of electric propulsion.

The idea of electric propulsion was explored further by Professor Hermann Oberth (fig. 20-2), a German rocket pioneer. In 1929, Professor Oberth described a possible electric rocket design which used high-voltage electric fields to accelerate charged particles to high exhaust velocities.

The acceleration of electrically charged particles requires a large quantity of electric power. In terms of propellant flow rate, the amount of electric power required is

$$\text{Power} = \frac{(\text{Propellant flow rate})(\text{Exhaust velocity})^2}{2}$$

In terms of rocket thrust,

$$\text{Power} = \frac{(\text{Thrust})(\text{Exhaust velocity})}{2}$$

Both of these equations show that electric power requirements increase as the exhaust velocity is increased. Suppose an electric rocket with a 1-pound thrust were to be built. For flights to the nearer planets, an exhaust velocity of 50 000 meters per second (about 100 000 mph) would be best for some electric rockets. More than 100 000 watts of electric power¹ are needed to accelerate enough charged particles to 50 000 meters per second in order to produce 4.45 newtons (1 lb) of thrust. That is enough electric power to light a thousand electric light bulbs or run a hundred electric washing machines.

In the time of Dr. Goddard and Professor Oberth, electric powerplants were very heavy, and conventional powerplants are still too heavy for use in electric rocket spacecraft. Moreover, they require large amounts of heavy fuel: coal, oil, or gas. Such powerplants are so heavy that very little payload could be carried.

The advent of practical atomic power improved the future of electric propulsion for space flight. As early as 1948, two British scientists, Dr. L. R. Shepherd and Mr. A. V. Cleaver (fig. 20-3), suggested that controlled nuclear fission could provide the lightweight power source needed for electric rockets. They described an electric generating system in which a nuclear reactor would heat a fluid to a high temperature. This fluid would drive a turbine, which would then drive an electric generator to provide the electricity required to accelerate charged particles to a high exhaust velocity. Although reactor structures and shields were quite heavy when Shepherd and Cleaver first proposed their plan, nuclear-energy technology has advanced rapidly, and their idea appears more practical today. The development of lightweight nuclear turboelectric systems for space propulsion power is one of today's most challenging problems. The solution of this problem may be one of the keys to practical interplanetary travel.

Once the theoretical feasibility of electric powerplants for space flight had been established, serious thought began to include another essential part of an electric spacecraft, the electric rocket engine or thruster. The first detailed discussion of the electric rocket engine appeared in 1954 when Dr. Ernst Stuhlinger (fig. 20-4) proposed designs for a cesium-ion engine, one of the types of electric rocket engine being tested today.

1

$$\text{Power} = \frac{(\text{Thrust})(\text{Exhaust velocity})}{2}$$

and 1 pound of thrust = 4.45 newtons; therefore,

$$\text{Power} = \frac{(4.45 \text{ newtons})(50\,000 \text{ meters per second})}{2}$$

Since 1 watt = 1 joule per second = (1 newton)(meters per second), power = 111 250 watts.



Dr. L. R. Shepherd



Mr. A. V. Cleaver

Figure 20-3. - Two British scientists who, as early as 1948, foresaw the use of controlled nuclear fission as a lightweight power source for electric rockets.



Figure 20-4. - Dr. Ernst Stuhlinger, who in 1954 presented the first detailed discussion on the electric rocket engine.

Many scientists and engineers have been working on electric propulsion for space flight since 1957. Research on electric propulsion has progressed to the point where electric rocket engines have actually been tested during short space flights. Much more research and development remains, particularly on advanced propulsion systems that convert nuclear to electric energy in new ways.

ELECTRIC THRUSTERS

The electric thruster is a device that converts electric power and propellant into a forward-directed force, or thrust. The general principle of operation is illustrated in figure 20-5. Electric power is used to accelerate propellant material to a high exhaust velocity. This velocity produces thrust. There are three general types of electric thrusters: electrothermal, electromagnetic, and electrostatic.

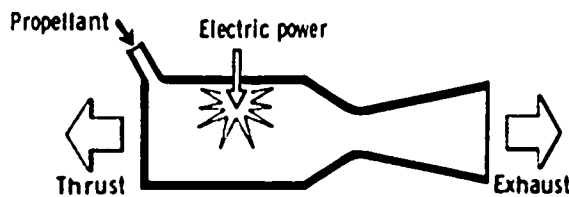


Figure 20-5. - Electric rocket engine.

Electrothermal Thrusters

The electrothermal thruster is similar in some respects to the chemical rocket. Although there is no combustion, the propellant gas is heated to high temperatures and expanded through a nozzle to produce thrust. This rocket can achieve exhaust velocities higher than those of chemical rockets because the energy added to the gas may be larger than the energy of combustion. Breakup or dissociation of the propellant gas molecules, which then absorb energy without raising gas temperature very much, places an upper practical limit on the amount of energy that can be added to the propellant. Other factors, such as material failure at high temperature, also limit the exhaust velocity.

The arcjet (fig. 20-6), in which an electric arc is used to heat the propellant, is one type of electrothermal thruster. The arcjet does not appear too promising as a thruster,

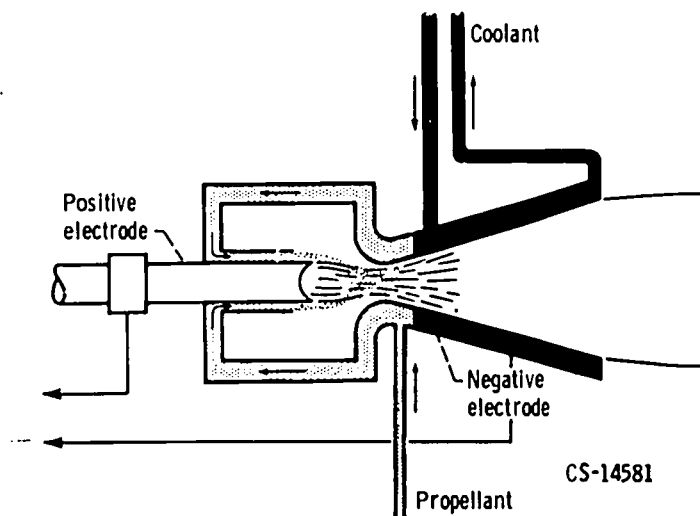
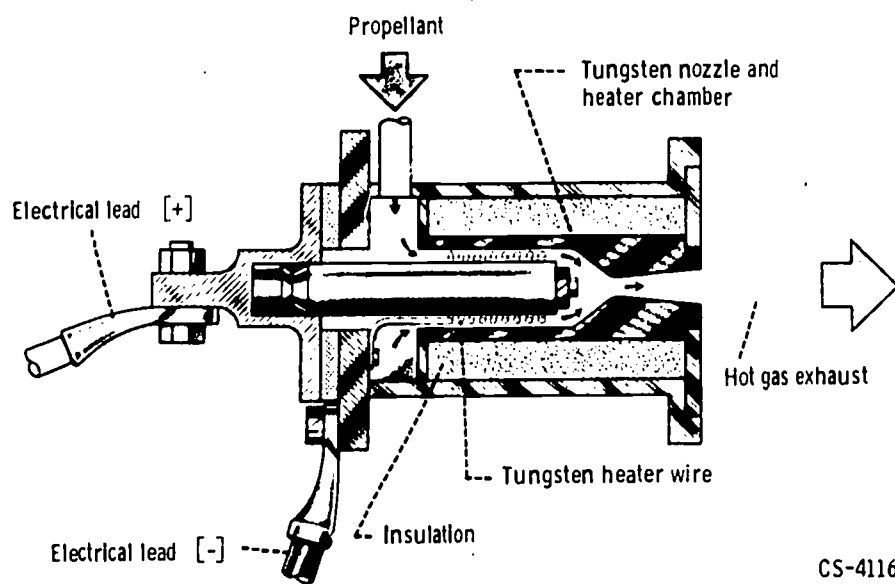


Figure 20-6. - Arcjet electric thruster.

but the technology gained in studying the arcjet has been useful for designing hypersonic wind tunnels and has led to the development of the MPD thruster, which will be described later. The second type of electrothermal thruster is the resistojet (fig. 20-7). In this thruster, a resistance heating element or hot wire is used to heat the propellant. The resistojet is simple, efficient, and reliable. The research effort on this thruster has been completed, and it is the one electric thruster that has already been used in a practical application - the station keeping of a satellite. Future missions will probably use one of the two types of electric thrusters to be discussed next, since they can produce even higher exhaust velocities than electrothermal thrusters.



CS-41165

Figure 20-7. - Resistojet electric thruster.

Electromagnetic Thruster

The electromagnetic thruster is often called the plasma engine (fig. 20-8). In this thruster, the propellant gas is ionized to form a plasma, which is then accelerated rearward by electric and magnetic fields.

A plasma is merely an ionized gas, that is, a gas in which electrons have been removed from many of the atoms. In a neutral atom, such as those comprising the propellant gas, there are as many electrons around the nucleus of each atom as there are protons in the nucleus. Neutrons have no electric charge, protons have one positive charge each, and electrons have one negative charge each. With an equal number of positive and negative charges, the atoms are electrically neutral. This is the normal state for atoms

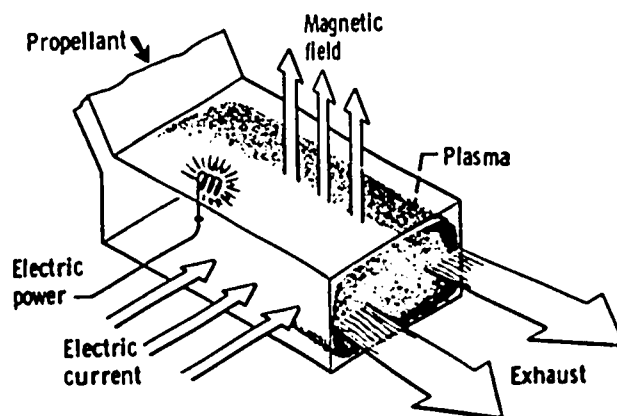


Figure 20-8. - Plasma engine.

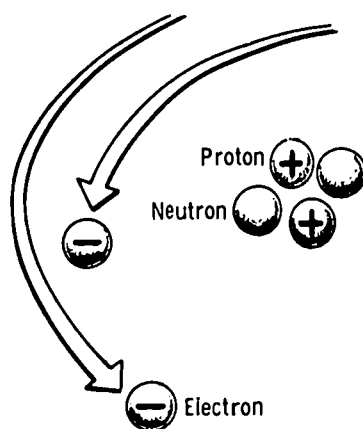


Figure 20-9. - Helium atom.

in a gas at ordinary temperatures. In figure 20-9, if one electron were knocked loose and away from the atom, the atom would have two protons and only one electron. Thus, a net value of one positive electric charge is left. The charged atom is called an ion.

The atom shown in figure 20-9 is a helium atom. It has a simple electronic structure. Other atoms have many more protons, neutrons, and electrons, but the principle of ionization is the same. An atom may be multiply ionized by the loss of several electrons. One of the significant properties of a plasma is that it can conduct electric current just as a copper wire can conduct current. It is this conductivity that makes it possible to accelerate the plasma as shown in figure 20-8. When an electric current is made to pass through the plasma in the presence of a magnetic field, a force is exerted on the plasma. Because of this force, the plasma is accelerated rearward to a high exhaust velocity. Thus, a plasma thruster is quite similar to an electric motor with the plasma taking the place of the moving rotor. This general acceleration principle has been used in many types of electromagnetic (or plasma) thrusters. Some of these have developed into potentially useful thrusters. Most are being used in various plasma physics experiments.

An even more promising electromagnetic thruster is the MPD or magnetoplasmadynamic arc type (fig. 20-10). It resembles an arcjet in general construction with the current passing between an anode and a cathode. It operates at a much lower propellant pressure than an arcjet, though, so that electromagnetic forces provide the dominant thrust-producing mechanism. The magnetic field either can be due to the current between the two electrodes, or it can be produced by a separate field coil as shown in figure 20-10. The advantages of the MPD thruster are its reasonable efficiency and the simplicity of associated electrical circuitry. It does not require much more than a source of low-voltage electric power. Considerable development remains, however, before the MPD thruster will be ready for use in space.

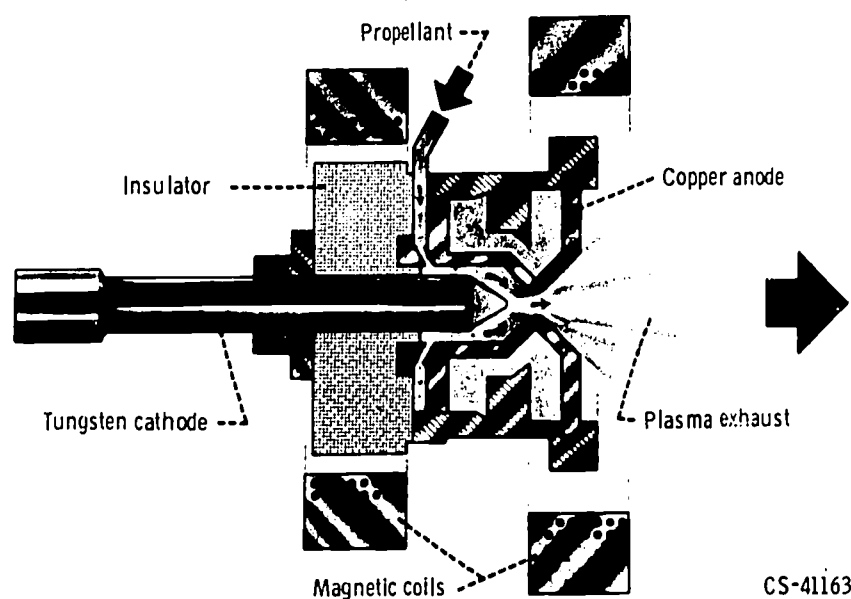


Figure 20-10. - Magnetoplasmadynamic (MPD) arc.

Electrostatic Thruster

The last general type of electric thruster, the electrostatic, is almost as well developed as the resistojet. It also uses ionized propellant, but the ions are accelerated without mixing in the electrons with them. After the ions are accelerated, the electrons must also be ejected. Otherwise the charge accumulation on the space vehicle would interfere with thruster operation. The mixing of the ejected electrons with the ion beam is called neutralization.

Simply stated, the operating principle of the electrostatic thruster is that like charges repel and unlike charges attract. The ion source has many like-charged ions which repel each other. The accelerator grid is charged with unlike charges, or electrons. This combination of repulsion and attraction serves to eject the ions with a high exhaust velocity.

There are different ways of producing ions. One is the contact ionization method (fig. 20-11) where a cesium propellant atom loses an electron (and thus becomes an ion) by passing through porous tungsten. The tungsten has to be hot enough to boil off the ions. The power needed to heat the tungsten is the largest loss in the contact-ionization thruster.

Contact-ionization thrusters appear best suited for low-thrust applications, such as station-keeping duty on a satellite. For larger sizes of electrostatic thrusters, electron bombardment appears to be a more efficient means of producing ions (fig. 20-12). Ions are produced in this type of thruster by striking propellant atoms with energetic electrons

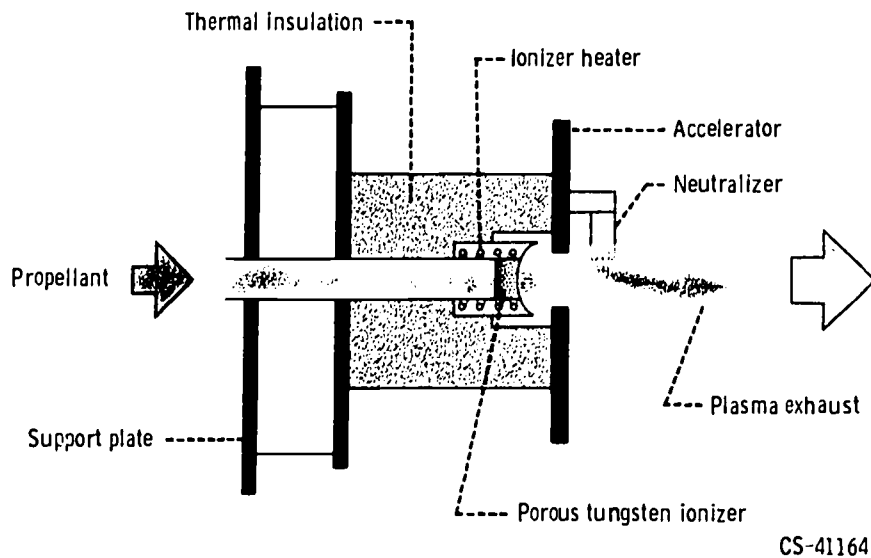


Figure 20-11. - Contact ionization thruster.

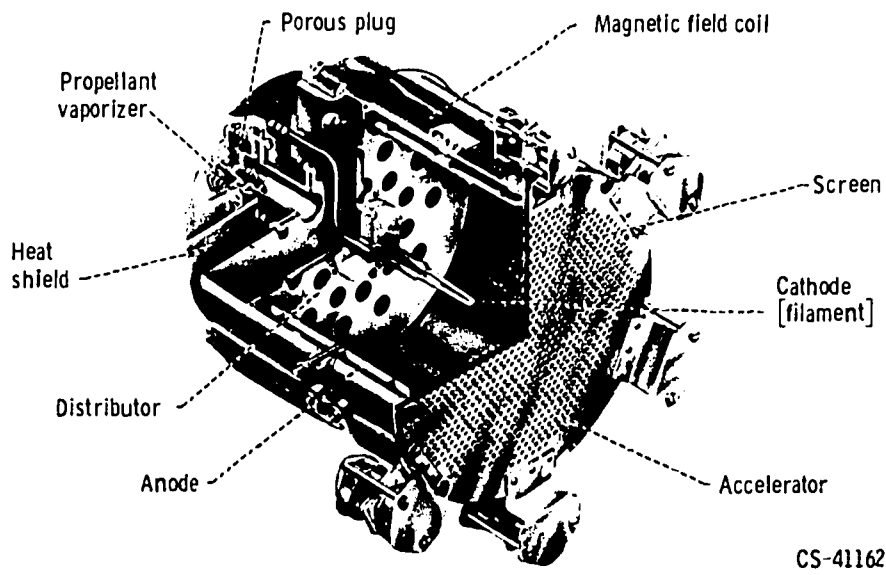


Figure 20-12. - Electron-bombardment thruster.

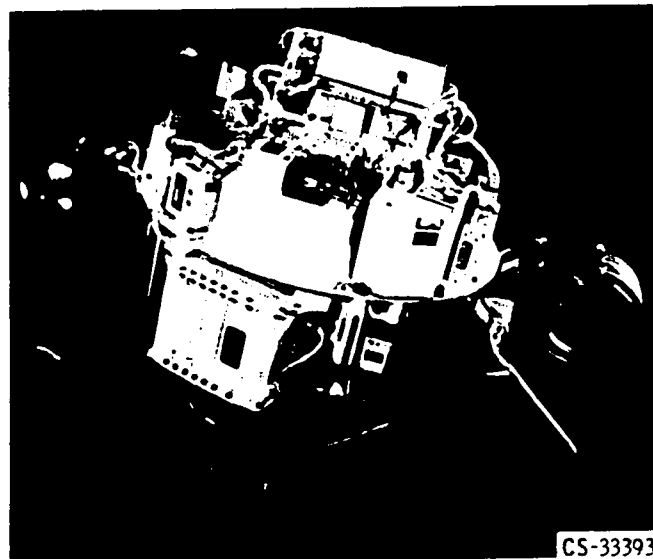


Figure 20-13. - SERT I spacecraft.

which are emitted from the hot cathode. The electron-bombardment thruster has already been tested in space for a short time on the SERT I payload (fig. 20-13). The letters SERT stand for Space Electric Rocket Test. SERT I was launched July 20, 1964, by NASA on a ballistic trajectory over the Atlantic Ocean. It was the first time that an ion engine of any type had been successfully operated in space. Measurements made during the flight conclusively proved that neutralization was not a problem and that an ion engine can generate thrust in space.

ELECTRIC POWERPLANTS

In the total electric propulsion system, the electric powerplant appears to be the heaviest component. For this reason, the specific mass of the powerplant is of major importance.

Space missions require very high total impulse, and the associated energy must be carried in a very lightweight form. Solar and nuclear energy sources appear to be the only forms of energy having sufficiently light weight. Solar energy itself is "free," but collection devices have an appreciable mass. Nuclear fission, radioisotope decay, and nuclear fusion all require onboard nuclear fuel, but the energy content is so high that fuel mass is a small part of the total mass for nuclear-electric powerplant schemes conceived so far.

A part of the solar spectrum is converted directly into electric power in solar cells by a photoelectric effect. Conventional solar cells are made of two thin layers of silicon, each of the two sheets having small amounts of artificially introduced impurity atoms.

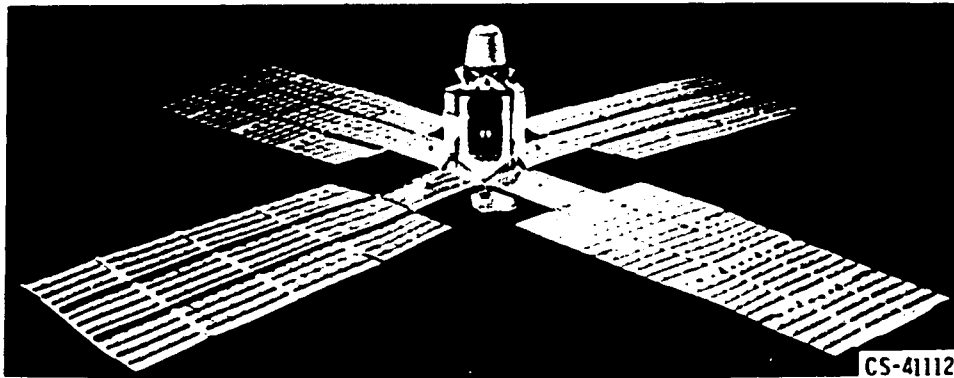


Figure 20-14. - Interplanetary probe with solar panels.

Collisions of solar photons with electrons in the top layer produce a current to the bottom layer, and hence electric power. Recent investigations with cadmium sulfide indicate that this material may be better than silicon for lightweight solar-cell arrays.

Studies of solar-cell panels based on present knowledge indicate that specific masses may be reduced to 25 to 50 kilograms per kilowatt for power levels in the range from 10 to 100 kilowatts operated in the vicinity of Earth. Such solar-cell panels would have an area of about 10 square meters for each kilowatt of electric power. The solar radiation varies inversely with the square of the distance from the Sun, so that solar-cell panels will produce less power for outward-bound missions. This effect is not severe for Earth-Mars missions, but is large for missions to planets beyond Mars. Future developments, such as the use of cadmium sulfide cells may permit the specific masses of solar-cell panels to be reduced to 10 to 25 kilograms per kilowatt. A design of a possible solar-powered interplanetary probe is shown in figure 20-14. The large solar-cell panels dwarf the rest of the vehicle.

Of the various powerplants being investigated for electric propulsion, the nuclear turboelectric is the most conventional in the sense that it has been used extensively for ground-based electric-power generation. The heat released in a nuclear reactor during fission is absorbed by a fluid passing through the reactor (fig. 20-15). The fluid carries

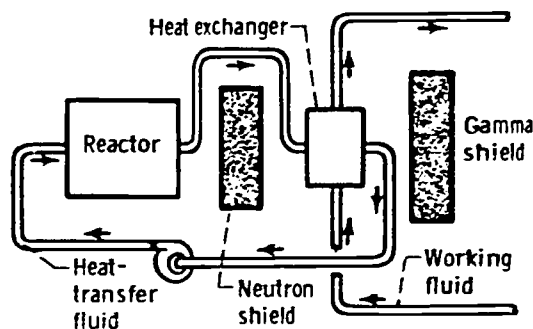


Figure 20-15. - Vapor-generating system of nuclear turboelectric powerplant.

this heat to a heat exchanger. There the heat of fusion is transferred from the heat-transfer fluid to the working fluid. The working fluid turns into vapor at a high pressure and drives a turbine. The turbine powers an electric generator to produce the electricity used to run the electric rocket engines.

Vapor being exhausted from the turbine must be cooled and condensed before it flows back to the heat exchanger, where it is heated and vaporized again. Because space is a vacuum, this cooling must be accomplished with a large radiator (fig. 20-16). There is

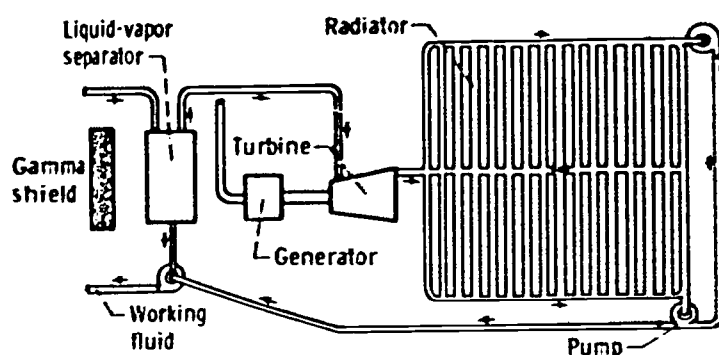


Figure 20-16. - Vapor-condensing system of nuclear turboelectric powerplant.

a greater probability of a micrometeoroid hitting a large area than a small one, and, therefore, the giant radiator must have tube walls thick enough to prevent punctures by micrometeoroids. Punctures would allow the working fluid to leak out. If this occurred, the spacecraft would stop thrusting and go into orbit around the Sun forever. Thick tube walls make the radiator heavy. Since very lightweight powerplants are needed for space flight, scientists are trying hard to design better, lighter radiators.

Analytical studies of nuclear-electric power sources for space use indicate that specific masses of 10 to 15 kilograms per kilowatt might be obtained. These low specific masses, though, require a powerplant which produces at least several hundred kilowatts. A powerplant with this capability is heavy, partly because a nuclear reactor must be large in order to function at all. This requirement for large size, together with the number of complicated components that are needed, means that such a nuclear-electric power source will be much more difficult to develop than a lightweight solar-cell power source. A nuclear-electric power source would, of course, have the advantage of being independent of solar radiation.

A design for an electrically propelled spacecraft using a nuclear-electric power source is shown in figure 20-17. Because a nuclear-electric powerplant has a low specific mass (kilograms per kilowatt) only in large sizes, the spacecraft of figure 20-17 is designed for a manned mission. To lighten the mass of the radiation shielding required,

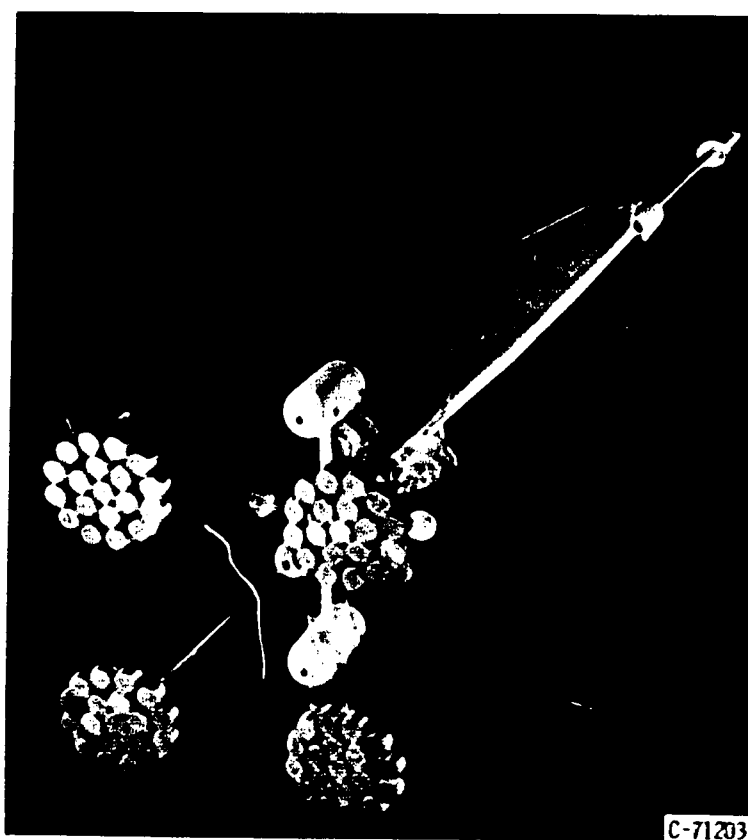


Figure 20-17. - Nuclear electric spacecraft.

the nuclear reactor is at the opposite end of the spacecraft from the crew cabins. The large panels in the middle of the spacecraft are the radiators, and the electric thrusters are in the four clusters next to the crew cabins.

There are several variations of nuclear-electric powerplants that have been proposed for electric propulsion. These variations use thermionic converters or MHD (magnetohydrodynamic) ducts to replace the turbine and generator. Although even less developed than the turbine-generator approach, these alternatives would have the advantage of fewer moving parts.

MISSIONS

As mentioned earlier, the chemical rocket has an upper limit to its exhaust velocity; for this reason, a large propellant mass must be used for long-distance flights that require a large total impulse. The electric rocket has a much higher exhaust velocity, with the result that much less propellant is needed.

The propellant mass required for a particular space flight (i. e., a particular total impulse) can be shown on a graph (fig. 20-18). The electric power requirement, how-

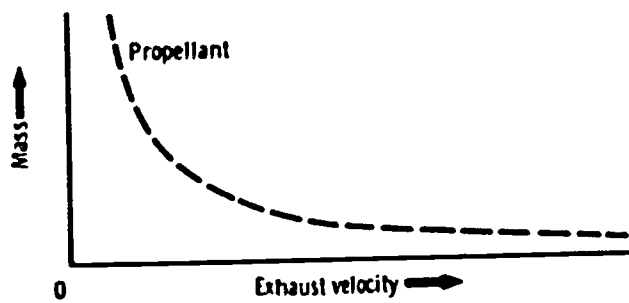


Figure 20-18. - Effect of changing exhaust velocity on propellant mass required for a specific flight.

ever, increases as the exhaust velocity increases. If the electric powerplant mass is directly proportional to its power output, the powerplant mass can also be shown on the graph as in figure 20-19. The sum of the propellant and the powerplant masses can now be shown with respect to the total spacecraft mass (fig. 20-20). The available payload mass is the shaded portion. There is a lower limit for the exhaust velocity; if the exhaust velocity is less than this lower limit, the propellant required would exceed the total mass of the vehicle. If the exhaust velocity is too high, the electric powerplant will have too much mass. In either case, the spacecraft cannot be built. It is evident that the best exhaust velocity to use is that which will allow the most payload to be carried (the lowest

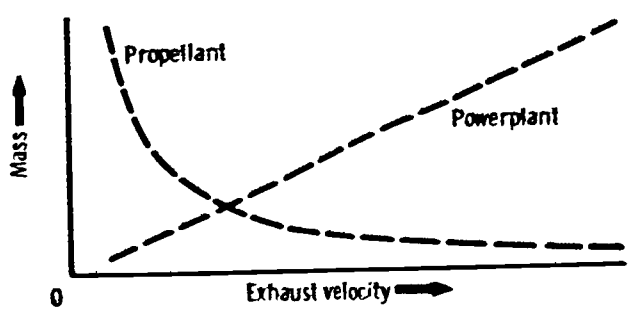


Figure 20-19. - Relation between powerplant mass and propellant mass for different exhaust velocities.

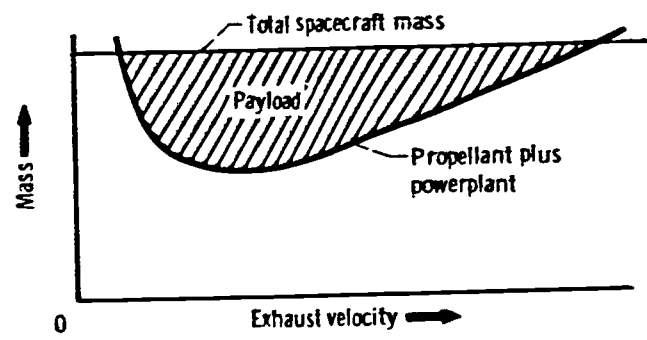


Figure 20-20. - Optimum mass and exhaust velocity for fixed total mass.

point on the shaded area of fig. 20-20). For trips to the nearest planets, the optimum exhaust velocity of electric rockets is almost always between 20 000 and 100 000 meters per second.

If a spacecraft is to take off from the Earth's surface, its thrust must be greater than its weight. For such a flight, the electric-rocket thrust would have to be much greater than the weight of the powerplant. The principles described so far can be used to show that extremely lightweight powerplants (of the order of 0.0001 kg/W) would be required. Thus, a powerplant with an output of 1000 watts could weigh only a few ounces. Space electric powerplants currently under development are hundreds of times heavier than this. Consequently, electric spacecraft currently being studied cannot be expected to take off from Earth. They must be boosted into orbit about Earth by chemical rockets.

Once in Earth orbit, electric spacecraft could fly very well with a small thrust. The electric rocket engine of an interplanetary vehicle would be started in orbit and the spacecraft would continue around the Earth in an ever-widening spiral until it effectively left the Earth's gravitational field (fig. 20-21). More precisely, it would enter a region in space where the gravity pull of the Earth is slight compared with the gravity of the Sun.

In this description of flight paths not much has been said of the actual speed of the spacecraft. Speed can be a misleading idea in the complex gravitational field of the solar system. Satellites decrease in speed as they move away from Earth. A low-level satellite moving at 7.7 kilometers per second (17 300 mph) takes about $1\frac{1}{2}$ hours to orbit the Earth. The Moon is a satellite of the Earth, too. It takes about 27 days to orbit the Earth, moving at a speed of about 1 kilometer per second (2300 mph). Thus, the Moon travels almost eight times slower with respect to the Earth than does the low-level satellite.

The electric rocket is also affected by this principle. It would move more slowly farther away from Earth. The work being done by the powerplant and the engine would be

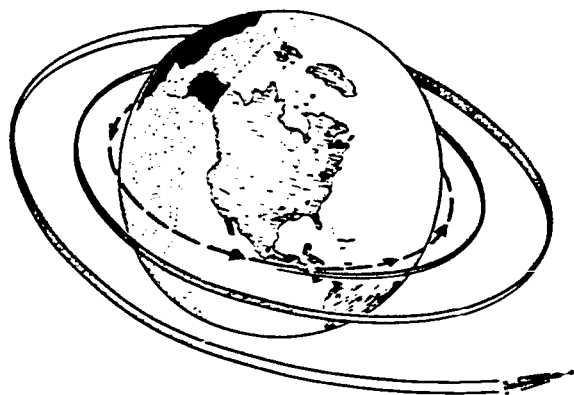


Figure 20-21. - Spacecraft departure path from Earth.

used in raising the ship up and out of the Earth's gravitational field. This work would not increase the ship's speed. The chemical rocket booster would provide the initial spurt in speed required to place the electric spacecraft in orbit. From there on, the electric rocket could provide the rest of the propulsion.

When the interplanetary electric spacecraft is hundreds of thousands of miles from Earth, the gravitational field of Earth becomes weaker than the gravitational field of the Sun. During the transition from dominance of Earth's field to dominance of the Sun's, the ship is attracted to both Earth and the Sun. This situation is so complicated that the ship's path must be calculated on a digital computer even when the rocket is coasting. When free from Earth, the ship still has the speed of Earth in addition to its speed with respect to Earth (fig. 20-22). For a mission to Mars, the electric spacecraft continues

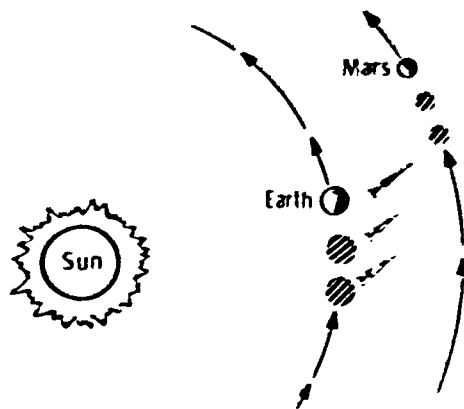


Figure 20-22. - Relative positions during spaceflight.

to thrust in the direction shown. Because it still has the speed impetus from Earth, it tends to move on around the Sun. The energy provided by the continued thrusting causes the ship to move farther away from the Sun, but because it is farther away from the Sun, it falls behind Earth in the race around the Sun. The initial speed provided by the Earth is important to any spacecraft. Without it the ship would fall into the Sun.

When the ship is about halfway to Mars, it is orbiting the Sun faster than Mars because it is closer to the Sun. In order to orbit Mars the ship must be swung around (fig. 20-23) to apply the reverse thrust necessary to slow it down to the speed of Mars. When the ship reaches the gravitational field of Mars, it must spiral down to a satellite orbit around Mars (fig. 20-24). The ship continues to thrust backward as it spirals down.

The low thrust of the electric rocket will not permit a direct landing on Mars. If the ship is manned, the crew may descend to the surface of Mars in a chemical rocket while the electric spacecraft continues to swing around Mars in its satellite orbit (fig. 20-25).

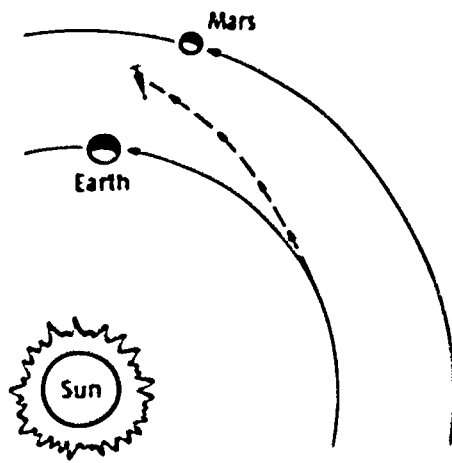


Figure 20-23. - Spacecraft assumes braking position.

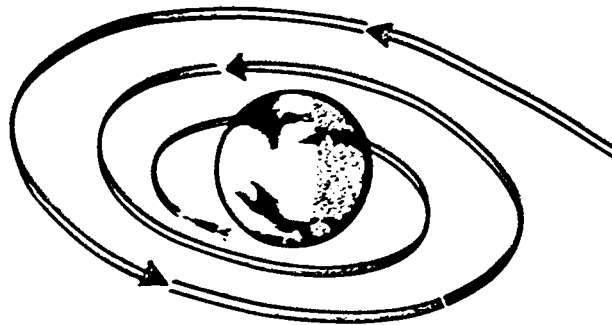


Figure 20-24. - Mars arrival path.

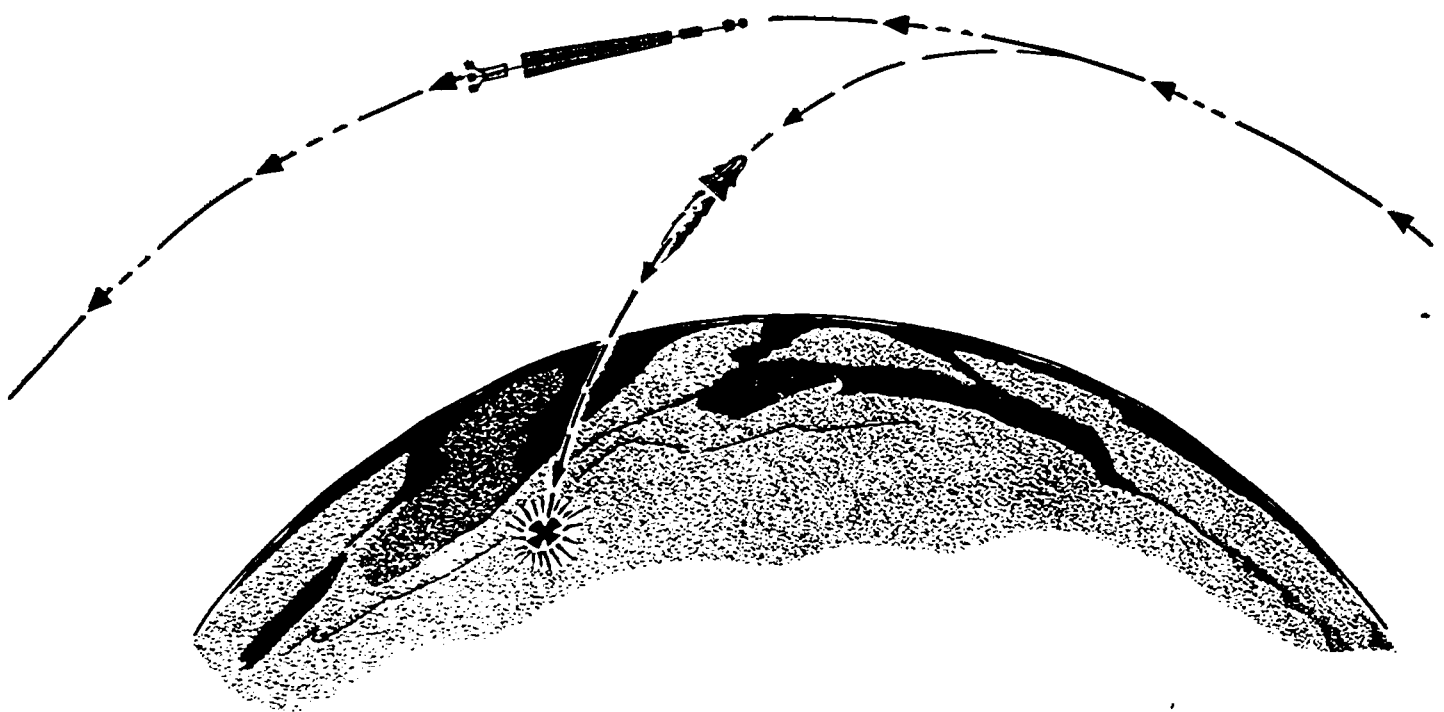


Figure 20-25. - Mars orbit and chemical rocket shuttle.

It is typical of interplanetary electric-propulsion missions that the thrusters are operated most of the time. This nearly continuous operation is necessary to make the best use of the limited power available for propulsion.

Figure 20-26 illustrates the theoretical performance of electric propulsion in orbiting a payload around Mars. The 25-kilograms-per-kilowatt curve is for power sources

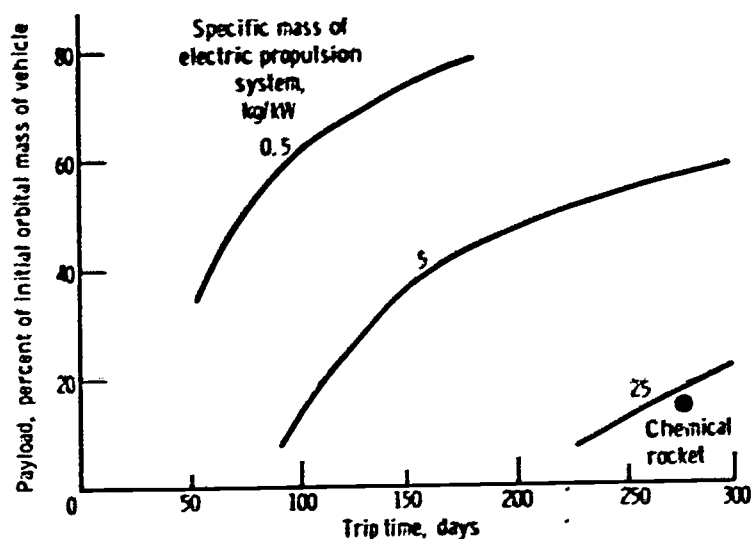


Figure 20-26. - Theoretical performance of electric propulsion system for Mars orbiter mission.

(either solar cell or nuclear electric) presently under development. The 5-kilograms-per-kilowatt curve is perhaps the best that might be hoped for with future development of these systems. Completely new approaches, though, may result in even lighter power sources, as indicated by the 0.5 kilogram per kilowatt curve. A word of caution must be included about these weights. The power source is the heaviest component of an electric propulsion system. Other components also have mass, as well as power losses, that must be included. Thus, the mass of the power source must be less than 25 kilograms per kilowatt if the complete system is to reach that value.

There are also various ways of conducting missions. Figure 20-26 is for a vehicle that uses electric propulsion starting from a low Earth orbit and ending in an orbit around Mars. If the space vehicle is first boosted to escape velocity from Earth (about 25 000 mi/hr) with a chemical rocket, the spiraling portion of the mission (fig. 20-21) can be omitted. The electric propulsion can then be confined to the portion of the mission that is in the Sun's gravitational field (figs. 20-22 and 20-23). This approach, called thrust augmentation, offers less gains for very light power sources, but substantially improves the performance of systems with 25 to 50 kilograms per kilowatt.

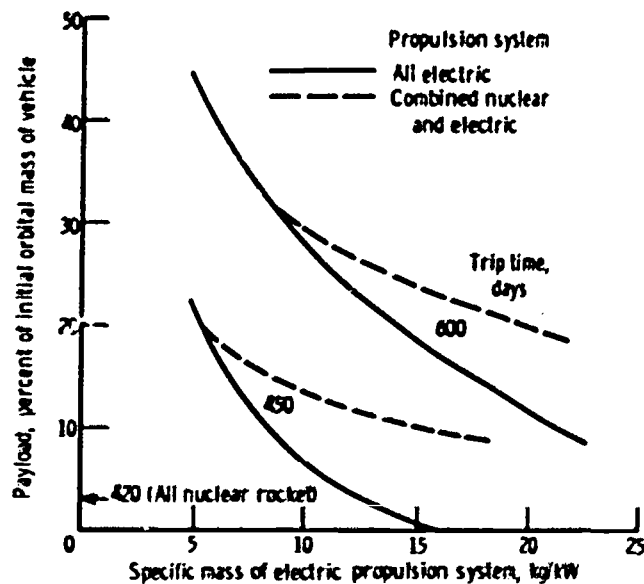


Figure 20-27. - Comparison of theoretical performance of nuclear and electric propulsion systems for Mars roundtrip mission.

The theoretical performance of nuclear and electric propulsion systems are compared in figure 20-27 for a Mars roundtrip mission. The percent payload was calculated on the basis of the starting mass in Earth orbit, as was also done for figure 20-26. Also, some atmospheric braking (11 km/sec) was assumed on return to Earth. Only one trip time is included for the nuclear rocket (420 days), inasmuch as additional time does not give payload advantages for the nuclear rocket in the same way as for electric propulsion. Two trip times are shown for electric propulsion. The 450-day trip time roughly matches the trip time of the nuclear rocket, and the 600-day trip time shows the effect of a substantial increase in this time. To approximate both the trip time and payload of the nuclear rocket, the electric propulsion system must weigh less than about 13 kilograms per kilowatt. If longer trip times are acceptable, though, the electric propulsion system can carry bigger payloads with even relatively heavy system weights. Also shown in figure 20-27 is the performance of a combined system. Roughly speaking, the nuclear rocket is used near planets (except for Earth atmospheric braking) and the electric propulsion system is used in interplanetary portions of the mission. For most of the range of interest, the combined approach shows advantages over either approach used alone.

Large interplanetary vehicles that use electric propulsion are many years away. The first practical applications of electric thrusters will be the control of satellites. In fact, as mentioned earlier, a resistojet has already been used in this application. Some satellites must be held in specific attitudes so that their instruments, antennas, or solar cells will work correctly. Other satellites must also be held in particular positions relative to Earth. For example, "synchronous" satellites must be held directly over a single spot on Earth. These are also called "24-hour satellites" because they orbit at

such an altitude over the equator that the satellite revolves around the center of the Earth once every 24 hours. Since the Earth also rotates once in a 24-hour period, the orbiting satellite is stationary in relation to Earth.

Forces tending to disturb the attitude or position of a satellite are many; they are due to the oblateness of Earth and the gravitational attractions of the Sun, the Moon, and other celestial bodies. These forces are small, but over a period of days or weeks they can appreciably affect the satellite. Ion rocket engines may be well suited to overcoming these perturbing forces on satellites. The ion rocket thrust is small, but so are the perturbing forces.

Ion engines have a low propellant consumption because of their high exhaust velocities. Solar cells can provide enough electric power to run the ion engines. For these reasons, ion engines can be satisfactorily used for attitude control and position keeping of long-life satellites.

21. BIOMEDICAL ENGINEERING

Kirby W. Hiller*

Listening to the heart by direct ear contact is said to have begun with Hippocrates in the late fourth century B. C. During the following 2200 years, the method was used with limited success for examining patients with suspected heart trouble. One of the main limitations was that the method could not be used on fat people because the fat muffled the sound. It was exactly this problem, a fat patient with suspected heart trouble, that faced René Laënnec in 1816, and his solution became an early example of the application of engineering principles to medicine. The following is a description of the incident in Laënnec's own words (ref. 1):

I happened to recollect a simple and well-known fact in acoustics . . . the great distinctness with which we hear the scratch of a pin at one end of a piece of wood on applying our ear to the other. Immediately, . . . I rolled a quire of paper into a kind of cylinder and applied one end of it to the region of the heart and the other to my ear, and was not a little surprised and pleased to find that I could thereby perceive the action of the heart in a manner much more clear and distinct than I had ever been able to do by the immediate application of the ear.

Laënnec called his instrument a stethoscope and experimented with many materials and configurations to improve it.

The recent dramatic increase in the applications of aerospace engineering principles to medicine has given rise to a new field of engineering - biomedical engineering. Market survey organizations have been studying the prospects for this field, and they predict that it will grow into a young giant, becoming one of the seven new industries to surpass the billion dollar mark in the 1970's. It should be worthwhile to examine the nature of this new field and to consider what factors may be responsible for its growth.

Engineering principles are applied to biology and medicine in four main areas: diagnostics, treatment, prosthetics, and biological research. These areas are discussed in the following sections.

DIAGNOSTICS

Diagnosis is the process by which a disease is identified from its symptoms. Engi-

*Head, Airbreathing Engine Controls Section.

neering equipment lends itself to a wide variety of these applications. The following are some examples.

X-ray photography. - Almost as soon as it was discovered in 1895, X-ray photography (fig. 21-1) became one of the best known and most useful applications of engineering to medicine and has remained so ever since. The X-ray machine demonstrates one of the most desirable features of any diagnostic equipment: in operation, it affects neither the patient nor the pathological condition it must examine. (A glossary of medical terms is given at the end of this chapter, p. 21.) It depends entirely on the differences in opacity to X-rays of the various tissues for its success. Radiopaque substances, if swallowed or injected, follow the motion of fluids through the body and these can then



(a) Normal foot in shoe (taken by D. C. Miller, probably in early 1896).



(b) Composite self-portrait of D. C. Miller (probably taken in early 1896).



(c) Dislocated thumb (taken by D. C. Miller on March 13, 1896).



(d) Hand with parts of fourth and fifth fingers removed by buzz saw (taken in April 1922). Note improvement in X-ray technique.

Figure 21-1. - Early examples of X-ray photography. (Original plates loaned to NASA by Professor Robert S. Shankland, Case Western Reserve University.)



(a) Before surgery.



(b) After surgery. (The dark area at the patient's mouth is a pipe.)

Figure 21-2. - Infrared photographs showing variation in skin temperature of patient with blocked carotid artery. Dark areas indicate lower temperatures. (Courtesy of Dr. Warren Zeph Lane, Norwalk Hospital, Norwalk, Conn.)

be studied. For rapid motion, as in the circulatory system, X-ray motion pictures are taken.

Infrared photography. - If infrared-sensitive film is used to photograph a patient, the resulting image indicates variations in skin temperature. The presence of cancer, for example, may show up as a slight decrease in temperature over the afflicted area of the body. Figure 21-2 is an example of an infrared photograph. Figure 21-2(a) shows the facial temperature pattern of a patient who has a blocked carotid artery (the principal artery of the neck). Before surgery, the patient's average facial temperature is about 94.3° F, and his nose is particularly cold. After surgical removal of the blockage (fig. 21-2(b)), the patient's average facial temperature is about 0.5° warmer. (The dark area at the side of the patient's mouth is a pipe.)

Blood-sample diagnosis. - A typical large hospital performs thousands of chemical analyses per week on blood samples from patients. These analyses are slow and subject to human error. A machine is now available that automatically separates a blood sample into a dozen or so subsamples which are fed into analysis modules. Reagents are added automatically, the mixture may be heated or filtered, the results are analyzed optically by photocells, and the results are printed.

Patient monitoring. - Automatic monitoring equipment in use for intensive-care patients provides continuous electronic sensing of the electrocardiogram (EKG) signal, pulse rate, blood pressure, and respiration rate. When one of these parameters falls outside of normal limits, an alarm is automatically sounded and an automatic chart printout is initiated.

Telemetry. - Small transmitters, in combination with patient monitoring sensors, can be carried on or in the patient and make it possible to monitor the patient in action. Microelectronic devices developed for space programs have advanced this field. It is possible to monitor the blood pressure and heartbeat of a patient while he is climbing stairs. A small capsule is available which, when swallowed, telemeters back a signal indicative of the temperature in the alimentary canal.

Computer diagnosis. - Today, one of the most common uses of computers is in the maintenance of centralized records and medical information. A knowledge of past medical history is often valuable in treating a specific illness, and with people traveling more, centralized records can make their medical history available to physicians all over the country. Travel, by exposing people to a wider variety of diseases, introduces another medical problem which computers are able to help solve: although a doctor in Colorado, for example, may be very familiar with tick fever, he seldom encounters a case of malaria; for a doctor in another place, the reverse may be true. Centralized medical information makes it easier for each doctor to use the experiences of the other.

Diagnostics summary. - The many fruitful techniques for applying engineering to diagnosis gives this branch of biomedical engineering a bright future. It will grow rapidly and, in so doing, will rely on miniature instruments to probe into hitherto inaccessible areas of the body. Automated medical analysis will encourage the clinical approach, in which the patient will be given a comprehensive series of tests that will then be interpreted by computers. The role of the physician will change; instead of a man who makes a diagnosis on the basis of broad experience and a few well-selected tests, he will become increasingly concerned with using and improving diagnostic equipment.

The education and experience requirements of the physician will change. There will be opportunities for physicians who are very knowledgeable about engineering equipment and for engineers who are well versed in anatomy and physiology.

TREATMENT

Medical engineering equipment is being developed which makes new treatment techniques possible. Some examples are now presented.

Heart-lung machine. - In the human circulatory system (fig. 21-3), blood returns from the body to the right atrium of the heart; from there, it passes into the right ventricle, which pumps it to the lungs for oxygenation. Following this, the blood reenters the heart at the left atrium, moves to the left ventricle, and is pumped back into the body.

During operations on the heart or lungs, it is generally dangerous to expect them to continue functioning normally. Moreover, even if they do, such activity may easily com-

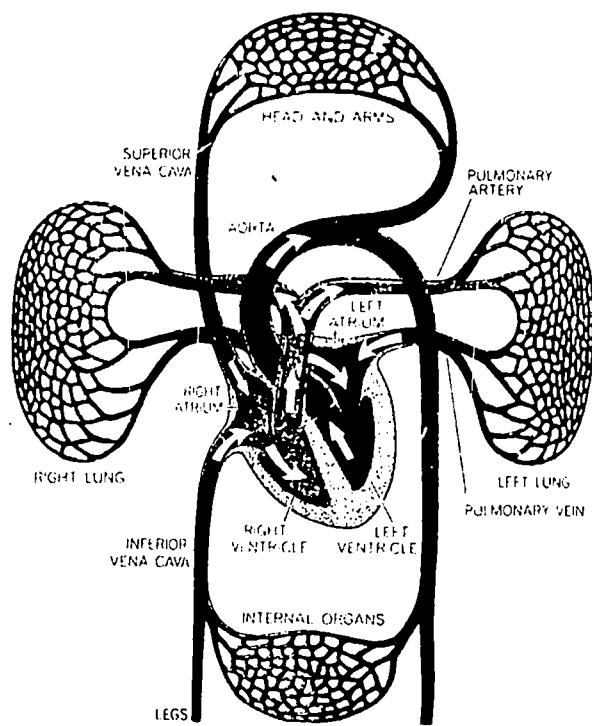


Figure 21-3. - Human circulatory system. (From "An Artificial Heart Inside the Body," by Willem J. Kolff. Copyright 1965 by Scientific American, Inc.)

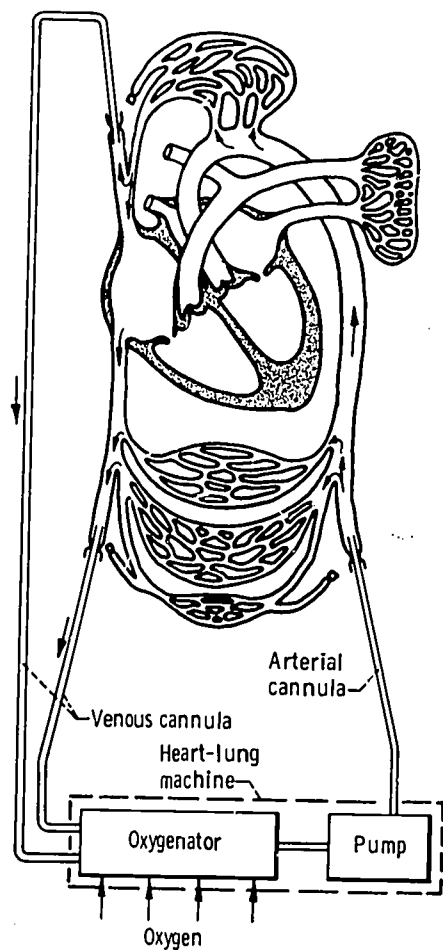


Figure 21-4. - Human circulatory system with heart-lung machine.

plicate the surgeon's problems. Surgery in this region of the body is much simpler when the heart and lungs can be inactivated without danger to the patient. This is the job of the heart-lung machine (fig. 21-4).

While the blood is outside the body for oxygenation and pumping, it is cooled by being run through a heat exchanger to reduce the patient's body temperature quickly to a state of deep hypothermia. This permits dry field surgery because cold tissues use oxygen at a lower rate and can live without circulation for a longer period.

Heart assist pump. - A person recovers much more quickly from a heart attack if his heart has a chance to rest for a while; the heart assist pump makes this possible. One of the major problems in developing this device was synchronizing the artificial pumping action with the natural heartbeat. This was solved by NASA engineers by allowing the patient's own heart to stimulate the artificial one through an electropneumatic relay which responds to myopotentials. Thus, an electrical signal as low as 1 millivolt, produced at the skin by a feeble natural heartbeat, is sufficient to trigger the heart assist pump.

According to the nature of the problem, several types of heart assist pumps are available. One is the left-heart bypass. It pumps blood in parallel with the left heart. Another is the counter-pulsation pump, which pushes blood in and out of the aorta in synchronization with the heartbeat. Both devices reduce the workload of the heart and hence are useful in helping a patient recover from open-heart surgery as well as from heart attacks.

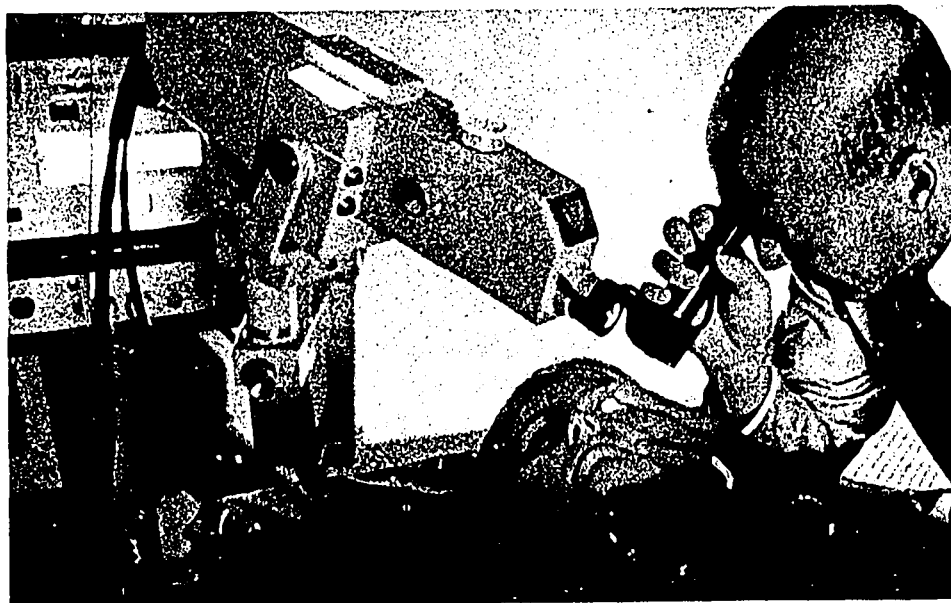


Figure 21-5. - Laser eye surgery. (Courtesy of Archie Liebermann.)

Laser. - The recent development of the laser device has created the new field of bloodless laser surgery. Ultraviolet lasers have been used to remove tumors. Lasers are also used for delicate eye surgery, as shown in figure 21-5. Here the surgeon aims a concentrated laser beam onto the back of the patient's eye. The resulting burn forms a pinpoint scar to seal down a dangerous tear of the retina.

Cryogenic probe. - The application of the cryogenic probe to the field of surgery has resulted in the technique of cryosurgery, which is the process of destroying diseased tissue by freezing. Cryogenic probes can be used to freeze the lens of an eye before removal of a cataract or to make a therapeutic lesion. Certain diseased areas of the brain can be killed by inserting a cryogenic probe to the proper depth and freezing the tissue (fig. 21-6).

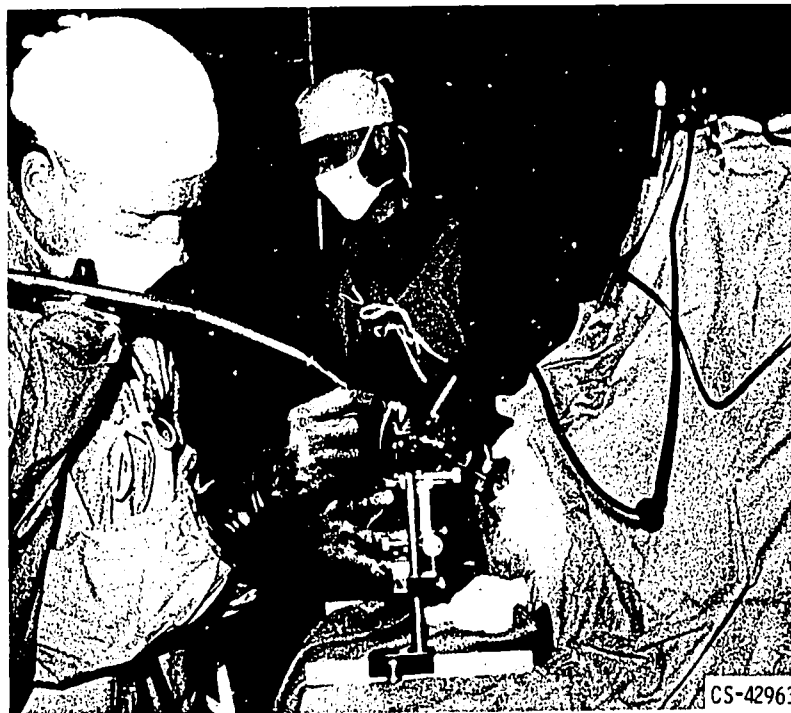


Figure 21-6. - Cryogenic brain surgery.

Air-inflated Hoverbed. - The principle and the technology of the Hovercraft, resulting from aeronautical research, have been applied in the development of the air-inflated Hoverbed, shown in figure 21-7. This bed is used for treating burn victims. The bag is pressurized by air from a compressor. The upper surface of the bag consists of segments of porous, light fabric. The pressure difference between the inside of the bag and the outside causes the upper surface to billow up. If an object is placed on the bag, a seal is made at the periphery of the object. Now the pressure on the bottom of the object becomes as high as the pressure inside the bag. Since a pressure difference

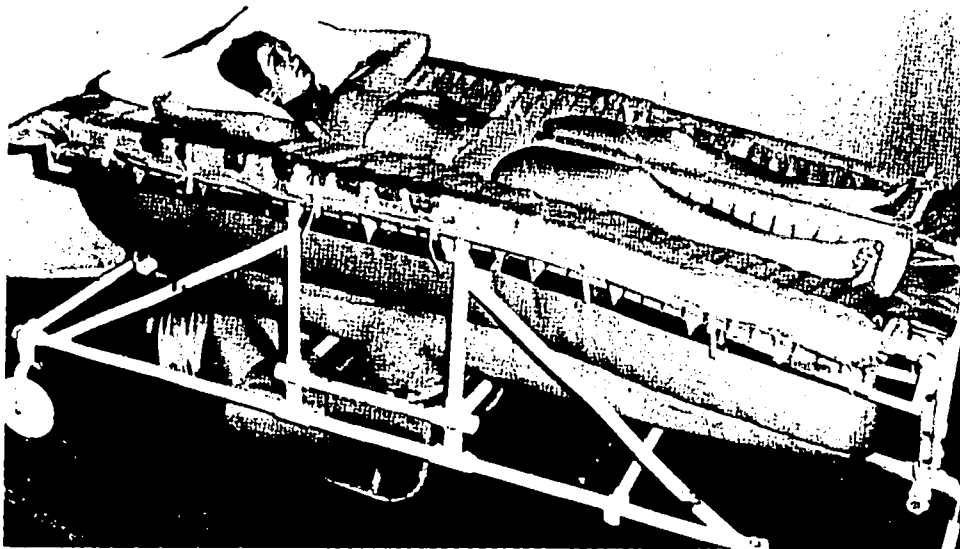


Figure 21-7. - Air-inflated Hoverbed. (Reprinted with the permission of Industrial Research, Inc.)

no longer exists across the fabric, it falls limply away. Now the object is essentially floating on air, except for a line of contact at its periphery. (This is the principle of Hovercraft.) The same thing happens when a patient lies down on the bag; the patient becomes almost completely airborne. Under this kind of treatment the weeping areas of burns dry rapidly.

Treatment summary. - Through the use of engineering equipment, entirely new treatment techniques, as well as better ways of doing the old jobs, have been made possible. As in diagnostics, the need for physicians who can deal with complicated engineering equipment is increasing. For the engineer, the design of equipment which will solve the needs of the physician is important. This field is already well underway with many fruitful applications.

PROSTHETICS

Prosthetics is the specialty which is concerned with the replacement of organs of the body with artificial devices. Some examples are now discussed.

Artificial heart. - The human heart is a four-chambered pump equipped with four valves (see fig. 21-3, p. 5). Recently, medical engineers have developed lightweight plastic pumps which can be substituted for the chambers of the heart. Figure 21-8 is a schematic diagram of one of these pumps. When pneumatic pressure in the drive line is reduced, blood pressure in the vein causes blood to open the inflow valve and fill the artificial ventricle. When pneumatic pressure in the drive line is increased, the resulting increased blood pressure in the ventricle closes the inflow valve, opens the outflow valve, and causes the blood to discharge into the artery.

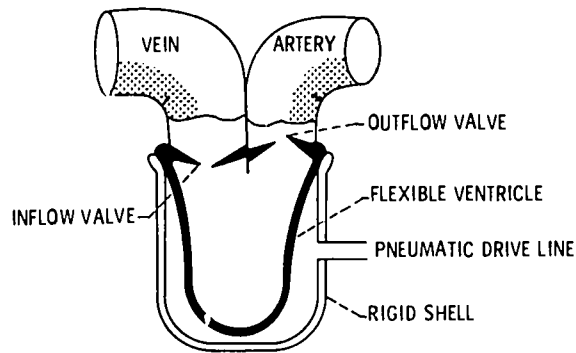
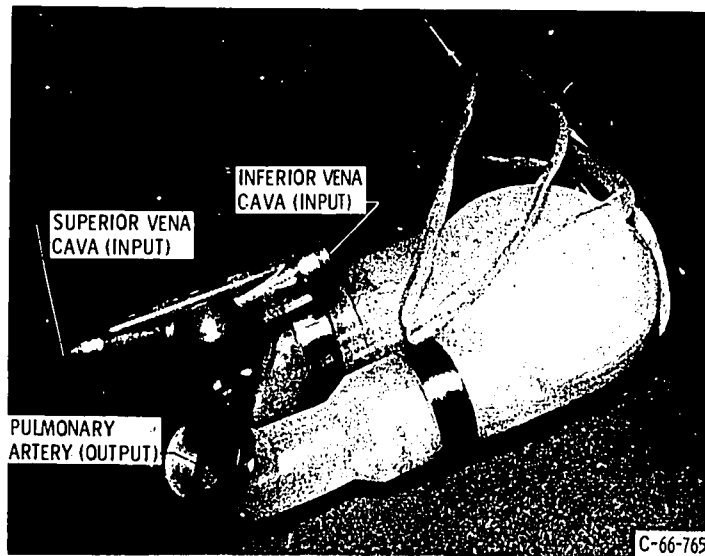
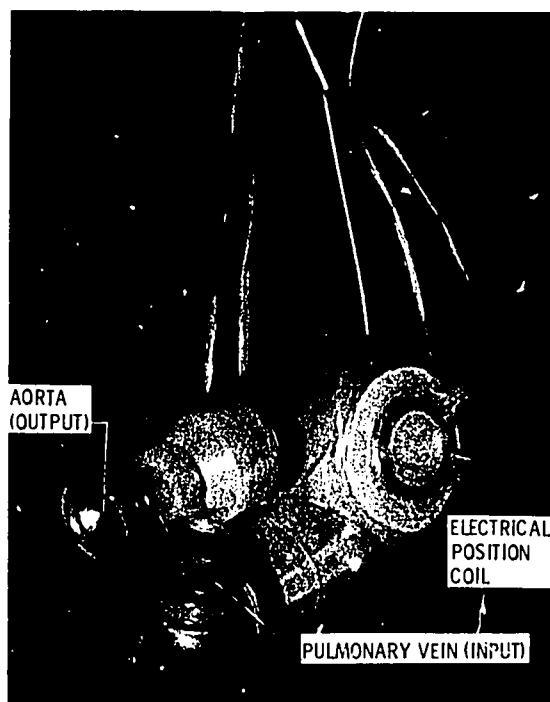


Figure 21-8. - Sac-type pneumatic artificial ventricle.



(a) Right chamber.



(b) Left chamber.

Figure 21-9. - Chambers of artificial heart.

345

Two such prosthetic ventricles (fig. 21-9) are required to replace a human heart. These ventricles, or chambers, are made of silicone rubber, a flexible material that is compatible with body fluids. The doughnut-shaped object on the side of the left chamber in figure 21-9 is an electrical position coil used to detect the blood volume in the artificial ventricle.

NASA engineers have contributed to the development of artificial heart systems, first by suggesting in 1960 the possibility of using air as an energy transfer medium for driving artificial hearts, and later by designing pneumatic control devices capable of reproducing physiologic pressure waveforms and pulse rates.

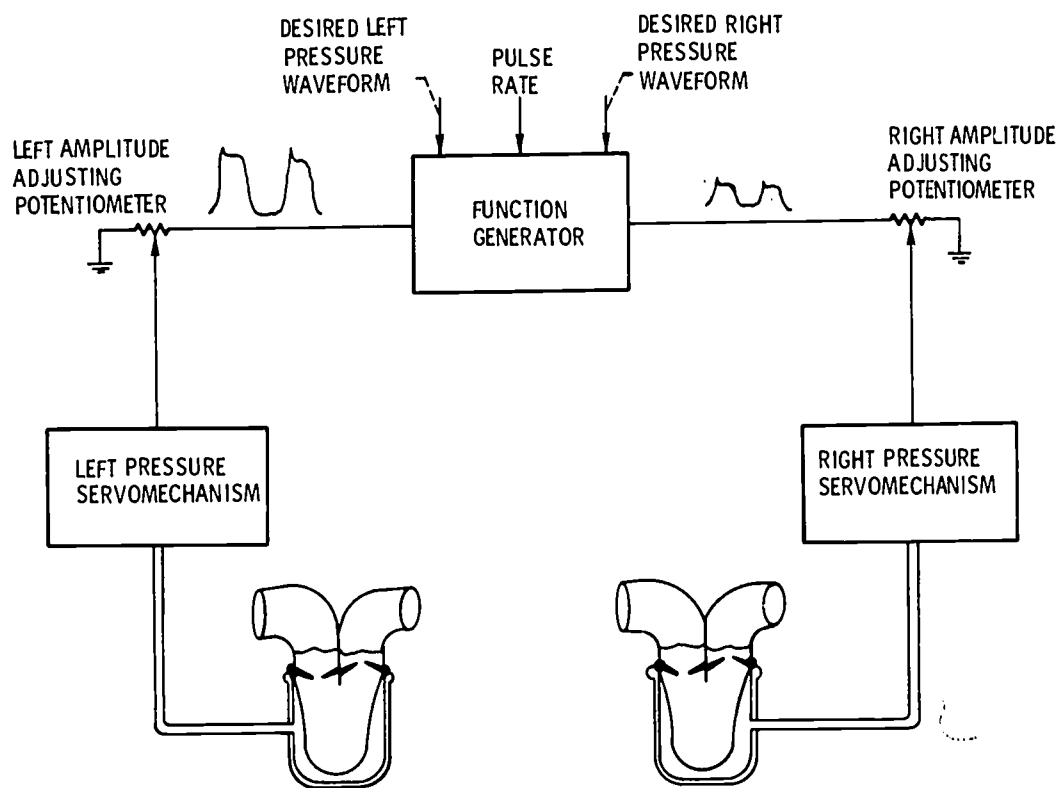


Figure 21-10. - Block diagram of artificial heart control system.

A block diagram of this NASA-developed control system for the artificial heart is shown in figure 21-10. The function generator is an electronic device which repetitively produces electrical voltages indicative of the desired left and right ventricular pressures. Since it is an electronic device, its waveforms can be adjusted to any desired functions of time, and it can be sped up or slowed down to provide variable pulse rates.

A desired fraction of the left and right voltages can be selected by means of the two amplitude adjusting potentiometers and fed to two pressure servomechanisms. These servos are slave devices which faithfully reproduce the voltages as pneumatic pressures.

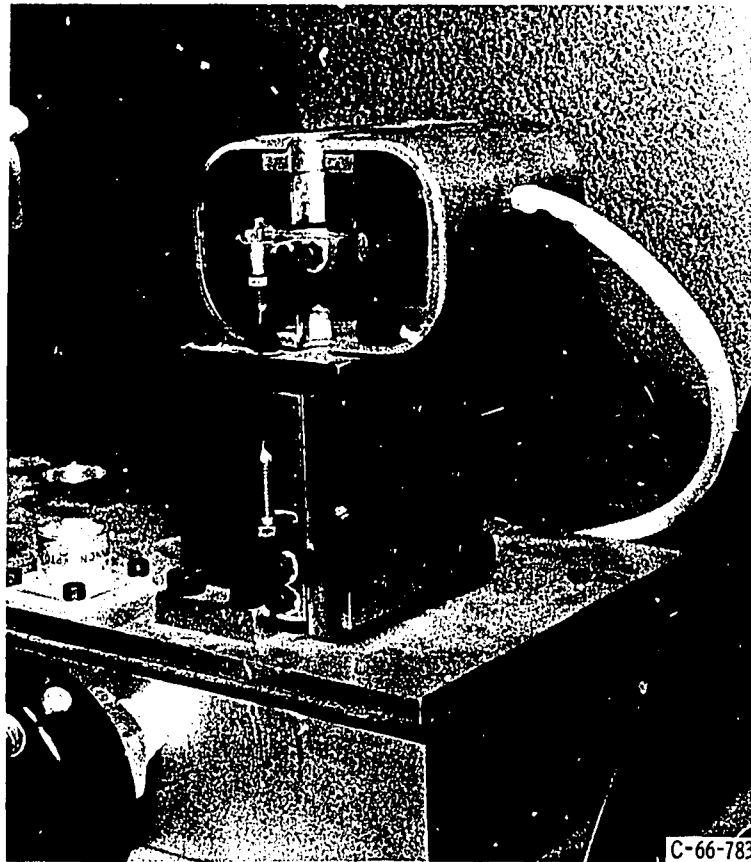


Figure 21-11. - Pneumatic servovalve for artificial heart.

Within each pressure servomechanism the electrical signal is transduced to a pneumatic pressure by a servovalve, shown in figure 21-11. The operating principle of the servovalve is similar to that of an electrical solenoid. An electrical current produces a motion of an armature. Through the use of a restraining spring, the motion of the armature is rendered proportional to the current in the coil. A valve element is connected to the armature by means of the long, thin drive rod shown in figure 21-11.

The complete control system, shown in figure 21-12, employs many sophistications necessitated by the nature of this medical research. The small analog computer at the top of the left console is used to lend flexibility to the control system. For example, the computer permits automatic adjustment of the amplitudes of the voltages going to the left and right pressure servos and eliminates the need for manual adjustment of the potentiometers shown in figure 21-10. This feature allows heart flow rate to respond to the body's needs through electronic sensing of physiological signals. Thus, the need for continual operator adjustment is reduced, and the system essentially makes its own adjustments. The bank of potentiometers in the lower portion of the left console (fig. 21-12)

347

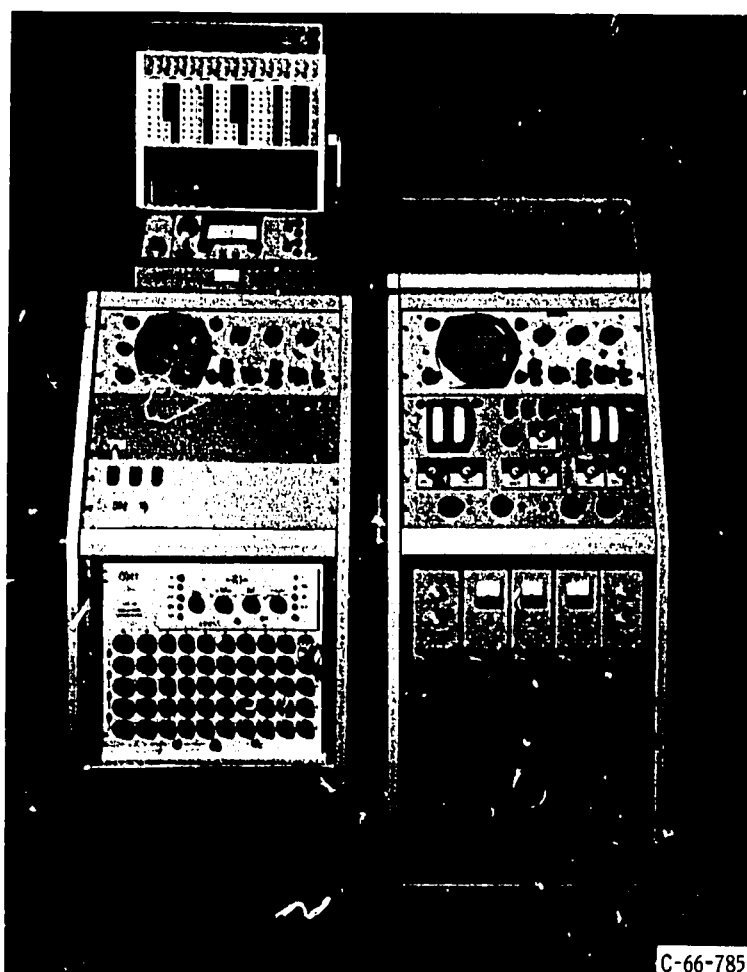


Figure 21-12. - Control system for artificial heart.

is used to set up the left and right heart pressure waveforms. The use of these 50 dual potentiometers permits a relatively exact setting of the desired waveforms.

The three electronic modules with square meters in the lower portion of the right console (fig. 21-12) are servoamplifiers for the pneumatic servovalves that are located in the pull-out drawer at the bottom of the console. Three channels of servosystems permit one to serve as a spare in case either the left or right channel fails. Automatic sensing of a failure and automatic substitution of the spare channel is accomplished by the large panel under the oscilloscope in the right console.

This control system is being used in a medical research program to develop artificial hearts for total heart replacement in humans. Present experimental work is being done with sheep and calves.

Pacemaker. - The pacemaker is an electronic heart-shocking device that replaces the nervous impulse that initiates the beat of the heart. Most pacemakers operate at a fixed pulse rate and consist of a free-running oscillator, a power amplifier, and batteries. Recently, the battery life has been increased, and the units can be implanted

under the skin; the requirements for electrical leads that penetrate the skin are thus eliminated.

Artificial kidney. - The artificial kidney is based on the principle of dialysis, which is the separation of substances in solution by means of differential diffusion through a semipermeable membrane. In the artificial kidney (fig. 21-13), blood from the body flows past semipermeable plastic membranes that are bathed by a dialyzing fluid. Impurities are removed from the blood by their diffusion through the membranes into the dialyzing solution. The artificial kidney shown in the figure was designed for home use to minimize cost to the patient.



Figure 21-13. - Artificial kidney for home use. (Courtesy of Dr. Yukihiko Nosé, Cleveland Clinic.)

Artificial limbs. - Work is being done in several organizations to develop powered artificial arms or legs. An artificial arm requires many degrees of freedom, and electric or hydraulic actuators with position or force feedback are required for each degree of freedom. Packaging all of this into a size compatible with the limb to be replaced presents a real engineering challenge. A variety of ways are available for obtaining the command signals. One way is to use biological electric signals caused by muscle contractions and called myopotentials. These signals from even minute muscle motions can be picked up on the skin's surface by electrodes, amplified, fed to a pattern-recognition computer similar to that used in recognizing aerial reconnaissance photos, and used to drive the actuators.

Prosthetics summary. - The ease with which engineering has been applied to diagnostics and treatment has not held true for prosthetics. One difficulty is that prosthetic

devices must serve as complete replacements for human organs during the remaining life of the patient. In the case of the artificial heart, for example, this requires approximately 100 000 beats a day, 3.6 million a year, or 720 million in 20 years. In contrast to this, the heart-lung machine, an operating-room device, need only function for about 6 hours, or about 25 000 beats. The researchers in prosthetics find themselves competing with nature in trying, in a few years, to develop an artificial organ as good as the natural one that developed over millions of years. The researcher gains a new respect for the capabilities of the human body. He also may find that the organ he is trying to replace was performing a function only partly understood by the physiologists. If the life of a patient depends on an artificial organ, the researcher is faced with several moral and legal problems. For example, if the artificial organ costs \$100 000 and requires a team of six experts to maintain it, could the resources being expended to keep one man alive keep several alive? If the machine fails because a simple part breaks, who is responsible? These are not arguments against working in this field, but they are arguments for working carefully. Moreover, advancing technology will solve many problems - new power sources, increased reliability, lower costs, and stronger materials are exactly what workers in this field are seeking.

BIOLOGICAL RESEARCH AND MAN-AUGMENTATION

The use of scientific and engineering equipment enables us to study the basic processes of nature, thereby expanding our knowledge of man. Special microscopes, electronic detectors, and chemical analysis techniques can be used in these studies. As this field expands, researchers may discover, on the molecular level, how the basic process of life takes place. The factors which determine and control intelligence, the basic nature of the thought process, heredity, aging, and disease will all become better understood.

When these basic biological subjects are understood in depth, improvements will be easier to make. A hint comes from Philco's Communications and Electronic Division, where work on the artificial limb control mentioned earlier has made it possible for man's nervous system to communicate directly with a computer by means of sensing myopotentials. At the same time, it is possible to communicate back to man's nervous system by electronics; experiments have been conducted in which electrodes have been implanted deep in the brains of monkeys. This has permitted stimulation of the monkeys that induced pleasure responses so great that the monkeys preferred pushing a lever to eating or sleeping - hence they levered themselves to exhaustion. A possible application of the myopotential work is remote control of industrial machines. It is hoped that a digging machine can be made to follow the arm motions of the operator. If detailed

intelligence-bearing information could be conveyed to and from the nervous system by electronics, the consequences to our society would be great. For example, speech at 200 words per minute is an awkward way to supply information to a computer, but electrical communication with the nervous system of man would permit individuals to communicate by electronics at speeds in excess of 1000 words per minute.

Electronic communication between man's mental processes and computers illustrates what may come about through the application of engineering principles to man himself. As technological development has advanced, man has produced sizable changes in his environment. He has surrounded himself with equipment that permits him to travel very fast, to speak over long distances, to raise crops, and to build roads with little expenditure of human energy. But, man's personal attributes have remained relatively unaffected. He still communicates verbally or in writing, the way men did when they thought that arteries were filled with air and that the heart was the body's source of heat, the site of love, and the habitat of the soul. During this time, man's machines have outstripped him. Technology has become so extensive that man, who still communicates and learns with the same old techniques, must spend an increasingly long time to learn enough to be useful; some professionals, like the surgeons, do not complete their education until they are past 30, or nearly at the chronological midpoint of their lives.

A further illustration of the incompatibility of man and his machine is the automobile. Each year, cars become faster and traffic patterns become more complicated. The proportion of people who are really capable of driving safely under these more difficult conditions is getting smaller. The need for an automobile control system using electronic sensors and computers which will augment the driver's sensory and decision-making capability is becoming very acute and is a fruitful area for future research.

Thus, a field which might be called man-augmentation is ready to be developed. It will bring man back into harmony with his machines. This will be done by both changing the machines so they are right for man and, through biological research, changing man so he can handle his new role in life. When this work is successful, man will become the master of his technology rather than a slave to it. Beyond these immediate goals, advances in basic biological research may, in the future, permit profound changes in man's physiology. It may be possible to regenerate diseased tissue, to enhance intelligence, to select the sex of progeny, or to slow down the aging process.

As with prosthetics, biological research and man-augmentation tends to be a more futuristic field than diagnostics and treatment. The idea of extending man's basic personal capabilities is far from present practice, but the future potential of this field is very great.

APPENDIX - CIRCULATORY SYSTEM PHYSIOLOGY

Purpose of Circulatory System

Any living organism depends for its existence on the exchange of material between itself and its surroundings. A spherical object like a single cell of radius R has a surface area of $4\pi R^2$ and a volume of $4\pi R^3/3$. Its surface-to-volume ratio is given by

$$\frac{S}{V} = \frac{3}{R} = \frac{6}{D}$$

This is the familiar surface-to-volume ratio which gives an insight into many phenomena of nature. It shows why larger plants and animals have had to develop specialized organisms for exchanging material with their surroundings. On a linear scale basis, man is about 5000 times as large as a single cell, so his material exchange problem, being a volume-to-surface-area related phenomenon, is 5000 times more difficult. To make life possible, organs like the lungs and digestive system have been developed with folded, crinkled surfaces to maximize their surface area. The circulatory system conducts materials around the body in liquid solution from these organs to nourish the cells of the body. These cells live in the interstitial fluid whose chemical composition is constantly maintained by the circulation of blood. Some reference numbers for man are as follows:

| | |
|--|------------|
| Body weight, kg (lb) | 70 (155) |
| Body volume, liters (qt) | 85 (89.7) |
| Interstitial fluid volume, liters (qt) | 14 (14.8) |
| Blood volume, liters (qt) | 5.3 (5.6) |
| Skin surface area, m^2 (ft^2) | 1.7 (18.3) |
| Lung effective surface area, m^2 (ft^2) | 90 (970) |
| Intestine effective surface area, m^2 (ft^2) | 10 (107) |
| Kidney effective surface area, m^2 (ft^2) | 1 (10.7) |

Function of Circulatory System

The circulatory system is composed primarily of the heart and a number of blood

vessels. Figure 21-3 (p. 5) shows a diagram of the system. The heart's only known function is to pump blood. The blood vessels essentially conduct blood to and away from the heart. The action of the heart is as follows: On diastole, the top part of the heart contracts (the two atria) and the bottom relaxes (the two ventricles). This causes blood to enter the two inflow valves and fill the ventricles. On systole, the bottom part of the heart contracts (the ventricles) and the top part relaxes (the atria). This causes blood to leave the heart through the two outflow valves. Thus, the heart is a four-chambered pump with four valves, two for each ventricle. Its external connections are four large veins and two large arteries, or six vessels in all. As the heart accepts blood on diastole and discharges it on systole, it exhibits an up-and-down motion because of the momentum of the entering and leaving blood. This motion, together with the pulsatile pressurization of the circulatory system which it causes, produces a two-pulsed sound on each beat. It also exerts a pulsating force on its owner. These sounds and motions are normally indicative of the presence or absence of life.

The flow path of blood in the circulatory system can be deduced by observing the vessel connections and knowing that the heart induces pulsatile, unidirectional flow of blood in its six connecting vessels. Starting from the superior and inferior venae cavae, blood enters the right atrium. On diastole, it enters the right ventricle through the tricuspid valve. On systole, blood leaves the right ventricle through the semilunar valve and enters the pulmonary artery. This artery divides to carry the blue blood to the two lungs. Red oxygenated blood returns from the lungs through the pulmonary veins to the left atrium. On diastole, it enters the left ventricle through the mitral valve. On systole, blood leaves the left heart through the aortic valve and enters the aorta. The ascending aorta divides to provide flows to the head and upper extremities while the remainder flows down the descending aorta to the trunk and lower extremities. The two sides of the circulatory system are the pulmonary system, and the systemic system.

The overall action of the heart and circulatory system is a fairly complex, ever-changing phenomenon. Pressures and flows in the vessels are not steady but pulsating. At locations near the heart, the amplitude of these pulsations are large, while at the ends of the small arteries the pulsations have been filtered, leaving steady flow conditions. In addition to the pulsatile conditions that exist in the circulatory system, the net overall flow rate, pulse rate, and pressure level change in response to stimulation of the organism. It has been found that both heart and blood vessels work together to produce these changes.

A graph of the time sequence of events in the left heart is shown in figure 21-14. The solid curve in the upper part of the figure shows pressure inside the ventricle. The upper dotted curve shows pressure in the aorta, while the lower dotted curve shows pressure in the left atrium. The next curve down shows a graph of heart sound output; the next curve shows the ventricular volume, and the last, the electrocardiogram (EKG).

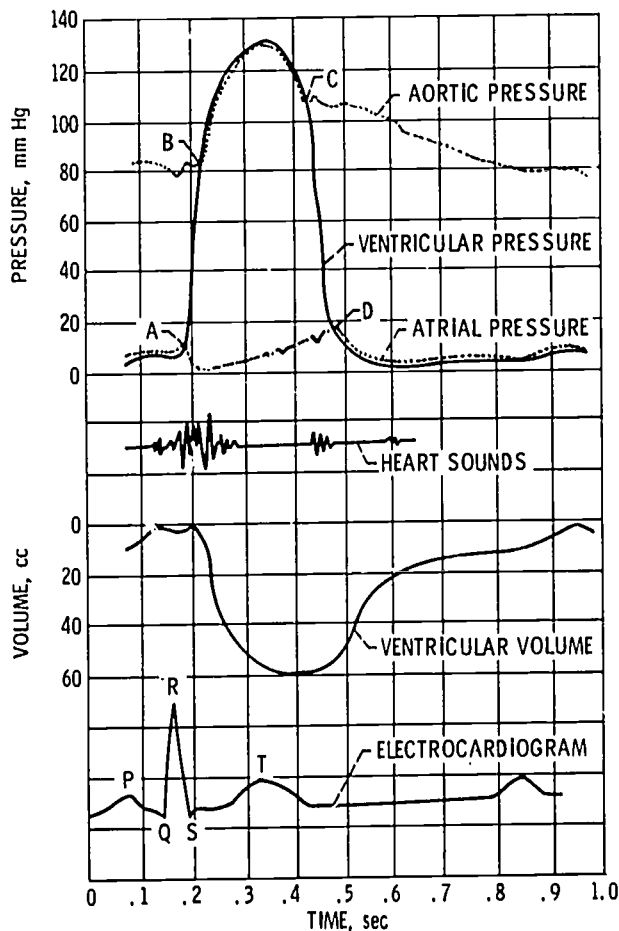


Figure 21-14. - Time history for left heart. (Based on Physiology In Health and Disease by C. J. Wiggers, Lea & Febiger, Publishers, 1949.)

At time 0.15 second on the graph, the heart gets a nervous impulse to beat. This causes a depolarization wave to sweep through the muscle cells of the heart, giving rise to the "QRS complex" part of the EKG signal and initiating contraction of the ventricles (systole). Shortly after this, the ventricle starts to contract. At point A (time = 0.18 sec) on the pressure curve, ventricular pressure exceeds atrial pressure and causes the mitral valve to close. Ventricular pressure rises rapidly from point A to point B (0.21 sec), at which point ventricular pressure exceeds aortic pressure and causes the aortic valve to open and outflow to begin. On the sound trace, it is seen that a fair amount of noise is associated with the rapid pressurization of the circulatory system and the action of the valves at points A and B.

From point B (0.21 sec) to point C (0.42 sec), ventricular pressure exceeds aortic pressure to cause outflow through the aortic valve. At point C, contraction of the ventricle is complete. This is the beginning of diastole. Ventricular pressure drops, thereby allowing the aortic valve to close. The heart first relaxes isometrically (i. e., without blood flow) from point C (0.42 sec) to point D (0.48 sec), both valves being closed. At point D, ventricular pressure drops below atrial pressure to cause the

mitral valve to open. This is followed by a relatively long inflow phase from point D (0.48 sec) to the beginning of the next systole, at about 0.98 second.

It is seen that the duration of systole is 0.24 second while that of diastole is 0.56 second. The period is 0.80 second, which corresponds to a pulse rate of 75 beats per minute. The percentage of the period for systole is 30 percent, with 70 percent of the time left for diastole.

The relatively short duration of systole is of interest. Since the entire outflow of the heart must be accomplished during this time, the peak instantaneous flow rate during systole is of the order of six times the average blood flow rate. Typical numbers are 30 liters per minute for peak instantaneous flow rate and 5 liters per minute for average flow rate.

Since 30 liters per minute equals about 8 gallons per minute, this peak flow rate is appreciable. (A typical flow rate from an open-ended garden hose is 5 gal/min.) One might wonder how high this peak flow rate might become during exercise. The situation is not as extreme as might be expected because the heart increases its rate mainly by shortening diastole. At very high pulse rates, systole and diastole are about equal in duration. This causes about a 4 to 1 ratio of peak instantaneous flow rate to average flow rate. At an average flow rate of 15 liters per minute, the peak value would be 60 liters per minute, or, at that instant, about three times the flow rate out of a garden hose.

A subject of additional interest is the power consumed by the human heart. Hydraulic power is found by multiplying pressure by flow rate and using the proper conversion factor. The following is a summary of average pressures in the circulatory system:

| Location | Pressure | |
|------------------|----------|------|
| | mm Hg | psi |
| Right atrium | 1.5 | 0.03 |
| Pulmonary artery | 15 | .3 |
| Left atrium | 5 | .1 |
| Aorta | 100 | 1.9 |

The right heart has to cause a pressure rise of 13.5 mm Hg (0.27 psi) while the left heart, 95 mm Hg (1.8 psi). With average flow rates of 5 liters per minute (resting) and 15 liters per minute (maximum), the hydraulic power outputs for the heart are as follows:

| | Output, W | |
|-------------|-----------|----------|
| | Rest | Exertion |
| Right heart | 0.16 | 0.48 |
| Left heart | 1.03 | 3.09 |
| Total | 1.19 | 3.57 |

This section has been a description of circulatory system physiology from the engineer's point of view. Special attention has been given to the timing of the heart's beat, the waveform of ventricular pressure, and hydraulic pumping power requirements.

GLOSSARY

anatomy. The science dealing with the structure of plants and animals.

aorta. The principal artery by which the blood leaves the heart and passes to the body.

aortic valve. The outflow valve from the left ventricle.

atrium. One of the two chambers of the heart by which the blood is received from the veins and forced into the ventricles. (The terms atrium and auricle are used interchangeably.)

cannula. A tube that is inserted into the body or into an organ for injecting or removing fluid.

depolarization. An object is polarized when it is charged electrically. A nervous impulse that depolarizes (discharges) the cells of a muscle causes that muscle to contract. This depolarization also induces a voltage (myopotential) that can be measured on the skin. The electrocardiogram (EKG) is a record of one of these voltages.

dialysis. The separation of substances in solution by means of their unequal diffusion through semipermeable membranes.

diastole. The period during which the heart muscle relaxes and the heart dilates. During this period the chambers of the heart fill with blood.

electropneumatic. Of or relating to a combination of electrical and pneumatic effects.

hypothermia. The state or condition of having a subnormal body temperature.

lesion. An injury to an organ or tissue.

mitral valve. The inflow valve to the left ventricle.

myopotential. A small electrical signal caused by the contraction of a muscle.

pathology. The study of the nature and progress of disease and of the changes it produces in structure and function. Thus, a pathological condition is the result of a disease.

physiology. The science dealing with the processes, activities, and phenomena characteristic of life.

radiopaque. Impenetrable to X-rays or other forms of radiation.

semilunar valve. The outflow valve from the right ventricle.

systole. The period during which the heart muscle is contracting and blood is expelled from the ventricles into the aorta and the arterial system.

therapeutic. Serving to cure or to heal.

tricuspid valve. The inflow valve to the right ventricle.

REFERENCE

1. Laënnec, R. T. H. (John Forbes, trans.): *A Treatise on the Diseases of the Chest and on Mediate Auscultation*. *Classics of Medicine and Surgery*. C. N. B. Camac, ed., Dover Publ., Inc., 1959, pp. 157-204 (originally published by W. B. Saunders Co., 1909).

22. PROJECTS IN ROCKETRY

James F. Connors*

The following is a brief description of the projects and activities undertaken by the Lewis Explorers during their rocketry studies. In its basic approach, each project was designed to simulate a practical working research environment. The Explorers were initially divided into six study, or research, teams, and each team was assigned a specific area of endeavor - propulsion, electronics, launch operations, aerodynamics, payloads and recovery, or tracking.

Within their assigned areas, members of these teams specialized during the first year of the program. They researched their topics to develop necessary operational skills and equipment for model rocketry. Guidance was provided to each team by NASA experts. To bring these activities into focus, a definite time allotment was made for the program. Project notebooks were maintained by each research team, and periodic oral progress reports were made to the Post membership. At the conclusion of this year of research effort, a formal research-and-development conference on aerospace rocketry was held for about 250 friends, family, teachers, and sponsors.

During the next year, the projects in model rocketry concentrated more on showing originality, exploring new ideas, and demonstrating craftsmanship. The objective was to achieve competition among the participants. Competitive categories (or events) similar to those used by the NAR (National Association of Rocketry) were established. The following events were included: (1) research and development, (2) parachute duration, (3) scale flight, (4) payload to maximum altitude, and (5) aerospace systems. The year's program culminated in the Explorer "Lunch-and-Launch" outing. A picnic was held, events were judged, and trophies were awarded. Some 60 or 70 models were launched before an appreciative audience of family, friends, school officials, and NASA and Boy Scouts of America sponsors.

Many of the Post activities are depicted in figures 22-1 to 22-36. These photographs are illustrative of the wide range of activities. Most are self-explanatory.

Some specific project work and field trips that the Post conducted are included in the photographs. Representative lecture-demonstration scenes are shown in figures 22-3 to 22-7. For pursuing the study of aerodynamics, a small wind tunnel (fig. 22-8) was

* Director of Technical Services.

improvised. It consisted simply of a three-speed floor fan with a metal cage to which were attached a cardboard honeycomb flow-straightening section and a center support tube. On this, rocket models (fig. 22-9) were mounted on a swivel to study the relation between center of pressure and center of gravity as they affect vehicle stability at high and low angles of attack. With a simple string-pulley-weight balance (fig. 22-10), the Explorers were able to evaluate fin geometries by measuring their relative lift effectiveness.

The aerodynamics group also evaluated the factors that enter into the determination of drag coefficient for parachutes (fig. 22-11). This evaluation was made by dropping a fixed-area chute with a known weight from a second-floor-level projection room and timing the fall from release to impact on the floor. Also, by using an inclined plane (in this case, ping-pong tables) and a wet, painted tennis ball (fig. 22-12), the Explorers traced a ballistic flight trajectory, which they determined to be parabolic.

In the propulsion area, commercial rocket engines were statically fired. An oscilloscope with a polaroid camera (fig. 22-13) was used to record the thrust-versus-time traces. The force produced by the rocket engine was measured by using a strain-gage flexure link or load cell. From the traces, engine performance and consistency could be evaluated. From measurements of the area under the curve of thrust-versus-time, the total impulse was determined.

In the electronics area, the project work concentrated on ignition circuitry and the firing console (fig. 22-14) for launch operations. Familiarity with common electronic instruments, direct-current bridge circuits, and the utilization and functions of the oscilloscope was also developed. In support of the launch operations, this group studied various methods available for providing communications between two tracking stations and the control center. Both walkie-talkie radios and wire-strung field phones were explored.

In shop areas, the Explorers were given the rudiments of model making (figs. 22-15, 22-16, and 22-17). In making balsa and cardboard models, techniques of wood selection, planing, turning, sanding, assembly, and finishing were practiced.

In all operations, procedures for personnel safety were observed. Before installing a model on the launch stand, each Explorer had to undergo a safety inspection of his model for workmanship and flight stability (figs. 22-18, 22-19, and 22-20). The Explorers installed their models on the launch stands and carried out their countdowns under the watchful eyes of the range safety officer.

With two tracking stations on a 1000-foot base line, theodolites (fig. 22-24) were used to track the rockets. Azimuthal and elevation angles were determined at the point where the model attained its maximum altitude. This information was communicated to the control center, where a plotting board (fig. 22-25) was set up. This board permitted graphical triangulation and the resultant determination of altitude.

Models were quite diversified in their basic designs and functions (figs. 22-26 and 22-27). Even a flying saucer was included. Most models were staged and had recoverable payloads, which varied from calibrated weights to fresh eggs and cameras.

Important adjuncts to the program were the special events, which were interspersed throughout the meetings schedule. These included a visit by NASA Spacemobile lecturers (fig. 22-28) and trips to the NASA-Lewis Plum Brook Station, with its nuclear test reactor (figs. 22-29, 22-30, and 22-31) and the rocket test facilities (fig. 22-32), the Cleveland Natural Science Museum and its planetarium, the Science Career Day at the Union Carbide Research Laboratory, and the National Explorer Delegate Conference at the University of Indiana (fig. 22-33). For 10 seniors, the climax of the program was a tour of the facilities at Cape Kennedy (figs. 22-34 and 22-35).



Figure 22-1. - Explorer officers.



Figure 22-2. - Member being welcomed to the group.



Figure 22-3. - Inside workings of a rocket thrust chamber.



Figure 22-4. - Lecture on basic principles of rocketry.



Figure 22-5. - Liquid-propellant mixing and vaporization.



Figure 22-6. - Solid propellants with different burning rates.



Figure 22-7. - Lift from air flowing over surfaces.

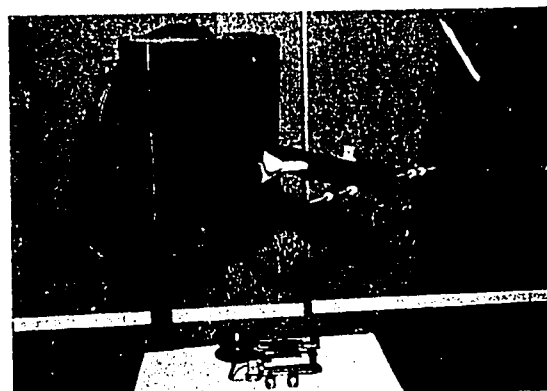


Figure 22-8. - Makeshift wind tunnel for evaluating fin effectiveness.



Figure 22-9. - Determination of rocket stability characteristics.

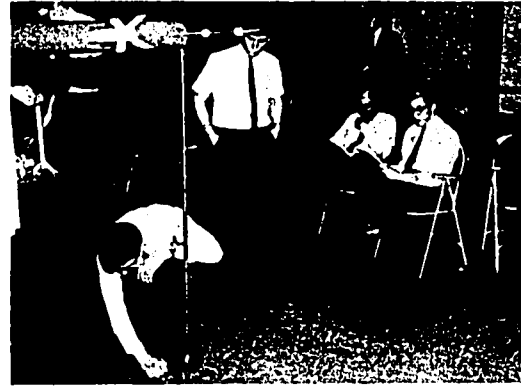


Figure 22-10. - Measuring relative lift effectiveness of rocket fins.

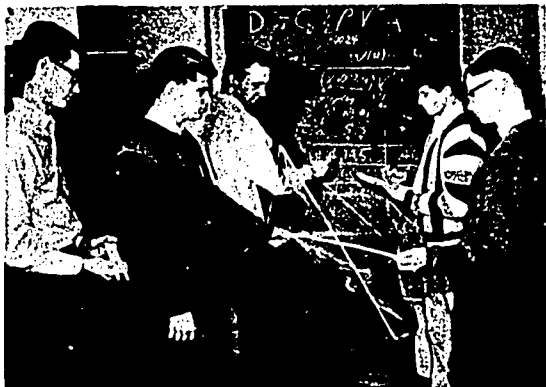


Figure 22-11. - Determination of parachute drag coefficient.



Figure 22-12. - Describing a ballistic rocket trajectory.

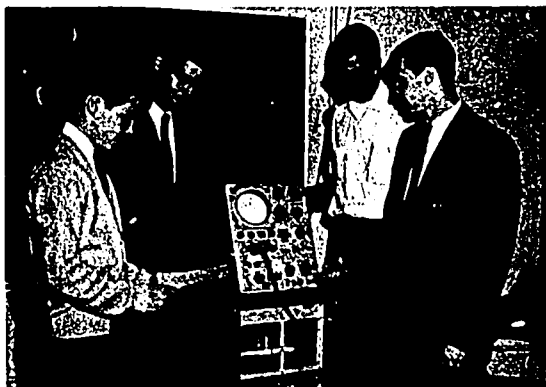


Figure 22-13. - Recording thrust versus time during static motor firing.



Figure 22-14. - Battery and firing-control console.



Figure 22-15. - Model fabrication.



Figure 22-16. - Model craftsmanship.



Figure 22-17. - Finished model boost glider.



Figure 22-18. - Preflight safety check of model rocket.



Figure 22-19. - Preparing the launch stand.

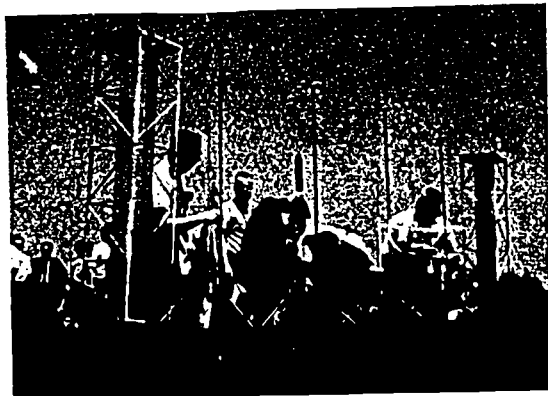


Figure 22-20. - Final preflight inspection.



Figure 22-21. - Scale model of Titan II rocket prepared for launch.

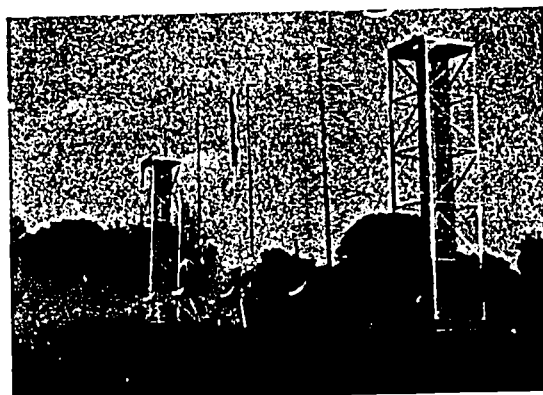


Figure 22-22. - Lift-off of Titan II model.



Figure 22-23. - Watching flight of model rocket.



Figure 22-24. - Remote tracking and communications station.



Figure 22-25. - Plotting board for altitude determinations.



Figure 22-26. - Preparing a six-stage rocket for launch.



Figure 22-27. - Preparing a flying saucer for launch.



Figure 22-28. - Demonstrations by NASA Spacemobile lecturers.



Figure 22-29. - Introduction to NASA-Lewis Plum Brook Reactor Facility.



Figure 22-30. - Water canals for transporting experiments out of Plum Brook Reactor Facility.



Figure 22-31. - Operating robot handling mechanisms in Hot Laboratory of Plum Brook Reactor Facility.

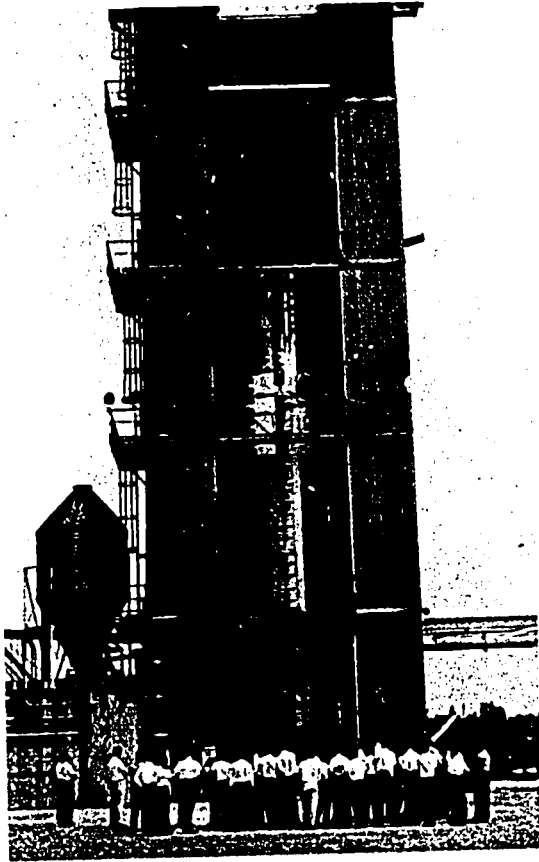


Figure 22-32. - Structural dynamic tests of the Atlas-Centaur at Plum Brook.

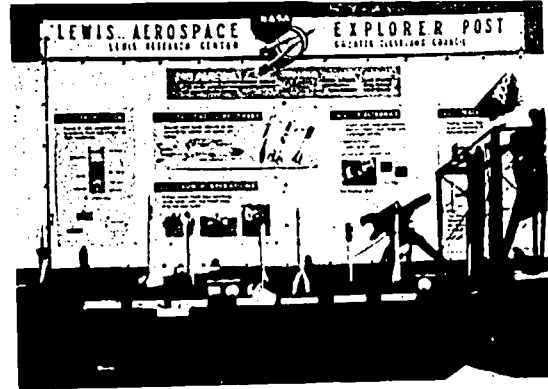


Figure 22-33. - Lewis Explorer exhibit for the National Delegate Conference at the University of Indiana.



Figure 22-34. - Monument to the original seven U.S. astronauts.

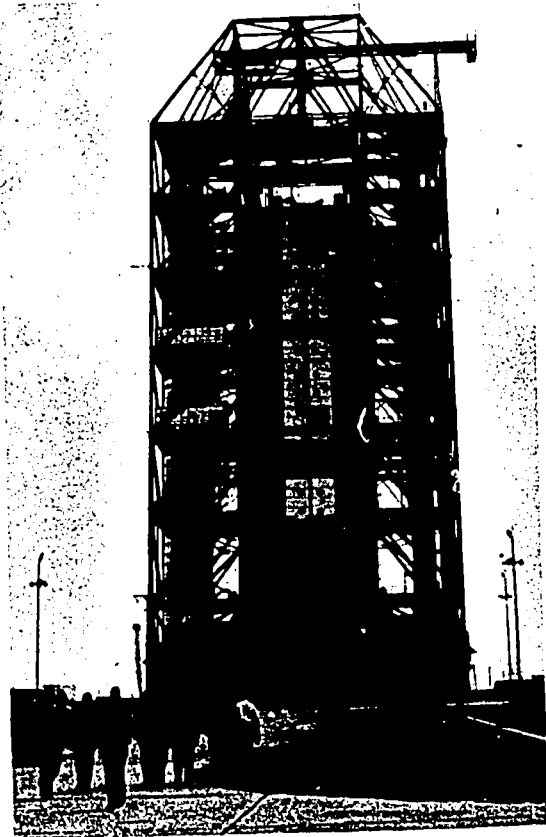


Figure 22-35. - NASA's moon terminal at Cape Kennedy.

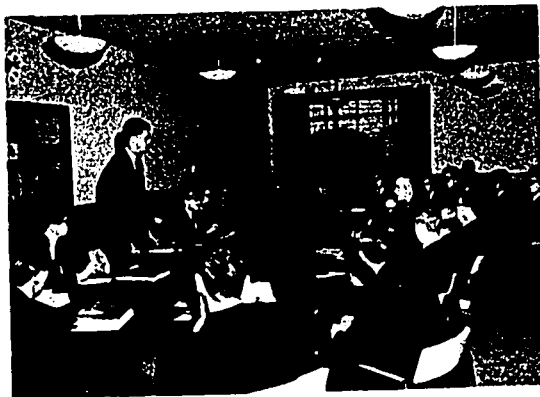


Figure 22-36. - Progress reporting on research-and-development projects.